ENDOCRINOLOGY IN CANCER AND AGING

EDITED BY: Ralf Jockers and Jianfeng Liu
PUBLISHED IN: Frontiers in Endocrinology

frontiers Research Topics

frontiers

ISSN 1664-8714
ISBN 978-2-88971-334-9
DOI 10.3389/978-2-88971-334-9

About Frontiers

Frontiers is more than just an open-access publisher of scholarly articles: it is a pioneering approach to the world of academia, radically improving the way scholarly research is managed. The grand vision of Frontiers is a world where all people have an equal opportunity to seek, share and generate knowledge. Frontiers provides immediate and permanent online open access to all its publications, but this alone is not enough to realize our grand goals.

Frontiers Journal Series

The Frontiers Journal Series is a multi-tier and interdisciplinary set of open-access, online journals, promising a paradigm shift from the current review, selection and dissemination processes in academic publishing. All Frontiers journals are driven by researchers for researchers; therefore, they constitute a service to the scholarly community. At the same time, the Frontiers Journal Series operates on a revolutionary invention, the tiered publishing system, initially addressing specific communities of scholars, and gradually climbing up to broader public understanding, thus serving the interests of the lay society, too.

Dedication to Quality

Each Frontiers article is a landmark of the highest quality, thanks to genuinely collaborative interactions between authors and review editors, who include some of the world's best academicians. Research must be certified by peers before entering a stream of knowledge that may eventually reach the public - and shape society; therefore, Frontiers only applies the most rigorous and unbiased reviews.
Frontiers revolutionizes research publishing by freely delivering the most outstanding research, evaluated with no bias from both the academic and social point of view. By applying the most advanced information technologies, Frontiers is catapulting scholarly publishing into a new generation.

What are Frontiers Research Topics?

Frontiers Research Topics are very popular trademarks of the Frontiers Journals Series: they are collections of at least ten articles, all centered on a particular subject. With their unique mix of varied contributions from Original Research to Review Articles, Frontiers Research Topics unify the most influential researchers, the latest key findings and historical advances in a hot research area! Find out more on how to host your own Frontiers Research Topic or contribute to one as an author by contacting the Frontiers Editorial Office: frontiersin.org/about/contact

ENDOCRINOLOGY IN CANCER AND AGING

Topic Editors:
Ralf Jockers, Université de Paris, France
Jianfeng Liu, Huazhong University of Science and Technology, China

Citation: Jockers, R., Liu, J., eds. (2021). Endocrinology in Cancer and Aging. Lausanne: Frontiers Media SA. doi: 10.3389/978-2-88971-334-9

Table of Contents

frontiers in Endocrinology

EDITORIAL
published: 15 July 2021
doi: 10.3389/fendo.2021.722929

Editorial: Endocrinology in Cancer and Aging

Ralf Jockers[1*] *and Jianfeng Liu*[2*]

[1] Université de Paris, Institut Cochin, INSERM, CNRS, Paris, France, [2] Cellular Signaling Laboratory, International Research Center for Sensory Biology and Technology of MOST, Key Laboratory of Molecular Biophysics of Ministry of Education, School of Life Science and Technology, Huazhong University of Science and Technology, Wuhan, China

Keywords: diabetes, obesity, dementia, pancreas, breast cancer

Editorial on the Research Topic

Endocrinology in Cancer and Aging

The Research Topic on "Endocrinology in Cancer and Aging" associated to the 7th edition of the International Congress on « Innovative therapeutics for Cancer and Ageing diseases » held in Wuhan (China) in October, 2019 generated a lot of interest with currently (June 2020) more than 22,000 views and more than 4,700 downloads of the 15 articles of this Research Topic.

Two articles of the Research Topic are authoritative review articles written by international experts in their fields. Duvillié et al. report on the interplay between type 2 diabetes and pancreatic ductal adenocarcinoma and insulinoma. The authors expose the complex landscape of the bidirectional interaction between diabetes and cancer that includes also obesity as a risk factor for diabetes, the influence of aging, genetic risk factors and pharmacological treatments. The authors try to consolidate the multiple interactions on the cellular and molecular level. Strous et al. focus in their review on growth hormone receptor (GHR) signaling pathways playing important roles in growth, metabolism, cancer and aging. As a cytokine receptor, GHR is regulated by signaling effectors that promote (i.e. JAK/STAT) or inhibiting (i.e. SOCS) GHR signaling as well as by ubiquitination followed by receptor proteasomal degradation, endocytosis and lysosomal degradation. The significance of GHR signaling for cancer development is demonstrated by mutations in the SOCS2-GHR axis that increases lung cancer risk as pointed out by the authors.

Several original articles of this Research Topic are studying the relation between diabetes and cancer in humans. In a prospective cohort study of 37,993 cancer survivors, Tao et al. found that diabetes increases the risk of all-cause mortality among breast, prostate, and colorectal cancer survivors but not for pre- or post-diagnosis diabetes.

In a case-control study on approximately 300 women with endometrial or ovarian cancer and a similar number of matched controls Liu et al. report that women with a history of gestational diabetes mellitus (GDM) or with the delivery of "large for gestational age" infants show increased the risk of developing endometrial cancer but not ovarian cancer. In contrast, the increase in risk of endometrial cancer was not observed in women with a history of preeclampsia. The authors speculate that increased placental leptin expression observed in GDM but not in preeclampsia might explain this difference.

Two association studies focused on elderlies. The study of Li et al. shows an association between polymorphisms in the Apolipoprotein E (*APOE*) gene, an important phospholipid and cholesterol transporter, with less depressive symptoms and higher serum LDL in Chinese elderly patients with schizophrenia, and a negative correlation between depressive symptoms and LDL. The study of Roh et al. shows that high body weight variability, i.e. repeated loss and regain of weight, is associated

OPEN ACCESS

Edited and reviewed by:
Paul Thomas Pfluger, Helmholtz-Gemeinschaft Deutscher Forschungszentren (HZ), Germany

***Correspondence:**
Ralf Jockers
ralf.jockers@inserm.fr
Jianfeng Liu
jfliu@mail.hust.edu.cn

Specialty section:
This article was submitted to Cellular Endocrinology, a section of the journal Frontiers in Endocrinology

Received: *09 June 2021*
Accepted: *30 June 2021*
Published: *15 July 2021*

Citation:
Jockers R and Liu J (2021) Editorial: Endocrinology in Cancer and Aging. Front. Endocrinol. 12:722929. doi: 10.3389/fendo.2021.722929

with an increased risk of dementia in a cohort of 19,987 elderly Korean. These studies highlight the increasingly recognized impact of metabolic dysfunction on dementia and schizophrenia.

Other articles report new biomarkers and advances in therapeutic solutions. Huang et al. analyzed the exosomal proteins present in the urine of 16 patients with papillary thyroid carcinoma and follicular thyroid carcinoma. By comparing the profiles before and after operation they identified serum thyroglobulin as a new biomarker for thyroid cancer. In a collection of 183 familial pancreatic neuroendocrine tumors Cuthbertson et al. showed that Ga-68 PET/CT imaging, a method based on the detection of somatostatin receptors present in 70-90 percent of neuroendocrine tumors, more accurately stages and guides the treatment of these patients.

In a retrospective study with 50 patients Wang et al. conclude that early diagnosis of primary adrenal lymphoma depends on a combination of biochemical examination, imaging studies, and pathological biopsy, and that a combined chemotherapy is associated with a good prognosis. Similarly, 58 patients with primary thyroid diffuse large B cell lymphoma having received a combination chemotherapy with radiotherapy had a better prognosis as reported by Yi et al. in a retrospective study.

The Research Topic includes also two insightful case reports. One on a 47-year-old female patient with primary adenoid cystic carcinoma of the upper anterior mediastinum mimicking a thyroid tumor (Wu et al.) and another on a 67-year-old man with a history of follicular thyroid carcinoma and papillary thyroid microcarcinoma (Wang et al.).

One original article uses an animal model, the MMTV-PyVT transgenic mouse model of spontaneous mammary tumors, to pinpoint the upregulation of quinolinate phosphoribosyltransferase (QPRT), an enzyme participating in NAD+ homeostasis (Liu et al.). Complementary *in vitro* studies in breast cancer cells indicate that QPRT enhanced breast cancer invasiveness probably through purinergic signaling and myosin light chain phosphorylation.

The two last original articles focus on *in vitro* studies to better understand the molecular mechanisms of cancer development. In the first study Wang et al. wanted to understand the effect of 17β-estradiol (E2) in the treatment of pelvic organ prolapse (POP) by determining the proliferation, apoptosis, and protein expressions of fibroblasts. The authors show that E2 can inhibit the progress of POP by inhibiting the expression level of mitofusin-2, a key regulator of mitochondrial fusion and division (Wang et al.). In second *in vitro* study starts from Czogalla et al. with a histological observation. The authors analyzed the expression of the scaffolding protein β-arrestin 2 in 156 patients with ovarian cancer. They show that high β-arrestin 2 expression correlates with high-grade serous histology and the expression of the gonadotropin receptors FSHR and LHCGR, as well as the membrane estrogen receptor GPER and hCGβ (Czogalla et al.). These results were confirmed by *in vitro* experiments in several cell lines. The authors propose β-arrestin 2 as a prognostic factor and a promising target for new therapeutic approaches in advanced ovarian cancer.

In conclusion, this Research Topic spans the full range of articles from case reports to studies on large cohorts, from original to review articles, from animal to human studies and from *in vitro* to *in vivo* studies. Altogether this collection makes a significant contribution to our understanding of endocrinology in cancer and aging.

AUTHOR CONTRIBUTIONS

Both authors contributed to the writing. All authors contributed to the article and approved the submitted version.

Conflict of Interest: The authors declare that the research was conducted in the absence of any commercial or financial relationships that could be construed as a potential conflict of interest.

frontiers in Endocrinology

ORIGINAL RESEARCH
published: 18 February 2020
doi: 10.3389/fendo.2020.00060

Pre- and Post-diagnosis Diabetes as a Risk Factor for All-Cause and Cancer-Specific Mortality in Breast, Prostate, and Colorectal Cancer Survivors: a Prospective Cohort Study

Huan Tao[1], *Adrienne O'Neil*[2,3], *Yunseon Choi*[4], *Wei Wang*[5], *Junfeng Wang*[6], *Yafeng Wang*[7]*, *Yongqian Jia*[1]* and *Xiong Chen*[8]*

[1] Department of Hematology and Research Laboratory of Hematology, West China Hospital, Sichuan University, Chengdu, China, [2] The Centre for Innovation in Mental and Physical Health and Clinical Treatment, Deakin University, Geelong, VIC, Australia, [3] Melbourne School of Population and Global Health, University of Melbourne, Carlton, VIC, Australia, [4] Department of Radiation Oncology, Busan Paik Hospital, Inje University College of Medicine, Busan, South Korea, [5] School of Mathematical Sciences, Shanghai Jiao Tong University, Shanghai, China, [6] Julius Center for Health Sciences and Primary Care, University Medical Center Utrecht, Utrecht University, Utrecht, Netherlands, [7] Department of Epidemiology and Biostatistics, School of Health Sciences, Wuhan University, Wuhan, China, [8] Department of Endocrinology, The First Affiliated Hospital of Wenzhou Medical University, Wenzhou, China

OPEN ACCESS

Edited by:
Ralf Jockers,
Université Paris-Sorbonne, France

Reviewed by:
Rosario Le Moli,
University of Catania, Italy
Alessandro Pizzocaro,
Milan University, Italy

***Correspondence:**
Yafeng Wang
wonyhfon@whu.edu.cn
Yongqian Jia
jia_yq@scu.edu.cn
Xiong Chen
chasecx@126.com

Specialty section:
This article was submitted to Cancer Endocrinology, a section of the journal Frontiers in Endocrinology

Received: *18 November 2019*
Accepted: *30 January 2020*
Published: *18 February 2020*

Citation:
Tao H, O'Neil A, Choi Y, Wang W, Wang J, Wang Y, Jia Y and Chen X (2020) Pre- and Post-diagnosis Diabetes as a Risk Factor for All-Cause and Cancer-Specific Mortality in Breast, Prostate, and Colorectal Cancer Survivors: a Prospective Cohort Study. Front. Endocrinol. 11:60. doi: 10.3389/fendo.2020.00060

Objective: The relationship between diabetes and all- and cause-specific mortality in individuals with common cancers (breast, colorectal, and prostate) remains both under-researched and poorly understood.

Methods: Cancer survivors (N = 37,993) from the National Health Interview Survey with linked data retrieved from the National Death Index served as our study participants. Cox proportional-hazards models were used to assess associations between pre- and post-diabetes and all-cause and cause-specific mortality.

Results: Over a median follow-up period of 13 years, 2,350 all-cause, 698 cancer, and 506 CVD deaths occurred. Among all cancer survivors, patients with diabetes had greater risk of: all-cause mortality [hazard ratio (HR) 1.35, 95% CI = 1.27–1.43], cancer-specific mortality (HR: 1.14, 95% CI = 1.03–1.27), CVD mortality (HR: 1.36, 95% CI = 1.18–1.55), diabetes related mortality (HR: 17.18, 95% CI = 11.51–25.64), and kidney disease mortality (HR: 2.51, 95% CI = 1.65–3.82), compared with individuals without diabetes. The risk of all-cause mortality was also higher amongst those with diabetes and specific types of cancer: breast cancer (HR: 1.28, 95% CI = 1.12–1.48), prostate cancer (HR: 1.20, 95% CI = 1.03–1.39), and colorectal cancer (HR: 1.29, 95% CI = 1.10–1.50). Diabetes increased the risk of cancer-specific mortality among colorectal cancer survivors (HR: 1.36, 95% CI = 1.04–1.78) compared to those without diabetes. Diabetes was associated with higher risk of diabetes-related mortality when compared to non-diabetic breast (HR: 9.20, 95% CI = 3.60–23.53), prostate (HR: 18.36, 95% CI = 6.01–56.11), and colorectal cancer survivors (HR: 12.18, 95% CI = 4.17–35.58). Both pre- and post-diagnosis diabetes increased the risk of all-cause mortality among

all cancer survivors. Cancer survivors with diabetes had similar risk of all-cause and CVD mortality during the second 5 years of diabetes and above 10 years of diabetes as compared to non-diabetic patients.

Conclusions: Diabetes increased the risk of all-cause mortality among breast, prostate, and colorectal cancer survivors, not for pre- or post-diagnosis diabetes. Greater attention on diabetes management is warranted in cancer survivors with diabetes.

Keywords: diabetes, all-cause, cancer, cardiovascular disease, mortality, cohort study

INTRODUCTION

Diabetes is a major public health burden. The prevalence of diabetes is projected to increase to 439 million adults by 2030. By this time, the disease burden in adults living with diabetes is estimated to increase by 20 and 69% in developing and developed countries, respectively (1, 2).

Diabetes mellitus (DM) and cancer are two common diseases affecting aging populations worldwide, which commonly co-occur. These associations are complex and may be cancer specific (3). On one hand, strong evidence links diabetes to an increased risk of breast and colorectal cancer onset (4, 5). On the other hand, there is some evidence it may be associated with decreased risk of prostate cancer onset (6). For those with a cancer diagnosis or history of the condition, there is evidence that diabetes may increase overall mortality risk. Previous studies have reported that diabetes increased the all-cause and cancer-specific mortality for cancer survivors compared to those without diabetes (7), including breast (8), colorectal (7–9), and prostate cancer survivors (10, 11). Interestingly, individuals with both diabetes and a history of cancer also have higher rates of cardiovascular mortality when compared to those without diabetes among the general population (12, 13). However, the relationship between diabetes and all- and cause-specific mortality in individuals with common cancers (breast, colorectal, and prostate) remains both under-researched and poorly understood.

This study aimed to estimate the associations of pre- and post-diagnosis diabetes, and duration of diabetes with all-cause, cancer-specific and CVD mortality among U.S. breast, prostate and colorectal cancer survivors in a large prospective cohort study.

METHODS

Study Population

The National Health Interview Survey (NHIS) is a stratified, multistage probability survey that samples an average of 57,000 adults per year to estimate the health of the U.S. population, the prevalence and incidence of disease, the extent of disability, and the use of health care services. One adult is randomly selected from each selected household for a detailed interview on health and other behaviors.

A total of 493,365 adults from the 13 cross-sectional waves (i.e., from 1997 to 2013) and their linked mortality data ending in December 31, 2015 was included in this analysis. After excluding missing data on diabetes, we identified 37,993 adults cancer survivors, including 6,330 breast cancer patients, 3,916 prostate cancer patients, and 2,656 colorectal cancer patients. A total of 5,174 cancer survivors diagnosed as diabetes, including 1,020 in breast cancer patients, 743 in prostate cancer patients and 509 in colorectal cancer patients. Totally, we identified 4,724 patients with diabetes prior to cancer diagnosis and 450 patients with diabetes after cancer diagnosis (**Figure 1**).

Diabetes

Self-reported diabetes was based on responses to questions "Have you ever been told by a doctor or other health professional that you had…" Women reporting diabetes occurring only during pregnancy, or adults who responded they had borderline diabetes were considered to not have diabetes. Diabetes was dichotomized into the presence or absence of diabetes (14, 15). Duration of diabetes was calculated by the present age minus the age at diagnosis of diabetes, and was categorized as <5, 5–10, and >10 years. After excluding individuals without diabetes and those with possible type 1 diabetes adults defined by using insulin and age of onset <30 years old which has been validated as accurate in 97% of cases (16).

Covariables

We included demographic variables (i.e., race, gender, education, and marital status), lifestyle variables (i.e., body mass index, physical activity, and alcohol consumption) and comorbid conditions [i.e., hypertension, coronary heart disease (CHD), and stroke]. Body mass index (BMI) was calculated as weight in kilograms divided by height squared (<25, 25–30, and >30 kg/m^2). A participant's physical activity was categorized into three groups according to metabolic equivalent task (MET) hours per week (low, 600 MET-h/wk; moderate, 600–3,000 MET-h/wk; high, >3,000 MET-h/wk). Alcohol consumption was categorized into three groups: lifetime abstainer; former drinker; current drinker. Cancer was defined as the presence of the same National Cancer Registry with a specific code (C code) more than three times within a year or an in patient hospitalization with a C code (17). Cancer diagnosed age was defined as the age at diagnosis of cancer and was categorized into <45, 45–65, and >65 years. Duration of cancer was calculated by the present age minus the cancer diagnosed age.

Abbreviations: NHIS, National Health Interview Survey; DM, Diabetes mellitus; CVD, Cardiovascular disease; CHD, Coronary heart disease; BMI, Body mass index; MET, Metabolic equivalent task; HRs, Hazard ratios; CI, Confidence intervals.

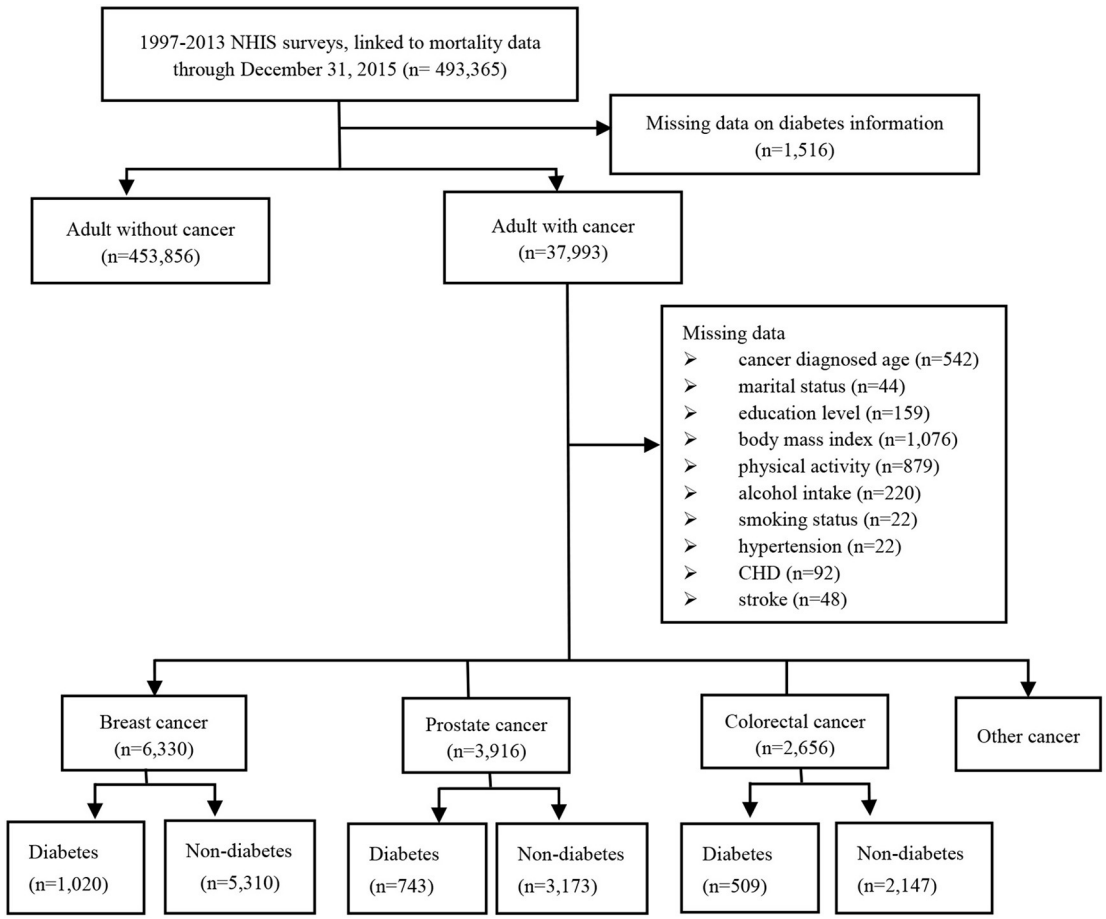

FIGURE 1 | Analytic sample selection.

Mortality

Ascertainment of mortality was established using the International Classification of Diseases-10th Revision codes, and study outcomes were defined using as follows: (1) all-cause mortality; (2) cancer-specific mortality (i.e., codes C00–C97); (3) CVD-mortality (i.e., codes I00–I09, I11, I13, and I20–I51, I60–I69); (4) diabetes mellitus (E10–E14); (5) chronic lower respiratory diseases (J40–J47); (6) influenza and pneumonia (J09–J18); (7) Alzheimer disease (G30) and (8) nephritis, Nephrotic syndrome and nephrosis (N00–N07, N17–N19, N25–N27).

Statistical Analysis

We compared participants with and without diabetes for basic characteristics using chi-square test to examine categorical differences in the weighted percentages. According to the baseline hazard to capture the increase in hazard due to aging, age was used as the underlying timescale. To evaluate the association of diabetes with all-cause, cancer and CVD mortality, we computed multivariable-adjusted hazard ratios (HRs) and 95% confidence intervals (CI) using cause-specific Cox proportional hazards models. All analyses were adjusted for age (using it as a timescale), sex, race, education level, income level, marital status, body mass index, smoking status, physical activity, alcohol intake, cancer diagnosed age, duration of cancer, history of hypertension, CHD, stroke, and missing data. We also analyzed the association between duration of diabetes and the risk of disease-specific and all-cause mortality. Besides, the relationship between pre- and post-diagnosis diabetes and mortality was examined among the 5,174 men and women cancer survivors. Two sensitivity analyses were also performed: (1) exclusion of individuals who died within the first 2 years; (2) exclusion of participants with CHD or stroke at interview; (3) excluding individuals with possible type 1 diabetes (defined by being on insulin and having an age of onset <30 years).

All analyses incorporated the complex survey design and were performed by using STATA version 15.0 (Stata Corp, College Station, TX, USA). Two-sided p-values <0.05 were considered significant for statistical inferences.

RESULTS

Descriptive statistics were reported in **Table 1**. The mean age of cancer survivors was 63 years at baseline. Compared to cancer

TABLE 1 | Basic characteristics.

Characteristics	Subgroups	Adult with diabetes (n = 5,174)	Adults without diabetes (n = 29,715)	P-value
		N (%)	N (%)	
Age				
	18–45 years	260 (5.08%)	5,059 (16.71%)	<0.001
	45–65 years	1,874 (35.91%)	11,424 (39.12%)	
	≥65 years	3,409 (59.01%)	15,425 (44.17%)	
Sex				<0.001
	Male	2,476 (49.13%)	12,036 (41.25%)	
	Female	3,067 (50.87%)	19,872 (58.75%)	
Race				<0.001
	Hispanic	500 (6.59%)	1,851 (3.93%)	
	Non-Hispanic White	4,143 (81.96%)	27,006 (88.99%)	
	Non-Hispanic Black	764 (9.22%)	2,363 (5.07%)	
	Non-Hispanic Other	136 (2.23%)	688 (2.01%)	
Education level				<0.001
	Less than high school degree	1,483 (24.10%)	5,531 (15.09%)	
	High school degree	1,717 (32.46%)	9,054 (28.75%)	
	More than high school degree	2,315 (43.44%)	17,187 (56.16%)	
Income level				<0.001
	Low	903 (12.02%)	3,796 (8.81%)	
	Moderate	3,306 (59.37%)	16,748 (49.84%)	
	High	1,334 (28.61%)	11,364 (41.35%)	
Marital status				<0.001
	Married/Living with partner	2,611 (61.74%)	16,273 (65.70%)	
	Widowed/Divorced/Separated	2,547 (32.83%)	12,804 (27.69%)	
	Never married	381 (5.43%)	2,791 (6.61%)	
Body mass index				<0.001
	<25 (kg/m^2)	1,078 (19.95%)	12,927 (41.04%)	
	25–30 (kg/m^2)	1,827 (33.88%)	11,161 (36.53%)	
	>30 (kg/m^2)	2,473 (46.17%)	6,885 (22.43%)	
Physical activity				<0.001
	Low (<600 MET-h/wk)	4,069 (73.19%)	19,331 (60.14%)	
	Moderate (600–3,000 MET-h/wk)	1,100 (22.05%)	9,107 (31.41%)	
	High (>3,000 MET-h/wk)	237 (4.76%)	2,462 (8.45%)	
Smoking status				<0.001
	Never smoking	2,424 (43.02%)	14,416 (45.28%)	
	Former smoking	2,382 (44.37%)	11,384 (36.75%)	
	Current smoking	700 (12.61%)	5,900 (17.96%)	
Alcohol intake				<0.001
	Lifetime abstainer	1,450 (25.17%)	6,224 (18.09%)	
	Former drinker	1,945 (34.76%)	7,100 (21.63%)	
	Current drinker	2,066 (40.07%)	18,129 (60.27%)	
Hypertension				<0.001
	Yes	4,243 (75.51%)	14,498 (43.49%)	
	No	1,297 (24.49%)	17,383 (56.51%)	
Stroke				<0.001
	Yes	707 (12.44%)	1,849 (5.38%)	
	No	4,826 (87.56%)	30,014 (94.62%)	
Coronary heart disease				<0.001
	Yes	1,270 (24.17%)	3,090 (9.52%)	
	No	4,241 (75.83%)	28,740 (90.48%)	
Cancer diagnosed age				<0.001
	<45	1,295 (24.04%)	11,599 (37.79%)	
	45–65	2,540 (46.63%)	12,537 (40.05%)	
	>65	1,708 (29.33%)	7,772 (22.15%)	

TABLE 2 | Mortality of cancer survivors with pre-diagnosis diabetes group compared to non-diabetic group.

Cancer sites	Mortality	Deaths	Adults without diabetes (n = 29,715)	Adults with diabetes (n = 5,174)			
				Pre-diagnosis diabetes (n = 4,724)		Post-diagnosis diabetes (n = 450)	
			HR	HR (95% CI)	*P*-value	HR (95% CI)	*P*-value
All cancer sites							
	All-cause mortality	2,350	1.00 (refer)	1.35 (1.27–1.44)	<0.001	1.35 (1.12–1.63)	0.002
	Cancer mortality	698	1.00 (refer)	1.14 (1.02–1.28)	0.02	1.23 (0.85–1.76)	0.267
	CVD mortality	506	1.00 (refer)	1.38 (1.20–1.59)	<0.001	1.07 (0.67–1.70)	0.771
	Chronic lower respiratory disease mortality	111	1.00 (refer)	1.12 (0.85–1.46)	0.429	1.73 (0.84–3.59)	0.138
	Diabetes mellitus mortality	189	1.00 (refer)	17.82 (11.86–26.79)	<0.001	8.62 (3.83–19.39)	<0.001
	Alzheimer's disease mortality	42	1.00 (refer)	1.66 (1.01–2.72)	0.044	0.37 (0.09–1.60)	0.185
	Influenza and pneumonia mortality	35	1.00 (refer)	0.98 (0.61–1.55)	0.917	2.18 (0.68–6.96)	0.188
	Kidney disease mortality	57	1.00 (refer)	2.45 (1.60–3.75)	<0.001	1.92 (0.66–5.61)	0.234
Breast (women)	All-cause mortality	425	1.00 (refer)	1.31 (1.10–1.57)	0.003	1.25 (1.02–1.52)	0.03
	Cancer mortality	125	1.00 (refer)	NA	NA	NA	NA
	CVD mortality	79	1.00 (refer)	2.05 (0.51–8.24)	0.313	NA	NA
	Diabetes mellitus mortality	30	1.00 (refer)	NA	NA	NA	NA
	Chronic lower respiratory disease mortality	25	1.00 (refer)	NA	NA	14.83 (3.67–59.88)	<0.001
	Alzheimer's disease mortality	11	1.00 (refer)	NA	NA	NA	NA
	Influenza and pneumonia mortality	8	1.00 (refer)	NA	NA	NA	NA
	Kidney disease mortality	11	1.00 (refer)	79.35 (4.93–1,277.73)	0.002	NA	NA
Prostate	All-cause mortality	333	1.00 (refer)	1.21 (1.01–1.43)	0.036	1.18 (0.93–1.51)	0.18
	Cancer mortality	103	1.00 (refer)	1.38 (0.38–4.98)	0.621	0.69 (0.07–6.71)	0.75
	CVD mortality	78	1.00 (refer)	NA	NA	NA	NA
	Diabetes mellitus mortality	21	1.00 (refer)	NA	NA	NA	NA
	Chronic lower respiratory disease mortality	15	1.00 (refer)	3.62 (1.12–11.72)	0.032	NA	NA
	Alzheimer's disease mortality	4	1.00 (refer)	16.44 (1.86–145.26)	0.012	NA	NA
	Influenza and pneumonia mortality	5	1.00 (refer)	NA	NA	NA	NA
	Kidney disease mortality	4	1.00 (refer)	NA	NA	NA	NA
Colorectal	All-cause mortality	272	1.00 (refer)	1.19 (0.77–1.84)	0.441	0.98 (0.33–2.93)	0.969
	Cancer mortality	96	1.00 (refer)	1.89 (0.51–7.02)	0.34	NA	NA
	CVD mortality	57	1.00 (refer)	NA	NA	NA	NA
	Diabetes mellitus mortality	24	1.00 (refer)	NA	NA	NA	NA
	Chronic lower respiratory disease mortality	8	1.00 (refer)	NA	NA	NA	NA
	Alzheimer's disease mortality	4	1.00 (refer)	NA	NA	NA	NA
	Influenza and pneumonia mortality	1	1.00 (refer)	NA	NA	NA	NA
	Kidney disease mortality	5	1.00 (refer)	NA	NA	NA	NA

CVD, cardiovascular disease; HR, hazard ratios.

Adjusted for age, sex, race, education level, income level, marital status, body mass index, smoking status, alcohol intake, physical activity, cancer diagnosed age, duration of cancer, history of hypertension, coronary heart disease and stroke, and missing data.

survivors without diabetes, cancer survivors with diabetes were more likely to be obesity (i.e., BMI > 30 kg/m^2) and be less physically active (i.e., low physical activity). Cancer survivors with diabetes tend to have a degree less than high school (24.1% in patients with diabetes, 15.09% in patients without diabetes). Patients with diabetes tend to have a history of hypertension (75.51% in patients with diabetes, 43.49% in patients without diabetes), CHD (24.17% in patients with diabetes, 9.52% in patients without diabetes), and stroke (12.44% in patients with diabetes, 5.38% in patients without diabetes).

After a median follow-up period of 13 years, 2,346 all-cause, 698 cancer-specific, and 506 CVD deaths occurred. **Figure 2** showed the risk of all-cause, cancer and CVD mortality among diabetic cancer survivors compared to non-diabetic cancer survivors. Compared to non-diabetes cancer survivors, cancer survivors with diabetes had a 35% higher risk of all-cause mortality (HR: 1.35, 95% CI = 1.27–1.43), 14% higher risk of cancer mortality (HR: 1.14, 95% CI = 1.03–1.27), and 36% higher risk of CVD mortality (HR: 1.36, 95% CI = 1.18–1.55). These relationships were

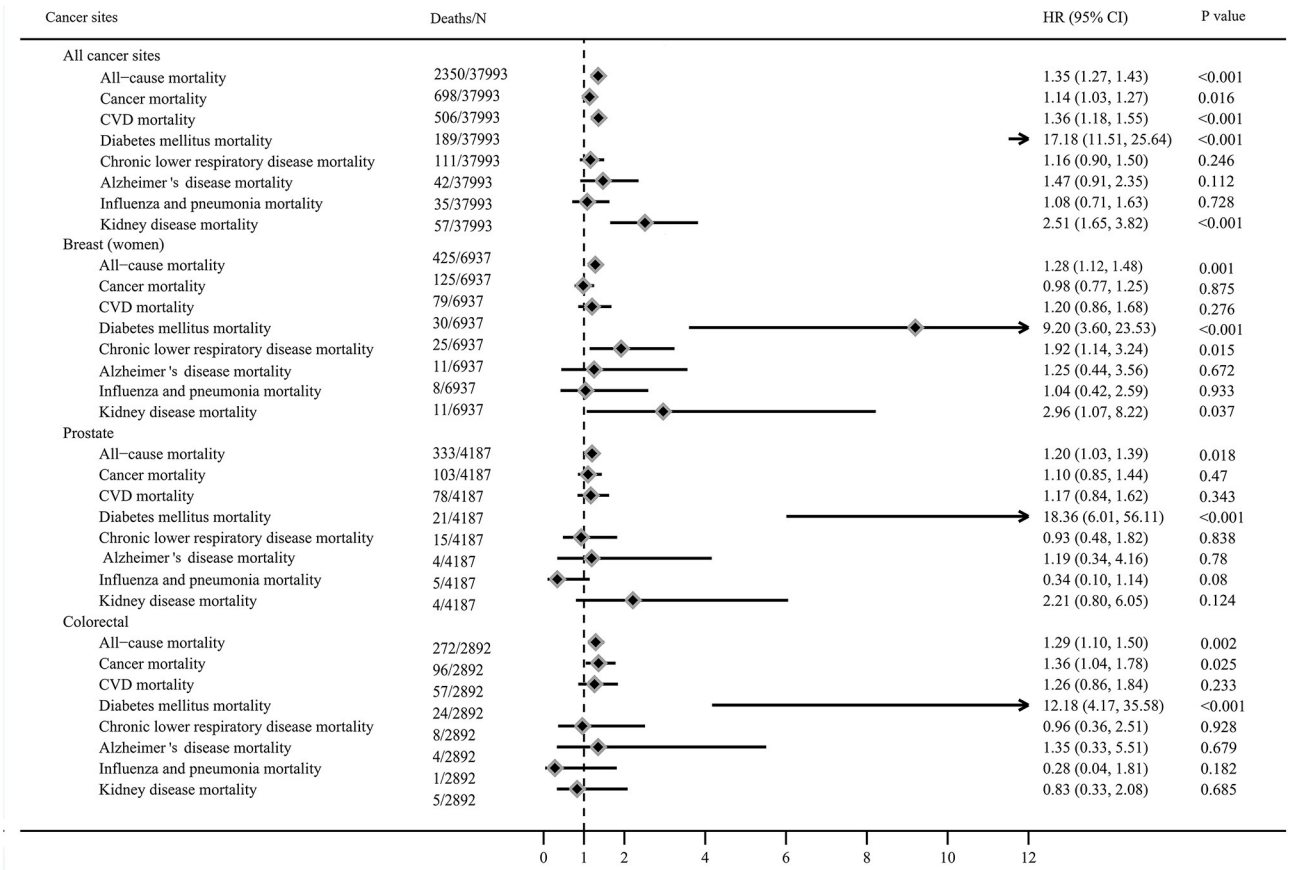

FIGURE 2 | Mortality of cancer survivors with diabetes compared to non-diabetic cancer survivors (adjusted for age, sex, race, education level, income level, marital status, body mass index, smoking status, alcohol intake, physical activity, cancer diagnosed age, duration of cancer, history of hypertension, coronary heart disease and stroke, and missing data).

stronger for diabetes related mortality (HR: 17.18, 95% CI = 11.51–25.64) and kidney disease mortality 2.51 for (95% CI = 1.65–3.82) who were diabetic survivors when compared to non-diabetic survivors, but no associations were observed between diabetes and risk of chronic lower respiratory disease, influenza and pneumonia, and Alzheimer disease mortality.

The HRs for all-cause mortality varied from 1.20 to 1.30 among survivors with diabetes diagnosed with breast cancer (HR: 1.28, 95% CI = 1.12–1.48), prostate cancer (HR: 1.20, 95% CI = 1.03–1.39), and colorectal cancer (HR = 1.29, 95% CI = 1.10–1.50). Diabetes increased the risk of cancer-specific mortality among colorectal cancer survivors (HR: 1.36, 95% CI = 1.04–1.78) compared to non-diabetic survivors, but not in breast and prostate cancer survivors. Diabetes was associated with higher risk of diabetes related mortality in breast (HR: 9.20, 95% CI = 3.60–23.53), prostate (HR: 18.36, 95% CI = 6.01–56.11), and colorectal cancer survivors (HR: 12.18, 95% CI = 4.17–35.58), compared to non-diabetic cancer survivors. Diabetes increased the risk of chronic lower respiratory disease mortality (HR: 1.92, 95% CI = 1.14–3.24) and kidney disease mortality (HR: 2.96, 95% CI = 1.07–8.22) among breast survivors compared to non-diabetic survivors, but not in colorectal and prostate cancer survivors.

Pre-diagnosis diabetes increased the risk of all-cause mortality (HR: 1.35, 95% CI = 1.27–1.44), cancer mortality (HR: 1.14, 95% CI = 1.02–1.28), CVD mortality (HR: 1.38, 95% CI = 1.20–1.59), diabetes mellitus mortality (HR: 17.82, 95% CI = 11.86–26.79), Alzheimer's disease mortality (HR: 1.66, 95% CI = 1.01–2.72), and kidney disease mortality (HR: 2.45, 95% CI = 1.60–3.75), respectively among all cancer survivors. Post-diagnosis diabetes increased the risk of all-cause mortality (HR: 1.35, 95% CI = 1.12–1.63) and diabetes mellitus mortality (HR: 8.62, 95% CI = 3.83–19.39), but not in other mortality. For specific cancer sites, pre-diagnosis diabetes increased the risk of all-cause mortality in prostate (HR: 1.21, 95% CI = 1.01–1.43) and breast cancer survivors (HR: 1.31, 95% CI = 1.10–1.57), not in colorectal cancer survivors. Post-diagnosis diabetes did not confer obvious increased risk of all-cause mortality for prostate and colorectal cancer sites except breast cancer (HR: 1.25, 95% CI = 1.02–1.52). Additional information were detailed in **Table 2**.

As summarized in **Table 3**, cancer survivors with diabetes had similar risk of all-cause and CVD mortality during the second 5 years of diabetes [(HR: 1.44, 95% CI = 1.29–1.60); (HR: 1.43,

TABLE 3 | Duration of diabetes among cancer survivors compared to those without diabetes.

Cancer sites	Mortality	Adults without diabetes	Adults with diabetes					
			0–5 years		5–10 years		>10 years	
		HR	HR (95% CI)	*P*-value	HR (95% CI)	*P*-value	HR (95% CI)	*P*-value
All cancer sites								
	All-cause mortality	1.00 (refer.)	1.21 (1.09, 1.33)	<0.001	1.44 (1.29–1.60)	<0.001	1.41 (1.30–1.52)	<0.001
	Cancer mortality	1.00 (refer.)	1.13 (0.97, 1.33)	0.123	1.40 (1.15–1.70)	0.001	1.04 (0.89–1.21)	0.624
	CVD mortality	1.00 (refer.)	1.14 (0.91, 1.43)	0.261	1.43 (1.13–1.82)	0.004	1.45 (1.22–1.71)	<0.001
	Chronic lower respiratory disease mortality	1.00 (refer.)	1.21 (1.10, 1.34)	<0.001	1.44 (1.29–1.60)	<0.001	1.41 (1.31–1.53)	<0.001
	Alzheimer's disease mortality	1.00 (refer.)	0.67 (0.26, 1.74)	0.408	2.20 (1.09–4.42)	0.027	1.71 (0.91–3.23)	0.098
	Diabetes mellitus mortality	1.00 (refer.)	10.97 (6.28, 19.16)	<0.001	11.04 (6.20–19.64)	<0.001	24.11 (15.55–37.38)	<0.001
	Influenza and pneumonia mortality	1.00 (refer.)	0.97 (0.43, 2.21)	0.95	0.55 (0.20–1.55)	0.258	1.29 (0.76–2.20)	0.342
	Kidney disease mortality	1.00 (refer.)	1.83 (0.84, 3.98)	0.129	4.29 (2.02–9.12)	<0.001	2.25 (1.35–3.73)	0.002
Breast (women)								
	All-cause mortality	1.00 (refer.)	1.22 (0.94, 1.56)	0.13	1.13 (0.88–1.46)	0.328	1.38 (1.16–1.64)	<0.001
	Cancer mortality	1.00 (refer.)	0.96 (0.62, 1.47)	0.849	1.26 (0.82–1.94)	0.283	0.89 (0.64–1.26)	0.521
	CVD mortality	1.00 (refer.)	1.18 (0.64, 2.18)	0.588	0.87 (0.41–1.87)	0.727	1.31 (0.87–1.99)	0.2
	Chronic lower respiratory disease mortality	1.00 (refer.)	1.22 (0.95, 1.57)	0.125	1.14 (0.88–1.47)	0.311	1.37 (1.15–1.63)	<0.001
	Alzheimer's disease mortality	1.00 (refer.)	0.16 (0.02, 1.21)	0.076	0.51 (0.06–4.14)	0.526	2.35 (0.73–7.56)	0.153
	Diabetes mellitus mortality	1.00 (refer.)	4.92 (1.42, 16.99)	0.012	5.61 (1.45–21.68)	0.013	13.45 (4.77–37.97)	<0.001
	Influenza and pneumonia mortality	1.00 (refer.)	1.63 (0.35, 7.53)	0.529	1.65 (0.38–7.07)	0.501	0.53 (0.11–2.48)	0.414
	Kidney disease mortality	1.00 (refer.)	0.66 (0.07, 6.62)	0.72	NA	NA	5.41 (1.84–15.87)	0.002
Prostate								
	All-cause mortality	1.00 (refer.)	1.11 (0.86, 1.42)	0.424	1.42 (1.07–1.89)	0.015	1.17 (0.96–1.41)	0.118
	Cancer mortality	1.00 (refer.)	1.31 (0.90, 1.91)	0.156	1.28 (0.74–2.20)	0.381	0.92 (0.65–1.31)	0.644
	CVD mortality	1.00 (refer.)	1.05 (0.58, 1.92)	0.871	1.51 (0.81–2.83)	0.194	1.12 (0.74–1.71)	0.592
	Chronic lower respiratory disease mortality	1.00 (refer.)	1.11 (0.86, 1.43)	0.41	1.43 (1.08–1.90)	0.014	1.17 (0.97–1.42)	0.107
	Alzheimer's disease mortality	1.00 (refer.)	0.96 (0.12, 7.74)	0.972	NA	NA	1.89 (0.42–8.56)	0.405
	Diabetes mellitus mortality	1.00 (refer.)	10.18 (2.16, 48.02)	0.003	16.29 (3.29–80.75)	0.001	25.25 (7.85–81.25)	<0.001
	Influenza and pneumonia mortality	1.00 (refer.)	0.21 (0.03, 1.57)	0.127	0.72 (0.09–5.91)	0.757	0.31 (0.05–1.73)	0.179
	Kidney disease mortality	1.00 (refer.)	2.72 (0.47, 15.59)	0.261	5.60 (2.41–13.03)	<0.001	0.60 (0.06–5.83)	0.661
Colorectal								
	All-cause mortality	1.00 (refer.)	1.19 (0.90, 1.58)	0.219	1.34 (0.98–1.82)	0.064	1.32 (1.08–1.60)	0.006
	Cancer mortality	1.00 (refer.)	1.29 (0.85, 1.98)	0.236	1.57 (0.91–2.72)	0.106	1.31 (0.90–1.89)	0.154
	CVD mortality	1.00 (refer.)	1.13 (0.55, 2.29)	0.743	0.98 (0.46–2.09)	0.956	1.42 (0.88–2.29)	0.149
	Chronic lower respiratory disease mortality	1.00 (refer.)	1.20 (0.91, 1.59)	0.198	1.34 (0.99–1.83)	0.059	1.33 (1.09–1.62)	0.005
	Alzheimer's disease mortality	1.00 (refer.)	1.21 (0.10, 14.85)	0.881	2.91 (0.54–15.76)	0.215	0.47 (0.06–3.82)	0.476
	Diabetes mellitus mortality	1.00 (refer.)	0.71 (0.08, 6.33)	0.756	5.54 (1.10–27.86)	0.038	23.47 (7.43–74.17)	<0.001
	Influenza and pneumonia mortality	1.00 (refer.)	NA	NA	NA	NA	0.49 (0.08–3.09)	0.444
	Kidney disease mortality	1.00 (refer.)	0.98 (0.10, 9.18)	0.985	0.99 (0.19–5.11)	0.994	0.73 (0.22–2.43)	0.604

CVD, cardiovascular disease; HR, hazard ratios.

Adjusted for age, sex, race, education level, income level, marital status, body mass index, smoking status, alcohol intake, physical activity, cancer diagnosed age, duration of cancer, history of hypertension, coronary heart disease and stroke, and missing data.

95% CI = 1.13–1.82)] and above 10 years [(HR = 1.41, 95% CI = 1.30–1.52); (HR: 1.45, 95% CI = 1.22–1.71)] as compared to non-diabetic participants. However, cancer survivors with duration of diabetes 5–10 years (HR: 1.40, 95% CI = 1.15–1.70) achieved the highest risk of cancer mortality compared to those with duration of diabetes <5 years or more than 10 years. Compared to non-diabetic survivors, cancer survivors with diabetes with duration for 0–5 years (HR: 10.97, 95% CI = 6.28–19.16), 5–10 years (HR: 11.04, 95% CI = 6.20–19.64), and more than 10 years (HR: 24.11, 95% CI = 15.55–37.38) were at increased risk of diabetes related mortality.

We conducted a sensitivity analysis excluding individuals who were followed up for less than the first 2 years, those with CHD, stroke. Exclusion of individuals with possible type 1 diabetes did not largely affect the HRs indicating the robustness of results (data not shown).

DISCUSSION

This large prospective study showed that compared to cancer survivors without diabetes, cancer survivors with diabetes had higher risk of all-cause, cancer-specific, and CVD mortality. Further they had an increased risk of all-cause, but not cancer specific mortality as the duration of diabetes increased. These findings add to a largely equivocal evidence base on this relationship.

Diabetes elevates all-cause and cancer specific mortality is consistent with a recent study which showed similar findings in individuals with established prostate cancer (11) as well as other studies in patients with breast and colorectal cancer (8). Some types of cancer are treated less aggressively in cancer survivors with diabetes than those without diabetes (18). In our study, pre-diagnosis diabetes increased the risk of all-cause mortality after adjusting for covariables in breast and prostate cancer sites, which is not consistent with previous findings (19, 20). But additional evidence indicated that pre-existing diabetes increased the risk of all-cause mortality among women with breast cancer after adjusting for covariables related to delayed diagnosis and therapy (21). In addition, pre-diagnosis diabetes increased the risk of all-cause mortality in colorectal cancer survivors in our study, which is consistent with findings in previous study (20).

Our second finding, that all-cause (but not cancer specific) mortality risk increased with diabetes duration has been observed previously in those with colorectal and breast cancer, respectively. With respect to the former group, diabetes duration of more than 10 years was associated with a 49% higher risk of all-cause mortality (22), which is slightly greater than the magnitude of association we observed (33%). With respect to the latter group, we found the risk of all-cause mortality increased in breast cancer patients who have had diabetes for more than 10 years, while others have shown increased risk from 7 years (23).

Among non-diabetic patients, hyperinsulinemia associated with reduced insulin sensitivity may play a role in the pathogenesis of prostate carcinoma (24). Thus, our study might underestimate the effect between insulin secretion or increase of insulin resistance and mortality among cancer survivors. Cancer survivor with diabetes have the same CVD risk of mortality during the second 5 years of diabetes and above 10 years as compared to non-diabetic patients. But this is not aspected since type 2 diabetes abnormalities (such as reduced insulin secretion, increase of insulin resistance) start several years before that the diabetes clinical manifestations appears.

Previous studies indicated the possible relationship between diabetic status and less aggressive oncological treatment and worse overall survival (18). In our study, all-cause mortality (but not cancer-specific) increase in long-standing diabetes diagnosis (>10 years) is likely to be related with the increase of potentially fatal events related to diabetic complications partially explaining the reduced cancer-mortality observed in this group in comparison with the 5–10 years group. A slight increase cancer-related mortality in recently diagnosed diabetic patient (0–5 years group) is likely to be related with short-time exposure to the risk of development of diabetes complications able to influence the oncological treatment strategies.

Diabetes could increase the risk of all-cause mortality among population with different diseases. In our study, both pre- and post-diagnosis diabetes increased the risk of all-cause mortality by 35% than non-diabetic cancer survivors, which was higher than that with 23% among tuberculosis patients (25). Previous studies indicated that patients with diabetes who underwent incident amputation have a 55% higher risk for all-cause mortality than non-diabetic patients (26), and diabetes increased the total mortality markedly with a higher 70% among patients hospitalized with a confirmed acute myocardial infarction than non-diabetic patients (27). In addition, individuals with vs. those without diabetes were at increased higher risk of all-cause mortality in the earlier (144%) and later time (95%) periods in the Framingham Heart Study (28).

There are several mechanistic pathways by which diabetes may confer elevated mortality risk in individuals with cancer history. Cancer patients with diabetes often have other diabetes-related comorbid conditions, which may influence physicians' clinical decision making (29). For example, cancer survivors with diabetes have been shown to be treated less aggressively with chemotherapy and radiotherapy (18, 30). This could partially explain the worse prognosis compared to those without diabetes. Secondly, individuals with co-morbid cancer and diabetes may have poor response to cancer treatment, including increased infection rates and intraoperative mortality (31). Thirdly, they may have a greater risk of chemotherapy-related toxicity (i.e., dilated cardiomyopathy in breast cancer) (30). Thus, conservative clinical decision making or side effects of conventional cancer treatments may impair survival time for individuals with this comorbidity.

The presence of diabetes may itself influence cancer progression via physiologic processes of hyperinsulinemia, hyperglycemia, immunodeficiency, and chronic inflammation. It is possible that most glucose uptake in cancer cells is constitutively high and independent of insulin binding to insulin-like growth factor receptor, which could stimulate cancer cell proliferation and metastasis (32, 33). Another potential pathway is that acute exposure to hyperglycemia may increase endothelial cell permeability for reasons of increased generation of reactive oxidative species and structural changes in the basement membrane, increasing the probability of metastasis (34). The third possible pathway is that hyperinsulinemia related to underlying insulin resistance might stimulate tumor growth (35). Multiple downstream signaling pathways are activated after insulin receptors interact with their ligands, and can stimulate multiple cancer phenotypes contribute to tumor initiation and progression (36). Decreased immunity induced by diabetes can also lead to cancer progression. In this study, the risk of diabetes related mortality increased obviously among cancer survivors with diabetes when compared to non-diabetic survivors. The increased mortality can be reversed when diabetes is managed well in clinical practice.

Limitations

Our study has several strengths including the large, prospective nature of the cohort used. The representativeness of the sample

further adds to the robustness of the findings. Nonetheless, our study had certain limitations. Firstly, we used an epidemiological definition of type 1 diabetes, which implies that misclassification of diabetes type is possible. However, a validation study has shown that those with possible type 1 diabetes adults defined by using insulin and age of onset <30 years old which has been validated as accurate in 97% of cases (16). This could be a potential bias for patients selection in our study. Secondly, we did not have extensive clinical parameters regarding disease status for diabetes and its comorbidities and cancer. For instance, insulin therapy has been associated with increased risk of newly developed colorectal cancer (37), however we could not account for this in the model. Thirdly, lacking of informations about pharmacological and/or surgical treatment received for either diabetes or cancer fail to identify subgroups of cancer survivors who may have been at risk of high mortality rate because of the cancer treatment they received. Fourthly, although diabetes assessments were from self-reports, it is always possible to include the participants who had never received the appropriate diagnostic tests of diabetes, and to misclassify the diabetes as non-diabetes. Self-report of cancer duration or diabetes implies high probability of incorrect data assumed as correct. Finally, our findings may not be generalizable to other cancer sites except for breast, colorectal, and prostate cancer.

CONCLUSION

Breast, prostate, and colorectal cancer survivors with diabetes had higher risk of all-cause mortality than did cancer survivors without diabetes. Pre-diagnosis diabetes increased risk of all-cause mortality after adjusting for covariables in breast and prostate cancer sites. Duration of diabetes is associated with increased risk of all-cause but not cancer specific mortality when compared to non-diabetic breast and prostate cancer survivors. Greater attention on diabetes control might be warranted in those with comorbid cancer and diabetes.

DATA AVAILABILITY STATEMENT

The datasets generated for this study are available on request to the corresponding author Yafeng Wang (wonyhfon@163.com).

ETHICS STATEMENT

The studies involving human participants were reviewed and approved by all procedures performed in studies involving adult participant provided a written informed consent and the NHIS was approved by the National Center for Health Statistics ethics review board. The patients/participants provided their written informed consent to participate in this study. Written informed consent was obtained from the individual(s) for the publication of any potentially identifiable images or data included in this article.

AUTHOR CONTRIBUTIONS

YW, XC, and YJ: conception and design of the study. YW and HT: acquisition of data and analysis, and statistical analysis. HT, YW, AO'N, YC, WW, JW, XC, and YJ: writing and revision of the manuscript. All authors read and approved the final manuscript.

FUNDING

This research was funded by the Department of Science and Technology of Sichuan Province (0040205302006) and Research Incubation Project of the First Affiliated Hospital of Wenzhou Medical University (FHY2019015).

ACKNOWLEDGMENTS

We would like to thank the NHIS for access to data and we greatly appreciate the support from other members of the study team who provided their generous contribution of time and efforts help during the research.

REFERENCES

1. Engelgau MM, Geiss LS, Saaddine JB, Boyle JP, Benjamin SM, Gregg EW, et al. The evolving diabetes burden in the United States. *Ann Intern Med.* (2004) 140:945–50. doi: 10.7326/0003-4819-140-11-200406010-00035
2. Shaw JE, Sicree RA, Zimmet PZ. Global estimates of the prevalence of diabetes for 2010 and 2030. *Diabetes Res Clin Pract.* (2010) 87:4–14. doi: 10.1016/j.diabres.2009.10.007
3. Renehan AG, Yeh HC, Johnson JA, Wild SH, Gale EA, Moller H. Diabetes and cancer (2): evaluating the impact of diabetes on mortality in patients with cancer. *Diabetologia.* (2012) 55:1619–32. doi: 10.1007/s00125-012-2526-0
4. Larsson SC, Orsini N, Wolk A. Diabetes mellitus and risk of colorectal cancer: a meta-analysis. *J Natl Cancer Inst.* (2005) 97:1679–87. doi: 10.1093/jnci/dji375
5. Johnson JA, Carstensen B, Witte D, Bowker SL, Lipscombe L, Renehan AG. Diabetes and cancer (1): evaluating the temporal relationship between type 2 diabetes and cancer incidence. *Diabetologia.* (2012) 55:1607–18. doi: 10.1007/s00125-012-2525-1
6. Kasper JS, Giovannucci E. A meta-analysis of diabetes mellitus and the risk of prostate cancer. *Cancer Epidemiol Biomarkers Prev.* (2006) 15:2056–62. doi: 10.1158/1055-9965.EPI-06-0410
7. Barone BB, Yeh HC, Snyder CF, Peairs KS, Stein KB, Derr RL, et al. Long-term all-cause mortality in cancer patients with preexisting diabetes mellitus: a systematic review and meta-analysis. *JAMA.* (2008) 300:2754–64. doi: 10.1001/jama.2008.824
8. De Bruijn KM, Arends LR, Hansen BE, Leeflang S, Ruiter R, van Eijck CH. Systematic review and meta-analysis of the association between diabetes mellitus and incidence and mortality in breast and colorectal cancer. *Br J Surg.* (2013) 100:1421–9. doi: 10.1002/bjs.9229
9. Luo W, Cao Y, Liao C, Gao F. Diabetes mellitus and the incidence and mortality of colorectal cancer: a meta-analysis of 24 cohort studies. *Colorectal Dis.* (2012) 14:1307–12. doi: 10.1111/j.1463-1318.2012.02875.x
10. Snyder CF, Stein KB, Barone BB, Peairs KS, Yeh HC, Derr RL, et al. Does pre-existing diabetes affect prostate cancer prognosis? A systematic review. *Prostate Cancer Prostatic Dis.* (2010) 13:58–64. doi: 10.1038/pcan.2009.39

11. Cai H, Xu Z, Xu T, Yu B, Zou Q. Diabetes mellitus is associated with elevated risk of mortality amongst patients with prostate cancer: a meta-analysis of 11 cohort studies. *Diabetes Metab Res Rev.* (2015) 31:336–43. doi: 10.1002/dmrr.2582
12. Rawshani A, Sattar N, Franzen S, Rawshani A, Hattersley AT, Svensson AM, et al. Excess mortality and cardiovascular disease in young adults with type 1 diabetes in relation to age at onset: a nationwide, register-based cohort study. *Lancet.* (2018) 392:477–86. doi: 10.1016/S0140-6736(18)31506-X
13. Sattar N, Rawshani A, Franzen S, Rawshani A, Svensson AM, Rosengren A, et al. Age at diagnosis of type 2 diabetes mellitus and associations with cardiovascular and mortality risks. *Circulation.* (2019) 139:2228–37. doi: 10.1161/CIRCULATIONAHA.118.037885
14. Miller EA, Tarasenko YN, Parker JD, Schoendorf KC. Diabetes and colorectal cancer screening among men and women in the USA: National Health Interview Survey: 2008, 2010. *Cancer Causes Control.* (2014) 25:553–60. doi: 10.1007/s10552-014-0360-z
15. Lipton BJ, Decker SL. Association between diagnosed diabetes and trouble seeing, National Health Interview Survey, 2011–13. *J Diabetes.* (2015) 7:743–6. doi: 10.1111/1753-0407.12311
16. Gregg EW, Cheng YJ, Srinivasan M, Lin J, Geiss LS, Albright AL, et al. Trends in cause-specific mortality among adults with and without diagnosed diabetes in the USA: an epidemiological analysis of linked national survey and vital statistics data. *Lancet.* (2018) 391:2430–40. doi: 10.1016/S0140-6736(18)30314-3
17. Hwangbo Y, Kang D, Kang M, Kim S, Lee EK, Kim YA, et al. Incidence of diabetes after cancer development: a Korean National Cohort Study. *JAMA Oncol.* (2018) 4:1099–105. doi: 10.1001/jamaoncol.2018.1684
18. van de Poll-Franse LV, Houterman S, Janssen-Heijnen ML, Dercksen MW, Coebergh JW, Haak HR. Less aggressive treatment and worse overall survival in cancer patients with diabetes: a large population based analysis. *Int J Cancer.* (2007) 120:1986–92. doi: 10.1002/ijc.22532
19. Kiderlen M, de Glas NA, Bastiaannet E, Engels CC, van de Water W, de Craen AJ, et al. Diabetes in relation to breast cancer relapse and all-cause mortality in elderly breast cancer patients: a FOCUS study analysis. *Ann Oncol.* (2013) 24:3011–6. doi: 10.1093/annonc/mdt367
20. Strele I, Pildava S, Repsa I, Kojalo U, Vilmanis J, Brigis G. Pre-existing diabetes mellitus and all-cause mortality in cancer patients: a register-based study in Latvia. *Acta Oncol.* (2018) 57:973–82. doi: 10.1080/0284186X.2017.1420909
21. Luo J, Hendryx M, Virnig B, Wen S, Chlebowski R, Chen C, et al. Pre-existing diabetes and breast cancer prognosis among elderly women. *Br J Cancer.* (2015) 113:827–32. doi: 10.1038/bjc.2015.249
22. Amshoff Y, Maskarinec G, Shvetsov YB, Raquinio PH, Grandinetti A, Setiawan VW, et al. Type 2 diabetes and colorectal cancer survival: the multiethnic cohort. *Int J Cancer.* (2018) 143:263–8. doi: 10.1002/ijc.31311
23. Maskarinec G, Shvetsov YB, Conroy SM, Haiman CA, Setiawan VW, Le Marchand L. Type 2 diabetes as a predictor of survival among breast cancer patients: the multiethnic cohort. *Breast Cancer Res Treat.* (2019) 173:637–45. doi: 10.1007/s10549-018-5025-2
24. Nandeesha H, Koner BC, Dorairajan LN. Altered insulin sensitivity, insulin secretion and lipid profile in non-diabetic prostate carcinoma. *Acta Physiol Hung.* (2008) 95:97–105. doi: 10.1556/APhysiol.95.2008.1.7
25. Ko PY, Lin SD, Hsieh MC, Chen YC. Diabetes mellitus increased all-cause mortality rate among newly-diagnosed tuberculosis patients in an Asian population: a nationwide population-based study. *Diabetes Res Clin Pract.* (2017) 133:115–23. doi: 10.1016/j.diabres.2017.08.011
26. Schofield CJ, Libby G, Brennan GM, MacAlpine RR, Morris AD, Leese GP, et al. Mortality and hospitalization in patients after amputation: a comparison between patients with and without diabetes. *Diabetes Care.* (2006) 29:2252–6. doi: 10.2337/dc06-0926
27. Mukamal KJ, Nesto RW, Cohen MC, Muller JE, Maclure M, Sherwood JB, et al. Impact of diabetes on long-term survival after acute myocardial infarction: comparability of risk with prior myocardial infarction. *Diabetes Care.* (2001) 24:1422–7. doi: 10.2337/diacare.24.8.1422
28. Preis SR, Hwang SJ, Coady S, Pencina MJ, D'Agostino RB Sr., Savage PJ, et al. Trends in all-cause and cardiovascular disease mortality among women and men with and without diabetes mellitus in the Framingham Heart Study, 1950 to 2005. *Circulation.* (2009) 119:1728–35. doi: 10.1161/CIRCULATIONAHA.108.829176
29. Richardson LC, Pollack LA. Therapy insight: influence of type 2 diabetes on the development, treatment and outcomes of cancer. *Nat Clin Pract Oncol.* (2005) 2:48–53. doi: 10.1038/ncponc0062
30. Srokowski TP, Fang S, Hortobagyi GN, Giordano SH. Impact of diabetes mellitus on complications and outcomes of adjuvant chemotherapy in older patients with breast cancer. *J Clin Oncol.* (2009) 27:2170–6. doi: 10.1200/JCO.2008.17.5935
31. Meyerhardt JA, Catalano PJ, Haller DG, Mayer RJ, Macdonald JS, Benson AB III, et al. Impact of diabetes mellitus on outcomes in patients with colon cancer. *J Clin Oncol.* (2003) 21:433–40. doi: 10.1200/JCO.2003.07.125
32. Giovannucci E. Insulin, insulin-like growth factors and colon cancer: a review of the evidence. *J Nutr.* (2001) 131:3109S—20. doi: 10.1093/jn/131.11.3109S
33. Zhang H, Pelzer AM, Kiang DT, Yee D. Down-regulation of type I insulin-like growth factor receptor increases sensitivity of breast cancer cells to insulin. *Cancer Res.* (2007) 67:391–7. doi: 10.1158/0008-5472.CAN-06-1712
34. Morss AS, Edelman ER. Glucose modulates basement membrane fibroblast growth factor-2 via alterations in endothelial cell permeability. *J Biol Chem.* (2007) 282:14635–44. doi: 10.1074/jbc.M608565200
35. Pollak M. Insulin, insulin-like growth factors and neoplasia. *Best Pract Res Clin Endocrinol Metab.* (2008) 22:625–38. doi: 10.1016/j.beem.2008.08.004
36. Mardilovich K, Pankratz SL, Shaw LM. Expression and function of the insulin receptor substrate proteins in cancer. *Cell Commun Signal.* (2009) 7:14. doi: 10.1186/1478-811X-7-14
37. Wong P, Weiner MG, Hwang WT, Yang YX. Insulin therapy and colorectal adenomas in patients with diabetes mellitus. *Cancer Epidemiol Biomarkers Prev.* (2012) 21:1833–40. doi: 10.1158/1055-9965.EPI-12-0771

Conflict of Interest: The authors declare that the research was conducted in the absence of any commercial or financial relationships that could be construed as a potential conflict of interest.

frontiers in Endocrinology

CASE REPORT
published: 22 April 2020
doi: 10.3389/fendo.2020.00235

Multidisciplinary Diagnosis of Subcutaneous Soft Tissue Metastasis of Follicular Thyroid Carcinoma: A Case Report

Yanfang Wang[1], *Fang Nie*[1]* *and Qingqing Fang*[2]

[1] Department of Ultrasound, Lanzhou University Second Hospital, Lanzhou University, Lanzhou, China, [2] Department of Pathology, Lanzhou University Second Hospital, Lanzhou University, Lanzhou, China

Background: Subcutaneous soft tissue metastasis of follicular thyroid carcinoma (FTC) is rarely diagnosed before surgery for clinicians.

Case Report: We present a case of a 67-year-old man with a history of FTC and papillary thyroid microcarcinoma for 5 years. Multiple protruding subcutaneous nodules of the neck were found and removed from the surface of the sternocleidomastoid muscle. Ultrasound, computed tomography and technetium-99 m pertechnetate single-photon emission computed tomography of the neck were performed before the operation, which unfortunately indicated suspicious malignant lesions. Serum Tg was > 300 ng/ml (0.83–68.0 ng/ml), TSH was 36.580 uIU/ml (0.380–4.340 uIU/ml) and AbTg was negative. The pathologic diagnosis was metastatic FTC, invading the surrounding striated muscle, adipose tissue and vessels. Immunohistochemical staining revealed the tumor cells to be positive for thyroglobulin and TTF-1. The specimens of these nodules were further investigated for TERT promoter mutation and the result revealed mutated type (position g 1,295, 228 C>T).

Conclusion: Preoperative diagnosis and prognostic prediction of metastatic FTC may be available through a combination of clinical, multimodal imaging and molecular genetic test (viz. multidisciplinary diagnosis). A long-term standardized follow-up is required for patients with a previous diagnosis of FTC.

Keywords: follicular thyroid carcinoma, metastasis, TERT promoter, diagnosis, case report

OPEN ACCESS

Edited by:
Jianfeng Liu,
Huazhong University of Science and Technology, China

Reviewed by:
Marialuisa Appetecchia,
Istituti Fisioterapici Ospitalieri (IRCCS), Italy
Agnese Barnabei,
Regina Elena National Cancer Institute, Italy

***Correspondence:**
Fang Nie
ery_nief@lzu.edu.cn

Specialty section:
This article was submitted to Cancer Endocrinology, a section of the journal Frontiers in Endocrinology

Received: *16 January 2020*
Accepted: *31 March 2020*
Published: *22 April 2020*

Citation:
Wang Y, Nie F and Fang Q (2020) Multidisciplinary Diagnosis of Subcutaneous Soft Tissue Metastasis of Follicular Thyroid Carcinoma: A Case Report. Front. Endocrinol. 11:235. doi: 10.3389/fendo.2020.00235

INTRODUCTION

Distant metastasis of follicular thyroid carcinoma (FTC) may occur commonly to lung, skeleton and brain, which accounted for 11–25% (1). Subcutaneous soft tissue metastasis is relatively rare and difficult to diagnose before surgery (2–4). There are few available data on subcutaneous soft tissue metastasis from FTC. The clinicopathologic features of uncommon metastases of thyroid are not well-defined, which represent potential diagnostic pitfalls and may lead to treatment uncertainties (3). Here we report a subcutaneous soft tissue metastasis from FTC to investigate the clinical multiple imaging and histopathologic and molecular genetic characteristics.

CASE REPORT

In Mar 2014, a 62-year-old male visited the local hospital (second-tier hospital) with a small egg-like mass on his anterior neck. According to his medical records in the local hospital, physical examination revealed a 5 × 6 cm mass on the left region of the thyroid, which is slightly hard in texture, unfixed, clearly demarcated and fully movable with swallowing. Neck ultrasonography (US) showed a 7.8 × 4.0 cm mixed mass on the left lobe of the thyroid with a central irregular liquid component and hyperechoic periphery. The mixed mass had clear boundaries and abundant flow signals in the hyperechoic area. On the right lobe, there were multiple solid and cystic nodules, and the larger one was 1.0 × 0.5 cm. No suspicious lymph node was found in the bilateral cervical lymph node region. Without further imaging examinations, the patient underwent subtotal lobectomy of the left thyroid gland at the local hospital. The pathological diagnosis was FTC and was further confirmed at the pathology department of our hospital. Half a month later, the patient was referred to our hospital for radical thyroidectomy (right total lobectomy, isthmic resection, left residual lobectomy and left central compartment lymph node dissection). Before the radical thyroidectomy, physical examination and US of the neck revealed no enlarged lymph nodes. The pathology revealed papillary thyroid microcarcinoma with surrounding nodular goiters in the right lobe, no tumor was found in the rest of the thyroid, and no metastatic lymph node was detected in the left central compartment. Soon the patient received iodine-131 (^{131}I) therapy (80 mCi) at another tertiary referral hospital. The serum thyroglobulin (Tg) before the ^{131}I therapy was 1.28 ng/ml (0.83–68.0 ng/ml), while TSH was 83.645 uIU/ml (0.380–4.340 uIU/ml) because of the suspension of Levothyroxine. A week after ^{131}I therapy, the Tg level elevated to 2.54 ng/ml (0.83–68.0 ng/ml), but neck US showed no abnormal findings in the thyroid area and bilateral lymph node region. The ^{131}I whole body scan was later performed and showed no uptake in the thyroid bed region and no abnormal uptake in the rest of the body. Since then, the patient took Levothyroxine replacement therapy and visited the local hospital for follow-up. During the follow-up period, Tg and AbTg were never checked (they should have been tested, but for some reasons they were not), and TSH raised to 48.91 uIU/ml (0.34–5.6 uIU/ml) in Jun 2015, declined to 20.84 uIU/ml in Apr 2016 and returned to normal level (3.19 uIU/ml) in Feb 2018. Neck US was performed in Dec 2017 and Feb 2018. In Dec 2017, the US showed no abnormal echo in the thyroid area after surgery. While in Feb 2018, US suggested there were several solid hypoechoic masses in the bilateral anterior neck, with the larger one (1.3 × 0.9 cm) in the right. Spot flow signals were observed within those masses. Other features were not recorded in the report. This US report may suggest disease progress, but the patient did not take any further examination and treatment measures other than taking the Levothyroxine during the following period.

In May 2019, the patient revisited our hospital with multiple asymptomatic, soft, protruding nodules on the anterior neck (**Figure 1A**). Thyroid function examination showed that Tg was > 300 ng/ml (0.83–68.0 ng/ml), AbTg was < 15 U/ml(0-60 U/ml), TSH was 36.580 uIU/ml (0.380–4.340 uIU/ml), FT4 was 8.28 pmol/L (10.44–24.88), and T3, FT3 and TPO-Ab were within normal levels. Physical examination found several soft, unfixed, well-defined mass in the lateral thoracic bone end of the bilateral sternocleidomastoid, immovable with swallowing. The larger one was in the right, about 3 × 3 cm. Subsequently, US, computed tomography (CT) and technetium-99 m pertechnetate single-photon emission CT ($^{99m}TcO_4$-SPECT) of the neck were performed. Neck US revealed several solid nodules with the similar US features in the left anterior neck, the larger one displayed a well-defined border and irregular margin (**Figure 1B**). In the right anterior neck, two solid nodules adjacent to each other with a partially well-defined border and partial regular margin (**Figure 1C**) were found. All of them showed solid hypoechogenicity, wider than tall, no calcification, absent peripheral halo and perinodular and intranodular flow, while CT revealed multiple low-density nodules in the subcutaneous tissue of the bilateral anterior neck (**Figure 1D**). SPECT found a shadow of a cold nodule in the right anterior neck region and a shadow of a nodule in the left anterior neck region (**Figure 1E**). Furthermore, the contrast-enhanced ultrasound showed hyper-vascular, larger nodules of bilateral neck with heterogeneous enhancement, no ring enhancement and partially clear enhanced boundary (**Figures 2A,B**). Elastosonography displayed both larger nodules mainly composed of blue color (at least 75% of the nodule was covered in blue) (**Figures 2C,D**). The elasticity score (ES) was classified into 4 (ES 4), which correlated with malignancy (5). As the patient refused ^{131}I whole body scan and 18-fluorodeoxyglucose positron-emission tomography/CT (18F-FDG-PET/CT) scan, $^{99m}TcO_4$-SPECT whole body scan was performed, showing no abnormal uptake in the whole body (**Figure 2E**). A surgical excision was performed and these nodules were removed from the surface of the sternocleidomastoid. The histopathologic examination of these nodules was FTC, invading the surrounding striated muscle, adipose tissue and vessels. Under the microscope, the tumor cells were arranged in the form of small follicles, with acidophilic cytoplasm, enlarged, hyperchromatic nuclei and vascular invasion (**Figure 3**). Immunohistochemistry revealed the tumor cells to be positive for Tg and TTF-1. According to the recent AJCC cancer staging manual (6), the TNM staging of this patient was T4aN0bM0. The TERT promoter mutation testing was positive (position g 1,295, 228 C>T) (**Figure 4**). Preoperative and postoperative US was performed by the same imaging doctor, with the latter suggesting no residual nodules and obvious abnormal echo on the bilateral anterior neck region. Up to 6 months of thyroid function and neck US follow-up, the patient has been doing well. The latest Tg was <0.1 ng/ml (0.83–68.0 ng/ml), AbTg was < 15 U/ml(0–60 U/ml), and TSH was 0.320 uIU/ml (0.380–4.340 uIU/ml). The latest neck US showed no abnormal echo in the thyroid area and bilateral anterior neck region. A long-term standardized follow-up is needed for this patient in the future.

DISCUSSION

FTC is the second most common differentiated thyroid malignancy. It is difficult to distinguish between thyroid follicular carcinoma and follicular adenoma before the operation. Around 5.4–11% of patients with FTC have distant metastasis, which

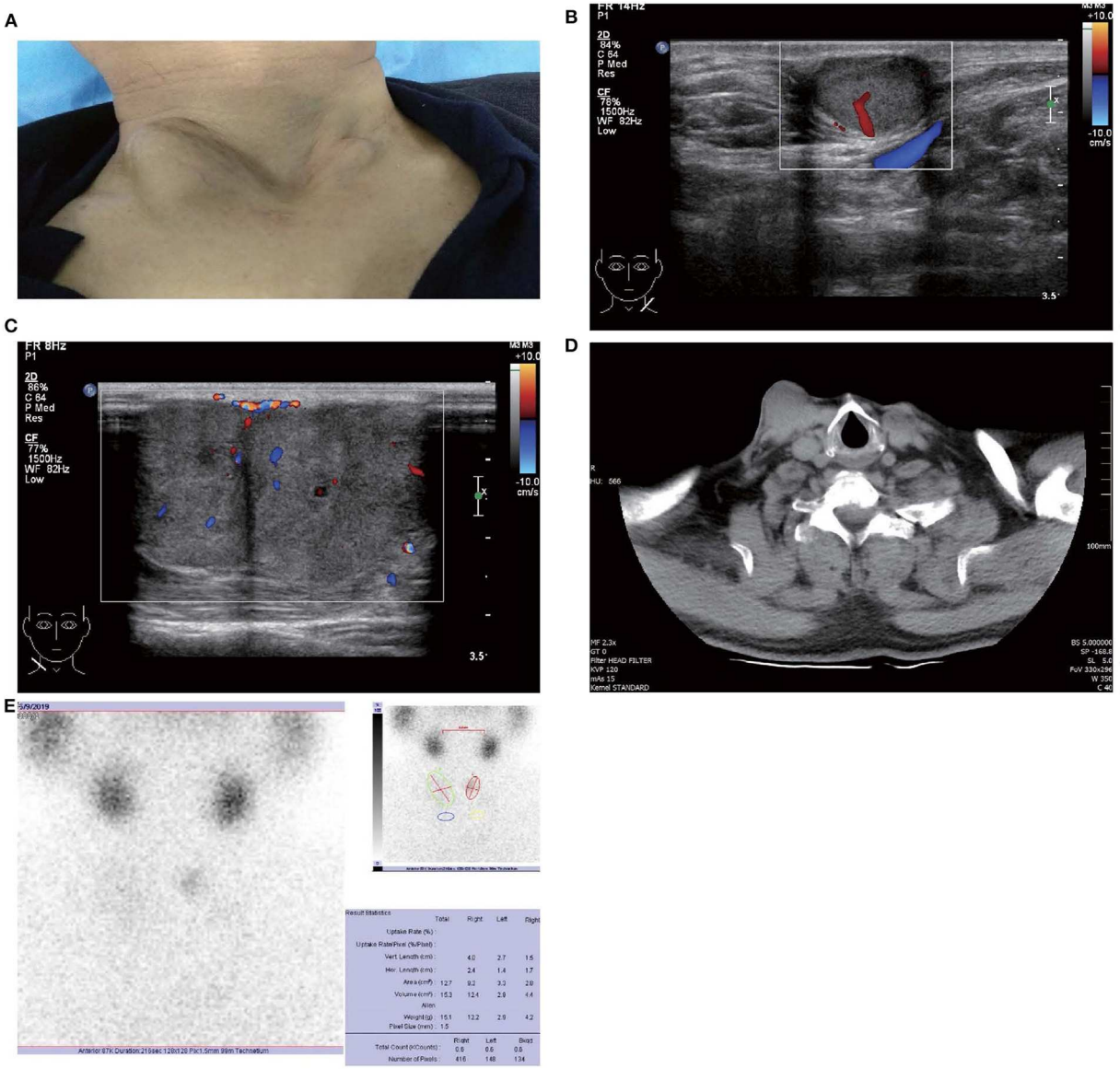

FIGURE 1 | Images of patient and subcutaneous nodules. **(A)** Multiple subcutaneous soft tissue nodules of metastatic follicular thyroid carcinoma on the anterior neck. **(B)** Gray-scale ultrasound shows a hypoechoic nodule in the subcutaneous soft tissue of left neck (size were 16 × 11 mm), with wider than taller, well-defined border, irregular margin, perinodular, and intranodular flow and absence of calcification and peripheral halo. **(C)** Gray-scale ultrasound shows two solid hypoechoic nodules adjacent to each other in the subcutaneous soft tissue of right neck (size of the larger one were 28 × 23 mm), with wider than taller, partially well-defined border, partially regular margin, perinodular and intranodular flow and absence of calcification and peripheral halo. **(D)** Computed tomography shows several low-density nodules in the subcutaneous of the anterior neck. **(E)** $^{99m}TcO_4$-SPECT reveals a shadow of a cold nodule in the right anterior neck region and a shadow of a nodule in the left anterior neck region.

usually has a poor prognosis and affects the survival of patients (7, 8). The most unusual metastatic site reported in the literature is the skin (3, 9). In our case, the metastatic site was the soft tissue between the skin and the surface of the sternocleidomastoid muscle. Adequate imaging follow-up and thyroid function follow-up are required despite surgical excision and ^{131}I therapy.

US is the most common non-invasive imaging method preferred for thyroid nodules, which can be used in differentiating benign and malignant lesions. Although extensive experience has been accumulated in diagnosing papillary thyroid carcinoma with US, there is limited and few data available in differentiating FTC (10, 11). Previous reports have suggested that larger size, absent sonographic halo, hypoechoic appearance, absence of cystic change and tubercle-in-nodule combination with calcification favored an FTC (12, 13). In this study, the sonographic findings of the metastatic

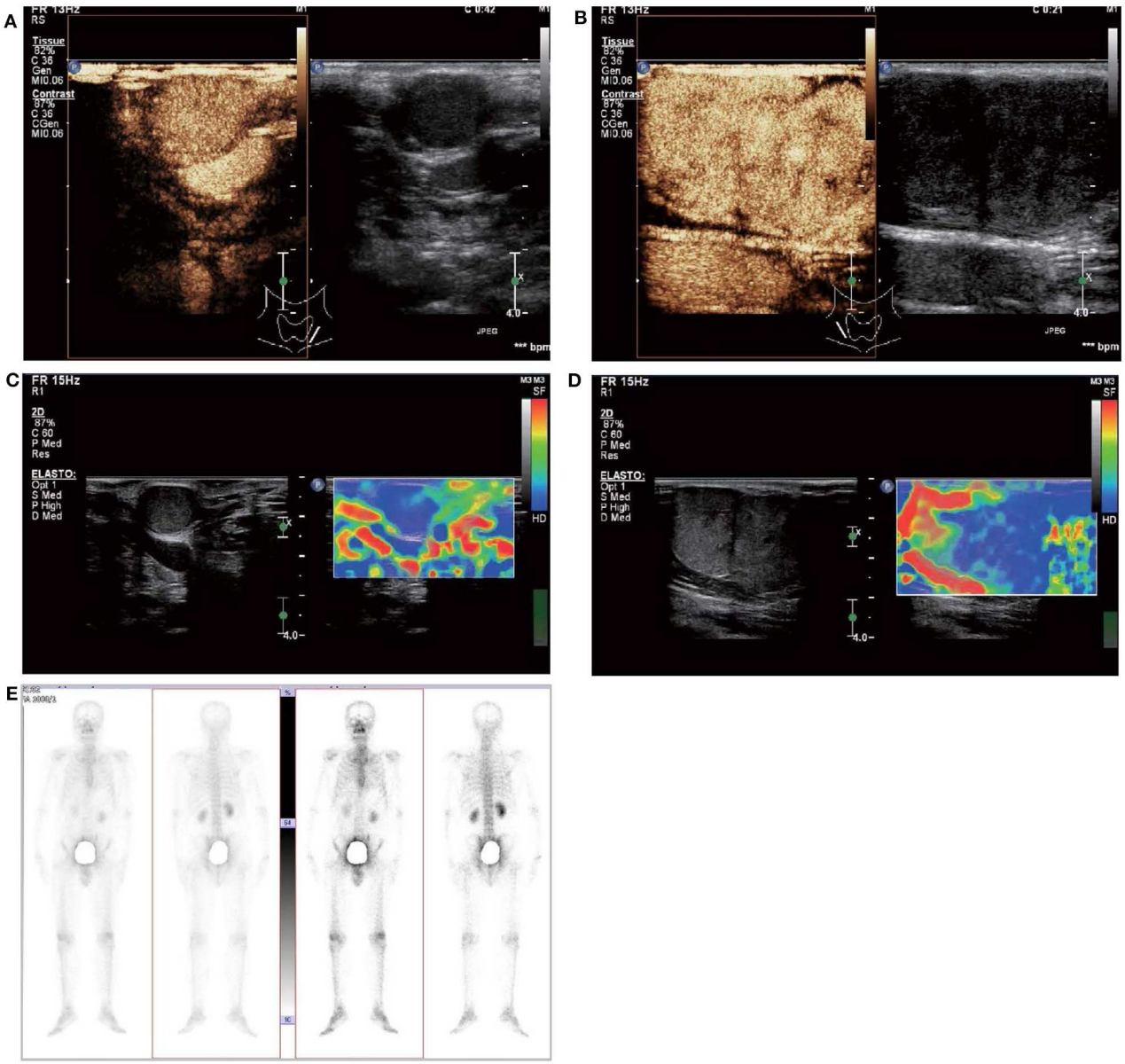

FIGURE 2 | Contrast-enhanced ultrasound and elastosonography appearance of the larger subcutaneous nodules on the bilateral neck. **(A,B)** Contrast-enhanced ultrasound showed both the larger nodule in the bilateral neck are hypervascular, heterogeneous enhancement, no ring enhancement, and partially clear enhanced boundary. **(C,D)** Elastosonography displayed both the larger one were mainly composed of blue color (at least 75% of the nodule was covered in blue). **(E)** $^{99m}TcO_4$-SPECT whole body scan was performed and showed no abnormal uptake in the whole body.

nodules were solid hypoechoic, partially clear border, irregular margin, absent calcification, absent peripheral halo, perinodular and intranodular flow, hyper-vascularity, heterogeneous enhancement, no ring enhancement, partially clear enhanced boundary and ES 4. These findings were unfortunately indicative of suspicious malignant lesions. However, there are no specific ultrasonic features for the diagnosis of FTC at present, let alone metastatic FTC. CT/MRI is more advantageous in staging but less advantageous in diagnosing than US. ^{131}I- or $^{99m}TcO_4$-SPECT is used to image thyroid metabolism to detect and localize abnormal thyroid tissue, especially in imaging ectopic or metastatic thyroid lesions. In the current case, ^{131}I therapy after radical thyroidectomy, there was no uptake in the thyroid bed region and no abnormal uptake in the rest of the body by the ^{131}I whole body scanning. It could be supposed that there was no metastatic, residual or ectopic thyroid tissue in the patient's body. But 5 years later, the $^{99m}TcO_4$-SPECT revealed shadows in the bilateral anterior neck region. Linking the history and previous examinations, we considered they were metastatic lesions. However, since SPECT is a projection image from

the radioactive nuclide, the image may be noisy and low in resolution. Furthermore, the lack of anatomic landmarks, as well as the possibility of physiologic or other benign uptake of this tracer, may make interpretation of images more difficult (14, 15). A further study is necessary to distinguish FTC by using image diagnostics in the future.

Immunohistochemical staining has helped confirm the tissue origin in dealing with metastatic lesions (16). From published data, immunohistochemical markers that are specific for FTC such as Tg and TTF-1 can be detected in over 95 and 100% of FTC cases (17). In our case, the Tg and TTF-1 were positive in subcutaneous metastasis nodules. Besides, the tumor cells under the microscope were arranged in the form of small follicles, with acidophilic cytoplasm, enlarged, hyperchromatic nuclei and vascular invasion. All of these findings support the diagnosis of metastatic FTC.

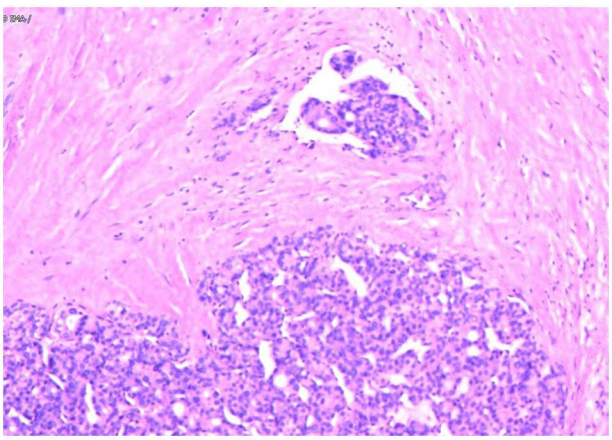

FIGURE 3 | Follicular thyroid carcinoma. (Hematoxylin and eosin staining of histological slides, × 200).

In thyroid cancer, TERT promoter mutations are usually presented in follicular-derived thyroid carcinoma and associated with more aggressiveness, distant metastasis, tumor recurrence and poor prognosis (18, 19). In our case, the metastasis nodules harbored TERT C228T mutation (**Figure 4**), which implies it may contribute to the aggressiveness of the FTC and distant metastasis. Indeed, the histopathological results showed these FTCs had invaded the surrounding striated muscle, adipose tissue and vessels. As the primary FTC was not performed in our hospital, we cannot make a molecular test for the original tumor. Therefore, we do not know whether there was a difference in molecular mutation between primary and metastatic tumors. Six months since the last surgical removal, the patient has been doing well. As the TERT mutation may indicate a poor prognosis, a long-term standardized follow-up is required for the patient.

Serum Tg is a very important laboratory indicator in clinical monitoring of recurrence and metastasis after thyroidectomy of thyroid cancer (20). Tg is a specific protein produced by the thyroid gland and secreted by thyroid follicular epithelial cells. In patients whose thyroid has been completely cleared (surgery and ^{131}I therapy), there should no longer be a source of Tg in the body. If detected in the serum, it often indicates residual disease or recurrence. However, serum Tg detection is susceptible to AbTg and TSH. When AbTg is positive, it will reduce the detection value of serum Tg by chemiluminescence immunoassay, thus affecting the accuracy of disease monitoring (21). It is noteworthy that the results of different Tg detection reagents may vary greatly, so the same detection reagent should be used in the follow-up (22). Under the TSH suppression, the ability of tumor cells to secret Tg is also inhibited. To better reflect

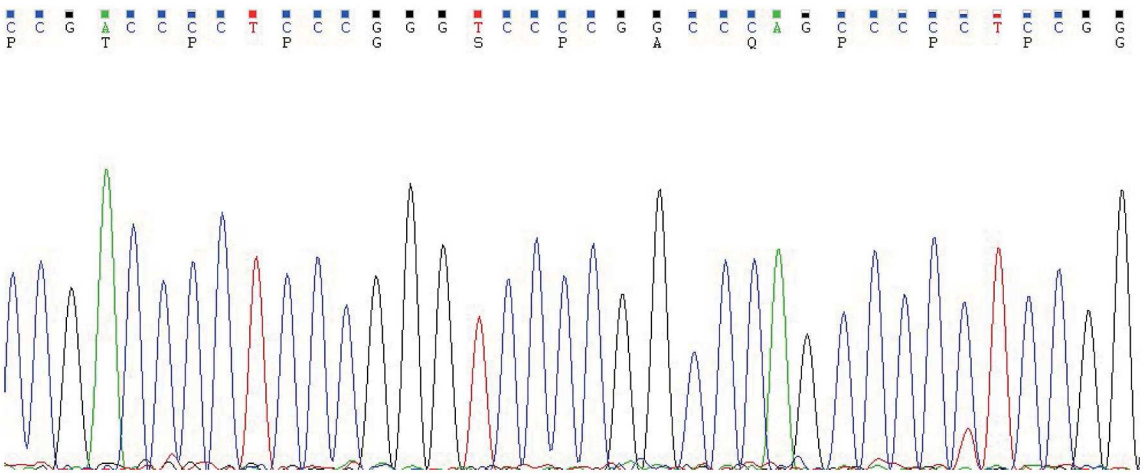

FIGURE 4 | The TERT promoter testing displayed a mutation type (position g 1,295, 228 C>T). Genomic DNA was isolated from four 5 μm-thick slices of formalin-fixed paraffin-embedded metastatic follicular thyroid carcinoma samples, using a commercial DNA extraction kit (TIANamp FFPE DNA Kit, TIANGEN, Catalog No. DP130608, China), according to the instruction of the manufacturer. The TERT promoter region (2 mutation hot spots—chr5:1,295, 228 C>T and chr5:1,295, 250 C>T) was amplified with a commercial kit (TERT Genetic Mutation Detection Kit, SinoMD, Catalog No. 20090031, China), according to the manufacturer's instructions. The amplified products were sequenced with Applied Biosystems 3,500 Genetic Analyzeror and mutations were recognized on sequencing electropherograms.

the disease status, Tg under the stimulation of TSH (TSH >30 uIU/ml) is usually preferred in clinical practice (23). And the cut-off value above 2 ng/mL following TSH stimulation is highly sensitive in identifying patients with persistent tumor (20). In this case, AbTg is negative and Tg (>300 ng/ml) was measured under the TSH stimulation (TSH: 36.580 uIU/ml). Metastasis or recurrence is highly suggestive of for this patient.

It should be noted that in this patient there could have been possible earlier progress; however, for certain reasons, it was delayed. This can be reflected by two aspects: first, during the follow-up period after ^{131}I therapy, Tg and AbTg were never checked; second, in Feb 2018, the US suggested there were several solid hypoechoic masses in the bilateral anterior neck. But the patient did not take any further management. If fundamental, standardized follow-up and timely treatment measurements were administered, the patient may have smaller surgical excision areas and lighter complications. This indicates that the regular standardized follow-up and timely treatment is completely necessary for FTC patients after thyroidectomy.

In summary, subcutaneous soft tissue metastasis from FTC is unusual. Multidisciplinary diagnosis, namely, combing clinical information with multimodal imaging materials and molecular genetic test, may help in diagnosing metastatic FTC and predicting prognosis before the operation. Immunohistochemical staining of Tg and TTF-1 plays a very important role in the final histopathological diagnosis of metastatic thyroid carcinoma. Postoperatively, monitoring of circulating Tg, AbTg and TSH together with neck US is very important in the follow-up of FTC. Since rare metastases identification could have a significant impact on patient management (3), the necessity for long-term standardized follow-up should be fully informed to patients, and the surgeons and physicians should take the metastasis into consideration in patients with a history of FTC.

DATA AVAILABILITY STATEMENT

The datasets generated for this study can be found in the article.

ETHICS STATEMENT

Written informed consent was obtained from the individual for the publication of any potentially identifiable images or data included in this article.

AUTHOR CONTRIBUTIONS

FN: case review. YW: clinical data, imaging data, design, analysis, and writing. QF: pathology data. All authors contributed to the manuscript work and approved the submitted version.

REFERENCES

1. Sevinc A, Buyukberber S, Sari R, Baysal T, Mizrak B. Follicular thyroid cancer presenting initially with soft tissue metastasis. *Jpn J Clin Oncol*. (2000) 30:27–9. doi: 10.1093/jjco/hyd007
2. Rodrigues G, Ghosh A. Synchronous bony and soft tissue metastases from follicular carcinoma of the thyroid. *J Korean Med Sci*. (2003) 18:914–6. doi: 10.3346/jkms.2003.18.6.914
3. Farina E, Monari F, Tallini G, Repaci A, Mazzarotto R, Giunchi F, et al. Unusual thyroid carcinoma metastases: a case series and literature review. *Endocr Pathol*. (2016) 27:55–64. doi: 10.1007/s12022-015-9410-7
4. Madani A, Jozaghi Y, Tabah R, How J, Mitmaker E. Rare metastases of well-differentiated thyroid cancers: a systematic review. *Ann Surg Oncol*. (2015) 22:460–6. doi: 10.1245/s10434-014-4058-y
5. Trimboli P, Guglielmi R, Monti S, Misischi I, Graziano F, Nasrollah N, et al. Ultrasound sensitivity for thyroid malignancy is increased by real-time elastography: a prospective multicenter study. *J Clin Endocrinol Metab*. (2012) 97:4524–30. doi: 10.1210/jc.2012-2951
6. Amin MB, Greene FL, Edge SB, Compton CC, Gershenwald JE, Brookland RK, et al. The eighth edition AJCC cancer staging manual: continuing to build a bridge from a population-based to a more "personalized" approach to cancer staging. *CA Cancer J Clin*. (2017) 67:93–9. doi: 10.3322/caac.21388
7. Kim H, Shin JH, Hahn SY, Oh YL, Kim SW, Park KW, et al. Prediction of follicular thyroid carcinoma associated with distant metastasis in the preoperative and postoperative model. *Head Neck*. (2019) 41:2507–13. doi: 10.1002/hed.25721
8. Sugino K, Ito K, Nagahama M, Kitagawa W, Shibuya H, Ohkuwa K, et al. Prognosis and prognostic factors for distant metastases and tumor mortality in follicular thyroid carcinoma. *Thyroid*. (2011) 21:751–7. doi: 10.1089/thy.2010.0353
9. Monti E, Dono M, Gonella E, Spina B, Pitto F, Petrogalli F, et al. An H-TERT mutated skin metastasis as first occurrence in a case of follicular thyroid carcinoma. *Front Endocrinol*. (2019) 10:513. doi: 10.3389/fendo.2019.00513
10. Segkos K, Porter K, Senter L, Ringel MD, Nabhan FA. Neck ultrasound in patients with follicular thyroid carcinoma. *Horm Cancer*. (2018) 9:433–9. doi: 10.1007/s12672-018-0345-6
11. Asteria C, Giovanardi A, Pizzocaro A, Cozzaglio L, Morabito A, Somalvico F, et al. US-elastography in the differential diagnosis of benign and malignant thyroid nodules. *Thyroid*. (2008) 18:523–31. doi: 10.1089/thy.2007.0323
12. Sillery JC, Reading CC, Charboneau JW, Henrichsen TL, Hay ID, Mandrekar JN. Thyroid follicular carcinoma: sonographic features of 50 cases. *AJR Am J Roentgenol*. (2010) 194:44–54. doi: 10.2214/AJR.09.3195
13. Kuo TC, Wu MH, Chen KY, Hsieh MS, Chen A, Chen CN. Ultrasonographic features for differentiating follicular thyroid carcinoma and follicular adenoma. *Asian J Surg*. (2020) 43:339–46. doi: 10.1016/j.asjsur.2019.04.016
14. Maruoka Y, Abe K, Baba S, Isoda T, Sawamoto H, Tanabe Y, et al. Incremental diagnostic value of SPECT/CT with 131I scintigraphy after radioiodine therapy in patients with well-differentiated thyroid carcinoma. *Radiology*. (2012) 265:902–9. doi: 10.1148/radiol.12112108
15. Freesmeyer M, Winkens T, Kuhnel C, Opfermann T, Seifert P. Technetium-99m SPECT/US hybrid imaging compared with conventional diagnostic thyroid imaging with scintigraphy and ultrasound. *Ultrasound Med Biol*. (2019) 45:1243–52. doi: 10.1016/j.ultrasmedbio.2019.01.003
16. Rico MJ, Penneys NS. Metastatic follicular carcinoma of the thyroid to the skin: a case confirmed by immunohistochemistry. *J Cutan Pathol*. (1985) 12:103–5. doi: 10.1111/j.1600-0560.1985.tb01609.x
17. Tatić S. Histopathological and immunohistochemical features of thyroid carcinoma. *Arch Oncol*. (2003) 11:173–4. doi: 10.2298/AOO0303173T
18. Liu R, Xing M. TERT promoter mutations in thyroid cancer. *Endocr Relat Cancer*. (2016) 23:R143–55. doi: 10.1530/ERC-15-0533
19. Yang J, Gong Y, Yan S, Chen H, Qin S, Gong R. Association between TERT promoter mutations and clinical behaviors in differentiated thyroid carcinoma: a systematic review and meta-analysis. *Endocrine*. (2019) 67:44–57. doi: 10.1007/s12020-019-02117-2
20. Haugen BR, Alexander EK, Bible KC, Doherty GM, Mandel SJ, Nikiforov YE, et al. American thyroid association management guidelines for adult

patients with thyroid nodules and differentiated thyroid cancer: the American thyroid association guidelines task force on thyroid nodules and differentiated thyroid cancer. *Thyroid*. (2016) 26:1–133. doi: 10.1089/thy.2015.0020

21. Spencer CA. Challenges of serum thyroglobulin (Tg) measurement in the presence of Tg autoantibodies. *J Clin Endocrinol Metab*. (2004) 89:3702–4. doi: 10.1210/jc.2004-0986
22. Woodmansee WW, Haugen BR. Uses for recombinant human TSH in patients with thyroid cancer and nodular goiter. *Clin Endocrinol*. (2004) 61:163–73. doi: 10.1111/j.1365-2265.2004.02025.x
23. Eustatia-Rutten CF, Smit JW, Romijn JA, van der Kleij-Corssmit EP, Pereira AM, Stokkel MP, et al. Diagnostic value of serum thyroglobulin measurements in the follow-up of differentiated thyroid carcinoma, a structured meta-analysis. *Clin Endocrinol*. (2004) 61:61–74. doi: 10.1111/j.1365-2265.2004.02060.x

Conflict of Interest: The authors declare that the research was conducted in the absence of any commercial or financial relationships that could be construed as a potential conflict of interest.

frontiers in Endocrinology

CASE REPORT
published: 23 April 2020
doi: 10.3389/fendo.2020.00242

Primary Adenoid Cystic Carcinoma of the Upper Anterior Mediastinum Mimicking a Thyroid Tumor: A Case Report and Review of Literature

Qiuji Wu[1†], *Weizi Sun*[1†], *Jiajun Bu*[2], *Yuanhang Xiang*[3] *and Yahua Zhong*[1*]

[1] Department of Radiation and Medical Oncology, Zhongnan Hospital of Wuhan University, Wuhan, China, [2] Department of Oncology, Wuhan Fourth Hospital, Wuhan, China, [3] Department of Pathology, Zhongnan Hospital of Wuhan University, Wuhan, China

Primary adenoid cystic carcinoma (ACC) of the upper anterior mediastinum mimicking a thyroid tumor has rarely been seen in clinical practice and lacks a standard of care therapy. Here, we report a 47-year old female patient with an ACC originated from the upper anterior mediastinum presenting as a thyroid gland tumor. The patient received gross surgical resection of the tumor and underwent post-surgical chemotherapy and radiotherapy. The patient was free from local recurrence 3-years following initial treatment, but developed multiple lung metastases. She remains under clinical observation without discomfort and is still followed as an outpatient. Here, we also summarized recent reports of similar cases with hope to provide some experience for future clinical practice.

Keywords: thyroid neoplasms, adenoid cystic carcinoma, diagnosis and treatment, case report, literature review

OPEN ACCESS

Edited by:
Ralf Jockers,
Université Paris-Sorbonne, France

Reviewed by:
Carl Friedrich Classen,
University Hospital Rostock, Germany
Lei Liu,
Huazhong University of Science and Technology, China

***Correspondence:**
Yahua Zhong
doctorzyh73@163.com

[†]*These authors share first authorship*

Specialty section:
This article was submitted to Cancer Endocrinology, a section of the journal Frontiers in Endocrinology

Received: *22 December 2019*
Accepted: *02 April 2020*
Published: *23 April 2020*

Citation:
Wu Q, Sun W, Bu J, Xiang Y and Zhong Y (2020) Primary Adenoid Cystic Carcinoma of the Upper Anterior Mediastinum Mimicking a Thyroid Tumor: A Case Report and Review of Literature. Front. Endocrinol. 11:242. doi: 10.3389/fendo.2020.00242

INTRODUCTION

Adenoid cystic carcinoma (ACC) is one of the most common malignancy in salivary glands, accounting for 1–2% of all head and neck malignancies and about 10% of all salivary gland tumors (1). Although quite rarely seen, ACC may also be found in uncommon sites including the larynx and trachea, as well as the lung, where submucosal seromucinous glands are thought to give rises to these tumors (2). ACC deriving from the thyroid gland is extremely rare, with most cases reported originating from the upper respiratory tract and invading into the thyroid gland, mimicking a thyroid tumor (3, 4). Distinct cytological characteristics and immunohistochemical profiles are important basis for the differentiation of ACC from other classical thyroid tumors such as papillary adenocarcinoma and medullary carcinoma (5). Surgery remains the principal treatment for locally advanced ACC of the upper respiratory tract invading the thyroid gland. However, given the infiltrative properties and the perineuronal invasion activities of ACC, postoperative radiotherapy is often delivered with the purpose of improving local control (6). Distant metastasis of ACC may eventually form and pose a difficult clinical problem, as there are no efficient treatments for metastatic ACC.

The most common sites of metastasis include the lung (20%), the bones (4%), and the liver (3%) (7). Three large retrospective studies using public database comprising more than 2,000 patients showed 5-year OS from 78 to 90.3%, 10-year OS from 59.6 to 79,9%, while 15-year OS differed from 35 to 69.2% (8–10). The mostly indicated prognostic factors included pathological types, patient age, disease stage, surgical margin status, site of origin, perineural invasion, etc. (11, 12).

Comprehensive understanding of molecular mechanisms of ACC might bring new opportunities to improve the prognosis of this disease. Critical molecular alterations such as *MYB-NFIB* translocation, *Sox 4, c-KIT*, and *Slug* gene activation, overexpression of epidermal growth factors (EGFs), vascular endothelial growth factors (VEGFs), nerve growth factors (NGFs), and their corresponding receptors have been demonstrated to play essential roles in the pathogenesis of ACC by recent studies (13). New targeted therapies such as anti-EGFR or anti-VEGF monoclonal antibodies provide potential anti-tumor activities, but larger clinical studies are warranted to evaluate their clinical benefits (14). A better understanding of the molecular mechanisms underlying ACC pathogenesis and tumor development is therefore in urgent need for novel and more efficient anti-tumor strategies.

Thyroid invasive tracheal ACC is a rare clinical presentation. Here, we report a 47-year old female patient with a thyroid gland tumor that was confirmed by post-surgical pathology to be an ACC originated from the upper anterior mediastinum, most likely from the trachea. We describe the clinical manifestations, diagnosis, treatment, and follow-up of this patient, with a hope to provide some experience for future clinical practice.

CASE PRESENTATION

A 47-year old female with no significant past medical history presented with a thyroid mass and a foreign body feeling when swallowing. The patient denied palpitation, dysphoria, fever, insomnia, cough, dyspnea, breathlessness, hoarseness, or other symptoms. The Doppler ultrasonography showed a hypoechoic solid mass about 67 × 40 mm with blood flow signals posterior to the lower border of the right lobe of the thyroid. Another hypoechoic solid mass about 70 × 43 mm with blood flow signals posterior to the lower part of the left lobe of the thyroid gland was also noted. Multiple enlarged lymph nodes with the largest ones measuring 18 × 6 mm in the right neck, and 15 × 5 mm in the left neck, were also detected. She then received a computed tomography (CT) scan of the neck and thorax that revealed a 85 × 54 mm hypodense-to-isodense space-occupying lesion in the posterior superior mediastinum, one solid mass in the right lobe, and another solid mass in the inferior posterior part of the left lobe of the thyroid. The lesions showed slight enhancement with a contrast-enhancement scan and caused compression of the trachea, esophagus and cervical vessels (**Figure 1**, left panel). An esophagogastroscopy also revealed stenosis of the esophagus 15–20 cm distal to the upper incisors. Two months following the initial presentation, the patient underwent surgical treatment with right and left thyroidectomy, upper mediastinal tumor resection, left recurrent laryngeal nerve exploration, right recurrent laryngeal nerve anastomosis, and tracheotomy. During the surgery, the thyroid gland was found to be adherent to the surrounding tissue and a tumor measuring about 10 × 8 × 6 cm was present within the dorsal part of the right lobe of the thyroid gland was noted. Specifically, the tumor was between the trachea and esophagus, but the border of the tumor was indistinct. The tumor involved the tracheal membranous wall, the upper esophagus, and the right recurrent laryngeal nerve. The left lobe of the thyroid gland was not directly involved by the tumor. Pathological investigations demonstrated an ACC of the upper mediastinum involving the left lobe of the thyroid gland, the tracheal cartilage, and the adjacent muscles. The immunohistochemical staining profile was as follows: Alcian blue (AB) (+), Periodic Acid Schiff (PAS) (–), CD56 (–), Syn (–), Calponin (+), smooth muscle actin (SMA) (+), P63 (+), epithelial membrane antigen (EMA) (+), cytokeratin (CK)5/6 (+), CK8/18 (+), CD117 (+), thyroid transcription factor-1 (TTF-1) (–), thyroglobulin (Tg) (–), chromogranin A (CgA) (–) (**Figure 2**). Perineuronal invasion was also noticed. The mass in the left lobe of the thyroid gland turned out to be a nodular goiter.

Postoperative CT scan showed changes in the area of the thyroid, with thickening of the upper thoracic esophageal wall, but no obvious abnormalities elsewhere in chest (**Figure 1**, middle panel). Other examinations including abdominal CT and bone scintigraphy were negative. The thyroid profile was as follows: free T3 3.27 pmol/L, free T4 10.76 pmol/L, TSH 48.400 μIU/mL, anti-Tg 12 IU/mL, anti-TPO 6 IU/mL. The patient was supplemented with oral thyroid hormone. The patient then received one cycle of chemotherapy in the form of 75 mg/m^2 of Cisplatin and 75 mg/m^2 of Docetaxel but were canceled because of intolerable gastrointestinal side effects. Since the tumor involved the tracheal cartilage and showed perineuronal invasion, radiation therapy was proposed. The patient underwent postoperative intensity-modulated radiation therapy (IMRT) with a prescribed dose of PTV-GTV of 70 Gy, PTV-CTV1 of 60 Gy, PTV-CTV2 of 54 Gy in 31 fractions (1 fraction per day, 5 fractions per week; **Figure 3**). She experienced grade II leucopenia, but the treatment was otherwise well tolerated.

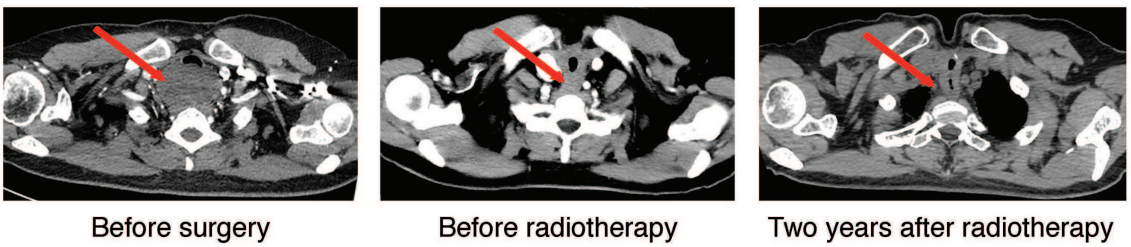

FIGURE 1 | Cervical-thoracic CT scans of the patient. Representative axial images of the disease before surgery, post-surgery/before radiotherapy, and 2-years after radiotherapy were shown. The red arrow highlighted the tumor and post-treatment changes in the tumor area.

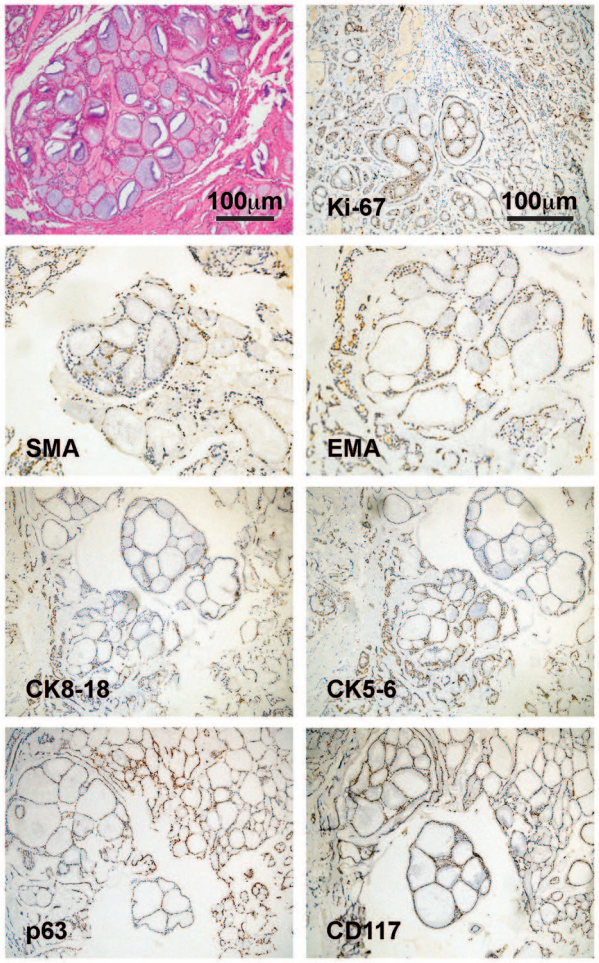

FIGURE 2 | Pathological features of the tumor. HE staining image indicated a cribriform ACC. Immunohistochemical staining images showed positive expression of Ki-67, SMA, EMA, CK8-18, CK5-6, p63, and CD117, which supported a diagnosis of ACC. ACC, adenoid cystic carcinoma; SMA, smooth muscle actin; EMA, epithelial membrane antigen; CK, cytokeratin; CD, cluster of differentiation.

The patient returned for post-treatment follow-up visit 3 months after the radiation therapy. CT scan showed no obvious changes compared with previous scans. The patient has undergone scheduled follow-up with CT scans as routine imaging since then.

Local control was quite satisfactory and the patient was free of local recurrence (**Figure 1**, right panel). However, multiple tiny nodules appeared in both lungs 2-years later following the initial presentation showing very slow increase in size. However, she declined any further treatment. The patient is still under follow-up 3-years after initial treatment and is not reporting any discomfort.

DISCUSSION

ACC mainly occurs in salivary glands with an relentless clinical course. However, local recurrence and distant metastasis are frequent in ACC patients due to the infiltrative characteristics of the tumor (15). Although ACC might also occur in other sites such as the trachea and the lung, primary thyroid ACC has not been described. To date, there were only few reported cases of ACC arising from the adjacent tissue of the thyroid such as the larynx and the trachea, where it invades into the thyroid gland mimicking a primary tumor. While other even rarer cases of thyroid metastasis of ACC from distant organs such as the salivary glands were also reported (**Table 1**).

Cytologically, ACC is characterized by monomorphic basaloid small round or oval tumor cells with round nuclei, small indistinct nucleoli, scant cytoplasm, and no inclusions, ranging in strands or clumps surrounding globules of acellular, homogenous spaces filled with mucoid or hyaline material (17). Three pathological patterns of ACC have been well-described, namely the cribriform, trabecular and solid types, with the cribriform type being the most prevalent. Cribriform ACC shows distinct microscopic "Swiss cheese" morphology and contains mucinous material strongly stained by alcian blue. Immunohistochemically, smooth muscle actin, S100, and vimentin, which are absent in thyroid malignancies. Primary thyroid tumor typically expresses thyroglobulin (Tg), thyroid transcription factor-1 (TTF-1), while these markers are absent in ACC (17).

Although CT scan and fine needle aspiration cytology (FNAC) are important diagnostic tools for thyroid tumors (17). ACC is rarely seemed in the thyroid gland and therefore misdiagnoses may occur. Post-surgical thorough histopathological examination and immunohistochemical procedures are therefore essential for an accurate diagnosis and proper differential diagnosis (5).

Surgery remains the major treatment for locally advanced ACC. However, the infiltrative properties of ACC render most surgeries non-radical. In our case, the tumor not only invaded the right lobe of the thyroid gland, but also involved the upper anterior mediastinum and the tracheal cartilage and displayed perineuronal infiltration. Therefore, postoperative radiotherapy was given in order to ensure optimal local control. Indeed, after 3-years of surgery and radiotherapy, the local control was satisfactory. However, lung metastases have developed.

On the other hand, the outcome of systemic treatment in metastatic ACC is far from satisfactory. In general, ACC is not sensitive to a variety of chemotherapeutic agents, although drugs including Cisplatin, Fluorouracil, and Taxol have shown low to moderate response rate (21). Novel targeted therapies such as anti-EGFR such as Cetuximab, and the small molecule inhibitor of VEGFR2, Apatinib, have entered clinical trials and yielded potential clinical benefit in recurrent or metastatic ACC patients (20, 22). Other agents targeting distinct molecular alterations such as *c-Kit* overexpression, *MYB-NFIB* fusion, *MYB* overexpression, and NF-κB over activation are still under investigations and might provide more choice for ACC patients (23).

Since ACC represents an indolent disease and patient with lung metastasis could still have relatively long overall survival (median OS 32.3 months), re-surgery for lung oligometastasis or close follow-up and best supportive care for multiple non-resected lung metastasis might also be a choice (23). For instance, Kukwa reported a case of 17-year old female patient who developed lung metastasis 3-years after the treatment of primary

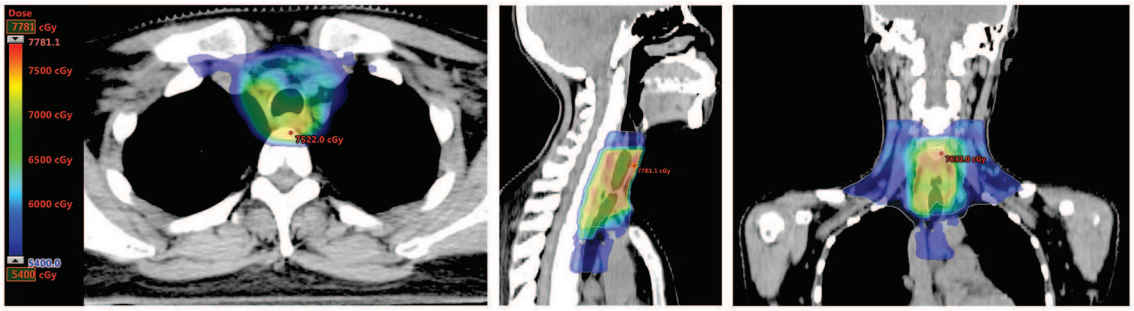

FIGURE 3 | Dose distribution of post-surgical radiotherapy. Representative axial, sagittal, and coronal images of dose distribution were shown. Areas with dose coverage of over 54 Gy were presented.

TABLE 1 | Cases of ACC with thyroid invasion reported in literature.

References	Sex	Age	Origin location	Size (cm)	Symptoms	Other metastasis location	Management	Survival (Months)
Kukwa et al. (4)	F	17	Trachea	3.7 × 2.6	Wheezing	Bilateral lungs	RR + RT (70 Gy)	>12 (live)
Aldrees et al. (16)	F	47	Trachea	3 × 4	Neck swelling, cough, shortness of breath, and hoarseness	None	RR	NA (live)
Nuwal et al. (17)	F	44	Trachea	2.5 × 2	Neck swelling	NA	RT (50 Gy)	Lost to follow-up
Shirian et al. (18)	M	45	Larynx	NA	Mild hoarseness and left-sided neck mass	NA	RR	NA
Qi et al. (3)	M	46	Trachea	NA	Dysphagia and associated dyspnea	NA	Bilateral partial mass resections	1 (dead)
Kashiwagi et al. (19)	F	33	Larynx	NA	Cough and wheeze	NA	RR	>24 (live)
Wang (20)	M	57	Trachea	NA	Cough, pressure and suffocation in the chest	Bilateral lungs	CH, RT (60 + 60 Gy), Apatinib	>120 (live)

F, female; M, male; NA, not available; RR, radical resection; RT, radiation therapy; CH, chemotherapy; ACC, adenoid cystic carcinoma.

tracheal ACC with thyroid metastasis (4). The patient underwent metastasis resection and no recurrence was detected 1-year after the surgery.

In conclusion, although ACC is less sensitive to radiotherapy than squamous cell carcinoma, it is still important treatment to reduce local recurrence. The long-term prognosis of remains ACC is still dismal, with the 10 and 20-year OS being 52 and 28%, respectively (24). The main cause of death is distant metastasis, in particular lung metastasis (24). Further research is needed to improve the survival of ACC patients. For patients with ACC invading the thyroid gland who underwent thyroid gland removal and post-operative radiotherapy, thyroid hormone therapy is also critical.

DATA AVAILABILITY STATEMENT

All datasets generated for this study are included in the article.

ETHICS STATEMENT

The studies involving human participants were reviewed and approved by Medical Ethics Committee of Zhongnan Hospital of Wuhan University. The patients/participants provided their written informed consent to participate in this study. Written informed consent was obtained from the individual(s) for the publication of any potentially identifiable images or data included in this article.

AUTHOR CONTRIBUTIONS

QW and WS designed the study and wrote the manuscript. JB and YX analyzed pathological and imaging data and participated in discussion. YZ supervised the study and corrected the manuscript.

FUNDING

This work was supported by the National Natural Science Foundation Youth Project (Grant no. 81803061) and the Foundation of Health Commission of Hubei Province of China (Grant no. WJ2019H064).

ACKNOWLEDGMENTS

We thank the patient for providing written informed consent for the publication of her data and associated images.

REFERENCES

1. Jang S, Patel PN, Kimple RJ, McCulloch TM. Clinical outcomes and prognostic factors of adenoid cystic carcinoma of the head and neck. *Anticancer Res.* (2017) 37:3045–52. doi: 10.21873/anticanres.11659
2. Meyers M, Granger B, Herman P, Janot F, Garrel R, Fakhry N, et al. Head and neck adenoid cystic carcinoma: a prospective multicenter REFCOR study of 95 cases. *Eur Ann Otorhinolaryngol Head Neck Dis.* (2016) 133:13–7. doi: 10.1016/j.anorl.2015.09.009
3. Qi D, Feng L, Li J, Liu B, Zhang Q. Primary adenoid cystic carcinoma of the trachea with thyroid invasion: a case report and literature review. *Onco Targets Ther.* (2016) 9:6291–6. doi: 10.2147/OTT.S112498
4. Kukwa W, Korzen P, Wojtowicz P, Sobczyk G, Kiprian D, Kawecki A, et al. Tracheal adenoid cystic carcinoma mimicking a thyroid tumor: a case report. *Oncol Lett.* (2014) 8:1312–6. doi: 10.3892/ol.2014.2282
5. Idowu MO, Reiter ER, Powers CN. Adenoid cystic carcinoma: a pitfall in aspiration cytology of the thyroid. *Am J Clin Pathol.* (2004) 121:551–6. doi: 10.1309/NKED4TJXUENR21M2
6. Balamucki CJ, Amdur RJ, Werning JW, Vaysberg M, Morris CG, Kirwan JM, et al. Adenoid cystic carcinoma of the head and neck. *Am J Otolaryngol.* (2012) 33:510–8. doi: 10.1016/j.amjoto.2011.11.006
7. Amit M, Binenbaum Y, Sharma K, Ramer N, Ramer I, Agbetoba A, et al. Analysis of failure in patients with adenoid cystic carcinoma of the head and neck. An international collaborative study. *Head Neck.* (2014) 36:998–1004. doi: 10.1002/hed.23405
8. Lloyd S, Yu JB, Wilson LD, Decker RH. Determinants and patterns of survival in adenoid cystic carcinoma of the head and neck, including an analysis of adjuvant radiation therapy. *Am J Clin Oncol.* (2011) 34:76–81. doi: 10.1097/COC.0b013e3181d26d45
9. Ellington CL, Goodman M, Kono SA, Grist W, Wadsworth T, Chen AY, et al. Adenoid cystic carcinoma of the head and neck: incidence and survival trends based on 1973-2007 surveillance, epidemiology, and end results data. *Cancer.* (2012) 118:4444–51. doi: 10.1002/cncr.27408
10. Ciccolallo L, Licitra L, Cantu G, Gatta G, Group EW. Survival from salivary glands adenoid cystic carcinoma in European populations. *Oral Oncol.* (2009) 45:669–74. doi: 10.1016/j.oraloncology.2008.10.010
11. Imanguli M, Sumer BD. Model to predict cause-specific mortality in patients with head and neck adenoid cystic carcinoma: a competing risk analysis. *Ann Surg Oncol.* (2017) 24:2069–70. doi: 10.1245/s10434-017-5862-y
12. Ko JJ, Siever JE, Hao D, Simpson R, Lau HY. Adenoid cystic carcinoma of head and neck: clinical predictors of outcome from a Canadian centre. *Curr Oncol.* (2016) 23:26–33. doi: 10.3747/co.23.2898
13. Liu J, Shao C, Tan ML, Mu D, Ferris RL, Ha PK. Molecular biology of adenoid cystic carcinoma. *Head Neck.* (2012) 34:1665–77. doi: 10.1002/hed.21849
14. Dillon PM, Chakraborty S, Moskaluk CA, Joshi PJ, Thomas CY. Adenoid cystic carcinoma: a review of recent advances, molecular targets, and clinical trials. *Head Neck.* (2016) 38:620–7. doi: 10.1002/hed.23925
15. Andreasen S, Agander TK, Bjorndal K, Erentaite D, Heegaard S, Larsen SR, et al. Genetic rearrangements, hotspot mutations, and microRNA expression in the progression of metastatic adenoid cystic carcinoma of the salivary gland. *Oncotarget.* (2018) 9:19675–87. doi: 10.18632/oncotarget.24800
16. Aldrees T, Alanazi A, Fatani HA, Samman A, Aldhahri SF. Adenoid cystic carcinoma of the upper airway mimicking a thyroid tumor: a case report. *Mol Clin Oncol.* (2016) 5:367–70. doi: 10.3892/mco.2016.931
17. Nuwal P, Dixit R, Singhal AK. Primary adenoid cystic carcinoma of trachea presenting as midline neck swelling and mimicking thyroid tumor: a case report and review of literature. *Lung India.* (2010) 27:167–9. doi: 10.4103/0970-2113.68330
18. Shirian S, Maghbool M, Aledavood A, Negahban S, Khademi B, Daneshbod Y. Adenoid cystic carcinoma of the larynx presenting as a thyroid mass and brief literature review. *Acta Cytol.* (2017) 61:237–41. doi: 10.1159/000464271
19. Kashiwagi T, Kanaya H, Konno W, Goto K, Hirabayashi H, Haruna S. Adenoid cystic carcinoma of the larynx presenting with unusual subglottic mass: case report. *Auris Nasus Larynx.* (2016) 43:562–5. doi: 10.1016/j.anl.2015.12.011
20. Wang H. Case report of apatinib mesylate treatment in rare advanced tracheal adenoid cystic carcinoma. *Thorac Cancer.* (2017) 8:729–33. doi: 10.1111/1759-7714.12506
21. Chae YK, Chung SY, Davis AA, Carneiro BA, Chandra S, Kaplan J, et al. Adenoid cystic carcinoma: current therapy and potential therapeutic advances based on genomic profiling. *Oncotarget.* (2015) 6:37117–34. doi: 10.18632/oncotarget.5076
22. Hitre E, Budai B, Takacsi-Nagy Z, Rubovszky G, Toth E, Remenar E, et al. Cetuximab and platinum-based chemoradio- or chemotherapy of patients with epidermal growth factor receptor expressing adenoid cystic carcinoma: a phase II trial. *Br J Cancer.* (2013) 109:1117–22. doi: 10.1038/bjc.2013.468
23. Coca-Pelaz A, Rodrigo JP, Bradley PJ, Vander Poorten V, Triantafyllou A, Hunt JL, et al. Adenoid cystic carcinoma of the head and neck–An update. *Oral Oncol.* (2015) 51:652–61. doi: 10.1016/j.oraloncology.2015.04.005
24. van Weert S, Bloemena E, van der Waal I, de Bree R, Rietveld DH, Kuik JD, et al. Adenoid cystic carcinoma of the head and neck: a single-center analysis of 105 consecutive cases over a 30-year period. *Oral Oncol.* (2013) 49:824–9. doi: 10.1016/j.oraloncology.2013.05.004

Conflict of Interest: The authors declare that the research was conducted in the absence of any commercial or financial relationships that could be construed as a potential conflict of interest.

frontiers in Endocrinology

ORIGINAL RESEARCH
published: 12 May 2020
doi: 10.3389/fendo.2020.00291

Body Weight Variability Increases Dementia Risk Among Older Adults: A Nationwide Population-Based Cohort Study

*Eun Roh[1], Soon Young Hwang[2], Jung A. Kim[1], You-Bin Lee[1], So-hyeon Hong[1], Nam Hoon Kim[1], Ji A. Seo[1], Sin Gon Kim[1], Nan Hee Kim[1], Kyung Mook Choi[1], Sei Hyun Baik[1] and Hye Jin Yoo[1]**

[1] Division of Endocrinology and Metabolism, Department of Internal Medicine, Korea University College of Medicine, Seoul, South Korea, [2] Department of Biostatistics, Korea University College of Medicine, Seoul, South Korea

OPEN ACCESS

Edited by:
Ralf Jockers,
Université Paris-Sorbonne, France

Reviewed by:
Marie-Christine Pardon,
University of Nottingham,
United Kingdom
Claudio Acuña-Castillo,
Universidad de Santiago, Chile

***Correspondence:**
Hye Jin Yoo
deisy21@naver.com

Specialty section:
This article was submitted to Endocrinology of Aging, a section of the journal Frontiers in Endocrinology

Received: 23 December 2019
Accepted: 17 April 2020
Published: 12 May 2020

Citation:
Roh E, Hwang SY, Kim JA, Lee Y-B, Hong S-h, Kim NH, Seo JA, Kim SG, Kim NH, Choi KM, Baik SH and Yoo HJ (2020) Body Weight Variability Increases Dementia Risk Among Older Adults: A Nationwide Population-Based Cohort Study. Front. Endocrinol. 11:291. doi: 10.3389/fendo.2020.00291

Background: Recent growing evidences suggest that body weight (Bwt) variability, a repeated loss and regain of weight within a specific period, causes metabolic disturbances and can be a marker for poor homeostasis. Although there have been many studies about the association between Bwt variability and various health status, its association with the incidence of dementia among elderly people has not been examined.

Methods: We performed a retrospective elderly cohort study from 19,987 participants with mean age 73 years old in the Korean National Health Insurance Service. We examined the risk of incident dementia, including Alzheimer's dementia and vascular dementia, according to the quartile of Bwt variability, represented as coefficient of variation (Bwt-CV), SD (Bwt-SD), and variability independent of the mean (Bwt-VIM).

Results: In fully adjusted model, the group with the highest Bwt variability (Bwt-VIM Q4) showed an increased risk of all-cause dementia (hazard ratio [HR] 1.39, 95% confidence interval [CI] 1.206–1.603) and Alzheimer's dementia (HR 1.46, CI 1.240–1.724) compared to the lowest quartile (Bwt-VIM Q1). We also found that subjects with the highest Bwt variability (Q4) and underweight BMI had a significantly increased risk of developing dementia (HR 1.994, 95% CI 1.302–3.054), while subjects with low Bwt variability (Q1 and Q2) and obese BMI had decreased risk of dementia (HR 0.664, 95% CI 0.505–0.872 and HR 0.648, 95% CI 0.493–0.852, respectively) compared to reference group (lowest Bwt variability (Q1) with normal baseline BMI). The effect of Bwt variability on the incidence of dementia was more prominent in subjects <75 years old and abnormal BMI groups (P for interaction < 0.05).

Conclusion: The present study revealed that high Bwt variability was associated with an increased risk of dementia in the elderly.

Keywords: body weight, variability, dementia, Alzheimer's dementia, older people, retrospective cohort study

INTRODUCTION

The worldwide epidemic of dementia is a major health problem with significant economic consequences. The number of patients with dementia has increased worldwide because of a growing population of older adults. Several risk factors for the development of dementia have been identified. Although increasing age is well-accepted as a risk factor for the development of dementia, dementia is not regarded as an inevitable consequence of aging (1). Dementia shares many modifiable risk factors, including high blood pressure, obesity, physical inactivity, and unhealthy diet, with other major chronic late-life disorders, such as ischemic heart disease and cerebrovascular disease (1). On the bases of epidemiological and clinical evidence, mid-life obesity has been identified as a risk factor for late-life dementia through the direct effect of adipocyte-derived hormones and cytokines on cognitive function as well as the indirect impact on vascular risk factors (2–6). In contrast, in late-life, a low body mass index (BMI) or being underweight late in life was a risk factor for dementia and age-related brain atrophy in several prospective and cross-sectional studies (5, 7–9). However, these studies require attention to interpretation because a low BMI in the elderly might result from decreased muscle mass, not fat mass (10), and weight loss is a potential preclinical marker for dementia 6–10 years before a clinical diagnosis (11). Therefore, body weight (Bwt) trajectory rather than Bwt at a specific time might provide more information on the risk of dementia late in life.

Recent growing evidences suggest that variability in metabolic parameters may have a role in predicting mortality and cardiovascular outcomes (12–17). A loss of physiological homeostasis in the elderly can lead to intrinsic variability in various physiological indices, ultimately impairing health or causing disease. Under physiological conditions, homeostatic adaptations protect against weight gain or loss (18). Bwt variability, same meaning as Bwt fluctuation or weight cycling, refers to the repeated loss and regain of weight within a specific period. A meta-analysis of 25 studies involving more than 400,000 participants, Bwt fluctuation was associated with a significant increase in risk of all-cause mortality, cardiovascular disease (CVD) mortality, and CVD (17). Although there have been some studies to examine the association between BMI at a specific time or Bwt changes with dementia (19–21), there has been no study to explore the effects of Bwt variability in late-life on the incidence of dementia.

Thus, to clarify the importance of healthy Bwt control in older people, which can help maintain cognitive function, the present study investigated the association between visit-to-visit Bwt variability and the risk for all-cause dementia and dementia subtypes in an elderly population by using the longitudinal National Health Insurance Service (NHIS)-Senior database. Because baseline BMI can influence the risk of dementia in the elderly, we also analyzed the association between Bwt variability and dementia according to baseline BMI.

MATERIALS AND METHODS

Study Population

The NHIS is a mandatory social health insurance program that enrolls about 98% of Koreans who participate in biannual standardized health examinations provided by the Korean government (22, 23). The NHIS-Senior database was used to randomly select ∼10% of NHIS participants who were aged more than 60 years. The NHIS-Senior database contains an eligibility database (including data such as age, sex, and socioeconomic variables), a health examination database (comprising questionnaires on health-related behavioral variables and results of laboratory measurements), and a medical history database (comprising information on diagnosis, medication, admission, and death). Quality control procedures were checked by the Korean Association of Laboratory Quality Control.

Data from participants who underwent the national health examinations in 2009 (index year), and three or more health examinations from January 1, 2005, to December 31, 2009 were included. A total of 67,235 participants who underwent only one or two examinations and 1,675 participants with missing on at least one variable were excluded. An additional 206 participants were excluded due to a previous diagnosis of any type of dementia, including Alzheimer's dementia and vascular dementia, based on diagnoses coded according to the International Classification of Diseases, 10th revision (ICD-10) and questionnaires about medical history before the index year. Subjects who had diseases that could change Bwt, such as any kinds of malignant neoplasm (C00–C97; $n = 16{,}087$), hypothyroidism or thyrotoxicosis (E03, E05; $n = 2{,}177$), were excluded. A total 19,987 individuals were finally included in the analysis (**Figure 1**). The protocols were approved by the NHIS review committee, and the Institutional Review Board of Korea University approved the study protocol in accordance with the Declaration of Helsinki of the World Medical Association (IRB No. K2018–1107-001). Informed consent was waived because anonymous and de-identified information was used for analysis.

Measurements and Definitions

Anthropometric and laboratory measurements were performed after an overnight fast. Body mass index (BMI) was calculated as Bwt in kilograms (kg) divided by the square of height in meters (m^2). Subjects were categorized into 4 groups according to the World Health Organization recommendation for Asian population: <18.5 kg/m^2 (underweight), 18.5–22.9 kg/m^2 (normal), 23.0–24.9 kg/m^2 (overweight), and BMI ≥ 25 kg/m^2 (obese) (19). Information on current smoking status, alcohol consumption (at least 1 drink per week), and regular exercise (strenuous physical activity on at least 3 times per week) were obtained from a questionnaire filled-in during the health examination. Income levels were dichotomized at the lower 10%.

Diabetes was defined as fasting glucose level ≥ 126 mg/dL or at least one prescription claim per year for antidiabetic medication under the International Classification of Diseases, 10th revision (ICD-10) codes (E10–E14). Hypertension was defined as systolic/diastolic blood pressure $\geq 140/90$ mmHg or

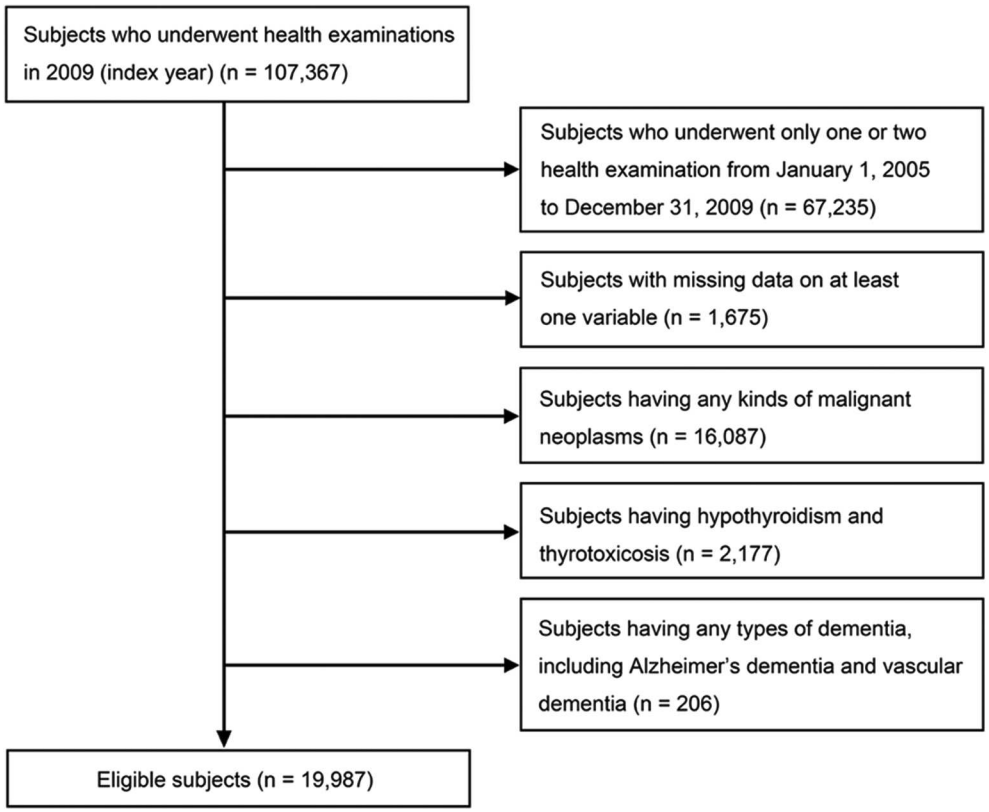

FIGURE 1 | Flowchart of the study population.

at least one prescription claim per year for an antihypertensive agent under ICD-10 codes (I10–I13, I15). Dyslipidemia was defined as total cholesterol levels ≥240 mg/dL or at least one prescription claim per year for an antihyperlipidemic agent under ICD-10 codes (E78). Ischemic heart disease (I20–25) and cerebrovascular disease (I60–69) were assessed by searching for ICD-10 codes.

Definition of Bwt Variability

Visit-to-visit Bwt variability was determined from at least three Bwt measurements for each participant. A total of 17,681 participants (88.5%) had three measurements, 1,548 participants (7.8%) had four measurements, and 758 participants (3.8%) had five measurements. We measured intra-individual Bwt variability using three indices of variability, namely variability independent of the mean (Bwt-VIM), coefficient of variation (Bwt-CV), and standard deviation (Bwt-SD). Bwt-SD can increase as the mean Bwt level increases. CV was defined as (SD/mean) × 100 (%) to exclude the effect of mean Bwt level, but it had concern that it does not completely rule out the effects of mean Bwt level. Bwt-VIM is another visit-to-visit Bwt variability measurement that has no correlation with mean Bwt level over visits. VIM was $(k \times SD(Bwt))/mean(Bwt)^x$, where x is calculated from fitting a power model: SD (Bwt) = a times $mean(Bwt)^x$ and k = $mean(mean(Bwt))^x$ (24, 25).

Outcomes

We examined new cases of dementia in the governmental database from January 1, 2009 to December 31, 2015. The incidence of all-cause dementia was determined through prescriptions for an anti-dementia drug (donepezil, galantamine, rivastigmine, or memantine), defined as ICD-10 codes (F00, F01, F02, F03, and G30) used as the first or second diagnosis for medical expense claims submitted to the NHIS until the end of follow-up. Alzheimer's dementia was specified by ICD-10 codes F00 or G30, while vascular dementia was defined by ICD-10 code F01. When both Alzheimer's disease and vascular dementia codes were used, the final diagnosis was defined as vascular dementia. This definition was applied to both outpatients and hospitalized patients. To submit a valid claim for an anti-dementia drug prescription, physicians need to document evidence of cognitive decline according to relatively strict criteria: (1) Mini Mental State Examination score ≤ 26 and (2) either a Clinical Dementia Rating ≥ 1 or a Global Deterioration Scale score ≥ 3 (26).

Statistical Analysis

Data were analyzed with SAS 9.4 (SAS Institute Inc., Cary, NC, USA). Results are presented as the median (interquartile range) for continuous variables and counts (percentage, %) for categorical variables. Normal distribution was determined by Kolmogorov-Smirnov test. Statistical analysis for between-group

comparisons was based on Kruskal-Wallis test or Mann-Whitney test for continuous variables or χ^2 test for categorical variables. Kaplan–Meier curves for cumulative incidence of dementia and dementia subgroups were obtained for four groups, classified as according to quartile of Bwt variability. Cox proportional hazards models were used to calculate hazard ratios (HRs) and 95% confidence intervals (CIs) for the risk of dementia by quartile of Bwt variability after adjusting for confounding factors including age, sex, BMI, alcohol consumption, current smoking, exercise, income, diabetes mellitus, hypertension, dyslipidemia, heart failure, ischemic heart disease, and cerebrovascular disease. HRs (95% CIs) for the incidence of dementia was also calculated according to quartiles of Bwt variability and four categories of baseline BMI with interaction effect after adjusting for multiple confounding factors. Subgroup analysis was conducted by stratifying for age, sex, BMI, current smoking status, alcohol consumption, regular exercise, income, diabetes, hypertension, dyslipidemia, ischemic heart disease, and cerebrovascular disease. In subgroup analyses, the HR and 95% CI of the highest quartile (Q4) group were compared with those of the lower three quartiles (Q1–Q3) as the reference group by using Cox proportional hazards regression models with interaction effect. Sensitivity analyses were also performed, excluding subjects over 85 years of age, or subjects with continuous weight loss or gain. Statistical significance was assumed at $P < 0.05$. All statistical analyses were performed by an experienced professional statistician, who was also one of authors.

RESULTS

Baseline Characteristics and Incidence of Dementia

Baseline characteristics of the study subjects according to the presence of dementia are presented in **Supplementary Table 1**. The mean age of our study population in 2009 (index year) was 73.1 years ($SD = 4.1$, range 67–98). Subjects with dementia were older and more likely to be female when compared to subjects without dementia. Individuals with dementia had lower BMI, Bwt, and waist circumference and a higher Bwt variability. The percentages of current smokers and alcohol consumers were lower in dementia group. They also had a higher prevalence of diabetes, dyslipidemia, cerebrovascular disease, and ischemic heart disease.

Table 1 shows the baseline characteristics of study subjects according to Bwt-VIM quartile. The mean values of anthropometric measurements, BMI, proportions of lifestyle characteristics, and the prevalence of diabetes, hypertension, and cerebrovascular disease differed significantly among the Bwt-VIM quartile. During the median follow-up period of 6.5 years (range, 6.2–6.8 years), 1,592 (7.97%) of the 19,987 subjects with complete follow-up data had all-cause dementia, of which 1,217 (6.09%) had Alzheimer's dementia and 304 (1.52%) had vascular dementia. The ratio of Alzheimer's dementia to vascular dementia was 4.0, similar to previous Korean prevalence studies (27).

Effects of Bwt Variability on Incident Dementia

A Kaplan-Meier plot was used to describe the cumulative incidence of dementia according to Bwt-VIM quartile (**Figure 2A**). The incidence of all-cause dementia and Alzheimer's dementia increased as Bwt variability increased. The annual incidence of all-cause dementia was 10.00 per 1,000 person-years in Bwt-VIM Q1 and 15.66 per 1,000 person-years in Bwt-VIM Q4. In Alzheimer's dementia, the annual incidence was 7.24 per 1,000 person-years in Bwt-VIM Q1 and 11.92 per 1,000 person-years in Bwt-VIM Q4 group. The risk of all-cause dementia and Alzheimer's dementia were highest in Bwt-VIM Q4 (log rank test, $P < 0.001$, both). These results were consistent when Bwt variability was determined with CV or SD (**Figures 2B,C**).

Table 2 indicates that the association between Bwt variability and the incidence of all-cause dementia and Alzheimer's dementia remained after adjusting for baseline covariates. Subjects in the Bwt-VIM Q4 had a higher risk of all-cause dementia (unadjusted, HR 1.570, 95% CI 1.363–1.808) than did subjects in the Bwt-VIM Q1. After adjusting for age, sex, BMI, alcohol consumption, smoking, exercise, income, diabetes, hypertension, dyslipidemia, ischemic heart disease, and cerebrovascular disease (Model 3), the association persisted (HR 1.390, 95% CI 1.206–1.603 for Q4 compared to Q1). The association between Bwt variability and risk of Alzheimer's dementia was especially significant. The fully adjusted HRs for the incidence of Alzheimer's dementia for the Bwt-VIM Q4 vs. Bwt-VIM Q1 was 1.462 (95% CI 1.240–1.724). For vascular dementia, the association between Bwt variability and the risk of dementia was attenuated in the adjusted models (Model 3, HR 1.204, 95% CI 0.880–1.647 for Q4 compared to Q1).

Effects of Baseline BMI and Bwt Variability on the Incidence of Dementia

We analyzed the baseline characteristics of study subjects according to baseline BMI (**Supplementary Table 2**). Underweight subjects had the highest Bwt variability indices and highest prevalence of all-cause dementia, Alzheimer's dementia, and vascular dementia. Subjects with a lower baseline BMI were more likely to be current smokers and less likely to exercise regularly. In contrast, obese subjects had the highest mean of Bwt, waist circumference, fasting glucose and total cholesterol, and prevalence of diabetes, hypertension, dyslipidemia and ischemic heart disease.

The association between Bwt variability and dementia differed according to baseline BMI category (**Figure 3** and **Supplementary Table 3**, P-value for interaction between Bwt variability and baseline BMI category = 0.034). To analyze the effect of Bwt variability on the risk of dementia according to baseline BMI, we performed analyses using a single reference group (normal baseline BMI with Bwt-VIM Q1). Subjects in underweight BMI with Bwt-VIM Q4 group had a significantly increased risk of developing dementia (HR 1.994, 95% CI 1.302–3.054). Subjects in obese BMI with Bwt-VIM Q1 and Q2 groups

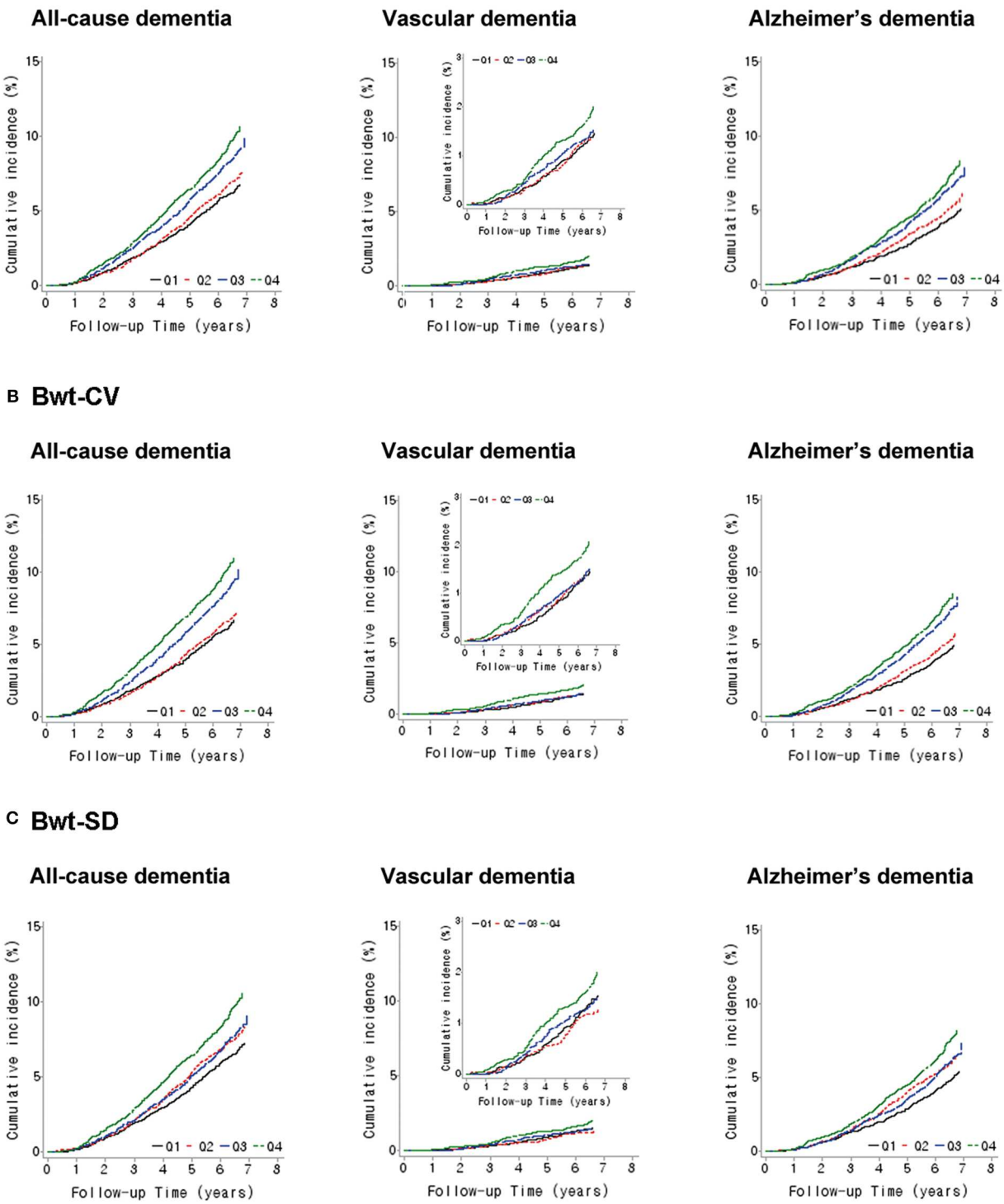

FIGURE 2 | Kaplan–Meier estimates of cumulative incidence of dementia according to quartiles of body weight (Bwt) variability **(A)** Bwt-VIM, **(B)** Bwt-CV, **(C)** Bwt-SD. CV, coefficients of variance; SD, standard deviation; VIM, variability independent of the mean.

TABLE 1 | Baseline characteristics of the subjects according to the quartiles of body weight (Bwt) variability.

	Q1 *N* = 4,996	Q2 *N* = 4,985	Q3 *N* = 5,011	Q4 *N* = 4,995	*P*-value
Age (years)	72 (70, 74)	72 (70, 75)	72 (70, 76)	72 (70, 76)	<0.001
Sex (male) (*n*, %)	3,131 (62.7)	2,946 (59.1)	2,940 (58.7)	3,008 (60.2)	<0.001
BMI (kg/m^2)	23.85 (22.05, 25.56)	23.53 (21.72, 25.46)	23.18 (21.17, 25.28)	23.39 (21.22, 25.51)	<0.001
Body weight (kg)	60 (55, 66)	59 (53, 66)	58 (50, 65)	59 (52, 66)	<0.001
Waist circumference (cm)	84 (79, 89)	83 (78, 88)	82 (76, 88)	83 (78, 90)	<0.001
Body weight variability	0.59 (0.57, 0.97)	1.21 (1.13, 1.5)	2 (1.73, 2.11)	3.13 (2.67, 4.01)	<0.001
VIM	0.59 (0.57, 0.97)	1.21 (1.13, 1.5)	2 (1.73, 2.11)	3.13 (2.67, 4.01)	<0.001
CV (%)	1.08 (0.89, 1.47)	2.17 (1.92, 2.45)	3.3 (2.96, 3.7)	5.41 (4.54, 6.93)	<0.001
SD (mg/dL)	0.58 (0.58, 1)	1.15 (1.15, 1.53)	2 (1.73, 2.08)	3.06 (2.65, 4.04)	<0.001
Incidence of dementia (*n*, %)					
All-cause dementia	318 (6.4)	351 (7.0)	432 (8.6)	491 (9.8)	<0.001
Vascular dementia	69 (1.4)	67 (1.3)	74 (1.5)	94 (1.9)	0.035
Alzheimer's dementia	232 (4.6)	268 (5.4)	339 (6.8)	378 (7.6)	<0.001
Systolic BP (mmHg)	130 (120, 140)	130 (120, 140)	130 (120, 139)	130 (120, 140)	0.059
Diastolic BP (mmHg)	80 (70, 83)	80 (70, 84)	80 (70, 84)	80 (70, 85)	0.322
Fasting plasma glucose (mg/dL)	97 (89, 109)	97 (89, 108)	96 (88, 108)	97 (89, 109)	0.001
Total cholesterol (mg/dL)	194 (172, 220)	195 (172, 220)	195 (171, 221)	193 (169, 219)	0.001
Aspartate transaminase (IU/L)	24 (20, 29)	24 (20, 29)	24 (20, 29)	24 (20, 30)	0.180
Alanine transaminase (IU/L)	19 (15, 25)	19 (15, 25)	19 (15, 25)	19 (15, 26)	0.009
Current smoker (*n*, %)	731 (14.6)	705 (14.1)	774 (15.5)	778 (15.6)	0.141
Alcohol consumption (*n*, %)	1,676 (33.6)	1,584 (31.8)	1,609 (32.1)	1,530 (30.6)	0.019
Regular exercise (*n*, %)	1,113 (22.3)	978 (19.6)	944 (18.8)	900 (18)	<0.001
Diabetes (*n*, %)	1,229 (24.6)	1,199 (24.1)	1,200 (24)	1,330 (26.6)	0.006
Hypertension (*n*, %)	3,107 (62.2)	3,182 (63.8)	3,177 (63.4)	3,324 (66.6)	<0.001
Dyslipidemia (*n*, %)	1,686 (33.8)	1,639 (32.9)	1,657 (33.1)	1,643 (32.9)	0.769
erebrovascular disease (*n*, %)	412 (8.3)	402 (8.1)	456 (9.1)	492 (9.9)	0.005
Ischemic heart disease (*n*, %)	547 (11)	584 (11.7)	584 (11.7)	610 (12.2)	0.268
Income (lower 10%)	547 (11)	565 (11.3)	550 (11)	569 (11.4)	0.845

P-value derived using Kruskal–Wallis test and χ^2 test.
Data are expressed as median (interquartile range), or n (%).
BMI, body mass index; BP, blood pressure; CV, coefficients of variance; SD, standard deviation; VIM, variability independent of the mean.

had a decreased risk of developing dementia (HR 0.664, 95% CI 0.505–0.872 and HR 0.648, 95% CI 0.493–0.852, respectively).

Subgroup Analysis

Stratified analyses were conducted by age, sex, smoking status, alcohol consumption, income and presence or absence of diabetes, hypertension, dyslipidemia, cerebrovascular disease, and ischemic heart disease. Bwt-VIM Q4 remained predictive of dementia in almost all subgroups when compared with Q1–Q3. In subgroup analysis, higher adjusted HRs of all-cause dementia were observed among subjects with younger age (age <75), subjects with abnormal BMI (underweight, overweight, and obese), and subjects who participated in regular exercise (**Figure 4**).

Sensitivity Analysis

The impact of body weight variability on the risk of dementia is very likely to be influenced by age. To exclude the possible effects of prodromal symptoms of Alzheimer's disease in oldest-old, an additional analysis was performed except for those over 85 years of age (**Supplementary Table 4**). The fully adjusted HRs for the incidence of all-cause dementia and Alzheimer's dementia for the Bwt-VIM Q4 vs. Bwt-VIM Q1 were 1.426 (95% CI 1.236–1.646) and 1.513 (95% CI 1.281–1.787), respectively. Bwt variability means intra-individual weight cycling within specific period, and it is different concept with the simple weight loss and weight gain. Thus, we conducted further analysis after excluding subjects with continuous weight loss or gain (**Supplementary Table 5**). Subjects in the Bwt-VIM Q4 had higher risks of all-cause dementia (HR 1.325, 95% CI 1.127–1.557) and Alzheimer's dementia (HR 1.352, 95% CI 1.122–1.63) than did subjects in the Bwt-VIM Q1 in Model 3.

DISCUSSION

The present study provides the first demonstration that high Bwt variability in the elderly was significantly associated with the risk of all-cause dementia and Alzheimer's dementia after extensive adjustment for possible covariates in the Korean population. This association remained statistical significant even

TABLE 2 | Hazard ratios and 95% confidence intervals of incidence dementia by quartiles of body weight (Bwt) variability.

	Total (n)	Events (n)	Follow-up duration (person years)	Incidence rate (per 1,000 person years)	Hazard ratio (95% confidence intervals)			
					Unadjusted	Model 1	Model 2	Model 3
All-cause dementia								
Q1	4,996	318	31791.3	10.00	1 (ref)	1 (ref)	1 (ref)	1 (ref)
Q2	4,985	351	31702.84	11.07	1.106 (0.951, 1.288)	1.079 (0.927, 1.256)	1.070 (0.919, 1.245)	1.074 (0.923, 1.250)
Q3	5,011	432	31607.93	13.67	1.369 (1.185, 1.583)	1.294 (1.119, 1.495)	1.268 (1.097, 1.467)	1.265 (1.094, 1.464)
Q4	4,995	491	31351.62	15.66	1.570 (1.363, 1.808)	1.421 (1.233, 1.637)	1.403 (1.217, 1.617)	1.390 (1.206, 1.603)
P for trend					<0.001	<0.001	<0.001	<0.001
Vascular dementia								
Q1	4,996	69	32433.34	2.13	1 (ref)	1 (ref)	1 (ref)	1 (ref)
Q2	4,985	67	32399.7	2.07	0.971 (0.694, 1.360)	0.953 (0.681, 1.334)	0.944 (0.674, 1.322)	0.945 (0.675, 1.324)
Q3	5,011	74	32523.6	2.28	1.070 (0.771, 1.486)	1.025 (0.738, 1.424)	1.004 (0.722, 1.395)	0.982 (0.706, 1.366)
Q4	4,995	94	32354.95	2.91	1.368 (1.002, 1.866)	1.268 (0.928, 1.732)	1.251 (0.915, 1.710)	1.204 (0.880, 1.647)
P for trend					0.040	0.122	0.149	0.242
Alzheimer's dementia								
Q1	4,996	232	32053.83	7.24	1 (ref)	1 (ref)	1 (ref)	1 (ref)
Q2	4,985	268	31934.62	8.39	1.159 (0.972, 1.381)	1.129 (0.947, 1.346)	1.118 (0.938, 1.333)	1.124 (0.943, 1.341)
Q3	5,011	339	31909.59	10.62	1.471 (1.245, 1.738)	1.386 (1.173,1.638)	1.357 (1.147, 1.605)	1.362 (1.151, 1.611)
Q4	4,995	378	31724.19	11.92	1.649 (1.400, 1.941)	1.483 (1.258, 1.748)	1.463 (1.241, 1.725)	1.462 (1.240, 1.724)
P for trend					<0.001	<0.001	<0.001	<0.001

Model 1: Adjusted for age, sex.
Model 2: model 1 + BMI.
Model 3: model 2 + alcohol, smoking, exercise, income, diabetes, hypertension, dyslipidemia, ischemic heart disease, cerebrovascular disease.

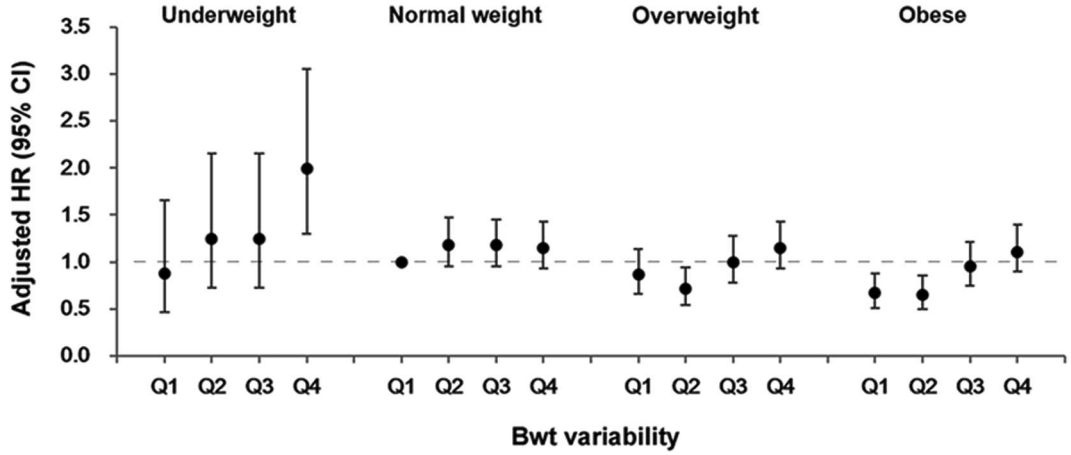

FIGURE 3 | Association between body weight (Bwt) variability and the risk of dementia according to baseline body mass index (BMI) category. CI, confidence intervals; HR, hazard ratios.

after excluding the subjects with continuous weight low or gain. Furthermore, in individuals with an obese BMI at baseline, lower Bwt variability was associated with decreased risk of dementia, whereas the subjects with underweight BMI and the highest Bwt variability showed a significantly increased risk of developing dementia.

Epidemiologic studies have shown that higher adiposity at mid-life, whether measured as BMI or central obesity, was associated with a higher risk of dementia (3, 5, 6). The mechanisms linking obesity with cognitive decline and dementia have been demonstrated in several studies. In middle aged adults, visceral fat volume was associated with global brain atrophy

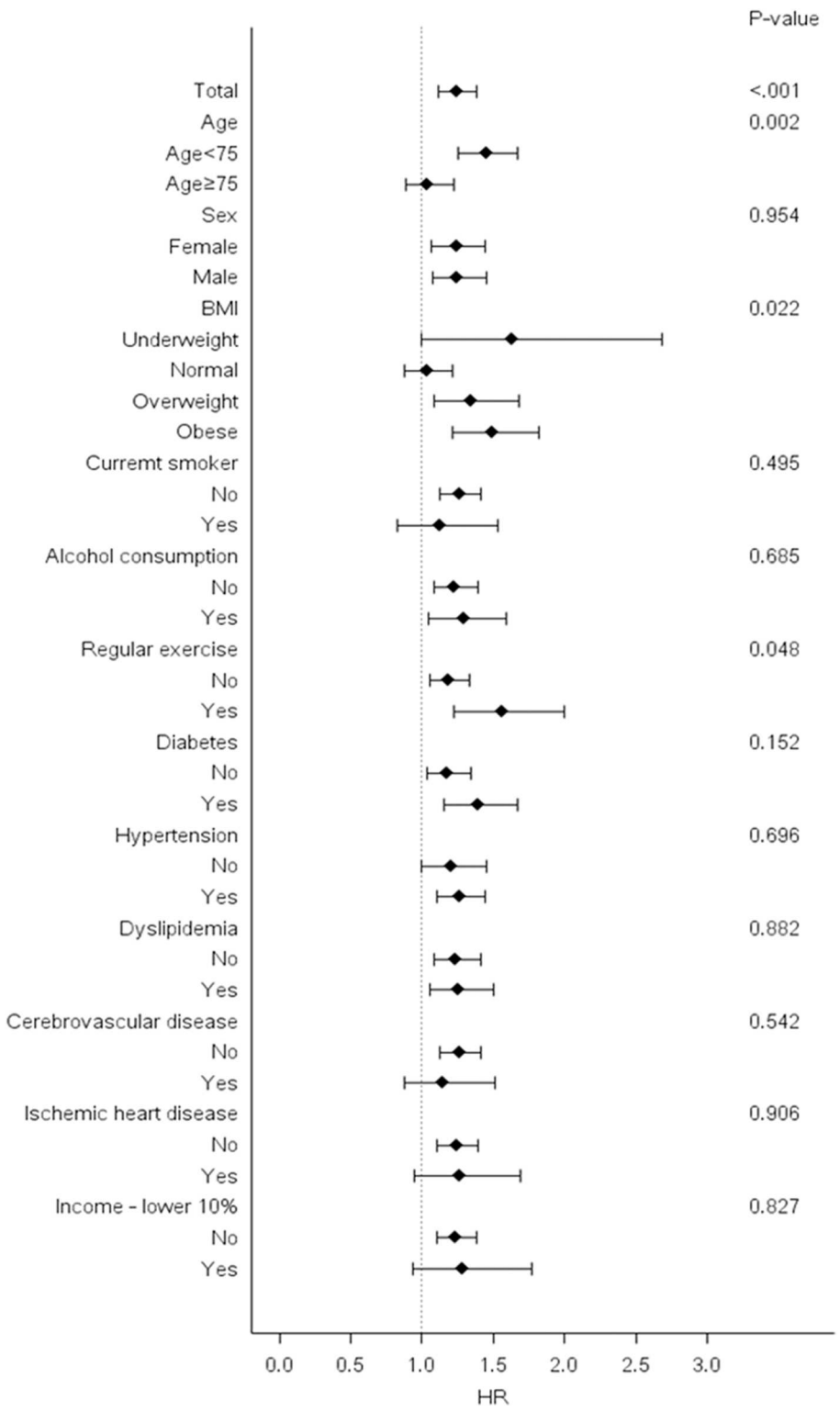

FIGURE 4 | Risk of dementia in the highest vs. lower three quartiles of body weight (Bwt) variability in subgroups. Hazard ratios and 95% confidence intervals for the risk of dementia in the highest quartile (Q4) vs. lower three quartiles (Q1–Q3) of Bwt variability in subgroups. BMI, body mass index; HR, hazard ratios.

measured by MRI (28). Furthermore, increased adiposity has been correlated with atrophy of several brain regions including the hippocampus (29, 30). Reduced hippocampal volume predicts cognitive function in the general population (31). Mid-life obesity was associated with earlier onset of Alzheimer's disease and greater severity of Alzheimer's neuropathology (4). Moreover, obesity increased the risk of cognitive impairment and dementia through vascular effects, such as atherosclerosis, endothelial dysfunction, arterial stiffness, and impairment of the blood-brain barrier (32, 33). Despite these definite direct and indirect links between mid-life obesity and dementia, epidemiological studies have focused on the association between late-life obesity and dementia and reported conflicting results. Weight reduction in midlife can lead to healthy condition via controlling various metabolic risk factors, whereas weight loss in late-life may reflect underlying illness and muscle reduction, causing unhealthy body composition. As a result, The association between a high Bwt and adverse clinical outcomes attenuates with age (10). Findings from the Whitehall II study published after the meta-analysis showed a higher risk of dementia for obesity at age 50, but not at ages 60–70 years (34). Furthermore, in the collaborative study of over 1.3 million adults, higher BMI was associated with increased dementia risk when weight was measured >20 years before dementia diagnosis, but this association was reversed when BMI was assessed <10 years before dementia diagnosis (35). Dementia-related weight loss appeared about 6 years before the onset of the clinical syndrome (36). Therefore, Bwt of elderly population cannot give accurate information for the risk of dementia.

Recently, several studies have demonstrated that Bwt variability was associated with increased risk of cardiovascular disease and mortality (12–14). According to the study in mice, weight cycling induced greater adipose tissue inflammation and insulin resistance than a consistently obese state (37) and a human study showed that Bwt fluctuation was related to poorer body-fat distribution (38). Sustained fluctuations in energy balance will lead to potential fluctuations of cardiometabolic risk variables, such as blood pressure, heart rate, blood glucose and lipids (39). In a 7-year follow-up French national cohort study, weight fluctuation was an independent risk factor for metabolic syndrome (40). Apart from this direct causal effect between Bwt variability and metabolic disturbances, Bwt fluctuation might reflect difficulty maintaining homeostasis, subsequent declining mental health. However, very few studies have assessed the effects of Bwt variability on dementia. One study suggested that mid-life Bwt variability was associated increased risk of dementia late in life (20). Another study of elderly women reported that Bwt variability was associated with increased risk of cognitive impairment or dementia, but the risk was attenuated after adjusting for covariates (21). However, those studies included a relative small-sized number with only women or men and did not utilize the accurate variability index such as CV, SD and VIM. Furthermore, the trajectory period was over 20-years covering both mid and late-life, which did not focus on the late-life Bwt variability like our research. We for the first time demonstrated that Bwt variability in the elderly was significantly associated with the increased risk for dementia after adjusting other covariates, suggesting that the inability to maintain one's weight might be an indication for poorer homeostatic control and general condition. This association remained statistical significance even after excluding the subject with continuous weight loss and very old age group (≥85 years), implying that the close relation between Bwt variability in late-life and dementia was independent from preclinical weight loss of dementia or age. Previously, Arnold et al. (41) reported that a history of weight cycling for the elderly with more than 65-years old increased the risk of physical disability by 28% after adjusting other risk factors including average weight and weight change per year. Considering that Bwt fluctuations in older persons are not benign condition, monitoring the weight of an older person for fluctuations as well as episodes of weight loss might be an important aspect of geriatric care.

Subgroup analyses in our study showed a stronger association between Bwt variability and dementia in people age <75 years compared with those older 75 years, because the older subgroup is easy to face with additional competing risk factors for dementia, such as age itself. The association between Bwt variability and dementia is stronger in subject with abnormal baseline BMI (underweight, overweight, and obese) compared to those with normal baseline BMI. Although the underlying mechanism of this association is not clear, individuals who exercised regularly had a higher risk of dementia according to Bwt variability quartile compared to those who did not (P-value for interaction = 0.048). Individuals without regular exercise might be more vulnerable to other risk factors of the dementia other than Bwt variability.

Our study has several limitations. We could not consider educational level or dietary factors due to lack of information. We could not consider the role of APOE e4, the major susceptibility allele for dementia, due to lack of data. Patients with dementia were identified according to ICD-10 codes and not confirmed by brain imaging. Thus, the prevalence of dementia may have been underestimated because we used information recorded in the claim database. The incidence of vascular dementia was relatively low, which may have reduced the significance of any associations. Finally, because of the intrinsic limitations of the observational study design, we could not define a causal relationship between Bwt variability and dementia. Despite these limitations, this study has the strength of using a large-scale nationwide database, which is standardized and validated by the Korean government and represents the entire elderly Korean population.

In conclusion, our study findings suggest that Bwt variability is an independent predictor for dementia in the elderly. The risk of developing dementia was significantly increased in subjects with highest Bwt variability and underweight BMI and significantly decreased in subjects with low Bwt variability and obese BMI. These results merit further study in order to confirm our results in different ethnic groups and to explore the mechanistic links between Bwt variability and dementia.

DATA AVAILABILITY STATEMENT

Data are available through the Korean National Health Insurance Sharing Service (NHISS). Researchers who wish to access the data can apply at (https://nhiss.nhis.or.kr/bd/ay/bdaya001iv.do) and request access to NHIS-2018–2-195.

ETHICS STATEMENT

The studies involving human participants were reviewed and approved by Institutional Review Board of Korea University. Written informed consent for participation was not required for this study in accordance with the national legislation and the institutional requirements.

AUTHOR CONTRIBUTIONS

ER and HY contributed to the study design, statistical analyses, data interpretation, and fund raising and drafted the manuscript. SHw contributed to the data collection and statistical analyses. JK, Y-BL, and SHo contributed to the study design and data interpretation. NHoK, JS, SK, NHeK, KC, and SB contributed to the data interpretation. All authors have approved the submitted manuscript.

FUNDING

This work was supported by National Research Foundation of Korea (NRF) funded by the Ministry of Education of Korea (2018R1D1A1B07047587, 2018R1D1A1B07050991). The funders had no role in the study design, data collection, analysis, and interpretation, decision to publish, or preparation of the manuscript.

ACKNOWLEDGMENTS

This work was performed in cooperation with the Korean National Health Insurance Sharing Service (NHISS).

SUPPLEMENTARY MATERIAL

The Supplementary Material for this article can be found online at: https://www.frontiersin.org/articles/10.3389/fendo.2020.00291/full#supplementary-material

REFERENCES

1. Winblad B, Amouyel P, Andrieu S, Ballard C, Brayne C, Brodaty H, et al. Defeating Alzheimer's disease and other dementias: a priority for European science and society. *Lancet Neurol*. (2016) 15:455–532. doi: 10.1016/S1474–4422(16)00062–4
2. Kivipelto M, Ngandu T, Fratiglioni L, Viitanen M, Kåreholt I, Winblad B, et al. Obesity and vascular risk factors at midlife and the risk of dementia and Alzheimer disease. *Arch Neurol*. (2005) 62:1556–60. doi: 10.1001/archneur.62.10.1556
3. Whitmer RA, Gunderson EP, Quesenberry CP, Zhou J, Yaffe K. Body mass index in midlife and risk of Alzheimer disease and vascular dementia. *Curr Alzheimer Res*. (2007) 4:103–9. doi: 10.2174/156720507780362047
4. Chuang Y-F, An Y, Bilgel M, Wong DF, Troncoso JC, O'Brien RJ, et al. Midlife adiposity predicts earlier onset of Alzheimer's dementia, neuropathology and presymptomatic cerebral amyloid accumulation. *Mol Psychiatry*. (2016) 21:910–5. doi: 10.1038/mp.2015.129
5. Fitzpatrick AL, Kuller LH, Lopez OL, Diehr P, O'Meara ES, Longstreth W, et al. Midlife and late-life obesity and the risk of dementia: cardiovascular health study. *Arch Neurol*. (2009) 66:336–42. doi: 10.1001/archneurol.2008.582
6. Whitmer R, Gustafson D, Barrett-Connor E, Haan M, Gunderson E, Yaffe K. Central obesity and increased risk of dementia more than three decades later. *Neurology*. (2008) 71:1057–64. doi: 10.1212/01.wnl.0000306313.89165.ef
7. Atti AR, Palmer K, Volpato S, Winblad B, De Ronchi D, Fratiglioni L. Late-life body mass index and dementia incidence: nine-year follow-up data from the Kungsholmen Project. *J Am Geriatr Soc*. (2008) 56:111–6. doi: 10.1111/j.1532–5415.2007.01458.x
8. Nourhashemi F, Deschamps V, Larrieu S, Letenneur L, Dartigues J-F, Barberger-Gateau P. Body mass index and incidence of dementia the PAQUID study. *Neurology*. (2003) 60:117–9. doi: 10.1212/01.wnl.0000038910.46217.aa
9. Grundman M, Corey-Bloom J, Jernigan T, Archibald S, Thal L. Low body weight in Alzheimer's disease is associated with mesial temporal cortex atrophy. *Neurology*. (1996) 46:1585–91. doi: 10.1212/wnl.46.6.1585
10. Stevens J, Cai J, Pamuk ER, Williamson DF, Thun MJ, Wood JL. The effect of age on the association between body-mass index and mortality. *N Engl J Med*. (1998) 338:1–7. doi: 10.1056/NEJM199801013380101
11. Knopman DS, Edland SD, Cha RH, Petersen RC, Rocca WA. Incident dementia in women is preceded by weight loss by at least a decade. *Neurology*. (2007) 69:739–46. doi: 10.1212/01.wnl.0000267661.65586.33
12. Lissner L, Odell PM, D'Agostino RB, Stokes J III, Kreger BE, Belanger AJ, et al. Variability of body weight and health outcomes in the framingham population. *N Engl J Med*. (1991) 324:1839–44. doi: 10.1056/NEJM199106273242602
13. Blair SN, Shaten J, Brownell K, Collins G, Lissner L. Body weight change, all-cause mortality, and cause-specific mortality in the multiple risk factor intervention trial. *Ann Intern Med*. (1993) 119:749–57. doi: 10.7326/0003–4819-119–7_part_2–199310011-00024
14. Bangalore S, Fayyad R, Laskey R, DeMicco DA, Messerli FH, Waters DD. Body-weight fluctuations and outcomes in coronary disease. *N Engl J Med*. (2017) 376:1332–40. doi: 10.1056/NEJMc1705832
15. Kim MK, Han K, Kim HS, Park YM, Kwon HS, Yoon KH, et al. Cholesterol variability and the risk of mortality, myocardial infarction, and stroke: a nationwide population-based study. *Eur Heart J*. (2017) 38:3560–6. doi: 10.1093/eurheartj/ehx585
16. Kim MK, Han K, Park Y-M, Kwon H-S, Kang G, Yoon K-H, et al. Associations of variability in blood pressure, glucose and cholesterol concentrations, and body mass index with mortality and cardiovascular outcomes in the general population. *Circulation*. (2018) 138:2627–37. doi: 10.1161/CIRCULATIONAHA.118.034978
17. Zou H, Yin P, Liu L, Liu W, Zhang Z, Yang Y, et al. Body-weight fluctuation was associated with increased risk for cardiovascular disease, all-cause and cardiovascular mortality: a systematic review and meta-analysis. *Front Endocrinol*. (2019) 10:728. doi: 10.3389/fendo.2019.00728
18. Morton GJ, Cummings DE, Baskin DG, Barsh GS, Schwartz MW. Central nervous system control of food intake and body weight. *Nature*. (2006) 443:289–95. doi: 10.1038/nature05026
19. Park S, Jeon SM, Jung SY, Hwang J, Kwon JW. Effect of late-life weight change on dementia incidence: a 10-year cohort study using claim data in Korea. *BMJ Open*. (2019) 9:e021739. doi: 10.1136/bmjopen-2018–021739
20. Ravona-Springer R, Schnaider-Beeri M, Goldbourt U. Body weight variability in midlife and risk for dementia in old age. *Neurology*. (2013) 80:1677–83. doi: 10.1212/WNL.0b013e3182904cee
21. LeBlanc ES, Rizzo JH, Pedula KL, Yaffe K, Ensrud KE, Cauley J, et al. Weight trajectory over 20 years and likelihood of mild cognitive impairment

or dementia among older women. *J Am Geriatr Soc*. (2017) 65:511–9. doi: 10.1111/jgs.14552
22. Kwon S. Thirty years of national health insurance in South Korea: lessons for achieving universal health care coverage. *Health Policy Plan*. (2008) 24:63–71. doi: 10.1093/heapol/czn037
23. Seong SC, Kim YY, Park SK, Khang YH, Kim HC, Park JH, et al. Cohort profile: the National Health Insurance Service-National Health Screening Cohort (NHIS-HEALS) in Korea. *BMJ Open*. (2017) 7:e016640. doi: 10.1136/bmjopen-2017–016640
24. Rothwell PM, Howard SC, Dolan E, O'Brien E, Dobson JE, Dahlof B, et al. Prognostic significance of visit-to-visit variability, maximum systolic blood pressure, and episodic hypertension. *Lancet*. (2010) 375:895–905. doi: 10.1016/s0140–6736(10)60308-X
25. Selvarajah V, Pasea L, Ojha S, Wilkinson IB, Tomlinson LA. Pre-dialysis systolic blood pressure-variability is independently associated with all-cause mortality in incident haemodialysis patients. *PLoS ONE*. (2014) 9:e86514. doi: 10.1371/journal.pone.0086514
26. Jeong S-M, Shin DW, Lee JE, Hyeon JH, Lee J, Kim S. Anemia is associated with incidence of dementia: a national health screening study in Korea involving 37,900 persons. *Alzheimers Res Ther*. (2017) 9:94. doi: 10.1186/s13195–017-0322–2
27. Kim YJ, Han JW, So YS, Seo JY, Kim KY, Kim KW. Prevalence and trends of dementia in Korea: a systematic review and meta-analysis. *J Korean Med Sci*. (2014) 29:903–12. doi: 10.3346/jkms.2014.29.7.903
28. Debette S, Beiser A, Hoffmann U, DeCarli C, O'donnell CJ, Massaro JM, et al. Visceral fat is associated with lower brain volume in healthy middle-aged adults. *Ann Neurol*. (2010) 68:136–44. doi: 10.1002/ana.22062
29. Gustafson D, Lissner L, Bengtsson C, Björkelund C, Skoog I. A 24-year follow-up of body mass index and cerebral atrophy. *Neurology*. (2004) 63:1876. doi: 10.1212/01.wnl.0000141850.47773.5f
30. Pannacciulli N, Del Parigi A, Chen K, Le DSNT, Reiman EM, Tataranni PA. Brain abnormalities in human obesity: A voxel-based morphometric study. *NeuroImage*. (2006) 31:1419–25. doi: 10.1016/j.neuroimage.2006.01.047
31. den Heijer T, van der Lijn F, Koudstaal PJ, Hofman A, van der Lugt A, Krestin GP, et al. A 10-year follow-up of hippocampal volume on magnetic resonance imaging in early dementia and cognitive decline. *Brain*. (2010) 133:1163–72. doi: 10.1093/brain/awq048
32. Gorelick PB, Scuteri A, Black SE, DeCarli C, Greenberg SM, Iadecola C, et al. Vascular contributions to cognitive impairment and dementia: a statement for healthcare professionals from the American heart association/American stroke association. *Stroke*. (2011) 42:2672–713. doi: 10.1161/STR.0b013e3182299496
33. Zlokovic BV. Neurovascular pathways to neurodegeneration in Alzheimer's disease and other disorders. *Nat Rev Neurosci*. (2011) 12:723–38. doi: 10.1038/nrn3114
34. Singh-Manoux A, Dugravot A, Shipley M, Brunner EJ, Elbaz A, Sabia S, et al. Obesity trajectories and risk of dementia: 28 years of follow-up in the whitehall II study. *Alzheimers Dement*. (2018) 14:178–86. doi: 10.1016/j.jalz.2017.06.2637
35. Kivimaki M, Luukkonen R, Batty GD, Ferrie JE, Pentti J, Nyberg ST, et al. Body mass index and risk of dementia: Analysis of individual-level data from 1.3 million individuals. *Alzheimers Dement*. (2018) 14:601–9. doi: 10.1016/j.jalz.2017.09.016
36. Stewart R, Masaki K, Xue Q-L, Peila R, Petrovitch H, White LR, et al. A 32-year prospective study of change in body weight and incident dementia: the Honolulu-Asia Aging Study. *Arch Neurol*. (2005) 62:55–60. doi: 10.1001/archneur.62.1.55
37. Anderson EK, Gutierrez DA, Kennedy A, Hasty AH. Weight cycling increases T-cell accumulation in adipose tissue and impairs systemic glucose tolerance. *Diabetes*. (2013) 62:3180–8. doi: 10.2337/db12–1076
38. van der Kooy K, Leenen R, Seidell JC, Deurenberg P, Hautvast JG. Effect of a weight cycle on visceral fat accumulation. *Am J Clin Nutr*. (1993) 58:853–7. doi: 10.1093/ajcn/58.6.853
39. Montani J-P, Viecelli A, Prévot A, Dulloo AG. Weight cycling during growth and beyond as a risk factor for later cardiovascular diseases: the 'repeated overshoot'theory. *Int J Obes*. (2006) 30:S58–66. doi: 10.1038/sj.ijo.0803520
40. Vergnaud AC, Bertrais S, Oppert JM, Maillard-Teyssier L, Galan P, Hercberg S, et al. Weight fluctuations and risk for metabolic syndrome in an adult cohort. *Int J Obes*. (2008) 32:315–21. doi: 10.1038/sj.ijo.0803739
41. Arnold AM, Newman AB, Cushman M, Ding J, Kritchevsky S. Body weight dynamics and their association with physical function and mortality in older adults: the Cardiovascular Health Study. *J Gerontol A Biol Sci Med Sci*. (2010) 65:63–70. doi: 10.1093/gerona/glp050

Conflict of Interest: The authors declare that the research was conducted in the absence of any commercial or financial relationships that could be construed as a potential conflict of interest.

frontiers in Endocrinology

ORIGINAL RESEARCH
published: 16 June 2020
doi: 10.3389/fendo.2020.00382

Urinary Exosomal Thyroglobulin in Thyroid Cancer Patients With Post-ablative Therapy: A New Biomarker in Thyroid Cancer

Tse-Ying Huang[1], Chih-Yuan Wang[1], Kuen-Yuan Chen[2] and Li-Ting Huang[1]*

[1] Department of Internal Medicine, National Taiwan University Hospital Yun-Lin/Hsin-Chu Branch, College of Medicine, National Taiwan University, Taipei, Taiwan, [2] Department of Surgery, National Taiwan University Hospital, College of Medicine, National Taiwan University, Taipei, Taiwan

Background: Most patients with thyroid cancer typically receive thyroidectomy with ablative radioactive iodine therapy. Such patients were followed with thyroid ultrasonography and serial serum thyroglobulin evaluation. Exosomes are nanovesicles secreted into extracellular environments, including plasma, saliva, urine, and other body fluids of patients with cancer. We try to find the early prognostic and exosomal biological markers of urine.

Methods: We analyzed urinary exosomal proteins, including thyroglobulin and galectin-3, to identify early prognostic biological markers in urine for patients receiving operation and radioactive iodine ablative therapy. We enrolled sixteen newly diagnosed patients with papillary thyroid carcinoma and follicular thyroid carcinoma. We collect all patient's urine samples before operation, immediately after operation, post-operatively at three and six months (4 collections per patient). The levels of pre-operative and post-ablative of U-Ex Tg and galectin-3 in patients with thyroid cancer were measured.

Results: Trends in urinary thyroglobulin concentrations in patients with post-ablative thyroid cancer were detected in the first sixteen patients. Importantly, serum thyroglobulin was not detected in five patients after operation and radioactive I-131 ablation, while U-Ex Tg still showed an increasing trend, which implicating the probable recurrence of thyroid cancer. This is the first study to evaluate whether U-Ex Tg is a future biological marker as a substitute for serum thyroglobulin.

Conclusion: Our study have developed a brand-new evaluation for tracking thyroid cancer. The most useful scenario in using a test that is potentially more sensitive than existing serological testing is to eliminate the suspicion of recurrence and remove subjects from long term follow up.

Trial Registration: ClinicalTrials.gov: NCT02862470; 5, August 2016. https://clinicaltrials.gov/ct2/show/NCT02862470?term=NCT02862470&rank=1. ClinicalTrials.gov: NCT03488134; 3, August 2018. https://clinicaltrials.gov/ct2/show/NCT03488134?term=NCT03488134&draw=2&rank=1.

Keywords: thyroid cancer, thyroglobulin, exosome, urine, galectin-3

OPEN ACCESS

Edited by:
Ralf Jockers, Université Paris-Sorbonne, France

Reviewed by:
Marialuisa Appetecchia, Istituti Fisioterapici Ospitalieri (IRCCS), Italy
Daniela Pasquali, University of Campania Luigi Vanvitelli, Italy

***Correspondence:**
Chih-Yuan Wang
cyw1965@gmail.com; cyw1965@ntu.edu.tw

Specialty section:
This article was submitted to Cancer Endocrinology, a section of the journal Frontiers in Endocrinology

Received: *17 February 2020*
Accepted: *14 May 2020*
Published: *16 June 2020*

Citation:
Huang T-Y, Wang C-Y, Chen K-Y and Huang L-T (2020) Urinary Exosomal Thyroglobulin in Thyroid Cancer Patients With Post-ablative Therapy: A New Biomarker in Thyroid Cancer. Front. Endocrinol. 11:382. doi: 10.3389/fendo.2020.00382

INTRODUCTION

Papillary and follicular thyroid cancers are low-grade endocrine malignancies, and, the core issue of differentiated thyroid cancer is surgical approach, which remain the primary mode of therapy (1–3), but reliable post-operation follow-up biomarker has remained further discussable issue. Most patients typically receive thyroidectomy with ablative radioactive iodine therapy (4, 5). These patients are followed with thyroid ultrasonography and serial serum thyroglobulin evaluation. Serum thyroglobulin is a pivotal biomarker for detecting possible residual tumors or recurrence of thyroid cancer (4). Generally, such patients appear to have a higher residual risk of isolated thyroglobulinemia, and postoperative serum thyroglobulin suggest distant metastases (4). Low-risk patients with non-stimulated postoperative serum thyroglobulin are typically defined as having less than 0.2 ng/mL or with thyroid hormone withdrawal thyroglobulin of less than 1.0 ng/mL (6, 7). However, costly recombinant human TSH (rhTSH) is often required to stimulate serum thyroglobulin for detecting local recurrence or distant metastasis (8). Thus, earlier biological markers for predicting the prognosis of thyroid cancer are needed.

Exosomes are nanovesicles secreted into extracellular environments. Cancer cell-derived exosomes are found in the plasma, saliva, urine, and other body fluids of patients with cancer. Increasing evidence suggests that exosomes can be used as biomarkers for the diagnosis and prognosis of malignant tumors (9, 10). Exosomes are 40–100 nm in diameter and correspond to the intraluminal vesicles of endosomal multivesicular bodies (11). Exosomes secreted by cells transfer molecular messages between cells and may be useful biological markers of cancer (11). In addition, exosomes can be collected from the serum, tissue fluid, and urine for diseases follow-up, and collecting urine as a biosample is easier to repeatedly obtain and non-invasive (12, 13). In this study, we enrolled patients with papillary and follicular thyroid carcinoma, and collected their urine samples before operation, immediately after operation, and post-operatively 3 and 6 months. We analyzed the urinary exosomal proteins to identify early prognostic biological markers in the urine in this prospective study.

MATERIALS AND METHODS

Patients

The prospective study enrolled patients with newly diagnosed thyroid cancer. This preliminary study report included sixteen patients who were followed-up for six months. We enrolled 23 patients in the very beginning, and 16 patients completed all 4-times check-ups in our study. All sixteen patients received total thyroidectomy under clinically surgical judgment, and twelve patients received radioactive I-131 ablation at approximately four weeks after operation.

Study Design

We enrolled the newly diagnosed patients with thyroid papillary, follicular cancer. After signing inform consent, we collect their urine samples before operation, immediately after operation, post-operatively at three and six months (4 collections per patient). This prospective study was approved by (Ethical Review Board approval) Institution Responsibility Board of National Taiwan University Hospital and complete patient inform consent. We identify the committee that approved the research and confirm that all research was carried out in accordance with relevant guidelines/regulations, and informed consent was obtained from all participants.

TABLE 1 | Peptide standards list and representative protein.

Peptide	Sequence	Molecular weight (Dalton)
Thyroglobulin	FLAVQSVISGR	1176.38
Galectin-3	IALDFQR	862.00

Peptide Sequences

Thyroglobulin sequence and galectin-3 sequence are available from Peptide Atlas (https://db.systemsbiology.net/sbeams/cgi/PeptideAtlas/GetSELExperiments) and UniProt (http://www.uniprot.org/) in **Table 1**. Standard peptides were synthesized by Mission Biotech, Ltd. (Taipei, Taiwan). The synthetic peptides were dried and precipitated with ether. Peptides were purified by reverse-phase high-performance liquid chromatography while monitoring peptide elution at 230 nm.

Urine Collection

Urinary exosome precipitation was performed. First, 200 mL of fresh human urinary sample was collected for exosome precipitation. These samples were centrifuged at 3000 $\times g$ for 15 min at 4°C to remove cells and cell debris, and then centrifuged at 10,000 $\times g$ for 30 min at 4°C to remove microvesicles. Amicon® Ultra 15-centrifugal filters, 100K (Millipore, Billerica, MA, USA) were used to concentrate the 200-mL urinary samples to 5–10 mL. Urinary exosomes were isolated using ExoQuick-TC (System Biosceinces, Palo Alto, CA, USA). Supernatants were transferred to new tubes, completeTM, EDTA-free Protease Inhibitor Cocktail (Roche, Basel, Switzerland) was added, and samples were stored at−80°C. Exosome pellets were resuspended in lysis buffer (7 M urea, 2 M thiourea, 4% CHAPS). Exosome protein samples were frozen at −80°C until multiple reaction monitor (MRM) analysis.

Reagents and Chemicals

All reagents were ACS grade or higher. All solvents used, including water, were liquid chromatography (LC)/mass spectrometry (MS) grade.

Tryptic Digestion

Urinary exosome samples were precipitated with three volumes of cold methanol at −20°C, followed by centrifugation at 10,000 $\times g$ for 10 min. The pellet was then suspended in lysis buffer (4 M urea, 25 mM ammonium bicarbonate, pH 8.5). The denatured samples were reduced with 200 mM dithiothreitol at ambient temperature for 1 h and then alkylated with 200 mM iodoacetamide in the dark for 1 h. The remaining iodoacetamide

was quenched by the addition of 200 mM DTT and incubated at ambient temperature for 20 min. Modified sequencing-grade trypsin (Promega, Madison, WI, USA) was added to samples. Digestion was carried out for 16 h at 37°C.

MRM Q1/Q3 Ion Pair Selection Using Direct Infusion

Synthetic standard peptides were diluted to 2 μg/mL in 0.1% formic acid for infusion at a flow rate of 10 μL/min using a syringe pump. The infused peptide solutions were analyzed by electrospray ionization using an AB SCIEX QTRAP 5500 mass spectrometer (Framingham, MA, USA) equipped with the TurboV source and controlled by Analyst software 1.5. MS analysis was conducted in positive ion mode with the ion spray voltage set to 5500 V. The source temperature was set to 550°C. Additional parameters were nebulizer and drying gas flow at 60 and 45 psi, respectively. Analyst software (version 1.5) was used to generate a list of all possible b- and y-series fragment ions for both 2+ and 3+ precursor ion-charge state spanning *m/z* range from 100 to 1000. MRM scans for optimization of MRM Q1/Q3 ion pairs were conducted with both Q1 and Q3 set to unit resolution (0.7 Da full width at half maximum), while the collision energy (CE) was ramped from 5 to 55 V in 1-V increments, with dwell time of 150 ms for each transition. From this data, the four transitions that produced the strongest signals were selected on a per-peptide basis.

Next, the three transitions producing the most abundant signals free of signal interferences were selected from these four transitions.

LC-MRM/MS Analysis of Urinary Exosome Digests

An Agilent 1260 Infinity HPLC system (Agilent Technologies, Santa Clara, CA, USA) was used to directly inject 10 μL of urine digest samples onto a reverse-phase analytical column (100 × 2.1 mm i.d., 2.7 μm, Agilent Poroshell 120 EC-C18) that was maintained at ambient temperature. Samples were separated using a 300 μL/min flow rate and gradient of 3–90% of mobile phase B over a total run time of 30 min. Mobile phase A consisted of 0.1% v/v formic acid, while mobile phase B consisted of ACN/0.1% formic acid. The gradient method is composed of multiple linear gradients as follows (time: %B) : 0.1 min, 10% B; 3.5 min, 11% B; 6.5 min, 20% B; 7 min, 21% B; 7.5 min, 22% B; 12.5 min, 22.5% B; 17 min, 25% B; 20 min, 30% B; 22.5 min, 42% B; 23.5 min, 90% B; 27 min, 3% B; 30 min, 3% B. An AB SCIEX QTRAP 5500 with a TurboV ionization source, controlled by Analyst software, was used for all LC-MRM/MS sample analyses. All acquisition methods used the following parameters: 5500 V ion spray voltage, nebulizer and drying gas flow of 60 and 45 psi, respectively, source temperature of 550°C, and Q1 and Q3 set to unit resolution (0.7 full width at half maximum).

MRM acquisition methods were initially composed of four ion pairs per peptide during determination of high-signal producing interference-free transitions and LC method development. The final analytical method was composed of one verified quantifier ion pair per peptide, and is a high-throughput, rapid 30-min method that has been evaluated for common urine interferences. However, urine analysis of the samples was performed with acquisition methods containing three verified ion-pair transitions per target peptide to ensure the detection of any minor sample-specific signals. MRM acquisition methods were constructed using fragment ion-specific tuned CE voltages and retention time constraints.

MRM Data Analysis

All MRM data were processed using AB SCIEX Analyst software (version 1.5) with the Integrator algorithm for peak integration set to default values. All integrated peaks were manually inspected to ensure correct peak detection and accurate integration. Linear regression of all calibration curves was performed using a standard 1/x2 (x = concentration) weighting option to aid in covering a wide dynamic range. The concentration of each peptide target was calculated based on the observed response and experimentally determined linear regression equation from the standard curve. The calculated concentration is reported in μM of urine and can be defined in ng/mL when the weight of the entire processed protein is taken into account.

Thyroglobulin and Anti-thyroglobulin Antibody

Thyroglobulin levels were determined using IMMULITE 2000 Thyroglobulin, a solid-phase, chemiluminescent immunometric assay. Its analytical sensitivity is 0.2 ng/mL (Siemens, Erlangen, Germany). An anti-thyroglobulin antibody survey was conducted in the ARCHITECT Anti-Tg assay, which is a two-step immunoassay for quantitative determination of thyroglobulin autoantibodies in human serum. Its sensitivity is ≤1.0 IU/mL (Abbott Laboratories, Chicago, IL, USA).

RESULTS

Patients Demographics

All patients receive pre-operative and post-operative investigation of thyroid function and serum thyroglobulin. All demographic information with surgical pathological findings are shown in **Table 2**.

Urinary Biomarkers

The initial quantification of U-Ex Tg and galectin-3 is shown in **Supplemental Data**. Peptide concentrations are shown in units of μM. We converted the unit of μM into ng/mL using the formula: (ng/mL) = (μM) (molecular weight in Dalton).

Urinary peptide biomarkers concentrations are shown in before conversion as μM and after conversion as ng/mL. Our data showed that thyroglobulin was not detected with high sensitivity (<0.2 ng/mL), but U-Ex Tg was detected by peptide sequencing. The trends in urinary thyroglobulin concentrations were recorded individually for each patient. Particularly, serum thyroglobulin was not detected in patients 1, 3, 4, and 7 after thyroidectomy and/or radioactive I-131 ablation; however, U-Ex

TABLE 2 | Demography of patients before and after operation.

Patient number	Gender	Age	Date of OP.	Date of radioactive I-131	I-131 Ablation Dose	FT4 Post-OP.	hsTSH Post-OP.	Tg Pre-OP.	Tg Post-OP. 6 months	Anti-Tg Ab Post-OP. 6 months	Pathology
1	F	49	20160820	20160929	30 mCi	0.981	0.212	93.6	<0.2	<3.0	PTC with minimally extra-thyroid soft tissue involvement, TNM: T3N0M0
2	F	58	20160908	NA	NA	1.13	2.12	NA	<0.2	50.4	PTC with clear surgical margin, TNM: T1aN0M0
3	F	57	20160912	20161014	30 mCi	1.24	2.96	NA	<0.2	<3.0	PTC with minimally extra-thyroid soft tissue involvement, central lymph nodes dissection TNM: T3N0M0
4	F	42	20160912	20161014	30 mCi	1.24	0.611	<0.2	<0.2	6.03	PTC TNM: T1bN1aM0
5	F	34	20161015	20161118	30 mCi	1.07	11.3	NA	<0.2	<3.0	PTC with minimally capsular invasion, TNM: T3N0M0
6	F	52	20161119	NA	NA	1.01	0.249	NA	3.8	4.47	PTC TNM: T2N0M0
7	F	43	20161208	20170120	30 mCi	<0.27	233	NA	<0.2	NA	PTC TNM: T1bN0M0
8	M	48	20161205	20170112	30 mCi	0.372	57.7	NA	<0.2	NA	Right thyroid follicular carcinoma TNM: T1bN0M0
9	M	41	20170422	20170720	150 mCi	2.23	0.059	NA	27.4	3.46	Papillary carcinoma, with minimal extrathyroid extension, TNM: T3N0M1 (lung)
10	F	59	20170410	NA	NA	1.27	0.96	NA	9.14	<3.0	Papillary microcarcinoma TNM: T1aN0M0
11	F	45	20170318	20170421	30 mCi	0.963	118	NA	<0.2	<3.0	PTC (multifoci) TNM: T3N0M0
12	F	41	20170501	20170726	125 mCi	1.32	0.998	1.34	<0.2	119.52	PTC TNM: T1bN1aM0
13	M	49	20161015	NA	NA	0.999	1.51	29.4	15.9	<3.0	PTC TNM: T3N0M0
14	F	39	20170619	20170721	30 mCi	1.25	1.9799	46.2	<0.2	<3.0	PTC TNM: T1aN1aM0
15	F	74	20170828	20170929	30 mCi	1.12	0.202	14.1	<0.2	<3.0	PTC TNM: T1aN1aM0
16	F	31	20171005	20180208	100 mCi	1.29	1.9095	57.6	0.217	<3.0	PTC TNM: T3N1bM0

T1 or T2: patients 2, 6, 7, 8, 10; T3 or lymph nodes metastasis: patients 1, 4, 5, 11, 12, 13, 14, 15, 16; T3 with distant metastasis or suspect delphian lymph nodes metastasis: patients 3, 9.

Tg showed an increasing trend. This condition may implicit the tumor burden and the recurrence of thyroid cancer in the future.

We classified U-Ex Tg level according to the thyroid cancer stage (**Figure 1**), fourteen patients (patient 3 and 9 were excluded due to distant metastasis or suspect delphian lymph node involvement) revealed that U-Ex Tg was statically significant higher in larger tumor, which point out that U-Ex Tg can implicit the tumor burden. In addition, pre-operative and

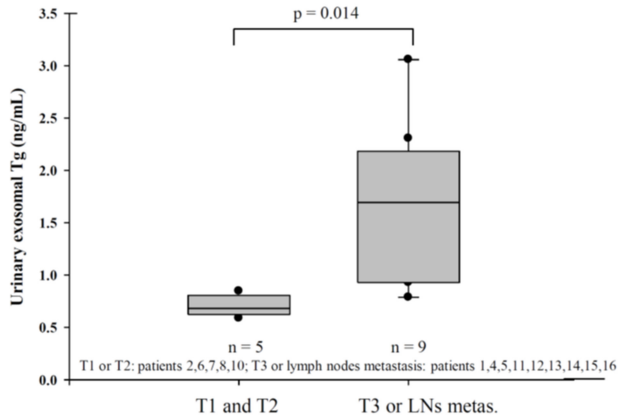

FIGURE 1 | Urinary exosomal thyroglobulin revealed statistically significant in larger tumor (T3) or lymph nodes metastasis in pathological report.

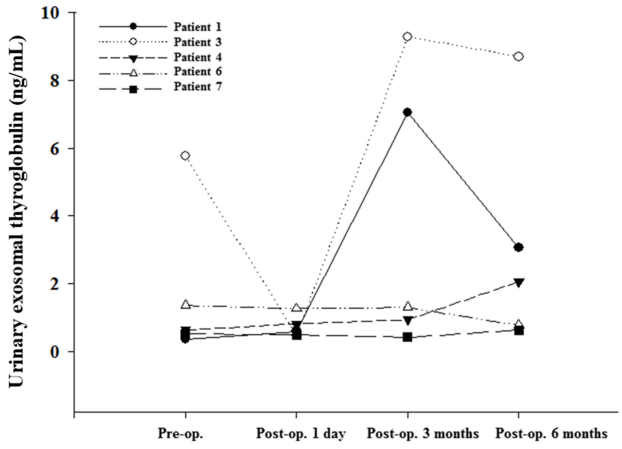

FIGURE 2 | Urinary exosomal thyroglobulin showed an increasing trend in patients of post thyroidectomy and/or I-131 ablation in comparison with serum thyroglobulin.

post-operative serial changes of U-Ex Tg in patients receiving total thyroidectomy and/or radio-active iodine ablation are revealed in **Figure 2**. The U-Ex Tg levels still showed trends of elevation in patients 1, 3, and 4, who were papillary thyroid cancer with soft tissue involvement or metastasis of level IV lymph nodes. However, serum thyroglobulin cannot be detected in such patients after ablative therapy.

We hope to emphasize the difference of U-Ex Tg between various surgical findings. The pathological findings of patients 1, 3, 4 revealed larger tumor (T3) or lymph nodes metastasis, in contrast to patients 6 and 7 with smaller tumor without lymph nodes metastasis. In addition, patient 1, 3, and 4 received ablative I-131 treatment without detectable serum thyroglobulin, but prominently elevated U-Ex Tg postoperatively. However, patient 6, who did not receive ablative I-131, was noted of detectable serum thyroglobulin, but very lower U-Ex Tg. The difference between these two groups revealed that U-Ex Tg will be an earlier and brand-new biomarker to predict the prognosis or recurrence for patients with DTC post-operatively.

DISCUSSION

Our study is the first study to evaluate whether urinary exosomal thyroglobulin (U-Ex Tg) is a reliable biological marker as a substitute for serum thyroglobulin. Such patients are not required to withdraw thyroid hormone or receive rhTSH stimulation. For patients with thyroid cancer who received thyroidectomy with or without ablative radioactive I-131 therapy, serum thyroglobulin is defined as a cancer biomarker during follow-up (4–8). If thyroglobulin cannot be detected in the serum, patients are considered to have completed treatment, independently of the interference of anti-thyroglobulin antibody (4). Typically, serum thyroglobulin cannot be detected even under costly rhTSH stimulation in patients with biochemically complete treatment. Therefore, currently no serial biomarkers are available for evaluating and predicting cancer recurrence.

Exosomes are membrane-derived extracellular vesicles with size about 40–100 nm, which are found in consistent concentrations in all body fluids, including blood, saliva and urine. In this study, U-Ex Tg was shown to be a non-invasive, reproducible, convenient, serial, and accurate follow-up marker for patients with thyroid cancer, as we used peptide sequences to quantify the levels of thyroglobulin in urine exosomes. Without the requirement for rhTSH, costs are reduced, and patients can continue the use of thyroid hormone during cancer follow-up. We also used galectin-3 for comparison to confirm the trends in thyroglobulin levels. Galectin-3 modulates cell growth via galactosidase-binding protein, which is correlated with occurrence and metastasis of papillary thyroid carcinoma (14–16). In this study, the trends in the changes of U-Ex Tg to be higher in patients with extra-thyroid invasion, metastasis of neck level IV lymph nodes, and lymph-vascular invasion. While the patients received ablation of radioactive I-131 therapy six months later, serum thyroglobulin was not detected. However, the increasing tendency of U-Ex Tg suggests that probable recurrence.

In recent years, progress in peptide mass spectrometry methods has provided a cost-effective, accurate method for identifying biomarkers. Large profiling of proteomics of human urine reveled different follow-up manners (17, 18). From the perspective of oncology, one option is to identify new biomarkers for earlier diagnosis of various cancers, while another option is to prevent follow-up residual tumor formation and cancer recurrence. The goal of our study is to identify a new pathway for tracking biomarkers in patients with thyroid cancer receiving ablative surgery and radioactive I-131 treatment. Exosomal proteins can influence cellular signaling, inflammation, immunity. In addition, inflammatory exosomal proteins contribute to various patho-physiological processes in cellular behavior (19). Compared with serum thyroglobulin, U-Ex Tg can be an important pro-inflammatory predictor and biomarker of thyroid cancer recurrence for certain patients.

For patients receiving total thyroidectomy and/or ablation with radioactive iodine, the increasing tendency of U-Ex Tg revealed that it can be used as a substitute for undetectable serum thyroglobulin in predicting the recurrence of thyroid cancer. U-Ex Tg could be an important alternative to serum thyroglobulin which advantages technology and eases requirements for patients. Our limitation is limited current patient numbers, but the study is still ongoing with a larger cohort in patients of thyroid cancer, who received thyroidectomy and/or radioactive iodine at least one year.

In our study, the most important and useful scenario in using a test that is potentially more sensitive than existing serological testing is to eliminate the suspicion of recurrence and remove subjects from long term follow up.

STRENGTHS AND LIMITATIONS OF THIS STUDY

1. The aim of the present study is to analyze the urinary exosomal proteins to identify early prognostic biological markers in the urine in this prospective study.
2. The significant and novel finding in the present study is that in comparison with serum thyroglobulin, urinary exosomal thyroglobulin (U-Ex Tg) can be an important pro-inflammatory predictor and biomarker of thyroid cancer recurrence. U-Ex Tg could be an important alternative to serum thyroglobulin which advantages technology and eases requirements for patients.
3. Current patient numbers are limited, but the study is still ongoing to collect more data from urinary exosomal proteins of patients with thyroid cancer.

DATA AVAILABILITY STATEMENT

The datasets presented in this article are not readily available because the study is still ongoing with a larger cohort in patients of thyroid cancer. Requests to access the datasets should be directed to Chih-Yuan Wang: cyw1965@gmail.com.

ETHICS STATEMENT

The studies involving human participants were reviewed and approved by Institution Review Board of National Taiwan University Hospital. The patients/participants provided their written informed consent to participate in this study. Written informed consent was obtained from the individual(s) for the publication of any potentially identifiable images or data included in this article.

AUTHOR'S NOTE

This study had accepted as a poster presentation at the 88th Annual Meeting of the American Thyroid Association, 2018; Poster ID: 409. https://www.liebertpub.com/doi/10.1089/thy.2018.29065.abstracts.

AUTHOR CONTRIBUTIONS

C-YW: conception and design and development of methodology. T-YH, C-YW, K-YC, and L-TH: acquisition of data (provided animals, acquired and managed patients, provided facilities, etc.). T-YH, C-YW, and L-TH: analysis and interpretation of data (e.g., statistical analysis, biostatistics, computational analysis). T-YH and C-YW: writing, review, and/or revision of the manuscript. C-YW and L-TH: administrative, technical, or material support (i.e., reporting or organizing data, constructing databases), Other (application to regional ethics committee), and Other (supply of reagents generated by herself). C-YW and K-YC: study supervision. All authors contributed to the article and approved the submitted version.

FUNDING

This research was funded by a grant from the Ministry of Science and Technology, Taiwan (MOST-105-2314-B-002—102 -MY2, MOST-107-2314-B-002—024 -MY3).

ACKNOWLEDGMENTS

We thank the staff of the 7th Core Lab, Department of Medical Research, National Taiwan University Hospital for technical support during the study.

SUPPLEMENTARY MATERIAL

The Supplementary Material for this article can be found online at: https://www.frontiersin.org/articles/10.3389/fendo.2020.00382/full#supplementary-material

REFERENCES

1. Wang TS, Sosa JA. Thyroid surgery for differentiated thyroid cancer - recent advances and future directions. *Nat Rev Endocrinol.* (2018) 14:670–83. doi: 10.1038/s41574-018-0080-7
2. Conzo G, Avenia N, Bellastella G, Candela G, de Bellis A, Esposito K, et al. The role of surgery in the current management of differentiated thyroid cancer. *Endocrine.* (2014) 47:380–8. doi: 10.1007/s12020-014-0251-9
3. Docimo G, Tolone S, Ruggiero R, Gubitosi A, Pasquali D, De Bellis A, et al. Total thyroidectomy without prophylactic central neck dissection combined with routine oral calcium and vitamin D supplements: is it a good option to achieve a low recurrence rate avoiding hypocalcemia? A retrospective study. *Minerva Chir.* (2013) 68:321–8.
4. Haugen BR, Alexander EK, Bible KC, Doherty GM, Mandel SJ, Nikiforov YE, et al. American Thyroid Association management guidelines for adult patients with thyroid nodules and differentiated thyroid Cancer. *Thyroid.* (2016) 26:1–133. doi: 10.1089/thy.2015.0020
5. Haugen BR. 2015 American Thyroid Association management guidelines for adult patients with thyroid nodules and differentiated thyroid Cancer: What is new and what has changed? *Cancer.* (2017) 123:372–81. doi: 10.1002/cncr.30360

6. Giovanella L, Ceriani L, Suriano S, Ghelfo A, Maffioli M. Thyroglobulin measurement before rhTSHaided 131I ablation in detecting metastases from differentiated thyroid carcinoma. *Clin Endocrinol (Oxf).* (2008) 69:659–63. doi: 10.1111/j.1365-2265.2008.03244.x
7. Rosario PW, Xavier AC, Calsolari MR. Value of postoperative thyroglobulin and ultrasonography for the indication of ablation and 131I activity in patients with thyroid cancer and low risk of recurrence. *Thyroid.* (2011) 21:49–53. doi: 10.1089/thy.2010.0145
8. Giovanella L, Clark PM, Chiovato L, Duntas L, Elisei R, Feldt-Rasmussen U, et al. Diagnosis of Endocrine disease: Thyroglobulin measurement using highly sensitive assays in patients with differentiated thyroid cancer: a clinical position paper. *Eur J Endocrinol.* (2014) 171:R33–46. doi: 10.1530/EJE-14-0148
9. Soung YH, Nguyen T, Cao H, Lee J, Chung J. Emerging roles of exosomes in cancer invasion and metastasis. *BMB Rep.* (2016) 49:18–25. doi: 10.5483/BMBRep.2016.49.1.239
10. Properzi F, Logozzi M, Fais S. Exosomes: the future of biomarkers in medicine. *Biomark Med.* (2013) 7:769–78. doi: 10.2217/bmm.13.63
11. Simpson RJ, Jensen SS, Lim WE. Proteomic profiling of exosomes: current perspectives. *Proteomics.* (2008) 8:4083–99. doi: 10.1002/pmic.200800109
12. Pisitkun T, Johnstone R, Knepper MA. Discovery of urinary biomarkers. *Mol Cell Proteomics.* (2006) 5:1760–71. doi: 10.1074/mcp.R600004-MCP200
13. Huebner AR, Somparn P, Benjachat T, Leelahavanichkul A, Avihingsanon Y, Fenton RA, et al. Exosomes in urinary biomarker discovery. *Adv Exp Med Biol.* (2015) 845:43–58. doi: 10.1007/978-94-017-9523-4_5
14. Rabinovich GA. Galectin-1 as a potential cancer target. *Br J Cancer.* (2005) 92:1188–92. doi: 10.1038/sj.bjc.6602493
15. Lin TW, Chang HT, Chen CH, Chen CH, Lin SW, Hsu TL, et al. Galectin-3 binding protein and galectin-1 interaction in breast cancer cell aggregation and metastasis. *J Am Chem Soc.* (2015) 137:9685–93. doi: 10.1021/jacs.5b04744
16. Tang WW, Huang CW, Tang CY, Xu J, Wang H. Galectin-3 may serve as a potential marker for diagnosis and prognosis in papillary thyroid carcinoma: a meta-analysis. *Onco Targets Ther.* (2016) 9:455–60. doi: 10.2147/OTT.S94514
17. Moon PG, You S, Lee JE, Hwang D, Baek MC. Urinary exosomes and proteomics. *Mass Spectrom Rev.* (2011) 30:1185–1202. doi: 10.1002/mas.20319
18. Street JM, Koritzinsky EH, Glispie DM, Star RA, Yuen PS. Urine exosomes: an emerging trove of biomarkers. *Adv Clin Chem.* (2017) 78:103–22. doi: 10.1016/bs.acc.2016.07.003
19. Desdín-Micó G, Mittelbrunn M. Role of exosomes in the protection of cellular homeostasis. *Cell Adh Migr.* (2017) 11:127–34. doi: 10.1080/19336918.2016.1251000

Disclaimer: Taiwan (No. 201915489); Taiwan Intellectual Property Office (TIPO) Invention Patent No. I 682176; BIOMARKER FOR PROGNOSIS OF THYROID CANCER; **G01N-033/574**(2006.01); **G01N-033/68**(2006.01). USA: This study has filed patent protection with the U.S. Patent and Trademark Office, Department of Commerce (EFS ID: 30401287), Application Number: (62/560,171 20170918).

Conflict of Interest: The authors declare that the research was conducted in the absence of any commercial or financial relationships that could be construed as a potential conflict of interest.

frontiers in Endocrinology

ORIGINAL RESEARCH
published: 28 August 2020
doi: 10.3389/fendo.2020.00542

A Multicenter Retrospective Study of 58 Patients With Primary Thyroid Diffuse Large B Cell Lymphoma

*Jianing Yi[1], Pingyong Yi[2], Wei Wang[3], Huan Wang[4], Xinyu Wang[5], Hanjia Luo[3] and Peizhi Fan[1]**

[1] Surgical Department of Breast and Thyroid Gland, The First Affiliated Hospital of Hunan Normal University/Hunan Provincial People's Hospital, Changsha, China, [2] Department of Oncology, Changsha Kexin Cancer Hospital, Changsha, China, [3] Department of Oncology, Affiliated Cancer Hospital of Xiangya School of Medicine, Central South University, Changsha, China, [4] Surgical Department of Breast and Thyroid Gland, Xiangya Second Hospital of Central South University, Changsha, China, [5] Surgical Department, Xiangya Hospital of Central South University, Changsha, China

Background: Primary thyroid diffuse large B cell lymphoma (DLBCL) is a rare type of extranodal lymphoma; optimal treatment methods and the key prognostic factors have not been established.

Methods: The clinical data of 58 patients with primary thyroid DLBCL from January 2007 to December 2017 were collected. The Kaplan–Meier method and log-rank tests were used for the survival analysis. Cox regression analysis was performed to evaluate the prognostic factors.

Results: The follow-up time was 6–120 months; 5-year overall survival (OS) and progression-free survival (PFS) were 73 and 61%, respectively. Single-factor analysis showed that IPI, Ki-67, treatment modalities, Hans classification, Myc/Bcl-2 protein co-expression, and administration of rituximab had a significant effect on the 5-year OS and PFS ($P < 0.05$), while age, sex, Bcl-2 protein expression, Myc protein expression, tumor stage, tumor size, Hashimoto's thyroiditis, and B symptoms were not associated with prognosis ($P > 0.05$). Multivariate risk regression analysis revealed that Myc/Bcl-2 protein co-expression, treatment modalities, and rituximab were independent prognostic factors ($P < 0.05$).

Conclusions: Patients with primary thyroid DLBCL who received combination chemotherapy with radiotherapy had a better prognosis. Surgical treatment alone was not associated with the prognosis and is used only for diagnosis. Rituximab could improve the survival time of patients.

Keywords: thyroid, lymphoma, large B-cell, prognosis, treatment

OPEN ACCESS

Edited by:
Jianfeng Liu,
Huazhong University of Science and Technology, China

Reviewed by:
Pasqualino Malandrino, University of Catania, Italy
Jason David Prescott, The Johns Hopkins Hospital, Johns Hopkins Medicine, United States

****Correspondence:***
Peizhi Fan
Fanpzh64@163.com

Specialty section:
This article was submitted to Cancer Endocrinology, a section of the journal Frontiers in Endocrinology

Received: *09 May 2020*
Accepted: *06 July 2020*
Published: *28 August 2020*

Citation:
Yi J, Yi P, Wang W, Wang H, Wang X, Luo H and Fan P (2020) A Multicenter Retrospective Study of 58 Patients With Primary Thyroid Diffuse Large B Cell Lymphoma. Front. Endocrinol. 11:542. doi: 10.3389/fendo.2020.00542

INTRODUCTION

Primary thyroid lymphoma (PTL) is an uncommon lymphoma that develops in the thyroid gland, accounting for ∼2% of all extranodal lymphomas; its morbidity is higher in elderly females with chronic Hashimoto's thyroiditis (1). Generally, the main complaint is neck swelling; some patients also show B symptoms such as night sweats, fever, and weight loss (2). Histopathologically, DLBCL is the main type of PTL; other pathological subtypes include follicular

lymphoma, mucosa-associated lymphoid tissue lymphoma, small lymphocytic lymphoma, and T-cell lymphoma (2, 3). Surgical biopsy or core needle biopsy can be performed to diagnose the disease. Previous studies on primary thyroid DLBCL were done on the basis of limited data due to the rarity of the disease, and there is no consensus on optimal treatment modalities and key prognostic factors. To address these issues, this study aimed to investigate treatment modalities and clinicopathological characteristics correlated with survival in patients with primary thyroid DLBCL, so as to find useful information about treatment option and key prognostic factors.

MATERIALS AND METHODS

Clinical Data

Clinical data were obtained from the medical records of 58 patients with primary thyroid DLBCL, who were diagnosed and treated at Hunan Provincial People's Hospital, Hunan Cancer Hospital, Changsha Kexin Cancer Hospital, Xiangya Hospital, and the Second Xiangya Hospital from January 2007 to December 2017. Age, sex, treatment modality, stage, Hashimoto's thyroiditis existence, LDH (lactate dehydrogenase), IPI (international prognostic index), tumor size, Hans classification, Ki-67 and Bcl-2 protein expression, Myc protein expression, B symptom, and overall survival status were evaluated. Core needle biopsy, surgical biopsy, and surgical excision were used for diagnosis. Patients who had systemic disease were excluded from the evaluation. Follow-up data were calculated from the time of initial surgery on the thyroid gland to the last follow-up. The clinical survey was finished through reviewing patient records, interview, and clinic visits. Ethical approval for this study was obtained from the ethical committee of The First Affiliated Hospital of Hunan Normal University/Hunan Provincial People's Hospital. Written informed consent was obtained from all of the local cohort participants.

Evaluation Standard

Primary thyroid DLBCL developed in the thyroid gland with or without the involvement of regional lymph nodes and without metastasis to other visceral tissues (1). All samples were reviewed by two pathologists for confirmation of the histological diagnosis. The clinical stages were defined in two categories through computed tomography, ultrasonography, and bone marrow aspiration biopsy: Stage IE refers to lesion localized within the thyroid, and stage IIE refers to lesion confined to the thyroid and regional lymph nodes (3). Fouty percentage was used for cutoff values of for Myc and 70% for Bcl-2 and Ki-67 (4, 5); the cutoff values of other markers assessed in this study were based on previous reports (6).

Patient Survival

The final follow-up was done on December 1, 2018. Overall survival (OS) was calculated from the time of initial surgery on the thyroid gland to death from any cause, while progression-free survival (PFS) was calculated from the date of diagnosis to the date of initial disease progression, relapse, or death.

Statistical Analysis

The Kaplan–Meier method was used for the survival analysis and univariate analysis. The Cox regression analysis was performed to evaluate the prognostic factors of patients with primary thyroid DLBCL. The chi-squared (χ^2) test was performed to compare clinical characteristics, and differences were tested using the two-tailed test. SPSS software (version 21.0, SPSS Inc., Chicago, IL, USA) was used for all statistical analyses. All p-values were 2-sided, and a $P < 0.05$ was considered statistically significant.

RESULTS

Clinical Characteristics

At the time of diagnosis, of the 58 patients with primary thyroid DLBCL, 43 were women and 15 were men; 15 patients presented bilateral involvement, 21 presented right lesions, and 22 presented left lesions; 18 patients had clinical B symptoms, and 40 had no B symptoms; 28 patients had stage IE lymphoma and 30 patients had stage IIE lymphoma; 31 patients had 0–1 IPI score, and 27 patients had 2–3 IPI score; 24 patients had elevated LDH; and 22 patients had a history of Hashimoto's thyroiditis. The median age of the patients was 65 years (range, 28–78 years), and the average size of the primary thyroid DLBCL was 3.8 cm (range, 1.5–7.6 cm). A total of 30 patients presented involvement of adjacent organs, including 18 patients with neck lymph-node invasion and 12 patients with mediastinal lymph-node invasion.

Pathological Characteristics

Histopathological diagnosis was carried out on the pathological tissue sections of the patients after hematoxylin–eosin (HE) staining and immunohistochemistry, revealing a total of 58 patients with primary thyroid DLBCL. B cells were labeled with antibodies to CD20 and CD79a in all patients, BCL-2 expression in 26 patients, BCL-6 expression in 37 patients, CD10 expression in 21 patients, MYC expression in 28 patients, Myc/Bcl-2 protein co-expression in 17 patients, multiple myeloma oncogene 1 (MUM1) expression in 32 patients, and PAX5 expression in 48 patients. A proliferation index of Ki-67 $\leq$70% was found in 36 patients, and Ki-67 $>$70% in 22 patients. 21 patients had germinal center B-cell-like (GCB) DLBCL, and 37 had non-GCB DLBCL.

Treatment and Follow-Up

Overall, 15 patients received only surgical excision (four lobectomy, eight partial lobectomy, three thyroidectomy), 31 underwent surgical biopsy, 12 underwent core needle biopsy, 18 received simple chemotherapy (CT), and 25 received chemotherapy combined with radiotherapy (RT). The radiotherapy dose ranged from 30 to 40 Gy with a median value of 36 Gy. While 26 patients were treated with rituximab, 32 did not receive the treatment. Regarding chemotherapy regimens, 17 patients received cyclophosphamide, doxorubicin, vincristine, and prednisone (CHOP) chemotherapy, whereas 26 received rituximab plus cyclophosphamide, doxorubicin, vincristine, and prednisone (R+CHOP) chemotherapy. The follow-up time was 6–120 months, with a median value of 60 months. All 58 patients had a follow-up rate of 100%. In the 58 patients with primary thyroid DLBCL, the 5-year

OS and 5-year PFS were 73% (95% confidence interval (CI), 68–96%, and 61% (95% CI, 45–69%), respectively. Forty-eight patients did not show disease recurrence, whereas 10 did. Among the 10 patients with relapse, two had ipsilateral thyroid involvement, two had lung involvement, one had neck lymph-node involvement, two had brain involvement, two had bone involvement, and one had liver involvement. All the patients who experienced relapse received chemotherapy, including GEMOX (gemcitabine and oxaliplatin), MINE (mesna, ifosfamide, mitoxantrone, etoposide), and ESHAP (etoposide, methylprednisolone, cisplatin and cytarabine). Additionally, two patients also received radiotherapy, and one patient received intrathecal chemotherapy for intracranial involvement, whereas five died of progressive disease.

Correlation Analysis of Clinical Characteristics and Treatment Methods With 5-Year PFS and OS Rates

Univariate analysis was performed for patients' age, sex, tumor size, stage, treatment modalities, B symptoms, serum LDH level, IPI score, administration of rituximab, BCL-2 protein expression level, MYC protein expression level, Myc/Bcl-2 protein co-expression, Hans classification, Ki-67, and presence of Hashimoto's thyroiditis, as listed in **Table 1**. The results showed that IPI score, treatment modalities, Hans classification, administration of rituximab, and Ki-67 and Myc/Bcl-2 protein co-expression were significantly associated with prognosis ($P < 0.05$), while patient age, sex, tumor size, B symptoms, Hashimoto's thyroiditis existence, BCL-2 expression level, MYC expression level, serum LDH level, and tumor stage were not significantly associated with prognosis ($P > 0.05$; **Table 1**).

For treatment modalities, first, stratification based on baseline demographic, and clinicopathological characteristics was performed for the patients treated with different treatment modalities; the results showed that the demographic and clinicopathological characteristics were generally well-balanced among different treatment groups at baseline (**Table 2**). Then, survival analysis revealed that the 5-year OS and PFS were 81.2 and 77.8%, respectively, for patients with CT plus RT, 60.9 and 53.9% for patients with CT alone, and 35.3 and 31.6% for patients that underwent surgical excision ($P < 0.05$; **Figures 1A**, **2A**), thus indicating that the patients that received CT with RT had better survival than CT or surgical excision alone and that surgical excision alone did not have any advantage over CT or CT plus RT.

For patients who received rituximab, the 5-year OS and PFS were 78.6 and 68.3%, while for those that did not receive rituximab, the values were 50.2 and 47.5%, respectively ($P < 0.01$; **Figures 1B**, **2B**), thus suggesting that rituximab could improve the survival rate of patients with primary thyroid DLBCL.

In patients with primary thyroid DLBCL with a positive Myc who received immunohistochemistry, the 5-year OS was 73.9% and 5-year PFS was 58.2%. In patients with primary thyroid DLBCL with a negative Myc treated by immunohistochemistry, the 5-year OS was 76.4% and the 5-year PFS was 63.4% ($P > 0.05$; **Table 1**). In patients with primary thyroid DLBCL with

TABLE 1 | Univariate analysis affecting OS and PFS of patients with primary thyroid DLBCL.

Clinicopathological parameters	*n*	5-year OS (%)	χ^2	*P*	5-year PFS (%)	χ^2	*P*
Age, years			0.58	>0.05		1.37	>0.05
≤60	20	78.3			64.2		
>60	38	73.8			59.5		
Sex			0.93	>0.05		1.23	>0.05
Male	15	79.1			63.5		
Female	43	71.8			58.8		
Stage			1.08	>0.05		1.32	>0.05
I E	28	78.6			65		
II E	30	73.2			57.8		
IPI score			9.16	<0.05		7.32	<0.05
0–1	31	80.6			68.9		
2–3	27	51.1			47.3		
Treatments			8.97	<0.05		9.06	<0.05
Surgical excision	15	35.3			31.6		
CT	18	60.9			53.9		
CT+RT	25	81.2			77.8		
Rituximab			10.6	<0.01		9.56	<0.01
Yes	26	78.6			68.3		
No	32	50.2			47.5		
Hans classification			12.7	<0.01		11.2	<0.01
GCB	21	79.2			69.4		
Non-GCB	37	50.7			48.7		
Ki-67			11.7	<0.01		9.48	<0.01
>70%	22	57.3			46.4		
≤70%	36	78.7			65.3		
Bcl-2			1.62	>0.05		1.31	>0.05
Positive	26	71.2			57.1		
Negative	32	79.1			64.6		
Myc			1.65	>0.05		1.52	>0.05
Positive	28	73.9			58.2		
Negative	30	76.4			63.4		
Myc/Bcl-2 protein co-expression			14.2	<0.01		12.3	<0.01
Yes	17	48.9			47.3		
No	41	82.3			68.4		
LDH level			1.37	>0.05		1.33	>0.05
Normal	34	77.8			63.9		
Elevated	24	74.1			59.4		
B symptom			1.51	>0.05		1.61	>0.05
Yes	18	70.9			60.6		
No	40	78.3			63.5		
Hashimoto's thyroiditis			1.22	>0.05		1.28	>0.05
Yes	22	76.9			57.9		
No	36	72.3			64.1		
Tumor size (cm)			1.68	>0.05		1.57	>0.05
≤5	30	79.4			65.7		
>5	28	70.8			56.4		0

n, case number; LDH, lactate dehydrogenase; IPI, international prognostic index; CT, chemotherapy; RT, radiotherapy.

TABLE 2 | The baseline characteristics of the patients treated with different treatment modalities.

	Treatment modalities					
	Surgical excision (*n* = 15)		CT (*n* = 18)		CT+RT (*n* = 25)	
Characteristics	***n***	**%**	***n***	**%**	***n***	**%**
Age, years						
≤60	5	33.3	7	38.9	8	32.0
>60	10	66.7	11	61.1	17	68.0
Sex						
Male	4	26.7	5	27.8	6	24.0
Female	11	73.3	13	73.2	19	76.0
Stage						
I E	7	46.7	9	50.0	12	48.0
II E	8	53.3	9	50.0	13	52.0
IPI score						
0–1	8	53.3	9	50.0	14	56.0
2–3	7	46.7	9	50.0	11	44.0
Hans classification						
GCB	5	33.3	7	38.9	9	36.0
Non-GCB	10	66.7	11	61.1	16	64.0
Ki-67						
>70%	6	40.0	7	38.9	9	36.0
≤70%	9	60.0	11	61.1	16	64.0
Bcl-2						
Positive	7	46.7	8	44.4	11	44.0
Negative	8	53.3	10	55.6	14	56.0
Myc						
Positive	7	46.7	9	50.0	12	48.0
Negative	8	53.3	9	50.0	13	52.0
Myc/Bcl-2 protein co-expression						
Yes	5	33.3	5	27.8	7	28.0
No	10	66.7	13	72.2	18	72.0
LDH level						
Normal	9	60.0	10	55.6	15	60.0
Elevated	6	40.0	8	44.4	10	40.0
B symptom						
Yes	5	33.3	5	27.8	8	32.0
No	10	66.7	13	72.2	17	68.0
Hashimoto's thyroiditis						
Yes	6	40.0	7	38.9	9	36.0
No	9	60.0	11	61.1	16	64.0
Tumor size (cm)						
≤5	8	53.3	9	50.0	13	52.0
>5	7	46.7	9	50.0	12	48.0

n, case number; LDH, lactate dehydrogenase; IPI, international prognostic index; CT, chemotherapy; RT, radiotherapy.

a positive Bcl-2 who underwent immunohistochemistry, the 5-year OS was 71.2% and 5-year PFS was 57.1%. In patients with primary thyroid DLBCL with a negative Bcl-2 who received immunohistochemistry, the 5-year OS was 79.2% and 5-year PFS was 64.6% ($P > 0.05$; **Table 1**). The 5-year OS and PFS in Myc/Bcl-2 protein co-expression patients were 48.9 and 47.3%, respectively, while those in patients without Myc/Bcl-2 protein co-expression were 82.3 and 68.4% respectively ($P < 0.05$; **Figures 1C**, **2C**). These findings indicate that Bcl-2 protein expression or Myc protein expression alone has no significant effect on survival, but Myc/Bcl-2 protein co-expression is negatively associated with prognosis, i.e., the patients with Myc/BCL-2 protein co-expression had a worse prognosis.

For Hans classification, the 5-year OS and 5-year PFS were 79.2 and 69.4% for the patients with GCB DLBCL and those of the patients with non-GCB DLBCL were 50.7 and 48.7%, respectively ($P < 0.05$; **Figures 1D**, **2D**), indicating that non-GCB subtype was significantly associated with poor prognosis.

For patients with an IPI score of 0–1, the 5-year OS was 80.6% and the 5-year PFS was 68.9%, while for patients with an IPI score of 2–3, the 5-year OS and the 5-year PFS were 51.1 and 47.3%, respectively ($P < 0.05$). Thus, the higher the IPI score, the worse the prognosis (**Figures 1E**, **2E**).

The 5-year OS of patients with a proliferation index of Ki-67 ≤70% was 78.7%, and the 5-year PFS was 65.3%; the 5-year OS of patients with a proliferation index of Ki-67 >70% was 57.3%, and the 5-year PFS was 46.4% ($P < 0.05$), indicating that patients with a proliferation index of Ki-67 >70% had a worse prognosis (**Figures 1F**, **2F**).

Furthermore, multivariate risk regression analysis using the Cox model revealed that Myc/Bcl-2 protein co-expression, treatment modalities, and rituximab were independent prognostic factors for patients with primary thyroid DLBCL ($P < 0.001$; **Table 3**).

DISCUSSION

PTL is a rare neoplasm of the thyroid gland, with the most common type of PTL being DLBCL. This was a larger study that evaluated the association of clinicopathological characteristics and treatments with a survival rate in patients with primary thyroid DLBCL. With 58 cases in the final analysis, some important findings were revealed for the first time in our study.

Optimal treatment methods for primary thyroid DLBCL have not been established (2, 3). The role of surgery in PTL has changed (7, 8); although it is usually used as diagnostic biopsies now, some patients with PTL were reported to have undergone surgical excision because of various reasons (3) In our study, 15 patients underwent surgical excision; however, even with lesion resection, these patients had no significant prognostic advantage. A study from the Mayo Clinic showed that surgical excision did not have any advantage over the simply performed surgical biopsy for diagnosis. Patients who underwent surgical biopsy and chemotherapy had better prognosis than those with surgical excision followed by adjuvant chemotherapy (9). Therefore, chemotherapy and RT have replaced surgery as the main treatment measure (8). Mian et al. (10) reported that patients who underwent chemotherapy followed by radiotherapy had a longer PFS than those who received single therapy. Doria et al. (11) reported that the recurrence rate was 7.7% with combined therapy of radiotherapy and chemotherapy for thyroid

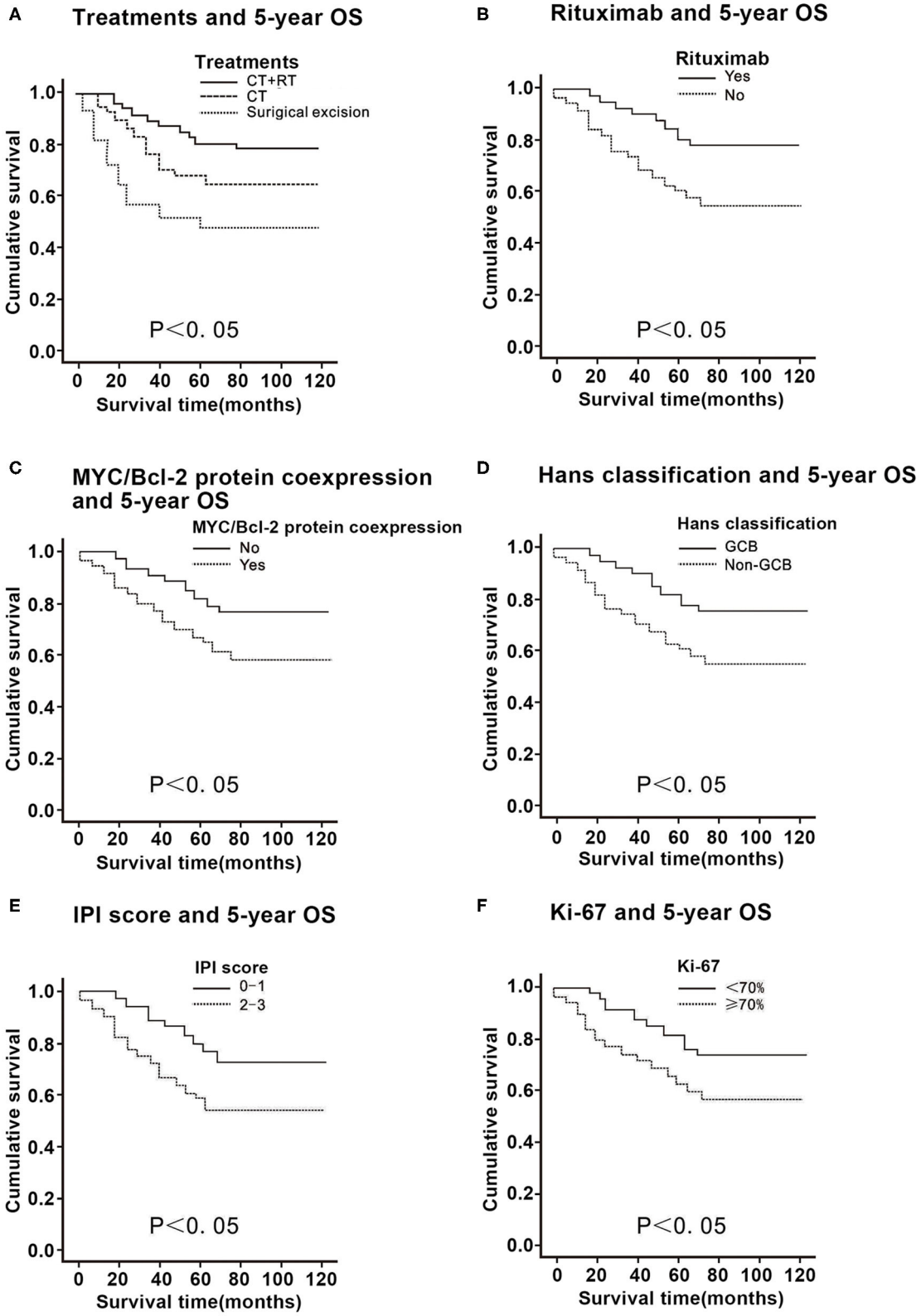

FIGURE 1 | Correlation of the 5-year overall survival (OS) with the clinicopathological features in 58 patients with primary thyroid diffuse large B cell lymphoma. **(A)** Comparison of the 5-year OS in patients with primary thyroid DLBCL according to treatments. **(B)** Comparison of the 5-year OS in patients with primary thyroid DLBCL according to rituximab. **(C)** Comparison of the 5-year OS in patients with primary thyroid DLBCL according to Myc/Bcl-2 protein co-expression. **(D)** Comparison of the 5-year OS in patients with primary thyroid DLBCL according to Hans classification. **(E)** Comparison of the 5-year OS in patients with primary thyroid DLBCL according to the international prognostic index (IPI) score. **(F)** Comparison of the 5-year OS in patients with primary thyroid DLBCL according to Ki-67 expression.

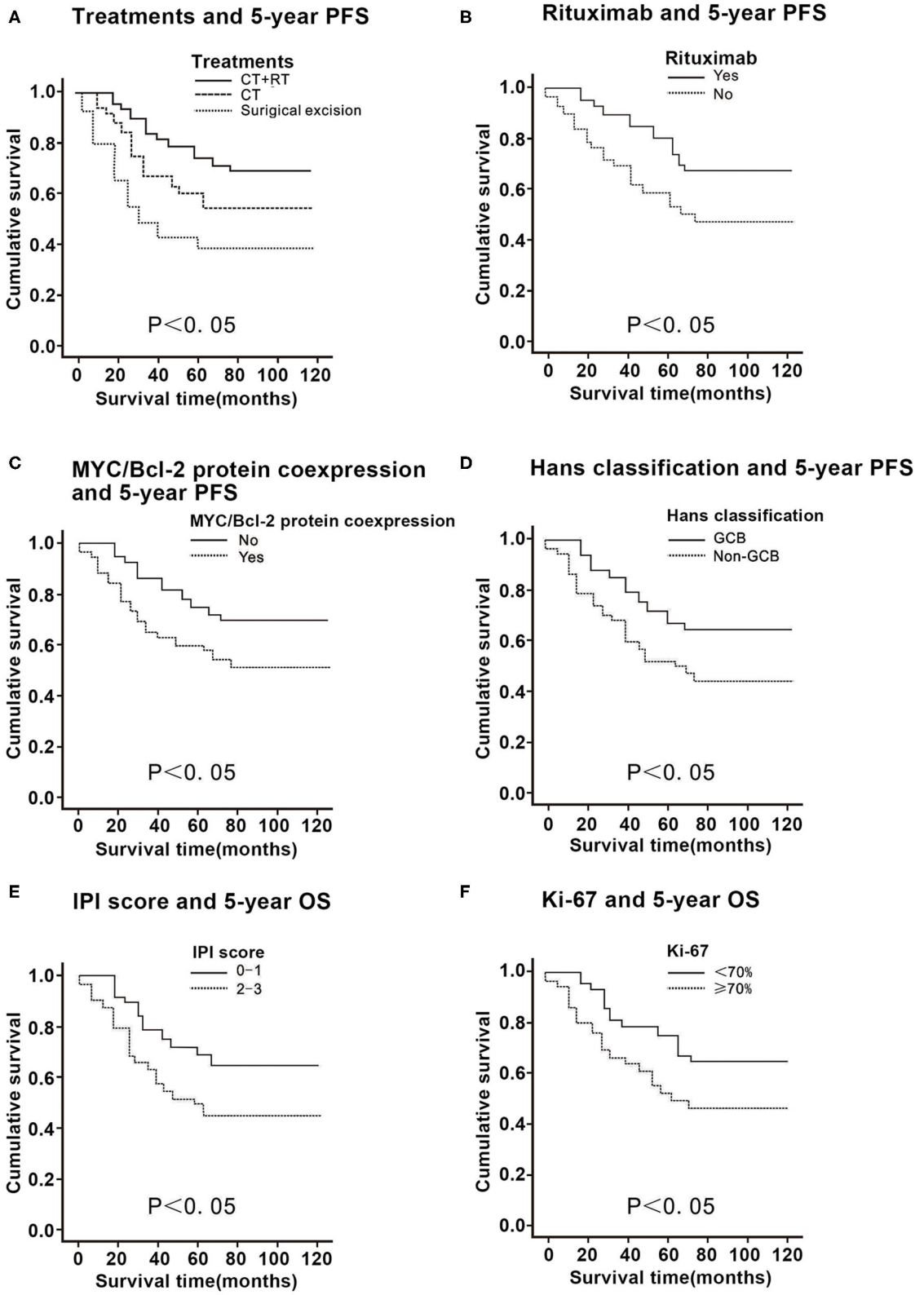

FIGURE 2 | Correlation of the 5-year progression-free survival (PFS) with the clinicopathological features in 58 patients with primary thyroid diffuse large B cell lymphoma. **(A)** Comparison of the 5-year PFS in patients with primary thyroid DLBCL according to treatments. **(B)** Comparison of the 5-year PFS in patients with primary thyroid DLBCL according to rituximab. **(C)** Comparison of the 5-year PFS in patients with primary thyroid DLBCL according to Myc/Bcl-2 protein

(Continued)

FIGURE 2 | co-expression. **(D)** Comparison of the 5-year PFS in patients with primary thyroid DLBCL according to Hans classification. **(E)** Comparison of the 5-year PFS in patients with primary thyroid DLBCL according to the international prognostic index (IPI) score. **(F)** Comparison of the 5-year PFS in patients with primary thyroid DLBCL according to Ki-67 expression.

primary DLBCL, 37.1% with radiotherapy alone, and 43% with chemotherapy alone. Matsuzuka et al. (12) reported the outcome of chemotherapy plus RT in patients with aggressive PTL, in which the survival rate at 8 years was 100%. Onal et al. (13) described the treatment effect of 60 patients with aggressive PTL; among those cases, there was a remarkable improvement in survival rate and local control with chemotherapy plus RT over RT or chemotherapy alone. The findings from our study also demonstrated that patients with primary thyroid DLBCL receiving CT plus RT had better prognosis, supporting the role for combined therapy of chemotherapy plus radiotherapy in those with aggressive histologic subtypes. Targeted CD20 therapy is widely being used for DLBCL with CD20 positive. CD20 is positive in primary thyroid DLBCL, and in the present study, CD20 is positive in all 58 cases with primary thyroid DLBCL; therefore, immunochemotherapy including rituximab might be a good treatment. In this study, chemotherapy combined with rituximab confers additional benefits to the patients with primary thyroid DLBCL. Consistent with our result, Vardell et al. (14) reported that CHOP plus rituximab showed better results for the management of primary thyroid DLBCL. Dralle et al. (15) suggested that rituximab could improve survival of patients with primary thyroid DLBCL. Watanabe et al. (16) showed that the inclusion of rituximab to combination therapy was effective for elderly patients with primary thyroid DLBCL. These findings suggested that chemotherapy including rituximab in combination with supplementary radiotherapy may be optimal treatment modality for patients with primary thyroid DLBCL.

Furthermore, this study also investigated the association between pathological features and prognosis in patients with primary thyroid DLBCL. Alterations in Myc gene and Bcl-2 gene, which are main regulators of cellular apoptosis and proliferation, may be related to the pathogenesis of DLBCL (17, 18). Some DLBCL also co-express high levels of Bcl-2 protein and Myc protein, which may be a key factor of pathogenesis in this disease. In DLBCLs, Myc overexpression, Bcl-2 overexpression, and Myc/Bcl-2 protein co-expression were detected by IHC staining in 29–47% and 50% and 20–35% of the cells, respectively, (19, 20). This study showed 44.8% were positive for Bcl-2, 48.3% were positive for Myc, and 29.3% were double positive for Myc and Bcl-2 protein expression. Whether Myc or Bcl-2 expression in IHC singly predicts survival outcome is controversial, with some studies showing an inferior outcome (19, 20) and others showing no association with outcome (21). However, Myc/Bcl-2 protein co-expression, the so-called double-expresser phenotype, is considered a useful prognostic tool for predicting survival outcome (19, 20). Despite that several studies showed an association of IHC-determined Myc and Bcl-2 expression with inferior outcomes in nodal DLBCL (20), there have been very few reports of Myc/Bcl-2 co-expression in primary thyroid DLBCL. Consistent with results from prior studies, this study showed that Bcl-2 or Myc protein expression alone had no significant effect on survival, while patients with primary thyroid DLBCL with Myc/Bcl-2 protein co-expression had poor clinical outcomes, with <30% rate of 5-year OS and PFS.

TABLE 3 | Multivariate analysis and regression analysis of COX model affecting the prognosis of patients with primary thyroid DLBCL.

Clinicopathological parameters	β	SE	OR	χ2	P	95% CI
CT+RT	2.19	0.58	1.85	12.01	0.001*	0.261∼0.662
IPI	−1.04	0.85	0.37	1.59	0.312	0.174∼2.791
Hans classification	0.46	0.56	0.45	1.47	0.347	0.374∼1.034
Rituximab	−1.07	0.36	1.37	9.06	0.001*	0.17∼0.79
Myc/Bcl-2 protein co-expression	2.21	0.59	1.65	11.08	0.005*	2.71∼3.46
Ki-67	0.39	0.67	0.19	0.29	0.762	0.348∼3.745

$P < 0.05$ was statistically significant. SE, standard error; OR, odds ratio; CI, confidence interval; CT, chemotherapy; RT, radiotherapy.

The positive cell rate of Ki-67 expression is referred to as the proliferation activity of cells. The prognostic value of Ki-67 expression in patients with DLBCL remains controversial. Some studies found a significantly negative relationship of prognosis with high Ki-67 expression (22); other studies showed no effect on prognosis (22). In this study, for patients with high Ki-67 expression (>70%), the 5-year OS and PFS were much lower than those in patients with low Ki-67 expression (≤70%). Thus, we inferred that Ki-67 expression status had a prognostic value to survival. Patients with high Ki-67 expression also seem to have a shorter survival. Probable explanations for the inter-report variations are differences in study populations and cutoff value of Ki-67 (22, 23).

Recent studies have shown that patients with DLBCL may be divided into two types by the Hans classification, such as GCB type and non-GCB type; previous studies showed that the majority of patients with primary extra-nodal DLBCL are of the non-GCB (24). Furthermore, the GCB type is correlated with a better prognosis than the non-GCB type (25). Consistent with prior studies, in the present study, 63.8% patients with primary thyroid DLBCL were of non-GCB type, accounting for a majority of these cases. 5-year OS and PFS in patients with GCB type were significantly higher than were patients with the non-GCB type.

IPI has been reported to stratify patients with aggressive lymphoma into distinct groups; IPI remains one of the main indices for assessing prognosis in DLBCL, even in the current era of immunochemotherapy including rituximab (26). This study also confirmed this finding; the results showed an association of high IPI scores with poor prognosis in primary thyroid DLBCL.

In our study, 26.5% of patients presented with B symptoms, 41.4% of patients had high serum levels of LDH, 51.7% of patients had stage IE lymphoma, and there were 43.8% of patients with tumor size >5 cm. Previous studies had shown that B symptoms, high serum LDH levels, bulky tumor, and advanced stage were positively correlated with poor prognosis in nodal DLBCL (3, 27, 28). However, in our study, B symptoms, serum levels of LDH, tumor size, and clinical stage were not associated with prognosis. We infer that primary thyroid DLBCL was different from nodal DLBCL in biological activity.

Hashimoto's thyroiditis is an established risk factor for PTL often accompanying PTL and a potential precursor that confers a 67- to 80-fold increase in risk (2, 29). In our study, 39% of the patients showed features of Hashimoto's thyroiditis; however, its presence was not significantly associated with 5-year OS and PFS.

In summary, this study suggested that surgery did not improve the prognosis of patients with primary thyroid DLBCL; chemotherapy including rituximab in combination with supplementary radiotherapy may be an optimal treatment modality for patients with primary thyroid DLBCL. Myc/Bcl-2 protein co-expression, rituximab, and treatment modalities were found to be independent factors of prognosis in patients with primary thyroid DLBCL. Due to the rarity of this disease, some multicenter, and prospective trials are required to guide the clinical treatment of primary thyroid DLBCL in future.

SIGNIFICANCE

This study revealed that patients with primary thyroid diffuse large B cell lymphoma who received combination immunochemotherapy with radiotherapy had a better prognosis and Myc/Bcl-2 protein co-expression, treatment modalities, and rituximab were independent prognostic factors.

DATA AVAILABILITY STATEMENT

The original contributions presented in the study are included in the article/supplementary material, further inquiries can be directed to the corresponding author/s.

ETHICS STATEMENT

Written informed consent was obtained from the individual(s) for the publication of any potentially identifiable images or data included in this article.

AUTHOR CONTRIBUTIONS

JY, PF, and PY designed this study. JY, PY, HL, and XW performed the search and collected the data. PF, WW, HW, and PY rechecked the data. JY, PF, and PY performed the analysis and wrote the manuscript. All authors approved the final version of the manuscript.

FUNDING

This work was supported by the Key Project of Hunan Provincial Health Commission (Grant No. A2017003); the Hunan Natural Science Foundation (Grant No. 2017JJ3171); and the Hunan Province Clinical Medical Technology Innovation Guide Program (Grant No. 2018SK50720).

REFERENCES

1. Ansell SM, Grant CS, Habermann TM. Primary thyroid lymphoma. *Semin Oncol.* (1999) 26:316–23.
2. Chai YJ, Hong JH, Koo DH, Yu HW, Lee JH, Kwon H, et al. Clinicopathological characteristics and treatment outcomes of 38 cases of primary thyroid lymphoma: a multicenter study. *Ann Surg Treat Res.* (2015) 89:295–9. doi: 10.4174/astr.2015.89.6.295
3. Graff-Baker A, Roman SA, Thomas DC, Udelsman R, Sosa JA. Prognosis of primary thyroid lymphoma: demographic, clinical, and pathologic predictors of survival in 1,408 cases. *Surgery.* (2009) 146:1105–15. doi: 10.1016/j.surg.2009.09.020
4. Green TM, Young KH, Visco C, Xu-Monette ZY, Orazi A, Go RS, et al. Immunohistochemical double-hit score is a strong predictor of outcome in patients with diffuse large B-cell lymphoma treated with rituximab plus cyclophosphamide, doxorubicin, vincristine, and prednisone. *J Clin Oncol.* (2012) 30:3460–7. doi: 10.1200/JCO.2011.41.4342
5. Li ZM, Huang JJ, Xia Y, Zhu YJ, Zhao W, Wei WX, et al. High Ki-67 expression in diffuse large B-cell lymphoma patients with non-germinal center subtype indicates limited survival benefit from R-CHOP therapy. *Eur J Haematol.* (2012) 88:510–7. doi: 10.1111/j.1600-0609.2012.01778.x
6. Visco C, Li Y, Xu-Monette ZY, Miranda RN, Green TM, Li Y, et al. Comprehensive gene expression profiling and immunohistochemical studies support application of immunophenotypic algorithm for molecular subtype classification in diffuse large B-cell lymphoma: a report from the international DLBCL rituximab-CHOP consortium program study. *Leukemia.* (2012) 26:2103–13. doi: 10.1038/leu.2012.83
7. Sakorafas GH, Kokkoris P, Farley DR. Primary thyroid lymphoma (correction of lympoma): diagnostic and therapeutic dilemmas. *Surg Oncol.* (2010) 19:e124–9. doi: 10.1016/j.suronc.2010.06.002
8. Udelsman R, Chen H. The current management of thyroid cancer. *Adv Surg.* (1999) 33:1–27.
9. Pyke CM, Grant CS, Habermann TM, Kurtin PJ, van Heerden JA, Bergstralh EJ, et al. Non-hodgkin's lymphoma of the thyroid: is more than biopsy necessary? *World J. Surg.* (1992) 16:604–9; discussion 609–10. doi: 10.1007/BF02067333
10. Mian M, Gaidano G, Conconi A, Tsang R, Gospodarowicz MK, Rambaldi A, et al. High response rate and improvement of long-term survival with combined treatment modalities in patients with poor-risk primary thyroid diffuse large B-cell lymphoma: an international extranodal lymphoma study group and intergruppo italiano linfomi study. *Leuk Lymphoma.* (2011) 52:823–32. doi: 10.3109/10428194.2011.555888
11. Doria R, Jekel JF, Cooper DL. Thyroid lymphoma. The case for combined modality therapy. *Cancer Am Cancer Soc.* (1994) 73:200–6.
12. Matsuzuka F, Miyauchi A, Katayama S, Narabayashi I, Ikeda H, Kuma K, et al. Clinical aspects of primary thyroid lymphoma: diagnosis and treatment based on our experience of 119 cases. *Thyroid.* (1993) 3:93–9. doi: 10.1089/thy.1993.3.93
13. Onal C, Li YX, Miller RC, Poortmans P, Constantinou N, Weber DC, et al. Treatment results and prognostic factors in primary thyroid lymphoma patients: a rare cancer network study. *Ann Oncol.* (2011) 22:156–64. doi: 10.1093/annonc/mdq310

14. Vardell NV, Ermann DA, Griffin EK, Silberstein PT. Primary thyroid lymphoma: an analysis of the national cancer database. *Cureus*. (2019) 11:e4088. doi: 10.7759/cureus.4088
15. Dralle H, Musholt TJ, Schabram J, Steinmuller T, Frilling A, Simon D, et al. German association of endocrine surgeons practice guideline for the surgical management of malignant thyroid tumors. *Langenbecks Arch Surg*. (2013) 398:347–75. doi: 10.1007/s00423-013-1057-6
16. Watanabe N, Narimatsu H, Noh JY, Kunii Y, Mukasa K, Matsumoto M, et al. Rituximab-including combined modality treatment for primary thyroid lymphoma: an effective regimen for elderly patients. *Thyroid*. (2014) 24:994–9. doi: 10.1089/thy.2013.0523
17. Lenz G, Staudt LM. Aggressive lymphomas. *N Engl J Med*. (2010) 362:1417–29. doi: 10.1056/NEJMra0807082
18. Adams JM, Harris AW, Pinkert CA, Corcoran LM, Alexander WS, Cory S, et al. The c-myc oncogene driven by immunoglobulin enhancers induces lymphoid malignancy in transgenic mice. *Nature*. (1985) 318:533–8. doi: 10.1038/318533a0
19. Horn H, Ziepert M, Becher C, Barth TF, Bernd HW, Feller AC, et al. MYC status in concert with BCL2 and BCL6 expression predicts outcome in diffuse large B-cell lymphoma. *Blood*. (2013) 121:2253–63. doi: 10.1182/blood-2012-06-435842
20. Hu S, Xu-Monette ZY, Tzankov A, Green T, Wu L, Balasubramanyam A, et al. MYC/BCL2 protein coexpression contributes to the inferior survival of activated B-cell subtype of diffuse large B-cell lymphoma and demonstrates high-risk gene expression signatures: a report from the international DLBCL rituximab-CHOP consortium program. *Blood*. (2013) 121:4021–31; quiz 4250. doi: 10.1182/blood-2012-10-460063
21. Swerdlow SH, Campo E, Harris NL, Jaffe ES, Pileri SA, Stein H, et al. *Classification of Tumours of Haematopoietic and Lymphoid Tissues, 4th Ed*. (2017). Lyon: International Agency for Research on Cancer.
22. Yoon DH, Choi DR, Ahn HJ, Kim S, Lee DH, Kim SW, et al. Ki-67 expression as a prognostic factor in diffuse large B-cell lymphoma patients treated with rituximab plus CHOP. *Eur J Haematol*. (2010) 85:149–57. doi: 10.1111/j.1600-0609.2010.01467.x
23. Llanos M, Alvarez-Arguelles H, Aleman R, Oramas J, Diaz-Flores L, Batista N. Prognostic significance of Ki-67 nuclear proliferative antigen, bcl-2 protein, and p53 expression in follicular and diffuse large B-cell lymphoma. *Med Oncol*. (2001) 18:15–22. doi: 10.1385/MO:18:1:15
24. Hosein PJ, Maragulia JC, Salzberg MP, Press OW, Habermann TM, Vose JM, et al. A multicentre study of primary breast diffuse large B-cell lymphoma in the rituximab era. *Br J Haematol*. (2014) 165:358–63. doi: 10.1111/bjh.12753
25. Nyman H, Adde M, Karjalainen-Lindsberg ML, Taskinen M, Berglund M, Amini RM, et al. Prognostic impact of immunohistochemically defined germinal center phenotype in diffuse large B-cell lymphoma patients treated with immunochemotherapy. *Blood*. (2007) 109:4930–5. doi: 10.1182/blood-2006-09-047068
26. Zhou Z, Sehn LH, Rademaker AW, Gordon LI, Lacasce AS, Crosby-Thompson A, et al. An enhanced international prognostic index (NCCN-IPI) for patients with diffuse large B-cell lymphoma treated in the rituximab era. *Blood*. (2014) 123:837–42. doi: 10.1182/blood-2013-09-524108
27. Evens AM, Rosen ST, Helenowski I, Kline J, Larsen A, Colvin J, et al. A phase I/II trial of bortezomib combined concurrently with gemcitabine for relapsed or refractory DLBCL and peripheral T-cell lymphomas. *Br J Haematol*. (2013) 163:55–61. doi: 10.1111/bjh.12488
28. Shipp M. Prognostic factors in non-hodgkin's lymphoma. *Curr Opin Oncol*. (1992) 4:856–62. doi: 10.1097/00001622-199210000-00007
29. Pasieka JL. Hashimoto's disease and thyroid lymphoma: role of the surgeon. *World J Surg*. (2000) 24:966–70. doi: 10.1007/s002680010159

Conflict of Interest: The authors declare that the research was conducted in the absence of any commercial or financial relationships that could be construed as a potential conflict of interest.

frontiers in Endocrinology

ORIGINAL RESEARCH
published: 18 September 2020
doi: 10.3389/fendo.2020.554733

β-arrestin 2 Is a Prognostic Factor for Survival of Ovarian Cancer Patients Upregulating Cell Proliferation

Bastian Czogalla[1†], Alexandra Partenheimer[1†], Udo Jeschke[1,2], Viktoria von Schönfeldt[1], Doris Mayr[3], Sven Mahner[1], Alexander Burges[1], Manuela Simoni[4,5,6,7], Beatrice Melli[4], Riccardo Benevelli[4], Sara Bertini[4], Livio Casarini[4,5‡] and Fabian Trillsch[1‡]*

[1] Department of Obstetrics and Gynecology, University Hospital, LMU Munich, Munich, Germany, [2] Department of Obstetrics and Gynecology, University Hospital Augsburg, Augsburg, Germany, [3] Institute of Pathology, Faculty of Medicine, LMU Munich, Munich, Germany, [4] Unit of Endocrinology, Department of Biomedical, Metabolic and Neural Sciences, University of Modena and Reggio Emilia, Modena, Italy, [5] Center for Genomic Research, University of Modena and Reggio Emilia, Modena, Italy, [6] Unit of Endocrinology, Department of Medical Specialties, Azienda Ospedaliero-Universitaria, Modena, Italy, [7] PRC, INRA, CNRS, IFCE, Université de Tours, Nouzilly, France

OPEN ACCESS

Edited by:
Jianfeng Liu,
Huazhong University of Science and Technology, China

Reviewed by:
Prathibha Ranganathan,
Centre for Human Genetics (CHG), India
Francesca Lovat,
The Ohio State University, United States

***Correspondence:**
Bastian Czogalla
bastian.czogalla@med.uni-muenchen.de

[†]These authors share first authorship

[‡]These authors share senior authorship

Specialty section:
This article was submitted to Cancer Endocrinology, a section of the journal Frontiers in Endocrinology

Received: *22 April 2020*
Accepted: *12 August 2020*
Published: *18 September 2020*

Citation:
Czogalla B, Partenheimer A, Jeschke U, von Schönfeldt V, Mayr D, Mahner S, Burges A, Simoni M, Melli B, Benevelli R, Bertini S, Casarini L and Trillsch F (2020) β-arrestin 2 Is a Prognostic Factor for Survival of Ovarian Cancer Patients Upregulating Cell Proliferation. Front. Endocrinol. 11:554733. doi: 10.3389/fendo.2020.554733

Establishing reliable prognostic factors as well as specific targets for new therapeutic approaches is an urgent requirement in advanced ovarian cancer. For several tumor entities, the ubiquitously spread scaffold protein β-arrestin 2, a multifunctional scaffold protein regulating signal transduction and internalization of activated G protein-coupled receptors (GPCRs), has been considered with rising interest for carcinogenesis. Therefore, we aimed to elucidate the prognostic impact of β-arrestin 2 and its functional role in ovarian cancer. β-arrestin 2 expression was analyzed in a subset of 156 samples of ovarian cancer patients by immunohistochemistry. Cytoplasmic expression levels were correlated with clinical as well as pathological characteristics and with prognosis. The biologic impact of β-arrestin 2 on cell proliferation and survival was evaluated, *in vitro*. Following transient transfection by increasing concentrations of plasmid encoding β-arrestin 2, different cell lines were evaluated in cell viability and death. β-arrestin 2 was detected in all histological ovarian cancer subtypes with highest intensity in clear cell histology. High β-arrestin 2 expression levels correlated with high-grade serous histology and the expression of the gonadotropin receptors FSHR and LHCGR, as well as the membrane estrogen receptor GPER and hCGβ. Higher cytoplasmic β-arrestin 2 expression was associated with a significantly impaired prognosis (median 29.88 vs. 50.64 months; $P = 0.025$). Clinical data were confirmed in transfected HEK293 cells, human immortalized granulosa cell line (hGL5) and the ovarian cancer cell line A2780 *in vitro*, where the induction of β-arrestin 2 cDNA expression enhanced cell viability, while the depletion of the molecule by siRNA resulted in cell death. Reflecting the role of β-arrestin 2 in modulating GPCR-induced proliferative and anti-apoptotic signals, we propose β-arrestin 2 as an important prognostic factor and also as a promising target for new therapeutic approaches in advanced ovarian cancer.

Keywords: β-arrestin 2, ovarian cancer, immunohistochemistry, survival analysis, G protein-coupled receptor, *in vitro* analyses

INTRODUCTION

Epithelial ovarian cancer (EOC) is the most lethal gynecological malignancy and is considered the fifth leading cause of death among women (1), mainly due to late diagnosis in advanced tumor stage leading to overall poor prognosis. Lack of inadequate screening methods and rising resistances toward chemotherapy over the clinical course further contribute to the relatively low 5-years survival at around 45% (1, 2). Standard treatment for advanced EOC consists of primary cytoreductive surgery, followed by platinum-based combination chemotherapy followed by targeted therapies like the anti-angiogenic antibody bevacizumab or PARP inhibitors. To date, the most reliable prognostic factors include volume of post-operative residual disease, tumor stage diagnosed according to the International Federation of Gynecology and Obstetrics (FIGO) staging system, patient's age and histology (2–7). EOCs are classified into four histological subtypes: serous, mucinous, endometrioid, and clear-cell, which vary in terms of phenotype, etiology and molecular background (8). Taking the heterogeneity of ovarian cancer into account appears crucial for developing new prognostic and therapeutic strategies.

β-arrestin 2 is a multifunctional scaffold protein regulating signal transduction and internalization of activated G protein-coupled receptors (GPCRs) like follicle-stimulating hormone receptor (FSHR) and luteinizing hormone/choriogonadotropin receptor (LHCGR) by promoting clathrin-dependent endocytosis (9). The β-arrestin family is a known activator of signaling pathways involved in tumorgenesis (10–12) and proliferation of certain tumor entities (13–17), including ovarian cancer (18). Functional association between FSHR/LHCGR and β-arrestin in granulosa cells could be demonstrated after gonadotropin treatment *in vitro* (19, 20). In immortalized ovarian cell lines, β-arrestin 2 triggers the activation of FSH-induced mitogen-activated protein (MAP) kinase signaling cascades linked to anti-apoptotic and proliferative events (21).

In this study, we aimed to evaluate the possible prognostic impact of β-arrestin 2 on clinical course of ovarian cancer. The role of β-arrestin 2 in modulating cell viability and survival was elucidated by functional analyses *in vitro*, suggesting new therapeutic approaches in ovarian cancer.

TABLE 1 | Patient characteristics.

Parameters	*N*	Percentage (%)
HISTOLOGY		
Serous	110	70.5
Clear cell	12	7.7
Endometrioid	21	13.5
Mucinous	13	8.3
LYMPH NODE		
pNX	61	39.1
pN0	43	27.6
pN1	52	33.3
DISTANT METASTASIS		
pM0/X	150	96.2
pM1	6	3.8
GRADING SEROUS		
Low	24	23.0
High	80	77.0
ENDOMETRIOID		
G1	6	31.6
G2	5	26.3
G3	8	42.1
MUCINOUS		
G1	6	50.0
G2	6	50.0
G3	0	0
CLEAR CELL		
G3	9	100
FIGO		
I	35	23.1
II	10	6.6
III	103	68.2
IV	3	2.0
AGE		
≤60 years	83	53.2
>60 years	73	46.8

MATERIALS AND METHODS

Patients and Specimens

156 ovarian cancer samples of patients that underwent surgery between 1990 and 2002 at the Department of Obstetrics and Gynecology, Ludwig Maximilian University in Munich, Germany, were analyzed (**Table 1**). The clinical data were received from the patient's charts, whereas the follow-up data from the Munich Cancer Registry (MCR). Only patients with a clear diagnosis of ovarian cancer and were included in this study, while benign tumors, just as borderline tumors were excluded. These patients had no history of previous or secondary cancers. Also, none of the patients had neoadjuvant chemotherapy. After the samples had been formalin-fixed and paraffin-embedded (FFPE), they were evaluated by a specialized pathologist at the department of Pathology, Ludwig Maximilian University, who classified them into histological subtypes [serous ($n = 110$), endometrioid ($n = 21$), mucinous ($n = 13$), clear-cell ($n = 12$)] and rated the tumor grading. The serous ovarian cancer samples were divided into low and high grading. Endometrioid ovarian cancer was graded according to G1–G3. For the mucinous carcinoma, there is no WHO classification; however, the subtype is often classified into G1–G3. The clear cell cancer was always categorized as G3. Staging was performed using the FIGO (WHO) and TNM classification. I ($n = 35$), II ($n = 10$,) III ($n = 103$), and IV ($n = 3$). Data on primary tumor extension was available in 155 cases: T1 ($n = 40$), T2 ($n = 18$), T3 ($n = 93$), T4 ($n = 4$), and on lymph node involvement in 95 cases: N0 ($n = 43$), N1 ($n = 52$). In nine cases available was the data on distant metastasis: M0 ($n = 3$), M1 ($n = 6$).

Ethical Approval

This study was approved by the Ethics Committee of the Ludwig-Maximilians-University, Munich, Germany (approval number 227-09 and 18-392). All tissue samples used for this study were obtained from leftover material from the archives of LMU Munich, Department Gynecology and Obstetrics, Ludwig-Maximilians-University, Munich, Germany, initially used for pathological diagnostics. The diagnostic procedures were completed before the current study was performed. During all experimental and statistical analysis, the observers were fully blinded to patient's data. All experiments were performed according to the standards of the Declaration of Helsinki (1975). As per declaration of our ethics committee no written informed consent of the participants or permission to publish is needed given the circumstances described above.

Immunohistochemistry

The formalin-fixed and paraffin-embedded ovarian cancer tissue samples were dewaxed in xylene for 20 min, before adding 100% ethanol to completely remove the Xylol. Unspecific color responses were avoided by blocking the endogenous peroxidase with 3% H_2O_2 in methanol (3 ml 30% H_2O_2 + 97 ml methanol), followed by rehydrating it in 70%, then 50% ethanol. Afterwards the slides were placed in a pressure cooker for 10 min, using sodium citrate buffer (pH = 6), made from 0.1 M citric acid and 0.1 M sodium citrate). After cooling down, this was followed by washing the samples first in distilled water, then in phosphate buffered saline (PBS) twice. After preprocessing, the slides were incubated in a blocking solution (ZytoChem Plus HRP Polymer System, Berlin, Germany, POLHRP-100) for 5 min to prevent an unspecific staining reaction. This was followed by a 16-h incubation overnight at 4°C with the primary antibodies: anti-β-arrestin 2, rabbit IgG, polyclonal, Abcam, ab151774 at a 1:1,500 dilution; anti-FSHR, rabbit IgG, polyclonal, Novus Biologicals, NLS2231 at a 1:100 dilution, anti-LHCGR, rabbit IgG, polyclonal, Acris, SP4594P at a 1:800 dilution; anti-GPER, rabbit IgG, polyclonal, Lifespan Biosciences, LS92467 at a 1:600 dilution and anti-hCGβ, rabbit IgG, polyclonal, Dako, A-0231 at a 1:300 dilution—then washed in PBS twice. Next step was the application of reagent 2 (ZytoChem Plus HRP Polymer System, Berlin, Germany, POLHRP-100), consisting of a corresponding biotinylated secondary anti-rabbit IgG antibody and the associated avidin-biotin-peroxidase complex, for 20 min. For the visualization reaction 3,3 Diaminobenzidine (DAB) and a substrate buffer (Liquid DAB and Substrate Chromogen System, Dako, Munich, Germany, K3468) was used for 30 min, followed by distilled water, to stop the reaction. After counterstaining the slides with Mayer's acidic hematoxylin (Waldeck-Chroma, Münster, Germany, catalog-number 2E-038) for 2 min, they were dehydrated in an ascending series of alcohol (70, 96, 100%), brightened by adding xylol and then covered. Negative and positive controls were used to assess the specificity of the immunoreactions. Negative controls (colored in blue) were performed in kidney, placental and uterine tissue by replacement of the primary antibodies by species-specific (rabbit) isotype control antibodies (Dako, Glostrup, Denmark). For positive controls, placental and kidney tissues were used.

Staining Evaluation

All EOC specimens were examined with a Leitz photomicroscope (Wetzlar, Germany) and specific β-arrestin 2 immunohistochemically staining reaction was observed in the cytoplasm of the cells. The intensity and distribution pattern of β-arrestin 2 staining was rated using the semi-quantitative immunoreactive score (IR score, Remmele's score). To obtain the IR score result, the optional staining intensity (0 = no, 1 = weak, 2 = moderate, and 3 = strong staining) and the percentage of positive stained cells (0 = no staining, 1 = <10% of the cells, 2 = 11–50% of the cells, 3 = 51–80% of the cells and 4 = >81%) were multiplied. Cut-off points for the IR scores were selected for the β-arrestin 2 staining considering the distribution pattern of IR scores in the collective. β-arrestin 2 staining was regarded as low with IRS 0–3 and as high with IRS ≥ 4. Renal biopsies from patients with different *ARRB2* expression levels served as positive and negative control staining (22) (**Figures 1E,F**).

Cell Lines and Transfection Protocol

The immortalized human granulosa (hGL5) cell line of ovarian origin (23), the human embryonic kidney (HEK293) and the ovarian carcinoma (A2780) cell lines were used for *in vitro* experiments. Cells were cultured and handled as previously described (21, 24–26). hGL5 cells culture medium was DMEM/F12 supplemented with 10% fetal bovine serum (FBS) and 2 mM L-glutamine (Sigma-Aldrich, St. Louis, MO, USA), 100 IU/mL penicillin and 50 µg/mL streptomycin (Thermo Fisher Scientific, Waltham, MA, USA) and 2% ITS + Premix Universal Culture Supplement (#354352; Corning Incorporated, Corning, NY, USA). The HEK293 cell line was cultured in DMEM additioned of 10% FBS, 2 mM L-glutamine, 100 IU/mL penicillin and 50 µg/mL streptomycin. The A2780 cell line served as a model of ovarian cancer and was cultured in RPMI1640 medium (Sigma-Aldrich) additioned of 10% FBS, 1% Hepes (Sigma-Aldrich), 2 mM L-glutamine, 100 IU/mL penicillin and 50 µg/mL streptomycin. Cell lines were maintained in an incubator at 37°C and 5% CO_2.

The transfection protocol was described previously (25–28). Briefly, 3.5×10^4 cells were transiently transfected in a 96-well plate using increasing amount (range: 0–200 ng/well) of β-arrestin 2-encoding pcDNA3.1 plasmid (29) or commercial siRNA probes against β-arrestin 2 (#14387; Life-Technologies, Carlsbad, CA, USA) (21), using an electroporator (Gene Pulser MXcell; Bio-Rad Laboratories Inc., Hercules, CA, USA) in accordance with established protocol and settings (21, 30). Control probes without specific target mRNAs were loaded for achieving equal amount of siRNA among wells.

Western Blot Analysis and Antibodies

Overexpression and knock-down of β-arrestin 2 and pro-caspase 3 were evaluated by Western blotting, as previously described (21, 24). Briefly, transfected cells were seeded in 24-well plates (1×10^5 cells/well) and cultured 48 h before to be lysed using 4°C RIPA buffer. β-arrestin 2 and pro-caspase 3 were evaluated by 12% SDS-page and Western blotting, using specific antibodies (#3857, Cell Signaling Technology Inc., Danvers, MA, USA; #MA1-91637, Thermo-Fisher Scientific,

respectively). β-actin signals served as loading controls and were detected using a horseradish peroxidase (HRP)-conjugated specific antibody (#A3854; Sigma-Aldrich). Signals were revealed by ECL chemiluminescent compound (GE HealthCare), after incubation of the membranes with a secondary anti-rabbit HRP-conjugated antibody (#NA9340V; GE HealthCare), except for β-actin. Western blotting signals were acquired by the Quantity One analysis software (Bio-Rad Laboratories Inc., Hercules, CA, USA).

Analysis of Cell Viability and Death

hGLC, HEK293, and A2780 cells were seeded in 96-well plates (1×10^4 cells/well) before viability assessment the by MTT colorimetric assay (31), using a previously validated protocol (21, 30). The absorbance was detected by a Victor3 plate reader (Perkin Elmer Inc., Waltham, MA, USA). A measure of death cells was obtained by incubating samples 30 min with propidium iodide (32). Cells were washed twice by PBS before excitation and light emission detection by a CLARIOstar microplate reader (BMG LabTech, Ortenberg, Germany), following the manufacturer's protocol. Data were represented as box and whiskers plots in a graph, as a measure of cell viability, and control of protein amount per well was performed by Bradford assay.

Statistical Analysis

IBM SPSS Statistics, version 25.0 (IBM Corporation, Armonk, NY, USA) was used for collecting and analyzing all the data for statistical significance. Overall-survival was compared with Kaplan-Meier curves and log-rank testing was used to detect differences in patients' overall survival times. The Spearman correlation coefficient (cc) was used for detecting correlations between immunohistochemical staining outcomes. For multivariate analyses, the cox regression was performed. Results obtained from cell lines were analyzed by D'Agostino and Pearson normality test before applying the Kruskal-Wallis test together with Dunn's correction for multiple comparisons, using the GraphPad Prism 6.0 software (GraphPad Software Inc., La Jolla, CA, USA). For all analysis a P-value of <0.05 was considered to be statistically significant.

RESULTS

β-arrestin 2 Expression and the Correlation to Clinical and Pathological Characteristics

The clinicopathologic characteristics of the analyzed ovarian cancer patients are listed in **Table 1**. 104 (67%) out of 156 ovarian cancer specimens showed positive cytoplasmic β-arrestin 2 expression. The median immunoreactive score (IRS) of cytoplasm staining was 2 (with a range of 0–12). Clear cell histology exhibited the strongest β-arrestin 2 staining (Kruskal-Wallis test; $p = 0.01$) when compared with different histological subtypes (**Figures 1A–D**).

Representative staining of benign ovarian and fallopian tube tissue show positive results in epithelial cells, granulosa cells and theca cells. The ovarian and fallopian tube stroma did not show a β-arrestin 2 staining (**Figures 2A,B**).

We analyzed the correlation between β-arrestin 2 and clinicopathological data, such as histology, grading, and FIGO classification (**Table 2**). A positive correlation was observed between high β-arrestin 2 expression and high-grade serous histology (Spearman's correlation analysis; $p = 0.041$; $cc = 0.169$). Moreover, no other correlations were observed.

β-arrestin 2 Correlates With Gonadotropin Receptors Expression

We then analyzed the correlation between β-arrestin 2 expression and other parameters previously examined (33–37) in the same ovarian cancer cohort (**Table 3**). A positive correlation was detected to the expression of the gonadotropin receptors FSHR ($p = 0.029$; $cc = 0.183$) and LHCGR ($p = 0.001$; $cc = 0.284$), the G protein-coupled membrane estrogen receptor GPER ($p = 0.0009$; $cc = 0.215$) as well as with the choriogonadotropin beta subunit (hCGβ) ($p < 0.001$; $cc = 0.36$). Representative stainings of the correlated parameters are shown in **Supplementary Figure 1**.

High β-arrestin 2 Expression Is Associated With Impaired Overall Survival

Age of the patient cohort was 58.7 ± 31.4 years (median ± standard deviation, SD; $n = 156$) with a range of 31–88 years. The overall survival of the EOC patients was 34.4 ± 57.8 months (median ± SD; $n = 156$). High β-arrestin 2 expression (IRS 4–12) is associated with shorter overall survival. As depicted on the Kaplan-Meier curve, higher cytoplasmic β-arrestin 2 expression correlates with a significantly impaired prognosis (**Figure 3**; 50.64 vs. 29.88 months, median; $p = 0.025$).

Clinicopathological Parameters as Independent Prognostic Factors

A multivariate cox-regression analysis was performed to detect which parameters were independent prognostic factors for overall survival in the present cohort. In this analysis, patients' age ($p = 0.014$) and FIGO stage ($p < 0.001$) were independent factors for overall survival. High β-arrestin 2 ($p = 0.152$), however, was not confirmed as an independent factor of prognostic independence (**Table 4**).

Effects of β-arrestin 2 Overexpression and Depletion on Cell Viability

Since β-arrestin 2 expression levels were found to correlate with overall survival of ovarian cancer patients, the impact of the molecule on cell proliferation and survival was evaluated, *in vitro*. Cell viability and death are represented by box and whiskers plots (**Figure 4**).

Western blot analysis demonstrated that β-arrestin 2 expression levels increase together with the amount of cDNA encoding the molecule, in the HEK293, hGL5 and A2780 cell lines (**Figure 4A**). We found increased viability of all cell models overexpressing β-arrestin 2, compared to mock-transfected cells used as controls (**Figures 4B–D**; Kruskal-Wallis test; $p < 0.01$; $n = 8$). Moreover, highest levels of cell viability corresponded to the highest amount of plasmid transfected. These results are corroborated by data from propidium iodide-stained HEK293

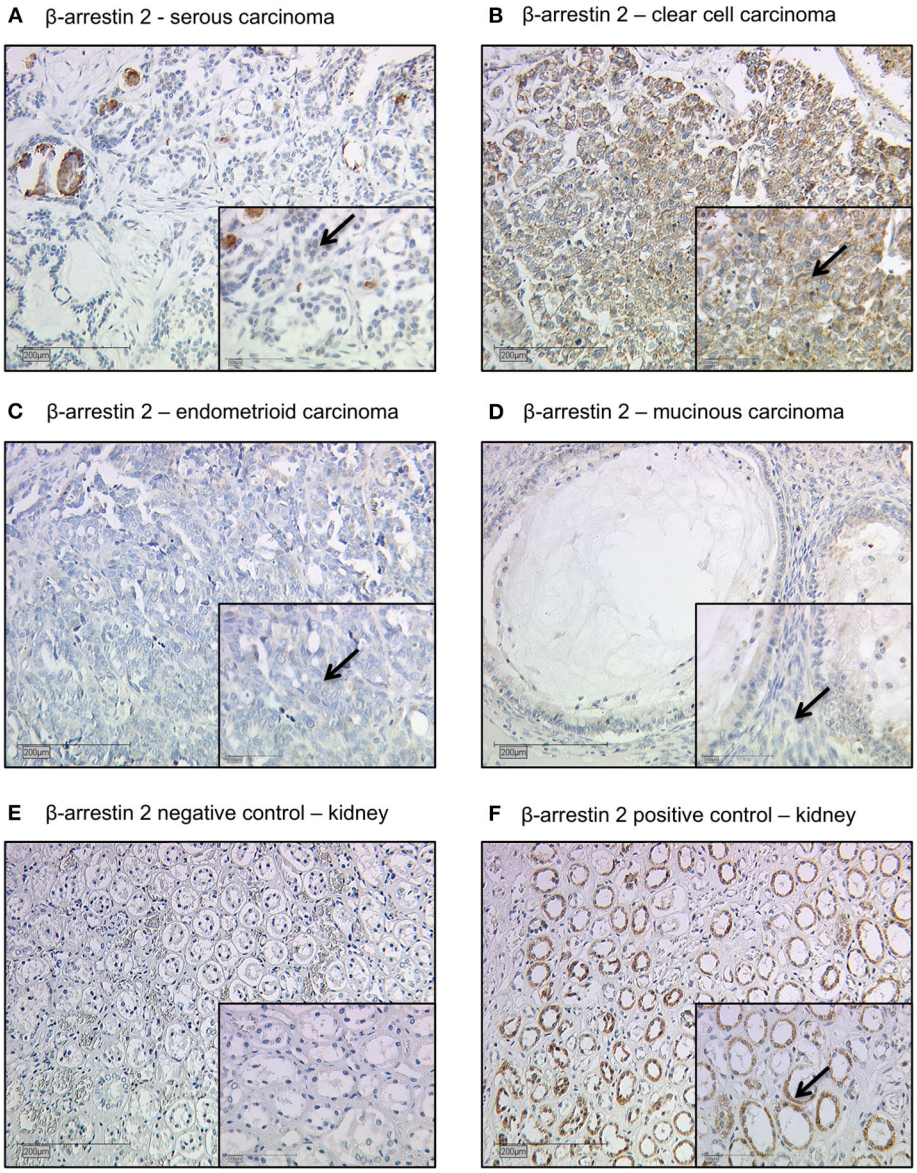

FIGURE 1 | Detection of β-arrestin 2 with immunohistochemistry. **(A)** Cytoplasmic β-arrestin 2 staining in ovarian cancer with serous, **(B)** clear cell, **(C)** endometrioid, and **(D)** mucinous histology. **(E)** β-arrestin 2 negative control **(F)** and positive control in human kidney tissue. Clear cell histology exhibited the strongest cytoplasmic β-arrestin 2 expression (Kruskal-Wallis test; $p = 0.01$) when compared with different histological subtypes. Arrows demonstrate representatively β-arrestin 2 stained cells. Images representative of three independent experiments.

and A2780 cells overexpressing β-arrestin 2, indicating that the least cell death occurs with the highest amounts of β-arrestin 2-encoding plasmid transfected (**Figures 4E–G**; Kruskal-Wallis test; $p < 0.01$; $n = 8$). However, data from transfected hGL5 cells did not reveal any association between β-arrestin 2 expression and cell death (**Figure 4F**; Kruskal-Wallis test; $p \geq 0.05$; $n = 8$).

Since a positive correlation between β-arrestin 2 expression and cell viability was found (**Figure 4**), control experiments were performed by evaluating the cell viability and death of cells maintained under β-arrestin 2 depletion, *in vitro*. Therefore, HEK293, hGL5, and A2780 cells were treated by increasing concentrations of siRNA probes silencing the endogenous molecule, then MTT assay and propidium iodide staining were performed (**Figure 5**).

The viability of all the cell lines is significantly reduced upon β-arrestin 2 depletion (**Figures 5A–C**; Kruskal-Wallis test; $p < 0.05$; $n = 8$). These data are reflected by increased propidium iodide signals occurring together with increasing amounts of siRNAs, in HEK293 cells (**Figure 5D**; Kruskal-Wallis test; $p < 0.05$; $n = 8$), while similar signals were found between siRNA-

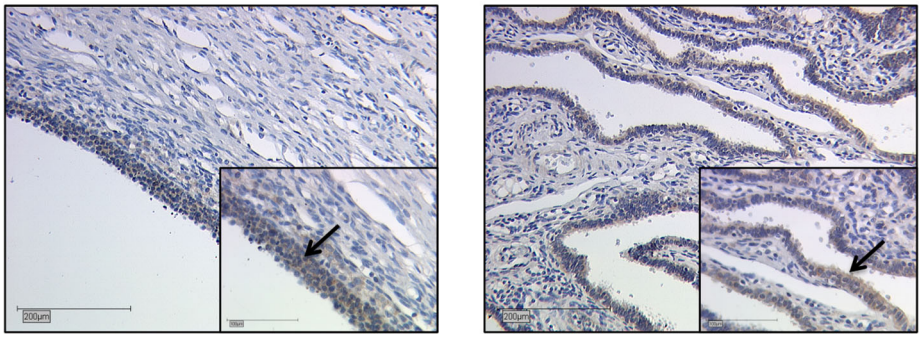

FIGURE 2 | Detection of β-arrestin 2 with immunohistochemistry in benign ovary and fallopian tube. Detection of β-arrestin 2 with immunohistochemistry in benign ovary **(A)** and fallopian tube **(B)**. Positive β-arrestin 2 staining was observed in epithelial cells, granulosa cells and theca cells. The ovarian and fallopian tube stroma did not show a β-arrestin 2 staining. Arrows demonstrate representatively β-arrestin 2 stained cells. Images representative of three independent experiments.

TABLE 2 | Correlation analysis between β-arrestin 2 expression and clinicopathological data.

Variable	*P*	Correlation coefficient
Histology	0.075	−0.083
FIGO stage	0.673	0.086
Age	0.206	0.105
GRADING		
Clear cell, endometrioid, and mucinous (G1–G3)	0.520	−0.088
Serous—low grading	0.052	−0.160
Serous—high grading	0.041*	0.169

*Clinicopathologic data and β-arrestin 2 expresssion were correlated to each other using Spearman's correlation analysis. Significant correlations are indicated by asterisks (*p < 0.05). p, two-tailed significance.*

TABLE 3 | Correlation analysis of β-arrestin 2.

Staining	β-arrestin 2	FSHR	LHCGR	GPER	hCGβ
β-ARRESTIN 2					
cc	1.000	0.183	0.284	0.215	0.360
p	–	0.029	0.001	0.009	0.000
n	148	143	146	148	137
FSHR					
cc	0.183	1.000	0.164	0.214	0.082
p	0.029	–	0.046	0.009	0.340
n	143	151	149	148	137
LHCGR					
cc	0.284	0.164	1.000	0.170	0.200
p	0.001	0.046	–	0.037	0.018
n	146	149	154	151	140
GPER					
cc	0.215	0.214	0.170	1.000	0.114
p	0.009	0.009	0.037	–	0.179
n	148	148	151	153	141
hCGβ					
cc	0.360	0.082	0.200	0.114	1.000
p	0.000	0.340	0.018	0.179	–
n	137	137	140	141	142

cc, correlation coefficient; p, two-tailed significance; n, number of patients.

and mock-treated hGL5 and A2780 cells (**Figures 5E,F**; Kruskal-Wallis test; $p \geq 0.05$; $n = 8$). Western blotting analysis confirmed the siRNA-dependence of β-arrestin 2 silencing, which is linked to pro-caspase 3 cleavage in all the cell lines (**Figure 5G**).

DISCUSSION

Our study revealed for the first time that β-arrestin 2 expression significantly correlates with impaired overall survival of ovarian cancer patients and these results are consistent with the proliferative role of β-arrestin 2 demonstrated *in vitro*. β-arrestins are known to act as scaffold proteins controlling multiple cellular functions, such as MAP kinase signaling, GPCR trafficking and transcriptional modulations (38, 39). Several studies demonstrated that β-arrestins are involved in carcinogenesis of the ovary (11, 18) and other types of cancer (10, 12–17). The relevance of the GPCR/β-arrestin pathway in ovarian cancer cells is demonstrated by the finding that endothelin-1 receptor/β-arrestin complex activates beta-catenin signaling pathways with impact on carcinogenesis and metastatic progression (11). Nevertheless, conflicting results have been reported with a positive impact of angiotensin-mediated β-arrestin expression in a clinical-genomic dataset from 820 ovarian cancer patients (40). Indicative results may be provided by the analysis of gene expression data stored in public cancer repositories. For instance, The Human Protein Atlas database (https://www.proteinatlas.org; last accession: 03 March 2020) revealed that β-arrestin 2-encoding gene (*ARRB2*) expression is an unfavorable prognostic marker of prostate cancer, although the association is not replicated for ovarian cancer. These data corroborate, at least in part, our finding although they should be considered cautiously, since gene expression levels

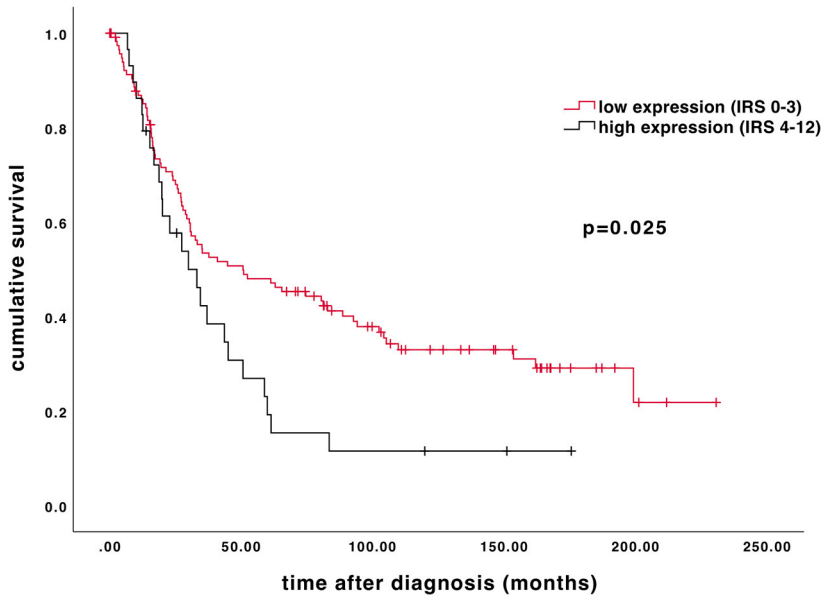

FIGURE 3 | Kaplan–Meier estimate of β-arrestin 2. β-arrestin 2 expression (IRS 4–12) was associated with impaired overall survival (50.64 vs. 29.88 months, median; $p = 0.025$). Censoring events have been marked in the graphs.

TABLE 4 | Multivariate analysis of the analyzed ovarian cancer patients ($n = 156$).

Covariate	Coefficient (b_i)	[HR Exp (b_i)]	95% CI		*P*-value
			Lower	Upper	
Patient's Age (≤60 vs. >60)	0.625	1.869	1.133	3.084	0.014
FIGO (I, II vs. III, IV)	0.813	2.255	1.499	3.393	<0.001
GRADING					
Clear cell, endometrioid, and mucinous (G1–G3)	0.142	1.153	0.749	1.774	0.517
Serous—low grading	−0.695	0.499	0.160	1.562	0.232
Serous—high grading	0.654	1.924	0.765	4.838	0.164
High β-arrestin 2	−0.097	0.907	0.795	1.036	0.152

are not necessarily corresponding to protein levels and the database does not allow to analyze all the specific histological tumor subtypes.

The link between GPCR/β-arrestins complexes and cancer is an established concept (41) and seems to be result of sustained intracellular signaling occurring upon dysregulation of intracellular β-arrestin protein levels (42). These molecules were associated with drug resistance of breast (43) and lung cancer cells (44), cancer cell migration and invasion (45), tumor progression (46) and metastasis (47), as well as a number of other tumors (48). Thus, β-arrestins were proposed as a target for therapeutic strategies (49). Our data *in vitro* confirm the proliferative role of β-arrestin 2 also in an ovarian cancer cell line, as well as in hGL5 and HEK293 cells. There are converging evidences that β-arrestin 2 depletion leads to decreasing cell viability and/or activating a caspase 3-mediated cell death, at least in HEK293 cells and confirmed in the ovarian cancer cell line A2780. Interestingly, in hGL5 cells, increased β-arrestin 2 expression is linked with upregulation of cell viability, while the depletion of this molecule by siRNA did not result in cell death. This is likely due to the integration of exogenous *E6* and *E7* oncogenes in the hGL5 cell line genome (23), which served for immortalizing them and, likely, results in increased resistance to caspase 3 activation. On the other hand, these oncogenes encode proteins inhibiting tumor protein 53 (p53) and retinoblastoma (Rb) molecules and interfering with apoptosis and cell cycle blockade. hGL5 have characteristics reflecting epithelial tumor cells, such as fibroblast-like spindle shape and relatively high proliferation rate, a feature depending on β-arrestins functioning (21), as well as in other ovarian cancer cell lines (40). However, these results underline that β-arrestins are modulators of proliferative signals exerted through a molecular signaling module with GPCRs and the extracellular-regulated MAP kinases 1 and

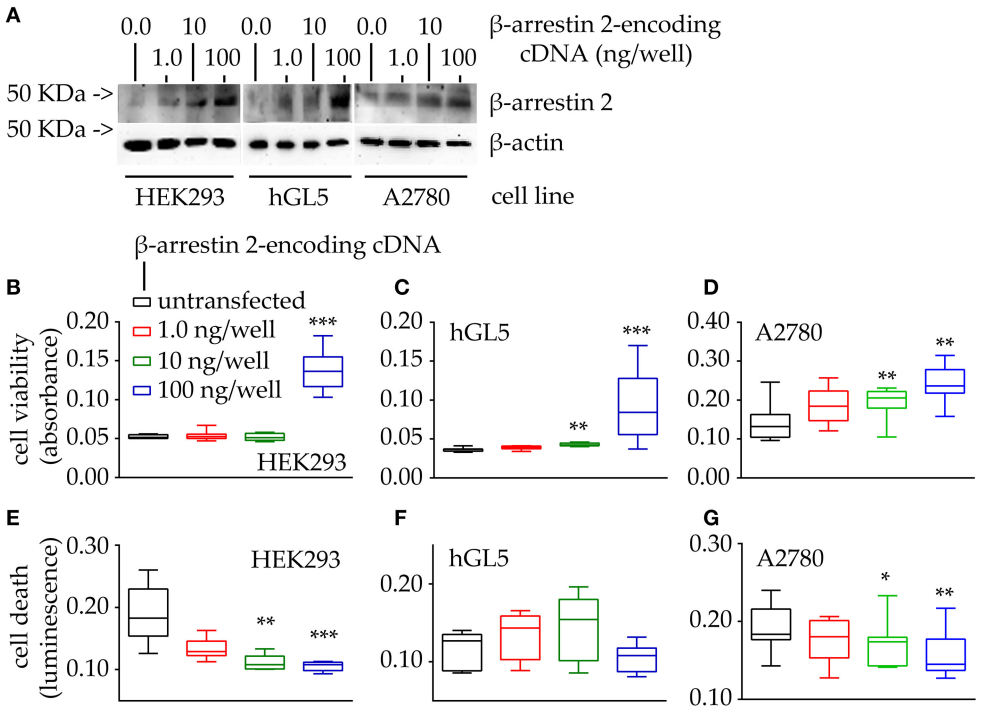

FIGURE 4 | Evaluation of cell viability and death under 48-h β-arrestin 2 overexpression. HEK293, hGL5, and A2780 cells were transfected by increasing amount of plasmid encoding β-arrestin 2 and cell viability and death were assessed by MTT and propidium iodide, respectively. Total protein content from 0.5×10^4 70% confluent log phase cells were loaded. **(A)** Representative image of β-arrestin 2 detected in cell lysates by Western blotting using a specific rabbit antibody using β-actin as a normalizer. **(B)** Box and Whiskers plot of MTT data, collected from transfected HEK293 cells overexpressing increasing levels of β-arrestin 2, representing cell viability. **(C)** hGL5 cell viability evaluated by MTT. **(D)** β-arrestin 2-dependent cell viability of the A2780 ovarian cancer cell line. **(E)** Data from the β-arrestin 2-overexpressing HEK293, representing cell death, in propidium iodide-stained samples. **(F)** β-arrestin 2-overexpressing hGL5 cell death. **(G)** β-arrestin 2-overexpressing A2780 ovarian cancer cell death. Brightness/contrast of Western blotting pictures were adjusted uniformly in all panels. Asterisks indicate significantly different data distribution than mock-transfected (untransfected) cells (Kruskal-Wallis test and Dunn's correction for multiple comparisons; $^*P < 0.05$; $^{**}P < 0.001$; $^{***}P < 0.0001$; $n = 8$).

2 (ERK1/2), in a number of cells (50), including ovarian cells (21). Gonadotropin receptors are expressed in ovarian cells and targeted by β-arrestin 2 (51). It is well-known that gonadotropin receptor expression is dysregulated in ovarian cancer (34, 36, 52) as well adrenal tumor (53), although the specific influence of these receptor on carcinogenesis is still not determined (54). One reason for this, may be the bi-directional regulation of pro- and anti-apoptotic signals which depend on FSHR and LHCGR expression levels (55). Interestingly, the depletion of β-arrestin 2 may be linked to increased tumor cell growth and angiogenesis, at least in certain cases, such as lung cancer (56). In this case, the absence of β-arrestin 2 would lead to uncontrolled activation of proliferative signals induced by other GPCRs, e.g., the interleukin 8 receptor beta (CXCR2). Taken together, we could speculate that β-arrestins may positively or negatively impact proliferative events, modulating the activity of various GPCRs specifically expressed in the tumor cells.

In correlation analyses, a link between β-arrestin 2 and the G-protein coupled estrogen receptor (GPER) was identified. This receptor is known for rapidly mediating non-genomic signals induced by estrogens and was found in both healthy and neoplastic human tissue (57, 58). Indeed, previous studies revealed that GPER is related to better overall survival in ovarian cancer patients (34, 59, 60). Since GPER belongs to the GPCRs family, we may suppose that β-arrestin 2 might interact with this membrane estrogen receptor and influence its physiological function. However, this issue must be further investigated because GPER recycling and intracellular trafficking seems to be regulated by mechanisms not involving β-arrestins (61).

Interestingly, we also found an association between β-arrestin 2 and one of the two LHCGR ligands, hCGβ. This hormone was shown to be associated with an increased 5-years survival in LHCGR positive/FSHR negative ovarian cancer cases (33). Although this study had limitations related to low specificity of the anti-gonadotropin receptor antibodies employed (62), it suggests that hCGβ and its receptor might be linked to survival in these patients. These data would be in line with the relatively high potency of hCGβ in inducing LHCGR-mediated intracellular cAMP increase (27), as an effect linked to the steroidogenic potential of the hormone and to pro-apoptotic effects (24). On the other hand, these data would

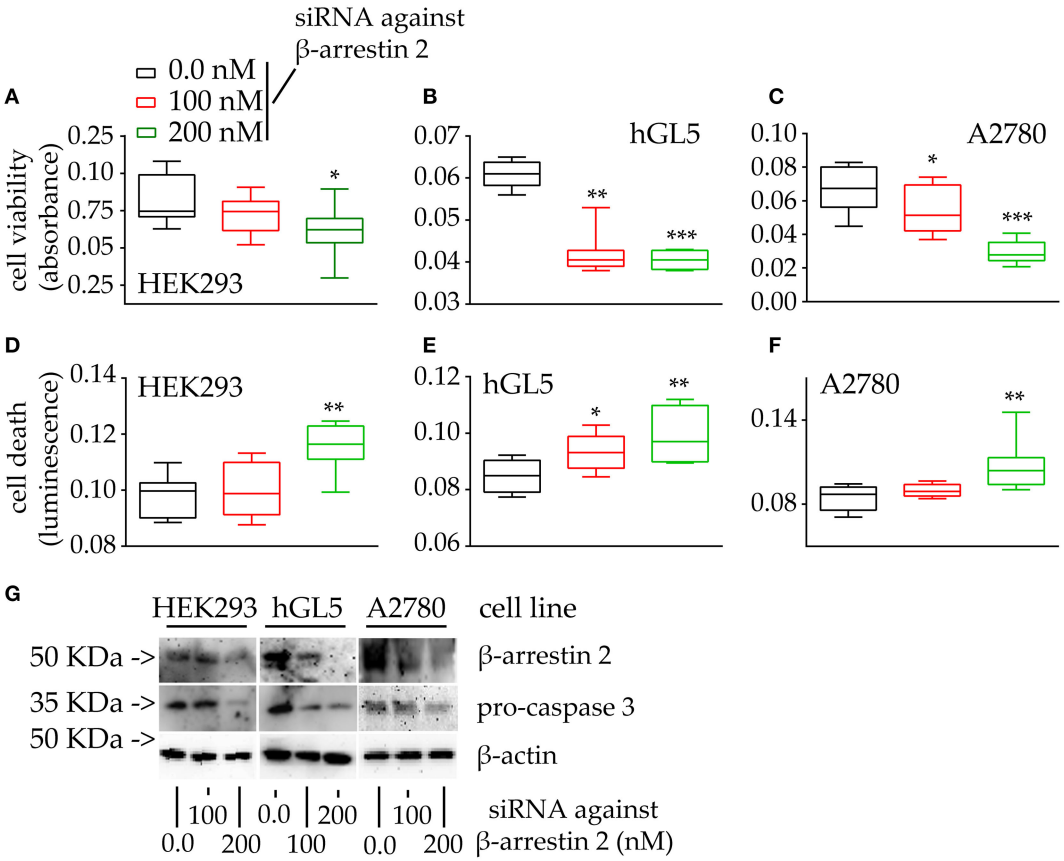

FIGURE 5 | Viability and death of 48-h β-arrestin 2-silenced HEK293, hGL5, and A2780 cells. Samples were transfected by increasing amount of siRNA probes targeting the β-arrestin 2 mRNA and 48-h cell viability and death were assessed by MTT and propidium iodide. Total protein content from 3×10^4 70% confluent log phase cells were loaded. **(A)** Box and Whiskers plot representing the HEK293 cell viability under β-arrestin 2 depletion. **(B)** β-arrestin 2-silenced hGL5 cell viability. **(C)** β-arrestin 2-silenced A2780 ovarian cancer cell viability. **(D)** Data from the β-arrestin 2-silenced HEK293, representing cell death evaluated using propidium iodide staining. **(E)** hGL5 cell death evaluated by propidium iodide. **(F)** Cell death in β-arrestin 2-silenced A2780 evaluated by propidium iodide. **(G)** Representative Western blotting images demonstrating β-arrestin 2 depletion and pro-caspase 3 cleavage in HEK293, hGL5, and A2780 cell lysates. β-actin was the normalizer. Brightness/contrast of Western blotting pictures were adjusted uniformly in all panels. Significantly different data distribution than mock-transfected (untransfected) cells were indicated by asterisks. Kruskal-Wallis test and Dunn's correction for multiple comparisons; $^*P < 0.05$; $^{**}P < 0.001$; $^{***}P < 0.0001$; $n = 8$).

be in contrast with the fact that hCGβ has been used as a marker of certain tumors, such as the choriocarcinoma (63), which reflects the involvement of β-arrestin 2 in the hCGβ-mediated intracellular signaling (29) and suggests that the connection between the two molecules in cancer merits further investigations.

β-arrestin 2 is associated with a significantly impaired overall survival of ovarian cancer patients. This finding is supported by *in vitro* data demonstrating that β-arrestin 2 upregulates the viability of an ovarian cancer cell line, and transfected HEK293 and hGL5 cells. Reflecting the role of β-arrestins as scaffold proteins linked to the GPCRs activity, correlations between the β-arrestin 2 and FSHR and LHCGR expression was identified ovarian cancer tissue. Taken together, we indicate that β-arrestin 2 may be a promising new target in ovarian cancer so that clinical implications should be further addressed in future research.

DATA AVAILABILITY STATEMENT

The raw data supporting the conclusions of this article will be made available by the authors, without undue reservation.

ETHICS STATEMENT

The studies involving human participants were reviewed and approved by Ethics Committee of the Ludwig-Maximilians-University, Munich, Germany. Written informed consent for participation was not required for this study in accordance with the national legislation and the institutional requirements.

AUTHOR CONTRIBUTIONS

BC, UJ, MS, LC, and FT: conceptualization. DM, SM, and AB: validation. BC, AP, UJ, and LC: formal analysis. AP, BM, RB,

and SB: investigation. BC, AP, LC, and FT: writing-original draft preparation. UJ, VS, DM, SM, AB, MS, BM, RB, and SB: writing—review and editing. AP, BC, and LC: visualization. UJ, SM, and MS: supervision. All authors have read and agreed to the published version of the manuscript.

FUNDING

MS was a Le Studium Research Fellow, Loire Valley Institute for Advanced Studies, Orléans & Tours, France, INRA—Centre Val de Loire, 37380 Nouzilly, France, receiving funding from the European Union's Horizon 2020 research and innovation programme under the Marie Skłodowska-Curie grant agreement No 665790. This research did not receive any specific grant from any funding agency in the public, commercial, or not-for-profit sector.

ACKNOWLEDGMENTS

The authors were grateful to Mrs. Christina Kuhn for excellent technical assistance and Professor Gaetano Marverti (University of Modena and Reggio Emilia, Modena, Italy) for providing the A2780 cell line. Authors were grateful to the Italian Ministry of University and Research for supporting the Department of Biomedical, Metabolic, and Neural Sciences (University of Modena and Reggio Emilia, Italy) in the context of the Departments of Excellence Programme.

SUPPLEMENTARY MATERIAL

The Supplementary Material for this article can be found online at: https://www.frontiersin.org/articles/10.3389/fendo.2020.554733/full#supplementary-material

REFERENCES

1. Siegel RL, Miller KD, Jemal A. Cancer statistics 2019. *CA Cancer J Clin.* (2019). 69:7–34. doi: 10.3322/caac.21551
2. Baldwin LA, Huang B, Miller RW, Tucker T, Goodrich ST, Podzielinski I, et al. Ten-year relative survival for epithelial ovarian cancer. *Obstet Gynecol.* (2012) 120:612–8. doi: 10.1097/AOG.0b013e318264f794
3. du Bois A, Reuss A, Pujade-Lauraine E, Harter P, Ray-Coquard I, Pfisterer J. Role of surgical outcome as prognostic factor in advanced epithelial ovarian cancer: a combined exploratory analysis of 3 prospectively randomized phase 3 multicenter trials: by the arbeitsgemeinschaft gynaekologische onkologie studiengruppe ovarialkarzinom (AGO-OVAR) and the groupe d'investigateurs nationaux pour les etudes des cancers de l'Ovaire (GINECO). *Cancer.* (2009) 115:1234–44. doi: 10.1002/cncr.24149
4. Aletti GD, Gostout BS, Podratz KC, Cliby WA. Ovarian cancer surgical resectability: relative impact of disease, patient status, and surgeon. *Gynecol Oncol.* (2006) 100:33–7. doi: 10.1016/j.ygyno.2005.07.123
5. Vergote I, De Brabanter J, Fyles A, Bertelsen K, Einhorn N, Sevelda P, et al. Prognostic importance of degree of differentiation and cyst rupture in stage I invasive epithelial ovarian carcinoma. *Lancet.* (2001) 357:176–82. doi: 10.1016/S0140-6736(00)03590-X
6. Dembo AJ, Davy M, Stenwig AE, Berle EJ, Bush RS, Kjorstad KK. Prognostic factors in patients with stage I epithelial ovarian cancer. *Obstet Gynecol.* (1990) 75:263–73.
7. Tomao F, Marchetti C, Romito A, Di Pinto A, Di Donato V, Capri O, et al. Overcoming platinum resistance in ovarian cancer treatment: from clinical practice to emerging chemical therapies. *Expert Opin Pharmacother.* (2017) 18:1443–55. doi: 10.1080/14656566.2017.1328055
8. Kossai M, Leary A, Scoazec JY, Genestie C. Ovarian cancer: a heterogeneous disease. *Pathobiology.* (2018) 85:41–9. doi: 10.1159/000479006
9. Shenoy SK, Lefkowitz RJ. β-arrestin-mediated receptor trafficking and signal transduction. *Trends Pharmacol Sci.* (2011) 32:521–33. doi: 10.1016/j.tips.2011.05.002
10. Mythreye K, Blobe GC. The type III TGF-beta receptor regulates epithelial and cancer cell migration through beta-arrestin2-mediated activation of Cdc42. *Proc Natl Acad Sci USA.* (2009) 106:8221–6. doi: 10.1073/pnas.0812879106
11. Rosano L, Cianfrocca R, Masi S, Spinella F, Di Castro V, Biroccio A, et al. Beta-arrestin links endothelin A receptor to beta-catenin signaling to induce ovarian cancer cell invasion and metastasis. *Proc Natl Acad Sci USA.* (2009) 106:2806–11. doi: 10.1073/pnas.0807158106
12. Alvarez CJP, Lodeiro M, Theodoropoulou M, Camina JP, Casanueva FF, Pazos Y. Obestatin stimulates Akt signalling in gastric cancer cells through beta-arrestin-mediated epidermal growth factor receptor transactivation. *Endocr Relat Cancer.* (2009) 16:599–611. doi: 10.1677/ERC-08-0192
13. Dasgupta P, Rizwani W, Pillai S, Davis R, Banerjee S, Hug K, et al. ARRB1-mediated regulation of E2F target genes in nicotine-induced growth of lung tumors. *J Natl Cancer Inst.* (2011) 103:317–33. doi: 10.1093/jnci/djq541
14. Buchanan FG, Gorden DL, Matta P, Shi Q, Matrisian LM, DuBois RN. Role of beta-arrestin 1 in the metastatic progression of colorectal cancer. *Proc Natl Acad Sci USA.* (2006) 103:1492–7. doi: 10.1073/pnas.0510562103
15. Moussa O, Ashton AW, Fraig M, Garrett-Mayer E, Ghoneim MA, Halushka PV, et al. Novel role of thromboxane receptors beta isoform in bladder cancer pathogenesis. *Cancer Res.* (2008) 68:4097–104. doi: 10.1158/0008-5472.CAN-07-6560
16. Li TT, Alemayehu M, Aziziyeh AI, Pape C, Pampillo M, Postovit LM, et al. Beta-arrestin/Ral signaling regulates lysophosphatidic acid-mediated migration and invasion of human breast tumor cells. *Mol Cancer Res.* (2009) 7:1064–77. doi: 10.1158/1541-7786.MCR-08-0578
17. Lin HK, Wang L, Hu YC, Altuwaijri S, Chang C. Phosphorylation-dependent ubiquitylation and degradation of androgen receptor by Akt require Mdm2 E3 ligase. *EMBO J.* (2002) 21:4037–48. doi: 10.1093/emboj/cdf406
18. Rosano L, Spinella F, Di Castro V, Nicotra MR, Dedhar S, de Herreros AG, et al. Endothelin-1 promotes epithelial-to-mesenchymal transition in human ovarian cancer cells. *Cancer Res.* (2005) 65:11649–57. doi: 10.1158/0008-5472.CAN-05-2123
19. Riccetti L, Klett D, Ayoub MA, Boulo T, Pignatti E, Tagliavini S, et al. Heterogeneous hCG and hMG commercial preparations result in different intracellular signalling but induce a similar long-term progesterone response *in vitro*. *Mol Hum Reprod.* (2017) 23:685–97. doi: 10.1093/molehr/gax047
20. Riccetti L, Sperduti S, Lazzaretti C, Klett D, De Pascali F, Paradiso E, et al. Glycosylation pattern and *in vitro* bioactivity of reference follitropin alfa and biosimilars. *Front Endocrinol.* (2019) 10:503. doi: 10.3389/fendo.2019.00503
21. Casarini L, Reiter E, Simoni, M. β-arrestins regulate gonadotropin receptor-mediated cell proliferation and apoptosis by controlling different FSHR or LHCGR intracellular signaling in the hGL5 cell line. *Mol Cell Endocrinol.* (2016) 437:11–21. doi: 10.1016/j.mce.2016.08.005
22. Liu J, Li QX, Wang XJ, Zhang C, Duan YQ, Wang ZY, et al. β-Arrestins promote podocyte injury by inhibition of autophagy in diabetic nephropathy. *Cell Death Dis.* (2016) 7:e2183. doi: 10.1038/cddis.2016.89

23. Rainey WH, Sawetawan C, Shay JW, Michael MD, Mathis JM, Kutteh W, et al. Transformation of human granulosa cells with the E6 and E7 regions of human papillomavirus. *J Clin Endocrinol Metab.* (1994) 78:705–10. doi: 10.1210/jcem.78.3.8126145
24. Casarini L, Riccetti L, De Pascali F, Gilioli L, Marino M, Vecchi E, et al. Estrogen modulates specific life and death signals induced by LH and hCG in human primary granulosa cells *in vitro*. *Int J Mol Sci.* (2017) 18:926. doi: 10.3390/ijms18050926
25. Sperduti S, Limoncella S, Lazzaretti C, Paradiso E, Riccetti L, Turchi S, et al. GnRH antagonists produce differential modulation of the signaling pathways mediated by GnRH receptors. *Int J Mol Sci.* (2019) 20:5548. doi: 10.3390/ijms20225548
26. Lazzaretti C, Riccetti L, Sperduti S, Anzivino C, Brigante G, De Pascali F, et al. Inferring biallelism of two FSH receptor mutations associated with spontaneous ovarian hyperstimulation syndrome by evaluating FSH, LH and HCG cross-activity. *Reprod Biomed Online.* (2019) 38:816–24. doi: 10.1016/j.rbmo.2018.12.021
27. Casarini L, Riccetti L, Limoncella S, Lazzaretti C, Barbagallo F, Pacifico S, et al. Probing the effect of sildenafil on progesterone and testosterone production by an intracellular FRET/BRET combined approach. *Biochemistry.* (2019) 58:799–808. doi: 10.1021/acs.biochem.8b01073
28. Brigante G, Riccetti L, Lazzaretti C, Rofrano L, Sperduti S, Poti F, et al. Abacavir, nevirapine, and ritonavir modulate intracellular calcium levels without affecting GHRH-mediated growth hormone secretion in somatotropic cells *in vitro*. *Mol Cell Endocrinol.* (2019) 482:37–44. doi: 10.1016/j.mce.2018.12.005
29. Riccetti L, Yvinec R, Klett D, Gallay N, Combarnous Y, Reiter E, et al. Human luteinizing hormone and chorionic gonadotropin display biased agonism at the LH and LH/CG receptors. *Sci Rep.* (2017) 7:940. doi: 10.1038/s41598-017-01078-8
30. Casarini L, Lispi M, Longobardi S, Milosa F, La Marca A, Tagliasacchi D, et al. LH and hCG action on the same receptor results in quantitatively and qualitatively different intracellular signalling. *PLoS ONE.* (2012) 7:e46682. doi: 10.1371/journal.pone.0046682
31. Mosmann, T. Rapid colorimetric assay for cellular growth and survival: application to proliferation and cytotoxicity assays. *J Immunol Methods.* (1983) 65:55–63. doi: 10.1016/0022-1759(83)90303-4
32. Kabakov AE, Gabai VL. Cell death survival assays. *Methods Mol Biol.* (2018) 1709:107–27. doi: 10.1007/978-1-4939-7477-1_9
33. Lenhard M, Tsvilina A, Schumacher L, Kupka M, Ditsch N, Mayr D, et al. Human chorionic gonadotropin and its relation to grade, stage and patient survival in ovarian cancer. *BMC Cancer.* (2012) 12:2. doi: 10.1186/1471-2407-12-2
34. Heublein S, Mayr D, Vrekoussis T, Friese K, Hofmann SS, Jeschke U, et al. The G-protein coupled estrogen receptor (GPER/GPR30) is a gonadotropin receptor dependent positive prognosticator in ovarian carcinoma patients. *PLoS ONE.* (2013) 8:e71791. doi: 10.1371/journal.pone.0071791
35. Heublein S, Vrekoussis T, Mayr D, Friese K, Lenhard M, Jeschke U, et al. Her-2/neu expression is a negative prognosticator in ovarian cancer cases that do not express the follicle stimulating hormone receptor (FSHR). *J Ovarian Res.* (2013) 6:6. doi: 10.1186/1757-2215-6-6
36. Scholz C, Heublein S, Lenhard M, Friese K, Mayr D, Jeschke U. Glycodelin A is a prognostic marker to predict poor outcome in advanced stage ovarian cancer patients. *BMC Res Notes.* (2012) 5:551. doi: 10.1186/1756-0500-5-551
37. Deuster E, Mayr D, Hester A, Kolben T, Zeder-Goss C, Burges A, et al. Correlation of the aryl hydrocarbon receptor with FSHR in ovarian cancer patients. *Int J Mol Sci.* (2019) 20:2862. doi: 10.3390/ijms20122862
38. DeWire SM, Ahn S, Lefkowitz RJ, Shenoy SK. Beta-arrestins cell signaling. *Annu Rev Physiol.* (2007) 69:483–510. doi: 10.1146/annurev.physiol.69.022405.154749
39. Kang DS, Tian X, Benovic JL. Role of beta-arrestins and arrestin domain-containing proteins in G protein-coupled receptor trafficking. *Curr Opin Cell Biol.* (2014) 27:63–71. doi: 10.1016/j.ceb.2013.11.005
40. Bush SH, Tollin S, Marchion DC, Xiong Y, Abbasi F, Ramirez IJ, et al. Sensitivity of ovarian cancer cells to acetaminophen reveals biological pathways that affect patient survival. *Mol Clin Oncol.* (2016) 4:399–404. doi: 10.3892/mco.2016.725
41. Suleymanova N, Crudden C, Shibano T, Worrall C, Oprea I, Tica A, et al. Functional antagonism of beta-arrestin isoforms balance IGF-1R expression and signalling with distinct cancer-related biological outcomes. *Oncogene.* (2017) 36:5734–44. doi: 10.1038/onc.2017.179
42. Thomsen ARB, Plouffe B, Cahill TJ III, Shukla AK, Tarrasch JT, Dosey AM, et al. GPCR-G protein-beta-arrestin super-complex mediates sustained G protein signaling. *Cell.* (2016) 166:907–19. doi: 10.1016/j.cell.2016.07.004
43. Jing X, Zhang H, Hu J, Su P, Zhang W, Jia M, et al. β-arrestin 2 is associated with multidrug resistance in breast cancer cells through regulating MDR1 gene expression. *Int J Clin Exp Pathol.* (2015) 8:1354–63.
44. Becker JH, Gao Y, Soucheray M, Pulido I, Kikuchi E, Rodriguez ML, et al. CXCR7 reactivates ERK signaling to promote resistance to EGFR kinase inhibitors in NSCLC. *Cancer Res.* (2019) 79:4439–52. doi: 10.1158/0008-5472.CAN-19-0024
45. Rosano L, Bagnato A. New insights into the regulation of the actin cytoskeleton dynamics by GPCR/beta-arrestin in cancer invasion and metastasis. *Int Rev Cell Mol Biol.* (2019) 346:129–55. doi: 10.1016/bs.ircmb.2019.03.002
46. Son D, Kim Y, Lim S, Kang HG, Kim DH, Park JW, et al. miR-374a-5p promotes tumor progression by targeting ARRB1 in triple negative breast cancer. *Cancer Lett.* (2019) 454:224–33. doi: 10.1016/j.canlet.2019.04.006
47. Ji H, Liu N, Li J, Chen D, Luo D, Sun Q, et al. Oxytocin involves in chronic stress-evoked melanoma metastasis via beta-arrestin 2-mediated ERK signaling pathway. *Carcinogenesis.* (2019) 40:1395–404. doi: 10.1093/carcin/bgz064
48. Song Q, Ji Q, Li Q. The role and mechanism of betaarrestins in cancer invasion and metastasis. *Int J Mol Med.* (2018) 41:631–9. doi: 10.3892/ijmm.2017.3288
49. Peterson YK, Luttrell LM. The diverse roles of arrestin scaffolds in G protein-coupled receptor signaling. *Pharmacol Rev.* (2017) 69:256–97. doi: 10.1124/pr.116.013367
50. Carmona-Rosas G, Alcantara-Hernandez R, Hernandez-Espinosa DA. Dissecting the signaling features of the multi-protein complex GPCR/beta-arrestin/ERK1/2. *Eur J Cell Biol.* (2018) 97:349–58. doi: 10.1016/j.ejcb.2018.04.001
51. Ayoub MA, Landomiel F, Gallay N, Jegot G, Poupon A, Crepieux P, et al. Assessing gonadotropin receptor function by resonance energy transfer-based assays. *Front Endocrinol.* (2015) 6:130. doi: 10.3389/fendo.2015.00130
52. Feng Z, Wen H, Bi R, Ju X, Chen X, Yang W, et al. A clinically applicable molecular classification for high-grade serous ovarian cancer based on hormone receptor expression. *Sci Rep.* (2016) 6:25408. doi: 10.1038/srep25408
53. Bernichtein S, Peltoketo H, Huhtaniemi I. Adrenal hyperplasia and tumours in mice in connection with aberrant pituitary-gonadal function. *Mol Cell Endocrinol.* (2009) 300:164–8. doi: 10.1016/j.mce.2008.10.005
54. Nordhoff V, Gromoll J, Simoni M. Constitutively active mutations of G protein-coupled receptors: the case of the human luteinizing hormone and follicle-stimulating hormone receptors. *Arch Med Res.* (1999) 30:501–9. doi: 10.1016/S0188-4409(99)00076-4
55. Casarini L, Santi D, Simoni M, Poti F. 'Spare' luteinizing hormone receptors: facts and fiction. *Trends Endocrinol Metab.* (2018) 29:208–17. doi: 10.1016/j.tem.2018.01.007
56. Raghuwanshi SK, Nasser MW, Chen X, Strieter RM, Richardson RM. Depletion of beta-arrestin-2 promotes tumor growth and angiogenesis in a murine model of lung cancer. *J Immunol.* (2008) 180:5699–706. doi: 10.4049/jimmunol.180.8.5699
57. Jala VR, Radde BN, Haribabu B, Klinge CM. Enhanced expression of G-protein coupled estrogen receptor (GPER/GPR30) in lung cancer. *BMC Cancer.* (2012) 12:624. doi: 10.1186/1471-2407-12-624
58. Ignatov A, Ignatov T, Weissenborn C, Eggemann H, Bischoff J, Semczuk A, et al. G-protein-coupled estrogen receptor GPR30 and tamoxifen resistance in breast cancer. *Breast Cancer Res Treat.* (2011) 128:457–66. doi: 10.1007/s10549-011-1584-1
59. Heublein S, Lenhard M, Vrekoussis T, Schoepfer J, Kuhn C, Friese K, et al. The G-protein-coupled estrogen receptor (GPER) is expressed in

normal human ovaries and is upregulated in ovarian endometriosis and pelvic inflammatory disease involving the ovary. *Reprod Sci.* (2012) 19:1197–204. doi: 10.1177/1933719112446085

60. Ignatov T, Modl S, Thulig M, Weissenborn C, Treeck O, Ortmann O, et al. GPER-1 acts as a tumor suppressor in ovarian cancer. *J Ovarian Res.* (2013) 6:51. doi: 10.1186/1757-2215-6-51
61. Cheng SB, Quinn JA, Graeber CT, Filardo EJ. Down-modulation of the G-protein-coupled estrogen receptor, GPER, from the cell surface occurs via a trans-Golgi-proteasome pathway. *J Biol Chem.* (2011) 286:22441–55. doi: 10.1074/jbc.M111.224071
62. Chrusciel M, Ponikwicka-Tyszko D, Wolczynski S, Huhtaniemi I, Rahman NA. Extragonadal FSHR expression and function-is it real? *Front Endocrinol.* (2019) 10:32. doi: 10.3389/fendo.2019.00032
63. Cole LA, Hartle RJ, Laferla JJ, Ruddon RW. Detection of the free beta subunit of human chorionic gonadotropin (HCG) in cultures of normal and malignant trophoblast cells, pregnancy sera, and sera of patients with choriocarcinoma. *Endocrinology.* (1983) 113:1176–8. doi: 10.1210/endo-113-3-1176

Conflict of Interest: Research support, advisory board, honoraria, and travel expenses from AstraZeneca, Clovis, Medac, MSD, Novartis, PharmaMar, Roche, Sensor Kinesis, Tesaro, Teva have been received by SM and from AstraZeneca, Medac, PharmaMar, Roche, Tesaro/GSK by FT. All above mentioned companies did not influence the study design, data collection and analysis, decision to publish, or preparation of the manuscript.

The remaining authors declare that the research was conducted in the absence of any commercial or financial relationships that could be construed as a potential conflict of interest.

frontiers in Endocrinology

ORIGINAL RESEARCH
published: 24 September 2020
doi: 10.3389/fendo.2020.00595

Clinical Features of 50 Patients With Primary Adrenal Lymphoma

Yan Wang[1,2†], *Yan Ren*[1†], *Lifen Ma*[1,3†], *Jian Li*[4], *Yuchun Zhu*[5], *Lianling Zhao*[1], *Haoming Tian*[1*] and *Tao Chen*[1*]

[1] Department of Endocrinology and Metabolism, Adrenal Center, West China Hospital of Sichuan University, Chengdu, China, [2] Department of Endocrinology and Metabolism, People's Hospital of Deyang City, Deyang, China, [3] Department of Endocrinology, Baoji Centre Hospital, Baoji, China, [4] Department of Hematology, West China Hospital of Sichuan University, Chengdu, China, [5] Department of Urology, West China Hospital of Sichuan University, Chengdu, China

Background and Objective: Primary adrenal lymphoma is a rare, progressive, easily misdiagnosed adrenal tumor with a poor prognosis. There are limited data on its clinical characteristics, and these have been derived from small sample studies. This study aimed to identify the clinical characteristics and prognosis of primary adrenal lymphoma.

Methods: This single-center study retrospectively analyzed data of 50 primary adrenal lymphoma patients treated between January 2008 and January 2018. Demographic information, biochemical indexes, computed tomography images, pathological findings, treatment regimens, and prognostic factors were analyzed.

Results: The median age of onset was 60.3 years, and 30 (60.0%) of 50 patients were male. Abdominal pain was the most common symptom, followed by incidentaloma and B symptoms. On average, patients presented with elevated lactate dehydrogenase (348 IU/L, normal range 110–220 IU/L) and hydroxybutyrate dehydrogenase levels (287 IU/L, normal range 72–182 IU/L) and decreased high-density lipoprotein cholesterol levels (0.88 mmol/L, normal range > 0.9 mmol/L). Bilateral lesions in the adrenal glands were observed in 30 (60.0%) patients. Computed tomography showed that 42 (84%) patients had signs of infiltration. Diffuse large B-cell lymphoma was present in 44 (88%) patients. Immunohistochemistry revealed that 70.6% (12/17), 89.5% (17/19), 92.0% (23/25), and 68.8% (11/16) of patients were positive for *MYC*, *p53*, *BCL2*, and both *MYC* and *BCL2*, respectively. Combined chemotherapy was associated with a good prognosis.

Conclusions: Early diagnosis of primary adrenal lymphoma depends on a combination of biochemical examination, imaging studies, and pathological biopsy, and combined chemotherapy may lead to a better prognosis.

Keywords: primary adrenal lymphoma, diffuse large B-cell lymphoma, high-density lipoprotein cholesterol, proto-oncogene, Epstein–Barr virus infection

OPEN ACCESS

Edited by:
Jianfeng Liu,
Huazhong University of Science and Technology, China

Reviewed by:
Andrea M. Isidori,
Sapienza University of Rome, Italy
Irina Bancos,
Mayo Clinic, United States

***Correspondence:**
Haoming Tian
hmtian999@126.com
Tao Chen
dr.chentao@qq.com

[†] *These authors have contributed equally to this work*

Specialty section:
This article was submitted to Cancer Endocrinology, a section of the journal Frontiers in Endocrinology

Received: *06 April 2020*
Accepted: *21 July 2020*
Published: *24 September 2020*

Citation:
Wang Y, Ren Y, Ma L, Li J, Zhu Y, Zhao L, Tian H and Chen T (2020) Clinical Features of 50 Patients With Primary Adrenal Lymphoma. Front. Endocrinol. 11:595. doi: 10.3389/fendo.2020.00595

INTRODUCTION

In clinical practice, adrenal masses are frequently incidental findings on imaging studies that are not specifically performed for adrenal diseases. A systematic review demonstrated that the estimated risk for malignancies was 0.2% in all incidentalomas (1). Computed tomography (CT) is helpful for the diagnosis of benign and malignant tumors. However, there are limited data (only two studies

involving 102 true incidentalomas) indicating that a CT density of >10 HU has high sensitivity for the detection of adrenal malignancies, This indicate that adrenal masses with a density of ≤10 HU are unlikely to be malignant (2). Among the diverse malignant causes of incidentalomas, a primary adrenal lymphoma (PAL) is rare causative tumor (2). In 2013, a systematic review indicated that <200 PAL cases have been reported in the English literature (3). Despite the rarity of this disease, PAL induces considerable clinical concern. First, despite the absence of benign characteristics, a PAL on CT and/or magnetic resonance imaging (MRI) may lead to misdiagnosis in the initial evaluation (4); furthermore in some cases, PAL is difficult to distinguish from adrenocortical carcinoma (ACC) (5) and pheochromocytoma (6). Second, PAL is a progressive disease with a poor prognosis, and some patients die before effective treatment can be administered (3). Therefore, early diagnosis is vitally important. Third, PAL belongs to non-Hodgkin lymphoma (NHL), While, diffuse large B-cell lymphoma (DLBCL) is the most common type, the pathophysiology of PAL has not been fully elucidated. Fourth, whether there is a strong association between NHL and decreased HDL-C is inconsistent in previous research (7, 8). Decreased average HDL-C levels and increased monocytes counts have been previously described in patients with non-Hodgkin lymphoma (9) and lymphoblastic leukemia (10). The underlying mechanism may be related to cytokines, such as interleukin-10, which are excessively secreted from lymphoma cells (11, 12). Inversely, a clear or strong association between these lipid traits and the most common NHL subtypes including DLBCL was not found, using the data of genome-wide association study from the Inter Lymph Consortium Mendelian randomization (MR) analysis (8). To date, the majority of published studies on PAL have been constrained by small sample size and insufficient clinical information. So far, this is the largest cohort of 50 patients with pathologically diagnosed PAL. Patients were evaluated retrospectively, to investigate the clinical characteristics and influence of treatment on prognosis over the course of a 2-year follow up period.

METHODS

From January 2008 to January 2018, 50 Chinese patients were pathologically diagnosed with PAL at the West China Hospital of Sichuan University in accordance with criteria that were suggested by a previous study. These diagnostic criteria included the following: a histologically proven lymphoma, no prior history of lymphoma, and dominant adrenal lesions in the presence of other organs and/or lymph nodes metastases (3). Histological classification of the lymphoma was based on the 2017 World Health Organization criteria (13). The positivity of molecular markers on immune-histochemical staining was attributed by the percentage of positive cells as follows: CD10 and BCL6 >30%, MYC >40% and BCL2 >50%. DLBCL was further classified into germinal center B-cell (GCB) and non-GCB subtypes by the Hans algorithm bases on the positivity of three markers (CD10, MUM1/IRF4, and BCL6) (14). The GCB subtype was characterized by $CD10^+/MUM1^-$, $CD10^+/MUM1^+$, or $CD10^-/MUM1^-/BCL6^+$. The non-GCB subtype was characterized by $CD10^-/BCL6^-$, and $CD10^-/MUM1^+/BCL6^+$ cases (14, 15). The presence of Epstein-Barr virus (EBV) RNA was examined by *in situ* hybridization (ISH) in lymphoma biopsy specimen. Moreover, fluorescence *in situ* hybridization (FISH) was performed to examine gene translocations (e.g., *MYC*, *BCL2*, and *BCL6*) (9).

Demographics information, biochemical indices, baseline cortisol, CT findings, pathological findings, treatment regimens, and prognosis, were collected for each patient. Adrenal insufficiency was defined as an early-morning (8–10 A.M.) serum cortisol <140 nmol/L and a plasma adrenocorticotropic hormone (ACTH) level 2-fold greater than the upper limit of the normal range (16). ACTH was determined using the electrochemiluminescence technique with the normal reference range being 7.2–63.3 pg/ml. Lipid profile was collected with the normal reference range being>0.9 mmol/L for HDL-C and 0.29–1.83 mmol/L for triglyceride (TG). The Ann Arbor classification was used for staging of PAL, based on the findings of the positron emission tomography–CT (PET-CT) or CT. This study was approved by the Ethical Committee of West China Hospital of Sichuan University (approval no. 2017-378) and adhered to the principles evinced in the Declaration of Helsinki and its later amendments.

Both MS Excel 2007 and R statistical software were used for the statistical analyses. Continuous data with normal and skewed distributions were described as the mean ± standard deviation (SD) and median (interquartile range), respectively, and were compared with an independent Student's *t*-test. Dichotomous data were compared using the chi-square test and Fisher's exact tests, and the results were described as percentages. The levels of high-density lipoprotein cholesterol (HDL-C), monocytes, lactate dehydrogenase (LDH), and hydroxybutyrate dehydrogenase (HBDH) were compared with the reference ranges of the general population from the same area. Cox proportional hazard models were used to evaluate the risk factors that contributed to the prognosis. A Kaplan–Meier approach was used to calculate overall survival. $P < 0.05$ was considered statistically indicative of statistical significance.

RESULTS

General Clinical Characteristics

In this study population, 30 (60.0%) of the 50 patients were male. The median age at PAL onset was 60.3 years (range 21–84 years). Bilateral involvement was observed in 30 (60%) patients. With regard to comorbidities, six patients had hepatitis B infection, three patients each had tuberculosis and type 2 diabetes, two had gastric ulcers, two had lymphomas in other parts of body, one had small cell lung cancer, one had uveitis, one had thrombotic thrombocytopenic purpura, one had hemolytic anemia, one had rheumatoid-arthritis, and one had a human immunodeficiency virus (HIV) infection. None of the patients had a history of cancer and autoimmune adrenalitis.

Except for three patients without data, 47 patients had a clear presentation of the characteristic clinical features of PAL. Abdominal pain was the most common symptom in 23 (48.9%) patients, followed by incidentaloma in 14 (29.8%) patients, B symptoms in 13 (27.7%, fever, night sweats, and weight loss), gastrointestinal symptoms in 7 (17.0%), fatigue in 2 (4.3%), and hyperpigmentation in 2 (2.1%) (**Figure 1**). In addition, hepatosplenomegaly was found in 4 of 37 patients (10.8%). Elevated LDH (30 of 37; 81.1%) and HBDH (28 of 37; 75.7%) levels were observed. The blood lipid profiles of patients were characterized by decreased HDL-C levels and elevated TG levels, whereas the total cholesterol and low-density lipoprotein cholesterol (LDL-C) levels were within the normal range. Patients' total white blood cell counts were within the normal range. An evaluation of the adrenal function in the 35 patients with available data showed that only 4 (11.4%) patients had baseline cortisol (17.64, 120.4, 79.24, and 94.86 nmol/L, respectively), and ACTH levels (216.2, 391.0, 219.9, and 325 pmol/L, respectively), that were suggestive of adrenal insufficiency, including 3 (8.5%) patients with bilateral adrenal involvement and 1 (2.9%) patient with unilateral adrenal involvement. All patients were treated with prednisone (5–10 mg daily). In 8 (38.1%) patients, EBV-RNA was detected in the serum (**Table 1**).

Radiography Findings

As shown in **Figure 2**, PAL patients demonstrated versatile CT findings with regard to tumor shape, edge, enhancement patterns, liquidation/necrosis, and local infiltration. Unenhanced CT findings were available for all patients and enhanced CT findings were available for 33 (66%) patients. Briefly, the adrenal glands were unilaterally and bilaterally affected in 20 (40.0%) and 30 (60%) patients, respectively. The median diameter of the lesions was 6.5 ± 2.7 cm (1.7–12.1 cm) and 6.6 ± 3.6 cm (1.4–16.8 cm) on the left and right sides, respectively. The edges of 26 lesions were well-defined, whereas 21 lesions had ill-defined edges. The median non-contrast CT density was 31.8 (25.8, 44.4HU). None of the lesions had a measurement value of <10 HU. On contrast imaging with iopamidol, moderate enhancement in the arterial and the parenchyma phases were observed bilaterally, and enhancement patterns were heterogeneous in 42.2% of patients. A total of 76.2% of patients presented with signs of infiltration of local organs or tissues (**Table 2**). Only two patients underwent MRI in our cohort, 1 case was characterized by an irregular mass with ambiguous boundary, measuring 5.3 × 4.1 × 3.9 cm^3, around the left kidney with uneven low signal in the T1-weighted image, slightly high signal in the T2-weighted image, and obvious inhomogeneous enhancement on the enhanced scan. The MRI data of the other case detail was not available because the patient was being examined in another hospital. Additionally, PET/CT were examined in three patients. The results showed that the glucose metabolism in the adrenal was obviously increased. Additionally, one case was accompanied by the increased metabolism of glucose involving the abdomen and neighboring lymph nodes and liver. Seventeen patients underwent head CT or MRI screening, and only one patient had lymphoma invasion in the central nervous system.

Pathological Features

A total of 36 patients were pathogenically diagnosed based on CT/ultrasound-guided needle core biopsy findings, and 14 patients were diagnosed after surgical resection. Of patients diagnosed with PAL, 44 (88%) patients were diagnosed with DLBCL, 4 (8.0%) with extra-nodal natural killer (NK)/T-cell lymphoma (nasal type), and 2 (4.0%) with peripheral T-cell lymphoma (PTCL). Of the 44 patients with DLBCL, 7 were further classified to have the GCB subtype, and 37 were classified into the non-GCB subtype. The seven patients

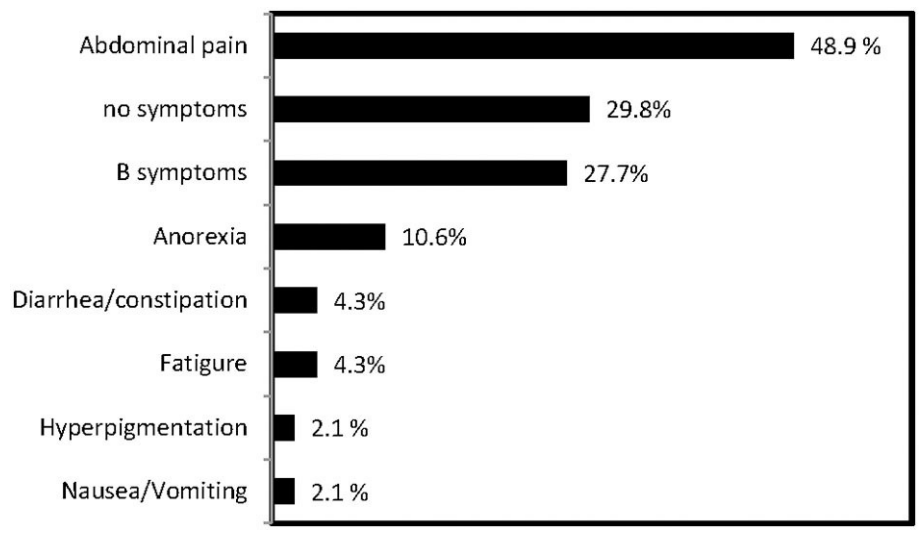

FIGURE 1 | Frequency of clinical presentations of PAL in this series.

TABLE 1 | Clinical characteristics of PAL patients.

	Total	Reference
n.	50	
Age(years)	60.3 ± 14.1	–
Male (n)	30 (60%)	–
Unilateral/bilateral involvement	22/28	–
BMI (kg/m^2)[a]	22.2 ± 3.2	–
Malignances(*n*, %)	1 (2.0%)	–
Autoimmune diseases(*n*, %)	5 (8.0%)	–
Infectious disease (*n*, %)	10 (20%)	–
TG (mmol/L)[b]	1.49 ± 0.69	0.29–1.83
HDL-C (mmol/L)[b]	0.88 ± 0.38	>0.9
UA (μmol/L)[b]	329.2 ± 296.9	240.0–490.0
LDH (IU/L)[b]	571.2 ± 358.0	110–220
LDH %(*n*, %)[b,d]	30 (81.1%)	–
HBDH (IU/L) [b]	444.5 ± 289.0	72–182
HBDH %(*n*, %) [b,d]	28 (75.5%)	–
WBC [b]	5.3 ± 2.2	3.5–9.5 × 10^9/L
Neutrophils %	62.8 ± 14.9	40–75.0%
Lymphocytes %	21.1 ± 9.41	20–50.0%
Monocytes %	8.7 ± 2.9	3–10.0%
Adrenal insufficiency (*n*)[c]	4 (11.4%)	–
Bilateral adrenal involvement	3 (8.5%)	
Unilateral adrenal involvement	1 (2.9%)	
Serum Epstein-Barr virus-encoded small	8 (38.1%)	
Bilateral lesions (*n*, %)	30 (60%)	–
Tumor Size (cm)		
Left (range)	6.5 (1.7, 12.1)	–
Right (range)	6.7(1.4, 16.8)	–

Adrenal insufficiency was defined as an early morning (8–10 A.M.) serum cortisol level <140 nmol/L and a plasma adrenocorticotropic hormone (ACTH) level that was 2-fold greater than the upper limit of the normal range (17), because a corticotropin stimulation test is not feasible in the western area of China. The cortisol level of four patients with adrenocortical insufficiency were 94.86, 79.24, 120.40, 17.64 nmol/L, and corresponding ACTH level were 325, 219.9, 391, 216.2 pmol/L, respectively. [a]Twenty-five patients with data regarding BMI; [b]37 patients with data regarding TG, HDL-C, UA, LDH, HBDH level, and WBC count; [c]34 patients with data regarding ACTH and early-morning cortisol level; [d](n) represented the number of patents whose LDH or HBDH level were above the upper limits of the reference range.

BMI: body mass index; TG triglyceride; UA uric acid; LDH: lactate dehydrogenase; HBDH: hydroxybutyrate dehydrogenase; HDL-C: high-density lipoprotein cholesterol.

6 HBV, 3 TB and diabetes respectively, 2 gastric ulcers, 2 lymphomas in other parts, 1 small cell lung cancer, 1 uveitis, 1 thrombotic thrombocytopenic, 1 hemolytic anemia and 1 rheumatoid arthritis. 1 HIV, and no patients with tumor history and autoimmune adrenalitis.

with the GCB subtype showed the following profiles: two patients, CD10$^+$/MUM1$^-$, two patients, CD10$^+$/MUM1$^+$; and three patients, CD10$^-$/MUM1$^-$/BCL6$^+$, The 37 patients with non-GCB subtypes showed the following profiles: four patients, CD10$^-$/BCL6$^-$ and 33 patients, CD10$^-$/MUM1$^+$/BCL6$^+$. In **Supplemental Figure 1**, we present the pathological findings of a 59-year-old woman who was diagnosed with DLBCL. Immunohistochemical analysis showed that the tumor cells were positive for CD20, BCL2, BCL6, and MUM-1 and were negative for CD5 and CD10.

All patients a except for two showed strong positivity for Ki-67 (most >50%). Immunohistochemical analysis revealed that 70.6% (12/17) of patients were positive for *MYC*, 89.5% (17/19) for *p53*, 92.0% (23/25) for *BCL2*, and 68.8% (11/16) for both *MYC* and *BCL2*. EBV-RNA screening was performed by ISH in 25 patients, and four patients had positive results. Gene rearrangements were screened in 14 patients, 78.6% (11/14) of whom exhibited *IGH*/*IGK* rearrangement. FISH was further performed in five patients, three of whom carried the *BLC6* translocation and 1 had a *MYC* translocation (**Supplemental Figure 2**). Moreover, two of the five patients with T-cell lymphoma had TCRγ gene rearrangement, and both patients tested positive for EBV-RNA in lymphoma cells. Twenty-five patients underwent bone marrow (BM) biopsy, and 8.0% ($n = 4$) were found to have BM involvement.

Factors Associated With the Prognosis

Of the 44 patients with available data, 14 patients had undergone surgical resection, and four subsequently accepted chemotherapy after surgical resection; A further 16 patients underwent chemotherapy after diagnosis based on CT/ultrasound-guided biopsy findings. Among the 20 patients who underwent chemotherapy, 15 had complete remission, four had partial remission, and one had one no remission. Fourteen patients only used glucocorticoid agents and/or supportive treatment due to poor clinical conditions at the time of diagnosis (**Table 3**).

The median follow-up duration was 22.45 months in 35 patients for whom data were available. The 1-year and 2-year overall survival rates were 79.5 and 72.5%, respectively, during follow-up. In this cohort, four patients died in the hospital without undergoing chemotherapy, and three patients died within 3 months to 2 years due to causes such as multi-organs failure (MOF) and severe infection.

Cox univariate proportional hazard models were employed to investigate the association of risk factors with the prognosis of PAL. The 2-year overall survival rate was 84.2% in patients who underwent chemotherapy, compared to 41.7% in patients who did not undergo chemotherapy (i.e., surgery alone and supportive treatment). The results showed that chemotherapy alone was associated with a lower risk of death ($P = 0.029$); and the mortality risk was 78.9% lower in patients who underwent chemotherapy compared to those who did not. The LDH, TG, and HDL-C levels, adrenal insufficiency, and international prognostic index scores were not associated with prognosis. Compared with the patients who were treated with chemotherapy and/or surgery to improve survival, the patients who only received palliative care had higher LDH and HBDH levels. In addition, baseline patient characteristics, including age, sex, HDL-C levels, pathologic type, and adrenal involvement, showed no differences between these two groups (**Supplemental Table 1**).

The Kaplan–Meier approach was used to examine the difference in the overall survival between the chemotherapy group and non-chemotherapy group (**Figure 3**). There were 19 patients in the chemotherapy group (including four patients who received postoperative chemotherapy) and 16 patients in the non-chemotherapy group (including nine patients who received supportive treatment, 5 who underwent surgery, and 2 with an unknown treatment strategy). After 24-months

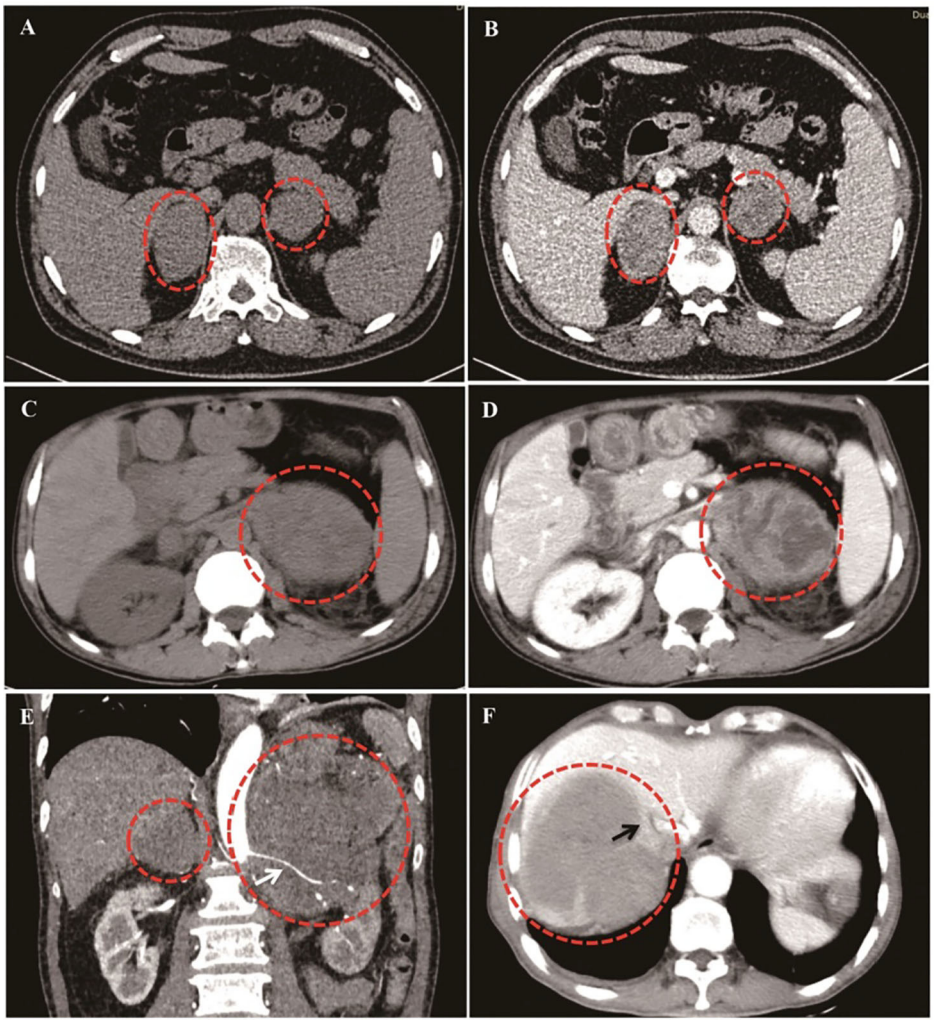

FIGURE 2 | Different CT imaging features of PAL patients. **(A,B)**: Bilateral PAL with oval/round shape, well-defined edge, moderately enhanced in parenchyma phase, and homogeneous enhancement patterns. **(C,D)**: Bilateral PAL with liquidation/necrosis in the left tumor mass, which was obvious after contrast by iodamide. **(E)**: Lymphoma cells surrounded the renal artery without invasion (White arrow). **(F)**: Right lymphoma mass invaded inferior vena cava (Black arrow).

follow-up, the survival rate was slightly significantly higher in the chemotherapy group than in the non-chemotherapy group ($P = 0.049$).

DISCUSSION

PAL is a rare but fatal disease, and understanding of its clinical manifestations, pathogenesis, and prognostic factors (3). Therefore, additional information is needed to better understand this disease. This study retrospectively analyzed the features of 50 PAL patients to evaluate their clinical presentations, laboratory results, imaging findings, pathologic details, potential mechanisms, and prognostic factors.

The median age at onset was ∼60 years, and there were more male patients included than females (1.4 times more men than women), consistent with the results reported in several previous studies (5, 18). Notably, 29.8% of patients were asymptomatic, and PAL was detected during routine health checkups. This result was considerably different from that of a previous large case series, in which only a few patients (<1%) were identified

TABLE 2 | Extra-adrenal infiltrations.

Affected organ/tissues	*n* (%)
Kidney vasculatures	19 (45.2)
Lymph nodes	16 (38.1)
Kidney	15 (35.7)
Inferior vena cava	10 (23.8)
Liver	7 (16.7)
Pancreas	6 (14.3)
Spleen	4 (9.5)
Osteomedullary invasion	4/25 (8.0)

Forty-two patients were found to have extra-adrenal infiltration.

incidentally (3). In another case series in Japan, two of five patients were asymptomatic (18). Furthermore, a few cases have been reported as adrenal incidentaloma without any symptoms (9, 19, 20). Strikingly, most of the asymptomatic patients had bilaterally disease, and three patients in this study and one patient in the previous study (18) developed a tumor mass with a maximum diameter of more than 8 cm. These results suggested the heterogeneity of PAL with regard to clinical manifestations and emphasized the differential diagnosis of adrenal incidentaloma, especially in those with bilateral lesions and larger sized tumors.

TABLE 3 | Types and schedules of chemotherapy and patient responses.

Chemotherapy type	Chemotherapy regimen (*)	Case (*n*)	Response
CHOP	1*	1	PR
	6*	2	2CR
	8*	3	3CR
	Unknown	3	1CR+1PR+1NR
R-CHOP	6*	2	2CR
	8*	1	CR
	Unknown	2	CR
CHOP+ R-CHOP+Gemox	CHOP × 2*+R-CHOP × 1*+Gemox × 6*	1	CR
R+V+P	1*	1	PR
Gemox	4*	1	CR
R-CHOP+ICE	R-CHOP × 8*+ICE × 4*	1	CR
GLIDE	4*	1	CR
P	2*	1	PR

*CHOP, Cyclophosphamide+ Doxorubicin+ Vincristine+ Prednisolone; R, Rituximab; V, Vincristine; P, Prednisolone; ICE, Ifosfamide+ Cisplatin+ Etoposide; GLIDE, Gemcitabino+ L-asparaginase+ Ifosfamide+ Dexamethasone+ Etoposide; Gemox, Gemcitabino+Oxaliplatin; CR, complete remission, PR, partial remission, NR, no remission; *, chemotherapy regimen.*

As expected, LDH and HBDH levels were increased in >80% of patients. In our series, the patients who only accepted palliative care had higher LDH and HBDH levels than those who were treated with chemotherapy and/or surgery to improve survival, whereas the patients who were treated with palliative care had worse conditions. Therefore, we speculate that high levels of LDH and HBDH are predictive factors for the poor prognosis of PAL. Moreover, this study demonstrated that lightly decreased average HDL-C levels and increased monocytes counts in PAL patients. Therefore, such changes in lipids profiles, white blood cell counts, and LDH/HBDH level seemed to be unique features of PAL in the setting of adrenal masses. However, our Cox multivariate proportional hazard model analysis also did not reveal an association between LDH, TG, and HDL-C levels and the prognosis of PAL.

It has been suggested that adrenal insufficiency in PAL is significantly related to older age, bilateral lesions, and hyper-segmentation (3). In our study, adrenal function was evaluated in 35 patients, and only 4 (11.4%) were found to have adrenal insufficiency: three patients had bilateral adrenal involvement, and one patient had unilateral adrenal involvement. Unilateral involvement may also be related to the patient's history of tuberculosis. The level of ACTH and baseline cortisol in patients with bilateral lymphoma who did not have adrenal insufficiency were 123.1 pmol/L (95% CI: 48.6, 197.6) and, 444.2 nmol/L (95% CI: 348.4, 540.1), respectively. In contrast, the incidence of adrenal insufficiency was largely less than those in previous studies, with a reported incidence of 61% (3). The unexpected commonness of adrenal insufficiency in PAL patients is likely due to biases related to publication and research methods (21). The data evaluated in this previous study were obtained from published literature, whereas our study used data from retrospective cases in a single medical center. Moreover, in our series, the incidence of bilateral involvement was 30 (60%), with an average age of 62 years vs. 75% bilateral involvement, with an average age of 60 years in previous research. Finally, only

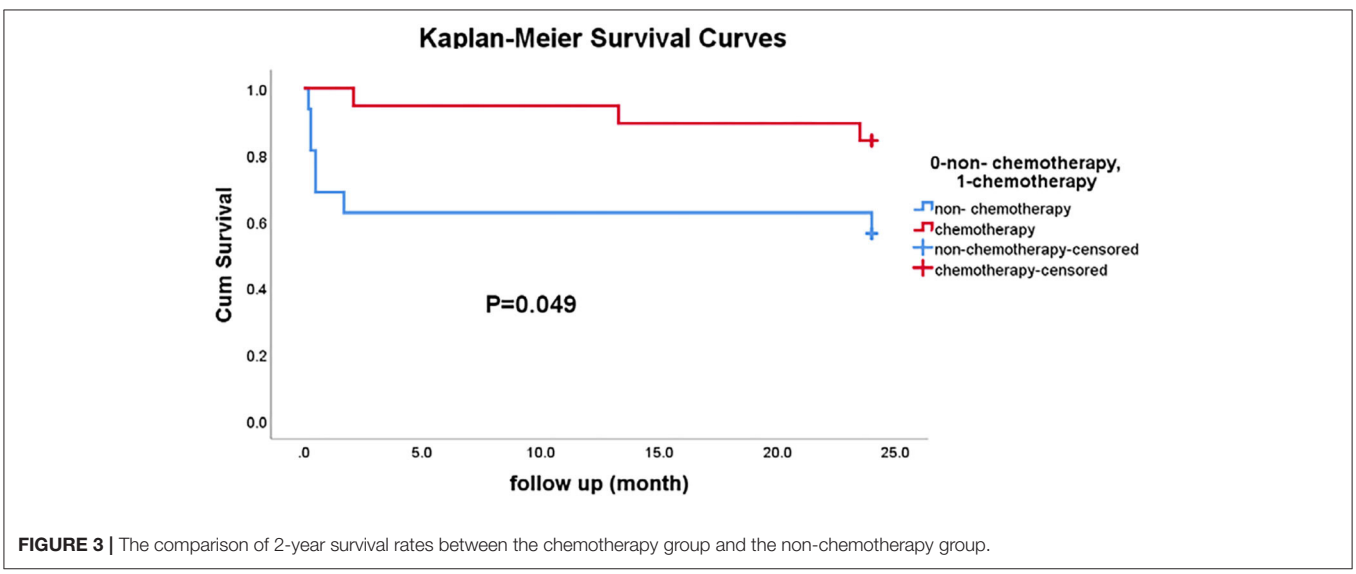

FIGURE 3 | The comparison of 2-year survival rates between the chemotherapy group and the non-chemotherapy group.

54% of the cases in this previous study were from Asia, while all cases in our study were from Asian. This poses the question of whether the differences in the incidence of adrenal insufficiency were related to race; however, further observations and research are necessary to demonstrate this possible correlation.

The CT findings were similar to those in previous studies (3), including large tumor size, the incidence of slightly hypodense values in non-contrast CT scans, slight to moderate enhancement after the administration of iopamidol, a frequently observed heterogeneous appearance, and adjacent infiltration. Among these features, necrosis or cysts were observed in several patients and were misdiagnosed as pheochromocytomas or ganglioneuromas in the initial evaluation (data not shown), which is consistent with other reports (3, 22). Therefore, diagnosis of PAL at the initial evaluation based on the findings of traditional imaging modalities is challenging (23). Generally, the density of the adenomas is equal to or slightly lower than that of the normal adrenal gland tissue unless they are necrotic and/or cystic. The density is usually <10 HU in lipid-rich adenomas(70%) and between 10 and 30 HU in lipid-poor adenomas (30%). Our series show that the non-contrast CT density of PAL was 31.8 (25.8, 44.4) HU. However, it is still indistinguishable because of the similar appearance in adrenal lymphoma, pheochromocytoma, metastasis, and ACC. Heterogeneous enhancement, necrosis, and hemorrhage can be seen. Only a little sign can provide profitable alert for differential diagnosis. The enlargement of the retroperitoneal lymph nodes is common in adrenal lymphoma. The diversity in size was found in pheochromocytomas (17), It is usually larger than adenomas, but smaller than metastatic tumors, and the attenuation values are often similar to those of the muscle tissue, and are significantly higher than those of adrenal adenomas. Common primary malignancies and possible calcification were both found in metastases. Large masses (usually >6 cm) and invasion of the inferior vena cava is a common finding of ACC. Otherwise, MRI might be extra helpful for the differential diagnosis of PAL and pheochromocytoma or ganglioneuroma (23). Although T1 hypo-intense and T2 hyper-intense lesions were typically characteristic, a mild to moderate enhancement can be seen on the enhanced scan in adrenal lymphoma, isointense with ring-like or uneven enhancement after contrast administration may be found in adrenal metastases, and heterogeneous hyper-intensity was manifested in ACC. Regrettably, the one 1 case that had data available, was characterized by obvious uneven enhancement, rather than mild to moderate enhancement, which was inconsistent with the characteristics of previous literature reports (23). The value of MRI in these cases should be further evaluated in the future.

DLBCL was the commonest pathologic type (86%) in this cohort, consistent with the findings from other studies (3). Additionally, three patients had extra-nodal NK/T-cell lymphoma (nasal type), and three patients had PTCL. This distribution was different from that in previous reports, in which PTCL was more common, and only 3 NK/T-cell (nasal types) were identified among 187 cases of PAL (3). Among patients with DLBCL, seven were further classified as having the GCB subtype. A previous study suggested that those with the GCB subtype might have a better prognosis (24, 25). The longest complete remission period (56 months) was seen in a patient with GCB subtype, but the available data were not sufficient to draw a firm conclusion.

The etiology of PAL has not been fully elucidated. Immune dysfunction, EBV infection, and mutations in the *p53* and proto-oncogenes have been implicated (3, 21). In this cohort, few patients had a clear history of cancer, HIV infection, or autoimmune diseases, and no patients had a history of autoimmune adrenalitis, except for Hepatitis B virus infection (16.2%). Notably, this study revealed high positivity of *P53* (17/19), *BCL2* (23/25), and *MYC* (12/17). The phenomenon of *MYC* and *BCL2* co-expression was also frequently observed (11/16). Data on gene rearrangement are limited but suggested that the presence of the *IGH/IGK* rearrangement with *BCL2* or *MYC* expression might play a significant role in lymphoma genesis. With regarding EBV infection, only 4 of 25 patients exhibited the EBV-DNA in PAL tissues, this frequency was lower than that reported previously (45%) (26). Furthermore, a study showed that EBV infection seemed more active in T-cell lymphoma (27). All three patients with extra-nodal NK/T-cell lymphoma had EBV genomes in PAL tissues, TCRγ gene rearrangement might mediate EBV-induced T-cell transformation.

PAL is an aggressive lymphoma with strong Ki-67 expression in almost all patients, different from Castleman's disease with high interleukin-6 (IL-6) expression, heterotopic ossification, and benign micro-nodular hyperplasia appeared in proximity to the lymphatic tissue invading the adrenal (28). The reported survival rate approximately almost 20%, is poor at the 12-month follow-up (3). Due to the rarity of PAL, few studies have presented follow-up data.

Moreover, the 1-year and 2-year overall survival rates in the 35 patients with available follow-up data were 79.5 and 72.5%, respectively. This survival rate is higher than previously reported. Kim et al. (29) summarized 31 PAL cases and found that for patients with DLBCL treated with a median of six cycles of R-CHOP (cyclophosphamide, doxorubicin, vincristine, prednisone) chemotherapy, the 2-year overall and progression-free survival rates were 68 and 51%, respectively. With regard to the difference, early diagnosis could be one of the possible reasons; the initial indication of PAL was an incidentaloma during routine healthy examination in 29.8% of patients, which was significantly higher than that previously reported (1%) (30). Second, central nervous system involvement in PAL has a negative impact on long-term prognosis. In our series, only one patient had lymphoma invasion in the central nervous system.

Consistent with the findings of previous studies, chemotherapy, especially with the addition of rituximab, significantly improved outcomes (3, 29, 30). In early studies, the 1-year survival rate was nearly 20%, while in a recent series with more patients receiving rituximab add-on therapy, the 2-year survival rate was nearly 62% (5). In our analysis, the overall survival rates were 84.2 and 41.7% in patients who did and did not receive chemotherapy (surgery alone and supportive treatment), respectively. Meanwhile, the 2-year survival rate in the chemotherapy group was slightly higher than

that in the non-chemotherapy group. The reasons for failure to undergo chemotherapy treatment included concerns about the effectiveness of the treatment, side effects, financial burdens, and severity of co-morbidities. Notably, two patients showed rapid deterioration and died in the hospital before chemotherapy could be administered, which further emphasizes the importance of early diagnosis of PAL according to clinical indications, e.g., adrenal imaging, alterations in LDH/HBDH levels, and changes in lipid profiles.

As a single center study, we collected the largest sample of PAL so far. Additionally we analyzed the clinical characteristics, pathological types, treatment, and prognosis. However, there are several limitations to the present study. A major limitation is its retrospective design, which may have led to missing or incorrect data; further, the assessment of adrenal function was insufficient. Another limitation is the incomplete follow-up data; only 15 patients completed a follow-up of more than 2 years. Furthermore, an inaccurate result could be deduced from the incomplete data. The third limitation is that more than half of the patients were diagnosed based on needle core biopsy findings, and in some cases insufficient tumor tissue was obtained for pathological analysis, especially for FISH. Otherwise, MRI was performed in only 2 cases. Hence, most of these deficiencies should be overcome when treating the adrenal incidentaloma again. The more complete evaluation including MRI was performed and clinical data were collected to accurately analyze the clinical characteristics of PAL and provide important reference for the choice of treatment strategy.

CONCLUSIONS

In summary, this study systematically analyzed the clinical characteristics of 50 patients with PAL. Most patients developed PAL at the age of 60 years, with men making up the majority of the study cohort. Abdominal pain, incidentaloma, and B symptoms were the most common manifestations. Decreased HDL-C levels and lymphocyte counts and elevated LDH/HBDH levels demonstrated potential value for the differential diagnosis of PAL. DLBCL (non-GCB subtype) and extra-nodal NK/T-cell lymphoma (nasal type) were the most common pathological types. Moreover, tumor masses exhibited an aggressive growth pattern. Gene mutations (*P53*, *MYC*, and *BCL2*) and EBV infection played important roles in lymphoma genesis. Early diagnosis and combined chemotherapy were associated with a better prognosis.

DATA AVAILABILITY STATEMENT

The raw data supporting the conclusions of this article will be made available by the authors, without undue reservation.

ETHICS STATEMENT

This study was approved by the Ethics Committee of West China Hospital of Sichuan University and adhered to the Declaration of Helsinki (No. 2017-378). The patients/participants provided their written informed consent to participate in this study. Written informed consent was obtained from the individual(s) for the publication of any potentially identifiable images or data included in this article.

AUTHOR CONTRIBUTIONS

TC and HT developed and designed the research. TC obtained funding, TC, YW, LM, and YR interpreted the data and drafted the manuscript. YZ and LZ contributed to data collection. All the authors revised and approved the final version of the manuscript.

FUNDING

This study was partially supported by a grant sponsored by the Science & Technology Department of Sichuan Province (2017FZ0066) and a 1.3.5 project for disciplines of excellence, West China Hospital, Sichuan University (ZYGD18022).

ACKNOWLEDGMENTS

We thank Prof. Shuyi Liu and Prof. Dong Wei for their kind help in collecting follow-up data from several patients. We thank all of the patients who kindly participated in the PAL survey.

SUPPLEMENTARY MATERIAL

The Supplementary Material for this article can be found online at: https://www.frontiersin.org/articles/10.3389/fendo.2020.00595/full#supplementary-material

REFERENCES

1. Cawood TJ, Hunt PJ, O'Shea D, Cole D, Soule S. Recommended evaluation of adrenal incidentalomas is costly, has high falsepositive rates and confers a risk of fatal cancer that is similar to the risk of the adrenal lesion malignant; time for a rethink? *Eur J Endocrinol.* (2009) 161:513–27. doi: 10.1530/EJE-09-0234
2. Fassnacht M, Arlt W, Bancos I, Dralle H, Newell-Price J, Sahdev A, et al. Management of adrenal incidentalomas: european society of endocrinology clinical practice guideline in collaboration with the european network for the study of adrenal tumors. *Eur J Endocrinol.* (2016) 175:G1–34. doi: 10.1530/EJE-16-0467
3. Rashidi A, Fisher SI. Primary adrenal lymphoma: a systematic review. *Ann Hematol.* (2013) 92:1583–93. doi: 10.1007/s00277-013-1812-3
4. Libe R, Dall'Asta C, Barbetta L, Baccarelli A, Beck-Peccoz P, Ambrosi B. Long-term follow-up study of patients with adrenal incidentalomas. *Eur J Endocrinol.* (2002) 147:489–94. doi: 10.1530/eje.0.1470489
5. Laurent C, Casasnovas O, Martin L, Chauchet A, Ghesquieres H, Aussedat G, et al. Adrenal lymphoma: presentation, management and prognosis. *QJM.* (2017) 110:103–9. doi: 10.1093/qjmed/hcw174
6. Joseph FG, Cook S, Gowda D. Primary adrenal lymphoma with initial presentation concerning for bilateral adrenal pheochromocytomas. *BMJ Case Rep.* (2017) 2017:bcr2016219136. doi: 10.1136/bcr-2017-220549

7. Lim U, Gayles T, Katki HA, Stolzenberg-Solomon R, Weinstein SJ, Pietinen P, et al. Serum high-density lipoprotein cholesterol and risk of non-hodgkin lymphoma. *Cancer Res.* (2007) 67:5569–74. doi: 10.1158/0008-5472.CAN-07-0212
8. Kleinstern G, Camp NJ, Berndt SI, Birmann BM, Nieters A, Bracci PM, et al. Lipid trait variants and the risk of non-hodgkin lymphoma subtypes: a mendelian randomization study. *Cancer Epidemiol Biomarkers Prev*. (2020) 29:1074–8. doi: 10.1158/1055-9965.EPI-19-0803
9. Rizzo C, Camilleri DJ, Betts A, Gatt A, Fava S. Primary bilateral non-hodgkin's lymphoma of the adrenal gland presenting as incidental adrenal masses. *Case Rep Med.* (2015) 2015:620381. doi: 10.1155/2015/620381
10. Halton JM, Nazir DJ, McQueen MJ, Barr RD. Blood lipid profiles in children with acute lymphoblastic leukemia. *Cancer.* (1998) 83:379–84. doi: 10.1002/(SICI)1097-0142(19980715)83:2<379::AID-CNCR24>3.0.CO;2-P
11. Moraitis AG, Freeman LA, Shamburek RD, Wesley R, Wilson W, Grant CM, et al. Elevated interleukin-10: a new cause of dyslipidemia leading to severe HDL deficiency. *J Clin Lipidol.* (2015) 9:81–90. doi: 10.1016/j.jacl.2014.09.014
12. Xiu B, Lin Y, Grote DM, Ziesmer SC, Gustafson MP, Maas ML, et al. IL-10 induces the development of immunosuppressive CD14(+)HLA-DR(low/-) monocytes in B-cell non-Hodgkin lymphoma. *Blood Cancer J.* (2015) 5:e328. doi: 10.1038/bcj.2015.56
13. Polyatskin IL, Artemyeva AS, Krivolapov YA. Revised WHO classification of tumors of hematopoietic and lymphoid tissues, 2017 (4th Edition): lymphoid tumors. *Arkh Patol.* (2019) 81:59-65. doi: 10.17116/patol20198103159
14. Hans CP, Weisenburger DD, Greiner TC, Gascoyne RD, Delabie J, Ott G, et al. Confirmation of the molecular classification of diffuse large B-cell lymphoma by immunohistochemistry using a tissue microarray. *Blood.* (2004) 103:275–82. doi: 10.1182/blood-2003-05-1545
15. Choi WW, Weisenburger DD, Greiner TC, Piris MA, Banham AH, Delabie J, et al. A new immunostain algorithm classifies diffuse large B-cell lymphoma into molecular subtypes with high accuracy. *Clin Cancer Res.* (2009) 15:5494–502. doi: 10.1158/1078-0432.CCR-09-0113
16. Bornstein SR, Allolio B, Arlt W, Barthel A, Don-Wauchope A, Hammer GD, et al. Diagnosis and treatment of primary adrenal insufficiency: an endocrine society clinical practice guideline. *J Clin Endocrinol Metab.* (2016) 101:364–89. doi: 10.1210/jc.2015-1710
17. Tsirlin A, Oo Y, Sharma R, Kansara A, Gliwa A, Banerji MA. Pheochromocytoma: a review. *Maturitas.* (2014) 77:229–38. doi: 10.1016/j.maturitas.2013.12.009
18. Harada K, Kimura K, Iwamuro M, Terasaka T, Hanayama Y, Kondo E, et al. The clinical and hormonal characteristics of primary adrenal lymphomas: the necessity of early detection of adrenal insufficiency. *Intern Med.* (2017) 56:2261–9. doi: 10.2169/internalmedicine.8216-16
19. Bourne AE, Bell SW, Wayment RO, Schwartz BF. Primary hodgkin lymphoma of the adrenal gland: a unique case presentation. *Can J Urol.* (2009) 16:4694–6.
20. Ohkura Y, Shindoh J, Haruta S, Kaji D, Ota Y, Fujii T, et al. Primary adrenal lymphoma possibly associated with epstein-barr virus reactivation due to immunosuppression under methotrexate therapy. *Medicine*. (2015) 94:e1270. doi: 10.1097/MD.0000000000001270
21. Mozos A, Ye H, Chuang WY, Chu JS, Huang WT, Chen HK, et al. Most primary adrenal lymphomas are diffuse large B-cell lymphomas with non-germinal center B-cell phenotype, BCL6 gene rearrangement and poor prognosis. *Mod Pathol.* (2009) 22:1210–7. doi: 10.1038/modpathol.2009.87
22. Falchook FS, Allard JC. CT of primary adrenal lymphoma. *J Comput Assist Tomogr.* (1991) 15:1048–50. doi: 10.1097/00004728-199111000-00030
23. Fuqin W, Junwei L, Ruoxi Z, Yonghua B, Cailin L, Bangguo L, et al. CT and MRI of adrenal gland pathologies. *Quant Imaging Med Surg.* (2018) 8:853–75. doi: 10.21037/qims.2018.09.13
24. Ide M, Fukushima N, Hisatomi T, Tsuneyoshi N, Tanaka M, Yokoo M, et al. Non-germinal cell phenotype and bcl-2 expression in primary adrenal diffuse large B-cell lymphoma. *Leuk Lymphoma.* (2007) 48:2244–6. doi: 10.1080/10428190701636450
25. Yoon SO, Jeon YK, Paik JH, Kim WY, Kim YA, Kim JE, et al. MYC translocation and an increased copy number predict poor prognosis in adult diffuse large B-cell lymphoma (DLBCL), especially in germinal centre-like B cell (GCB) type. *Histopathology.* (2008) 53:205–17. doi: 10.1111/j.1365-2559.2008.03076.x
26. Ohsawa M, Tomita Y, Hashimoto M, Yasunaga Y, Kanno H, Aozasa K. Malignant lymphoma of the adrenal gland: its possible correlation with the Epstein-Barr virus. *Mod Pathol.* (1996) 9:534–43.
27. Ali AS, Al-Shraim M, Al-Hakami AM, Jones IM. Epstein- barr virus: clinical and epidemiological revisits and genetic basis of oncogenesis. *Open Virol J.* (2015) 9:7–28. doi: 10.2174/1874357901509010007
28. Müssig K, Horger M, Wehrmann M. Adrenal castleman's disease. *Ann Hematol.* (2007) 86:63–5. doi: 10.1007/s00277-006-0200-7
29. Kim YR, Kim JS, Min YH, Hyunyoon D, Shin HJ, Mun YC, et al. Prognostic factors in primary diffuse large B-cell lymphoma of adrenal gland treated with rituximab-CHOP chemotherapy from the consortium for improving survival of lymphoma (CISL). *J Hematol Oncol.* (2012) 5:49. doi: 10.1186/1756-8722-5-49
30. Ichikawa S, Fukuhara N, Inoue A, Katsushima H, Ohba R, Katsuoka Y, et al. Clinicopathological analysis of primary adrenal diffuse large B-cell lymphoma: effectiveness of rituximab-containing chemotherapy including central nervous system prophylaxis. *Exp Hematol Oncol.* (2013) 2:19. doi: 10.1186/2162-3619-2-19

Conflict of Interest: The authors declare that the research was conducted in the absence of any commercial or financial relationships that could be construed as a potential conflict of interest.

frontiers in Endocrinology

MINI REVIEW
published: 30 September 2020
doi: 10.3389/fendo.2020.563267

Interplay Between Diabetes and Pancreatic Ductal Adenocarcinoma and Insulinoma: The Role of Aging, Genetic Factors, and Obesity

Bertrand Duvillié[1,2,3,4,5]*, *Rayane Kourdoughli*[1,2,3,4,5], *Sabine Druillennec*[1,2,3,4,5], *Alain Eychène*[1,2,3,4,5] and *Celio Pouponnot*[1,2,3,4,5]

[1] Department of Signaling, Radiobiology and Cancer, Institut Curie, Orsay, France, [2] INSERM U1021, Centre Universitaire, Orsay, France, [3] CNRS UMR 3347, Centre Universitaire, Orsay, France, [4] Université Paris-Saclay, Orsay, France, [5] PSL Research University, Paris, France

OPEN ACCESS

Edited by:
Jianfeng Liu,
Huazhong University of Science and Technology, China

Reviewed by:
Eva Surmacz,
Allysta Pharmaceuticals, Inc., United States
Silvio Naviglio,
University of Campania Luigi Vanvitelli, Italy

***Correspondence:**
Bertrand Duvillié
bertrand.duvillie@curie.fr

Specialty section:
This article was submitted to Cancer Endocrinology, a section of the journal Frontiers in Endocrinology

Received: 18 May 2020
Accepted: 14 September 2020
Published: 30 September 2020

Citation:
Duvillié B, Kourdoughli R, Druillennec S, Eychène A and Pouponnot C (2020) Interplay Between Diabetes and Pancreatic Ductal Adenocarcinoma and Insulinoma: The Role of Aging, Genetic Factors, and Obesity. Front. Endocrinol. 11:563267. doi: 10.3389/fendo.2020.563267

Epidemiologic analyses have shed light on an association between type 2 diabetes (T2D) and pancreatic ductal adenocarcinoma (PDAC). Recent data also suggest a potential relationship between T2D and insulinoma. Under rare circumstances, type 1 diabetes (T1D) can also be implicated in tumorigenesis. The biological mechanisms underlying such relationships are extremely complex. Some genetic factors contributing to the development of T2D are shared with pancreatic exocrine and endocrine tumors. Obesity and overweight can also contribute to the initiation and severity of T2D, while aging may influence both endocrine and exocrine tumors. Finally, pharmacological treatments of T2D may have an impact on PDAC. On the other hand, some treatments for insulinoma can trigger diabetes. In the present minireview, we discuss the cellular and molecular mechanisms that could explain these interactions. This analysis may help to define new potential therapeutic strategies.

Keywords: diabetes, pancreas, cancer, aging, insulinoma, obesity

INTRODUCTION

Diabetes is a metabolic disorder characterized by chronic hyperglycemia. Type 1 diabetes (T1D) is less frequent (5.6%) than type 2 diabetes (T2D) and is caused by autoimmune destruction of pancreatic beta-cells. T2D represents 91.2% of diabetes cases and is generally associated with insulin resistance and compensatory hyperinsulinemia, an early indicator of metabolic dysfunction. In the longer term, T2D leads to progressive functional defects of beta-cells. The remaining cases are primarily gestational diabetes, which are represented by hyperglycemia that generally disappears after delivery. Pancreatic adenocarcinoma (PDAC), the most frequent (95%) exocrine pancreatic cancer, is also the most lethal, with a 5-year overall survival of less than 8% (1). Insulinomas are functional neuroendocrine tumors originating from beta-cells. They are generally benign but can metastasize in 5%–10% of cases (2). Interestingly, T2D and pancreatic cancers share several common risk factors, and long standing T2D represents a recognized risk for carcinogenesis. Inversely, PDAC may also be responsible for diabetes (3). This link between diabetes and cancer was first suggested by epidemiologic observations. In particular, PDAC is strongly associated with

diabetes (4). Although T2D is a well-established risk factor for PDAC (5), this association is less clear for T1D. Indeed, a clinical prospective study on patients with T1D showed an increased risk of stomach, cervical and endometrium cancers, but only a very modest association with PDAC (6). These differences between T1D and T2D in the risk of developing PDAC may be attributed to differences in insulin levels, which is a risk factor (6). Finally, recent data has suggested a potential association between T2D and insulinoma (7). Despite this evidence, the causative link between T2D and PDAC, as well as insulinoma is not completely understood. The possible molecular mechanisms of this association will be discussed in this review.

COMMON DETERMINANTS OF DIABETES AND PANCREATIC CANCER

T2D and PDAC have common determinants, including aging, obesity, and genetic factors (**Figure 1**), in addition to some environmental factors that include tobacco smocking, alcohol consumption and low level of physical activity (8). T2D and insulinoma also share causative signals.

Aging

The Effect of Aging in T2D

Aging is the time-dependent deterioration of physiological functions affecting both diabetes and PDAC. The incidence of diabetes increases with age: with 1.8 million patients aged 20–39, 11.7 millions at 40–59, to 19.3 millions at 60–79 in the European Union in 2017 (9). Moreover, the mass of islet cells increases during maturation, but slowly decreases after age 40 (10). Islet amyloidis, which is associated with insulin resistance and T2D, is more commonly found in older individuals (11). Finally, metabolic sensing pathways, such as the mTOR, AMP-activated protein kinase, and insulin/insulin-like growth factors (IGFs) pathways (12, 13) are age-dependent. Interestingly, mTOR, a kinase activated by metabolic signaling, also plays an important role in T2D (14) and PDAC (15).

Aging and PDAC

Aging dramatically increases the risk of pancreatic carcinogenesis (16). Indeed, pancreatic intraepithelial neoplasia (PanINs) is one precursor of PDAC. In an autopsy study, high grade PanIN lesions were found more frequently in T2D patients and old individuals, suggesting a role of both aging and diabetes (17). Moreover, PanINs are associated with chromosomal instability, telomere shortening (18), and DNA damage, which all depend on aging (19). Several cellular mechanisms involved in aging also play an important role in PDAC. For example, lobulocentric atrophy, a combination of atrophy of acinar parenchyma, acinar to ductal metaplasia and fibrosis, promotes proliferation of small ductular structures and PanINs. This process is found in patients at high risk of PDAC and is age-dependent (20). Moreover, senescence is also important in cancer cells: after oncogenic transformation, cells can undergo senescence, with a reduction of their proliferation. However, some malignant cells often escape this process (21). In addition, age-related senescent-associated secretory phenotype (SASP) cells in the stromal micro-environment support cancer progression (21). In the $KRAS^{G12D}$ model of PDAC, knock-out of the senescence-

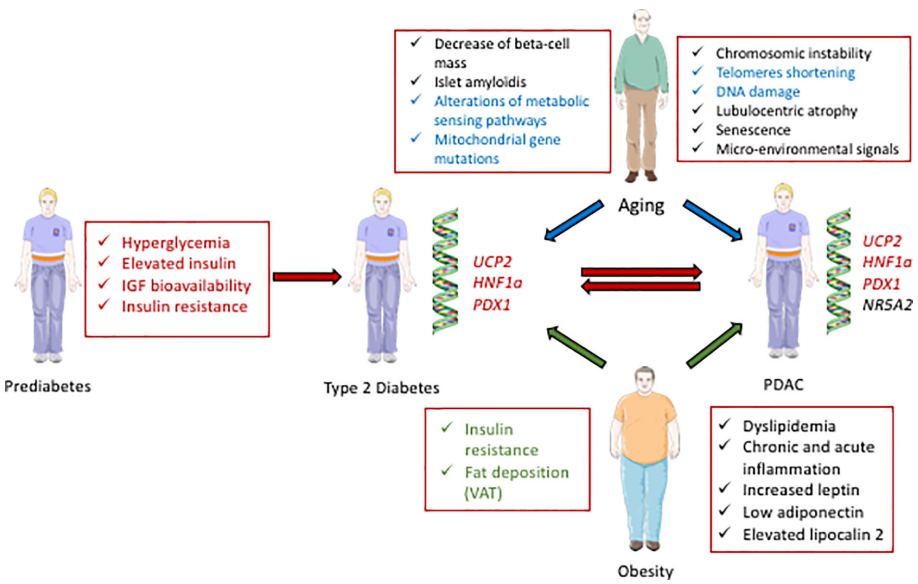

FIGURE 1 | Schematic representation of the interactions between diabetes and PDAC. Some biological parameters occurring during prediabetes, including hyperglycemia, elevated insulin, and IGF bioavailability contribute to diabetes (T2D) and can further lead to PDAC (red arrows). Some genetic factors; *UCP2*, *HNF1a*, and *PDX1*, are also common determinants of diabetes and PDAC (written in red). Some parameters in relation with aging can cause T2D and/or PDAC (blue arrows, and the common determinants for T2D and PDAC development are written in blue). Some characteristics of obesity can contribute to T2D and/or PDAC (green arrows, and the common determinants for T2D and PDAC development are written in green).

inducing factor SIN3B reduced the initiation and progression of pancreatic lesions, while decreasing secretion of the SASP factor IL-1α (22). Moreover, the conditional knock-out of IL-1α also reduces the number of neoplastic lesions. Finally, mitochondrial gene mutations, which accumulate with age, affect cell metabolism. Consequently, a selective growth advantage that promotes cancer is confered to the cells present in the aging environment (23, 24). Importantly, such mitochondrial events also enhance tumor progression in PDAC (25). Together, these data highlight the strong impact of aging in PDAC.

The Role of Aging in Insulinoma

Men1 knock-out mice provide a model of insulinoma, in which tumors develop late. Indeed, early inactivation of *Men1* specific to beta-cells leads to multiple insulinoma only by 60 weeks (26), suggesting the requirement of additional somatic events. Notably, in *Men1* knock-out tumors, an increase in the number of entire chromosome 11 was also found in insulinomas, and of chromosome 15 in pituitary prolactinomas. Several oncogenes, including *c-MYC* and *ErbB2/Her2/Neu* are present in these duplicated regions (26). The age-related penetrance of MEN1 in patients is 7%, 52%, 87%, 98%, 99%, and 100% at 10, 20, 30, 40, 50, and 60 years of age, respectively (27), suggesting that aging also influences tumorigenesis in human MEN1 tumors. Interestingly, different phenotypes in MEN1 monozygotic twins were observed: in (28), both twins developed parathyroidism, but only one had a pancreatic tumor. This observation suggests that one single mutation in *MEN1* is insufficient to induce insulinoma. The variant *V109G* of p27 and inactivating mutations of *CDKN1B* were shown to influence the clinical phenotype of MEN1 patients (29). Moreover, some cell-cycle regulators, whose expression is age-dependent (30), are also differentially expressed in human beta-cells from insulinoma as compared to healthy tissue (31). For example, p16 is more heavily expressed at the adult stage than in prenatal beta-cells (32). Such expression restricts beta-cell proliferation with aging (30) and also promotes senescence. Interestingly, its expression is considerably reduced in insulinoma cells (31). Together, these data suggest that aging influences beta-cell proliferation, but that insulinoma cells develop a specific proliferation pattern evading this control.

Obesity

Obesity and Diabetes

Obesity, characterized by excessive accumulation of body fat, with a body mass index (BMI) of 30 kg/m^2 or greater, is a well-known risk factor of diabetes (**Figure 1**) (33). Indeed, 87.5% of adults with T2D are also obese or overweight [BMI>25 (34, 35). The first causative link between obesity and T2D is insulin resistance. Indeed, both obesity and insulin resistance precede altered glycemia (36). Moreover, fat deposition has deleterious effects that depend on its anatomical location. The visceral adipose tissue (VAT), located in the abdominal cavity is linked to a higher risk of T2D as compared to subcutaneous adipose tissue (SCAT) (37).

Obesity and PDAC

Infiltration of adipose tissue favors pancreatic precancerous lesions (38). Indeed, in obese patients, fat has an effect on PanIN lesions and PDAC development. Obesity promotes inflammation that activates tumor associated neutrophils, and consequently pancreatic stellate cells, leading to increased desmoplasia and tumor growth (39). Moreover, chronic inflammation can promote EMT in PanIN cells, driving tumor progression and cell dissemination, leading to PDAC (40). Insulin resistance associated with obesity promotes dislypidemia (41), with elevated concentrations of triglycerides (42), and increased cholesterol synthesis (43). Hypertriglyceridemia is the third most common cause of acute pancreatitis (44), which also represents a risk for PDAC (45). Indeed, patients with acute pancreatitis had a 2-fold increased risk of pancreatic cancer when compared to the matched population. Moreover, adipokines, which include leptin, adiponectin, and lipocalin 2, also establish a connection between obesity and PDAC. In animals and humans, the leptin receptor Ob-Rb plays an important role in obesity (46). While leptin is produced by mature adipocytes, human PDAC cell lines and tissues both express the leptin receptor. Overexpression of leptin in an orthotopic model of human pancreatic cancer promotes tumor growth and lymph node metastasis (47), indicating that leptin is a key factor for PDAC. Recently, a possible interconnection between leptin and the Notch pathway, which is responsible for transformation, proliferation, tumor progression, EMT and chemoresistance, was described (48). Adiponectin is found in adipose tissue and its expression is very low in obese subjects. Prospective epidemiologic studies have shown that low concentration of adiponectin is linked to a higher risk of PDAC (49). Interestingly, adiponectin treatment inhibits the proliferation of human pancreatic cancer cells (50). Knocking-down adiponectin receptors abolished these effects, and enhanced the growth of human pancreatic cancer xenografts in nude mice. Moreover, this antiproliferative effect of adiponectin was shown to be mediated by the β-catenin signaling pathway. However, the roles of leptin and adiponectin are still debated, as a higher adiponectin/leptin ratio and lower leptin levels were found in patients with PDAC as compared to controls (51). Finally, lipocalin 2, a protein involved in innate immunity, also plays an important role in the cellular microenvironment that contributes to PDAC. Lipocalin 2 was found to be a regulator of VAT hypertrophy in animals treated with high fat diet (HFD). The deletion of *Lipocalin2* decreases PDAC incidence in KRAS-G12D transgenic mice (52). More generally, diet has a strong impact on pancreatic cancer. Recently, Chang et al. showed that HFD dramatically increases the incidence of PDAC in KRAS-G12D mice. Indeed, the PanIN lesions express new genetic variants, suggesting that genetic alterations may participate to this process (53).

Obesity and Insulinoma

Obesity has thus far not been identified as a cause of insulinoma, but the reverse has been described. Insulinoma can be linked to hyperphagia in some cases by induction of hypoglycemia and hunger. This may lead to weight gain in 20%–40% of patients and even to overt obesity (54, 55). Interestingly, the orexigenic hormone ghrelin is associated with obesity (56). Co-expression of ghrelin and its receptor was detected in several pancreatic

endocrine tumors, and specifically in insulinoma, but elevated circulating ghrelin is rare in these patients (57).

The Genetic Factors

The Genetics of Diabetes and PDAC

Genome wide association studies (GWAS) have been used to identify relationships between diabetes and pancreatic cancers. Several pancreatic developmental genes, *NR5A2*, *PDX1*, and *HNF1A*, were identified as susceptibility factors for PDAC (**Figure 1**) (58). Moreover, heterozygous mutations in some of these genes, *PDX1* and *HNF1α*, are also responsible for different monogenic forms of maturity onset diabetes of the young (MODY 4 and MODY 5). Some variants of *PDX1* and *HNF1α* are also associated with increased risks of T2D (59, 60), obesity (61), or hyperglycemia (62). The antioxidant mitochondrial uncoupling protein 2 (UCP2), which controls pancreatic development and insulin secretion (63), is overexpressed in PDAC tumors compared to normal adjacent tissues (64), suggesting that *UCP2* overexpression is a biomarker of bad prognosis. However, other recent studies using the pancreatic cancer cell line Mia PACA2 showed that UCP2 inhibits cancer cell proliferation and tumorigenesis (65). This effect is mediated by retrograde mitochondrial signaling on the Warburg effect that reorients mitochondrial function toward oxidative phosphorylation rather than glycolysis. Additional analyses are needed to elucidate the discrepancy between these two studies involving *UCP2*. Taken together, these data indicate a link between genes controlling pancreas development, diabetes and PDAC.

The Genetic Links Between Diabetes and Insulinoma

Recently, a strong link between T2D and insulinoma has been established (**Figure 2**). A p.Ser64Phe mutation in *MAFA* that prevents GSK3-mediated MAFA phosphorylation (42, 44) was identified in 25 individuals from two independent families (7). These patients develop either insulinoma or diabetes with 90% penetrance. Interestingly, the MAF proteins are well established oncoproteins (66) and their tumorigenic activity is regulated by GSK3-mediated phosphorylation in different cancers (67, 68). Moreover, other studies have also revealed a role of *MAFA* in diabetes. Within the pancreas, *MAFA* is exclusively expressed in developing and mature beta-cells. MafA activates the insulin promoter in response to glucose, and regulates genes involved in beta-cell function such as glucose transporter 2, glucagon-like peptide 1 receptor and prohormone convertase 1/3 (69). Accordingly, glucose-stimulated insulin secretion (GSIS) is impaired in *MafA* knock-out mice, and the architecture of the islets is disorganized. Moreover, these mice develop T2D at 50 weeks after birth (70). In humans, data have also established a link between *MAFA* and different forms of diabetes. Indeed, expression of *MAFA* is decreased in islets from T2D patients and a polymorphism in *MAFA* is associated with T1D (71).

Cases of insulinoma with pre-existing diabetes are very rare (72, 73). In (7), a 27 year-old female patient with a *MAFA*

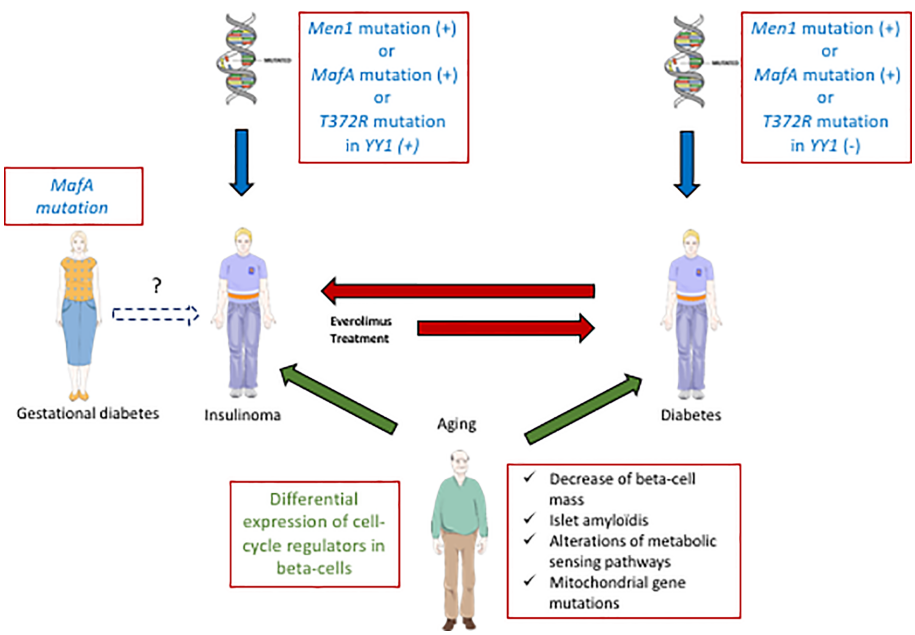

FIGURE 2 | Interactions between diabetes and insulinoma. Some specific *MafA* mutations can predispose to diabetes (T2D) or insulinoma. In some rare cases with such mutations of *MafA*, gestational diabetes precedes insulinoma. Moreover, other genes (*Men1*, *YY1*) are also involved positively (+) or negatively (–) in the development of diabetes or insulinoma (blue arrows). Aging also contributes to both pathologies (green arrows, common aging determinant for T2D and insulinoma written in green). Some inulinoma treatments (everolimus) can enhance the risk of diabetes (red arrow). On the other hand, exceptional cases of T1D can induce insulinoma (red arrow).

mutation preventing its phosphorylation by GSK3 first developed gestational diabetes, and subsequent insulinoma at 55 years old. This finding suggests that the *MAFA* mutation may have caused metabolic disorders in relation to diabetes, that would lead to insulinoma in the long term. Another genetic link between diabetes and insulinoma was suggested by the presence of a recurrent somatic T372R mutation in YY1 (Yin and Yang 1 protein) in 30% of tumors (74). YY1 is a transcription factor that belongs to the GLI-Kruppel class of zinc finger proteins and is a target of mTOR inhibitors. In beta-cells, YY1 regulates the transcription of CXCL12, which also has antidiabetogenic potential (75). In some cases, insulinoma develop in a context of hereditary predisposition to pancreatic endocrine tumors. Indeed, *MEN1*, type-1 multiple endocrine neoplasm, represents the most frequent predisposition gene for insulinoma (76). Moreover, a relationship between *MEN 1* and *MAFA* genes was also established: altered *MEN1* expression was shown to disrupt the *MAFA* differentiation pathway in human and mice insulinoma cells (77).

IS DIABETES A RISK FACTOR FOR PANCREATIC CANCERS?

Hyperglycemia

Hyperglycemia and PDAC

In T2D, hyperglycemia is caused by excessive hepatic gluconeogenesis, decreased incretin activity, and peripheral glucose uptake, as well as altered insulin signaling. T2D results from a long history of metabolic disorders before diagnosis. These events can cause carcinogenesis and particularly PDAC (**Figure 1**) (76). Indeed, patients can remain asymptomatic for many years, with undiscovered glucose intolerance and transient hyperglycemia (78). This prediabetic period considerably increases the probability of developing PDAC (79). One possible mechanism is the activation of the TGFβ pathway by glucose, leading to reduced E-cadherin levels in pancreatic ductal cells and to a pronounced mesenchymal phenotype promoting tumor growth and metastasis (5). Hyperglycemia may also increase genomic instability leading to *KRAS* mutations through activation of O-GlcNAcylation and nucleotides deficiency (80). Finally, the mTOR pathway controls protein synthesis and autophagy, and its deregulation is implicated in diabetes, cancer, and the aging process (81). Interestingly, mTOR inhibition in mouse models of KRAS-dependent PDAC subtypes reduces tumorigenesis (15).

Hyperglycemia and Insulinoma

Glucose controls beta-cell proliferation both *in vitro* and *in vivo* (82). In the context of insulin demand, beta-cells undergo hypertrophy or hyperplasia to normalize glycemia (83). One hypothesis is that pre-existing diabetes leads to insulinoma through hyperglycemia. However, such cases are extremely rare. Recently, two patients with pre-existing T1D developed insulinoma (84, 85). In (84), a 31-year-old man experienced T1D for 28 years. Surprisingly, frequent hypoglycemic episodes occurred, leading to the arrest of insulin therapy. After resection, histopathology revealed a grade-2 insulinoma. One unsolved issue is the absence of an autoimmune response against tumor cells in this patient (84). Further analyses will be necessary to investigate the mechanisms involved in tumor progression in such patients.

Insulin and Insulin-Like Growth Factors (IGFs) in Diabetes and Tumorigenesis

The insulin/IGF signalization plays an important role in diabetes. Epidemiological studies have associated serum level variations of IGF-1 (86, 87), IGF-2 (88), IGF binding proteins 1 (89, 90), 2 (91), 3 (86, 90), 4 (91) with T2D. Moreover, obese subjects also exhibit alterations of the IGF system (88, 92, 93) influenced by the presence or absence of T2D (93). Non-diabetic obese subjects have elevated free IGF-1 and IGF-2, total IGF-2, IGF-BP3, and reduced IGF-BP1 and 2 levels. In obese T2D patients, IGFBP-2 is further reduced (93).

PDAC

PDAC originates from both ductal and acinar cells of the pancreas (94), which are exposed to high levels of insulin. Such proxicrine signals promote growth of pancreatic cancer cells (**Figure 1**) (3). Indeed, the effects of insulin and IGFs 1 and 2 are mediated by the insulin receptor (IR) and IGF1 receptor (IGF1R) (95, 96). As previously discussed, obesity and T2D are associated with increased risk of PDAC. These metabolic disorders are characterized by insulin resistance, compensatory overproduction of insulin and increased bioavailability of IGF-1 (97). To examine the role of insulin in PDAC initiation, Ptf1aCre^{ER}LSL-KRAS^{G12D}*Ins*1$^{+/-}$ *Ins*2$^{-/-}$ mice, which have a sustain reduction of insulin but no altered glycemia, were used (98). Mice with reduced insulin had a significant decrease in the number of PanINs and pancreatic tumors when compared to controls. Thus, these results demonstrate that insulin regulates PDAC development. Interestingly, altered expression of the tumor suppressor p53, observed in 50% to 75% of PDAC (99), was shown to stimulate the insulin/IGF1 pathway (100). Moreover, polymorphisms in the IGF genes have been associated with decreased survival of patients with PDAC (101). Taken together, these data strongly support a role of the insulin/IGF axis in pancreatic cancer.

Insulinoma

In animals and human, some associations between IGF2 and diabetes have been shown. In particular, IGF2 overexpression in transgenic mice leads to beta-cell dysfunction (102), by inducing beta-cell de-differentiation and reticulum stress. Moreover, in a mouse model of multistage carcinogenesis induced by the SV40 large T antigen in pancreatic beta-cells, IGF2 was increased and contributed to insulinoma development (103). Recently, studies have shown that the IGF pathway is activated in insulinoma (104). Glutamine can also stimulate biosynthesis and secretion of IGF2 in mouse insulinoma cells, which regulate beta-cell mass and function in an autocrine manner (105). Interestingly, hypermethylation of the differentially methylated region 2 of *IGF2* was discovered in human insulinoma, leading to loss of imprinting and overexpression of *IGF2* (106). Finally, IGF2

overexpression was also detected in *Men1*-mutated mouse insulinoma (107). IGF signaling thus appear to be an important hallmark of insulinoma.

DIABETES TREATMENT TO PREVENT PANCREATIC CANCERS?

PDAC

Metformin (108) is the most frequently prescribed, first-line treatment drug for T2D (109). Metformin decreases glycemia by lowering hepatic gluconeogenesis and improves insulin sensitivity by promoting glucose uptake in skeletal muscle and adipose tissue. Several epidemiological studies have demonstrated that metformin administration reduces incidence, recurrence and mortality of pancreatic cancer in diabetic patients (110, 111). Clinical trials using metformin in combination with other drugs used to treat PDAC are actually under investigation (https://clinicaltrials.gov/ct2/results?term=metformin&cond=Pancreatic+Cancer). To delineate the molecular mechanisms involved in this protective effect of metformin, animal models were used. Metformin significantly decreased the incidence of PDAC promoted by diet-induced obesity in the conditional KRAS-G12D knock-in mouse (112). Together, these findings demonstrate that metformin, a treatment for diabetes, represents an important pharmacological tool for PDAC prevention, strengthening the link between these two pathologies. Moreover, AdipoRon, which acts as an adiponectin receptor agonist (113), has antidiabetic properties and can inhibit tumor growth of pancreatic cancer cells MIAPACa-2 in xenografts. AdipoRon can also induce cell death in cells derived from PDAC patients (114). These data suggest that AdipoRon could be a therapeutic agent for both diabetes and PDAC. Finally, several studies analyzed the antidiabetic and protective effects of aspirin against PDAC. Indeed, inflammation is a hallmark of T2D, and aspirin reduces inflammation by regulating T-cell function (115). Interestingly, clinical analysis of a subgroup of patients with diabetes showed a protective role of aspirin against PDAC (116). However, the effects of aspirin against PDAC seem to be heterogenous and controversial (116–118). Further analysis is thus required to better understand these effects.

Insulinoma

Anti-cancer drugs are used to treat insulinoma. Recently, a combination of mTOR inhibitors and streptozotocin was shown to have synergistic antitumor effects in insulinoma cells, both *in vitro* and *in vivo* (119). Everolimus, an mTOR inhibitor, was successfully used to treat advanced pancreatic neuroendocrine tumors in a phase 3 clinical trial (120) (RADIANT-3 ClinicalTrials.gov number, NCT00510068). However, other data indicate that such anti-cancer therapy also has endocrine side effects, such as increased plasma triglycerides, LDL cholesterol, and high incidence of hyperglycemia (121). Thus, despite its benefits in cancer, this treatment may enhance the risk of diabetes.

CONCLUSION

Pre-clinical and clinical data provide clear evidence of common characteristics shared by T2D and PDAC, as well as T2D and insulinoma. The association between diabetes and PDAC is frequent, while it is more unusual between diabetes and insulinoma. Some specific gene mutations contribute to both T2D and insulinoma, strengthening the link between these diseases, while others mutations have opposite effects on T2D and insulinoma. Diabetes and PDAC share several metabolical disorders, that are also found during obesity. Accordingly, obesity often contributes to PDAC initiation, whereas obesity is a consequence of insulinoma. Understanding the relation between T2D and PDAC and between T2D and insulinoma may have important consequences. Indeed, treatments of T2D can limit PDAC progression, while treatment for insulinoma may induce T2D. These important findings should be taken into consideration to develop new pharmacological strategies to limit tumor progression.

AUTHOR CONTRIBUTIONS

All authors contributed to the article and approved the submitted version.

FUNDING

BD is supported by Société Francophone du Diabète (SFD) (Grant number 26866).

ACKNOWLEDGMENTS

For the figures, SERVIER MEDICAL ART was used. We thank Eleanor Hawkins for proofreading our manuscript.

REFERENCES

1. Siegel RL, Miller KD, Jemal A. Cancer statistics, 2018: Cancer Statistics, 2018. *CA: A Cancer J Clinicians* (2018) 68:7–30. doi: 10.3322/caac.21442
2. Halfdanarson TR, Rubin J, Farnell MB, Grant CS, Petersen GM. Pancreatic endocrine neoplasms: epidemiology and prognosis of pancreatic endocrine tumors. *Endoc Relat Cancer* (2008) 15:409–27. doi: 10.1677/ERC-07-0221
3. Andersen DK, Korc M, Petersen GM, Eibl G, Li D, Rickels MR, et al. Diabetes, Pancreatogenic Diabetes, and Pancreatic Cancer. *Diabetes* (2017) 66:1103–10. doi: 10.2337/db16-1477
4. Aggarwal G, Kamada P, Chari ST. Prevalence of Diabetes Mellitus in Pancreatic Cancer Compared to Common Cancers. *Pancreas* (2013) 42:198–201. doi: 10.1097/MPA.0b013e3182592c96
5. Rahn S, Zimmermann V, Viol F, Knaack H, Stemmer K, Peters L, et al. Diabetes as risk factor for pancreatic cancer: Hyperglycemia promotes epithelial-mesenchymal-transition and stem cell properties in pancreatic ductal epithelial cells. *Cancer Lett* (2018) 415:129–50. doi: 10.1016/j.canlet.2017.12.004
6. Zendehdel K. Cancer Incidence in Patients With Type 1 Diabetes Mellitus: A Population-Based Cohort Study in Sweden. *Cancer Spectrum Knowledge Environ* (2003) 95:1797–800. doi: 10.1093/jnci/djg105

7. Iacovazzo D, Flanagan SE, Walker E, Quezado R, de Sousa Barros FA, Caswell R, et al. *MAFA* missense mutation causes familial insulinomatosis and diabetes mellitus. *Proc Natl Acad Sci USA* (2018) 115:1027–32. doi: 10.1073/pnas.1712262115
8. Giovannucci E, Harlan DM, Archer MC, Bergenstal RM, Gapstur SM, Habel LA, et al. Diabetes and Cancer: A Consensus Report. *CA: A Cancer J Clinicians* (2010) 60:207–21. doi: 10.3322/caac.20078
9. OECD/EU. *Health at a Glance: Europe 2018: State of Health in the EU Cycle*. Paris: OECD Publishing (2018). doi: 10.1787/health_glance_eur-2018-en
10. Mizukami H, Takahashi K, Inaba W, Osonoi S, Kamata K, Tsuboi K, et al. Age-associated changes of islet endocrine cells and the effects of body mass index in Japanese. *J Diabetes Invest* (2014) 5:38–47. doi: 10.1111/jdi.12118
11. Campbell F, Verbeke CS. *Pathology of the Pancreas*. London: Springer London (2013). doi: 10.1007/978-1-4471-2449-8
12. Johnson SC, Rabinovitch PS, Kaeberlein M. mTOR is a key modulator of ageing and age-related disease. *Nature* (2013) 493:338–45. doi: 10.1038/nature11861
13. Kennedy BK, Lamming DW. The Mechanistic Target of Rapamycin: The Grand ConducTOR of Metabolism and Aging. *Cell Metab* (2016) 23:990–1003. doi: 10.1016/j.cmet.2016.05.009
14. Guillén C, Benito M. mTORC1 Overactivation as a Key Aging Factor in the Progression to Type 2 Diabetes Mellitus. *Front Endocrinol* (2018) 9:621. doi: 10.3389/fendo.2018.00621
15. Iriana S, Ahmed S, Gong J, Annamalai AA, Tuli R , Hendifar AE. Targeting mTOR in Pancreatic Ductal Adenocarcinoma. *Front Oncol* (2016) 6:99. doi: 10.3389/fonc.2016.00099
16. Matsuda Y. Age-related morphological changes in the pancreas and their association with pancreatic carcinogenesis. *Pathol Int* (2019) 69:450–62. doi: 10.1111/pin.12837
17. Matsuda Y, Furukawa T, Yachida S, Nishimura M, Seki A, Nonaka K, et al. The Prevalence and Clinicopathological Characteristics of High-Grade Pancreatic Intraepithelial Neoplasia: Autopsy Study Evaluating the Entire Pancreatic Parenchyma. *Pancreas* (2017) 46:658–64. doi: 10.1097/MPA.0000000000000786
18. van Heek NT, Meeker AK, Kern SE, Yeo CJ, Lillemoe KD, Cameron JL, et al. Telomere shortening is nearly universal in pancreatic intraepithelial neoplasia. *Am J Pathol* (2002) 161:1541–7. doi: 10.1016/S0002-9440(10)64432-X
19. Aunan JR, Cho WC, Søreide K. The Biology of Aging and Cancer: A Brief Overview of Shared and Divergent Molecular Hallmarks. *A&D* (2017) 8:628. doi: 10.14336/AD.2017.0103
20. Shi C, Hruban RH, Klein AP. Familial pancreatic cancer. *Arch Pathol Lab Med* (2009) 133:365–74. doi: 10.1043/1543-2165-133.3.365
21. Fane M, Weeraratna AT. How the ageing microenvironment influences tumour progression. *Nat Rev Cancer* (2020) 20:89–106. doi: 10.1038/s41568-019-0222-9
22. Rielland M, Cantor DJ, Graveline R, Hajdu C, Mara L, Diaz B de D, et al. Senescence-associated SIN3B promotes inflammation and pancreatic cancer progression. *J Clin Invest* (2014) 124:2125–35. doi: 10.1172/JCI72619
23. Rozhok AI, Salstrom JL, DeGregori J. Stochastic modeling indicates that aging and somatic evolution in the hematopoietic system are driven by non-cell-autonomous processes. *Aging* (2014) 6:1033–48. doi: 10.18632/aging.100707
24. Tidwell TR, Søreide K, Hagland HR. Aging, Metabolism, and Cancer Development: from Peto's Paradox to the Warburg Effect. *A&D* (2017) 8:662. doi: 10.14336/AD.2017.0713
25. Hopkins JF, Denroche RE, Aguiar JA, Notta F, Connor AA, Wilson JM, et al. Mutations in Mitochondrial DNA From Pancreatic Ductal Adenocarcinomas Associate With Survival Times of Patients and Accumulate as Tumors Progress. *Gastroenterology* (2018) 154:1620–4. doi: 10.1053/j.gastro.2018.01.029
26. Crabtree JS, Scacheri PC, Ward JM, McNally SR, Swain GP, Montagna C, et al. Of Mice and MEN1: Insulinomas in a Conditional Mouse Knockout. *Mol Cell Biol* (2003) 23:6075–85. doi: 10.1128/MCB.23.17.6075-6085.2003
27. Bassett JH, Forbes SA, Pannett AA, Lloyd SE, Christie PT, Wooding C, et al. Characterization of mutations in patients with multiple endocrine neoplasia type 1. *Am J Hum Genet* (1998) 62:232–44. doi: 10.1086/301729
28. Namihira H, Sato M, Miyauchi A, Ohye H, Matsubara S, Bhuiyan MM, et al. Different phenotypes of multiple endocrine neoplasia type 1 (MEN1) in monozygotic twins found in a Japanese MEN1 family with MEN1 gene mutation. *Endocr J* (2000) 47:37–43. doi: 10.1507/endocrj.47.37
29. Longuini VC, Lourenço DM, Sekiya T, Meirelles O, Goncalves TD, Coutinho FL, et al. Association between the p27 rs2066827 variant and tumor multiplicity in patients harboring MEN1 germline mutations. *Eur J Endocrinol* (2014) 171:335–42. doi: 10.1530/EJE-14-0130
30. Köhler CU, Olewinski M, Tannapfel A, Schmidt WE, Fritsch H, Meier JJ. Cell cycle control of β-cell replication in the prenatal and postnatal human pancreas. *Am J Physiol-Endocrinol Metab* (2011) 300:E221–30. doi: 10.1152/ajpendo.00496.2010
31. Ueberberg S, Tannapfel A, Schenker P, Viebahn R, Uhl W, Schneider S, et al. Differential expression of cell-cycle regulators in human beta-cells derived from insulinoma tissue. *Metab Clin Exp* (2016) 65:736–46. doi: 10.1016/j.metabol.2016.02.007
32. Helman A, Avrahami D, Klochendler A, Glaser B, Kaestner KH, Ben-Porath I, et al. Effects of ageing and senescence on pancreatic β-cell function. *Diabetes Obes Metab* (2016) 18 Suppl 1:58–62. doi: 10.1111/dom.12719
33. Ozcan U. Endoplasmic Reticulum Stress Links Obesity, Insulin Action, and Type 2 Diabetes. *Science* (2004) 306:457–61. doi: 10.1126/science.1103160
34. World Health Organization. *Obesity: preventing and managing the global epidemic: report of a WHO consultation*. Geneva: World Health Organization (2000).
35. Malone JI, Hansen BC. Does obesity cause type 2 diabetes mellitus (T2DM)? Or is it the opposite? *Pediatr Diabetes* (2019) 20:5–9. doi: 10.1111/pedi.12787
36. Reaven GM. Pathophysiology of insulin resistance in human disease. *Physiol Rev* (1995) 75:473–86. doi: 10.1152/physrev.1995.75.3.473
37. Ibrahim MM. Subcutaneous and visceral adipose tissue: structural and functional differences. *Obes Rev* (2010) 11:11–8. doi: 10.1111/j.1467-789X.2009.00623.x
38. Rebours V, Gaujoux S, d'Assignies G, Sauvanet A, Ruszniewski P, Levy P, et al. Obesity and Fatty Pancreatic Infiltration Are Risk Factors for Pancreatic Precancerous Lesions (PanIN). *Clin Cancer Res* (2015) 21:3522–8. doi: 10.1158/1078-0432.CCR-14-2385
39. Incio J, Liu H, Suboj P, Chin SM, Chen IX, Pinter M, et al. Obesity-Induced Inflammation and Desmoplasia Promote Pancreatic Cancer Progression and Resistance to Chemotherapy. *Cancer Discovery* (2016) 6:852–69. doi: 10.1158/2159-8290.CD-15-1177
40. Rhim AD, Mirek ET, Aiello NM, Maitra A, Bailey JM, McAllister F, et al. EMT and Dissemination Precede Pancreatic Tumor Formation. *Cell* (2012) 148:349–61. doi: 10.1016/j.cell.2011.11.025
41. Klop B, Elte J, Cabezas M. Dyslipidemia in Obesity: Mechanisms and Potential Targets. *Nutrients* (2013) 5:1218–40. doi: 10.3390/nu5041218
42. Otvos JD, Mora S, Shalaurova I, Greenland P, Mackey RH, Goff DC. Clinical implications of discordance between low-density lipoprotein cholesterol and particle number. *J Clin Lipidol* (2011) 5:105–13. doi: 10.1016/j.jacl.2011.02.001
43. Pihlajamäki J, Gylling H, Miettinen TA, Laakso M. Insulin resistance is associated with increased cholesterol synthesis and decreased cholesterol absorption in normoglycemic men. *J Lipid Res* (2004) 45:507–12. doi: 10.1194/jlr.M300368-JLR200
44. Mosztbacher D, Hanák L, Farkas N, Szentesi A, Mikó A, Bajor J, et al. Hypertriglyceridemia-induced acute pancreatitis: A prospective, multicenter, international cohort analysis of 716 acute pancreatitis cases. *Pancreatology* (2020) 20:608–16. doi: 10.1016/j.pan.2020.03.018
45. Kirkegård J, Cronin-Fenton D, Heide-Jørgensen U, Mortensen FV. Acute Pancreatitis and Pancreatic Cancer Risk: A Nationwide Matched-Cohort Study in Denmark. *Gastroenterology* (2018) 154:1729–36. doi: 10.1053/j.gastro.2018.02.011
46. Zhang Y, Proenca R, Maffei M, Barone M, Leopold L, Friedman JM. Positional cloning of the mouse obese gene and its human homologue. *Nature* (1994) 372:425–32. doi: 10.1038/372425a0
47. Fan Y, Gan Y, Shen Y, Cai X, Song Y, Zhao F, et al. Leptin signaling enhances cell invasion and promotes the metastasis of human pancreatic cancer via increasing MMP-13 production. *Oncotarget* (2015) 6:16120–34. doi: 10.18632/oncotarget.3878
48. Cascetta P, Cavaliere A, Piro G, Torroni L, Santoro R, Tortora G, et al. Pancreatic Cancer and Obesity: Molecular Mechanisms of Cell Transformation and Chemoresistance. *IJMS* (2018) 19:3331. doi: 10.3390/ijms19113331

49. Grote VA, Rohrmann S, Dossus L, Nieters A, Halkjaer J, Tjønneland A, et al. The association of circulating adiponectin levels with pancreatic cancer risk: A study within the prospective EPIC cohort. *Int J Cancer* (2012) 130:2428–37. doi: 10.1002/ijc.26244
50. Jiang J, Fan Y, Zhang W, Shen Y, Liu T, Yao M, et al. Adiponectin Suppresses Human Pancreatic Cancer Growth through Attenuating the β-Catenin Signaling Pathway. *Int J Biol Sci* (2019) 15:253–64. doi: 10.7150/ijbs.27420
51. Krechler T, Zeman M, Vecka M, Macasek J, Jachymova M, Zima T, et al. Leptin and adiponectin in pancreatic cancer: connection with diabetes mellitus. *neo* (2011) 58:58–64. doi: 10.4149/neo_2011_01_58
52. Gomez-Chou SB, Swidnicka-Siergiejko AK, Badi N, Chavez-Tomar M, Lesinski GB, Bekaii-Saab T, et al. Lipocalin-2 Promotes Pancreatic Ductal Adenocarcinoma by Regulating Inflammation in the Tumor Microenvironment. *Cancer Res* (2017) 77:2647–60. doi: 10.1158/0008-5472.CAN-16-1986
53. Chang H-H, Moro A, Takakura K, Su H-Y, Mo A, Nakanishi M, et al. Incidence of pancreatic cancer is dramatically increased by a high fat, high calorie diet in KrasG12D mice. *PloS One* (2017) 12:e0184455. doi: 10.1371/journal.pone.0184455
54. Bonfig W, Kann P, Rothmund M, Schwarz HP. Recurrent hypoglycemic seizures and obesity: delayed diagnosis of an insulinoma in a 15 year-old boy–final diagnostic localization with endosonography. *J Pediatr Endocrinol Metab* (2007) 20:1035–8. doi: 10.1515/jpem.2007.20.9.1035
55. Mathur A, Gorden P, Libutti SK. Insulinoma. *Surg Clin North Am* (2009) 89:1105–21. doi: 10.1016/j.suc.2009.06.009
56. Cummings DE. Ghrelin and the short- and long-term regulation of appetite and body weight. *Physiol Behav* (2006) 89:71–84. doi: 10.1016/j.physbeh.2006.05.022
57. Ekeblad S, Lejonklou MH, Grimfjärd P, Johansson T, Eriksson B, Grimelius L, et al. Co-expression of ghrelin and its receptor in pancreatic endocrine tumours. *Clin Endocrinol* (2006) 66(1):115–22 doi: 10.1111/j.1365-2265.2006.02695.x
58. Li D, Duell EJ, Yu K, Risch HA, Olson SH, Kooperberg C, et al. Pathway analysis of genome-wide association study data highlights pancreatic development genes as susceptibility factors for pancreatic cancer. *Carcinogenesis* (2012) 33:1384–90. doi: 10.1093/carcin/bgs151
59. Holmkvist J, Cervin C, Lyssenko V, Winckler W, Anevski D, Cilio C, et al. Common variants in HNF-1 α and risk of type 2 diabetes. *Diabetologia* (2006) 49:2882–91. doi: 10.1007/s00125-006-0450-x
60. Tallapragada DSP, Bhaskar S, Chandak GR. New insights from monogenic diabetes for "common" type 2 diabetes. *Front Genet* (2015) 6:251. doi: 10.3389/fgene.2015.00251
61. MAGIC, on behalf of Procardis Consortium, Speliotes EK, Willer CJ, Berndt SI, Monda KL, Thorleifsson G, et al. Association analyses of 249,796 individuals reveal 18 new loci associated with body mass index. *Nat Genet* (2010) 42:937–48. doi: 10.1038/ng.686
62. DIAbetes Genetics Replication And Meta-analysis (DIAGRAM) Consortium and The Multiple Tissue Human Expression Resource (MUTHER) Consortium, Manning AK, Hivert M-F, Scott RA, Grimsby JL, et al. A genome-wide approach accounting for body mass index identifies genetic variants influencing fasting glycemic traits and insulin resistance. *Nat Genet* (2012) 44:659–69. doi: 10.1038/ng.2274
63. Broche B, Ben Fradj S, Aguilar E, Sancerni T, Bénard M, Makaci F, et al. Mitochondrial Protein UCP2 Controls Pancreas Development. *Diabetes* (2018) 67:78–84. doi: 10.2337/db17-0118
64. Donadelli M, Dando I, Pozza ED, Palmieri M. Mitochondrial uncoupling protein 2 and pancreatic cancer: A new potential target therapy. *WJG* (2015) 21:3232–8. doi: 10.3748/wjg.v21.i11.3232
65. Esteves P, Pecqueur C, Ransy C, Esnous C, Lenoir V, Bouillaud F, et al. Mitochondrial Retrograde Signaling Mediated by UCP2 Inhibits Cancer Cell Proliferation and Tumorigenesis. *Cancer Res* (2014) 74:3971–82. doi: 10.1158/0008-5472.CAN-13-3383
66. Eychène A, Rocques N, Pouponnot C. A new MAFia in cancer. *Nat Rev Cancer* (2008) 8:683–93. doi: 10.1038/nrc2460
67. Herath NI, Rocques N, Garancher A, Eychène A, Pouponnot C. GSK3-mediated MAF phosphorylation in multiple myeloma as a potential therapeutic target. *Blood Cancer J* (2014) 4:e175–5. doi: 10.1038/bcj.2013.67
68. Rocques N, Abou Zeid N, Sii-Felice K, Lecoin L, Felder-Schmittbuhl M-P, Eychène A, et al. GSK-3-Mediated Phosphorylation Enhances Maf-Transforming Activity. *Mol Cell* (2007) 28:584–97. doi: 10.1016/j.molcel.2007.11.009
69. Aramata S, Han S-I, Kataoka K. Roles and regulation of transcription factor MafA in islet beta-cells. *Endocr J* (2007) 54:659–66. doi: 10.1507/endocrj.kr-101
70. Zhang C, Moriguchi T, Kajihara M, Esaki R, Harada A, Shimohata H, et al. MafA Is a Key Regulator of Glucose-Stimulated Insulin Secretion. *Mol Cell Biol* (2005) 25:4969–76. doi: 10.1128/MCB.25.12.4969-4976.2005
71. Guo S, Dai C, Guo M, Taylor B, Harmon JS, Sander M, et al. Inactivation of specific β cell transcription factors in type 2 diabetes. *J Clin Invest* (2013) 123:3305–16. doi: 10.1172/JCI65390
72. Kamocki ZK, Wodyńska NA, Pryczynicz A. Co-existence of insulinoma and diabetes: A case report. *Oncol Lett* (2014) 8:1697–700. doi: 10.3892/ol.2014.2338
73. Sakurai A, Aizawa T, Katakura M, Sato Y, Kaneko G, Yoshizawa K, et al. Insulinoma in a Patient with Non-Insulin-Dependent Diabetes Mellitus. *Endocr J* (1997) 44:473–7. doi: 10.1507/endocrj.44.473
74. Cao Y, Gao Z, Li L, Jiang X, Shan A, Cai J, et al. Whole exome sequencing of insulinoma reveals recurrent T372R mutations in YY1. *Nat Commun* (2013) 4:2810. doi: 10.1038/ncomms3810
75. Marković J, Grdović N, Dinić S, Karan-Djurašević T, Uskoković A, Arambašić J, et al. PARP-1 and YY1 Are Important Novel Regulators of CXCL12 Gene Transcription in Rat Pancreatic Beta Cells. *PloS One* (2013) 8:e59679. doi: 10.1371/journal.pone.0059679
76. Jensen RT, Berna MJ, Bingham DB, Norton JA. Inherited pancreatic endocrine tumor syndromes: Advances in molecular pathogenesis, diagnosis, management, and controversies. *Cancer* (2008) 113:1807–43. doi: 10.1002/cncr.23648
77. Hamze Z, Vercherat C, Bernigaud-Lacheretz A, Bazzi W, Bonnavion R, Lu J, et al. Altered MENIN expression disrupts the MAFA differentiation pathway in insulinoma. *Endocr-Relat Cancer* (2013) 20:833–48. doi: 10.1530/ERC-13-0164
78. Paternoster S, Falasca M. The intricate relationship between diabetes, obesity and pancreatic cancer. *Biochim Biophys Acta (BBA) - Rev Cancer* (2020) 1873:188326. doi: 10.1016/j.bbcan.2019.188326
79. Pang Y, Kartsonaki C, Guo Y, Bragg F, Yang L, Bian Z, et al. Diabetes, plasma glucose and incidence of pancreatic cancer: A prospective study of 0.5 million C hinese adults and a meta-analysis of 22 cohort studies. *Int J Cancer* (2017) 140:1781–8. doi: 10.1002/ijc.30599
80. Hu C-M, Tien S-C, Hsieh P-K, Jeng Y-M, Chang M-C, Chang Y-T, et al. High Glucose Triggers Nucleotide Imbalance through O-GlcNAcylation of Key Enzymes and Induces KRAS Mutation in Pancreatic Cells. *Cell Metab* (2019) 29:1334–49. doi: 10.1016/j.cmet.2019.02.005
81. Saxton RA, Sabatini DM. mTOR Signaling in Growth, Metabolism, and Disease. *Cell* (2017) 168:960–76. doi: 10.1016/j.cell.2017.02.004
82. Alonso LC, Yokoe T, Zhang P, Scott DK, Kim SK, O'Donnell CP, et al. Glucose Infusion in Mice: A New Model to Induce -Cell Replication. *Diabetes* (2007) 56:1792–801. doi: 10.2337/db06-1513
83. Cerf ME. High Fat Programming of β-Cell Failure. *Adv Exp Med Biol* (2010) 654:77–89. doi: 10.1007/978-90-481-3271-3_5
84. Lablanche S, Chobert-Bakouline M, Risse O, Laverrière M-H, Chabre O, Benhamou P-Y. Malignant insulinoma may arise during the course of type 1 diabetes mellitus: A case report. *Diabetes Metab* (2015) 41:258–61. doi: 10.1016/j.diabet.2014.08.004
85. Oikawa Y, Katsuki T, Kawasaki M, Hashiguchi A, Mukai K, Handa K, et al. Insulinoma may mask the existence of Type 1 diabetes: Insulinoma may mask Type 1 diabetes. *Diabetic Med* (2012) 29:e138–41. doi: 10.1111/j.1464-5491.2012.03615.x
86. Drogan D, Schulze MB, Boeing H, Pischon T. Insulin-Like Growth Factor 1 and Insulin-Like Growth Factor–Binding Protein 3 in Relation to the Risk of Type 2 Diabetes Mellitus: Results From the EPIC–Potsdam Study. *Am J Epidemiol* (2016) 183:553–60. doi: 10.1093/aje/kwv188
87. Sandhu MS, Heald AH, Gibson JM, Cruickshank JK, Dunger DB, Wareham NJ. Circulating concentrations of insulin-like growth factor-I and development of glucose intolerance: a prospective observational study. *Lancet* (2002) 359:1740–5. doi: 10.1016/S0140-6736(02)08655-5
88. Sandhu MS, Gibson JM, Heald AH, Dunger DB, Wareham NJ. Low Circulating IGF-II Concentrations Predict Weight Gain and Obesity in Humans. *Diabetes* (2003) 52:1403–8. doi: 10.2337/diabetes.52.6.1403

89. Heald AH, Cruickshank JK, Riste LK, Cade JE, Anderson S, Greenhalgh A, et al. Close relation of fasting insulin-like growth factor binding protein-1 (IGFBP-1) with glucose tolerance and cardiovascular risk in two populations. *Diabetologia* (2001) 44:333–9. doi: 10.1007/s001250051623
90. Rajpathak SN, He M, Sun Q, Kaplan RC, Muzumdar R, Rohan TE, et al. Insulin-Like Growth Factor Axis and Risk of Type 2 Diabetes in Women. *Diabetes* (2012) 61:2248–54. doi: 10.2337/db11-1488
91. Hjortebjerg R, Laugesen E, Høyem P, Oxvig C, Stausbøl-Grøn B, Knudsen ST, et al. The IGF system in patients with type 2 diabetes: associations with markers of cardiovascular target organ damage. *Eur J Endocrinol* (2017) 176:521–31. doi: 10.1530/EJE-16-0940
92. Heald AH, Kärvestedt L, Anderson SG, McLaughlin J, Knowles A, Wong L, et al. Low Insulin-like Growth Factor-II Levels Predict Weight Gain in Normal Weight Subjects with Type 2 Diabetes. *Am J Med* (2006) 119:167.e9–167.e15. doi: 10.1016/j.amjmed.2005.08.001
93. Frystyk J, Skjaerbaek C, Vestbo E, Fisker S, Orskov H. Circulating levels of free insulin-like growth factors in obese subjects: the impact of type 2 diabetes. *Diabetes Metab Res Rev* (1999) 15:314–22. doi: 10.1002/(sici)1520-7560(199909/10)15:5<314::aid-dmrr56>3.0.co;2-e
94. Xu Y, Liu J, Nipper M, Wang P. Ductal vs. acinar? Recent insights into identifying cell lineage of pancreatic ductal adenocarcinoma. *Ann Pancreat Cancer* (2019) 2:11–1. doi: 10.21037/apc.2019.06.03
95. Duvillié B, Cordonnier N, Deltour L, Dandoy-Dron F, Itier JM, Monthioux E, et al. Phenotypic alterations in insulin-deficient mutant mice. *Proc Natl Acad Sci USA* (1997) 94:5137–40. doi: 10.1073/pnas.94.10.5137
96. Leroux L, Desbois P, Lamotte L, Duvillié B, Cordonnier N, Jackerott M, et al. Compensatory responses in mice carrying a null mutation for Ins1 or Ins2. *Diabetes* (2001) 50 Suppl 1:S150–153. doi: 10.2337/diabetes.50.2007.s150
97. Alemán JO, Eusebi LH, Ricciardiello L, Patidar K, Sanyal AJ, Holt PR. Mechanisms of Obesity-Induced Gastrointestinal Neoplasia. *Gastroenterology* (2014) 146:357–73. doi: 10.1053/j.gastro.2013.11.051
98. Zhang AMY, Magrill J, de Winter TJJ, Hu X, Skovsø S, Schaeffer DF, et al. Endogenous Hyperinsulinemia Contributes to Pancreatic Cancer Development. *Cell Metab* (2019) 30:403–4. doi: 10.1016/j.cmet.2019.07.003
99. Rozenblum E, Schutte M, Goggins M, Hahn SA, Panzer S, Zahurak M, et al. Tumor-suppressive pathways in pancreatic carcinoma. *Cancer Res* (1997) 57:1731–4.
100. Feng Z, Levine AJ. The regulation of energy metabolism and the IGF-1/mTOR pathways by the p53 protein. *Trends Cell Biol* (2010) 20:427–34. doi: 10.1016/j.tcb.2010.03.004
101. Dong X, Javle M, Hess KR, Shroff R, Abbruzzese JL, Li D. Insulin-Like Growth Factor Axis Gene Polymorphisms and Clinical Outcomes in Pancreatic Cancer. *Gastroenterology* (2010) 139:464–73. doi: 10.1053/j.gastro.2010.04.042
102. Casellas A, Mallol C, Salavert A, Jimenez V, Garcia M, Agudo J, et al. Insulin-like Growth Factor 2 Overexpression Induces β-Cell Dysfunction and Increases Beta-cell Susceptibility to Damage. *J Biol Chem* (2015) 290:16772–85. doi: 10.1074/jbc.M115.642041
103. Christofori G, Naik P, Hanahan D. Deregulation of both imprinted and expressed alleles of the insulin–like growth factor 2 gene during β–cell tumorigenesis. *Nat Genet* (1995) 10:196–201. doi: 10.1038/ng0695-196
104. Henfling MER, Perren AA, Schmitt AM, Saddig CM, Starke AA, Riedl RG, et al. The IGF pathway is activated in insulinomas but downregulated in metastatic disease. *Endocr-Relat Cancer* (2018) 25:1005–18. doi: 10.1530/ERC-18-0222
105. Modi H, Cornu M, Thorens B. Glutamine Stimulates Biosynthesis and Secretion of Insulin-like Growth Factor 2 (IGF2), an Autocrine Regulator of Beta Cell Mass and Function. *J Biol Chem* (2014) 289:31972–82. doi: 10.1074/jbc.M114.587733
106. Dejeux E, Olaso R, Dousset B, Audebourg A, Gut IG, Terris B, et al. Hypermethylation of the IGF2 differentially methylated region 2 is a specific event in insulinomas leading to loss-of-imprinting and overexpression. *Endocr-Relat Cancer* (2009) 16:939–52. doi: 10.1677/ERC-08-0331
107. Fontanière S, Tost J, Wierinckx A, Lachuer J, Lu J, Hussein N, et al. Gene expression profiling in insulinomas of Men1 β-cell mutant mice reveals early genetic and epigenetic events involved in pancreatic β-cell tumorigenesis. *Endocr-Relat Cancer* (2006) 13:1223–36. doi: 10.1677/erc.1.01294
108. Palmer SC, Strippoli GFM. Metformin as first-line treatment for type 2 diabetes. *Lancet* (2018) 392:120. doi: 10.1016/S0140-6736(18)31541-1
109. Kahn BB, Alquier T, Carling D, Hardie DG. AMP-activated protein kinase: Ancient energy gauge provides clues to modern understanding of metabolism. *Cell Metab* (2005) 1:15–25. doi: 10.1016/j.cmet.2004.12.003
110. Li D, Yeung SJ, Hassan MM, Konopleva M, Abbruzzese JL. Antidiabetic Therapies Affect Risk of Pancreatic Cancer. *Gastroenterology* (2009) 137:482–8. doi: 10.1053/j.gastro.2009.04.013
111. Li X, Li T, Liu Z, Gou S, Wang C. The effect of metformin on survival of patients with pancreatic cancer: a meta-analysis. *Sci Rep* (2017) 7:5825. doi: 10.1038/s41598-017-06207-x
112. Chang H-H, Moro A, Chou CEN, Dawson DW, French S, Schmidt AI, et al. Metformin Decreases the Incidence of Pancreatic Ductal Adenocarcinoma Promoted by Diet-induced Obesity in the Conditional KrasG12D Mouse Model. *Sci Rep* (2018) 8:5899. doi: 10.1038/s41598-018-24337-8
113. Sapio L, Nigro E, Ragone A, Salzillo A, Illiano M, Spina A, et al. AdipoRon Affects Cell Cycle Progression and Inhibits Proliferation in Human Osteosarcoma Cells. *J Oncol* (2020) 2020:1–12. doi: 10.1155/2020/7262479
114. Akimoto M, Maruyama R, Kawabata Y, Tajima Y, Takenaga K. Antidiabetic adiponectin receptor agonist AdipoRon suppresses tumour growth of pancreatic cancer by inducing RIPK1/ERK-dependent necroptosis. *Cell Death Dis* (2018) 9:804. doi: 10.1038/s41419-018-0851-z
115. Nyambuya TM, Dludla PV, Mxinwa V, Mokgalaboni K, Ngcobo SR, Tiano L, et al. The impact of metformin and aspirin on T-cell mediated inflammation: A systematic review of in vitro and in vivo findings. *Life Sci* (2020) 255:117854. doi: 10.1016/j.lfs.2020.117854
116. Khalaf N, Yuan C, Hamada T, Cao Y, Babic A, Morales-Oyarvide V, et al. Regular Use of Aspirin or Non-Aspirin Nonsteroidal Anti-Inflammatory Drugs Is Not Associated With Risk of Incident Pancreatic Cancer in Two Large Cohort Studies. *Gastroenterology* (2018) 154:1380–1390.e5. doi: 10.1053/j.gastro.2017.12.001
117. Sun J, Li Y, Liu L, Jiang Z, Liu G. Aspirin use and pancreatic cancer risk: A systematic review of observational studies. *Medicine* (2019) 98:e18033. doi: 10.1097/MD.0000000000018033
118. Zhang Y-P, Wan Y-D, Sun Y-L, Li J, Zhu R-T. Aspirin might reduce the incidence of pancreatic cancer: A meta-analysis of observational studies. *Sci Rep* (2015) 5:15460. doi: 10.1038/srep15460
119. Bollard J, Patte C, Massoma P, Goddard I, Gadot N, Benslama N, et al. Combinatorial Treatment with mTOR Inhibitors and Streptozotocin Leads to Synergistic *In Vitro* and *In Vivo* Antitumor Effects in Insulinoma Cells. *Mol Cancer Ther* (2018) 17:60–72. doi: 10.1158/1535-7163.MCT-17-0325
120. Yao JC, Shah MH, Ito T, Bohas CL, Wolin EM, Van Cutsem E, et al. Everolimus for Advanced Pancreatic Neuroendocrine Tumors. *N Engl J Med* (2011) 364:514–23. doi: 10.1056/NEJMoa1009290
121. Vergès B, Walter T, Cariou B. Endocrine Side Effects of Anti-Cancer Drugs: Effects of anti-cancer targeted therapies on lipid and glucose metabolism. *Eur J Endocrinol* (2014) 170:R43–55. doi: 10.1530/EJE-13-0586

Conflict of Interest: The authors declare that the research was conducted in the absence of any commercial or financial relationships that could be construed as a potential conflict of interest.

frontiers in Endocrinology

ORIGINAL RESEARCH
published: 15 October 2020
doi: 10.3389/fendo.2020.00642

Homozygosity in the *APOE* 3 Polymorphism Is Associated With Less Depression and Higher Serum Low-Density Lipoprotein in Chinese Elderly Schizophrenics

Wei Li[1,2†], *Chunxia Ban*[3†], *Ling Yue*[1,2†], *Lin Sun*[1,2*], *Xia Li*[1,2*] *and Shifu Xiao*[1,2*]

[1] Department of Geriatric Psychiatry, Shanghai Mental Health Center, Shanghai Jiao Tong University School of Medicine, Shanghai, China, [2] Alzheimer's Disease and Related Disorders Center, Shanghai Jiao Tong University, Shanghai, China, [3] General Psychiatry, Jiading District Mental Health Center, Shanghai, China

OPEN ACCESS

Edited by:
Ralf Jockers,
Université Paris-Sorbonne, France

Reviewed by:
Rami M. El Zein,
INSERM U1016 Institut Cochin, France
Xiaolong Zhao,
Sichuan Provincial People's Hospital, China

***Correspondence:**
Lin Sun
xiaosuan2004@126.com
Xia Li
ja_1023@hotmail.com
Shifu Xiao
xiaoshifu@msn.com

[†] These authors have contributed equally to this work

Specialty section:
This article was submitted to Endocrinology of Aging, a section of the journal Frontiers in Endocrinology

Received: 21 December 2019
Accepted: 06 August 2020
Published: 15 October 2020

Citation:
Li W, Ban C, Yue L, Sun L, Li X and Xiao S (2020) Homozygosity in the APOE 3 Polymorphism Is Associated With Less Depression and Higher Serum Low-Density Lipoprotein in Chinese Elderly Schizophrenics. Front. Endocrinol. 11:642. doi: 10.3389/fendo.2020.00642

Background: Depressive symptoms are common comorbidities in schizophrenia. However, the effect of APOE E3 on depressive symptoms has never been investigated in an aging Chinese population with schizophrenia. This cross-sectional study aimed to investigate the effects of APOE E3 on blood lipid metabolism and depressive symptoms in elderly schizophrenics in China.

Methods: Three Hundred and one elderly schizophrenics (161 males, age ranges from 60 to 92 years, with an average age of 67.31 ± 6.667) were included in the study. Depressive symptoms were assessed using the Geriatric Depression Scale (GDS). APOE gene polymorphism was determined by polymerase chain reaction (PCR). We assessed the correlations of GDS and serum low-density lipoprotein (LDL) with APOE genotypes.

Results: The concentration of LDL in the Homozygous APOE E3 group was significantly higher than that in the non-homozygous APOE E3 group, while the scores of GDS of the Homozygous APOE E3 group were lower than that in the non-homozygous APOE E3 group. Using partial correlation analysis and controlling age, gender, duration of disease, and hyperlipidemia, we found that the scores of GDS were significantly correlated with LDL ($r = -0.194$, $p = 0.016$).

Conclusions : APOE E3 is associated with less depressive symptoms and higher serum LDL in Chinese elderly patients with schizophrenia, and there is a negative correlation between depressive symptoms and LDL.

Keywords: aging, APOE E3, depressive symptom, Chinese, schizophrenia

INTRODUCTION

Schizophrenia is associated with an increased prevalence of depressive symptoms. According to previous studies, ∼59% of schizophrenia patients suffer from either minor or major depression (1, 2). Depressive symptoms are commonly seen in all stages of schizophrenia, particularly in the acute phase (3). They have been found to correlate with positive symptoms, negative symptoms,

and general psychopathology in patients with schizophrenia (4). The accumulated evidence from previous studies suggests that the presence of depressive symptoms in patients with schizophrenia has been associated with worse overall outcomes, greater comorbidity, work impairment, poorer quality of life, deterioration of psychosocial functioning, greater risk of relapse, and increased risk of suicide (5, 6). It is therefore extremely important to understand the prevalence and influencing factors of depression in schizophrenics and to develop effective interventions.

Various physiological factors increase the risk of depressive symptoms or depression, including lipid metabolism and genetic variations related to lipids (7). A potential genetic variant that affects lipid metabolism symptoms is the Apolipoprotein E (APOE) gene. APOE is critical in the modulation of phospholipid and cholesterol transport between cells, and it is also believed to play a significant role in neuronal growth and repair (8). Human APOE is a polymorphic protein, APOE E2, E3, and E4, which are encoded by three alleles, ϵ2, ϵ3, and ϵ4, respectively (9). Meta-analyses of genetic studies reported an association of APOE allele ϵ2 with major depressive disorder (10). Skoog et al. (11) proved that the presence of APOE allele ϵ4 predicted future depression and might be an identifier for aging people who are at high risk of clinically significant depression.

The APOE E3 allele is the most frequent allele in all human groups (12) and has been reported to have protection against cardiovascular diseases by maintaining lipid homeostasis (13). However, the effect of APOE E3 on depressive symptoms in schizophrenia has never been investigated. In response, we conducted a cross-sectional study to investigate the effects of homozygosity in the APOE 3 polymorphism on lipid metabolism and depressive symptoms in elderly Chinese schizophrenics.

MATERIALS AND METHODS

Participants

This cross-sectional study was conducted between July 1, 2015, and December 31, 2015, and included 301 hospitalized elderly schizophrenics (age ranges from 60 to 92 years, with an average age of 67.31 ± 6.667; among them, 161 were males, accounting for 53.5%), who were recruited from three mental health centers (including the Shanghai Mental Health Center, the Mental Health Center of Fengxian District in Shanghai, and the Mental Health Center of Jiading District in Shanghai). The method of sampling has been described in our previous studies (14). The inclusion criteria were as follows: (1) aged 60 or more; (2) diagnosed with schizophrenia, which was diagnosed by a senior psychiatrist according to the International Classification of Diseases 10 diagnostic standard; (3) without major medical abnormalities, including unstable, acute, or life-threatening medical illness and central nervous system diseases; (4) was able to cooperate and complete relevant inspections. Subjects with a history of major medical abnormalities (e.g., cancer and infection) and those who chose not to take part were excluded. Through face-to-face interviews, we obtained general demographic data (for example, age, education, gender, BMI, duration of disease), daily living habits (smoking, drinking, drinking tea, physical exercise, and hobbies), disease history (hypertension, diabetes, and hyperlipidemia) and currently prescribed medicines (including clozapine, olanzapine, quetiapine, risperidone, and aripiprazole).

This study was approved by the Research Ethical Committee of the affiliated mental health center of the Shanghai Jiaotong University, School of Medicine. Written informed consent was obtained from all participants before the study. All research processes were conducted according to the principles of the Declaration of Helsinki.

Neuropsychological Assessment

Depression Evaluation

Depression is a condition characterized by a depressed mood or loss of pleasure or interest in nearly all activities almost every day for at least 2 weeks (15). The presence of depressive symptoms was determined using the Geriatric Depression Scale (GDS) (16). The GDS consists of 30 items (hereafter referred to as the GDS-30), and participants were asked to answer "yes" or "no" to these items based on how they felt over the past week, and those with a score higher than 10 points were considered to have depression (17).

Cognitive Assessment

The Montreal Cognitive Assessment (MoCA) was used to evaluate the cognitive function of these subjects. MoCA is a widely used 10-min cognitive screening test for the detection of mild cognitive impairment (MCI), with high sensitivity (90%) and specificity (87%) (18). It has been proven to be effective in detecting cognitive impairment in schizophrenics (19).

Symptom Assessment

The Positive and Negative Syndrome Scale (PANSS) was utilized to assess the symptoms and severity of schizophrenia, as it is a reliable and valid instrument that has served the scientific research community for decades (20). The PANSS includes four scales measuring positive and negative syndromes, aggressiveness, as well as general severity of illness (21). Several subsequent studies have shown that it has strong psychometric properties in terms of reliability, validity, and sensitivity (22).

Genotyping of APOE and Biochemical Detection of Blood Lipids

The genomic DNA was removed from peripheral blood (Morning fasting whole blood) by using a Blood Genomic DNA Extraction Kit (spin column, Tiangen Biochemical Science and Technology Co., Ltd., Beijing, China). The APOE genotype was determined by multiplex amplification refractory mutation system polymerase chain reaction (PCR). The multiplex PCR reactions based on the two SNP cores of the APOE gene were measured using the rs7412 and rs429358 design primers as follows: P1:5-′GCCTACAAATCGGAACTGGACAGCT CCTCGGTGCTCTG-3′ and P2:5 ′-TAAGCGGCTCCTCCGCGATGCCCCGGCCTGGTACACTG-3′. We verified the primers on Nucleotide-nucleotide BLAST: (https://ncbiinsights.ncbi.nlm.nih.gov/tag/nucleotide-blast).

According to the methods previously described (23), the 301 subjects were divided into two groups, the Homozygous APOE E3 group (ε3/ε3, $n = 205$) and the non-homozygous APOE E3 group (ε2/ε2, ε2/ε3, ε3/ε4, and ε4/ε4, $n = 96$) group. **Tables 1** and **2** list the information about gene distribution in detail. The values of serum triglyceride, cholesterol, fasting blood glucose, low-density lipoprotein, and high-density lipoprotein were obtained by using the hexokinase method on an auto-analyzer (Dimension Xpand plus).

TABLE 1 | Allele frequencies and prevalence of APOE among Chinese elderly with schizophrenia.

APOE	Male ($n = 161$)	Female ($n = 140$)	Combined ($n = 301$)
E2 (ϵ2/ϵ2, ϵ2/ϵ3)	23 (14.3%)	17 (12.1%)	40 (13.3%)
E3(ϵ3/ϵ3)	109 (67.7%)	96 (68.6%)	205 (68.1%)
E4(ϵ2/ϵ4, ϵ3/ϵ4, ϵ4/ϵ4)	29 (18.0%)	27 (19.3%)	56 (18.6%)
ϵ2/ϵ2	1 (0.6%)	1 (0.7%)	2 (0.7%)
ϵ2/ϵ3	22 (13.7%)	16 (11.4%)	38 (12.6%)
ϵ2/ϵ4	2 (1.2%)	4 (2.9%)	6 (2.0%)
ϵ3/ϵ3	109 (67.7%)	96 (68.6%)	205 (68.1%)
ϵ3/ϵ4	23 (14.3%)	20 (14.3%)	43 (14.3%)
ϵ4/ϵ4	4 (2.5%)	3 (2.1%)	7 (2.3%)

Statistical Analysis

Continuous variables were expressed as mean ± SD and categorical variables were expressed as frequencies (%). A single sample Kolmogorov-Smirnov test was used to test whether the data conformed to the normal distribution and an independent sample *t*-test was used to compare the data of normal distribution between the Homozygous APOE E3, and the non-homozygous APOE E3 group. The Mann-Whitney U test was used to compare the data of non-normal distribution, while the Chi-square test was used to categorical variables between the two groups. The partial correlation analysis was then used to explore the association between neuropsychological tests and blood lipids (age, education, duration of disease, and hyperlipidemia were controlled). All statistical analyses were performed using SPSS 22.0 (IBM Corporation, Armonk, NY, USA), and two-tailed tests were utilized at a significance level of $P < 0.05$.

RESULTS

Table 1 presents the results of the allele and genotype frequencies. Frequencies of APOE E3 were greatest (68.1%). **Table 2** displays

TABLE 2 | General demographic data of the Chinese elderly with schizophrenia based on APOE E3.

Variables	Homozygous APOE E3 ($N = 205$)	Non-homozygous APOE E3 ($N = 96$)	F or X^2	*P*
Age, y	67.10 ± 6.542	67.73 ± 6.888	−0.768	0.443
Education, y	8.21 ± 3.652	7.63 ± 3.807	1.272	0.204
Duration of disease, y	35.45 ± 13.241	37.71 ± 13.066	−1.374	0.170
BMI, kg/m^2	23.95 ± 4.217	23.56 ± 3.989	0.749	0.455
Fasting blood glucose, mmol/L	5.50 ± 1.491	5.47 ± 1.264	0.177	0.859
Triglyceride, mmol/L	1.38 ± 0.836	1.39 ± 0.808	0.076	0.927
High density lipoprotein, mmol/L	1.29 ± 0.406	1.31 ± 0.412	−0.055	0.956
Low density lipoprotein, mmol/L	2.83 ± 0.752	2.62 ± 0.858	2.140	0.033*
Male, n (%)	109 (53.2)	52 (54.2)	0.026	0.902
Hypertension, n (%)	78 (38.0)	33 (34.4)	0.379	0.609
Diabetes, n (%)	52 (25.4)	26 (27.1)	0.100	0.779
Hyperlipidemia, n (%)	72 (35.1)	48 (50.0)	6.037	0.016*
Smoker, n (%)	69 (33.7)	28 (29.2)	0.604	0.509
Drinker, n (%)	24 (11.7)	9 (9.4)	0.364	0.693
Tea drinker, n (%)	44 (21.5)	22 (22.9)	0.081	0.767
Physical exercise, n (%)	66 (32.2)	29 (30.2)	0.119	0.791
Hobby, n (%)	78 (38.0)	31 (32.3)	0.938	0.369
Clozapine, n (%)	33 (16.1)	15 (15.6)	0.011	1.000
Olanzapine, n (%)	54 (26.3)	28 (29.2)	0.263	0.677
Quetiapine, n (%)	26 (12.7)	16 (16.7)	0.864	0.375
Risperidone, n (%)	61 (29.8)	26 (27.1)	0.227	0.684
Aripiprazole, n (%)	38 (18.5)	17 (17.7)	0.030	1.000
MoCA	14.23 ± 6.740	12.99 ± 7.203	1.335	0.183
GDS	9.46 ± 5.927	11.71 ± 5.514	−2.765	0.006*
PANSS	63.95 ± 21.100	65.70 ± 22.823	−0.603	0.547

*$p < 0.05$.

the characteristic of subjects with different APOE genotypes. By using a single sample Kolmogorov-Smirnov test, we found that BMI ($p > 0.05$) was in the normal distribution, while age, education, duration of disease, fasting blood sugar, triglyceride, high- density lipoprotein, low-density lipoprotein, and scores of MoCA, GDS, and PANSS ($p < 0.05$) were in non-normal distribution.

By using the Independent sample *t*-test (Normal distribution), Mann-Whitney U test (Non-normal distribution), and Chi-square test (Categorical variable), we found that there were statistical differences between the two groups in terms of low density lipoprotein ($p = 0.033$), the score of GDS ($p = 0.006$), and hyperlipidemia ($p = 0.016$). There was no significant difference ($p > 0.05$) in age, education, duration of disease, BMI, fasting blood sugar, triglyceride, high-density lipoprotein, gender, hypertension, diabetes, smoker, drinker, tea drinker, physical exercise, hobby, clozapine, olanzapine, quetiapine, risperidone, aripiprazole, and scores of MoCA and PANSS between the two groups (**Table 2**). The concentration of LDL in the Homozygous APOE E3 group was significantly higher than the non-homozygous APOE E3 group, while the scores of GDS in the Homozygous APOE E3 group were lower than that in the non-homozygous APOE E3 group. **Table 2**, **Figures 1**, **2** show the results. By using partial correlation analysis and controlling age, gender, duration of disease, and hyperlipidemia, we found that the scores of GDS were significantly correlated with low-density lipoprotein ($r = -0.194$, $p = 0.016$).

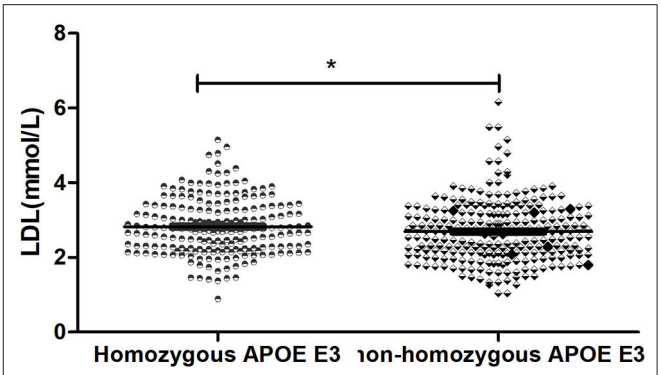

FIGURE 1 | Comparsion of LDL between two groups. *means $p < 0.05$.

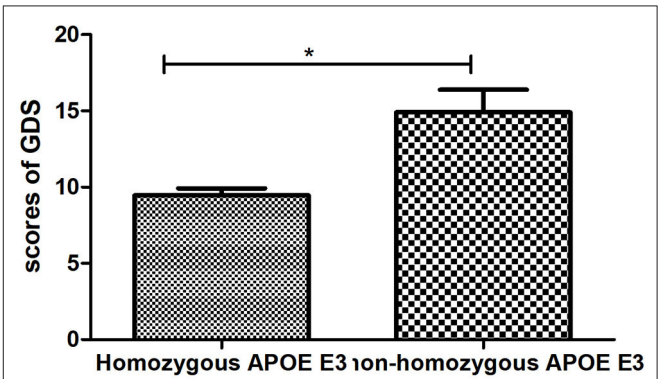

FIGURE 2 | Comparsion of GDS between two groups. *means $p < 0.05$.

DISCUSSION

To the best of our knowledge, this is the first study to explore the effect of homozygosity in the APOE 3 polymorphism on depressive symptoms in a Chinese elderly population with schizophrenia. The study revealed several interesting findings: (1) that the APOE E3 genotype was associated with less depressive symptoms in elderly patients with schizophrenia; (2) the APOE E3 genotype was associated with higher serum low-density lipoprotein; and, (3) that there was a negative correlation between low-density lipoprotein and depression score.

The present study recruited 301 hospitalized elderly schizophrenics. All participants completed a neuropsychological assessment (MoCA, GDS, and PANSS), APOE gene polymorphism test, and blood lipid test. Using the Mann-Whitney U test, we found that APOE E3 was associated with lower depressive symptoms and higher concentrations of LDL. By using partial correlation analysis and controlling age, gender, duration of disease, and hyperlipidemia, we proved that scores of GDS were significantly correlated with low density lipoprotein ($r = -0.194$, $p = 0.016$).

To verify whether the above conclusions still exist in a non-schizophrenic elderly population, we recruited 154 participants as controls (age ranges from 60 to 78 years, with an average age of 68.54 ± 6.632). Among them, 72 were male, accounting for 46.8%, and there was no statistical difference in the above indexes between the schizophrenia group and control group. After controlling for age and gender, there was no statistical difference in the concentration of LDL between the Homozygous APOE E3 group and the non-homozygous APOE E3 group. However, the scores of GDS in the Homozygous APOE E3 group were still lower than those in the non-homozygous APOE E3 group. **Table 3** presents these results.

The relationship between APOE gene polymorphism and schizophrenia is very complicated. Gibbons et al. (24) have pointed out that alterations in APOE expression might lead to either the risk of developing schizophrenia or clinical manifestations, as APOE was important in CNS functions such as modulating cell signaling, protein phosphorylation, intraneuronal calcium, and storage-induced synaptic sprouting. However, other related conclusions are not consistent. For example, a French association study and meta-analysis suggested that there was no major role for APOE gene variants in schizophrenia as a whole (25). However, another study supported that the APOE epsilon 4/epsilon 4 genotypes might be associated with early-onset

TABLE 3 | Characteristics of Chinese normal elderly subjects with different APOE groups.

Characteristics	Homozygous APOE E3 ($n = 97$)	Non-homozygous APOE E3 ($n = 57$)	t or X^2	p
Age, y	68.30 ± 6.515	68.95 ± 6.867	−0.585	0.560
Low density lipoprotein, mmol/L	2.874 ± 0.870	2.930 ± 0.809	−0.401	0.689
Male, n (%)	45 (46.4)	27 (47.4)	0.014	1.000
GDS	4.769 ± 3.947	6.887 ± 4.718	−2.887	0.005*

*$p < 0.05$.

schizophrenia, while the APOE epsilon 3 allele might function protectively in later onset in this disease (26). Therefore, a large sample of longitudinal studies is needed to further examine the association between APOE gene polymorphism and schizophrenia.

It is well-known that lipid metabolism could be affected by the frequency of APOE (27). In our study, we found that APOE E3 was associated with higher LDL in Chinese aging patients with schizophrenia and there was a negative correlation between LDL and depression score. A systematic review and meta-analysis (28) showed that patients with depression tend to have lower LDL (Mean difference $= -4.29$, 95% $CI = -8.19$, -0.40, $p = 0.03$). Beasley et al. (29) found that cholesterol levels were 13% lower in major depressive disorder ($p = 0.018$) and 10% lower in bipolar disorder ($p = 0.052$) compared with controls, while there was no significant difference ($p > 0.05$) between schizophrenia and controls. Another study by Olsson et al. (30) also indicated that low LDL might increase the risk of depression and the mechanism might involve immunity, inflammation, and brain dysfunction. However, a previous study suggested that stroke patients with the APOE genotype $\epsilon 3/\epsilon 3$ had more symptoms of depression compared to the other genotypes (13). Another study showed that there was no significant association between depression and APOE genotype (31). Our findings are partially consistent, and different human populations and different disease types might be responsible for these differences.

Several mechanisms might be used to explain why the APOE E3 genotype helps prevent depression. First, APOE E3 can inhibit amyloid accumulation and increase LDL receptor levels. Second, APOE E3 also plays a crucial role in cholesterol efflux and reverse cholesterol transport, and bears anti-inflammatory and anti-oxidant properties (32). Third, E3 ubiquitin ligase IDOL determines the level of ApoER2 protein in the synapse in response to neuronal activation and regulates the morphogenesis and plasticity of dendritic spines. Furthermore, APOE E3 contributes toward maintaining the integrity of endothelial function and the blood-brain barrier (BBB) at the neurovascular junction (33).

There are some limitations to our research. First, this is a cross-sectional study, unable to establish the causal relationship between APOE E3, LDL, and depressive symptoms. Second, the relatively small sample size reduces the reliability of the study. Third, these subjects have been taking antipsychotics, which could have influenced the research conclusion.

CONCLUSIONS

The APOE E3 genotype is associated with less depressive symptoms and higher serum low-density lipoprotein in Chinese elderly patients with schizophrenia. There is a negative correlation between depressive symptoms and low-density lipoprotein. Therefore, it may be possible to improve depressive symptoms by increasing blood lipid concentration in patients with schizophrenia, but this conclusion needs to be verified by a large sample of longitudinal research.

DATA AVAILABILITY STATEMENT

The datasets analyzed in this article are not publicly available, because the database is less than ten years old, and it needs to be authorized by the data owner to be public. Requests to access the datasets should be directed to ja_1023@hotmail.com.

ETHICS STATEMENT

The studies involving human participants were reviewed and approved by Research Ethical Committee of the affiliated mental health center of Shanghai jiaotong university school of medicine. The patients/participants provided their written informed consent to participate in this study. Written informed consent was obtained from the individual(s) for the publication of any potentially identifiable images or data included in this article.

AUTHOR CONTRIBUTIONS

WL and LS contributed to the study concept and design. LY and CB acquired the data. XL and SX analyzed the data and drafted the manuscript. All authors read and approved the final manuscript.

FUNDING

This work was supported by grants from the National Natural Science Foundation of China (no. 81671402), the National Key R&D Program of China (2017YFC1310501500), the Cultivation of Multidisciplinary Interdisciplinary Project in Shanghai Jiaotong University (YG2019QNA10), the Clinical research center project of Shanghai Mental Health Center (CRC2017ZD02), Shanghai Clinical Research Center for Mental Health (SCRC-MH) (19MC1911100), and the Feixiang Program of Shanghai Mental Health Center(2020-FX-03).

REFERENCES

1. Felmet K, Zisook S, Kasckow JW. Elderly patients with schizophrenia and depression: diagnosis and treatment. *Clin. Schizophr. Relat. Psychoses.* (2011) 4:239–50. doi: 10.3371/CSRP.4.4.4
2. Xu YM, Li F, Liu XB, Zhong BL. Depressive symptoms in Chinese male inpatients with schizophrenia: prevalence and clinical correlates. *Psychiatry Res.* (2018) 264:380–84. doi: 10.1016/j.psychres.2018.04.016
3. Baynes D, Mulholland C, Cooper SJ, Montgomery RC, MacFlynn G, Lynch G, et al. Depressive symptoms in stable chronic schizophrenia: prevalence and relationship to psychopathology and treatment. *Schizophr. Res.* (2000) 45:47–56. doi: 10.1016/S0920-9964(99)00205-4
4. Peitl V, Vidrih B, Karlovic Z, Getaldic B, Peitl M, Karlovic D. Platelet serotonin concentration and depressive symptoms in patients with schizophrenia. *Psychiatry Res.* (2016) 239:105–10. doi: 10.1016/j.psychres.2016.03.006
5. Majadas S, Olivares J, Galan J, Diez T. Prevalence of depression and its relationship with other clinical characteristics in a sample of patients with stable schizophrenia. *Compr. Psychiatry.* (2012) 53:145–51. doi: 10.1016/j.comppsych.2011.03.009
6. Cotton SM, Lambert M, Schimmelmann BG, Mackinnon A, Gleeson JF, Berk M, et al. Depressive symptoms in first episode schizophrenia spectrum disorder. *Schizophr. Res.* (2012) 134:20–6. doi: 10.1016/j.schres.2011.08.018
7. Zhou X, Wang J, Lu Y, Chen C, Hu Y, Liu P, et al. Anti-depressive effects of Kai-Xin-San on lipid metabolism in depressed patients and CUMS rats using metabolomic analysis. *J Ethnopharmacol.* (2020) 252:112615. doi: 10.1016/j.jep.2020.112615
8. Verghese PB, Castellano JM, Holtzman DM. Apolipoprotein E in Alzheimer's disease and other neurological disorders. *Lancet Neurol.* (2011) 10:241–52. doi: 10.1016/S1474-4422(10)70325-2
9. Poirier J, Davignon J, Bouthillier D, Kogan S, Bertrand P, Gauthier S. Apolipoprotein E polymorphism and Alzheimer's disease. *Lancet.* (1993) 342:697–99. doi: 10.1016/0140-6736(93)91705-Q
10. Lopez-Leon S, Janssens AC, Gonzalez-Zuloeta Ladd AM, Del-Favero J, Claes SJ, Oostra BA, et al. Meta-analyses of genetic studies on major depressive disorder. *Mol. Psychiatry.* (2008) 13:772–85. doi: 10.1038/sj.mp.4002088
11. Skoog I, Waern M, Duberstein P, Blennow K, Zetterberg H, Börjesson-Hanson A, et al. A 9-year prospective population-based study on the association between the APOE*E4 allele and late-life depression in Sweden. *Biol. Psychiatry.* (2015) 78:730–36. doi: 10.1016/j.biopsych.2015.01.006
12. Corbo RM, Scacchi R. Apolipoprotein E (APOE) allele distribution in the world. Is APOE*4 a 'thrifty' allele? *Ann. Hum. Genet.* (1999) 63(Pt 4):301–10. doi: 10.1046/j.1469-1809.1999.6340301.x
13. Leduc V, Domenger D, De Beaumont L, Lalonde D, Belanger-Jasmin S, Poirier J. Function and comorbidities of apolipoprotein e in Alzheimer's disease. *Int. J. Alzheimers Dis.* (2011) 2011:974361. doi: 10.4061/2011/974361
14. Ban C, Zhang Q, Feng J, Li H, Qiu Q, Tian Y, et al. Low prevalence of lipid metabolism abnormalities in APOE epsilon2-genotype and male patients 60 years or older with schizophrenia. *BMC Psychiatry.* (2017) 17:399. doi: 10.1186/s12888-017-1530-9
15. Smith K. Mental health: a world of depression. *Nature.* (2014) 515:181. doi: 10.1038/515180a
16. Lin X, Haralambous B, Pachana NA, Bryant C, LoGiudice D, Goh A, et al. Screening for depression and anxiety among older Chinese immigrants living in Western countries: the use of the Geriatric Depression Scale (GDS) and the Geriatric Anxiety Inventory (GAI). *Asia Pac. Psychiatry.* (2016) 8:32–43. doi: 10.1111/appy.12191
17. Albinski R, Kleszczewska-Albinska A, Bedynska S. Geriatric depression scale (GDS). validity and reliability of different versions of the scale—review. *Psychiatr. Pol.* (2011) 45:555–62.
18. Nasreddine ZS, Phillips NA, Bedirian V, Charbonneau S, Whitehead V, Collin I, et al. The Montreal Cognitive Assessment, MoCA: a brief screening tool for mild cognitive impairment. *J. Am. Geriatr. Soc.* (2005) 53:695–99. doi: 10.1111/j.1532-5415.2005.53221.x
19. Fisekovic S, Memic A, Pasalic A. Correlation between moca and mmse for the assessment of cognition in schizophrenia. *Acta Inform. Med.* (2012) 20:186–89. doi: 10.5455/aim.2012.20.186-189
20. Aboraya A, Nasrallah HA. Perspectives on the positive and negative syndrome scale (PANSS): use, misuse, drawbacks, and a new alternative for schizophrenia research. *Ann. Clin. Psychiatry.* (2016) 28:125–31.
21. Kay SR, Fiszbein A, Opler LA. The positive and negative syndrome scale (PANSS) for schizophrenia. *Schizophr. Bull.* (1987) 13:261–76. doi: 10.1093/schbul/13.2.261
22. Rabinowitz J, Schooler NR, Anderson A, Ayearst L, Daniel D, Davidson M, et al. Consistency checks to improve measurement with the positive and negative syndrome scale (PANSS). *Schizophr Res.* (2017) 190:74–6. doi: 10.1016/j.schres.2017.03.017
23. Donohoe GG, Salomaki A, Lehtimaki T, Pulkki K, Kairisto V. Rapid identification of apolipoprotein E genotypes by multiplex amplification refractory mutation system PCR and capillary gel electrophoresis. *Clin Chem.* (1999) 45:143–46. doi: 10.1093/clinchem/45.1.143
24. Gibbons AS, Udawela M, Jeon WJ, Seo MS, Brooks L, Dean B. The neurobiology of APOE in schizophrenia and mood disorders. *Front. Biosci.* (2011) 16:962–79. doi: 10.2741/3729
25. Schurhoff F, Krebs MO, Szoke A, Loze JY, Goldberger C, Quignon V, et al. Apolipoprotein E in schizophrenia: a French association study and meta-analysis. *Am. J. Med. Genet. B Neuropsychiatr. Genet.* (2003) 119b:18–23. doi: 10.1002/ajmg.b.20007
26. Kampman O, Anttila S, Illi A, Mattila KM, Rontu R, Leinonen E, et al. Apolipoprotein E polymorphism is associated with age of onset in schizophrenia. *J. Hum. Genet.* (2004) 49:355–59. doi: 10.1007/s10038-004-0157-0
27. Guan S, Yang J, Tang Z, Fang X, Wu X, Sun F, et al. The relationship between apolipoprotein (apo) E polymorphism and lipid changes: an 8-year cohort study in Beijing elderly persons. *Arch. Gerontol. Geriatr.* (2012) 55:713–17. doi: 10.1016/j.archger.2011.12.001
28. Persons JE, Fiedorowicz JG. Depression and serum low-density lipoprotein: a systematic review and meta-analysis. *J. Affect. Disord.* (2016) 206:55–67. doi: 10.1016/j.jad.2016.07.033
29. Beasley CL, Honer WG, Bergmann K, Falkai P, Lutjohann D, Bayer TA. Reductions in cholesterol and synaptic markers in association cortex in mood disorders. *Bipolar Disord.* (2005) 7:449–55. doi: 10.1111/j.1399-5618.2005.00239.x
30. Olsson AG, Angelin B, Assmann G, Binder CJ, Björkhem I, Cedazo-Minguez A, et al. Can LDL cholesterol be too low? Possible risks of extremely low levels. *J. Intern. Med.* (2017) 281:534–53. doi: 10.1111/joim.12614
31. Lyketsos CG, Baker L, Warren A, Steele C, Brandt J, Steinberg M, et al. Depression, delusions, and hallucinations in Alzheimer's disease: no relationship to apolipoprotein E genotype. *J. Neuropsychiatr. Clin. Neurosci.* (1997) 9:64–7. doi: 10.1176/jnp.9.1.64
32. Liao F, Yoon H, Kim J. Apolipoprotein E metabolism and functions in brain and its role in Alzheimer's disease. *Curr. Opin. Lipidol.* (2017) 28:60–7. doi: 10.1097/MOL.0000000000000383
33. Jofre-Monseny L, Minihane AM, Rimbach G. Impact of apoE genotype on oxidative stress, inflammation and disease risk. *Mol. Nutr. Food Res.* (2008) 52:131–45. doi: 10.1002/mnfr.200700322

Conflict of Interest: The authors declare that the research was conducted in the absence of any commercial or financial relationships that could be construed as a potential conflict of interest.

frontiers in Endocrinology

REVIEW
published: 18 November 2020
doi: 10.3389/fendo.2020.597573

Growth Hormone Receptor Regulation in Cancer and Chronic Diseases

Ger J. Strous[1,2], Ana Da Silva Almeida[1†], Joyce Putters[1†], Julia Schantl[1], Magdalena Sedek[1†], Johan A. Slotman[1†], Tobias Nespital[1†], Gerco C. Hassink[1†] and Jan A. Mol[3]**

[1] Department of Cell Biology, Centre for Molecular Medicine, University Medical Centre Utrecht, Utrecht, Netherlands, [2] BIMINI Biotech B.V., Leiden, Netherlands, [3] Department of Clinical Sciences of Companion Animals, Faculty of Veterinary Medicine, Utrecht University, Utrecht, Netherlands

The GHR signaling pathway plays important roles in growth, metabolism, cell cycle control, immunity, homeostatic processes, and chemoresistance *via* both the JAK/STAT and the SRC pathways. Dysregulation of GHR signaling is associated with various diseases and chronic conditions such as acromegaly, cancer, aging, metabolic disease, fibroses, inflammation and autoimmunity. Numerous studies entailing the GHR signaling pathway have been conducted for various cancers. Diverse factors mediate the up- or down-regulation of GHR signaling through post-translational modifications. Of the numerous modifications, ubiquitination and deubiquitination are prominent events. Ubiquitination by E3 ligase attaches ubiquitins to target proteins and induces proteasomal degradation or starts the sequence of events that leads to endocytosis and lysosomal degradation. In this review, we discuss the role of first line effectors that act directly on the GHR at the cell surface including ADAM17, JAK2, SRC family member Lyn, Ubc13/CHIP, proteasome, βTrCP, CK2, STAT5b, and SOCS2. Activity of all, except JAK2, Lyn and STAT5b, counteract GHR signaling. Loss of their function increases the GH-induced signaling in favor of aging and certain chronic diseases, exemplified by increased lung cancer risk in case of a mutation in the SOCS2-GHR interaction site. Insight in their roles in GHR signaling can be applied for cancer and other therapeutic strategies.

Keywords: aging, cancer, ubiquitin, endocytosis, GH/IGF-1 axis, GH sensitivity

OPEN ACCESS

Edited by:
Ralf Jockers,
Université de Paris, France

Reviewed by:
Vincent Goffin,
Université Paris Descartes, France
Roman L. Bogorad,
Puretech Health, Inc., United States

****Correspondence:***
Ger J. Strous
gstrous@umcutrecht.nl;
ger.strous@biminibiotech.nl
Jan A. Mol
j.a.mol@uu.nl

†Present addresses:
Ana Da Silva Almeida,
Biogen, Cambridge, MA, United States
Joyce Putters,
Department of Life, Environment, and Health, Dutch Research Council (NWO) The Hague, Netherlands
Magdalena Sedek,
Merck Chemicals B.V., Amsterdam, Netherlands
Johan A. Slotman,
Optical Imaging Centre, Erasmus Medical Center Rotterdam, Rotterdam, Netherlands
Tobias Nespital,
Biological Mechanisms of Ageing, Max-Planck Institute for Biology of Ageing, Cologne, Germany
Gerco C. Hassink,
Clinical Neurophysiology, Technical Medical Centre, University of Twente, Enschede, Netherlands

Specialty section:
This article was submitted to Cellular Endocrinology, a section of the journal Frontiers in Endocrinology

Received: *21 August 2020*
Accepted: *14 October 2020*
Published: *18 November 2020*

INTRODUCTION

In 1989 with a background of posttranslational modifications and intracellular transport of membrane glycoproteins our lab decided to focus on studying the role of ubiquitination in membrane trafficking. Knowledge on the role of ubiquitination as a major regulator of cell functions had just started to emerge (1). To address the question of whether ubiquitination and membrane trafficking are connected processes, we sought a model membrane protein to focus on. Some evidence suggested that the growth hormone receptor (GHR), isolated from rabbit liver, is

ubiquitinated (2). We choose this as our model and very soon, it became clear that the two fields were indeed connected (3). Now, we know that both the ubiquitin system and the GHR are crucially important for the regulation of cellular life and metabolism. The state-of-the-art of both fields has been described in excellent recent reviews (4–11). In this review we will connect both systems.

Loss of the GHR is not lethal, but results in sub-optimal health, short stature, decreased bone mineral density, decreased muscle strength, thin skin and hair, increased adiposity, and hepatic steatosis. Interestingly, people with non-functional GH signaling have very low plasma insulin growth factor 1 (IGF-1) concentrations, are highly resistant to cancer and diabetes type 2 and seem to have a slow cognitive decline (12, 13). GHR, whose function is more a modulator of cellular processes, may deteriorate healthy aging and act as an important stimulator of carcinogenesis. Our focus will therefore be on the mechanisms involved in the regulation of this important receptor, wherein ubiquitination and phosphorylation enzymes play major parts, and on the impact of these in health and disease.

THE GROWTH HORMONE RECEPTOR

The Prototype Cytokine Receptor

GHR is a single membrane spanning protein of 638 amino acids, isolated for the first time from rabbit liver (14). Cloning from several species revealed a strong sequence homology (15). The human *GHR* is composed by 9 exons (16) encoding a cleavable amino acid signal peptide of 18 (exon 2), an extracellular domain of 246 (exon 3 to 7), a transmembrane domain of 24 (exon 8), and an intracellular domain of 350 residues (exon 9 and 10). GHR belongs to the class 1 superfamily of cytokine receptors, which includes 27 ligands and 34 human type I cytokine receptors (17). The GHR was the first member of the family to be characterized (2) and is expressed in most cells of the human body.

The class 1 cytokine receptors share many features. In the extracellular domain they contain conserved cysteine residues and a WSxWS motif (18). In the case of GHR, this motif is different, although homologous, YGEFS. Alteration of the sequence disrupts ligand binding and receptor signaling (19). Despite the limited amino acid homology, the structures of GHR, EPOR and PRLR are similar, consisting of two fibronectin- (FN) type 3 domains (β-sandwich composed of seven β strands). In GHR the N-terminal domain is composed of amino acids 19–141 and the C-terminal composed of amino acids 146–264, separated by a four-amino acid hinge region (20). The GHR extracellular domain contains 3 disulfide bridges, formed by 6 of its 7 cysteine residues (**Figure 1**) (23). The intracellular domain contains two conserved membrane-proximal conserved sequences, referred to as box1 and box2, equivalent to the UbE/TPR motif, with functions in JAK2 binding and GHR endocytosis, respectively. Additionally, a conserved DSGxxS degradation motif is present downstream of box2, whose function is explained later in this review.

GHR Life Cycle

While being translated on ribosomes, GHR is inserted in the endoplasmic reticulum (ER) membrane due the presence of the signal peptide (**Figure 2**). In the ER, the disulfide bonds are formed and GHR dimerizes (29). GHR is glycosylated with high mannose oligosaccharides important for the process of quality control in the ER. When correctly folded, higher order (presumably tetrameric) complexes assemble, and GHR continues its route in to the Golgi apparatus (27). In the Golgi, the high mannose oligosaccharides of GHR are processed into complex oligosaccharides.

In 2003, we identified both SGTA and BAG6 as binding partners for the GHR (30, 31). The binding depends on an intact UbE/TPR motif, similar as for CHIP and βTrCP. Also pentatricopeptide motif-containing proteins like LRP130 were identified (30). The binding was lost if F345 was mutated. Bag6/Bat3 localized to the nucleus, the Golgi complex and to mitochondria. Inhibition of protein synthesis as well as UV-treatment resulted in a reduction of Bag6 to mitochondria. According to current insight Bag6 can bind to both precursor and mature GHR *via* SGTA and Ubl4a (32–34). Silencing of UBL4 had no effect on GHR function at the cell surface and its endocytosis (35). Most likely the SGTA/Bag6 complex plays a role in GHR dimerization, and multimerization at the endoplasmic reticulum and in the Golgi complex (27, 36).

After this step, the GHRs traffic to the cell surface (**Figure 2**). Unlike most growth factor receptors, the GHR is continuously synthesized and degraded with a half-life of 30-60 min (37–39). GHR is constitutively endocytosed independently of GH binding (39, 40). GH binding at the cell surface initiates signaling, and accelerates endocytosis of the GH-GHR complex (41, 42). GHR is sorted into the multivesicular bodies (MVB), and eventually degraded in the lysosome (43). Additionally, when at the cell surface, GHRs can be cleaved by the metalloprotease tumor necrosis factor-α-converting enzyme (TACE, ADAM17), a process called shedding (44, 45). The cleaved extracellular domain circulates in the blood and is referred to as growth hormone binding protein (GHBP); the intracellular part is endocytosed and degraded. GHBP levels in the blood have been used as an indication of the amounts of GHR in the cells (46). When GH is bound to GHR or if a tri-peptide (E260–D262) is deleted or mutated, shedding is inhibited (39, 47, 48). In the bloodstream, GHBP may antagonize GH actions by competing for its binding with GHR at the cell surface (49). Alternatively, the GH-GHBP complex may increase the bioavailability of GH in the circulation. Another function of the shedding process is downregulation of the responsiveness of the cells to GH. The availability for GH at the cells surface is determined by the rate of GHR endocytosis (75%), the rate of shedding (10%), and other (unknown) mechanisms (15%) (50). Control of GHR endocytosis is crucially important. The high turnover rate allows cells to quickly respond to stresses and changing metabolic conditions.

Both GHR and its kinase, JAK2, can translocate to the nucleus. The JAK2 transport can be facilitated by the sumoylation machinery (24).Under certain conditions at defined cell cycle- regulated times in proliferative cells, activated GHR escapes *via* the cytoplasm to the nucleus by the importin- α/β mediated classical import pathway.

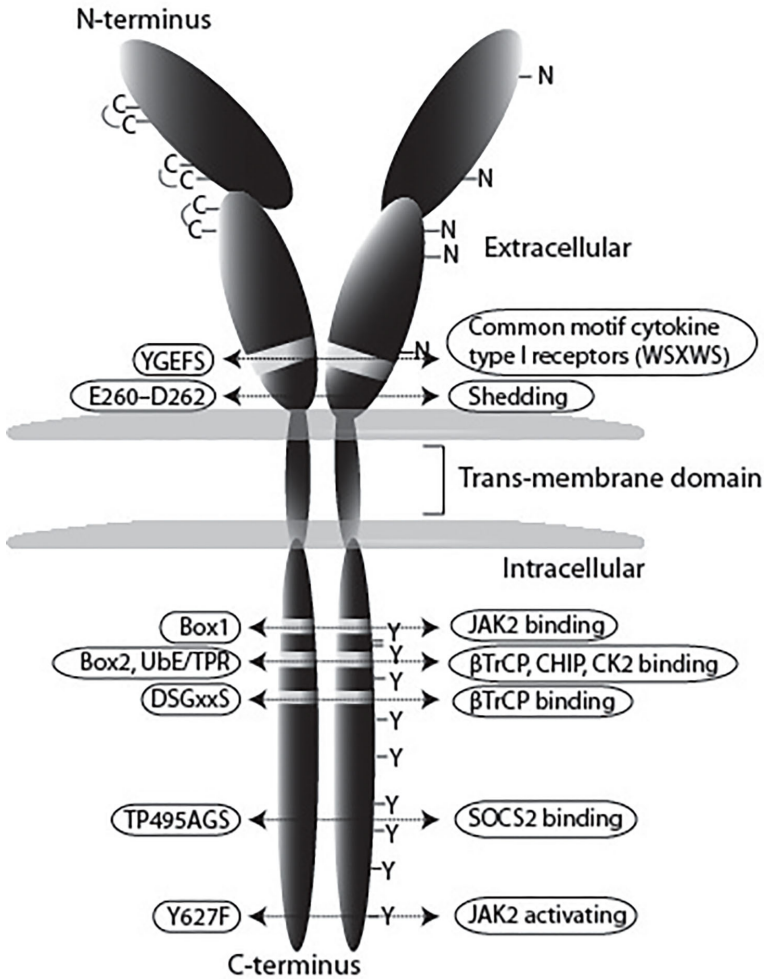

FIGURE 1 | Schematic representation of the GHR. In this review we use the notation of the human GHR protein (GenBank: AAA52555). The GHR consists of an extracellular domain of 246 amino acids, a transmembrane domain (TMD) of 24 residues, and a cytoplasmic region of 350 amino acids. The extracellular domain contains 5 potential glycosylation sites (N), and seven cysteine residues, from which 6 form disulfide bonds. The YGEFS domain is located at the C-terminal part of the extracellular domain. The intracellular domain contains 9 tyrosine residues that can be phosphorylated upon receptor activation by GH. E260-D262 are involved in ADAM17 shedding activity, Box1 is responsible for JAK2 binding, the membrane-proximal 150 amino acids contain the SRC (Lyn) binding site; UbE/TPR and DSGxxS are for GHR internalization and degradation, TP495AG serves as SOCS2 binding site (21), and Y627F causes constitutive JAK2 activation (22).

This process requires interaction with the nuclear localization signal-containing protein Co-activator activator (CoAA). Through its N-terminal domain nuclear GHR can act as a transcriptional activator in conjunction with CoAA to initiate transcription of a subset of target genes to regulate cell cycle progression. Most likely, the nuclear GHR together with CoAA increases the proliferative action of GH (25, 26). Details as whether dimeric, phosphorylated GHR, or whether JAK2, or GH are needed, are currently lacking.

GROWTH HORMONE PHYSIOLOGY

GH Family and Structure

Growth Hormone (GH), also known as somatotropin or somatotropic hormone, is a peptide hormone produced in the anterior pituitary gland which promotes cell division, regeneration and growth (6). Phylogenetically, GH is an ancestral hormone that has been found in the pituitary of primitive vertebrates, such as the jawless sea lamprey fish (51). In primates, GH is part of a family of highly similar genes consisting of GH1 which is mainly expressed in the pituitary, a placental GH variant gene known as GH2, and three placental lactogens also known as chorionic somatomammotropin genes (CSH1 and CSH2) and chorionic somatomammotropin-like gene (CSHL1). Several GH isoforms have been identified, but in humans the majority of the circulating GH is the 22,000 GH1 form from the pituitary gland (52, 53). Some extra-pituitary tissues (e.g. neural, immune, reproductive, digestive, respiratory systems among others) have also been found to produce GH (54). Thus, GH and also PRL expression is widely spread in many tissues throughout the body where it has autocrine or paracrine functions and may play a

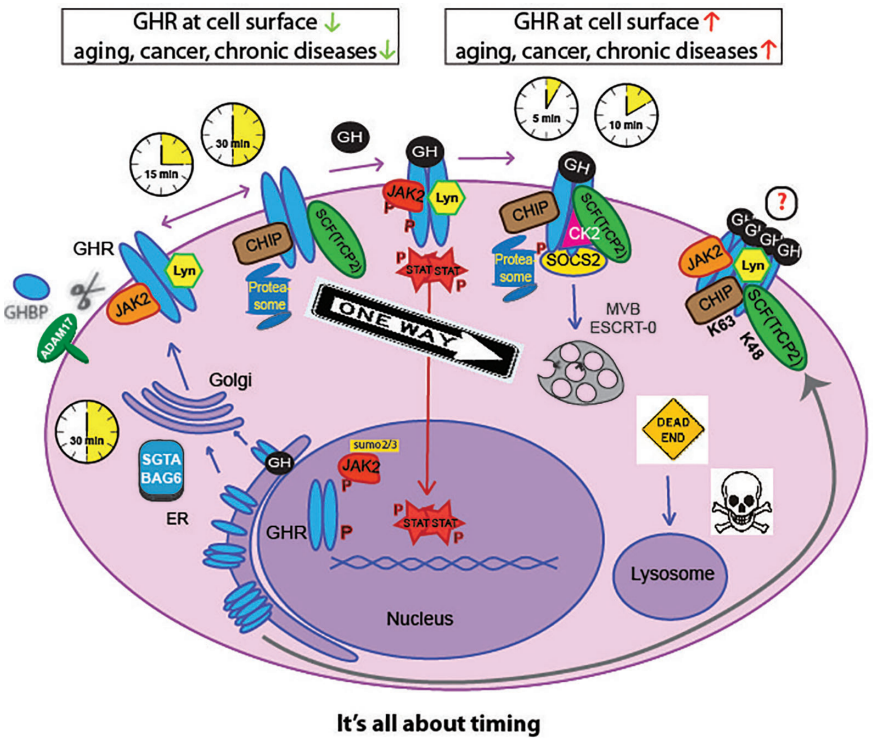

FIGURE 2 | Life cycle of the GHR. GHR is synthesized in the endoplasmic-reticulum (ER) where it undergoes N-glycosylation and dimerization. The small glutamine-rich tetratricopeptide repeat-containing protein SGTA together with Large proline-rich protein BAG6 (or BCL2-associated athanogene 6), SGTA/BAG6, probably act as chaperone in GHR complex formation toward the Golgi complex. After complex glycosylation in the Golgi the GHR arrives at the plasma membrane within 30 min. With no GH present, the GHR endocytoses *via* coated pits catalyzed by βTrCP (on DSGxxS motif, **Figure 1**), Ubc13/CHIP, and the proteasome, within 30 min after arrival. Alternatively, the GH binding domain (GHBP) is shedded into the blood by the action of ADAM17. If GH binds to the GHR, signal transduction is initiated *via* JAK2, Lyn, and CK2; in addition, SOCS2 is recruited to the degron sequence $TP^{495}AGS$, downstream of the STAT5b-interacting pY487. The activated GHR uses the same ubiquitination machinery but a different motif (UbE/TPR) for βTrCP binding and endocytosis. This shortens the residence time to 5-10 min, as explained below and in **Figure 5**. The endocytosed GHRs are then transported through endosomes, selected by the ESCRT-0 complexes at the multivesicular bodies (MVB) and degraded in the lysosomes. The CK2 involvement is hypothetical. Upon GH binding, JAK2 and Lyn phosphorylate downstream effectors. Phosphorylated STATs translocate to the nucleus and activate many genes. Both GHRs and JAK2 can be translocated to the nucleus (24–26). High-order functional GH-GHR complexes may occur that upon activation are phosphorylated and act as signaling platforms (27, 28). If GH and GHR are expressed in the same cell, they bind in the ER and the signaling starts from the Golgi complex.

role in various diseases. Autocrine GH may have an even greater role in cancer development than endocrine GH (55). In mammary tissue GH1 expression has been found to be regulated by progesterone (56–58). GH belongs to the same family as prolactin (59), and in primates GH binds also to the PRLR, which presumably implicates all PRLR-mediated actions including mammary gland differentiation and lactation. Two disulfide bounds are necessary for its biological activity (60). Before closure of the growth plates, recombinant GH can be given to promote growth in children with short statue (61).

GH Secretion and Availability

GH is released from the somatotropic cells in the anterior pituitary in a pulsatile manner (**Figure 3**). In man, GH is secreted episodically with a major surge at the onset of the slow-wave sleep, and less pronounced secretory episodes a few hours after meals (62–64). The pulsatility of GH secretion has a major impact on the pattern of GH-induced hepatic gene expression (65–67). Sexually-dimorphic patterns of genes manifest themselves in the liver through the pulsatile nuclear and DNA occupancy of STAT5b in males, while In females a more continuous pattern leads to dramatic differences in gene expression (68–70). Pulses are regulated primarily by the interplay of hypothalamic hormones: a stimulatory GH-releasing hormone (GHRH) and an inhibitory hormone, somatostatin (SS). These factors act *via* their respective receptors, expressed at the cell surface of the somatotropic cells. In addition, other peptides, called secretagogues (GHS), were identified to regulate GH secretion, such as GH releasing peptides (GHRP) originating from the brain (71), and Ghrelin, produced by stomach tissue (72). Additionally, insulin-like growth factors (IGFs), of which the transcription depends on GH/STAT5b signaling, are able to inhibit GH release in a negative feedback loop (73). Expression and release of GH are mainly regulated by the transcription factor Pit-1, which has additional functions in the differentiation and maintenance of

somatotropic cells (74, 75). GH secretion is also affected by other factors such as physical stress, body composition, metabolic status and others (**Figure 3**). For instance, during fasting and certain conditions of physical stress, GH secretion is increased, and excess of glucose or lipid intermediates inhibits GH release in healthy man (63, 76–78). After maximal GH secretion at puberty (79), adulthood is associated with its gradual decline (80). Besides the tight regulation of GH secretion, the availability of GH is also influenced by its clearance by the kidneys and by internalization through its receptor. During pregnancy, the pulsatile GH secretion is completely abolished due to the placental GH2 secretion which evokes elevated plasma IGF-1 concentrations inhibiting pituitary GH1 release by feedback inhibition. Because of this, insulin-resistance may develop eventually leading to pregnancy diabetes (81).

GHR ACTIVATION, SIGNALING, AND DESENSITIZATION

GH signaling not only depends on the amounts of GH in circulation, but also on the levels of GHR at the cell surface. The responsiveness (sensitivity) of the cells to GH is dynamically regulated, reflecting a balance of receptor endocytosis/degradation, and transport of newly synthesized receptors to the plasma membrane (50).

If GH and GHR are synthesized in the same cell, autocrine signaling occurs. Binding and complex formation takes place in the ER, but signaling starts only in the Golgi complex (27, 82). As it is a continuous process, the kinetics of downstream signaling certainly differ from the endocrine mode. While for the latter, JAK2-induced phosphorylation is rapidly counteracted by SOCS activity and endocytosis, the autocrine signaling occurs continuously from inside and there is no information about the exact role of the different factors discussed in this review. Most likely, cells that synthesize GH, already carry GH-GHR complexes at the cell surface and react differently upon GH from outside the cell.

Receptor Activation Mechanisms

The class 1 cytokine receptors do not have intrinsic kinase activity (83). This role is mediated by JAK2 and the SRC kinase family member, Lyn, that associate with sequences in the cytosolic tail: box1 for JAK2 (84), and the membrane proximal 150 residues of the cytoplasmic domain for Lyn (85). In this review we choose Lyn as a member of the SRC family, but also c-Src and Fyn may be involved (86).

The first step in GH action is its binding to the GHR. The crystal structure of the extracellular domain of GHR bound to GH revealed that one GH molecule binds with two asymmetric binding sites two molecules of GHR (20) (**Figure 4**). For a long time, it was thought that GH binding to one GHR monomer at the plasma membrane recruits the second monomer of GHR to

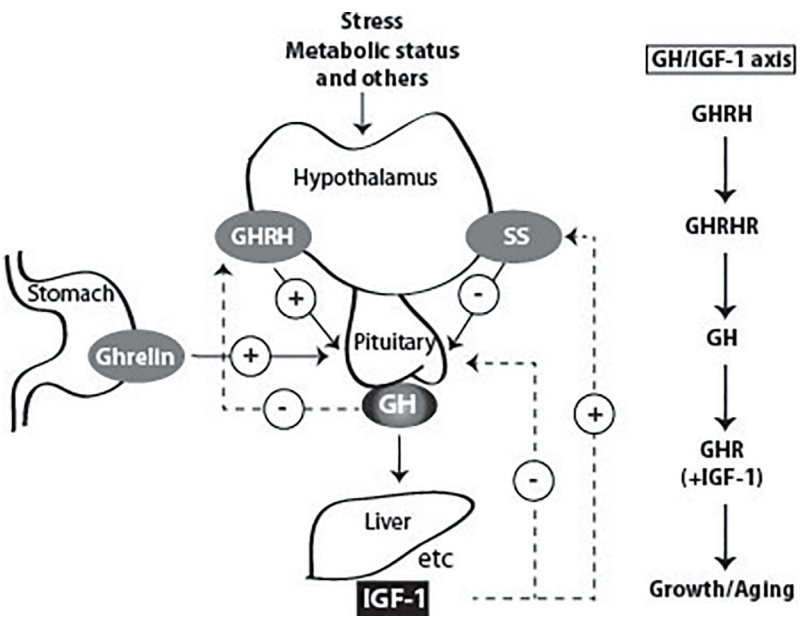

FIGURE 3 | Factors that stimulate and suppress GH secretion under physiological conditions. Several factors influence GH secretion including stress, nutrition, and exercise among others. However, two factors are the main regulators: GH releasing Hormone (GHRH) and somatostatin (SS), which stimulate and inhibit GH secretion, respectively. Ghrelin produced in the stomach also stimulates GH release. GH stimulates the synthesis of IGF-1 by the liver, and in other peripheral tissues. Both GH and IGF-1 are involved in negative feedback loops. High GH levels inhibit its own secretion by inhibiting the release of GHRH. High blood levels of IGF-1 lead to decreased secretion of GH by direct suppression in the pituitary and by stimulating the release of SS.

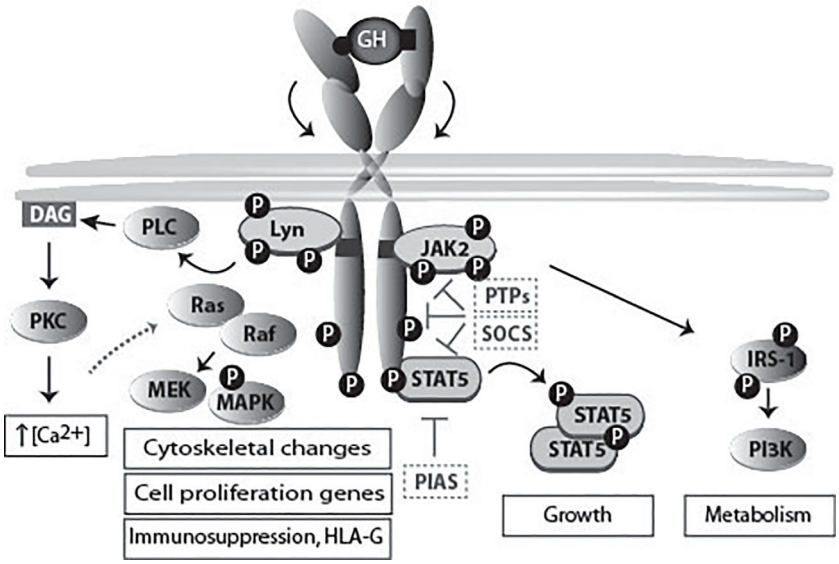

FIGURE 4 | GHR activation and signaling. The binding of the two asymmetric binding sites of one GH molecule to the GHR dimer causes its rotation and subsequent activation of downstream signaling pathways, and ultimately specific gene transcription. The activation of different signaling pathways accounts for the multitude of GH functions. JAK2 binds to box1, while the SRC family member (Lyn) binding is to the membrane proximal 150 residues (85). Lyn activates PLCγ, which leads to an increase in the cytoplasmic calcium ion concentration. This process results in RAS activation and initiation of the ERK1/2 signaling pathway. In the scheme also molecules involved in signal termination (PTPs, SOCS and PIAS) are indicated. In **Figure 7** the physiology and pathophysiology are further detailed.

its second binding site. JAK2 activation was proposed to occur due to GHR dimerization itself. However, subsequent studies disproved this model. Studies by Gent and collaborators showed that GHR dimerizes in the ER, independently of GH, and travels to the cell surface as a pre-formed dimer (29). Subsequently, work by the group of Waters suggested that a change in conformation, induced by GH, rather than GHR dimerization, is responsible for GHR activation. In this study, the comparison of the crystal structure of the extracellular domain of GHR alone and the previous structure of GH-bound GHR revealed differences in conformation (87). Based on this knowledge, the current model for GHR activation proposes that GH binding to the GHR dimer causes a change in conformation in the extracellular binding domain This structural change causes the receptor transmembrane domain to change from a parallel to a left-handed crossover interaction. This structural transition leads to a separation of the intracellular domain, at least to the Box1–Box2 motif, dissociates the JAK2 kinase/pseudokinase trans-interaction and brings the JAK2 kinase domains in proximity, allowing trans-phosphorylation and activation (88, 89). As described for many cytokine receptors, high-order functional GH-GHR complexes of 900,000 Mr occur that upon activation are phosphorylated and act as signaling platforms as identified by native polyacrylamide gel electrophoresis (27, 28, 90).

The phosphorylation of specific tyrosine residues, brought about by JAK2 and Lyn, has extensively been studied as intermediaries for recruiting downstream signaling effectors (91). Herewith in agreement, we confirmed that tyrosine residues 487, 534, and 627, but not residue 566, are most important for GHR and STAT5b phosphorylation. In addition, we showed that the GHR(Y627F) mutation constitutively (independent of GH binding) activates JAK2 and downstream effectors (92).

JAK2 Activation

JAK2 is composed of four major domains: a N-terminal FERM (4.1 protein, ezrin, radixin, and moesin) domain, followed by a SH2 (Src homology 2) domain, pseudokinase and kinase domains. The binding to the box1 of GHR occurs through the FERM domain (93). Normally JAK2 is held in an inactive conformation, where the kinase and pseudokinase domain interact with each other (94). The activation of JAK2 requires that two catalytic domains are brought in close proximity. This was concluded after realizing that often in human leukemia there is oligomerization of JAK2 molecules which renders them constitutively active; this aggregation is due to the occurrence of a genetic fusion between the JAK2 catalytic domain and the oncogenic transcription factor TEL (95). Analysis of other mutation also contributed to the understanding of JAK2 physiology. The mutation V617A, which turns JAK2 into a constitutively active state, is found in patients with myeloproliferative disorders (96). This mutation probably disrupts the inhibitory interaction between the pseudokinase and kinase domain (97). Following mutational analysis, the SH2-pseudokinase domain linker turned out to be important for JAK2 activation (98). JAK2 activation results in the phosphorylation of multiple tyrosines. Several of these have been identified as important in the regulation of JAK2 function. For example, phosphorylation at tyrosine 1,007 is thought to expose the substrate and/or ATP binding sites (99), and phosphorylation of tyrosine 119 is thought to promote JAK2 dissociation from its receptor (100). Phosphorylation of tyrosine 813 appears to enhance JAK2 activity (101), whereas phosphorylation of tyrosine 221

decreases it (102). The importance of many of the JAK2 tyrosines is related to their roles in recruiting ancillary molecules needed for signaling propagation or signal termination.

Unexpectedly, the JAK/STAT signaling pathway is downregulated at febrile temperatures (103). JAK2 protein levels rapidly decrease in cells exposed to thermal stress, while its synthesis remains normal. The analogy of these findings in a variety of cell lines, as well as in PBMCs isolated from human blood, indicate the universal validity of this effect. Although JAK2 is a stable protein, it is degraded in a ubiquitin-dependent manner *via* the ubiquitin proteasome pathway (104). The significance of this process was illustrated in mouse 3T3 cells that showed a decreased GH response at 40°C. JAK2 underwent aggregation in an irreversible manner. Interestingly, kinase-inactive JAK2 did not show aggregation, although the effect of degradation in the cytoplasm at elevated temperatures was conserved. The findings predict that elevated body temperatures lower the responsiveness of cytokine receptors.

SRC Activation

For a long time JAK2 has been regarded as the only kinase activated directly *via* the GHR. However, recent data, indicating that not all the GH signaling events rely on JAK2, brought controversy to the field. In particular, the activation of Lyn (SRC family kinase member) can occur independently of JAK2. First evidence came from a study by Zhu et al, who showed this by using pharmacological inhibitors and kinase inactive proteins (105). Additional evidence came from Rowlinson and co-workers, who reported that interfering with the GH-induced GHR conformational change affects JAK2 and Lyn activation differently (85). Activation of STAT5b by GH seems to require only JAK2, while activation of the small GTPases RalA, RalB, Rap1 and Rap2 by GH requires both Lyn and JAK2 (105). Lyn activation by GH was shown to activate MAPKs, also referred to as extracellular signal-regulated kinase 1 and 2 (ERK1 and ERK2), through the phospholipase Cγ-Ras pathway, signaling that might promote oncogenesis (85). Genes exclusively regulated by Lyn include genes involved in mRNA transcription and metabolism, including the GHR itself: the basal GHR expression level *via* Lyn is 4.8-fold higher, comparing GHR Box1-/- vs. GHR-/- (106). GHR signaling *via* this pathway induces also HLA-G, a powerful immunosuppressive protein for NK cells and macrophages. GH-enhanced immunosuppression in tumors might evade immune attack. On the other hand, it might be used to stop excessive inflammation after partial hepatectomy allowing liver regeneration and survival, Figs. 4 and 7 (107). For 3T3-F442A preadipocytes and H4IIE hepatoma cells it has been shown that relative levels of JAK2 and SRC family kinase in any particular cell might determine which kinase is the major signaling element, with JAK2 predominating in most cases (108). Barclay and co-workers showed that targeted mutation in the box1 of GHR in mice, although abrogating JAK2 activation, did not decrease the hepatic activation of MAPK *via* Lyn (106). The importance of this pathway came from studies with exon 3-deleted GHR, which results in the deletion of 22 amino acids in the extracellular domain of the GHR. Males with this genotype exhibit reduced basal but enhanced ERK signaling after GH stimulation. Exon 3-deleted GHR individuals showed lower serum IGF-1 levels, and were found to be of higher stature with extended lifespan (10 years) (109).

Signaling Pathways of GH

The main pathways activated by GH are: the signal transducer and activator of transcription (STAT) pathway, the mitogen-activated protein kinase (MAPK) pathway, and the phosphoinositide-3 kinase (PI3K) pathway (**Figure 4**). The extent by which each pathway is activated depends on the cell types, related to differences in relative expression levels of the components of each pathway.

The STAT Pathway

STATs are latent transcription factors that upon activation by certain hormones or cytokines undergo tyrosine phosphorylation in the cytoplasm, dimerize *via* phosphotyrosine-SH2 interactions, and translocate into the nucleus where they activate transcription of specific genes (110). In mammals seven members of STAT have been identified with molecular weights ranging from 95 to 111,000 Mr (111). GH stimulation creates STATs binding sites in the GHR-JAK2 complex. The activation of STAT5b is critical for many of the GH biological functions, including metabolic changes, body growth and sex-dependent liver gene regulation (112, 113). Sex-biased genetic programs in liver metabolism and liver fibrosis are controlled by EZH1 and EZH2 downstream of GH-activated STAT5b (114). STATs 1 and 3 also become activated in response to GH (112), but their importance is still unclear.

STAT5b binds to the promoter elements of the IGF-1 gene, regulating its transcription in a GH-dependent manner (115, 116). A mutation in STAT5b, affecting its GH-induced tyrosine phosphorylation, caused severe growth retardation and immunodeficiency in one patient (117). Since then, more germline STAT5b missense variants with demonstrable dominant-negative effects, associated with short stature and mild immune dysregulation were identified in three unrelated families (118). This reiterates the importance of STAT5b for IGF-1 expression. STAT5b, but not STAT3, requires an intact and tyrosine phosphorylated GHR cytoplasmic tail for full activation (119). The key GHR tyrosines necessary for this event were identified (120, 121).

The MAPK Pathway

The Ras/MAPK, or ERK/MAPK has also been shown to be activated by GH. GHR phosphorylation creates docking sites for Src homology 2 domain-containing transforming protein C (Shc) (122). Shc gets then phosphorylated by JAK2, and binds growth factor receptor-bound protein 2 (Grb2) which binds Son of Sevenless (SOS), a guanine nucleotide exchange protein. Subsequently, Ras, Raf, mitogen-activated protein kinase/extracellular-regulated protein kinase (MEK), and ultimately MAPKs are sequentially activated (123). Phosphorylated MAPKs translocate to the nucleus where they transactivate transcription factors, and change gene expression to promote growth differentiation or mitosis. Data suggest that GH-dependent activation of the Ras/MEK/MAPK pathway

contribute to GH-stimulated c-fos expression through serum response element (SRE). It remains controversial whether and how MAPK activation affects GH-induced proliferation and anti-apoptosis (124). As explained above, the activation of MAPKs may occur in a Lyn-dependent, JAK2 independent way. As STATs are also serine phosphorylated for full activity (125), it was suggested that this is mediated by MAPK pathway (126).

Some evidence suggests that GH signaling *via* MAPK pathway may engage in cross-talk with signaling pathways induced by other stimuli. Yamauchi and co-workers propose an interesting mechanism by which GH activates MAPK through stimulating the phosphorylation of a Grb2 binding site in the epidermal growth factor (EGF) receptor (127). Additionally, studies by Kim and co-workers show that GH stimulation alters the phosphorylation status of ErbB-2, a tyrosine kinase growth factor receptor member of the EGF receptor family, in a MAPK dependent manner (128). GH has also been described to activate other members of MAPK pathway, namely p38 MAP kinase and c-Jun amino-terminal kinase (JNK) (129, 130).

The PI3K Pathway

GH has also been shown to stimulate the PI-3K pathway, probably through tyrosyl phosphorylation of the large adaptor proteins, the insulin receptor substrates (IRS). GH stimulates the phosphorylation of IRS-1, -2, and -3 by JAK2, which leads to their association with multiple signaling molecules including the p85 subunit of PI-3 kinase (122, 131). This pathway is shared by the insulin signaling pathway, which may justify the insulin-like effects of acute GH stimulation under certain conditions, as discussed above. Particularly, activation of PI-3 kinase mediates the GH-induced increase in glucose transport, *via* induction of translocation of the glucose transporter 4 (GLUT4) to the cell surface (132), and has been suggested to mediate the ability of GH to stimulate lipid synthesis (133, 134). Additionally, PI-3 kinase activation results in AKT activation, which has been implicated in GH-promotion of cell survival. Activation of AKT depends on JAK2 binding to box1 in the GHR (135). Another kinase, p70S6K, involved in the control of cell proliferation and differentiation was shown to be activated by GH through PI-3 kinase and protein kinase C (PKC) (136). The NFκB pathway has also been shown to be activated by PI3-K and downstream AKT after GH stimulation (137).

GH Desensitization

Termination of the GHR signaling is an important mechanism for controlling GH actions (**Figure 4**). Protein tyrosine phosphatases (PTPs) are employed by the cells for negative regulation of GH signaling, namely SH2 domain-containing protein-tyrosine phosphatase (SHP-1), SHP-2, protein-tyrosine phosphatase (PTP)-H1, PTP1, TC-PTP, and PT1b (138). Mice, deficient in SHP-1, have prolonged JAK-2 phosphorylation and STAT5b activity, which represents strong evidence for an important role of this phosphatase in the deactivation of GH signaling (139). There are conflicting reports concerning the physiologic importance of SHP-2 in GHR: while Frank et al. concluded that SHP-2 is a positive regulator (140), Stofega et al. proposed SHP-2 as an inhibitor of GH signaling (141). GH stimulation has been shown to trigger the phosphorylation of JAK2-associated SIRP-α, signal regulatory protein alpha. This was suggested to promote SHP-2 recruitment and consequent attenuation of GH signaling (142). A study by Pasquali has identified PTP-H1, PTP1, PTP1b, and TC-PTP as specific interactors of phosphorylated GHR (143). PTP1b knockout mice display increased JAK2 and STAT5b phosphorylation, while PTP-H1 knockout mice display enhanced growth (144, 145). CD45 was shown to be a JAK2 phosphatase, being able to suppress its activity and regulate cytokine receptor signaling (146).

Other regulators are PIAS, "protein inhibitors of the activated STATs", which display SUMO ligase activity. PIAS can bind STAT proteins, and prevent their association to the DNA. Although the majority of the PIAS interactor proteins are prone to modification by SUMO, the exact mechanism by which PIAS influences STAT5b function is still unclear (147). Some studies have also implicated the adaptor protein Grb10 as regulator of GH signaling. Grb10 interacts with GHR upon GH stimulation, and downregulates GH signaling pathways downstream of JAK2 and independently of STAT5b (148). Work of Carter-Su and colleagues found that SH2B-β association with JAK2 enhances its activity (149). Thus, decrease in SH2B-β levels could contribute for GH-signaling termination. Other cellular factors that modulate GH sensitivity are insulin, thyroid and sex hormones, as well as inflammatory cytokines (150, 151).

In addition to direct interference with the signaling molecules, cells have the capacity to tune the number of GHRs at the cell surface in several ways. As described above, the extracellular domain of GHR can be cleaved in a process called shedding. One of the consequences of this process is the reduction of the number of signaling competent receptors at the cell surface, and consequent regulation of the cell sensitivity to GH (124). Since GH binding to GHR inhibits its shedding, this mechanism cannot be regarded as signal terminator (152, 153). However, the most powerful and best studied mechanism to control GH sensitivity of cells is endocytosis. Opposite to other type 1 cytokine receptors, GHR is endocytosed both in the presence and absence of ligand (154, 155). Therefore, besides regulating the responsiveness of the cells to GH, endocytosis of GHR provides a very efficient way for GH signaling attenuation. The next paragraph will be dedicated to the advances made in understanding GHR endocytosis.

THE UBIQUITIN SYSTEM IN RECEPTOR TRAFFICKING

Ubiquitin is a small molecule of 76 amino acids which C-terminus is attached to proteins upon sequential action of three enzymes: a ubiquitin activating enzyme (E1), a ubiquitin conjugating enzyme (E2), and a ubiquitin protein ligase (E3). Ubiquitin may be added as a single monomer or multiple monomers, or as a polyubiquitin chain. The addition of ubiquitin to target proteins covers a great variety of functions. Endocytosis is the main way used by the cells to achieve the

homeostatic regulation of plasma membrane protein abundance. Once a protein is endocytosed it is either recycled back to the cell surface or captured in the intraluminal vesicles of the MVBs, and eventually guided to lysosomes for degradation (156).

Ubiquitination has emerged as a central mechanism governing the subcellular trafficking of proteins, reviewed in (7). It is critically important for the regulation of the number of receptors and transporters at the plasma membrane. The first evidence for a role of ubiquitin in the membrane trafficking came from the work of Kölling and collaborators with the ABC-transporter Step6 in yeast (157). In mammalian cells, the first receptor reported to depend on the ubiquitination system for its endocytosis and degradation was GHR (3). From then on, many more receptors were shown to depend on the ubiquitin system to be endocytosed, often in response to ligand binding (7, 158).

Ubiquitination works as an engagement tool of the proteins with the endosomal sorting complexes required for transport (ESCRTs) (159). In fact, ubiquitination has been reported at several points along the endocytic pathway. Although monoubiquitination has been regarded as a sufficient signal for sorting, K63 linked polyubiquitin chain are now considered as the primary sorting factor. Studies with the GAP-1 permease indicated that monoubiquitination is sufficient for initial internalization, but further sorting in the endosomes requires K63-linked polyubiquitin (160). Also studies of the mammalian TrkA and MHC class 1 proteins showed the importance of this type of chains in their MVB sorting (161, 162). Within the endocytic system, ubiquitin acts as an interaction module that is recognized by a variety of ubiquitin binding domains (UBDs), including UIM, CUE, NZF, and certain VHS and SH3 domains present in several proteins (163). As illustrated in **Figure 2**, after endocytosis, the next step in the sorting route is the selection by the ESCRT-0 complex, which acts at a branch point in endosomal traffic: binding to certain cargo (like the GHR) commits it to degradation in the lysosome, while cargo that does not bind (like transferrin and Low Density Lipoprotein receptors will be recycled to the plasma membrane. ESCRT-0 is composed of HRS and STAM, both of which bearing UIM (ubiquitin interacting motif) and VHS (Vps27, HRS and STAM) domains, important for ubiquitin binding and cargo recognition (164–166).

Other important components to consider in the endocytic regulation are the deubiquitinating enzymes (DUBs), which are specific proteinases able to remove ubiquitin moieties from proteins. Besides the catalytic domain, DUBs contain domains that allow them to associate with scaffolding proteins and adaptors. The ESCRT machinery associates with at least two DUBs: AMSH and USP8 (UBPY). In yeast, Doa4 has been identified as an additional DUB, important for receptor recycling. Deubiquitination of endocytosed receptors before or after delivery into the MVBs may profoundly affect receptor trafficking, and ultimately substrate turnover rate (167). It remains unclear how the ubiquitinated cargo is handed from one sorting step to the other. Models have been put forward based on a gradient of sorting proteins containing ubiquitin binding domains of increasing binding affinities. More complexity can be added to this model if we consider ubiquitin ligases such as Triad1 and DUBs along the sorting pathway, which could perform additional chain editing (156, 168). In **Figure 5**, the different controlling factors are depicted with reference to their effects on residence time at the cell surface and consequences of loss of function for the GH/IGF-1 axis.

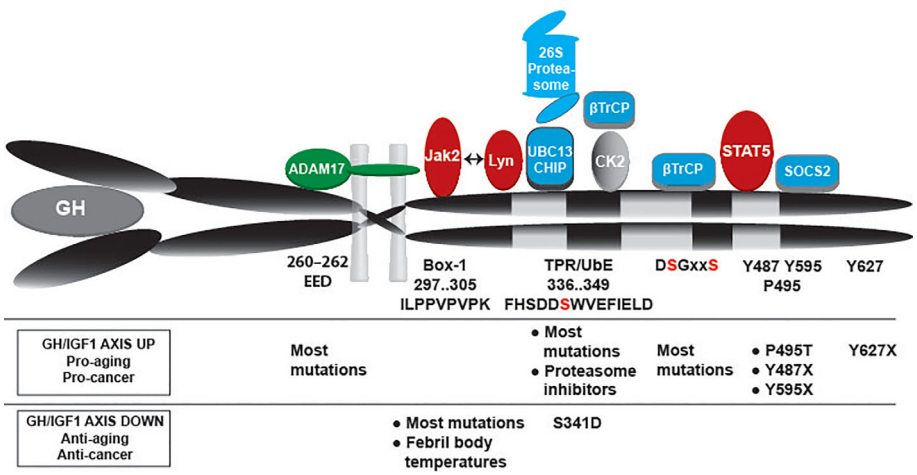

FIGURE 5 | GHR controlling factors: ADAM17, JAK2, Lyn, Ubc13/CHIP, proteasome, βTrCP, STAT5b, SOCS2 and possibly CK2. Their respective bindings sites are indicated. JAK2 and Lyn bind to the same membrane-proximal region, with overlapping substrate binding sites. Under basal conditions βTrCP binds to the constitutively phosphorylated DSGxxS sequence. The kinases responsible for DSGxxS phosphorylation are unknown. Under conditions of GH stimulation JAK2 is released from the receptor, and the serine 341 of the UbE motif gets phosphorylated probable by CK2. These events increase the affinity of βTrCP for the UbE motif, reduce the role of the DSGRTS sequence, and recruit STAT5b and SOCS2 to their respective binding sites (pY containing motifs). Overall, GH stimulation shortens the residence time at the plasma membrane and results in faster GHR endocytosis. The lower part indicates the effects of mutations and other conditions that might impact the GH sensitivity of cells: increased GH/IGF-1 activity acts pro-aging and pro-cancer, while lower activity acts anti-aging and anti-cancer.

Role of SCF^{TrCP1} in GHR Endocytosis

The SCF (SKP1-CUL1-F box protein) subfamily of E3 ligases was originally discovered and studied in budding yeast *Saccharomyces cerevisae* (Patton et al., 1998). They are the best characterized mammalian cullin RING ubiquitin ligases. The determination of the crystal structure of SCF complex by Zheng and co-workers added some insights in the roles of each of its components and the mechanistic aspects of their interlinked actions (Zheng et al., 2002; Frescas and Pagano, 2008).

The endocytosis and degradation of GHR depends on the ubiquitin conjugation system, as shown for the first time in a Chinese hamster lung cell line (ts20) with a temperature-sensitive mutation in the E1 enzyme. Whereas at the permissive temperature the endocytosis of GHR occurred normally, when the cells were put at non-permissive temperature the GHRs accumulate at the cell surface (3). Further evaluation revealed that GHR ubiquitination and clathrin dependent-GHR endocytosis are coupled events (40, 41). An important achievement in the mechanistic understanding of GHR endocytosis was the discovery of the "Ubiquitin-dependent endocytosis motif", UbE, 340-349, which consists in the amino acid sequence DSWVEFIELD (169). If this motif is mutated the ubiquitination and endocytosis of GHR are strongly inhibited. Besides this motif, there is a di-leucine motif at the position 365-366. This motif mediates fast ubiquitin-independent, clathrin-dependent GHR endocytosis only if the receptor is truncated at position 367, probably due to its complete exposure in this case. The functionality of the di-leucine motif in the context of full-length receptor is not apparent (170). Surprisingly, a GHR truncation (at amino acid 417), where all its lysines were mutated to arginines, although not being ubiquitinated, was normally endocytosed in a ubiquitin-system dependent manner. This indicates that the ubiquitination of GHR itself is neither needed for its endocytosis nor for its degradation (169). One reason that justifies the importance of the UbE motif in GHR endocytosis is its binding site for the $SCF^{\beta TrCP}$ E3 ligase (171). The role of the UbE motif and βTrCP has been also extended to sorting at the MVB and degradation at the lysosomes (172). JAK2 was also identified as a stoichiometric regulator of GHR endocytosis. Besides its role in signaling, merely binding of JAK2 to GHR is inhibitory for its endocytosis. As many cytokine receptors are JAK2 clients, cellular levels of JAK2 play a role in cytokine sensitivity, best illustrated by its sensitivity to febrile temperatures (103). The model is that GHR can only be endocytosed if JAK2 has detached from it, which was proposed to occur after GH stimulation. It is possible that JAK2 binding/dissociation cycles have direct effects in the ubiquitination events mediated by $SCF^{\beta TrCP}$, and thereby affect rate of GHR endocytosis (92). Not surprisingly, the life cycle of JAK2 is controlled by E3 ubiquitin ligases of the CBL family as has been shown in hematopoietic stem cells and myeloid malignancies (173).

The UbE motif works as a recruitment platform for βTrCP, the F-box substrate recognition subunit of $SCF^{\beta TrCP}$ E3 ligase, necessary for GHR endocytosis (171). Generally, $SCF^{\beta TrCP}$ recognizes the classical DSGxxS motif in its substrates (174), including receptors homologous to GHR, such as prolactin receptor (PRLR) (175), interferon-α receptor (IFNAR) (176), and erythropoietin receptor (EpoR) (177). In these receptors, βTrCP binds only upon ligand binding when the serine residues in the DSGxxS motif are phosphorylated, which leads to their endocytosis and signal termination. The GHR also contains a D^{383}SGxxS motif. This is constitutively phosphorylated, able to bind βTrCP, and contributes to the steady state endocytosis of the GHR (the half-life of unligated (mature) GHR is 30 min) (39, 42). Therefore, in contrast with other cytokine receptor family members, GHR DSGxxS motif does not seem to contribute to signal termination. This role is carried out by the UbE motif, important for both steady state and GH-induced endocytosis (42, 92). NMR experiments demonstrated that the UbE motif is essentially unstructured, and, together with functional mapping of the UbE and βTrCP revealed a unique interaction model of βTrCP with GHR-UbE (178). Since the regulation of βTrCP-substrates interactions involves serine phosphorylation, we evaluated the potential role of the UbE serine phosphorylation (S341) as a modulator of UbE-βTrCP interaction. Binding studies comparing affinities of the interaction of βTRCP to unphosphorylated vs phosphorylated S341 peptides (Surface plasmon resonance and pulldowns) showed 100 times increase in binding affinity upon S341 phosphorylation. Accordingly, ^{125}I-GH binding/internalisation assays in cell lines stably expressing S341A or S341D (phosphomimetic) suggest that GH stimulation triggers faster GHR endocytosis by causing phosphorylation of S341 in the GHR UbE motif and subsequent increase in UbE-βTrcP binding affinity (179). S341 phosphorylation might constitute a very efficient mechanism for signal termination after GH stimulation.

The kinase responsible for S341 phosphorylation is unknown yet. S341 is contained in a minimal consensus site for CK2 phosphorylation, which has been identified to be S-X-X-Acidic. The acidic residue may be glutamate, aspartate, or phosphorylated serine and tyrosine: in case of S341 this sequence is S^{341}WVE (180, 181). Preliminary studies on the evaluation of a potential role for CK2 in S341 phosphorylation, by using the CK2 inhibitor 4,5,6,7-tetra-bromo-benxotriazole (TBB) (182), revealed that CK2 is a promising target. It has become apparent that the regulation of CK2 involves regulated expression, assembly and subcellular localization, post-translational modifications, and regulatory interactions with molecules and proteins (183, 184). Interestingly, there are reports of increased CK2 activation by insulin, EGF, IGF-1 (185, 186) and TNF (187, 188). EGF-activated ERK2 binds directly CK2α enhancing its activity (189). TNFα-induced activation of CK2 was also related to ERK1/2 activity (187). It is interesting to evaluate whether CK2 can be activated by GH. Other stressors or pathways that activate ERK1/2 may result in increased activity of CK2 towards S341 in GHR, resulting in increased GHR endocytosis. Future studies will elucidate this hypothesis.

The SOCS Family and GHR

The suppressor of cytokine signaling (SOCS) family of proteins plays a very important role in the GH-signal termination. This family is composed of eight members, and the expression of four

of them is stimulated by GH, namely SOCS1, -2, -3, and CIS (cytokine inducible SH2-constaining protein) (138, 190). Structurally, SOCS proteins contain a central SH2 domain and a motif called SOCS box at their C-termini (138). The SOCS box mediates the formation of multi-subunit ubiquitin ligases, containing elongin BC, cullin 2 or 5 and the RING finger proteins Rbx1 or Rbx2 (191). SOCS1 and SOCS3 contain an additional kinase inhibitory region at their N-termini (KIR). Different SOCS apply different mechanisms for GH signaling downregulation. SOCS1 is thought to bind Y1007 on JAK2 activation loop, and by doing so, to inhibit JAK2 activity through KIR (192). SOCS3, besides binding to the same residue in JAK2 (193), also binds to phosphorylated tyrosines in GHR. Also, SOCS2 and CIS have been shown to bind to phosphorylated GHR, which was suggested to interfere with STAT5b-GHR binding (194). SOCS1, and possibly SOCS2 and SOCS3 use their ubiquitination activity to mediate GHR and JAK2 degradation and, therefore, signal termination (21, 104, 138). A role of CIS as a stimulator of GHR internalization and proteasomal degradation has been proposed (195). Interestingly, there is evidence that some stimuli that reduce GH sensitivity, such as estrogen or sepsis, do so by increasing expression of certain SOCS proteins (196, 197). The physiological importance of SOCS in GH signaling regulation is unclear since $SOCS1^{-/-}$, $CIS^{-/-}$ and liver specific $SOCS3^{-/-}$ are not bigger than normal (198–200). Only SOCS2 knockout mice are larger than wild-type (201). SOCS2 inhibits the GHR *via* binding to pY487 and pY595 (202, 203). SOCS may play a key role in shifting GH action from growth-promotion to lipolysis. Two independent studies showed that a single-nucleotide polymorphism in GHR resulting in a P495T substitution was associated with lung cancer (204, 205). Y595 (and Y487) were previously indicated as a binding site for the phosphatase SHP2 (141) Recently, Chhabra and collaborators showed a causative relation with SOCS2 binding to the GHR in which both P495 and pY487 are required (21). They show that GH-induced signaling increased AKT pT308 signaling significantly in GHRP495T cells. This is a strong prognostic indicator for non-small cell lung cancer (206). In addition, STAT3 was activated. Activated STAT3 is an important oncogenic factor during carcinogenesis and metastasis of both small cell lung cancer and squamous cell lung carcinoma (207). Taken together, SOCS family members, especially SOCS2, play an important role in the regulation of the GHR.

CHIP and GHR

In an effort to identify additional ubiquitination factors involved in the fate of GH receptors we used a small siRNA library targeting a selection of ubiquitination factors (35). As K63-linked ubiquitin chains have been implied in the regulation of membrane receptor trafficking, we search for such factors (160, 208). Silencing of the ubiquitin conjugase (E2) UBC13 came up as a GHR-specific endocytosis factor (165, 209). Previously, pull-down experiments showed that the UbE motif has an affinity for tetratricopeptide repeat-containing (TPR) proteins (30). As UBC13 can serve as E2 for a ubiquitin ligase that binds substrates *via* its TPR motif we tested both (C-terminus of Hsp70 interacting protein) CHIP and UBC13 for endocytosis and degradation of the GHR: both factors were required and collaborated in GH-induced endocytosis of the GHR (209). Using blue native electrophoresis, Sedek et al. confirmed K63-linked proteins in large GHR-containing protein complexes stimulated and isolated through streptavidin pull-down during endocytosis (27).

CHIP is an E3 ubiquitin ligase that plays a pivotal role in the protein quality control system by shifting the balance of the folding-refolding machinery toward the degradative pathway in order to maintain balanced proteostasis networks (33, 210–212). CHIP is highly expressed in tissues with high metabolic activity and protein turnover. In addition, as a regulator of growth and metabolism, CHIP mediates monoubiquitination and subsequent endocytic-lysosomal turnover of the insulin receptor (INSR). CHIP deficiency results in increased INSR levels that lead to premature aging in various organisms. The detrimental effects of the increased INSR level are mainly due to a PI3K/AKT signaling (213). In line with this, CHIP ubiquitinates AKT independent of its phosphorylation state (214). Remarkably, transcription of CHIP is also modulated in response to changes in AKT levels (215). Similar to AKT regulation, CHIP indirectly impacts the FOXO function on various levels through modulation of upstream substrates of the insulin/IGF-1 signaling pathway, a pivotal genetic program regulating cell growth, tissue development, metabolic physiology, and longevity of multicellular organisms (210). Thus, CHIP integrates proteostasis and aging by regulation the turnover of the INSR (211). In cancer the pathogenic mechanisms of CHIP are less clear (216). Several studies on breast cancer cells have indicated CHIP as tumor suppressor (212, 217–219).

PHYSIOLOGICAL ROLES OF GH

Promotion of Growth

The promotion of postnatal growth is a major physiological function of GH. Initially, it was thought that GH indirectly stimulates growth *via* triggering the production of IGFs, or somatomedins, exclusively in the liver. This was called the "somatomedin hypothesis". This theory was challenged when direct actions of GH on several peripheral tissues were reported (220). In fact, liver-specific IGF-1 gene-deleted mice show normal postnatal growth and development despite the low levels of IGF-1 in circulation. This indicates that direct effects of GH in target tissues (adipose tissue, bone and skeletal muscle) are involved in growth promotion, and probably in stimulation of local IGF-1 production (221). According to the dual effector hypothesis of Green et al. GH may stimulate early recruitment of stem cells followed by further clonal expansion due to GH-induced IGF1 expression (222). The critical importance of GH as the main endocrine mediator of growth is proven either by the dwarf phenotype occurring when the levels of GH are insufficient during early development, or by gigantism, due to hyper-secretion of GH before puberty (53). Apart from GH secretion, also defects in GHR and post-receptor signaling may result in

phenotypes similar to GH hypo-secretion. Laron and coworkers described for the first time the clinical phenotype of severe growth defect, and for that reason it is named "Laron Syndrome" (223). Deletions and mutations in GHR have been described as causative for this phenotype (224, 225). Studies on a large cohort of individuals in northeastern Brazil who were homozygous for a mutation in the GH-releasing hormone receptor gene revealed comparable phenotypes. These individuals are characterized by severe dwarfism, due to very low GH and IGF-1 levels, increased adiposity, and increased insulin sensitivity (226). Lean body mass (LBM) is reduced, but muscle function is adequate. Their longevity and quality of life are normal, and they are largely protected from cancer and less prone to atherosclerosis (227).

Postnatal growth of mice has been shown to rely on signaling mediated by JAK2 and STAT5. GHR-/- mice with knock-in GHR1-391, which eliminates all GH-mediated STAT5b signaling while still allowing activated hepatic JAK2 and ERK2, showed substantially decreased growth (228). This study identified many genes as STAT5b-regulated, such as IGF-1, Igfals, Socs2, P450 cytochrome, Cyp2b9, and some metabolic enzymes. Eleven of these were upregulated (e.g., Sth2, Hao3, and Ang), and nine were downregulated (e.g., Igfals, IGF-1, EgfR, and Comt). These results confirm the importance of STAT5b in growth promotion. On the other hand, pituitary adenomas that cause hypersecretion of GH result into excessive growth called gigantism when present before puberty, whereas in adulthood it results in a clinical condition called acromegaly (229). In these patients excess of GH, besides affecting the size of hands, feet, and fingers, has important metabolic consequences, suggesting additional functions for GH, that will be discussed next in this review.

Metabolic Regulation

GH holds important roles in metabolic regulation (**Figure 6**). As soon as human pituitary extracts became available it was shown that injection of large amounts of GH both in healthy subjects and GH-deficient patients stimulated lipolysis and led to hyperglycemia (230–232). Indeed, as expected, hyperinsulinemia, impaired glucose tolerance, and overt diabetes mellitus are common features of acromegaly (233). GH works as a metabolic switch between carbohydrate and lipid utilization: in conditions of energy surplus GH acts in concert with IGF-1 to promote nitrogen retention, while during starvation GH switches fuel consumption from carbohydrates and protein to lipids. This guarantees the preservation of protein stores and consequently maintains LBM. The direct acute metabolic effects of GH in the basal state are the stimulation of lipolysis and the consequent increase of free fatty acids (FFA) in the blood. Repetitive GH pulses in presence of adequate energy supply and concomitant increased insulin levels induces IGF-1 production (234, 235). Consequently, in the long range, protein stores and LBM increases, while body fat mass decreases. GH stimulates the cell growth of the skeletal muscle by facilitating myoblasts fusion. Like in more peripheral tissues GH does not regulate IGF-1 expression in myotubes. On the other hand IGF-1 has been implicated in skeletal muscle hypertrophy, attenuation of age-related skeletal muscle atrophy, and restoring and improvement of muscle mass (236, 237).

Studies evaluating the acute effects of GH on protein metabolism in the basal state have produced inconsistent conclusions. While some studies indicated that acute GH stimulation leads to increased muscle protein synthesis, others did not detect any effects of GH withdrawal in protein metabolism (238). Less controversial are the studies evaluating the effects of

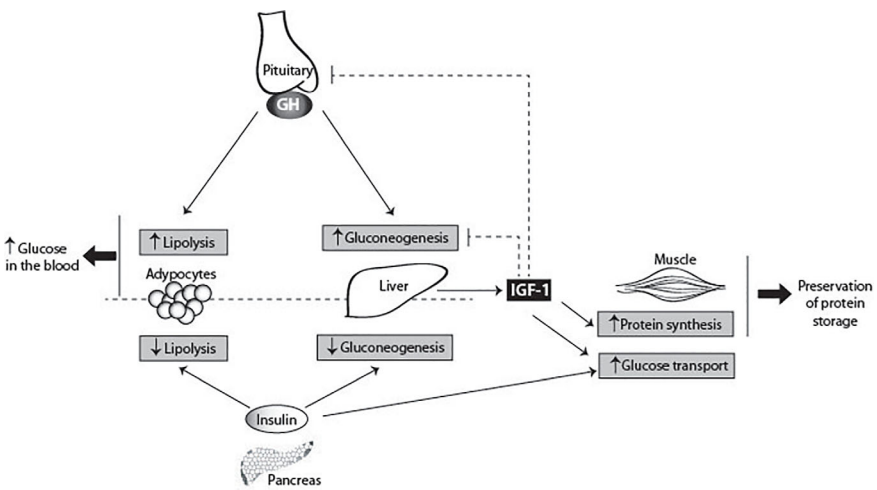

FIGURE 6 | GH metabolic actions. GH has pleiotropic effects on carbohydrate, lipid, and protein metabolism. GH antagonizes the effects of insulin, secreted by the pancreas, by two direct ways: inhibiting gluconeogenesis in the liver, and increasing lipolysis in adipocytes. GH also stimulates the production of IGF-1 by the liver. IGF-1 suppresses gluconeogenesis in the liver *via* the insulin receptor. In the muscle, IGF-1 stimulates directly glucose uptake, and stimulates protein synthesis. IGF-1 inhibits GH secretion by the pituitary gland, and therefore indirectly blocks the insulin antagonizing effects of GH, contributing for the glucose homeostasis. The main consequences of GH metabolic actions are the increase of glucose levels in the blood and preservation of protein storages.

GH on protein metabolism in pathological states (acromegaly and GH deficiency) and in stress (exercise and fasting). Stress conditions are the natural domains of GH, in which the body benefits from GH effects on substrate metabolism (238). During fasting GH is the only anabolic hormone to increase (239). GH administration has been shown to be beneficial for protein preservation in conditions of dietary restriction (240). Moreover, fasting in GH-deficient subjects resulted in 50% increase in urea-nitrogen excretion and 25% increase in muscle protein breakdown (241, 242). Also, obesity has been associated with decreased levels of circulating GH, and consequent protein loss (243). Treatment of these patients with GH has been successful in preserving the protein stores and LBM (244). Although the metabolic functions of GH are well recognized, the underlying mechanisms of these actions are not yet well described.

Under certain conditions (e.g. if cells are deprived of GH for some hours), GH has acute and transient insulin-like effects (134). These effects include increased glucose utilization, increased glucose uptake, anti-lipolysis among others. It has been suggested that these effects are mediated by the insulin receptor substrate-1 (IRS-1) and phosphoinositide 3-kinase (PI3-K), which get activated by GH stimulation (245).

There is an extensive interest in taking advantage of the anabolic effects of GH for improving athletic performance (246). During moderate exercise GH appears to stimulate lipolysis without any effect on protein and glucose metabolism. Prolonged GH administration results in prevalent lipolysis and decreased protein oxidation (238). Although administration of supra-physiological doses of GH to athletes exerts potentially beneficial effects on body composition, it remains unclear whether these effects translate to improved performance (247). Nevertheless, GH abuse has been widespread among the athletes for more than 20 years, with consequences such as edema, carpal tunnel syndrome, arthralgias, myalgias, glucose intolerance and diabetes mellitus (248, 249).

Roles in the Immune System

At the cellular level, GH stimulates differentiation and mitogenesis and prevents apoptosis (137, 145, 250). There are also reports that GH signaling results in tubulin polymerization (251), cell migration and chemotaxis (252). These cellular effects are implicated in a variety of biological actions of GH in immune cells. Both GH and its receptor are expressed in various immune cells as T lymphocytes, B lymphocytes, monocytes and neutrophils. GH enhances thymopoiesis and T cell development, modulates cytokine production, enhances B cell development and antibody production, activates neutrophils and monocytes, enhances neutrophil adhesion and monocyte migration, and it has an anti-apoptotic action (253). Additionally, GH is involved in the formation and functional activation of mature blood cells (254).

GHR clearly acts in favor of an active immune system. In aging people the immune response gradually deteriorates due to a downregulated GH/IGF-1 axis (238). This became particularly clear during the Covid-19 pandemic in 2020 when death rates were very high among elderly. Lowered GH/IGF-1 activity promote inflammatory activity, causing long term tissue damage and systemic chronic inflammation due to decreased levels of anti-inflammatory adipokines such as adiponectin (255). Somewhat counterintuitive, studies of long living mutants and caloric restricted animals show decreased pro-inflammatory activity with increased levels of anti-inflammatory adipokines such as adiponectin. This suggests that reduced inflammation promoting healthy metabolism may represent one of the major mechanisms of extended longevity in long-lived mutant mice and likely also in the human. Together it shows that there is a need for insight in the molecular mechanisms underlying the relation between the GH/IGF-1 axis and immunity. Recently, Ishikawa et al. found that induction of the mouse major histocompatibility complex (MHC) antigen blastocyst H2 (H2-Bl) expression by GH is critical for suppressing innate immune cells such as natural killer (NK) cells/NK T cells (NKTs) and macrophage-mediated hepatocyte apoptosis, which favors C57BL/6 mice liver regeneration and survival after partial hepatectomy. Application of human leukocyte antigen G (HLA-G, the human homolog of H2-Bl) gave similar results (107). They used a series of knock-in mice to prove that, rather than the JAK/STAT pathway, GHR signaling from SRC, presumably Lyn, bound to the GHR receptor, activates ERK *via* RAS (85, 106). Thus, H2-Bl expression is crucial for reducing innate immune-mediated apoptosis and promoting survival after partial hepatectomy. This is important progress on the long road to understand the relation between GH/IGF-1 signaling and immunity regulation.

Roles in the Brain

The activity of GH/GHR in the brain is still a matter of debate. GH has been described as modulator of stress response and behavior by acting directly on the brain (256). Recent studies show that GH has direct trophic effects on the formation of proopiomelanocortin- and agouti-related peptide-expressing neurons and provide evidence that GH regulates hypothalamic neurocircuits controlling energy homeostasis (257). IGF-1 is well known to be critical for neuronal structure and function, and models of IGF-1 deficiency demonstrate important hippocampal deficits, as reduced structural complexity, excitability, learning, and memory (258–261). Interestingly, low IGF-1 levels have been associated with risk for vascular dementias (262). On the contrary, studies with growth hormone deficient (GHD) people and mouse models support the notion that a decrease in GH action is beneficial for maintenance of CNS integrity and functions as learning and memory during aging (263–265). Both in humans and rodents, circulating GH and IGF-1 levels decline with age, including in the central nervous system (CNS) (266). However, despite low overall GH/IGF-1 levels, old Ames dwarf mice have elevated levels of GH and IGF-1 in the hippocampus. Also, human subjects with Laron syndrome show improved rather than impaired memory (13). A likely explanation for the disconnect between IGF-1 and GH roles in the brain was provided by Sun et al. who demonstrated that hippocampal IGF-1 expression is not reduced in GH-deficient mice (267). Importantly, studies by Efstratiadis provided

evidence that in contrast to hepatic IGF-1 expression, IGF-1 expression in the brain is not GH-dependent (268). GHD and GHR deficient mice, which have longer life expectancies than wild-type, also perform better on cognitive tasks (255). Furthermore, three prominent models of GH signaling disruption—Snell dwarf, Ames dwarf, and GHRKO mice—all suggest reduced GH is beneficial to the CNS. Ames dwarf mice, which carry a homozygous loss-of-function mutation at the Prop-1 locus, are deficient in GH, thyroid-stimulating hormone (TSH), and prolactin-producing cells in the adenohypophysis. Despite their smaller body size and unique phenotype, these mice have a significantly increased lifespan and maintain physiological and cognitive function at youthful levels longer than controls (269, 270).

GH and Aging

Knockout mice for GHR ("Laron Dwarf") and mice with mutations causing GH deficiency or resistance ("Ames dwarf", and "Snell dwarf", and "Little") live longer than their genetically normal siblings (4, 227, 271–274). This extended longevity is remarkable and reproducible, ranging from 25% to over 60%. These long-lived mice present many signs and indicators of a healthy delayed aging process. These results would lead to the conclusion that GH normally released by the pituitary limits life expectancy, probably due to acceleration of the aging process. This conclusion is supported by reports showing that reduced levels of IGF-1, or mutations interfering with IGF-1 signaling also result in increased mice longevity (275, 276). As expected, transgenic mice with elevated levels of GH and IGF-1 live shortly and reflect characteristics of an accelerated aging process (277). Studies analyzing the influence of GH signaling and lifespan in several species have been performed. Exciting new findings come from numerous tissue-specific GHRKO mice and include the role of GH in pancreatic β-cells to stimulate insulin following glucose challenge, in weight loss regulation in ablated AgRP neurons and in glucose homeostasis in LepR neurons. In muscle GHR disruption enhances insulin sensitivity and extends lifespan, while adult-onset global disruption of GHR extends female lifespan, reviewed in (278).

While Besson and co-workers reported that individuals with congenital GH deficiency live shorter (279), others reported that GH-deficient/resistant subjects live long with decreased incidence of cancer, atherosclerosis and vascular pathology, in spite of being obese (11, 280, 281). These conflicting results may be connected to another key factor influencing the aging process: the insulin sensitivity. In mouse models, GH-deficiency is associated with insulin sensitivity (low levels of circulating insulin), while GH-deficient people are insulin resistant (high levels of circulating insulin). In these models, GH-deficiency allied with insulin sensitivity contributes to low blood glucose level. This biochemical feature has been negatively correlated with oxidative stress (282). Since oxidative stress is recognized as one of the major causes of aging (283), GH may influence the aging process by acting on oxidative stress pathways. Accordingly, Ames dwarf mice produce less metabolic oxidants, and have increased levels of anti-oxidants (284, 285). On the other hand, in GH-deficient humans, insulin resistance increases the oxidative damage (282), induces accumulation of visceral fat mass (286), and increases the risk of several age-related diseases (12, 210, 287). Thus, differences in the aging process between mice and humans suffering from GH-deficiency may be explained by their difference in insulin sensitivity.

Recent studies show physical and functional interactions of GHR with IGF-1R, which might strengthen its role in aging (and cancer). Although absent in hepatocytes, IGF-1R can serve as a component of the GH signaling pathway, modulating GHR's signaling strength and allowing for more local heterogeneity of GH/IGF-1 actions (86). Not only the GH-induced IGF-1 expression in the liver, also its secretion is subject of regulation. Studies of the energy sensing liver kinase B1-AMP-activated protein kinase (LKB1–AMPKa1) pathway implicate this pathway in the IGF-1 secretion *via* the small GTPase, Rab8a: the LKB1–AMPK pathway inhibits IGF-1 secretion. How this relates to the tumor suppressor functions of LKB1 remains unclear. Independent of the LKB1–AMP–activity, the insulin sensitizer and anti–aging/cancer agent, metformin also inhibits IGF-1 secretion (288–290). Once again, these studies illustrate the complexity of the GH/IGF-1 axis for metabolism, in homeostasis, as well in aging and cancer.

In humans, during aging the GH/IGF-1 axis is down regulated (238). On one hand, this probably contributes to the effects of aging on body composition, skin characteristics and functional changes that decrease the quality of life. On the other hand, decrease in the amounts of GH with age may offer protection from cancer and other age-related diseases. Therefore, GH replacement is controversial as an anti-aging therapy and involves both benefits and risks (274, 291).

GH and Cancer

There is an overwhelming number of studies that implicate GH/IGF-I in cancer growth. Organisms that lack GHR activity are virtually devoid of cancer (4, 292–299). In addition to the pituitary, GH is expressed in colon, prostate, lung, meningiomas and breast, where it binds the GHR to signal in a paracrine/autocrine fashion (21, 297, 300–303). Elegant experiments with rodents reveal an important role of GH in tumor development. Crossing GHR KO mice with mice predisposed to develop carcinomas significantly slowed down tumor progression (304). Additionally, GH deficient rats crossed with rats predisposed to prostatic cancer showed significantly reduced tumor incidence and burden (305). Interestingly, GH-deficient female rats are resistant to chemical induction of mammary carcinogenesis, whereas GH replacement restores the risk of tumor development (306). Intracellular (autocrine) GH promotes breast cancer cell transformation (292, 294, 301, 307, 308) and induces an invasive phenotype by triggering an epithelial–mesenchymal transition (EMT), cell motility, and increased cell survival (295, 297, 300–302).

Strong epidemiological evidence shows that people without GHR (Laron dwarfism) live healthy normal lives despite low IGF-1 levels. Strikingly, they do not develop cancer (nor diabetes), while overabundance of GH/IGF-1 links to cancer incidence (280, 292, 309). For common cancers (breast, colon, prostate, melanoma) tall size relates to cancer risk (308, 310–314). Most importantly, studies

with cells, tissues and animals show that GH/IGF-1 stimulates growth of these same cancers, while cancer growth without GH/IGF-1 activity is absent (57, 294, 300, 301, 305). Recent data suggest that also pancreatic ductal adenocarcinomas and small-cell and squamous-cell lung cancer are driven by GH/IGF-1 (21, 315, 316). Thus, there is solid evidence that both GH and IGF-1 are important cancer drivers in humans.

Most cancer cells express GH. This raises the possibility that autocrine GHR activation might be a cancer-driver. In breast cancer tissue, that is devoid of pituitary-specific POU domain transcription factor 1, GH expression is stimulated by progesterone (58, 317). Approximately two-thirds of human breast cancers are steroid hormone receptor (ER/PR) positive and treated with combinations of selective estrogen receptor modulators. It is currently unknown whether their effect relies on inhibition of GH expression. Whether triple-negative breast cancer (TNBC) cells, that do not respond to these modulators, also depend on GH expression, is unknown. The GH-antagonist, pegvisomant, has been successfully used in cancer-derived cell lines (295), but does not inhibit autocrine-acting GH in cancer patients as it probably cannot interfere with intracellular GH/GHR signaling (82). Direct targeting of GH signaling is therefore most probably the only possibility for therapeutic intervention in most cancers.

GH treatment of intestinal organoids closely recapitulating normal human intestinal mucosa resulted in p53 suppression and increased Wnt (318). GH treatment leads to down-regulation of E-cadherin, which controls cell adhesion and prevents tumor cell dissemination (318, 319). An interesting JAK-STAT3 and Wnt–β-catenin pathway connection was revealed that fuels the growth of intestine tumors. The study presents evidence that partial suppression of systemic JAK-STAT3 signaling is sufficient to limit tumor growth by reducing Bmi-1–dependent repression of p21 and p16. Normally p21 is repressed by Bmi-1 in APC-mutant tumors (320, 321). This connection provides a route to use the GHR-STAT3 pathway for a therapeutic modality to inhibit APC mutant cancers.

A growing number of studies implicate GH also in development of therapeutic resistance in a variety of human cancers (322). Both JAK2- and Lyn-initiated pathways activate, upon anti-cancer treatment, many different systems that upregulate ABC-multidrug efflux pumps (ABCG2), block apoptosis, DNA repair (p53), and pro-apoptotic molecules (Bax, PPARγ), suppresses caspase activation, and induce EMT and markers of stemness like ALDH1, NANOG, and CD24. In melanoma, GH upregulates the melanocyte-inducing transcription factor (MITF), that targets the oncogene MET, and organizes the resistance to radiation therapy (323).

THE REGULATION OF THE GHR AT THE CELLULAR LEVEL

Given the many factors that control the GHR activity it is important to integrate this knowledge into a concept. Except for autocrine signaling, the number of GHRs at the cell surface determines the sensitivity for GH. This is tightly controlled by the factors discussed above.

Within 20–30 min after synthesis in the ER, the GHR arrives at the cell surface, is available for GH binding during ~30 min, is endocytosed, and degraded within 5 min. A good indication for this can be delineated from the ratio between the precursor form in the endoplasmic reticulum (110,000 Mr) and the mature form at the cell surface (130,000 Mr) if separated by SDS-PAGE and immunoblotted from a crude cell extract using an anti-GHR antibody: If this ratio is approximately 1:1 at steady state, it implies that each GHR is present at the cell surface for only 30 min. Protease K treatment on ice shows that almost no 130,000-Mr species is inside, on route to the lysosomes. In **Figures 2**, **5** the controlling factors are shown.

Based on data from literature combined with our own data we propose the following concept for GHR endocytosis. The major regulators are: ADAM17, JAK2, Ubc13/CHIP/Proteasome, CK2/βTrCP, βTrCP (DSGxxS), and SOCS2. In steady state (no GH), endocytosis is enabled by Ubc13/CHIP and βTrCP (DSGxxS). Both systems are necessary and sufficient. If JAK2 is activated, S341 is phosphorylated, presumably by an activated CK2, SOCS2 binds to pY487/pY595, and all 4 ubiquitination systems are necessary and sufficient for endocytosis. Inactivation of each impedes endocytosis and prolongs GHR signaling capacity. Summarizing the contribution of each enzyme system to GH sensitivity is as follows:

ADAM17 (TACE) contributes ~10% to the inactivation of GHR (**Figure 2**). It is involved in the shedding of many membrane proteins and receptors. Its activation, whether that means increased presence at the cell surface, increased enzymatic activity *via* phosphorylation, or increased residence time at the cell surface is poorly documented. Many signaling pathways are known to promote ADAM17 phosphorylation including PKCs, ERKs, p38 MAPK and PLK2 (324). Shedding of the GH-GHR complex is prohibited (39, 48, 152). Interestingly, Uev1A-Ubc13 (see below) mediates the classical TNFα-induced NF-κB signaling pathway, and at the same time provides for a feedback loop together with CHIP to terminate NF-κB signaling by facilitating ADAM17 maturation *via* RHBDF2 ubiquitination (325). It would not be surprising if GHR signaling would act on ADAM17 in an analogous way.

High JAK2 levels inhibit GHR endocytosis, but in normal cells and tissues this might be not relevant. In IM9 lymphoblasts high levels of JAK2 may prolong the life time at the cell surface (92), but in γ2A cells, that do not express JAK2, GHR has a normal half-life (326). In addition to being controlled by ancillary factors such as SH2-B (91), their activities are subjected to auto-activation, they trans-phosphorylate tyrosine residues in specific patterns (327), they detach from activated receptors to be recycled by phosphatases (92), and in particular, JAK2 responds to heat stress by irreversible aggregation (103). Thus, elevated body temperatures lower the responsiveness of cytokine receptors, and consequently, contribute to a balanced immune system e.g. during a cytokine storm (328, 329).

Ubc13/CHIP/Proteasome are required for both unstimulated and GH-stimulated (pGHR) endocytosis (35). The exact

mechanism is still unknown. The bottom-line is that endocytosis of the GHR is not possible if either proteasome activity, CHIP or Ubc13 are lacking. Other observations include: Endocytosis does not require lysine residues, and proteasome-independent endocytosis is only possible if the tail is partly truncated (40, 170). Given its nature as co-chaperone Ubc13/CHIP/Proteasome most likely act in a late step in GHR endocytosis, analogous to TPR proteins in quality control of mislocalized membrane proteins (34, 330). In an analogous way, we propose that CHIP binds with its first TPR motif to the UbE motif, with its central TPR motif to the proteasome and with its U-box to the ubiquitin conjugase Ubc13/UEV1a. Recruited by CHIP, the proteasome might remove the C-terminal part of the GHR downstream of the DSGxxS motif at amino acid 383: an action that explains why endocytosis of a truncated GHR requires both UbE and DSGxxS motifs, but no proteasomal activity (43). This is in line with our observation that degradation of the GHR cytosolic domain precedes degradation of the GH-binding domain (331). In this role CHIP cleans up and definitively terminates GH signaling at the cell surface. In such a scenario, proteasome inhibitors might be considered pro-cancer and pro-aging, as they prolong the residence time of the GHR at the cell surface (39, 209).

Phosphorylation of S341 in the UbE/TPR motif, presumably by CK2, is responsible for an 150% increase of the rate of GHR endocytosis and degradation (179). We showed that this is GH-induced, but also other conditions and stressors might stimulate S341 phosphorylation. Insulin has been suggested to reduce GHR levels and GH signaling in PI-3 kinase- and MAPK-dependent manners (332–334). Also, IGF-1 and estrogen might use phosphorylation of S341 to decrease the pool of GHRs at the cell surface (335, 336). Pro-inflammatory cytokines such as TNFα and IL-6 have been described to induce GH insensitivity. In the latter case, the kinase acts to desensitize cells for GH (337). Coincidentally or not, neighboring JAK2 that binds 45 amino acid residues upstream also is a CK2 client (338). If stressors phosphorylate the S341 in the UbE/TPR motif, the GHR endocytosis rate is increased, independent of SOCS2 (see below).

Phosphorylation of the DSGxxS motif: The DSGRTS sequence in GHR seems to be phosphorylated in basal conditions, without applying any special treatment or stressor to the cells (42). However, it is possible that under physiological conditions the phosphorylation status of DSGRTS might also be regulatable upon certain stimuli, as for the UbE/TPR motif. Additionally, in some situations that require high levels of GH signaling, the body would benefit from higher sensitivity to GH at steady state, e.g. in the process of chondrogenesis at children's growth plate, or during adolescence to stimulate breast growth, or at the end of mitosis if cells need to growth (339, 340). A decreased kinase activity towards the DSGRTS serine residues would result in decreased basal degradation of GHR, increase in cellular levels of GHR, and consequently increase in GH sensitivity.

SOCSs induce proteasomal degradation of targets through ubiquitination (341, 342). However, in case of transmembrane receptors like GHR and prolactin receptors it is less clear, whether they contribute only to their signal termination or also to their endocytosis/lysosomal targeting/degradation. SOCS2 binds to a degron sequence $TP^{495}AGS$ downstream of the STAT5b-interacting pY487. If P495 is mutated to threonine, the binding to SOCS2 is prevented, and the degradation of activated GHR (pGHR) is delayed (21). Assuming that the GHR-JAK2 complex *initiates* signaling only from the cell surface, the results of Chhabra and co-workers imply that pGHR can endocytose and be send to lysosomes, only after SOCS2 has acted on the pGHR (at the cell surface). In that case, SOCS2 is part of a concerted action together with JAK2, βTrCP, and CHIP in initiating signal transduction and preparing the GHR for endocytosis (**Figures 2** and **5**). Increased time span between signal initiation and endocytosis intensifies GH-induced signaling per GHR complex. In a previous study we showed that signal transduction can continue after endocytosis (343). At that time a clear distinction between events starting at the cell surface and continuing inside was difficult to make. Endocytosis of GHR with all tyrosine residues deleted is near normal (92). Thus, SOCS2 contributes only to the deactivation and endocytosis of pY487, pY595-GHR. If the GH/GHR signaling comes from inside (autocrine activation), as is assumed in many cancer cells, there are many open questions: Do the activated GH/GHR complexes reach the cell surface or are they directly transported to MVBs, what are the signaling modes and capacities of these complexes and (how) is it regulated? These are important open questions to understand the role of the GHR in cancer growth.

STAT5b binding to tyrosine residues 487, 534, and 627 are most important for its activation (22). Like GHR knock-out mice, mice that express GHR(1-391) show insulin sensitivity with obesity (344). GH-mediated STAT5b activation acts on multiple sites in the major insulin responsive tissues to promote insulin sensitivity. These actions are regulated at both transcriptional and posttranscriptional levels, and although ChIP analysis indicates direct STAT5b action at the promoter level of key genes, it is apparent that many of the insulin-sensitizing actions of GH-STAT5b deficiency are indirect.

Tyr627: In an effort to determine the contribution of individual tyrosine residues to the STAT5b and MAPK signaling pathways, we found that the Y627F mutation resulted in constitutive GHR, JAK2 and MAPK phosphorylation and activation (22). It is expected that this mutation would act as pro-cancer and pro-aging, but to our knowledge, this variant has not been reported in humans yet (345, 346).

In this summary, the role of Lyn *per se* has not been discussed, as the molecular details as how it functionally interacts with JAK2 and the endocytosis machinery are unknown.

CONCLUSIONS AND PERSPECTIVES

In this review, we discussed enzyme systems that regulate the GH-sensitivity of cells by direct interaction (ADAM17, JAK2, βTrCP, CHIP, SOCS2). As discussed in the previous section, except for JAK2, delayed activity of each of the systems predicts

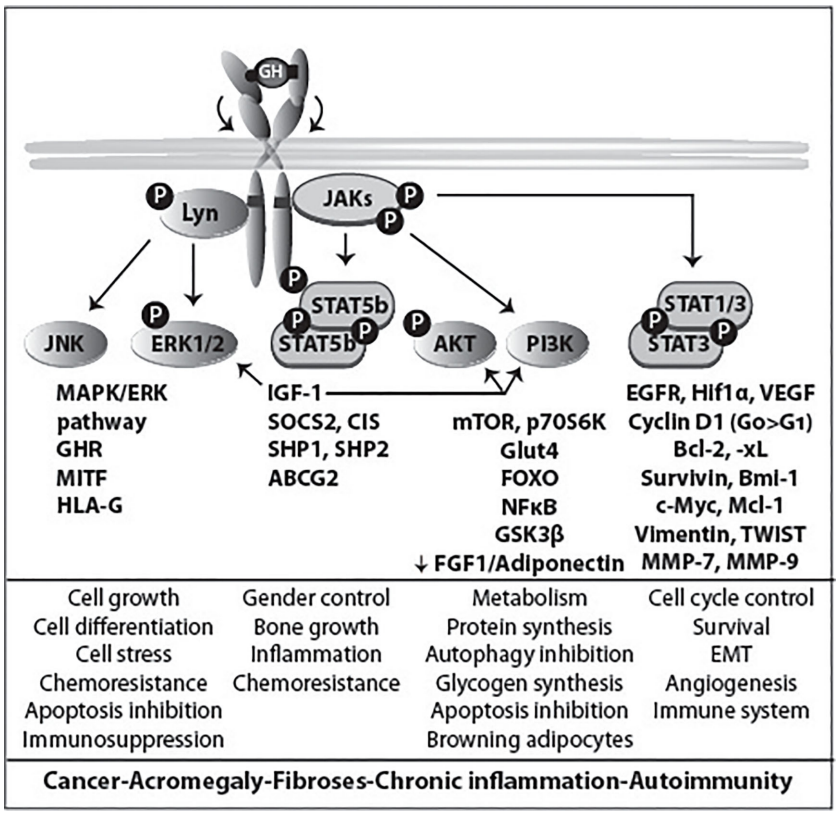

FIGURE 7 | GHR signaling and its span of control. GHR acts *via* JAK/STAT and Lyn, and controls many aspects of cell growth and differentiation, gender, metabolism and cell cycle (middle panel). The general scheme is in **Figure 4**. Deregulated downstream effectors have been studied in great detail in promoting many cancers and chronic diseases (lower panel).

prolongation of the GHR at the cell surface. As GHR synthesis continues, delayed endocytosis results in increased GH-sensitivity. This is illustrated for SOCS2: prolonged GH signaling, due to a defective GHR-SOCS2 interaction, promotes cancer progression in human lung cancer (21, 202). Although the GH/IGF-1 axis is clearly involved in cancer, none of the other binding sites have yet been identified in genome-wide association study (204, 205). Apparently, these sites are highly relevant for life and do not allow mutations.

Considering the GH/IGF-1 axis as the mains switch, downstream effectors are the executers of the many tasks (**Figure 7**) (116). Without exception, these factors function in various signaling pathways and are regulated not only by signaling receptors but also in networks of other stressors. Obviously, mutations in these crucial "house-hold factors" contribute to several chronic diseases. However, in many instances, they need the *supervision* of the GH/IGF-1 axis. As each of the enzyme systems impact the activity of the GHR similarly (less interaction results in higher GH-sensitivity) it is plausible that their presence in the regulation of the hierarchical command-and-control mode of the GHR indicates their importance for major control systems. Accordingly, their loss of function would result in the same effect as GHR gain of function. Upregulation of the GH/IGF-1 axis in adult species leads to chronic diseases as illustrated in **Figure 7** (4–10, 12, 13, 347). Indeed, there are many studies that validate this hypothesis. Taken together, literature on CHIP and SOCS shows striking analogy with the regulatory potential of the GHR: organisms with increased CHIP and SOCS2 activity live longer and suffer less from chronic diseases. This is also observed for some of the downstream GHR effectors like mTOR (348). Controlling GHR *turnover* in the axis: GHRH → GHRHR → GH → GHR (+IGF-1) → Growth/Aging, is a challenging mission. Accomplishment will be highly rewarding as it might offer novel tools to fight the conditions, that underlie the major diseases of aging populations.

AUTHOR CONTRIBUTIONS

All the authors contributed equally. All authors contributed to the article and approved the submitted version.

FUNDING

This work was supported by the European Network of Excellence, RUBICON "Role of ubiquitin and ubiquitin-like modifiers in cellular regulation", grant LSHG-CT-2005-018683; two European Union Marie Curie Networks, grant MRTNCT-2006-034555 (UbiRegulators) and ERBFMRXCT96-0026; by the Dutch Technology Foundation Stichting Technische Wetenschappen (STW), which is the applied science division of the Nederlandse Organisatie voor Wetenschappelijk Onderzoek (NWO), and the Technology Program of the Ministry of Economic Affairs, Grant 11155: "Targeting the Jak2-GH receptor interaction for treatment of cancer", The Netherlands Proteomics Centre, "Proteomic analysis of ubiquitylation in membrane trafficking, NPC3.1, and the Netherlands Organization for Scientific Research Grants NWO-ALW 814-02-011 and NWO-902-23-192.

ACKNOWLEDGMENTS

The authors thank all the collaborators who participated in the studies, in particular Peter van Kerkhof (UMC, Utrecht), Agnes van Rossum (Psychologie & Coaching Praktijken, Utrecht), Marcel Roza (Genmab, Utrecht), Monique van den Eijnden, Elpetra Timmermans-Sprang (UU, Utrecht), and Lieke van der Velden (CBG, Utrecht).

REFERENCES

1. Hershko A, Ciechanover A. The ubiquitin system for protein degradation. *Annu Rev Biochem* (1992) 61:761–807. doi: 10.1146/annurev.bi.61.070192.003553
2. Leung DW, Spencer SA, Cachianes G, Hammonds RG, Collins C, Henzel WJ, et al. Growth hormone receptor and serum binding protein: purification, cloning and expression. *Nature* (1987) 330:537–43. doi: 10.1038/330537a0
3. Strous GJ, van Kerkhof P, Govers R, Ciechanover A, Schwartz AL. The ubiquitin conjugation system is required for ligand-induced endocytosis and degradation of the growth hormone receptor. *EMBO J* (1996) 15:3806–12. doi: 10.1002/j.1460-2075.1996.tb00754.x
4. Basu R, Qian Y, Kopchick JJ. Mechanisms In Endocrinology: Lessons from growth hormone receptor gene-disrupted mice: are there benefits of endocrine defects? *Eur J Endocrinol* (2018) 178:R155–81. doi: 10.1530/EJE-18-0018
5. Ciechanover A. Intracellular protein degradation: From a vague idea thru the lysosome and the ubiquitin-proteasome system and onto human diseases and drug targeting. *Best Pract Res Clin Haematol* (2017) 30:341–55. doi: 10.1016/j.beha.2017.09.001
6. Dehkhoda F, Lee CMM, Medina J, Brooks AJ. The Growth Hormone Receptor: Mechanism of Receptor Activation, Cell Signaling, and Physiological Aspects. *Front Endocrinol (Lausanne)* (2018) 9:35. doi: 10.3389/fendo.2018.00035
7. Foot N, Henshall T, Kumar S. Ubiquitination and the Regulation of Membrane Proteins. *Physiol Rev* (2017) 97:253–81. doi: 10.1152/physrev.00012.2016
8. Junnila RK, List EO, Berryman DE, Murrey JW, Kopchick JJ. The GH/IGF-1 axis in ageing and longevity. *Nat Rev Endocrinol* (2013) 9:366–76. doi: 10.1038/nrendo.2013.67
9. Waters MJ. The growth hormone receptor. *Growth Horm IGF Res* (2016) 28:6–10. doi: 10.1016/j.ghir.2015.06.001
10. Wit JM, Oostdijk W, Losekoot M, van Duyvenvoorde HA, Ruivenkamp CA, Kant SG. Mechanisms In Endocrinology: Novel genetic causes of short stature. *Eur J Endocrinol* (2016) 174:R145–173. doi: 10.1530/EJE-15-0937
11. Guevara-Aguirre J, Guevara A, Palacios I, Perez M, Procel P, Teran E. GH and GHR signaling in human disease. *Growth Horm IGF Res* (2018) 38:34–8. doi: 10.1016/j.ghir.2017.12.006
12. Guevara-Aguirre J, Balasubramanian P, Guevara-Aguirre M, Wei M, Madia F, Cheng CW, et al. Growth hormone receptor deficiency is associated with a major reduction in pro-aging signaling, cancer, and diabetes in humans. *Sci Transl Med* (2011) 3:70ra13. doi: 10.1126/scitranslmed.3001845
13. Nashiro K, Guevara-Aguirre J, Braskie MN, Hafzalla GW, Velasco R, Balasubramanian P, et al. Brain Structure and Function Associated with Younger Adults in Growth Hormone Receptor-Deficient Humans. *J Neurosci* (2017) 37:1696–707. doi: 10.1523/JNEUROSCI.1929-16.2016
14. Posner BI, Kelly PA, Shiu RP, Friesen HG. Studies of insulin, growth hormone and prolactin binding: tissue distribution, species variation and characterization. *Endocrinology* (1974) 95:521–31. doi: 10.1210/endo-95-2-521
15. Kelly PA, Djiane J, Postel-Vinay MC, Edery M. The prolactin/growth hormone receptor family. *Endocr Rev* (1991) 12:235–51. doi: 10.1210/edrv-12-3-235
16. Godowski PJ, Leung DW, Meacham LR, Galgani JP, Hellmiss R, Keret R, et al. Characterization of the human growth hormone receptor gene and demonstration of a partial gene deletion in two patients with Laron-type dwarfism. *Proc Natl Acad Sci U.S.A.* (1989) 86:8083–7. doi: 10.1073/pnas.86.20.8083
17. Boulay JL, O'Shea JJ, Paul WE. Molecular phylogeny within type I cytokines and their cognate receptors. *Immunity* (2003) 19:159–63. doi: 10.1016/S1074-7613(03)00211-5
18. Bagley CJ, Woodcock JM, Stomski FC, Lopez AF. The structural and functional basis of cytokine receptor activation: lessons from the common á subunit of the granulocyte-macrophage colony-stimulating factor, interleukin-3 (il-3), and il-5 recept. *Blood* (1997) 89:1471–82. 1471-1482. doi: 10.1182/blood.V89.5.1471.1471_1471_1482
19. Baumgartner JW, Wells CA, Chen CM, Waters MJ. The role of the WSXWS equivalent motif in growth hormone receptor function. *J Biol Chem* (1994) 269:29094–101.
20. de Vos AM, Ultsch M, Kossiakoff AA. Human growth hormone and extracellular domain of its receptor: crystal structure of the complex. *Science* (1992) 255:306–12. doi: 10.1126/science.1549776
21. Chhabra Y, Wong HY, Nikolajsen LF, Steinocher H, Papadopulos A, Tunny KA, et al. A growth hormone receptor SNP promotes lung cancer by impairment of SOCS2-mediated degradation. *Oncogene* (2018) 37:489–501. doi: 10.1038/onc.2017.352
22. Putters J. *Phosphorylation and Ubiquitination in Growth Hormone Receptor Endocytosis and Signalling, Chapter V, The contribution of tyrosine residues to growth hormone receptor signalling*. Thesis, Utrecht: Utrecht University (2010). Available at: http://dspace.library.uu.nl/handle/1874/396613.
23. Fuh G, Mulkerrin MG, Bass S, McFarland N, Brochier M, Bourell JH, et al. The human growth hormone receptor. Secretion from Escherichia Coli and disulphide bonding pattern of the extracellular domain. *J Biol Chem* (1990) 265:3111–5.
24. Sedek M. *Posttranslational modifications of the regulation of GHR and Jak2. Chapter V: SUMO2/3 regulates GHR trafficking*. Thesis, Utrecht: Utrecht University (2012). Available at: https://dspace.library.uu.nl/handle/1874/397232.
25. Conway-Campbell BL, Wooh JW, Brooks AJ, Gordon D, Brown RJ, Lichanska AM, et al. Nuclear targeting of the growth hormone receptor results in dysregulation of cell proliferation and tumorigenesis. *Proc Natl Acad Sci U S A* (2007) 104:13331–6. doi: 10.1073/pnas.0600181104
26. Waters MJ, Brooks AJ. Growth hormone and cell growth. *Endocr Dev* (2012) 23:86–95. doi: 10.1159/000341761
27. Sedek M, van der Velden LM, Strous GJ. Multimeric growth hormone receptor complexes serve as signaling platforms. *J Biol Chem* (2014) 289:65–73. doi: 10.1074/jbc.M113.523373
28. Liu Y, Zhang Y, Jiang J, Lobie PE, Paulmurugan R, Langenheim JF, et al. GHR/PRLR Heteromultimer Is Composed of GHR Homodimers and PRLR Homodimers. *Mol Endocrinol* (2016) 30:504–17. doi: 10.1210/me.2015-1319
29. Gent J, van Kerkhof P, Roza M, Bu G, Strous GJ. Ligand-independent growth hormone receptor dimerization occurs in the endoplasmic reticulum and is required for ubiquitin system-dependent endocytosis. *Proc Natl Acad Sci U S A* (2002) 99:9858–63. doi: 10.1073/pnas.152294299
30. Schantl JA, Roza M, de Jong AP, Strous GJ. Small glutamine-rich tetratricopeptide repeat-containing protein interacts with the ubiquitin-dependent endocytosis

motif of the growth hormone receptor. *Biochem J* (2003) 373:855–63. doi: 10.1042/bj20021591
31. Schantl JA. *Growth Hormone Receptor Interacting Proteins, Chapter III: The anti-apoptotic protein Scythe interacts with the ubiquitin-dependent endocytosis motif of the growth hormone receptor and localizes to mitochondria*. Thesis, Utrecht: Utrecht University (2003). Available at: http://dspace.library.uu.nl/handle/1874/396614.
32. Benarroch R, Austin JM, Ahmed F, Isaacson RL. The roles of cytosolic quality control proteins, SGTA and the BAG6 complex, in disease. *Adv Protein Chem Struct Biol* (2019) 114:265–313. doi: 10.1016/bs.apcsb.2018.11.002
33. Shao S, Rodrigo-Brenni MC, Kivlen MH, Hegde RS. Mechanistic basis for a molecular triage reaction. *Science* (2017) 355:298–302. doi: 10.1126/science.aah6130
34. Leznicki P, Korac-Prlic J, Kliza K, Husnjak K, Nyathi Y, Dikic I, et al. Binding of SGTA to Rpn13 selectively modulates protein quality control. *J Cell Sci* (2015) 128:3187–96. doi: 10.1242/jcs.165209
35. Slotman JA, van Kerkhof P, Hassink GC, Kuiken HJ, Strous GJ. Identification of Ubiquitin System Factors in Growth Hormone Receptor Transport. In: *In Tech, Molecular Regulation of Endocytosis*, vol. 15. London: IntechOpen Limited, London, UK (2012). p. 391–410. 391-410.
36. Gent J, Van Den Eijnden M, Van Kerkhof P, Strous GJ. Dimerization and signal transduction of the growth hormone receptor. *Mol Endocrinol* (2003) 17:967–75. doi: 10.1210/me.2002-0261
37. Amit T, Hartmann K, Shoshany G, Baruch Y, Youdim MBH, Hochberg Z. The turnover of growth hormone (gh)-binding protein and gh receptor in rabbit and rat. *Mol Cell Endocrinol* (1993) 94:149–54. doi: 10.1016/0303-7207(93)90163-E
38. Murphy LJ, Lazarus L. The mouse fibroblast growth hormone receptor: ligand processing and receptor modulation and turnover. *Endocrinology* (1984) 115:1625–32. doi: 10.1210/endo-115-4-1625
39. van Kerkhof P, Smeets M, Strous GJ. The ubiquitin-proteasome pathway regulates the availability of the GH receptor. *Endocrinology* (2002) 143:1243–52. doi: 10.1210/endo.143.4.8755
40. Govers R, van Kerkhof P, Schwartz AL, Strous GJ. Linkage of the ubiquitin-conjugating system and the endocytic pathway in ligand-induced internalization of the growth hormone receptor. *EMBO J* (1997) 16:4851–8.internalization of the growth hormone receptor. Embo J 1997, 16:4851-4858. doi: 10.1093/emboj/16.16.4851
41. van Kerkhof P, Sachse M, Klumperman J, Strous GJ. Growth hormone receptor ubiquitination coincides with recruitment to clathrin-coated membrane domains. *J Biol Chem* (2000) 276:3778–84. doi: 10.1074/jbc.M007326200
42. da Silva Almeida AC, Strous GJ, van Rossum AG. betaTrCP controls GH receptor degradation via two different motifs. *Mol Endocrinol* (2012) 26:165–77. doi: 10.1210/me.2011-1211
43. van Kerkhof P, Alves dos Santos CM, Sachse M, Klumperman J, Bu G, Strous GJ. Proteasome inhibitors block a late step in lysosomal transport of selected membrane but not soluble proteins. *Mol Biol Cell* (2001) 12:2556–66. doi: 10.1091/mbc.12.8.2556
44. Sotiropoulos A, Goujon L, Simonin G, Kelly PA, PostelVinay MC, Finidori J. Evidence for generation of the growth hormone-binding protein through proteolysis of the growth hormone membrane receptor. *Endocrinology* (1993) 132:1863–5. doi: 10.1210/endo.132.4.8462483
45. Zhang Y, Jiang J, Black RA, Baumann G, Frank SJ. Tumor necrosis factor-alpha converting enzyme (TACE) is a growth hormone binding protein (GHBP) sheddase: the metalloprotease TACE/ADAM-17 is critical for (PMA-induced) GH receptor proteolysis and GHBP generation. *Endocrinology* (2000) 141:4342–8. doi: 10.1210/endo.141.12.7858
46. Amit T, Youdim MB, Hochberg Z. Clinical review 112: Does serum growth hormone (GH) binding protein reflect human GH receptor function? *J Clin Endocrinol Metab* (2000) 85:927–32. doi: 10.1210/jcem.85.3.6461
47. Zhang JG, Metcalf D, Rakar S, Asimakis M, Greenhalgh CJ, Willson TA. et al: The SOCS box of suppressor of cytokine signaling-1 is important for inhibition of cytokine action invivo. *Proc Natl Acad Sci U.S.A.* (2001) 98:13261–5. doi: 10.1073/pnas.231486498
48. Conte F, Salles JP, Raynal P, Fernandez L, Molinas C, Tauber M, et al. Identification of a region critical for proteolysis of the human growth hormone receptor. *Biochem Biophys Res Commun* (2002) 290:851–7. doi: 10.1006/bbrc.2001.6261
49. Baumann G. Growth hormone binding protein 2001. *J Pediatr Endocrinol Metab* (2001) 14:355–75. doi: 10.1515/JPEM.2001.14.4.355
50. Strous GJ, van Kerkhof P. The ubiquitin-proteasome pathway and the regulation of growth hormone receptor availability. *Mol Cell Endocrinol* (2002) 197:143–51. doi: 10.1016/S0303-7207(02)00258-7
51. Kawauchi H, Sower SA. The dawn and evolution of hormones in the adenohypophysis. *Gen Comp Endocrinol* (2006) 148:3–14. doi: 10.1016/j.ygcen.2005.10.011
52. Baumann G. Growth hormone heterogeneity: genes, isohormones, variants, and binding proteins. *Endocrine Rev* (1991) 12:424–49. doi: 10.1210/edrv-12-4-424
53. Okada S, Kopchick JJ. Biological effects of growth hormone and its antagonist. *Trends Mol Med* (2001) 7:126–32. doi: 10.1016/S1471-4914(01)01933-5
54. Harvey S. Extrapituitary growth hormone. *Endocrine* (2010) 38:335–59. doi: 10.1007/s12020-010-9403-8
55. Harvey S, Martinez-Moreno CG, Luna M, Aramburo C. Autocrine/paracrine roles of extrapituitary growth hormone and prolactin in health and disease: An overview. *Gen Comp Endocrinol* (2015) 220:103–11. doi: 10.1016/j.ygcen.2014.11.004
56. Mol JA, Lantinga-van Leeuwen IS, van Garderen E, Selman PJ, Oosterlaken-Dijksterhuis MA, Schalken JA, et al. Mammary growth hormone and tumorigenesis–lessons from the dog. *Vet Q* (1999) 21:111–5. doi: 10.1080/01652176.1999.9695004
57. Lombardi S, Honeth G, Ginestier C, Shinomiya I, Marlow R, Buchupalli B. et al: Growth hormone is secreted by normal breast epithelium upon progesterone stimulation and increases proliferation of stem/progenitor cells. *Stem Cell Rep* (2014) 2:780–93. doi: 10.1016/j.stemcr.2014.05.005
58. Timmermans-Sprang EPM, Gracanin A, Mol JA. Molecular Signaling of Progesterone, Growth Hormone, Wnt, and HER in Mammary Glands of Dogs, Rodents, and Humans: New Treatment Target Identification. *Front Vet Sci* (2017) 4:53. doi: 10.3389/fvets.2017.00053
59. Goffin V, Shiverick KT, Kelly PA, Martial JA. Sequence-function relationships within the expanding family of prolactin, growth hormone, placental lactogen, and related proteins in mammals. *Endocr Rev* (1996) 17:385–410. doi: 10.1210/er.17.4.385
60. Besson A, Salemi S, Deladoey J, Vuissoz JM, Eble A, Bidlingmaier M, et al. Short stature caused by a biologically inactive mutant growth hormone (GH-C53S). *J Clin Endocrinol Metab* (2005) 90:2493–9. doi: 10.1210/jc.2004-1838
61. Ranke MB, Wit JM. Growth hormone - past, present and future. *Nat Rev Endocrinol* (2018) 14:285–300. doi: 10.1038/nrendo.2018.22
62. Hartman ML, Faria AC, Vance ML, Johnson ML, Thorner MO, Veldhuis JD. Temporal structure of in vivo growth hormone secretory events in humans. *Am J Physiol* (1991) 260:E101–110. doi: 10.1152/ajpendo.1991.260.1.E101
63. Ho KY, Veldhuis JD, Johnson ML, Furlanetto R, Evans WS, Alberti KG. et al: Fasting enhances growth hormone secretion and amplifies the complex rhythms of growth hormone secretion in man. *J Clin Invest* (1988) 81:968–75. doi: 10.1172/JCI113450
64. Takahashi Y, Kipnis DM, Daughaday WH. Growth hormone secretion during sleep. *J Clin Invest* (1968) 47:2079–90. doi: 10.1172/JCI105893
65. Choi HK, Waxman DJ. Pulsatility of growth hormone (GH) signalling in liver cells: role of the JAK-STAT5b pathway in GH action. *Growth Horm IGF Res* (2000) 10 Suppl B:S1–8. doi: 10.1016/S1096-6374(00)80002-7
66. Gustafsson JA, Mode A, Norstedt G, Skett P. Sex steroid induced changes in hepatic enzymes. *Annu Rev Physiol* (1983) 45:51–60. doi: 10.1146/annurev.ph.45.030183.000411
67. Norstedt G, Palmiter R. Secretory rhythm of growth hormone regulates sexual differentiation of mouse liver. *Cell* (1984) 36:805–12. doi: 10.1016/0092-8674(84)90030-8
68. Clodfelter KH, Holloway MG, Hodor P, Park SH, Ray WJ, Waxman DJ. Sex-dependent liver gene expression is extensive and largely dependent upon signal transducer and activator of transcription 5b (STAT5b): STAT5b-dependent activation of male genes and repression of female genes revealed by microarray analysis. *Mol Endocrinol* (2006) 20:1333–51. doi: 10.1210/me.2005-0489
69. Laz EV, Sugathan A, Waxman DJ. Dynamic in vivo binding of STAT5 to growth hormone-regulated genes in intact rat liver. Sex-specific binding at

low- but not high-affinity STAT5 sites. *Mol Endocrinol* (2009) 23:1242–54. doi: 10.1210/me.2008-0449
70. Zhang Y, Laz EV, Waxman DJ. Dynamic, sex-differential STAT5 and BCL6 binding to sex-biased, growth hormone-regulated genes in adult mouse liver. *Mol Cell Biol* (2012) 32:880–96. doi: 10.1128/MCB.06312-11
71. Chen C. Growth hormone secretagogue actions on the pituitary gland: multiple receptors for multiple ligands? *Clin Exp Pharmacol Physiol* (2000) 27:323–9. doi: 10.1046/j.1440-1681.2000.03258.x
72. Kojima M, Hosoda H, Date Y, Nakazato M, Matsuo H, Kangawa K. Ghrelin is a growth-hormone-releasing acylated peptide from stomach. *Nature* (1999) 402:656–60. doi: 10.1038/45230
73. Hartman ML, Clayton PE, Johnson ML, Celniker A, Perlman AJ, Alberti KG, et al. A low dose euglycemic infusion of recombinant human insulin-like growth factor I rapidly suppresses fasting-enhanced pulsatile growth hormone secretion in humans. *J Clin Invest* (1993) 91:2453–62.91:2453-2462. doi: 10.1172/JCI116480
74. Pellegrini I, Roche C, Quentien MH, Ferrand M, Gunz G, Thirion S, et al. Involvement of the pituitary-specific transcription factor pit-1 in somatolactotrope cell growth and death: an approach using dominant-negative pit-1 mutants. *Mol Endocrinol* (2006) 20:3212–27. doi: 10.1210/me.2006-0122
75. Andersen B, Rosenfeld MG. Pit-1 determines cell types during development of the anterior pituitary gland. A model for transcriptional regulation of cell phenotypes in mammalian organogenesis. *J Biol Chem* (1994) 269:29335–8.
76. Roth J, Glick SM, Yalow RS, Berson SA. Secretion of human growth hormone: physiologic and experimental modification. *Metabolism* (1963) 12:577–9.
77. Hansen AP. Abnormal serum growth hormone response to exercise in maturity-onset diabetics. *Diabetes* (1973) 22:619–28. doi: 10.2337/diab.22.8.619
78. Melmed S, Polonsky KS, Larsen PR, H. K. *Williams Textbook of Endocrinology*. Philadelphia: Elsevier (2015).
79. Veldhuis JD, Roemmich JN, Richmond EJ, Bowers CY. Somatotropic and gonadotropic axes linkages in infancy, childhood, and the puberty-adult transition. *Endocr Rev* (2006) 27:101–40. doi: 10.1210/er.2005-0006
80. Corpas E, Harman SM, Blackman MR. Human growth hormone and human aging. *Endocr Rev* (1993) 14:20–39. doi: 10.1210/edrv-14-1-20
81. McIntyre HD, Zeck W, Russell A. Placental growth hormone, fetal growth and the IGF axis in normal and diabetic pregnancy. *Curr Diabetes Rev* (2009) 5:185–9. doi: 10.2174/157339909788920947
82. van den Eijnden MJ, Strous GJ. Autocrine growth hormone: effects on growth hormone receptor trafficking and signaling. *Mol Endocrinol* (2007) 21:2832–46. doi: 10.1210/me.2007-0092
83. Firmbach-Kraft I, Byers M, Shows T, Dalla-Favera R, Krolewski JJ. tyk2, prototype of a novel class of non-receptor tyrosine kinase genes. *Oncogene* (1990) 5:1329–36.
84. Argetsinger LS, Campbell GS, Yang XN, Witthuhn BA, Silvennoinen O, Ihle JN, et al. Identification of JAK2 as a growth hormone receptor-associated tyrosine kinase. *Cell* (1993) 74:237–44. doi: 10.1016/0092-8674(93)90415-M
85. Rowlinson SW, Yoshizato H, Barclay JL, Brooks AJ, Behncken SN, Kerr LM, et al. An agonist-induced conformational change in the growth hormone receptor determines the choice of signalling pathway. *Nat Cell Biol* (2008) 10:740–7. doi: 10.1038/ncb1737
86. Frank SJ. Classical and novel GH receptor signaling pathways. *Mol Cell Endocrinol* (2020) 518:110999. doi: 10.1016/j.mce.2020.110999
87. Brown RJ, Adams JJ, Pelekanos RA, Wan Y, McKinstry WJ, Palethorpe K. et al: Model for growth hormone receptor activation based on subunit rotation within a receptor dimer. *Nat Struct Mol Biol* (2005) 12:814–21. doi: 10.1038/nsmb977
88. Waters MJ, Brooks AJ. JAK2 activation by growth hormone and other cytokines. *Biochem J* (2015) 466:1–11. doi: 10.1042/BJ20141293
89. Brooks AJ, Dai W, O'Mara ML, Abankwa D, Chhabra Y, Pelekanos RA. et al: Mechanism of activation of protein kinase JAK2 by the growth hormone receptor. *Science* (2014) 344:1249783. doi: 10.1126/science.1249783
90. Wilmes S, Hafer M, Vuorio J, Tucker JA, Winkelmann H, Lochte S. et al: Mechanism of homodimeric cytokine receptor activation and dysregulation by oncogenic mutations. *Science* (2020) 367:643–52. doi: 10.1126/science.aaw3242
91. Carter-Su C, Schwartz J, Argetsinger LS. Growth hormone signaling pathways. *Growth Horm IGF Res* (2016) 28:11–5. doi: 10.1016/j.ghir.2015.09.002
92. Putters J, da Silva Almeida AC, van Kerkhof P, van Rossum AG, Gracanin A, Strous GJ. Jak2 is a negative regulator of ubiquitin-dependent endocytosis of the growth hormone receptor. *PloS One* (2011) 6:e14676. doi: 10.1371/journal.pone.0014676
93. Frank SJ, Yi W, Zhao Y, Goldsmith JF, Gilliland G, Jiang J, et al. Regions of the JAK2 tyrosine kinase required for coupling to the growth hormone receptor. *J Biol Chem* (1995) 270:14776–85. doi: 10.1074/jbc.270.24.14776
94. Saharinen P, Vihinen M, Silvennoinen O. Autoinhibition of Jak2 tyrosine kinase is dependent on specific regions in its pseudokinase domain. *Mol Biol Cell* (2003) 14:1448–59. doi: 10.1091/mbc.e02-06-0342
95. Lacronique V, Boureux A, Valle VD, Poirel H, Quang CT, Mauchauffe M, et al. A TEL-JAK2 fusion protein with constitutive kinase activity in human leukemia. *Science* (1997) 278:1309–12. doi: 10.1126/science.278.5341.1309
96. Kralovics R, Passamonti F, Buser AS, Teo SS, Tiedt R, Passweg JR, et al. A gain-of-function mutation of JAK2 in myeloproliferative disorders. *N Engl J Med* (2005) 352:1779–90. doi: 10.1056/NEJMoa051113
97. Lee TS, Ma W, Zhang X, Giles F, Kantarjian H, Albitar M. Mechanisms of constitutive activation of Janus kinase 2-V617F revealed at the atomic level through molecular dynamics simulations. *Cancer* (2009) 115:1692–700. doi: 10.1002/cncr.24183
98. Zhao L, Dong H, Zhang CC, Kinch L, Osawa M, Iacovino M, et al. A JAK2 interdomain linker relays Epo receptor engagement signals to kinase activation. *J Biol Chem* (2009) 284:26988–98. doi: 10.1074/jbc.M109.011387
99. Feng J, Witthuhn BA, Matsuda T, Kohlhuber F, Kerr IM, Ihle JN. Activation of Jak2 catalytic activity requires phosphorylation of Y1007 in the kinase activation loop. *Mol Cell Biol* (1997) 17:2497–501. doi: 10.1128/MCB.17.5.2497
100. Funakoshi-Tago M, Pelletier S, Matsuda T, Parganas E, Ihle JN. Receptor specific downregulation of cytokine signaling by autophosphorylation in the FERM domain of Jak2. *EMBO J* (2006) 25:4763–72. doi: 10.1038/sj.emboj.7601365
101. Kurzer JH, Argetsinger LS, Zhou YJ, Kouadio JL, O'Shea JJ, Carter-Su C. Tyrosine 813 Is a Site of JAK2 Autophosphorylation Critical for Activation of JAK2 by SH2-Bbeta Influence of growth hormone on the mandibular condylar cartilage of rats. *Mol Cell Biol* (2004) 24:4557–70. doi: 10.1128/MCB.24.10.4557-4570.2004
102. Argetsinger LS, Kouadio JL, Steen H, Stensballe A, Jensen ON, Carter-Su C. Autophosphorylation of JAK2 on Tyrosines 221 and 570 Regulates Its Activity. *Mol Cell Biol* (2004) 24:4955–67. doi: 10.1128/MCB.24.11.4955-4967.2004
103. Nespital T, Strous GJ. The Jak/STAT signaling pathway is downregulated at febrile temperatures. *PloS One* (2012) 7:e49374. doi: 10.1371/journal.pone.0049374
104. Ungureanu D, Saharinen P, Junttila I, Hilton DJ, Silvennoinen O. Regulation of Jak2 through the Ubiquitin-Proteasome Pathway Involves Phosphorylation of Jak2 on Y1007 and Interaction with SOCS-1. *Mol Cell Biol* (2002) 22:3316–26.doi: 10.1128/MCB.22.10.3316-3326.2002
105. Zhu T, Ling L, Lobie PE. Identification of a JAK2 independent pathway regulating growth hormone (GH) stimulated p44/42 MAP kinase activity: GH activation of RAL and phospholipase D is Src dependent. *J Biol Chem* (2002) 277:45592–603. doi: 10.1074/jbc.M201385200
106. Barclay JL, Kerr LM, Arthur L, Rowland JE, Nelson CN, Ishikawa M, et al. In vivo targeting of the growth hormone receptor (GHR) Box1 sequence demonstrates that the GHR does not signal exclusively through JAK2. *Mol Endocrinol* (2010) 24:204–17. doi: 10.1210/me.2009-0233
107. Ishikawa M, Brooks AJ, Fernandez-Rojo MA, Medina J, Chhabra Y, Minami S, et al. Growth hormone stops excessive inflammation after partial hepatectomy allowing liver regeneration and survival via induction of H2-Bl/HLA-G. *Hepatology* (2020) 258:119–133. doi: 10.1002/hep.31297
108. Jin H, Lanning NJ, Carter-Su C. JAK2, but Not Src Family Kinases, is Required for STAT, ERK and Akt Signaling in Response to Growth Hormone in Preadipocytes and Hepatoma Cells. *Mol Endocrinol* (2008) 22:1825–41. doi: 10.1210/me.2008-0015
109. Ben-Avraham D, Govindaraju DR, Budagov T, Fradin D, Durda P, Liu B. et al: The GH receptor exon 3 deletion is a marker of male-specific exceptional longevity associated with increased GH sensitivity and taller stature. *Sci Adv* (2017) 3:e1602025. doi: 10.1126/sciadv.1602025

110. Ihle JN. The Stat family in cytokine signaling. *Curr Opin Cell Biol* (2001) 13:211–7. doi: 10.1016/S0955-0674(00)00199-X
111. Chatterjee-Kishore M, van den Akker F, Stark GR. Association of STATs with relatives and friends. *Trends Cell Biol* (2000) 10:106–11. doi: 10.1016/S0962-8924(99)01709-2
112. Herrington J, Smit LS, Schwartz J, CarterSu C. The role of STAT proteins in growth hormone signaling. *Oncogene* (2000) 19:2585–97. doi: 10.1038/sj.onc.1203526
113. Waxman DJ, O'Connor C. Growth Hormone Regulation of Sex-dependent Liver Gene Expression*. *Mol Endocrinol* (2006) 20:2613–29. doi: 10.1210/me.2006-0007
114. Lau-Corona D, Bae WK, Hennighausen L, Waxman DJ. Sex-biased genetic programs in liver metabolism and liver fibrosis are controlled by EZH1 and EZH2. *PloS Genet* (2020) 16:e1008796. doi: 10.1371/journal.pgen.1008796
115. Woelfle J, Chia DJ, Rotwein P. Mechanisms of growth hormone action: identification of conserved Stat5 binding sites that mediate GH-induced insulin-like growth factor-I gene activation. *J Biol Chem* (2003) 278:51261–6. doi: 10.1074/jbc.M309486200
116. Rotwein P. Regulation of gene expression by growth hormone. *Mol Cell Endocrinol* (2020), 57:110788. doi: 10.1016/j.mce.2020.110788
117. Rosenfeld RG, Kofoed E, Buckway C, Little B, Woods KA, Tsubaki J, et al. Identification of the first patient with a confirmed mutation of the JAK-STAT system. *Pediatr Nephrol* (2005) 20:303–5. doi: 10.1007/s00467-004-1678-7
118. Klammt J, Neumann D, Gevers EF, Andrew SF, Schwartz ID, Rockstroh D, et al. Dominant-negative STAT5B mutations cause growth hormone insensitivity with short stature and mild immune dysregulation. *Nat Commun* (2018) 9:2105. doi: 10.1038/s41467-018-04521-0
119. Yi WS, Kim SO, Jiang J, Park SH, Kraft AS, Waxman DJ, et al. Growth hormone receptor cytoplasmic domain differentially promotes tyrosine phosphorylation of signal transducers and activators of transcription 5b and 3 by activated JAK2 kinase. *MolEndocrinol* (1996) 10:1425–43. doi: 10.1210/me.10.11.1425
120. Hansen LH, Wang X, Kopchick JJ, Bouchelouche P, Nielsen JH, Galsgaard ED, et al. Identification of tyrosine residues in the intracellular domain of the growth hormone receptor required for transcriptional signaling and Stat5 activation. *J Biol Chem* (1996) 271:12669–73. doi: 10.1074/jbc.271.21.12669
121. Smit LS, Meyer DJ, Billestrup N, Norstedt G, Schwartz J, Carter-Su C. The role of the growth hormone (GH) receptor and Jak1 and Jak2 kinases in the activation of stats 1,3, and 5 by GH. *Mol Endocrinol* (1996) 10:519–33. doi: 10.1210/mend.10.5.8732683
122. Thirone ACP, Carvalho CRO, Saad MJA. Growth hormone stimulates the tyrosine kinase activity of JAK2 and induces tyrosine phosphorylation of insulin receptor substrates and Shc in rat tissues. *Endocrinology* (1999) 140:55–62. doi: 10.1210/endo.140.1.6417
123. Vanderkuur JA, Butch ER, Waters SB, Pessin JE, Guan KL, Carter-Su C. Signaling molecules involved in coupling growth hormone receptor to mitogen-activated protein kinase activation. *Endocrinology* (1997) 138:4301–7. doi: 10.1210/endo.138.10.5453
124. Frank SJ. Growth hormone signalling and its regulation: Preventing too much of a good thing. *Growth Horm IGF Res* (2001) 11:201–12. doi: 10.1054/ghir.2001.0237
125. Decker T, Kovarik P. Serine phosphorylation of STATs. *Oncogene* (2000) 19:2628–37. doi: 10.1038/sj.onc.1203481
126. Pircher TJ, Petersen H, Gustafsson JA, Haldosen LA. Extracellular signal-regulated kinase (ERK) interacts with signal transducer and activator of transcription (STAT) 5a. *Mol Endocrinol* (1999) 13:555–65. doi: 10.1210/mend.13.4.0263
127. Yamauchi T, Ueki K, Tobe K, Tamemoto H, Sekine N, Wada M, et al. Tyrosine phosphorylation of the EGF receptor by the kinase Jak2 is induced by growth hormone. *Nature* (1997) 390:91–6. doi: 10.1038/36369
128. Kim SO, Houtman JCD, Jiang J, Ruppert JI, Bertics PJ, Frank SJ. Growth hormone-induced alteration in ErbB-2 phosphorylation status in 3T3-F442A fibroblasts. *J Biol Chem* (1999) 274:36015–24. doi: 10.1074/jbc.274.50.36015
129. Zhu T, Lobie PE. Janus kinase 2-dependent activation of p38 mitogen-activated protein kinase by growth hormone. Resultant transcriptional activation of ATF-2 and CHOP, cytoskeletal re-organization and mitogenesis. *J Biol Chem* (2000) 275:2103–14. doi: 10.1074/jbc.275.3.2103
130. Zhu T, Goh ELK, Leroith D, Lobie PE. Growth hormone stimulates the formation of a multiprotein signaling complex involving p130(Cas) and CrkII - Resultant activation of c-Jun N-terminal kinase/stress-activatedprotein kinase (JNK/SAPK). *J Biol Chem* (1998) 273:33864–75. doi: 10.1074/jbc.273.50.33864
131. Yamauchi T, Kaburagi Y, Ueki K, Tsuji Y, Stark GR, Kerr IM, et al. Growth hormone and prolactin stimulate tyrosine phosphorylation of insulin receptor substrate-1, -2, and -3, their association with p85 phosphatidylinositol 3-kinase (PI3-kinase), and concomitantly PI3-kinase activation via JAK2 kinase. *J Biol Chem* (1998) 273:15719–26. doi: 10.1074/jbc.273.25.15719
132. Yokota I, Hayashi H, Matsuda J, Saijo T, Naito E, Ito M, et al. Effect of growth hormone on the translocation of GLUT4 and its relation to insulin-like and anti-insulin action. *Biochim Biophys Acta - Mol Cell Res* (1998) 1404:451–6. doi: 10.1016/S0167-4889(98)00077-9
133. Ridderstrale M, Tornqvist H. PI-3-kinase inhibitor Wortmannin blocks the insulin-like effects of growth hormone in isolated rat adipocytes. *Biochem Biophys Res Commun* (1994) 203:306–10. doi: 10.1006/bbrc.1994.2182
134. Ridderstrale M. Signaling mechanism for the insulin-like effects of growth hormone–another example of a classical hormonal negative feedback loop. *Curr Drug Targets Immune Endocr Metabol Disord* (2005) 5:79–92. doi: 10.2174/1568008053174787
135. Costoya JA, Finidori J, Moutoussamy S, Searis R, Devesa J, Arce VM. Activation of growth hormone receptor delivers an antiapoptotic signal: evidence for a role of Akt in this pathway. *Endocrinology* (1999) 140:5937–43. doi: 10.1210/endo.140.12.7209
136. MacKenzie SJ, Yarwood SJ, Peden AH, Bolger GB, Vernon RG, Houslay MD. Stimulation of p70S6 kinase via a growth hormone-controlled phosphatidylinositol 3-kinase pathway leads to the activation of a PDE4A cyclic AMP-specific phosphodiesterase in 3T3-F442A preadipocytes. *Proc Nat Acad Sci USA* (1998) 95:3549–54. doi: 10.1073/pnas.95.7.3549
137. Jeay S, Sonenshein GE, Postel-Vinay MC, Kelly PA, Baixeras E. Growth hormone can act as a cytokine controlling survival and proliferation of immune cells: new insights into signaling pathways. *Mol Cell Endocrinol* (2002) 188:1–7. doi: 10.1016/S0303-7207(02)00014-X
138. Flores-Morales A, Greenhalgh CJ, Norstedt G, Rico-Bautista E. Negative Regulation of Growth Hormone Receptor Signaling. *Mol Endocrinol* (2006) 20:241–53. doi: 10.1210/me.2005-0170
139. Hackett RH, Wang YD, Sweitzer S, Feldman G, Wood WI, Larner AC. Mapping of a cytoplasmic domain of the human growth hormone receptor that regulates rates of inactivation of jak2 and stat proteins. *J Biol Chem* (1997) 272:11128–32. doi: 10.1074/jbc.272.17.11128
140. Kim SO, Jiang J, Yi W, Feng GS, Frank SJ. Involvement of the Src homology 2-containing tyrosine phosphatase SHP-2 in growth hormone signaling. *J Biol Chem* (1998) 273:2344–54. doi: 10.1074/jbc.273.4.2344
141. Stofega MR, Herrington J, Billestrup N, Carter-Su C. Mutation of the SHP-2 binding site in growth hormone (GH) receptor prolongs GH-promoted tyrosyl phosphorylation of GH receptor, JAK2, and STAT5B. *Mol Endocrinol* (2000) 14:1338–50. doi: 10.1210/mend.14.9.0513
142. Stofega MR, Argetsinger LS, Wang H, Ullrich A, Carter-Su C. Negative regulation of growth hormone receptor/JAK2 signaling by signal regulatory protein alpha. *J Biol Chem* (2000) 275:28222–9. doi: 10.1074/jbc.M004238200
143. Pasquali C, Curchod ML, Walchli S, Espanel X, Guerrier M, Arigoni F, et al. Identification of Protein Tyrosine Phosphatases with specificity for the ligand-activated GH Receptor. *Mol Endocrinol* (2003) 17:2228–39. doi: 10.1210/me.2003-0011
144. Gu F, Dube N, Kim JW, Cheng A, Ibarra-Sanchez Md Mde J, Tremblay ML, et al. Protein Tyrosine Phosphatase 1B Attenuates Growth Hormone-Mediated JAK2-STAT Signaling. *Mol Cell Biol* (2003) 23:3753–62. doi: 10.1128/MCB.23.11.3753-3762.2003
145. Pilecka I, Whatmore A, Hooft van Huijsduijnen R, Destenaves B, Clayton P. Growth hormone signalling: sprouting links between pathways, human genetics and therapeutic options. *Trends Endocrinol Metab* (2007) 18:12–8. doi: 10.1016/j.tem.2006.11.004
146. Irie-Sasaki J, Sasaki T, Matsumoto W, Opavsky A, Cheng M, Welstead G, et al. CD45 is a JAK phosphatase and negatively regulates cytokine receptor signalling. *Nature* (2001) 409:349–54. doi: 10.1038/35053086

147. Rakesh K, Agrawal DK. Controlling cytokine signaling by constitutive inhibitors. *Biochem Pharmacol* (2005) 70:649–57. doi: 10.1016/j.bcp.2005.04.042
148. Moutoussamy S, Renaudie F, Lago F, Kelly PA, Finidori J. Grb10 identified as a potential regulator of growth hormone (GH) signaling by cloning of GH receptor target proteins. *J Biol Chem* (1998) 273:15906–12. doi: 10.1074/jbc.273.26.15906
149. Rui L, Carter-Su C. Identification of SH2-bbeta as a potent cytoplasmic activator of the tyrosine kinase Janus kinase 2. *Proc Natl Acad Sci U.S.A.* (1999) 96:7172–7. doi: 10.1073/pnas.96.13.7172
150. Birzniece V, Sata A, Ho KK. Growth hormone receptor modulators. *Rev Endocr Metab Disord* (2009) 10:145–56. doi: 10.1007/s11154-008-9089-x
151. von Laue S, Ross RJ. Inflammatory cytokines and acquired growth hormone resistance. *Growth Horm IGF Res* (2000) 10 Suppl B:S9–14. doi: 10.1016/S1096-6374(00)80003-9
152. Zhang Y, Guan R, Jiang J, Kopchick JJ, Black RA, Baumann G. et al: Growth hormone (GH)-induced dimerization inhibits phorbol ester-stimulated GH receptor proteolysis. *J Biol Chem* (2001) 276:24565–73. doi: 10.1074/jbc.M101281200
153. Loesch K, Deng L, Cowan JW, Wang X, He K, Jiang J. et al: Janus Kinase 2 Influences Growth Hormone Receptor Metalloproteolysis. *Endocrinology* (2006) 147:2839–49. doi: 10.1210/en.2005-1484
154. Sawyer ST, Hankins WD. The functional form of the erythropoietin receptor is a 78-kDa protein: correlation with cell surface expression, endocytosis, and phosphorylation. *Proc Natl Acad Sci U.S.A.* (1993) 90:6849–53. doi: 10.1073/pnas.90.14.6849
155. Genty N, Paly J, Edery M, Kelly PA, Djiane J, Salesse R. Endocytosis and degradation of prolactin and its receptor in Chinese hamster ovary cells stably transfected with prolactin receptor cDNA. *Mol Cell Endocrinol* (1994) 99:221–8. doi: 10.1016/0303-7207(94)90011-6
156. Hurley JH, Stenmark H. Molecular Mechanisms of Ubiquitin-Dependent Membrane Traffic. *Annu Rev Biophys* (2011) 40:119–42. doi: 10.1146/annurev-biophys-042910-155404
157. Kölling R, Hollenberg CP. The ABC-transpporter Ste6 accumulates in the plasma membrane in a ubiquitinated form in endocytosis mutants. *EMBO J* (1994) 13:3261–71. doi: 10.1002/j.1460-2075.1994.tb06627.x
158. Critchley WR, Pellet-Many C, Ringham-Terry B, Harrison MA, Zachary IC, Ponnambalam S. Receptor Tyrosine Kinase Ubiquitination and De-Ubiquitination in Signal Transduction and Receptor Trafficking. *Cells* (2018) 7(3):22. doi: 10.3390/cells7030022
159. Clague MJ, Urbe S. Endocytosis: the DUB version. *Trends Cell Biol* (2006) 16:551–9. doi: 10.1016/j.tcb.2006.09.002
160. Lauwers E, Jacob C, Andre B. K63-linked ubiquitin chains as a specific signal for protein sorting into the multivesicular body pathway. *J Cell Biol* (2009) 185:493–502. doi: 10.1083/jcb.200810114
161. Duncan LM, Piper S, Dodd RB, Saville MK, Sanderson CM, Luzio JP, et al. Lysine-63-linked ubiquitination is required for endolysosomal degradation of class I molecules. *EMBO J* (2006) 25:1635–45. doi: 10.1038/sj.emboj.7601056
162. Geetha T, Wooten MW. TrkA Receptor Endolysosomal Degradation is both Ubiquitin and Proteasome Dependent. *Traffic* (2008) 9:1146–56. doi: 10.1111/j.1600-0854.2008.00751.x
163. Dikic I. Proteasomal and Autophagic Degradation Systems. *Annu Rev Biochem* (2017) 86:193–224. doi: 10.1146/annurev-biochem-061516-044908
164. Ren X, Hurley JH. VHS domains of ESCRT-0 cooperate in high-avidity binding to polyubiquitinated cargo. *EMBO J* (2010) 29:1045–54. doi: 10.1038/emboj.2010.6
165. Erpapazoglou Z, Walker O, Haguenauer-Tsapis R. Versatile roles of k63-linked ubiquitin chains in trafficking. *Cells* (2014) 3:1027–88. doi: 10.3390/cells3041027
166. Sachse M, Strous GJ, Klumperman J. ATPase-deficient hVPS4 impairs formation of internal endosomal vesicles and stabilizes bilayered clathrin coats on endosomal vacuoles. *J Cell Sci* (2004) 117:1699–708. doi: 10.1242/jcs.00998
167. Wright MH, Berlin I, Nash PD. Regulation of endocytic sorting by ESCRT-DUB-mediated deubiquitination. *Cell Biochem Biophys* (2011) 60:39–46. doi: 10.1007/s12013-011-9181-9
168. Hassink G, Slotman J, Oorschot V, Van Der Reijden BA, Monteferrario D, Noordermeer SM. et al: Identification of the ubiquitin ligase Triad1 as a regulator of endosomal transport. *Biol Open* (2012) 1:607–14. doi: 10.1242/bio.2012778
169. Govers R, ten Broeke T, van Kerkhof P, Schwartz AL, Strous GJ. Identification of a novel ubiquitin conjugation motif, required for ligand-induced internalization of the growth hormone receptor. *EMBO J* (1999) 18:28–36. doi: 10.1093/emboj/18.1.28
170. Govers R, van Kerkhof P, Schwartz AL, Strous GJ. Di-leucine-mediated internalization of ligand by a truncated growth hormone receptor is independent of the ubiquitin conjugation system. *J Biol Chem* (1998) 273:16426–33. doi: 10.1074/jbc.273.26.16426
171. van Kerkhof P, Putters J, Strous GJ. The ubiquitin ligase SCF(betaTrCP) regulates the degradation of the growth hormone receptor. *J Biol Chem* (2007) 282:20475–83. doi: 10.1074/jbc.M702610200
172. van Kerkhof P, Westgeest M, Hassink G, Strous GJ. SCF(TrCP) acts in endosomal sorting of the GH receptor. *Exp Cell Res* (2011) 317:1071–82. doi: 10.1016/j.yexcr.2010.12.020
173. Lv K, Jiang J, Donaghy R, Riling CR, Cheng Y, Chandra V, et al. CBL family E3 ubiquitin ligases control JAK2 ubiquitination and stability in hematopoietic stem cells and myeloid malignancies. *Genes Dev* (2017) 31:1007–23.31:1007-1023. doi: 10.1101/gad.297135.117
174. Frescas D, Pagano M. Deregulated proteolysis by the F-box proteins SKP2 and beta-TrCP: tipping the scales of cancer. *Nat Rev Cancer* (2008) 8:438–49. doi: 10.1038/nrc2396
175. Li Y, Suresh Kumar KG, Tang W, Spiegelman VS, Fuchs SY. Negative Regulation of Prolactin Receptor Stability and Signaling Mediated by SCF {beta}-TrCP E3 Ubiquitin Ligase. *Mol Cell Biol* (2004) 24:4038–48. doi: 10.1128/MCB.24.9.4038-4048.2004
176. Kumar KG, Tang W, Ravindranath AK, Clark WA, Croze E, Fuchs SY. SCF (HOS) ubiquitin ligase mediates the ligand-induced down-regulation of the interferon-alpha receptor. *EMBO J* (2003) 22:5480–90. doi: 10.1093/emboj/cdg524
177. Meyer L, Deau B, Forejtnikova H, Dumenil D, Margottin-Goguet F, Lacombe C, et al. Beta-Trcp mediates ubiquitination and degradation of the erythropoietin receptor and controls cell proliferation. *Blood* (2007) 109:5215–22. doi: 10.1182/blood-2006-10-055350
178. da Silva Almeida AC, Hocking HG, Boelens R, Strous GJ, van Rossum AG. betaTrCP interacts with the ubiquitin-dependent endocytosis motif of the GH receptor in an unconventional manner. *Biochem J* (2013) 453:291–301. doi: 10.1042/BJ20121843
179. da Silva Almeida AC. *Understanding the Growth Hormone Receptor-βTrCP interactions: Molecular Tools for controlling Growth Hormone Sensitivity. Chapter IV, Growth hormone receptor endocytosis and degradation are regulated by phosphorylation of serine 323 in the ubiquitin-dependent endocytosis moti£*. Utrecht: Thesis, Utrecht University (2011). Available at: http://dspace.library.uu.nl/handle/1874/350510.
180. Pinna LA. Casein kinase 2: an 'eminence grise' in cellular regulation? *Biochim Biophys Acta* (1990) 1054, 267–84. doi: 10.1016/0167-4889(90)90098-X
181. Bian Y, Song C, Cheng K, Dong M, Wang F, Huang J, et al. An enzyme assisted RP-RPLC approach for in-depth analysis of human liver phosphoproteome. *J Proteomics* (2014) 96:253–62. doi: 10.1016/j.jprot.2013.11.014
182. Szyszka R, Grankowski N, Felczak K, Shugar D. Halogenated benzimidazoles and benzotriazoles as selective inhibitors of protein kinases CK I and CK II from Saccharomyces cerevisiae and other sources. *Biochem Biophys Res Commun* (1995) 208:418–24.Biochem Biophys Res Commun 1995, 208:418-424. doi: 10.1006/bbrc.1995.1354
183. Litchfield DW. Protein kinase CK2: structure, regulation and role in cellular decisions of life and death. *Biochem J* (2003) 369:1–15. doi: 10.1042/bj20021469
184. Montenarh M. Cellular regulators of protein kinase CK2. *Cell Tissue Res* (2010) 342:139–46. doi: 10.1007/s00441-010-1068-3
185. Sommercorn J, Mulligan JA, Lozeman FJ, Krebs EG. Activation of casein kinase II in response to insulin and to epidermal growth factor. *Proc Natl Acad Sci U S A* (1987) 84:8834–8. doi: 10.1073/pnas.84.24.8834

186. Klarlund JK, Czech MP. Insulin-like growth factor I and insulin rapidly increase casein kinase II activity in BALB/c 3T3 fibroblasts. *J Biol Chem* (1988) 263:15872–5.
187. Van Lint J, Agostinis P, Vandevoorde V, Haegeman G, Fiers W, Merlevede W, et al. Tumor necrosis factor stimulates multiple serine/threonine protein kinases in Swiss 3T3 and L929 cells. Implication of casein kinase-2 and extracellular signal-regulated kinases in the tumor necrosis factor signal transduction pathway. *J Biol Chem* (1992) 267:25916–21.
188. Kim S, Ham S, Yang K, Kim K. Protein kinase CK2 activation is required for transforming growth factor beta-induced epithelial-mesenchymal transition. *Mol Oncol* (2018) 12:1811–26. doi: 10.1002/1878-0261.12378
189. Ji H, Wang J, Nika H, Hawke D, Keezer S, Ge Q, et al. EGF-induced ERK activation promotes CK2-mediated disassociation of alpha-Catenin from beta-Catenin and transactivation of beta-Catenin. *Mol Cell* (2009) 36:547–59. doi: 10.1016/j.molcel.2009.09.034
190. Starr R, Willson TA, Viney EM, Murray LJ, Rayner JR, Jenkins BJ, et al. A family of cytokine-inducible inhibitors of signalling. *Nature* (1997) 387:917–21. doi: 10.1038/43206
191. Kile BT, Schulman BA, Alexander WS, Nicola NA, Martin HM, Hilton DJ. The SOCS box: a tale of destruction and degradation. *Trends Biochem Sci* (2002) 27:235–41. doi: 10.1016/S0968-0004(02)02085-6
192. Yasukawa H, Misawa H, Sakamoto H, Masuhara M, Sasaki A, Wakioka T, et al. The JAK-binding protein JAB inhibits Janus tyrosine kinase activity through binding in the activation loop. *EMBO J* (1999) 18:1309–20. doi: 10.1093/emboj/18.5.1309
193. Sasaki A, Yasukawa H, Suzuki A, Kamizono S, Syoda T, Kinjyo I, et al. Cytokine-inducible SH2 protein-3 (CIS3/SOCS3) inhibits Janus tyrosine kinase by binding through the N-terminal kinase inhibitory region as well as SH2 domain. *Genes Cells* (1999) 4:339–51. doi: 10.1046/j.1365-2443.1999.00263.x
194. Ram PA, Waxman DJ. SOCS/CIS protein inhibition of growth hormone-stimulated STAT5 signaling by multiple mechanisms. *J Biol Chem* (1999) 274:35553–61. doi: 10.1074/jbc.274.50.35553
195. Landsman T, Waxman DJ. Role of the Cytokine-induced SH2 Domain-containing Protein CIS in Growth Hormone Receptor Internalization. *J Biol Chem* (2005) 280:37471–80. doi: 10.1074/jbc.M504125200
196. Leung KC, Doyle N, Ballesteros M, Sjogren K, Watts CK, Low TH, et al. Estrogen inhibits GH signaling by suppressing GH-induced JAK2 phosphorylation, an effect mediated by SOCS-2. *Proc Natl Acad Sci U.S.A.* (2003) 100:1016–21. doi: 10.1073/pnas.0337600100
197. Yumet G, Shumate ML, Bryant DP, Lang CH, Cooney RN. Hepatic growth hormone resistance during sepsis is associated with increased suppressors of cytokine signaling expression and impaired growth hormone signaling. *Crit Care Med* (2006) 34:1420–7. doi: 10.1097/01.CCM.0000215113.66070.E0
198. Alexander WS, Starr R, Fenner JE, Scott GL, Handman E, Sprigg NS, et al. SOCS1 is a critical inhibitor of interferon gamma signaling and prevents the potentially fatal neonatal actions of this cytokine. *Cell* (1999) 98:597–608. doi: 10.1016/S0092-8674(00)80047-1
199. Croker BA, Krebs DL, Zhang JG, Wormald S, Willson TA, Stanley EG, et al. SOCS3 negatively regulates IL-6 signaling in vivo. *Nat Immunol* (2003) 4:540–5. doi: 10.1038/ni931
200. Starr R, Metcalf D, Elefanty AG, Brysha M, Willson TA, Nicola NA, et al. Liver degeneration and lymphoid deficiencies in mice lacking suppressor of cytokine signaling-1. *Proc Natl Acad Sci U.S.A.* (1998) 95:14395–9. doi: 10.1073/pnas.95.24.14395
201. Metcalf D, Greenhalgh CJ, Viney E, Willson TA, Starr R, Nicola NA, et al. Gigantism in mice lacking suppressor of cytokine signalling-2. *Nature* (2000) 405:1069–73. doi: 10.1038/35016611
202. Greenhalgh CJ, Rico-Bautista E, Lorentzon M, Thaus AL, Morgan PO, Willson TA, et al. SOCS2 negatively regulates growth hormone action in vitro and in vivo. *J Clin Invest* (2005) 115:397–406. doi: 10.1172/JCI22710
203. Kung WW, Ramachandran S, Makukhin N, Bruno E, Ciulli A. Structural insights into substrate recognition by the SOCS2 E3 ubiquitin ligase. *Nat Commun* (2019) 10:2534. doi: 10.1038/s41467-019-10190-4
204. Rudd MF, Webb EL, Matakidou A, Sellick GS, Williams RD, Bridle H, et al. Variants in the GH-IGF axis confer susceptibility to lung cancer. *Genome Res* (2006) 16:693–701. doi: 10.1101/gr.5120106
205. Cao G, Lu H, Feng J, Shu J, Zheng D, Hou Y. Lung cancer risk associated with Thr495Pro polymorphism of GHR in Chinese population. *Jpn J Clin Oncol* (2008) 38:308–16. doi: 10.1093/jjco/hyn007
206. Vincent EE, Elder DJ, Thomas EC, Phillips L, Morgan C, Pawade J, et al. Akt phosphorylation on Thr308 but not on Ser473 correlates with Akt protein kinase activity in human non-small cell lung cancer. *Br J Cancer* (2011) 104:1755–61. doi: 10.1038/bjc.2011.132
207. Yu Y, Zhao Q, Wang Z, Liu XY. Activated STAT3 correlates with prognosis of non-small cell lung cancer and indicates new anticancer strategies. *Cancer Chemother Pharmacol* (2015) 75:917–22. doi: 10.1007/s00280-015-2710-2
208. Kamsteeg EJ, Hendriks G, Boone M, Konings IB, Oorschot V, van der Sluijs P, et al. Short-chain ubiquitination mediates the regulated endocytosis of the aquaporin-2 water channel. *Proc Natl Acad Sci U S A* (2006) 103:18344–9. doi: 10.1073/pnas.0604073103
209. Slotman JA, da Silva Almeida AC, Hassink GC, van de Ven RH, van Kerkhof P, Kuiken HJ, et al. Ubc13 and COOH terminus of Hsp70-interacting protein (CHIP) are required for growth hormone receptor endocytosis. *J Biol Chem* (2012) 287:15533–43. doi: 10.1074/jbc.M111.302521
210. Balaji V, Pokrzywa W, Hoppe T. Ubiquitylation Pathways In Insulin Signaling and Organismal Homeostasis. *Bioessays* (2018) 40:e1700223. doi: 10.1002/bies.201700223
211. Tawo R, Pokrzywa W, Kevei E, Akyuz ME, Balaji V, Adrian S, et al. The Ubiquitin Ligase CHIP Integrates Proteostasis and Aging by Regulation of Insulin Receptor Turnover. *Cell* (2017) 169:470–482 e413. doi: 10.1016/j.cell.2017.04.003
212. Sun C, Li HL, Shi ML, Liu QH, Bai J, Zheng JN. Diverse roles of C-terminal Hsp70-interacting protein (CHIP) in tumorigenesis. *J Cancer Res Clin Oncol* (2014) 140:189–97. doi: 10.1007/s00432-013-1571-5
213. Manning BD, Toker A. AKT/PKB Signaling: Navigating the Network. *Cell* (2017) 169:381–405. doi: 10.1016/j.cell.2017.04.001
214. Su CH, Wang CY, Lan KH, Li CP, Chao Y, Lin HC, et al. Akt phosphorylation at Thr308 and Ser473 is required for CHIP-mediated ubiquitination of the kinase. *Cell Signal* (2011) 23:1824–30. doi: 10.1016/j.cellsig.2011.06.018
215. Dickey CA, Koren J, Zhang YJ, Xu YF, Jinwal UK, Birnbaum MJ, et al. Akt and CHIP coregulate tau degradation through coordinated interactions. *Proc Natl Acad Sci U.S.A.* (2008) 105:3622–7. doi: 10.1073/pnas.0709180105
216. Cao Z, Li G, Shao Q, Yang G, Zheng L, Zhang T, et al. CHIP: A new modulator of human malignant disorders. *Oncotarget* (2016) 7:29864–74. doi: 10.18632/oncotarget.8219
217. Kajiro M, Hirota R, Nakajima Y, Kawanowa K, So-ma K, Ito I, et al. The ubiquitin ligase CHIP acts as an upstream regulator of oncogenic pathways. *Nat Cell Biol* (2009) 11:312–9. doi: 10.1038/ncb1839
218. Wang T, Wang W, Wang Q, Xie R, Landay A, Chen D. The E3 ubiquitin ligase CHIP in normal cell function and in disease conditions. *Ann N Y Acad Sci* (2020) 1460:3–10. doi: 10.1111/nyas.14206
219. Chung C, Yoo G, Kim T, Lee D, Lee CS, Cha HR, et al. The E3 ubiquitin ligase CHIP selectively regulates mutant epidermal growth factor receptor by ubiquitination and degradation. *Biochem Biophys Res Commun* (2016) 479:152–8. doi: 10.1016/j.bbrc.2016.07.111
220. D'Ercole AJ, Applewhite GT, Underwood LE. Evidence that somatomedin is synthesized by multiple tissues in the fetus. *Dev Biol* (1980) 75:315–28. doi: 10.1016/0012-1606(80)90166-9
221. Le Roith D, Bondy C, Yakar S, Liu JL, Butler A. The somatomedin hypothesis: 2001. *Endocr Rev* (2001) 22:53–74. doi: 10.1210/edrv.22.1.0419
222. Green H, Morikawa M, Nixon T. A dual effector theory of growth-hormone action. *Differentiation* (1985) 29:195–8. doi: 10.1111/j.1432-0436.1985.tb00316.x
223. Laron Z, Pertzelan A, Mannheimer S. Genetic pituitary dwarfism with high serum concentation of growth hormone–a new inborn error of metabolism? *Isr J Med Sci* (1966) 2:152–5.
224. Laron Z. Growth Hormone Insensitivity (Laron Syndrome). *Rev Endocr Metab Disord* (2002) 3:347–55. doi: 10.1023/A:1020905725012
225. Laron Z. Lessons from 50 Years of Study of Laron Syndrome. *Endocr Pract 2* (015) 21:1395–402. doi: 10.4158/EP15939.RA
226. Salvatori R, Fan X, Phillips JA,3, Espigares-Martin R, Martin De Lara I, Freeman KL, et al. Three new mutations in the gene for the growth hormone (gh)-releasing hormone receptor in familial isolated gh deficiency type ib. *J Clin Endocrinol Metab* (2001) 86:273–9. doi: 10.1210/jc.86.1.273

227. Aguiar-Oliveira MH, Bartke A. Growth Hormone Deficiency: Health and Longevity. *Endocr Rev* (2019) 40:575–601. doi: 10.1210/er.2018-00216
228. Rowland JE, Lichanska AM, Kerr LM, White M, d'Aniello EM, Maher SL. et al: In vivo analysis of growth hormone receptor signaling domains and their associated transcripts. *Mol Cell Biol* (2005) 25:66–77. doi: 10.1128/MCB.25.1.66-77.2005
229. Reddy R, Hope S, Wass J. Acromegaly. *BMJ* (2010) 341:c4189. doi: 10.1136/bmj.c4189
230. Fineberg SE, Merimee TJ. Acute metabolic effects of human growth hormone. *Diabetes* (1974) 23:499–504. doi: 10.2337/diab.23.6.499
231. Rabinowitz D, Klassen GA, Zierler KL. Effect of Human Growth Hormone on Muscle and Adipose Tissue Metabolism in the Forearm of Man. *J Clin Invest* (1965) 44:51–61. doi: 10.1172/JCI105126
232. Zierler KL, Rabinowitz D. Roles of Insulin and Growth Hormone, Based on Studies of Forearm Metabolism in Man. *Med (Baltimore)* (1963) 42:385–402. doi: 10.1097/00005792-196311000-00002
233. Sonksen PH, Greenwood FC, Ellis JP, Lowy C, Rutherford A, Nabarro JD. Changes of carbohydrate tolerance in acromegaly with progress of the disease and in response to treatment. *J Clin Endocrinol Metab* (1967) 27:1418–30. doi: 10.1210/jcem-27-10-1418
234. Wurzburger MI, Prelevic GM, Sonksen PH, Balint-Peric LA, Wheeler M. The effect of recombinant human growth hormone on regulation of growth hormone secretion and blood glucose in insulin-dependent diabetes. *J Clin Endocrinol Metab* (1993) 77:267–72. doi: 10.1210/jcem.77.1.8325951
235. Clemmons DR, Underwood LE. Nutritional regulation of IGF-I and IGF binding proteins. *Annu Rev Nutr* (1991) 11:393–412. doi: 10.1146/annurev.nu.11.070191.002141
236. Sotiropoulos A, Ohanna M, Kedzia C, Menon RK, Kopchick JJ, Kelly PA. et al: Growth hormone promotes skeletal muscle cell fusion independent of insulin-like growth factor 1 up-regulation. *PNAS* (2006) 103:7315–20. doi: 10.1073/pnas.0510033103
237. Barton-Davis ER, Shoturma DI, Musaro A, Rosenthal N, Sweeney HL. Viral mediated expression of insulin-like growth factor I blocks the aging-related loss of skeletal muscle function. *Proc Natl Acad Sci U.S.A.* (1998) 95:15603–7. doi: 10.1073/pnas.95.26.15603
238. Moller N, Jorgensen JO. Effects of growth hormone on glucose, lipid, and protein metabolism in human subjects. *Endocr Rev* (2009) 30:152–77. doi: 10.1210/er.2008-0027
239. Gjedsted J, Gormsen LC, Nielsen S, Schmitz O, Djurhuus CB, Keiding S, et al. Effects of a 3-day fast on regional lipid and glucose metabolism in human skeletal muscle and adipose tissue. *Acta Physiol (Oxf)* (2007) 191:205–16. doi: 10.1111/j.1748-1716.2007.01740.x
240. Manson JM, Wilmore DW. Positive nitrogen balance with human growth hormone and hypocaloric intravenous feeding. *Surgery* (1986) 100:188–97.
241. Norrelund H, Moller N, Nair KS, Christiansen JS, Jorgensen JO. Continuation of growth hormone (GH) substitution during fasting in GH-deficient patients decreases urea excretion and conserves protein synthesis. *J Clin Endocrinol Metab* (2001) 86:3120–9. doi: 10.1210/jc.86.7.3120
242. Norrelund H, Nair KS, Jorgensen JO, Christiansen JS, Moller N. The protein-retaining effects of growth hormone during fasting involve inhibition of muscle-protein breakdown. *Diabetes* (2001) 50:96–104. doi: 10.2337/diabetes.50.1.96
243. Veldhuis JD, Iranmanesh A, Ho KK, Waters MJ, Johnson ML, Lizarralde G. Dual defects in pulsatile growth hormone secretion and clearance subserve the hyposomatotropism of obesity in man. *J Clin Endocrinol Metab* (1991) 72:51–9. doi: 10.1210/jcem-72-1-51
244. Felig P, Marliss EB, Cahill GFJr. Metabolic response to human growth hormone during prolonged starvation. *J Clin Invest* (1971) 50:411–21. doi: 10.1172/JCI106508
245. Carter-Su C, King AP, Argetsinger LS, Smit LS, Vanderkuur J, Campbell GS. Signalling pathway of GH. *Endocr J* (1996) 43 Suppl:S65–70. doi: 10.1507/endocrj.43.Suppl_S65
246. Liu H, Bravata DM, Olkin I, Friedlander A, Liu V, Roberts B, et al. Systematic review: the effects of growth hormone on athletic performance. *Ann Intern Med* (2008) 148:747–58. doi: 10.7326/0003-4819-148-10-200805200-00215
247. Gibney J, Healy ML, Sonksen PH. The growth hormone/insulin-like growth factor-I axis in exercise and sport. *Endocr Rev* (2007) 28:603–24. doi: 10.1210/er.2006-0052
248. Birzniece V, Nelson AE, Ho KK. Growth hormone and physical performance. *Trends Endocrinol Metab* (2011) 22:171–8. doi: 10.1016/j.tem.2011.02.005
249. Irwig MS, Fleseriu M, Jonklaas J, Tritos NA, Yuen KCJ, Correa R, et al. Off-Label Use and Misuse of Testosterone, Growth Hormone, Thyroid Hormone, and Adrenal Supplements: Risks and Costs of a Growing Problem. *Endocr Pract* (2020) 26:340–53. doi: 10.4158/PS-2019-0540
250. Colosi P, Wong K, Leong SR, Wood WI. Mutational analysis of the intracellular domain of the human growth hormone receptor. *J Biol Chem* (1993) 268:12617–23.
251. Goh EL, Pircher TJ, Lobie PE. Growth hormone promotion of tubulin polymerization stabilizes the microtubule network and protects against colchicine-induced apoptosis. *Endocrinology* (1998) 139:4364–72. doi: 10.1210/endo.139.10.6237
252. Wiedermann CJ, Reinisch N, Braunsteiner H. Stimulation of monocyte chemotaxis by human growth hormone and its deactivation by somatostatin. *Blood* (1993) 82:954–60. doi: 10.1182/blood.V82.3.954.bloodjournal823954
253. Hattori N. Expression, regulation and biological actions of growth hormone (GH) and ghrelin in the immune system. *Growth Horm IGF Res* (2009) 19:187–97. doi: 10.1016/j.ghir.2008.12.001
254. Merchav S. The haematopoietic effects of growth hormone and insulin-like growth factor-I. *J Pediatr Endocrinol Metab* (1998) 11:677–85. doi: 10.1515/JPEM.1998.11.6.677
255. Masternak MM, Bartke A. Growth hormone, inflammation and aging. *Pathobiol Aging Age Relat Dis* (2012) 2:1–6. doi: 10.3402/pba.v2i0.17293
256. Yoshizato H, Fujikawa T, Soya H, Tanaka M, Nakashima K. The growth hormone (GH) gene is expressed in the lateral hypothalamus: enhancement by GH-releasing hormone and repression by restraint stress. *Endcrinology* (1998) 139:2545–51. doi: 10.1210/endo.139.5.6009
257. Wasinski F, Furigo IC, Teixeira PDS, Ramos-Lobo AM, Peroni CN, Bartolini P, et al. Growth Hormone Receptor Deletion Reduces the Density of Axonal Projections from Hypothalamic Arcuate Nucleus Neurons. *Neuroscience* (2020) 434:136–47. doi: 10.1016/j.neuroscience.2020.03.037
258. Ashpole NM, Sanders JE, Hodges EL, Yan H, Sonntag WE. Growth hormone, insulin-like growth factor-1 and the aging brain. *Exp Gerontol* (2015) 68:76–81. doi: 10.1016/j.exger.2014.10.002
259. Logan S, Pharaoh GA, Marlin MC, Masser DR, Matsuzaki S, Wronowski B, et al. Insulin-like growth factor receptor signaling regulates working memory, mitochondrial metabolism, and amyloid-beta uptake in astrocytes. *Mol Metab* (2018) 9:141–55. doi: 10.1016/j.molmet.2018.01.013
260. Sonntag WE, Deak F, Ashpole N, Toth P, Csiszar A, Freeman W, et al. Insulin-like growth factor-1 in CNS and cerebrovascular aging. *Front Aging Neurosci* (2013) 5:27. doi: 10.3389/fnagi.2013.00027
261. Labandeira-Garcia JL, Costa-Besada MA, Labandeira CM, Villar-Cheda B, Rodriguez-Perez AI. Insulin-Like Growth Factor-1 and Neuroinflammation. *Front Aging Neurosci* (2017) 9:365. doi: 10.3389/fnagi.2017.00365
262. Quinlan P, Horvath A, Nordlund A, Wallin A, Svensson J. Low serum insulin-like growth factor-I (IGF-I) level is associated with increased risk of vascular dementia. *Psychoneuroendocrinology* (2017) 86:169–75. doi: 10.1016/j.psyneuen.2017.09.018
263. Colon G, Saccon T, Schneider A, Cavalcante MB, Huffman DM, Berryman D, et al. The enigmatic role of growth hormone in age-related diseases, cognition, and longevity. *Geroscience* (2019) 41:759–74. doi: 10.1007/s11357-019-00096-w
264. Basu A, McFarlane HG, Kopchick JJ. Spatial learning and memory in male mice with altered growth hormone action. *Horm Behav* (2017) 93:18–30. doi: 10.1016/j.yhbeh.2017.04.001
265. Guevara-Aguirre J, Teran E, Lescano D, Guevara A, Guevara C, Longo V, et al. Growth hormone receptor deficiency in humans associates to obesity, increased body fat percentage, a healthy brain and a coordinated insulin sensitivity. *Growth Horm IGF Res* (2020) 51:58–64. doi: 10.1016/j.ghir.2020.02.004
266. Sonntag WE, Csiszar A, deCabo R, Ferrucci L, Ungvari Z. Diverse roles of growth hormone and insulin-like growth factor-1 in mammalian aging:

progress and controversies. *J Gerontol A Biol Sci Med Sci* (2012) 67:587–98. doi: 10.1093/gerona/gls115
267. Sun LY, Al-Regaiey K, Masternak MM, Wang J, Bartke A. Local expression of GH and IGF-1 in the hippocampus of GH-deficient long-lived mice. *Neurobiol Aging* (2005) 26:929–37. doi: 10.1016/j.neurobiolaging.2004.07.010
268. Lupu F, Terwilliger JD, Lee K, Segre GV, Efstratiadis A. Roles of growth hormone and insulin-like growth factor 1 in mouse postnatal growth. *Dev Biol* (2001) 229:141–62. doi: 10.1006/dbio.2000.9975
269. Ikeno Y, Bronson RT, Hubbard GB, Lee S, Bartke A. Delayed occurrence of fatal neoplastic diseases in ames dwarf mice: correlation to extended longevity. *J Gerontol A Biol Sci Med Sci* (2003) 58:291–6. doi: 10.1093/gerona/58.4.B291
270. Bartke A, Wright JC, Mattison JA, Ingram DK, Miller RA, Roth GS. Extending the lifespan of long-lived mice. *Nature* (2001) 414:412. doi: 10.1038/35106646
271. Coschigano KT, Holland AN, Riders ME, List EO, Flyvbjerg A, Kopchick JJ. Deletion, but not antagonism, of the mouse growth hormone receptor results in severely decreased body weights, insulin, and insulin-like growth factor I levels and increased life span. *Endocrinology* (2003) 144:3799–810. doi: 10.1210/en.2003-0374
272. Borg KE, Brown-Borg HM, Bartke A. Assessment of the primary adrenal cortical and pancreatic hormone basal levels in relation to plasma glucose and age in the unstressed Ames dwarf mouse. *Proc Soc Exp Biol Med* (1995) 210:126–33. doi: 10.3181/00379727-210-43931
273. Flurkey K, Papaconstantinou J, Miller RA, Harrison DE. Lifespan extension and delayed immune and collagen aging in mutant mice with defects in growth hormone production. *Proc Natl Acad Sci U.S.A.* (2001) 98:6736–41. doi: 10.1073/pnas.111158898
274. Bartke A, Darcy J. GH and ageing: Pitfalls and new insights. *Best Pract Res Clin Endocrinol Metab* (2017) 31:113–25. doi: 10.1016/j.beem.2017.02.005
275. Holzenberger M, Dupont J, Ducos B, Leneuve P, Geloen A, Even PC, et al. IGF-1 receptor regulates lifespan and resistance to oxidative stress in mice. *Nature* (2003) 421:182–7. doi: 10.1038/nature01298
276. Selman C, Lingard S, Choudhury AI, Batterham RL, Claret M, Clements M, et al. Evidence for lifespan extension and delayed age-related biomarkers in insulin receptor substrate 1 null mice. *FASEB J* (2008) 22:807–18. doi: 10.1096/fj.07-9261com
277. Bartke A. Can Growth Hormone (GH) Accelerate Aging? Evidence from GH-Transgenic Mice. *Neuroendocrinology* (2003) 78:210–6. doi: 10.1159/000073704
278. List EO, Duran-Ortiz S, Kopchick JJ. Effects of tissue-specific GH receptor knockouts in mice. *Mol Cell Endocrinol* (2020) 515:110919. doi: 10.1016/j.mce.2020.110919
279. Besson A, Salemi S, Gallati S, Jenal A, Horn R, Mullis PS, et al. Reduced longevity in untreated patients with isolated growth hormone deficiency. *J Clin Endocrinol Metab* (2003) 88:3664–7. doi: 10.1210/jc.2002-021938
280. Laron Z. Do deficiencies in growth hormone and insulin-like growth factor-1 (IGF-1) shorten or prolong longevity? *Mech Ageing Dev* (2005) 126:305–7. doi: 10.1016/j.mad.2004.08.02
281. Shevah O, Laron Z. Patients with congenital deficiency of IGF-I seem protected from the development of malignancies: a preliminary report. *Growth Horm IGF Res* (2007) 17:54–7. doi: 10.1016/j.ghir.2006.10.007
282. Paolisso G, Giugliano D. Oxidative stress and insulin action: is there a relationship? *Diabetologia* (1996) 39:357–63. doi: 10.1007/s001250050454
283. Romano AD, Serviddio G, de Matthaeis A, Bellanti F, Vendemiale G. Oxidative stress and aging. *J Nephrol* (2010) 23 Suppl 15:S29–36. doi: E8657B83-848C-46BE-856E-5377F6875270
284. Brown-Borg HM, Bode AM, Bartke A. Antioxidative mechanisms and plasma growth hormone levels: potential relationship in the aging process. *Endocrine* (1999) 11:41–8. doi: 10.1385/ENDO:11:1:41
285. Brown-Borg HM, Johnson WT, Rakoczy SG. Expression of oxidative phosphorylation components in mitochondria of long-living Ames dwarf mice. *Age (Dordr)* (2012) 34:43–57. doi: 10.1007/s11357-011-9212-x
286. Cefalu WT, Wang ZQ, Werbel S, Bell-Farrow A, Crouse JR,3, Hinson WH, et al. Contribution of visceral fat mass to the insulin resistance of aging. *Metabolism* (1995) 44:954–9. doi: 10.1016/0026-0495(95)90251-1
287. Facchini FS, Hua N, Abbasi F, Reaven GM. Insulin resistance as a predictor of age-related diseases. *J Clin Endocrinol Metab* (2001) 86:3574–8. doi: 10.1210/jcem.86.8.7763
288. Chen L, Chen Q, Rong P, Wang HY, Chen S. The energy sensing LKB1-AMPKalpha1 pathway regulates IGF1 secretion and consequent activation of the IGF1R-PKB pathway in primary hepatocytes. *FEBS J* (2017) 284:2096–109. doi: 10.1111/febs.14106
289. Chen L, Chen Q, Xie B, Quan C, Sheng Y, Zhu S, et al. Disruption of the AMPK-TBC1D1 nexus increases lipogenic gene expression and causes obesity in mice via promoting IGF1 secretion. *Proc Natl Acad Sci U.S.A.* (2016) 113:7219–24. doi: 10.1073/pnas.1600581113
290. Russo GL, Russo M, Ungaro P. AMP-activated protein kinase: a target for old drugs against diabetes and cancer. *Biochem Pharmacol* (2013) 86:339–50. doi: 10.1016/j.bcp.2013.05.023
291. Bartke A. Growth hormone and aging: a challenging controversy. *Clin Interv Aging* (2008) 3:659–65. doi: 10.2147/CIA.S3697
292. Bartke A, List EO, Kopchick JJ. The somatotropic axis and aging: Benefits of endocrine defects. *Growth Horm IGF Res* (2016) 27:41–5. doi: 10.1016/j.ghir.2016.02.002
293. Bartke A, Sun LY, Longo V. Somatotropic signaling: trade-offs between growth, reproductive development, and longevity. *Physiol Rev* (2013) 93:571–98. doi: 10.1152/physrev.00006.2012
294. Basu R, Wu S, Kopchick JJ. Targeting growth hormone receptor in human melanoma cells attenuates tumor progression and epithelial mesenchymal transition via suppression of multiple oncogenic pathways. *Oncotarget* (2017) 8:21579–98. doi: 10.18632/oncotarget.15375
295. Dagnaes-Hansen F, Duan H, Rasmussen LM, Friend KE, Flyvbjerg A. Growth hormone receptor antagonist administration inhibits growth of human colorectal carcinoma in nude mice. *Anticancer Res* (2004) 24:3735–42.
296. Farabaugh SM, Boone DN, Lee AV. Role of IGF1R in Breast Cancer Subtypes, Stemness, and Lineage Differentiation. *Front Endocrinol (Lausanne)* (2015) 6:59. doi: 10.3389/fendo.2015.00059
297. van Garderen E, van der Poel HJA, Swennenhuis JF, Wissink EHJ, Rutteman GR, Hellmen E, et al. Expression and molecular characterization of the growth hormone receptor in canine mammary tissue and mammary tumors. *Endocrinology* (1999) 140:5907–14. doi: 10.1210/endo.140.12.7189
298. Hoppe R, Fan P, Buttner F, Winter S, Tyagi AK, Cunliffe H, et al. Profiles of miRNAs matched to biology in aromatase inhibitor resistant breast cancer. *Oncotarget* (2016) 7:71235–54. doi: 10.18632/oncotarget.12103
299. Jung EJ, Santarpia L, Kim J, Esteva FJ, Moretti E, Buzdar AU, et al. Plasma microRNA 210 levels correlate with sensitivity to trastuzumab and tumor presence in breast cancer patients. *Cancer* (2012) 118:2603–14. doi: 10.1002/cncr.26565
300. Chesnokova V, Zonis S, Zhou C, Recouvreux MV, Ben-Shlomo A, Araki T, et al. Growth hormone is permissive for neoplastic colon growth. *Proc Natl Acad Sci U.S.A.* (2016) 113:E3250–3259. doi: 10.1073/pnas.1600561113
301. Mukhina S, Mertani HC, Guo K, Lee KO, Gluckman PD, Lobie PE. Phenotypic conversion of human mammary carcinoma cells by autocrine human growth hormone. *Proc Natl Acad Sci U.S.A.* (2004) 101:15166–71. doi: 10.1073/pnas.0405881101
302. Waters MJ, Conway-Campbell BL. The oncogenic potential of autocrine human growth hormone in breast cancer. *Proc Natl Acad Sci U.S.A.* (2004) 101:14992–3. doi: 10.1073/pnas.0406396101
303. Zhu T, Starling-Emerald B, Zhang X, Lee KO, Gluckman PD, Mertani HC, et al. Oncogenic transformation of human mammary epithelial cells by autocrine human growth hormone. *Cancer Res* (2005) 65:317–24.
304. Zhang X, Mehta RG, Lantvit DD, Coschigano KT, Kopchick JJ, Green JE, et al. Inhibition of estrogen-independent mammary carcinogenesis by disruption of growth hormone signaling. *Carcinogenesis* (2007) 28:143–50. doi: 10.1093/carcin/bgl138
305. Wang Z, Luque RM, Kineman RD, Ray VH, Christov KT, Lantvit DD, et al. Disruption of growth hormone signaling retards prostate carcinogenesis in the Probasin/TAg rat. *Endocrinology* (2008) 149:1366–76. doi: 10.1210/en.2007-1410
306. Shen Q, Lantvit DD, Lin Q, Li Y, Christov K, Wang Z, et al. Advanced rat mammary cancers are growth hormone dependent. *Endocrinology* (2007) 148:4536–44. doi: 10.1210/en.2007-0513

307. Raccurt M, Lobie PE, Moudilou E, Garcia-Caballero T, Frappart L, Morel G, et al. High stromal and epithelial human gh gene expression is associated with proliferative disorders of the mammary gland. *J Endocrinol* (2002) 175:307–18.Endocrinol 2002, 175:307-318. doi: 10.1677/joe.0.1750307
308. Zhu X, Li Y, Xu G, Fu C. Growth hormone receptor (GHR) promotes breast cancer progression via the BRAF/MEK/ERK signaling pathway. *FEBS Open Bio* (2020), 10(6):1013–20. doi: 10.1002/2211-5463.12816
309. Perry JK, Wu ZS, Mertani HC, Zhu T, Lobie PE. Tumour-Derived Human Growth Hormone As a Therapeutic Target in Oncology. *Trends Endocrinol Metab* (2017) 28(8):587–96. doi: 10.1016/j.tem.2017.05.003
310. Jensen BW, Gamborg M, Gogenur I, Renehan AG, Sorensen TIA, Baker JL. Childhood body mass index and height in relation to site-specific risks of colorectal cancers in adult life. *Eur J Epidemiol* (2017) 32:1097–106. doi: 10.1007/s10654-017-0289-0
311. Meyle KD, Gamborg M, Sorensen TIA, Baker JL. Childhood Body Size and the Risk of Malignant Melanoma in Adulthood. *Am J Epidemiol* (2017) 185:673–80. doi: 10.1093/aje/kww128
312. Perez-Cornago A, Appleby PN, Pischon T, Tsilidis KK, Tjonneland A, Olsen A, et al. Tall height and obesity are associated with an increased risk of aggressive prostate cancer: results from the EPIC cohort study. *BMC Med* (2017) 15:115. doi: 10.1186/s12916-017-0876-7
313. Sohn K. Now, the Taller Die Earlier: The Curse of Cancer. *J Gerontol A Biol Sci Med Sci* (2016) 71:713–9. doi: 10.1093/gerona/glv065
314. Subramani R, Nandy SB, Pedroza DA, Lakshmanaswamy R. Role of Growth Hormone in Breast Cancer. *Endocrinology* (2017) 158:1543–55. doi: 10.1210/en.2016-1928
315. Brittain AL, Basu R, Qian Y, Kopchick JJ. Growth Hormone and the Epithelial-to-Mesenchymal Transition. *J Clin Endocrinol Metab* (2017) 102:3662–73. doi: 10.1210/jc.2017-01000
316. Hirakawa T, Yashiro M, Doi Y, Kinoshita H, Morisaki T, Fukuoka T, et al. Pancreatic Fibroblasts Stimulate the Motility of Pancreatic Cancer Cells through IGF1/IGF1R Signaling under Hypoxia. *PloS One* (2016) 11: e0159912. doi: 10.1371/journal.pone.0159912
317. Lantinga-van Leeuwen IS, Timmermans-Sprang EA, Mol JA. Cloning and characterization of the 5'-flanking region of the canine growth hormone gene. *Mol Cell Endocrinol* (2002) 197:133–41. doi: 10.1016/S0303-7207(02)00257-5
318. Lamouille S, Xu J, Derynck R. Molecular mechanisms of epithelial-mesenchymal transition. *Nat Rev Mol Cell Biol* (2014) 15:178–96. doi: 10.1038/nrm3758
319. Kopchick JJ, List EO, Kelder B, Gosney ES, Berryman DE. Evaluation of growth hormone (GH) action in mice: discovery of GH receptor antagonists and clinical indications. *Mol Cell Endocrinol* (2014) 386:34–45.antagonists and clinical indications. Mol Cell Endocrinol 2014, 386:34-45. doi: 10.1016/j.mce.2013.09.004
320. Lee SK, Hwang JH, Choi KY. Interaction of the Wnt/beta-catenin and RAS-ERK pathways involving co-stabilization of both beta-catenin and RAS plays important roles in the colorectal tumorigenesis. *Adv Biol Regul* (2018) 68:46–54. doi: 10.1016/j.jbior.2018.01.001
321. Phesse TJ, Buchert M, Stuart E, Flanagan DJ, Faux M, Afshar-Sterle S, et al. Partial inhibition of gp130-Jak-Stat3 signaling prevents Wnt-beta-catenin-mediated intestinal tumor growth and regeneration. *Sci Signal* (2014) 7:ra92. doi: 10.1126/scisignal.2005411
322. Basu R, Kopchick JJ. The effects of growth hormone on therapy resistance in cancer. *Cancer Drug Resistance* (2019) 2:827–46. doi: 10.20517/cdr.2019.27
323. Basu R, Kulkarni P, Qian Y, Walsh C, Arora P, Davis E, et al. Growth Hormone Upregulates Melanocyte-Inducing Transcription Factor Expression and Activity via JAK2-STAT5 and SRC Signaling in GH Receptor-Positive Human Melanoma. *Cancers (Basel)* (2019) 11:1352. doi: 10.3390/cancers11091352
324. Dusterhoft S, Babendreyer A, Giese AA, Flasshove C, Ludwig A. Status update on iRhom and ADAM17: It's still complicated. *Biochim Biophys Acta Mol Cell Res* (2019) 1866:1567–83. doi: 10.1016/j.bbamcr.2019.06.017
325. Zhang Y, Li Y, Yang X, Wang J, Wang R, Qian X, et al. Uev1A-Ubc13 catalyzes K63-linked ubiquitination of RHBDF2 to promote TACE maturation. *Cell Signal* (2018) 42:155–64. doi: 10.1016/j.cellsig.2017.10.013
326. Alves dos Santos CM, ten Broeke T, Strous GJ. Growth hormone receptor ubiquitination, endocytosis, and degradation are independent of signal transduction via Janus kinase 2. *J Biol Chem* (2001) 276:32635–41. doi: 10.1074/jbc.M103583200
327. Matsuda T, Feng J, Witthuhn BA, Sekine Y, Ihle JN. Determination of the transphosphorylation sites of Jak2 kinase. *Biochem Biophys Res Commun* (2004) 325:586–94. doi: 10.1016/j.bbrc.2004.10.071
328. Li G, Zhou L, Zhang C, Shi Y, Dong D, Bai M, et al. Insulin-Like Growth Factor 1 Regulates Acute Inflammatory Lung Injury Mediated by Influenza Virus Infection. *Front Microbiol* (2019) 10:2541. doi: 10.3389/fmicb.2019.02541
329. Behrens EM, Koretzky GA. Review: Cytokine Storm Syndrome: Looking Toward the Precision Medicine Era. *Arthritis Rheumatol* (2017) 69:1135–43. doi: 10.1002/art.40071
330. Graham JB, Canniff NP, Hebert DN. TPR-containing proteins control protein organization and homeostasis for the endoplasmic reticulum. *Crit Rev Biochem Mol Biol* (2019) 54:103–18. doi: 10.1080/10409238.2019.1590305
331. van Kerkhof P, Strous GJ. The ubiquitin-proteasome pathway regulates lysosomal degradation of the growth hormone receptor and its ligand. *Biochem Soc Trans* (2001) 29:488–93. doi: 10.1042/bst0290488
332. Ji S, Guan R, Frank SJ, Messina JL. Insulin inhibits growth hormone signaling via the growth hormone receptor/JAK2/STAT5B pathway. *J Biol Chem* (1999) 274:13434–42. doi: 10.1074/jbc.274.19.13434
333. Bergan-Roller HE, Sheridan MA. The growth hormone signaling system: Insights into coordinating the anabolic and catabolic actions of growth hormone. *Gen Comp Endocrinol* (2017) 258:119–33. doi: 10.1016/j.ygcen.2017.07.028
334. Bergan-Roller HE, Ickstadt AT, Kittilson JD, Sheridan MA. Insulin and insulin-like growth factor-1 modulate the lipolytic action of growth hormone by altering signal pathway linkages. *Gen Comp Endocrinol* (2017) 248:40–8. doi: 10.1016/j.ygcen.2017.04.005
335. Leung KC, Waters MJ, Markus I, Baumbach WR, Ho KK. Insulin and insulin-like growth factor-I acutely inhibit surface translocation of growth hormone receptors in osteoblasts: a novel mechanism of growth hormone receptor regulation. *Proc Natl Acad Sci U S A* (1997) 94:11381–6.94:11381-11386. doi: 10.1073/pnas.94.21.11381
336. Leung KC, Johannsson G, Leong GM, Ho KK. Estrogen regulation of growth hormone action. *Endocr Rev* (2004) 25:693–721. doi: 10.1210/er.2003-0035
337. Wang P, Li N, Li JS, Li WQ. The role of endotoxin, TNF-alpha, and IL-6 in inducing the state of growth hormone insensitivity. *World J Gastroenterol* (2002) 8:531–6. doi: 10.3748/wjg.v8.i3.531
338. Zheng Y, Qin H, Frank SJ, Deng L, Litchfield DW, Tefferi A, et al. A CK2-dependent mechanism for activation of the JAK-STAT signaling pathway. *Blood* (2011) 118:156–66. doi: 10.1182/blood-2010-01-266320
339. De Luca F. Impaired growth plate chondrogenesis in children with chronic illnesses. *Pediatr Res* (2006) 59:625–9. doi: 10.1203/01.pdr.0000214966.60416.1b
340. Gevers EF, Hannah MJ, Waters MJ, Robinson IC. Regulation of rapid signal transducer and activator of transcription-5 phosphorylation in the resting cells of the growth plate and in the liver by growth hormone and feeding. *Endocrinology* (2009) 150:3627–36. doi: 10.1210/en.2008-0985
341. Ahmed SF, Farquharson C. The effect of GH and IGF1 on linear growth and skeletal development and their modulation by SOCS proteins. *J Endocrinol* (2010) 206:249–59. doi: 10.1677/JOE-10-0045
342. Zhang J-G, Farley A, Nicholson SE, Willson TA, Zugano LM, Simpson RJ, et al. The conserved SOCS box motif in suppressors of cytokines signalling binds to elongins B and C and may couple bound proteins to proteasomal degradation. *Proc Nat Acad Sci USA* (1999) 96:2071–6.
343. Alves dos Santos CM, van Kerkhof P, Strous GJ. The signal transduction of the growth hormone receptor is regulated by the ubiquitin/proteasome system and continues after endocytosis. *J Biol Chem* (2001) 276:10839–46. doi: 10.1074/jbc.M003635200
344. Chhabra Y, Nelson CN, Plescher M, Barclay JL, Smith AG, Andrikopoulos S, et al. Loss of growth hormone-mediated signal transducer and activator of transcription 5 (STAT5) signaling in mice results in insulin sensitivity with obesity. *FASEB J* (2019) 33:6412–30. doi: 10.1096/fj.201802328R
345. Derr MA, Fang P, Sinha SK, Ten S, Hwa V, Rosenfeld RG. A novel Y332C missense mutation in the intracellular domain of the human growth hormone receptor does not alter STAT5b signaling: redundancy of GHR intracellular tyrosines involved in STAT5b signaling. *Horm Res Paediatr* (2011) 75:187–99. doi: 10.1159/000320461
346. Glad CA, Barbosa EJ, Filipsson Nystrom H, Carlsson LM, Nilsson S, Nilsson AG. et al: SNPs within the GH-signaling pathway are associated with the

early IGF1 response to GH replacement therapy in GHD adults. *Eur J Endocrinol* (2014) 170:101–7. doi: 10.1530/EJE-13-0685
347. Chhabra Y, Waters MJ, Brooks AJ. Role of the growth hormone-IGF-1 axis in cancer. *Expert Rev Endocrinol Metab* (2011) 6:71–84. doi: 10.1586/eem.10.73
348. Saxton RA, Sabatini DM. mTOR Signaling in Growth, Metabolism, and Disease. *Cell* (2017) 168:960–76. doi: 10.1016/j.cell.2017.02.004

Conflict of Interest: GS was employed by BIMINI Biotech. B.V., Leiden.

The remaining authors declare that the research was conducted in the absence of any commercial or financial relationships that could be construed as a potential conflict of interest.

Citation: *Strous GJ, Almeida ADS, Putters J, Schantl J, Sedek M, Slotman JA, Nespital T, Hassink GC and Mol JA (2020) Growth Hormone Receptor Regulation in Cancer and Chronic Diseases.*
Front. Endocrinol. 11:597573. doi: 10.3389/fendo.2020.597573

frontiers in Endocrinology

ORIGINAL RESEARCH
published: 25 November 2020
doi: 10.3389/fendo.2020.586242

Therapeutic Effects of 17β-Estradiol on Pelvic Organ Prolapse by Inhibiting Mfn2 Expression: An *In Vitro* Study

*Xiao-Qing Wang, Rui-Ju He, Bing-Bing Xiao and Ye Lu**

Department of Obstetrics and Gynecology, Peking University First Hospital, Beijing, China

Objective: To assess the effects of 17β-estradiol (E2) on proliferation, apoptosis, and protein expressions of fibroblasts at different concentrations and time intervals to reveal the mechanism of E2 in the treatment of pelvic organ prolapse (POP).

Study Design: The uterosacral ligament fibroblasts were collected from seven POP patients for primary culture of fibroblasts. The culture media containing 0, 10^{-6}, 10^{-7}, 10^{-8}, and 10^{-9} mol/L E2 were used for 24, 48, 72, and 96 h.

Main Outcome Measures: The cells were collected for cell counting kit-8 (CCK-8), apoptosis, quantitative reverse transcription polymerase chain reaction (qRT-PCR), and Western blotting assays.

Results: Compared with the control group, in the values of fibroblasts cultured in 10^{-8} mol/L E2 for 72 h, the proliferation, mRNA and protein expression of Mitofusin-2 (Mfn2) separately increased ($P < 0.05$), decreased ($P<0.001$) and decreased ($P<0.001$). However, the expression level of procollagen 1A1/1A2/3A1 and cyclinD1 markedly increased ($P<0.001$, all), which was consistent with the results of protein level. What's more, the expression of estrogen receptor α(ERα), estrogen receptor β(ERβ) and G protein-coupled receptor 30(GPR30) were significantly increased in 10^{-8} mol/L E2 group.

Conclusions: E2 can inhibit the progress of POP by inhibiting the expression level of Mfn2, as well as promoting expression of procollagens and proliferation of fibroblasts. This effect is time- and concentration-dependent. Only when the estrogen concentration reaches 10^{-8} mol/L, the therapeutic effect is the greatest after 72 h.

Keywords: pelvic organ prolapse, 17β-estradiol, Mitofusin2, uterosacral ligament fibroblasts, procollagen

OPEN ACCESS

Edited by:
Ralf Jockers, Université de Paris, France

Reviewed by:
Alessandra Santillo, Second University of Naples, Italy
Sergio Minucci, University of Campania Luigi Vanvitelli, Italy

****Correspondence:***
Ye Lu
songqinlu@sina.com

Specialty section:
This article was submitted to Cellular Endocrinology, a section of the journal Frontiers in Endocrinology

Received: *12 August 2020*
Accepted: *21 October 2020*
Published: *25 November 2020*

Citation:
Wang X-Q, He R-J, Xiao B-B and Lu Y (2020) Therapeutic Effects of 17β-Estradiol on Pelvic Organ Prolapse by Inhibiting Mfn2 Expression: An In Vitro Study. Front. Endocrinol. 11:586242. doi: 10.3389/fendo.2020.586242

INTRODUCTION

Pelvic Organ Prolapse (POP) seriously affects women's quality of life. The symptom that most strongly correlates with POP is a vaginal bulge that can be seen or felt (1). It is now established and widely accepted that the decreased collagen fiber synthesis or increased degradation in pelvic floor tissue leads to POP (1–3). The most effective treatment method is surgery (1, 3). Estrogen can be used in the clinical treatment of POP (4, 5), making the vaginal mucosa thicker, as well as improving

local blood supply, while the specific molecular mechanism has still remained elusive. It has been reported that the quality of vaginal tissue can be improved by placing a continuous low-dose estradiol releasing vaginal ring immediately after pelvic floor reconstruction (4). Local estrogen therapy can increase the blood flow to the genitourinary area and increase the lubrication of vagina (6, 7). However, the evidence-based medical data and mechanism of estrogen treatment for POP are still insufficient (5). Therefore, the present study aimed to reveal the possible role of estrogen in the treatment of POP.

Mitochondria are highly dynamic organelles. They constantly migrate, fuse, and divide to regulate their shape, size, number, and biological function. Mitofusn2 (Mfn2) is a key regulator of mitochondrial fusion and division. It affects cell metabolism, function, proliferation and apoptosis by regulating a variety of signal pathways (8–11). Previous studies on Mfn2 mostly focused on pulmonary fibrosis (10), breast cancer (9), liver fibrosis (10), and Alzheimer's disease (11), and there was little research on pelvic floor dysfunction. To our knowledge, POP is an aging-related disease, and its relationship with the aging related protein, Mfn2 (12–14), has been rarely reported. However, our previous study (15–17) showed that the expression level of Mfn2 increased, while the expression of procollagen decreased in uterosacral ligament fibroblasts of POP patients. The increased expression level of Mfn2 could inhibit the proliferation and cell cycle of fibroblasts by mediating Ras/Raf/ERK pathway, and led to the decrease of collagen synthesis and secretion, eventually resulting in prolapse. On the basis of previous studies, we, in the current research, attempted to assess the effects of estrogen on proliferation and apoptosis of uterosacral ligament fibroblasts, Mfn2, and procollagen 1A1/1A2/3A1 in POP patients by setting different concentrations and time gradients of estrogen, and also indicate whether estrogen can affect the occurrence and development of POP *via* influencing the expression level of Mfn2.

MATERIALS AND METHODS

Study Subjects

From October to December, 2017, the uterosacral ligament tissues of seven POP patients were collected with the help of the Department of Gynecology and Obstetrics, the First Hospital of Peking University, Beijing, China. The baseline characteristics of 7 patients were as follows: Pelvic Organ Prolapse Quantification (POP-Q) stages (14) II-IV, age of 67.43 ± 7.55 (range, 57.00–77.00) years old, body mass index (BMI) of 23.57 ± 3.33 (range, 17.00–26.30), gravidity at 3.14 ± 1.35 (range, 2.00–5.00), parity 2.14 ± 1.69 (1, 3), and menopausal period of 18.00 ± 7.11 (range, 8.00–25.00) days. The uterosacral ligament was retained for primary culture. All patients had no urinary tract infection, history of vaginal surgery, and/or diseases affecting collagen metabolism, and had not taken 17β-estradiol (E2) within 3 months. The specimens were obtained with the informed consent of the patient. The study was approved by the Ethics Committee of Peking University First Hospital Approval No. 2016(1173).

Main Reagents and Instruments

Dimethyl sulfoxide (DMSO, A3672) was purchased from AppliChem GmbH (Darmstadt, Germany). TRIzol reagent and reverse transcription polymerase chain reaction polymer kit (AQ131-02) were purchased from Beijing Full-Type Gold Biotechnology Co., Ltd. (Beijing, China); besides, DMEM/F12 (11330-032), antibiotics-antimycotic (15240-062), fetal bovine serum (FBS; 10099141), 0.25% trypsin-EDTA digestive juices (25200-056) were purchased from Gibco (New York, NY, USA). The cell counting kit-8 (CCK-8) was provided by Dojindo Molecular Technologies, Inc. (Rockville, MD USA). Mfn2 monoclonal antibody (dilution, 1/1000; Ab56889) was purchased from Abcam (Cambridge, UK). Anti-procollagen 1A1/1A2/3A1 antibodies (dilution, 1/200; Sc-293182, Sc-166572, and Sc-166333, respectively) were purchased from Santa Cruz Biotechnology Inc. (Dallas, Texas, USA). Anti-ERα (D8H8) Rabbit mAb antibody (dilution, 1/1000) and Anti-cyclinD1 (92G2) Rabbit mAb antibody (dilution, 1/1000) were purchased from Cell Signaling Technology, Inc. (USA). Horseradish peroxidase (HRP) goat anti-mouse IgG (dilution, 1/5000, ab6789), Anti-ERβ(dilution, 1/1000, ab196787) and Anti-GPR30 (dilution, 1/1000, ab39742) were purchased from Abcam (Cambridge, UK). Procedural cooling box was purchased from Sigma-Aldrich (St. Louis, MO, USA).

Primary Cell Culture, Subculture, and Cryopreservation

During hysterectomy, the fresh uterosacral ligament tissues were taken with the size of 0.5×0.5×0.5 cm^3. The tissues were washed with phosphate-buffered saline (PBS) containing 1% antibiotics, and the tissues were cut into slices with a diameter of less than 0.1 cm, which were evenly distributed to the bottom of the 25 cm^2 bottle. Herein, upside-down containers were used and the bottle was carefully turned over after 4–6 h to avoid floating tissue blocks. The medium was prepared with 20% FBS, 69% DMEM/F12, and 1% antibiotics. Besides, passaging the cells was performed after about 15 days. When the cells grew to 70%–80% confluence, the digestion of the cells was conducted with 2.5% trypsin for about 1–2 min, and the reactions were terminated by aspirating the medium. The samples were placed in fridge/cool storage in boxes at -80°C.

E2 Dissolves Configurations and Stimulates Cells

First, E2 was dissolved with anhydrous alcohol in 20 ug/ml mother liquor, and stored at -20°C. The cells were then incubated with the concentrations of 0, 10^{-6}, 10^{-7}, 10^{-8}, and 10^{-9} mol/L of serum-free Dulbecco's modified Eagle's medium (DMEM), respectively. When the cells were grown to 2 ~ 4 generations, they were collected after 0, 24, 48, 72 and 96h of treating with concentrations of 0, 10^{-6}, 10^{-7}, 10^{-8}, and 10^{-9} mol/L E2.

Cell Proliferation

Cell proliferation was detected after 0, 24, 48, 72 and 96h of stimulation by E2. After addition of 10 ul CCK-8 detection solution to each well, cells were cultured for 1.5 h, and the optical density (OD) value was measured at the wavelength of 450 nm

using a microplate analyzer. Absolute cell numbers were calculated according to a previously prepared standard curve.

Apoptosis

The rates of cell apoptosis were detected by acridine orange/ethidium bromide (AO/EB) staining after 0, 24, 48, 72 and 96h of E2 stimulation. AO/EB fluorescent staining was carried out by mixing AO (100 ug/ml) and EB (100 ug/ml). After washing thrice with PBS, AO/EB working solution was added. After incubation at 37°C for 30 min, the cells were washed with PBS again for 3 times. The whole process was carried out in the dark condition. The samples stained with fluorescent dyes are observed with a fluorescence microscope. Five fields were randomly selected from each sample, and apoptotic cells were counted separately for subsequent analyses. Cells treated with E2 were digested and collected without EDTA trypsin, washed twice with PBS, centrifuged at 2000 rpm for 5 min, and 5×10^5 cells were collected per sample. The cells were re-suspended in binding buffer, and then, the cells were stained with PE-Annexin V and 7AAD for 10 min at room temperature. The data were analyzed by FlowJo software.

The mRNA Expression Levels of Mfn2 and Procollagen

Total RNA was extracted by TRIzol reagent after 0, 24, 48, 72 and 96h of stimulation with E2. In each case 1 μg of total RNA was retro-transcribed *via* TransScript One-Step gDNA Removal and cDNA Synthesis SuperMix which contained DNase (AT311-03, TransGen Biotech, China) and 0.05 μg of total RNA was used for the follow-up quantitative reverse transcription polymerase chain reaction (RT-qPCR). Herein, we detected the expression levels of Mfn2, procollagen 1A1/1A2/3A1 and β-actin (housekeeping gene) using RT-qPCR. The relative expressions of genes were calculated using $2^{-\Delta\Delta CT}$. The primers were as follows: Mfn2: forward: 5'-CATCAGCTACACTGGCTCCA ACT-3'; reverse 5'-GATGAGCAAAGGTCCCAGACA-3'; Procollagen1A1: forward: 5'-CGAGGGCCAAGACGAAGA-3'; reverse: 5'-CACGTCTCGGTCATGGTACCT-3'; Procollagen1A2: forward: 5'-TGGATACGCGGACTTTGTTG-3'; reverse: 5'-GGCTGGGCCCTTTCTTACAG-3'; Procollagen3A1:forward: 5'-TCGCCCTCCTAATGGTCAAG-3'; reverse: 5'-GGTCACCATTTCTCCCAGGAA-3'; ESR1 (ERα):forward: 5' - ACTTGCTCTTGGACAGGAACC-3'; reverse: 5'- TTCAGGGTGCTGGACAGAAA-3'; ESR2(ERβ): forward: 5' -TGCTCCCACTTAGAGGTCAC-3'; reverse: 5'-GAAAAGATCA CAAGCGACTTAACG-3'; GPR30: forward: 5' - ACGAGACTGTGAAATCCGCA-3'; reverse: 5'- CTCTCT GGGTACCTGCCGTC-3'; cyclinD1: forward 5'-CAATGACCC CGCACGATTTC-3', reverse5'-CATGGAGGGCGG ATTGGAA-3'; β-actin forward: 5'-CACGGCTGCTTCC AGCTC-3'; reverse: 5'-CACAGGACTCCATGCCCAG-3'.

The Protein Expression of Mfn2 and Procollagen in Fibroblasts

The total protein was extracted by radioimmunoprecipitation assay (RIPA), and the protein concentration was determined by the bicinchoninic acid (BCA) assay. The protein samples with known concentrations were added in a predetermined order, with 20 ug protein per well. The proteins were separated by sodium dodecyl sulfate polyacrylamide gel electrophoresis (SDS-PAGE) and transferred onto a polyvinylidene difluoride (PVDF) membrane. The membrane was blocked with 5% milk in Tris-Buffered Saline and Tween 20 (TBST) and incubated with primary antibodies overnight at 4°C. Next, the membrane was washed thrice with TBST and incubated with a HRP goat anti-mouse IgG secondary antibody (dilution, 1:5,000) at room temperature for 1 h. Membranes were washed three times, and enhanced chemiluminescence (ECL) was used for visualizing the proteins of interest as marked by HRP. Image J software was used for quantifications of Western blots bands.

Statistical Analysis

All data were statistically analyzed by SPSS 23.0 software (BM, Armonk, NY, USA). The patients' age, BMI, and other measured data were represented by mean ± standard deviation (SD). Normally distributed data were compared by one-way analysis of variance (ANOVA) or independent-sample t-test. K-W test or one-way ANOVA was applied for comparison non-normal distributed data. $P<0.05$ was considered statistically significant.

RESULTS

Primary Culture of Fibroblasts

After inoculation into the culture bottle, a small number of cells were observed, and the cells locally fused into a piece in the tissue block after around 7–10 days, which almost covered areas of the bottle bottom. After about 15 days, the cells were fully fused approximately. The cells were elongated and spindle-shaped or polygonal (**Figure 1**). The growth rate of cells was accelerated after passage, and the cells were then transferred for 3–5 days. The cells were in relatively satisfactory condition within 10 generations.

Proliferation of Fibroblasts After E2 Stimulation

It was noted that proliferation of fibroblasts increased after E2 stimulation, especially after addition of 10^{-8} mol/L E2, and the proliferation rate of the cells was significantly different from that of the non-E2 group (**Figure 2**). In the NC group(non-treated cells) and the E2 group with concentrations of 10^{-6}, 10^{-7}, 10^{-8}, and 10^{-9} mol/L, the mean optical density (OD) values at hours 0 (0 h), 24, 48, 72, and 96 were as follows: (0 h: 0.333, 0.343, 0.332, 0.312, and 0.324); (24 h: 0.615, 0.604, 0.699, 0.814, and 0.749); (48 h: 0.831, 0.911, 0.980, 1.212, and 0.921); (72 h: 1.025, 1.278, 1.222, 1.725, and 1.156); and (96 h: 1.312, 1.547, 1.554, 2.121, and 1.333). The differences were statistically significant. This indicated that 10^{-8} mol/L E2 had the most significant effect on the proliferation of POP fibroblasts. Therefore, we focused on this concentration of E2.

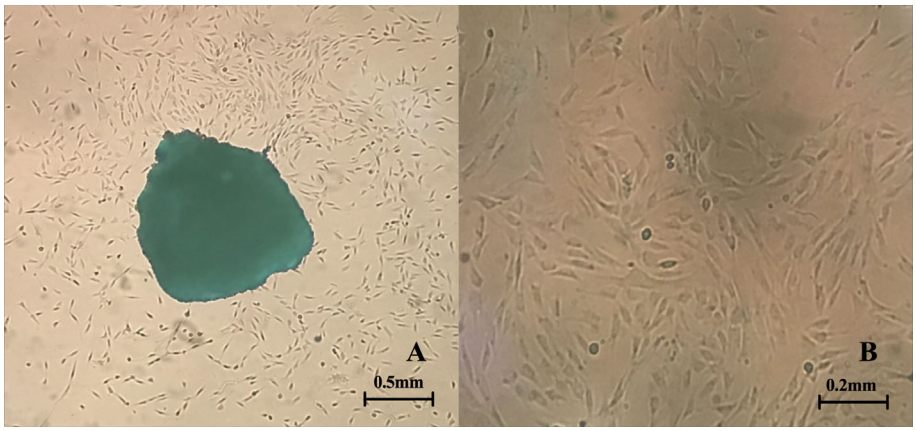

FIGURE 1 | Primary culture of fibroblasts. **(A)** Fibroblasts crawl out of the tissue fragments (the clumps can be observed in the center of the picture) (4X inverted microscope) **(B)** Morphology of fibroblasts after passage (10X inverted microscope).

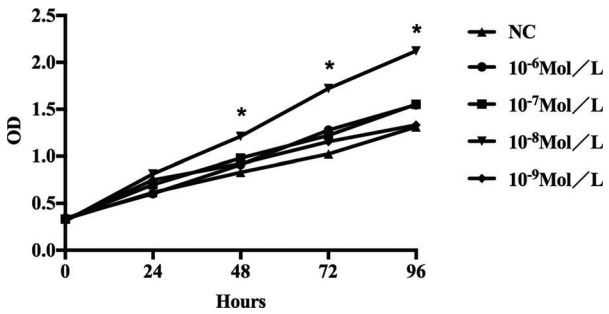

FIGURE 2 | Proliferation of sacral ligament fibroblasts in POP patients stimulated by E2 at different concentrations. The proliferation of fibroblasts increased after E2 stimulation, especially after addition of 10^{-8} mol/L E2, and the proliferation rate of the cells was significantly different from that of the non-E2 group (*P < 0.05).

Apoptosis of Fibroblasts After E2 Stimulation

After 24, 48, 72, and 96 h of E2 stimulation, there was no significant difference in the number of apoptotic cells in each group treating with concentrations of 0, 10^{-6}, 10^{-7}, 10^{-8}, and 10^{-9} mol/L E2. The AO penetrates the intact cell membrane and inserts nuclear DNA into the cell, causing emission of a bright green fluorescence. The EB can only penetrate cells with damaged membranes, embed nuclear DNA in agar, and emit orange fluorescence (18–20). Among them, normal cells appeared green. Late apoptotic cells observed in orange color and dead cells appeared red were extremely rare. There was no statistical difference in the number of early apoptotic cells between different groups of E2 whose nuclei were greenish yellow color and presented as dense plaques or fragments. For instance, after 72 h of stimulation (0, 10^{-6}, 10^{-7}, 10^{-8}, and 10^{-9} mol/L E2), the apoptosis was shown in **Figures 3A** and **4A**. In the meantime, the differences in fibroblast apoptosis (10^{-8} mol/L E2) among 0, 24, 48, 72, and 96 h were shown in **Figures 3B** and **4B**.

RT-qPCR After E2 Stimulation

According to the previous results, the groups affected by 10^{-8} mol/L E2 were selected for intensive observation. After 48 h of treatment, compared with the NC group, the mRNA level of Mfn2 remarkably reduced (0.194, P = 0.000), and the expression levels of procollagen 1A1 (2.252, P = 0.007), 1A2 (2.813, P = 0.003), 3A1 (2.990, P=0.012), ERα(2.177, P=0.008), ERβ(10.037, P=0.000), GPR30(5.041, P=0.000), and cyclinD1(2.526, P=0.002) were noticeably elevated in E2 group with concentration of 10^{-8} mol/L (**Figure 5A**).

At the same time, we did a time gradient experiment under the stimulation of 10^{-8} mol/L E2 (**Figure 5B**). Compared with the results of 0 h, the results of Mfn2, procollagen1A1/1A2/3A1, ERα, ERβ, GPR30 and cyclinD1 in 48, 72, and 96 h groups were as follows: (48 h: 0.098; 11.549; 6.079; 4.216; 2.661; 2.957; 4.988; 3.654); (72 h: 0.049; 3.199; 2.304; 6.042; 1.463; 2.723; 1.882; 3.505); (96 h: 0.022; 2.617; 1.520; 4.988; 1.852; 1.487; 1.525; 5.231).

Western Blotting After E2 Stimulation

Similarly, we first did a concentration gradient experiment (**Figure 5C**). We found that compared with NC group, the protein level of Mfn2 significantly reduced (0.201, P=0.000), and the protein levels of procollagen 1A1 (0.974, P=0.000), 1A2 (1.683, P=0.000), 3A1 (1.041, P=0.000), ERα(1.061, P=0.000), ERβ(0.626, P=0.000), GPR30(1.425, P=0.000), and cyclinD1 (1.644, P=0.000) were markedly increased.

In **Figure 5D**, we did a time gradient experiment under the stimulation of 10^{-8} mol/L E2. Compared with the results of 0 h, the changes of Mfn2, procollagen1A1/1A2/3A1, ERα, ERβ, GPR30, and cyclinD1 in 72 and 96 h groups were the most significant: 72 h (0.028; 1.268; 1.692; 1.876; 1.306; 1.502; 0.308; 1.763; P=0.000, all), 96 h(0.017; 1.284; 1.516; 1.814; 1.204; 1.558;

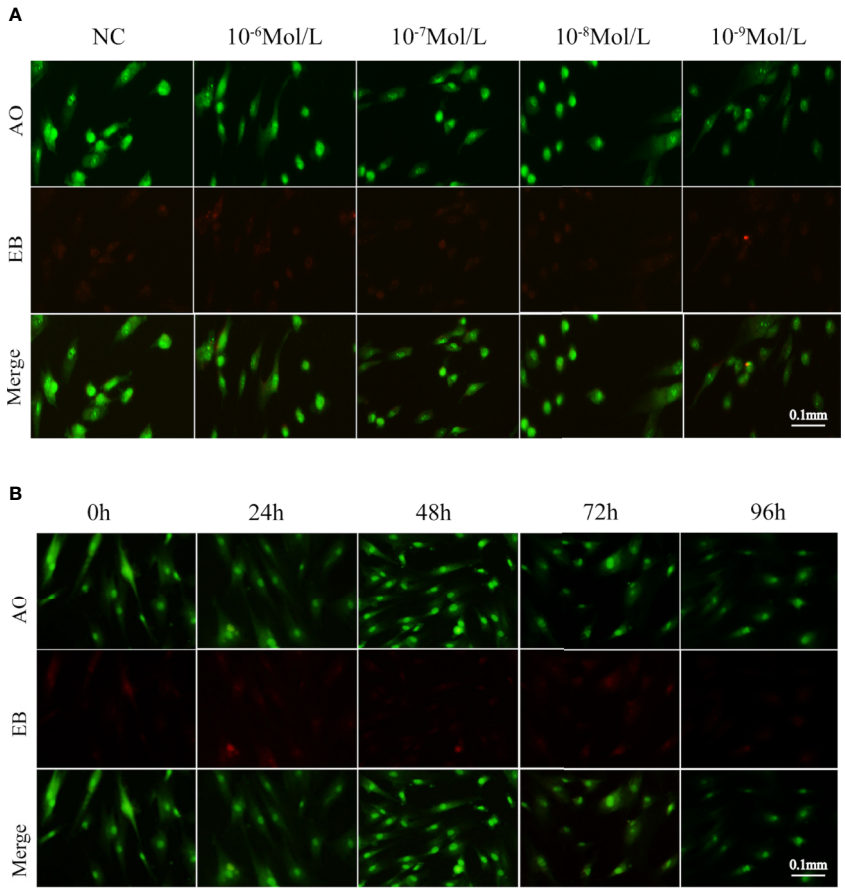

FIGURE 3 | Apoptosis of fibroblasts treated with E2 for 72 h at different concentrations. **(A)** Concentration gradient result of AO/EB after the stimulation for 72h. **(B)** Time gradient result of AO/EB with 10^{-8} mol/L E2. Late apoptotic cells observed in orange color and dead cells(red) were rare among different groups. Normal cells appeared green. There was no statistical difference between early apoptotic cells observed in greenish yellow color treating with concentrations of 0, 10^{-6}, 10^{-7}, 10^{-8}, and 10^{-9} mol/L E2 for 72 h. NC: E2 concentration was 0. Acridine orange (AO): an acridine orange that penetrates the intact cell membrane and inserts nuclear DNA into the cell, causing emission of a bright green fluorescence. Ethidium bromide (EB) can only penetrate cells with damaged membranes, embed nuclear DNA, and emit orange fluorescence.

0.415; 1.780; P=0.000, all). These result were consistent with those achieved by RT-qPCR.

DISCUSSION

Previous studies demonstrated that the majority of patients with POP are postmenopausal women who have low estrogen levels (12–14). A research showed a strong negative correlation between serum estrogen levels and POP-Q scores in patients with POP (21). Therefore, understanding the effects of estrogen on POP, especially the molecular mechanism, is highly essential for prevention and treatment of POP.

In the present study, after culturing the uterosacral ligament fibroblasts and stimulating them with different concentrations of estrogen, we found that compared with medium with concentrations of 0, 10^{-6}, 10^{-7}, and 10^{-9} mol/L E2, 10^{-8} mol/L E2 medium had more significant effect on inhibiting Mfn2 expression, promoting fibroblast proliferation and procollagen synthesis. At the same time, under the effect of 10^{-8} mol/L E2, Mfn2 expression was significantly inhibited and fibroblast proliferation and procollagen1A1/1A2/3A1 synthesis were significantly increased by 72 and 96 h treatment. What's more, the expression of ERα, ERβ and GPR30 were significantly increased in 10^{-8} mol/L E2 group.

After E2 stimulation, the proliferation of fibroblasts markedly elevated. Previous study (22) has found that E2 could promote cell growth by up-regulating the expression of cyclinD1, which was related to cell proliferation. This was consistent with the results of our study. Meanwhile, the protein and mRNA expressions of procollagen 1A1/1A2/3A1 significantly increased, which was closely related to POP. A number of scholars demonstrated that supportive structure of pelvic floor is mainly uterosacral ligament, and the change of collagen fiber content in ligament has a great influence on supportive function of pelvic floor (23). Types I and III collagen are the major constituents of collagen fibers, with type I collagen accounting for approximately 90% and type III accounting for the remainder (24). The type III collagen molecule is more flexible than the type

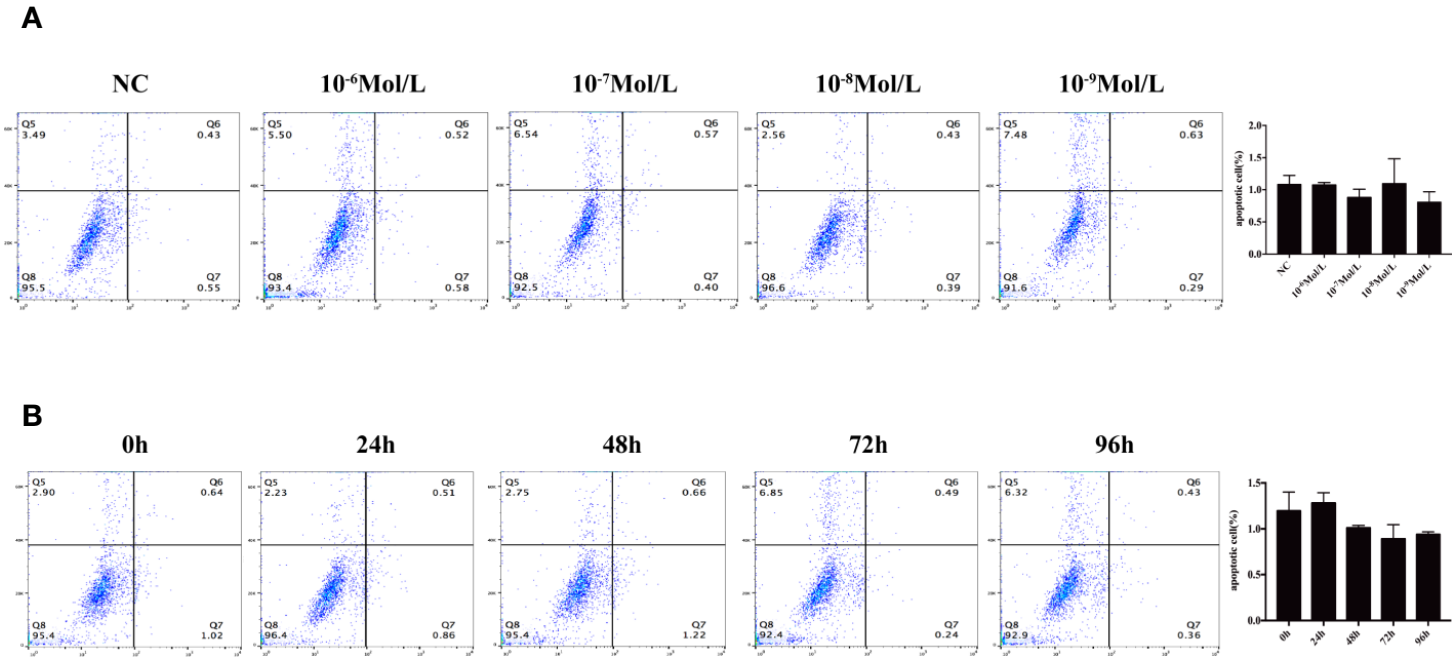

FIGURE 4 | Flow cytometry to detect apoptosis. **(A)** Concentration gradient experiment after the stimulation for 72 h. **(B)** Time gradient experiment with 10^{-8} mol/L E2 Q5: percentage of dead cells, Q6: early apoptotic cells, Q7: late apoptotic cells, and Q8: normal living cells. There was no statistical difference between different groups.

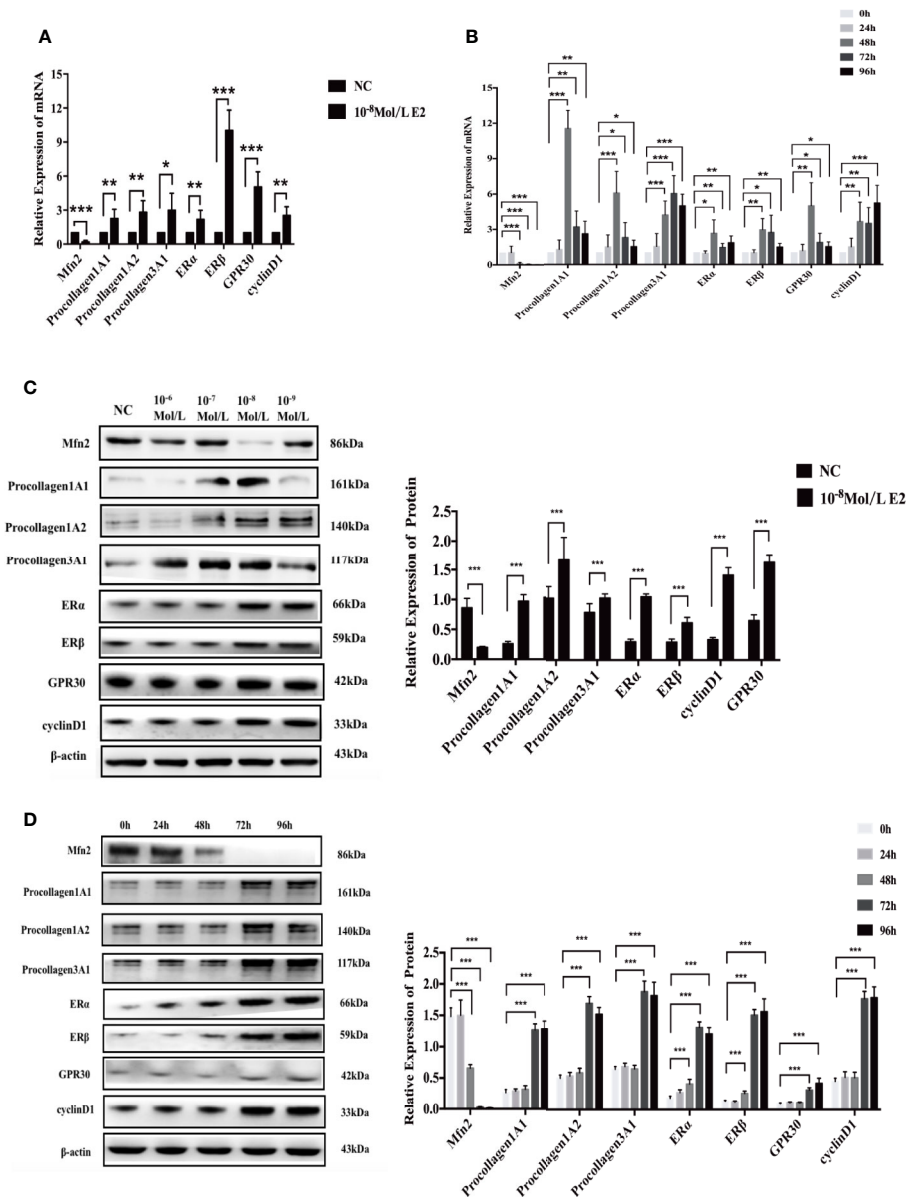

FIGURE 5 | mRNA and protein expression after stimulation of 10^{-8} mol/L E2. **(A, B)** After E2 stimulation of 10^{-8} mol/L for 72 and 96 h, the mRNA level of Mfn2 was decreased, while the mRNA level of procollagen 1A1/1A2/3A1, ERα, ERβ, GPR30, and cyclinD1 were increased. **(C, D)** When uterosacral ligament fibroblasts in POP patients were stimulated by E2 at concentration of 10^{-8} mol/L for 72 and 96 h, the protein level of Mfn2 significantly decreased, whereas the expression of procollagen1A1/1A2/3A1, ERα, ERβ, GPR30, and cyclinD1 were gradually increased. (*P < 0.05, **P < 0.01, ***P < 0.001).

I collagen molecule; thus, fibers rich in type III collagen are more extensible than those rich in type I collagen (i.e., type III collagen is less stiff than type I collagen) (25, 26). In other words, the number of fibroblasts and the procollagen secreted by the two types are important clues to explore the cause of POP. Therefore, the stimulation of E2 can ultimately enhance the elasticity and ductility of ligaments. However, cell proliferation without estrogen stimulation is weaker, and procollagen expression is lower, which may explain why POP is more serious in postmenopausal women. Analyzing the pathogenesis of POP from the perspective of fibroblast-procollagen production source is an innovative point of the present study as well.

In the current research, when estrogen was used to stimulate cells, Mfn2 expression was inhibited at both protein level and mRNA level, indicating that estrogen can play a role by inhibiting Mfn2 expression. Mfn2 is a protein that crosses the mitochondrial bilayer membrane twice (8–11). It is not only related to the fusion and division of mitochondria, but also cell proliferation, apoptosis, and signal transduction pathway (8–11). Additionally, Mfn2 is also related to aging (12–14). Our previous

in vivo and *in vitro* research revealed the relationship between Mfn2 and aging-related diseases; it was unveiled that compared with non-POP patients, Mfn2 has a higher expression in uterosacral ligament fibroblasts of POP patients, and Mfn2 can reduce the supporting effect of ligament and promote the occurrence and development of POP *via* inhibiting the proliferation of fibroblasts and the secretion of procollagen (15–17). The results of the present study further supported our previous results that Mfn2 may play a pivotal role in the occurrence and development of POP. However, estrogen may improve the symptoms of POP by inhibiting the expression level of Mfn2, promoting the proliferation of fibroblasts and the synthesis of procollagen. However, a limited number of reports concentrated on the relationship between Mfn2, estrogen, and POP, which is also a novelty of the present study.

At present, the interaction between Mfn2 and E2 is not clear. Some scholars have confirmed that (27) E2 can inhibit the proliferation of breast cancer cells by inhibiting the expression of Mfn2. Denardo et al. (28) identified a group of estrogen induced genes, including Mfn2. In our study, when we stimulated POP fibroblasts with E2, Mfn2 decreased and cell proliferation increased. These were consistent with the results of previous study. According to traditional studies (29–31), functions of E2 were mainly mediated by receptors, including nuclear receptors (including ERα and ERβ) and membrane receptor GPR30 (GPER-1). After binding with the receptor, E2 activated the transcription and translation of specific genes, and synthesized new functional proteins, thus producing biological effects. There are relatively few studies on the relationship between these receptors and Mfn2. For example, ERα transcription factor was a key regulator of Mfn2 transcription (29). It has been found that a specific region of Mfn2 promoter could bind to and be activated by ERα (30). In addition, E2/GPER/ERK pathway could promote cell proliferation by up-regulating cyclinD1 (31). So far, the relationship between ERβ and Mfn2 is not clear. In this study, we found that the mRNA and protein expression of three receptors increased after E2 stimulation. Therefore, we speculated that the interaction between these three receptors and Mfn2 might play an important role in the effect of E2 on fibroblasts from POP patients. We will continue to explore the mechanism of their interaction in the follow-up study.

The researchers believed that (32, 33) E2 could play a protective role by regulating oxidative stress and preventing mitochondrial dysfunction, leading to the reduction of caspase activation and inhibition of apoptosis. In this project, we used AO/EB and flow cytometry to detect the level of apoptosis. However, there was no significant difference in apoptosis among these groups. These indicated that E2 did not affect the apoptosis of primary fibroblasts from POP patients under the concentration gradient and time gradient set in this study.

We, in the current research, found that only 10^{-8} mol/L of estrogen can significantly change the function of cells, while higher concentrations (10^{-6} and 10^{-7} mol/L) of E2 are not satisfactory, indicating that for *in vitro* tests, higher concentrations of estrogen are not superior. The 10^{-8} mol/L concentration of estrogen is also the physiological concentration (34). In clinical practice, the influence of estrogen concentration in blood on women's health is highly significant. Especially for postmenopausal women, high estrogen level may increase the risk of some diseases, such as breast cancer, endometrial cancer, Alzheimer's disease, diabetes, cardiovascular disease, etc. (34–37). For instance, People (34) found that high estrogen levels are independent predictors of dementia, especially in postmenopausal diabetic women. Additionally, a number of scholars demonstrated that (37) the health characteristics of senior females who use estrogen alone or in form of long-term combination of estrogen and progesterone are more pronounced than those who have never used them. This suggests that in terms of drug safety, in order to prevent or control the progress of POP and avoid the high blood concentration caused by systemic drug use, clinicians may further pay attention to local medication. How to control estrogen in blood at a reasonable level, not only to control POP, but also not to cause other diseases, remains to be further studied. According to the results of different time gradients, it can be concluded that the results of 72 and 96 h *in vitro* test are more significant than those of 24 and 48 h, indicating that it is reasonable to recommend the application of E2 once or twice a week.

CONCLUSIONS

In conclusion, the use of estrogen possesses certain benefits for the function of uterosacral ligament fibroblasts in POP patients. Estrogen can promote the expression of downstream procollagen and the proliferation of fibroblasts by inhibiting the expression level of Mfn2 in uterosacral ligament fibroblasts. This effect is time and concentration-dependent (the effect is the greatest when estrogen concentration is 10^{-8} mol/L for 72 and 96 h). The limitation of the present study was that the sample size was extremely small and the observation time after estrogen stimulation was not long enough, requiring further improvement. However, in order to avoid the interference of estrogen in serum, we used serum-free medium for cell culture. After being treated with E2 for more than 96 h (e.g. 120 h or more), the cells were in relatively poor condition and they were no longer suitable for objective analysis of their proliferation, apoptosis and protein expression. In addition, the interaction between E2, Mfn2, and ERs, GPR30 needs to be further improved in future research. In addition, we will further verify our findings through animal experiments.

DATA AVAILABILITY STATEMENT

The raw data supporting the conclusions of this article will be made available by the authors, without undue reservation.

ETHICS STATEMENT

The studies involving human participants were reviewed and approved by the Ethics Committee of Peking University First

Hospital Approval No. 2016(1173). The patients/participants provided their written informed consent to participate in this study.

AUTHOR CONTRIBUTIONS

Conception, design and obtaining funding, YL. Drafting of the manuscript, X-QW. Analysis and interpretation of data, X-QW and B-BX. Communicating with patients, R-JH. Critical revision of the manuscript for important intellectual content, YL. All authors contributed to the article and approved the submitted version.

FUNDING

The present study was supported by a grant from the Beijing Natural Science Foundation (grant No. 7182167) and the National Natural Science Foundation of China NSFC (grant No. 81401185).

ACKNOWLEDGMENTS

The authors wish to express their sincere gratitude to Dr Yu Qi from Peking University First Hospital, for his instructive advice and professional guidance on the experiment design.

REFERENCES

1. Barber Matthew D. Pelvic organ prolapse. *BMJ* (2016) 354:i3853. doi: 10.1136/bmj.i3853
2. Jin M, Chen Y, Zhou Y, Mei Y, Liu W, Pan C, et al. Transplantation of bone marrow-derived mesenchymal stem cells expressing elastin alleviates pelvic floor dysfunction. *Stem Cell Res Ther* (2016) 7:51. doi: 10.1186/s13287-016-0308-1
3. Cheung RYK, Lee LLL, Chung TKH, Chan SSC. Predictors For Dislodgment Of Vaginal Pessary Within One Year In Women With Pelvic Organ Prolapse. *Maturitas* (2018) 108:53–7. doi: 10.1016/j.maturitas.2017.11.008
4. Karp DR, Jean-Michel M, Johnston Y, Suciu G, Aguilar VC, Davila GWA. Randomized Clinical Trial Of The Impact Of Local Estrogen On Postoperative Tissue Quality After Vaginal Reconstructive Surgery. *Female Pelvic Med Re* (2012) 18:211–5. doi: 10.1097/SPV.0b013e31825e6401
5. Fuermetz A, Schoenfeld M, Ennemoser S, Muetzel E, Jeschke U, Jundt K. Change Of Steroid Receptor Expression In The Posterior Vaginal Wall After Local Estrogen Therapy. *Eur J Obstet Gyn R B* (2015) 187:45–50. doi: 10.1016/j.ejogrb.2015.02.021
6. Tzur T, Yohai D, Weintraub AY. The Role Of Local Estrogen Therapy In The Management Of Pelvic Floor Disorders. *Climacteric* (2016) 19:162–71. doi: 10.3109/13697137.2015.1132199
7. Johari V, Loke C. The role of local vaginal estrogen for treatment of vaginal atrophy in postmenopausal women: 2007 position statement of The North American Menopause Society. *Menopause* (2007) 14:355–69. doi: 10.1097/gme.0b013e31805170eb
8. Giugale Lauren E, Carter-Brooks Charelle M, Ross James H, Shepherd Jonathan P, Zyczynski Halina M. Outcomes of a Staged Midurethral Sling Strategy for Stress Incontinence and Pelvic Organ Prolapse. *Obstet Gynecol* (2019) 134(4):736–44. doi: 10.1097/AOG.0000000000003448
9. Purohit PK, Edwards R, Tokatlidis K, Saini N. MiR-195 regulates mitochondrial function by targeting mitofusin-2 in breast cancer cells. *RNA Biol* (2019) 16(7):918–29. doi: 10.1080/15476286.2019.1600999
10. Das N, Mandala A, Naaz S, Giri S, Jain M, Bandyopadhyay D, et al. Melatonin protects against lipid-induced mitochondrial dysfunction in hepatocytes and inhibits stellate cell activation during hepatic fibrosis in mice. *J Pineal Res* (2017) 62(4):e12404. doi: 10.1111/jpi.12404
11. Han S, Nandy P, Austria Q, Siedlak SL, Torres S, Fujioka H, et al. Mfn2 Ablation in the Adult Mouse Hippocampus and Cortex Causes Neuronal Death. *Cells* (2020) 9(1):116. doi: 10.3390/cells9010116. undefined.
12. Chun SK, Lee S, Flores-Toro J, Y R U, Yang MJ, Go KL, et al. Loss Of Sirtuin1 And Mitofusin2 Contributes To Enhanced Ischemia/Reperfusion Injury In Aged Livers. *Aging Cell* (2018) 17:E12761. doi: 10.1111/acel.12761
13. Du F, Yu Q, Yan S, Hu G, Lue LF, Walker DG, et al. PINK1 Signalling Rescues Amyloid Pathology And Mitochondrial Dysfunction In Alzheimer's Disease. *Brain* (2017) 140:3233–51. doi: 10.1093/brain/awx258
14. Nivison MP, Ericson NG, Green VM, Bielas JH, Campbell JS, Horner PJ. Age-Related Accumulation Of Phosphorylated Mitofusin 2 Protein In Retinal Ganglion Cells Correlates With Glaucoma Progression. *Exp Neurol* (2017) 296:49–61. doi: 10.1016/j.expneurol.2017.07.001
15. Chen KH, Dasgupta A, Ding J, Indig FE, Ghosh P, Longo DL. Role Of Mitofusin 2 (Mfn2) In Controlling Cellular Proliferation. *FASEB J* (2014) 28:382–94. doi: 10.1096/fj.13-230037
16. Lu Y, Chen HY, Wang XQ, Wang JX. Correlations Between Mitofusin 2 Expression In Fibroblasts And Pelvic Organ Prolapse: An In Vitro Study. *Chin Med J* (2017) 130:2951–9. doi: 10.4103/0366-6999.220307
17. Wang XQ, Wang XX, Zhou YF, Chao P, Chen HY, Lu Y. Mitofusin2 regulates the proliferation and function of fibroblasts: The possible mechanisms underlying pelvic organ prolapse development. *Mol Med Rep* (2019) 20:2859–66. doi: 10.3892/mmr.2019.10501
18. Zhang J, Zheng S, Wang S, Liu Q, Xu S. Cadmium-induced oxidative stress promotes apoptosis and necrosis through the regulation of the miR-216a-PI3K/AKT axis in common carp lymphocytes and antagonized by selenium. *Chemosphere* (2020) 258:127341. doi: 10.1016/j.chemosphere.2020.127341
19. Narayani Sivasankara S, Saravanan S, Ravindran J, Ramasamy MS, Chitra J. In vitro anticancer activity of fucoidan extracted from Sargassum cinereum against Caco-2 cells. *Int J Biol Macromol* (2019) 138:618–28. doi: 10.1016/j.ijbiomac.2019.07.127
20. Liu J, Gong Y, Shi J, Hao X, Wang Y, Zhou Y, et al. Design, synthesis and biological evaluation of novel N-[4-(2-fluorophenoxy)pyridin-2-yl] cyclopropanecarboxamide derivatives as potential c-Met kinase inhibitors. *Eur J Med Chem* (2020) 194:112244. doi: 10.1016/j.ejmech.2020.112244
21. Barbara BA, Klaus B, Oliver K, Ksenia H, Heinz K, Wolfgang U. Association of endogenous circulating sex steroids and condition-specific quality of life domains in postmenopausal women with pelvic floor disorders. *Arch Gynecol Obstet* (2018) 297:725–30. doi: 10.1007/s00404-018-4650-7
22. Yu T, Liu M, Luo H, Wu C, Tang X, Tang S, et al. GPER mediates enhanced cell viability and motility via non-genomic signaling induced by 17β-estradiol in triple-negative breast cancer cells. *J Steroid Biochem* (2014) 143:392–403. doi: 10.1016/j.jsbmb.2014.05.003
23. Liapis A, Bakas P, Pafiti A, Frangos-Plemenos M, Arnoyannaki N, Creatsas G. Changes of collagen type III in female patients with genuine stress incontinence and pelvic floor prolapse. *Eur J Obstet Gynecol Reprod Biol* (2001) 97:76–9. doi: 10.1016/S0301-2115(00)00478-4
24. Cameron GJ, Alberts IL, Laing JH, Wess TJ. Structure of type I and type III heterotypic collagen fibrils: an X-ray diffraction study. *J Struct Biol* (2002) 137:15–22. doi: 10.1006/jsbi.2002.4459
25. Bailey AJ. Molecular mechanisms of ageing in connective tissues. *Mech Ageing Dev* (2001) 122:735–55. doi: 10.1016/S0047-6374(01)00225-1
26. Ramachandran GN, Kartha G. Structure of collagen. *Nature* (1955) 176:593–5. doi: 10.1038/176593a0
27. Ma L, Liu Y, Geng C, Qi X, Jiang J. Estrogen receptor β inhibits estradiol-induced proliferation and migration of MCF-7 cells through regulation of mitofusin 2. *Int J Oncol* (2013) 42(6):1993–2000. doi: 10.3892/ijo.2013.1903
28. Denardo DG, Hee-Tae K, Susan H, Valerie C, Anna T, Brown PH. Global gene expression analysis of estrogen receptor transcription factor cross talk in breast cancer: identification of estrogen-induced/activator protein-1-dependent genes. *Mol Endocrinol* (2005) 19:362–78. doi: 10.1210/me.2004-0267
29. Zorzano A. Regulation of mitofusin-2 expression in skeletal muscle. *Appl Physiol Nutr Metab* (2009) 34:433–9. doi: 10.1139/H09-049

30. Li P, Zhu S, Wu X, Zhu X, Li J, Li P, et al. Association of polymorphisms in mitofusin-2 gene with type 2 diabetes in han chinese. *J Biomedicine Biotechnol* (2012) 2012:205752. doi: 10.1155/2012/205752
31. Russell AP, Wada S, Vergani L, Hock MB, Akimoto T. Disruption of skeletal muscle mitochondrial network genes and mirnas in amyotrophic lateral sclerosis. *Neurobiol Dis* (2013) 49:107–17. doi: 10.1016/j.nbd.2012.08.015
32. Hu G, Zhang J, Zhou X, Liu J, Wang Q, Zhang B. Roles of estrogen receptor α and β in the regulation of proliferation in endometrial carcinoma. *Pathol Res Pract* (2020) 216(10):153149. doi: 10.1016/j.prp.2020.153149
33. Azcoitia I, Barreto George E, Garcia-Segura Luis M. Molecular mechanisms and cellular events involved in the neuroprotective actions of estradiol. *Anal sex Dif* (2019) 55:100787. doi: 10.1016/j.yfrne.2019.100787
34. Carcaillon L, Brailly-Tabard S, Ancelin ML, Rouaud O, Dartigues JF, Guiochon-Mantel A, et al. High plasma estradiol interacts with diabetes on risk of dementia in older postmenopausal women. *Neurology* (2014) 82:504–11. doi: 10.1212/WNL.0000000000000107
35. Franco B, Paola M, Andrea M, Gianfranco B, Vittorio K, Raffaella S, et al. Serum Sex Hormone Levels After Menopause and Subsequent Breast Cancer. *JNCI-J Natl Cancer I* (2004) 88:291–7. doi: 10.1093/jnci/88.5.291
36. Dunbier AK, Anderson H, Ghazoui Z, Folkerd EJ, A"Hern R, Crowder RJ, et al. Relationship between plasma estradiol levels and estrogen-responsive gene expression in estrogen receptor–positive breast cancer in postmenopausal women. *J Clin Oncol* (2010) 28:1161–7. doi: 10.1200/JCO.2009.23.9616
37. Kang JH, Weuve J, Grodstein F. Postmenopausal hormone therapy and risk of cognitive decline in community-dwelling aging women. *Neurology* (2004) 63:101–7. doi: 10.1212/01.WNL.0000132522.13574.67

Conflict of Interest: The authors declare that the research was conducted in the absence of any commercial or financial relationships that could be construed as a potential conflict of interest.

frontiers in Endocrinology

ORIGINAL RESEARCH
published: 04 February 2021
doi: 10.3389/fendo.2020.621944

Quinolinate Phosphoribosyltransferase Promotes Invasiveness of Breast Cancer Through Myosin Light Chain Phosphorylation

*Chien-Liang Liu[1,2,3], Shih-Ping Cheng[1,2,3], Ming-Jen Chen[1,2,3], Chi-Hsin Lin[3,4], Shan-Na Chen[3], Yi-Hue Kuo[3] and Yuan-Ching Chang[1,2,3]**

[1] Department of Surgery, MacKay Memorial Hospital, Taipei, Taiwan, [2] Department of Surgery, School of Medicine, Mackay Medical College, New Taipei City, Taiwan, [3] Department of Medical Research, MacKay Memorial Hospital, Taipei, Taiwan, [4] Department of Bioscience Technology, Chung Yuan Christian University, Taoyuan City, Taiwan

OPEN ACCESS

Edited by:
Ralf Jockers, Université de Paris, France

Reviewed by:
Jean-Marc Vanacker, Centre National de la Recherche Scientifique (CNRS), France
Guillermo Romero, University of Pittsburgh, United States

***Correspondence:**
Yuan-Ching Chang
changyc@mmh.org.tw

Specialty section:
This article was submitted to Cellular Endocrinology, a section of the journal Frontiers in Endocrinology

Received: *28 October 2020*
Accepted: *16 December 2020*
Published: *04 February 2021*

Citation:
Liu C-L, Cheng S-P, Chen M-J, Lin C-H, Chen S-N, Kuo Y-H and Chang Y-C (2021) Quinolinate Phosphoribosyltransferase Promotes Invasiveness of Breast Cancer Through Myosin Light Chain Phosphorylation. Front. Endocrinol. 11:621944. doi: 10.3389/fendo.2020.621944

Perturbed Nicotinamide adenine dinucleotide (NAD^+) homeostasis is involved in cancer progression and metastasis. Quinolinate phosphoribosyltransferase (QPRT) is the rate-limiting enzyme in the kynurenine pathway participating in NAD^+ generation. In this study, we demonstrated that QPRT expression was upregulated in invasive breast cancer and spontaneous mammary tumors from MMTV-PyVT transgenic mice. Knockdown of QPRT expression inhibited breast cancer cell migration and invasion. Consistently, ectopic expression of QPRT promoted cell migration and invasion in breast cancer cells. Treatment with QPRT inhibitor (phthalic acid) or $P2Y_{11}$ antagonist (NF340) could reverse the QPRT-induced invasiveness and phosphorylation of myosin light chain. Similar reversibility could be observed following treatment with Rho inhibitor (Y16), ROCK inhibitor (Y27632), PLC inhibitor (U73122), or MLCK inhibitor (ML7). Altogether, these results indicate that QPRT enhanced breast cancer invasiveness probably through purinergic signaling and might be a potential prognostic indicator and therapeutic target in breast cancer.

Keywords: quinolinate phosphoribosyltransferase, NAD, myosin light chain, neoplasm invasiveness, breast cancer

INTRODUCTION

Breast cancer is the most common malignant disease among women and represents a major healthcare burden (1). The incidence of breast cancer has been increasing worldwide, including in Taiwan (2, 3). Despite tremendous advances in the diagnosis and treatment of breast cancer, an increase in breast cancer mortality rates without regional disparities has been observed (4). Developing new therapeutic strategies that target cancer progression and metastasis will be essential to improve patient outcomes.

Nicotinamide adenine dinucleotide (NAD^+) and its reduced form NADH play an important role in biogenesis and redox balance of the human body (5). There is growing evidence of perturbed

NAD^+ homeostasis contributing to various disease states, including cancer and aging (6). In multiple cancer types, enzymes involving NAD^+ metabolism are aberrantly expressed or dysregulated. One of the well-studied targets is nicotinamide phosphoribosyltransferase (NAMPT), the rate-limiting enzyme of the NAD^+ salvage pathway (7). High NAMPT expression was associated with aggressive biological features in breast cancer and other malignancies (8, 9). Translational potential by genetic knockdown of NAMPT or pharmacologic inhibition has been rigorously evaluated in preclinical models.

In addition to the salvage pathway, NAD^+ can be synthesized from a simple amino acid, tryptophan, *via* the *de novo* pathway (10). Quinolinate phosphoribosyltransferase (QPRT) is the final and rate-limiting enzyme in the kynurenine pathway (11). The role of QPRT in cancer has not been well studied. Higher QPRT expression was noted in aggressive glioblastomas than in low-grade gliomas (12). Recently, QPRT was identified as a crucial prognostic gene that was significantly associated with breast cancer overall survival (13). In this study, we aimed to explore the clinicopathological significance of QPRT expression in breast cancer and its potential biological mechanisms.

MATERIALS AND METHODS

Cell Lines and Reagents

Human breast cancer cell lines (BT-20, T-47D, SK-BR-3, MCF-7, MDA-MB-468, MDA-MB-157, BT-474, DU4475, and MDA-MB-231) were all purchased from the American Type Culture Collection, Manassas, VA. An additional MCF-7 cell line derived from Dr. Jose Baselga's laboratory (Memorial Sloan Kettering Cancer Center, New York, NY) was kindly provided by Dr. Yen-Shen Lu (National Taiwan University Hospital, Taipei, Taiwan) (14). Cell line authentication by short tandem repeat sequencing was performed to check for cross-contamination. BT-20 cells were grown in Eagle's Minimum Essential Medium supplemented with 10% fetal bovine serum (FBS). MDA-MB-468 and MDA-MB-231 cells were grown in Leibovitz's L-15 Medium supplemented with 10% FBS. All cells were maintained at 37°C in a 5% CO_2 humidified atmosphere.

Cisplatin was purchased from Fresenius Kabi, Viman Nagar, India. Phthalic acid was obtained from Sigma-Aldrich, Merck KGaA, Darmstadt, Germany. For specific inhibitors, Y16 was obtained from MedChemExpress, Monmouth Junction, NJ; selisistat and olaparib from Selleck Chemicals, Houston, TX; NF340, Y27632, U73122, and ML7 from ApexBio Technology, Houston, TX.

Public Databases and Bioinformatic Analysis

The clinicopathologic profile and mRNA expression data of The Cancer Genome Atlas (TCGA) breast cancer dataset were downloaded through the Genomic Data Commons Data Portal (https://portal.gdc.cancer.gov/) (15). High and low QPRT expression groups were assigned by the median split method, and overall survival between the groups was compared with the log-rank test statistic. Transcriptome data from tumor samples of the top 25 percent and the bottom 25 percent of QPRT expression were further examined, and gene set enrichment analysis (GSEA) was performed to explore the potential significance of differential QPRT expression (16). Additionally, we used a meta-analysis of databases, the KM Plotter Online Tool (https://kmplot.com/analysis/), to validate the relationship between QPRT expression and clinical outcomes (recurrence-free survival and distant metastasis-free survival) (17).

Immunohistochemical (IHC) Staining

Tissue microarrays of breast neoplasms were obtained from Pantomics Inc., Fairfield, CA. The BB08015 set contained 48 tissue cores from 24 patients, and BC08118a contained 100 cores from 100 patients. Overall, 10 normal breast tissues, 20 cases of ductal carcinoma *in situ* (DCIS), and 94 cases of invasive carcinoma were included in the analysis. Mouse anti-human QPRT antibody was purchased from GeneTex, Irvine, CA. The tissue microarray slides were deparaffinized using xylene and rehydrated using serial gradient ethanol. The anti-QPRT antibody was diluted to 1:100. IHC staining was performed as we previously reported (18). Negative control slides were obtained by omitting the primary antibody incubation, and normal liver tissues were used as positive controls.

QPRT protein expression was quantified according to the intensity and extent of immunoreactivity. When the breast epithelial cells showed no positivity or <10% positive staining, they were scored as 0 and 1, respectively. When 10%–50% or >50% positive staining was observed, they were scored as 2 and 3, respectively. The IHC scores of two cores from the same patient were averaged.

Transfection

Lentiviral plasmid vector pLKO.1-puro with short hairpin RNA (shRNA) specific for QPRT and lentiviral vector with control shRNA were purchased from Sigma-Aldrich. To knock down the QPRT expression, MDA-MB-468 and BT-20 cells were transduced with lentivirus in the presence of polybrene (Sigma-Aldrich) and selected with puromycin (InvivoGen, San Diego, CA). Knockdown efficacy was confirmed by real-time quantitative polymerase chain reaction and western blotting.

To overexpress QPRT in breast cancer cells, pCMV6-entry empty vector and pCMV6-entry QPRT expression constructs were purchased from OriGene Technologies, Rockville, MD. We transfected MDA-MB-231 cells with the constructs using Lipofectamine 3000 reagent (Thermo Fisher Scientific, Waltham, MA) according to the manufacturer's protocol. QPRT overexpression was confirmed by western blotting 72 h after transfection.

Cell Viability

Cell growth was evaluated in MDA-MB-468 and BT-20 cells stably transfected with a control shRNA or QPRT-targeting shRNA for 24 to 96 h. MDA-MB-231 cells transfected with pCMV6-entry or pCMV6-QPRT were treated with increasing doses (0.1, 1, 10, 100, and 1000 μM) of cisplatin for 24 or 48 h. Cell viability was determined by the CellTiter Aqueous One

Solution Cell Proliferation (MTS) Assay (Promega, Madison, WI) as previously described (19).

Migration and Invasion Assay

The migration and invasion assays were performed as described (20). Cells in serum-free medium were seeded onto the upper Transwell insert with 8-μm pores of polycarbonate membrane (Corning Life Sciences, Tewksbury, MA). For invasion assay, BioCoat cell culture inserts pre-coated with Matrigel matrix (Corning Life Sciences) were used. The lower chamber contained the complete culture medium. The cells migrated or invaded through the insert membrane were fixed and stained with Diff-Quick (Sysmex, Kobe, Japan). The numbers of migrated or invaded cells were counted under the microscope from five random fields.

NAD^+ Quantification

Intracellular NAD^+ and NADH levels were measured using the NAD/NADH Assay Kit (ab65348; Abcam, Cambridge, UK) according to the manufacturer's protocol. Briefly, cells were extracted with the NAD/NADH extraction buffer and filtered through a 10 kD spin column to remove enzymes that consume NADH. To detect the NADH only, decomposition was performed by heating the samples at 60°C for 30 min. As such, NAD^+ was decomposed while the NADH was intact. The decomposition step was omitted in the detection of total NAD^+ and NADH. NAD^+ in the samples was then converted to NADH by adding NADH developer. Concentrations of NADH in the samples were derived from the standard curve. NAD^+/NADH ratio was calculated as ((total NAD^+ and NADH) - NADH)/NADH.

Immunoblot

Proteins extracted from total cellular lysates were subjected to SDS-PAGE followed by transfer to polyvinylidene fluoride membranes (21). The membranes were incubated with the following primary antibodies: anti-QPRT (GTX83743; GeneTex), anti-phospho-ERK1/2 $^{Thr202/Tyr204}$ (#9101), anti-phospho-AKT ^{Ser473} (#9271), anti-phospho-GSK3β ^{Ser9} (#9336), anti-phospho-Smad2 $^{Ser465/467}$/Smad3 $^{Ser423/425}$ (#8828), anti-phospho-MLC2 ^{Ser19} (#3671), and MLC2 (#8505). All antibodies were obtained from Cell Signaling Technology, Danvers, MA unless otherwise specified. Anti-β-actin (A5441; Sigma-Aldrich) or α-tubulin (T5168; Sigma-Aldrich) signal served as loading controls. The immunoblot band intensities were quantified using ImageJ software.

RNA Sequencing (RNA-seq) Analysis

Total RNA was isolated from MDA-MB-468 and BT-20 cells stably transfected with a control shRNA or QPRT-targeting shRNA. RNA-seq libraries were prepared and sequenced on an Illumina NovaSeq 6000 System (Illumina, San Diego, CA). Raw reads were trimmed to remove adaptor contamination and low-quality reads. Expression levels of the annotated genes were estimated using fragments per kilobase of transcript sequence per millions of base pairs (FPKM). RNA-seq data are available at the Gene Expression Omnibus (GEO) repository (https://www.ncbi.nlm.nih.gov/geo/), with GEO accession number GSE151521.

Hierarchical cluster analysis was performed as described (22). Differential gene expression calculations were done in DESeq2. GSEA was used to identify significant pathways associated with QPRT silencing.

MMTV-PyVT Transgenic Mice

All animal experiments (MMH-AS-108-22) were conducted according to the guidelines established by the institutional animal care and use committee of MacKay Memorial Hospital. Male FVB/N-Tg(MMTV-PyVT)634Mul/J were randomly bred with wild-type C57BL/6J females (BioLASCO, Taipei, Taiwan) to obtain female mice heterozygous for the expression of the Polyoma Virus middle T antigen. Hemizygous MMTV-PyVT mice develop spontaneous mammary tumors that closely resemble the progression and morphology of human breast cancer (23). Mammary tumor formation was monitored by palpation twice a week. Upon the formation of palpable tumors, the mice were further observed for 3–4 weeks for tumor progression (24). Normal mammary gland tissue samples were obtained from wild-type female mice. Proteins extracted from mammary tumors and normal mammary tissues were subjected to western blot analysis. Anti-mouse Qprt antibody was purchased from Biorbyt, Cambridge, UK. Murine liver tissues were used as positive controls.

Statistical Analysis

Data were expressed as mean ± SD. Statistical analyses were performed using Prism 8.3.0 (GraphPad, San Diego, CA). Comparisons of the subgroups were performed by an unpaired t-test or Jonckheere-Terpstra trend test. A two-sided P-value < 0.05 was considered statistically significant.

RESULTS

Clinical Significance of QPRT Expression in Breast Cancer

To explore the potential significance of QPRT expression in breast cancer, we set out to analyze TCGA transcriptome data. As shown in **Figure 1A**, primary breast tumors and metastatic lesions had significantly higher QPRT expression levels than normal breast tissues. Among breast cancer samples with available staging information (n = 1,071), a positive correlation between QPRT expression levels and disease stage was observed (**Figure 1B**). Divided by the median split, breast cancer patients with high QPRT expression had significantly shorter overall survival than those with low QPRT expression (P < 0.001, **Figure 1C**). Consistently, data from the KM Plotter indicated that breast cancer patients with high QPRT expression had significantly shorter recurrence-free and distant metastasis-free survival (**Figure 1D**). Taken together, these data indicate that higher QPRT expression may represent a negative prognostic factor in breast cancer.

GSEA was performed to identify possible alterations in association with differential QPRT expression. Interestingly,

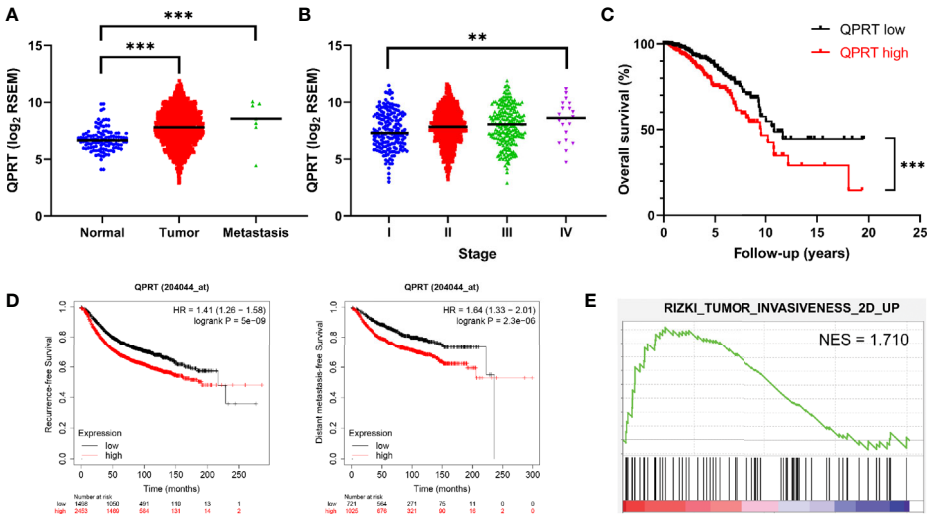

FIGURE 1 | Bioinformatic analysis of the clinical significance of quinolinate phosphoribosyltransferase (QPRT) expression in breast cancer. **(A)** Expression of QPRT quantified by RNA-Seq by Expectation Maximization (RSEM) from The Cancer Genome Atlas (TCGA) breast cancer (BRCA) dataset. Significance was calculated using an unpaired t-test. ***$P < 0.001$. Horizontal lines represent median values. **(B)** Expression of QPRT from TCGA BRCA dataset. Significance was calculated using the Jonckheere-Terpstra trend test (n = 1071). **$P_{for\ trend} < 0.01$. Horizontal lines represent median values. **(C)** Overall survival illustrated for patients from TCGA BRCA dataset. Significance was calculated using the log-rank test. ***$P < 0.001$. **(D)** Recurrence-free survival and distant metastasis-free survival data from the KM Plotter. **(E)** Gene set enrichment analysis (GSEA) of differential QPRT expression using TCGA BRCA dataset NES, normalized enrichment score.

tumor invasiveness was associated with higher QPRT expression in breast cancer (**Figure 1E**).

QPRT Protein Expression in Human and Murine Breast Neoplasms

We next performed IHC staining in clinical breast samples. As shown in **Figure 2A**, normal breast tissue or DCIS generally showed weak QPRT immunoreactivity. Invasive ductal or lobular carcinoma exhibited moderate to strong cytoplasmic staining for QPRT. The IHC scores significantly increased from normal breast tissue (n = 10) and DCIS (n = 20) to invasive carcinoma (n = 94) of different disease stages (**Figure 2B**). A total of 76 samples of invasive carcinoma had available information of tumor grade. Among them, the IHC scores were positively correlated with higher tumor grade. Taken together, the results suggest that the QPRT protein expression in breast neoplasms was associated with the aggressiveness of breast cancer.

QPRT overexpression in breast cancer was further validated in spontaneous mammary tumors from MMTV-PyVT transgenic mice. While normal mammary gland tissues from wild-type mice exhibited virtually undetectable QPRT expression, mammary tumors of MMTV-PyVT mice had relatively abundant QPRT protein expression (**Figure 2C**).

We next screened the QPRT expression in a panel of breast cancer cell lines in our laboratory. While breast cancer cell lines had variable QPRT expression, DU4475 and MDA-MB-231 cells were negative for QPRT expression (**Figure 2D**). Accordingly, triple-negative cancer cell line MDA-MB-231 was used for gain-of-function assays, and two triple-negative cancer cell lines MDA-MB-468 and BT-20 were used for loss-of-function assays in the subsequent experiments.

QPRT Depletion Suppressed the Migratory and Invasive Capacity

Gene silencing by lentiviral shRNA transduction remarkably reduced the QPRT expression in MDA-MB-468 and BT-20 cells (**Figure 3A**). QPRT depletion did not have adverse effects on cell viability or growth in breast cancer cells (**Figure S1**). Nonetheless, the migratory and invasive capacity were significantly suppressed by QPRT knockdown (**Figures 3B, C**).

To identify differentially expressed genes in association with QPRT silencing, RNA-seq analysis was performed in MDA-MB-468 and BT-20 cells transfected with a control shRNA or QPRT-targeting shRNA. A heatmap of selected differentially expressed genes was shown in **Figure 3D**. The GSEA further suggested enrichment for gene sets associated with breast cancer bone relapse and RhoA pathway in breast cancer cells with higher QPRT expression.

Ectopic QPRT Expression Increased the Migratory and Invasive Capacity

MDA-MB-231 cells showed undetectable QPRT expression and were transfected with pCMV6-QPRT. Abundant QPRT protein expression following transfection was confirmed by Western blot (**Figure 4A**). In malignant glioma cells, QPRT expression prevented apoptosis and increased resistance to oxidative stress induced by chemoradiotherapy (12). To test the hypothesis that QPRT overexpression may exert anti-apoptotic effects in breast cancer cells, MDA-MB-231 cells transfected with pCMV6-empty

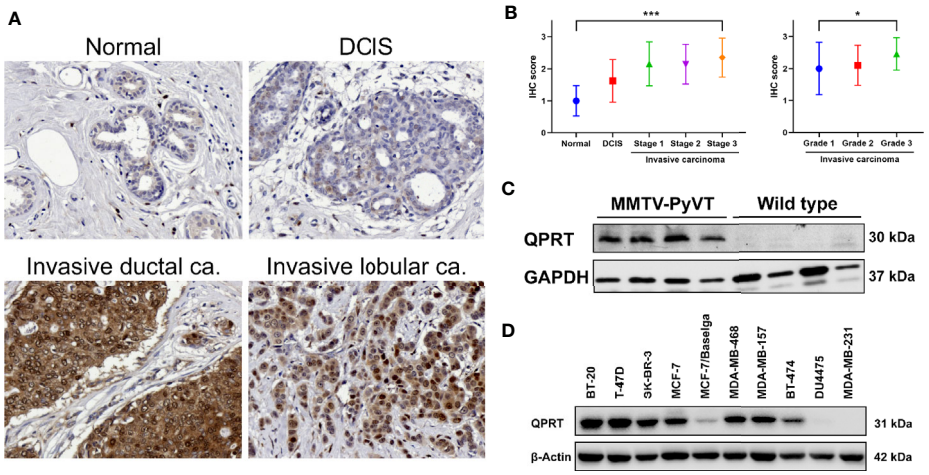

FIGURE 2 | Expression of quinolinate phosphoribosyltransferase (QPRT) in human and murine breast neoplasms. **(A)** Representative QPRT immunostaining of normal breast tissue, ductal carcinoma *in situ* (DCIS), and invasive ductal/lobular carcinoma in female patients. Original magnification, 200X. **(B)** Error bar plots showing means and standard deviations of immunohistochemical (IHC) scores. Significance was calculated using the Jonckheere-Terpstra trend test (normal n = 10, DCIS n = 20, invasive cancer n = 94). $^{*}P_{for\ trend} < 0.05$; $^{***}P_{for\ trend} < 0.001$. **(C)** Western blot analysis of QPRT protein expression in mammary tumors and normal mammary tissues from MMTV-PyVT and wild-type mice, respectively. **(D)** Protein expression of QPRT in a panel of breast cancer cell lines.

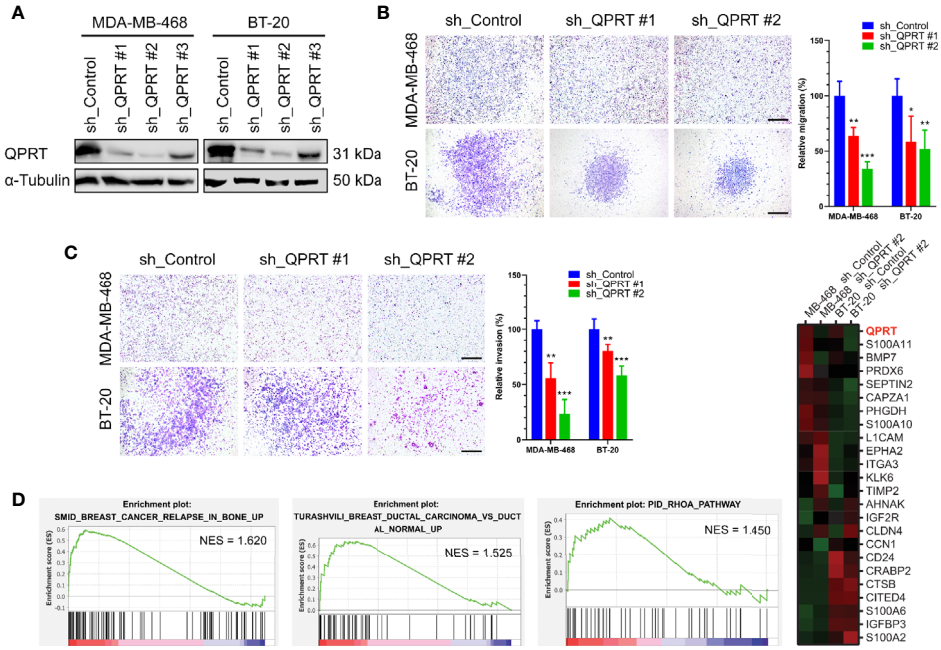

FIGURE 3 | Effects of quinolinate phosphoribosyltransferase (QPRT) silencing in breast cancer cells. **(A)** Protein expression of QPRT in MDA-MB-468 and BT-20 breast cancer cells stably transfected with a control shRNA or QPRT-targeting shRNA. **(B)** Migration and **(C)** invasion determined by the Transwell assay in breast cancer cells transfected with a control shRNA or QPRT-targeting shRNA. Significance was calculated using an unpaired t-test (n = 6). $^{*}P < 0.05$, $^{**}P < 0.01$, $^{***}P < 0.001$. Data represent means ± standard deviations. Scale bars, 500 μm. **(D)** Heatmap of selected differentially expressed genes analyzed by RNA-seq in MDA-MB-468 and BT-20 cells transfected with a control shRNA or QPRT-targeting shRNA. Significantly enriched gene sets generated by Gene set enrichment analysis (GSEA) are shown. NES, normalized enrichment score.

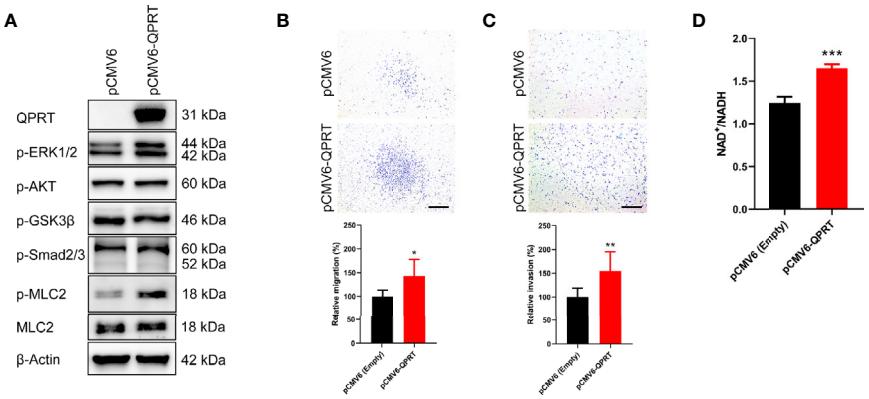

FIGURE 4 | Effects of ectopic quinolinate phosphoribosyltransferase (QPRT) expression in breast cancer cells. **(A)** Protein expression of QPRT and relevant phosphorylated molecules in MDA-MB-231 cells transfected with pCMV6-empty vector or pCMV6-QPRT. **(B)** Migration and **(C)** invasion determined by the Transwell assay in MDA-MB-231 cells transfected with pCMV6-empty vector or pCMV6-QPRT. Significance was calculated using an unpaired t-test (n = 6). $^{*}P < 0.05$, $^{**}P < 0.01$. Data represent means ± standard deviations. Scale bars, 500 μm. **(D)** The ratio of intracellular NAD^+ to NADH levels in MDA-MB-231 cells transfected with pCMV6-empty vector or pCMV6-QPRT. Significance was calculated using an unpaired t-test (n = 3). $^{***}P < 0.001$. Data represent means ± standard deviations.

vector or pCMV6-QPRT were treated with increasing doses of cisplatin. Nonetheless, we found no augmentation of cell viability in QPRT-overexpressing cells (**Figure S2**).

Following QPRT overexpression, MDA-MB-231 cells had significantly increased migratory and invasive capacity (**Figures 4B, C**). It is consistent with the results of loss-of-function assays in MDA-MB-468 and BT-20 cells. As expected, the NAD^+/NADH ratio was increased in MDA-MB-231 cells transfected with pCMV6-QPRT (**Figure 4D**).

QPRT Overexpression Increased the Phosphorylation of Myosin Light Chain

We next asked whether canonical oncogenic signaling pathways are involved in the QPRT-mediated increase in cellular migration and invasion. Following QPRT overexpression, the phosphorylation of ERK1/2 and myosin light chain was increased, while there was no alteration in the phosphorylation of AKT, GSK3β, and Smad2/3 (**Figure 4A**). Phosphorylation of the myosin light chain is a prime regulatory event of the contractile mechanism of stress fibers (25). Considering that the involvement of the RhoA pathway was suggested by our GSEA enrichment results, we hypothesized that the phosphorylation of myosin light chain might be the main effector of QPRT-associated invasiveness.

Sirtuins and poly(ADP-ribose) polymerases (PARPs) are important NAD^+-consuming enzymes and play important roles in breast cancer biology (10). Furthermore, NAD^+ can act as a ligand for the $P2Y_{11}$ purinoreceptor (26). To further delineate the association between QPRT and the RhoA pathway, we used QPRT inhibitor (phthalic acid), SIRT1 inhibitor (selisistat), PARP inhibitor (olaparib), and $P2Y_{11}$ antagonist (NF340) to examine the reversibility of the QPRT-enhanced invasiveness. At concentrations of no significant impact on the invasiveness in control cells, phthalic acid effectively reversed the augmented invasiveness in association with QPRT overexpression (**Figure 5A**). Paradoxically, selisistat heightened the invasiveness in MDA-MB-231 cells transfected with pCMV6-empty vector or pCMV6-QPRT. Olaparib and NF340 were able to reverse the QPRT-enhanced invasiveness, while the latter showed a better efficacy.

Subsequently, we evaluated the effects of treatment with phthalic acid or NF340 in QPRT-overexpressing MDA-MB-231 cells. Either treatment did not alter the phosphorylation of ERK1/2, AKT, and GSK3β. Nonetheless, both agents attenuated the phosphorylation of myosin light chain induced by ectopic QPRT expression (**Figure 5B**).

QPRT Involved Both Rho GTPase and Phospholipase C (PLC) Pathways

G-protein-coupled $P2Y_{11}$ receptors activate PLC and stimulate inositol trisphosphate generation and calcium mobilization (27). Subsequently, Ca^{2+}/calmodulin-dependent myosin light chain kinase (MLCK) is activated, resulting in phosphorylation of myosin light chain and cell contraction. Furthermore, Gαq/11 could enhance p63RhoGEF-induced RhoA activation by direct protein-protein interaction (28). RhoA and its effector, Rho kinase (ROCK), modulate the phosphorylation of myosin light chain and its dephosphorylation by myosin phosphatase (29). Accordingly, we used Rho inhibitor (Y16), ROCK inhibitor (Y27632), PLC inhibitor (U73122), and MLCK inhibitor (ML7) to assess the reversibility of the QPRT-enhanced invasiveness. At concentrations of no significant impact on the invasiveness in control cells, all inhibitors could effectively reverse the QPRT-enhanced invasiveness (**Figure 6A**).

Treatment with inhibitors of Rho, ROCK, PLC, or MLCK did not affect the QPRT expression. While the phosphorylation of ERK1/2 was reduced by the MLCK inhibitor, the most consistent finding was that the QPRT overexpression-induced phosphorylation of myosin light chain was decreased by treatment with either Rho, ROCK, PLC, or MLCK inhibitor

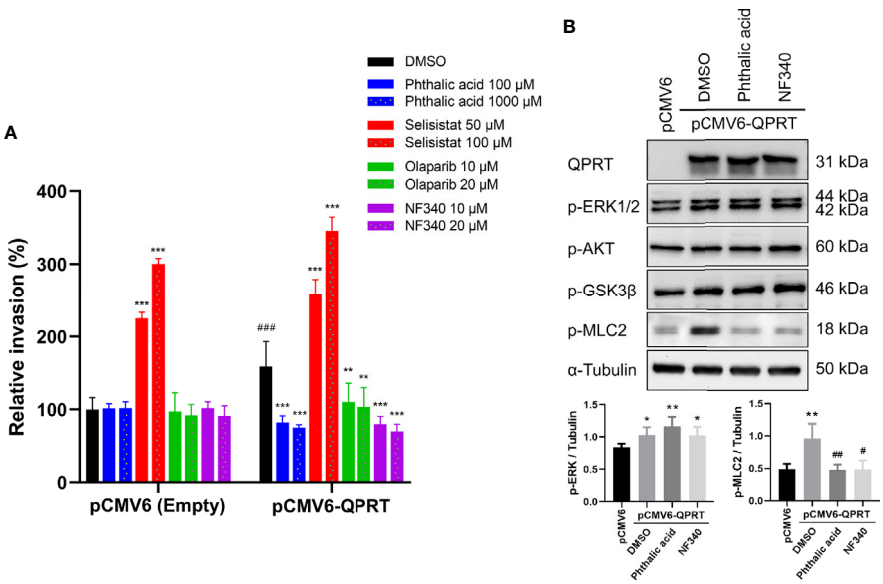

FIGURE 5 | Effects of inhibitors on quinolinate phosphoribosyltransferase (QPRT)-induced invasiveness in breast cancer cells. **(A)** MDA-MB-231 cells transfected with pCMV6-empty vector or pCMV6-QPRT were treated with vehicle control (dimethyl sulfoxide; DMSO), QPRT inhibitor (phthalic acid), SIRT1 inhibitor (selisistat), PARP inhibitor (olaparib), or $P2Y_{11}$ antagonist (NF340) for 24 h. Cell invasive ability was determined by the Transwell assay. Significance was calculated using an unpaired t-test (n = 4). $^{**}P < 0.01$, $^{***}P < 0.001$ compared to DMSO control. $^{###}P < 0.001$ compared to pCMV6-empty vector. Data represent means ± standard deviations. **(B)** Protein expression of QPRT and relevant phosphorylated molecules in MDA-MB-231 cells transfected with pCMV6-empty vector or pCMV6-QPRT and treated with vehicle control (DMSO), QPRT inhibitor (phthalic acid 100 μM), or $P2Y_{11}$ antagonist (NF340 20 μM) for 24 h. Significance was calculated using an unpaired t-test (n = 4). $^{*}P < 0.05$, $^{**}P < 0.01$ compared to pCMV6-empty vector. $^{#}P < 0.05$, $^{##}P < 0.01$ compared to DMSO control. Data represent means ± standard deviations.

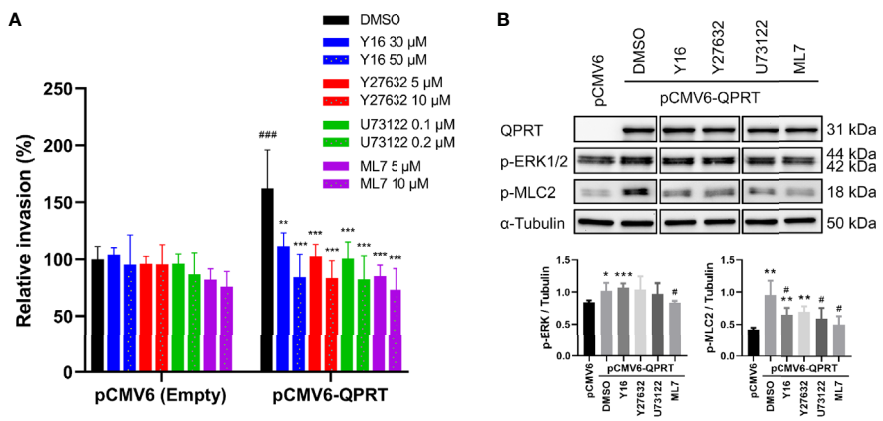

FIGURE 6 | Effects of inhibitors on quinolinate phosphoribosyltransferase (QPRT)-induced invasiveness in breast cancer cells. **(A)** MDA-MB-231 cells transfected with pCMV6-empty vector or pCMV6-QPRT were treated with vehicle control (dimethyl sulfoxide; DMSO), Rho inhibitor (Y16), ROCK inhibitor (Y27632), PLC inhibitor (U73122), or MLCK inhibitor (ML7) for 24 h. Cell invasive ability was determined by the Transwell assay. Significance was calculated using an unpaired t-test (n = 4). $^{**}P < 0.01$, $^{***}P < 0.001$ compared to DMSO control. $^{###}P < 0.001$ compared to pCMV6-empty vector. Data represent means ± standard deviations. **(B)** Protein expression of QPRT and relevant phosphorylated molecules in MDA-MB-231 cells transfected with pCMV6-empty vector or pCMV6-QPRT and treated with vehicle control (DMSO), Rho inhibitor (Y16 50 μM), ROCK inhibitor (Y27632 10 μM), PLC inhibitor (U73122 0.2 μM), or MLCK inhibitor (ML7 10 μM) for 24 h. Significance was calculated using an unpaired t-test (n = 4). $^{*}P < 0.05$, $^{**}P < 0.01$, $^{***}P < 0.001$ compared to pCMV6-empty vector. $^{#}P < 0.05$ compared to DMSO control. Data represent means ± standard deviations.

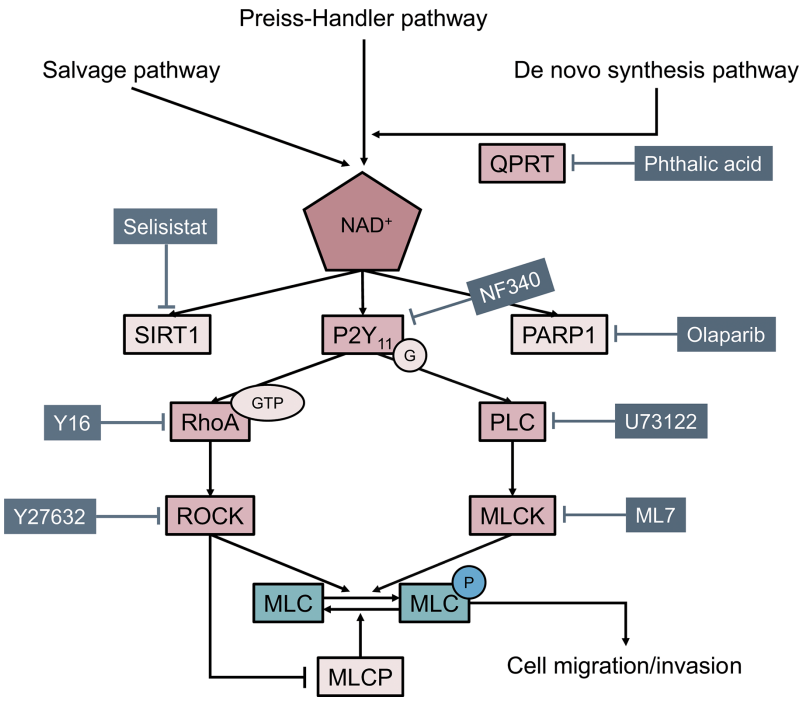

FIGURE 7 | Model illustrating how quinolinate phosphoribosyltransferase (QPRT) promoting cell migration and invasion through phosphorylation of myosin light chain (MLC) in breast cancer.

(**Figure 6B**). Taken together, these results indicate that the Rho-ROCK and PLC-MLCK pathways are both involved in the phosphorylation of myosin light chain as a downstream of the $P2Y_{11}$ activation.

DISCUSSION

In this study, we provided strong evidence supporting the association between QPRT upregulation and tumor progression in breast cancer. First, QPRT expression was positively associated with disease stage and tumor grade, whereas normal breast tissue exhibited low or undetectable QPRT expression. Second, spontaneous mammary tumors from MMTV-PyVT transgenic mice showed a similar trend of QPRT overexpression. Third, QPRT depletion significantly hindered the invasiveness of breast cancer cells.

NAD^+ participates in various cellular physiologic processes including glycolysis and oxidative phosphorylation. In mammalian cells, NAD^+ can be synthesized from nicotinic acid using the Preiss-Handler pathway, synthesized from tryptophan *via* the *de novo* pathway, or generated from nicotinamide or nicotinamide riboside *via* the salvage pathway. The source of NAD^+ generation appears to be tissue and cellular context-dependent (30). Targeting NAMPT of the salvage pathway has received much attention in recent years. Nonetheless, the metabolic plasticity of cancer cells generally leads to acquired resistance to NAMPT inhibition, and increased expression or activity of QPRT is a novel resistance mechanism (31, 32). It, therefore, highlights the need to further investigate the role of QPRT in cancer biology.

The expression of QPRT in malignant neoplasms was evaluated in only a few tumor types. Increased QPRT expression was observed in glioblastomas and follicular thyroid carcinomas (12, 33). Conversely, QPRT expression was decreased in renal cell carcinoma in comparison to normal kidney tissue (34). Furthermore, QPRT expression was decreased in metastatic melanoma after the acquisition of resistance to BRAF inhibitors (35). In the present study, upregulation of QPRT expression was validated in clinical samples and spontaneous murine tumors.

Increased QPRT expression would enhance the synthesis of nicotinic acid mononucleotide and in turn NAD^+. A reduction in intracellular NAD^+ in breast cancer cells may induce apoptosis and suppress cell survival (36). On the contrary, nonlethal reduction of NAD^+ may render tumor cells more aggressive and increase metastasis (37). Although QPRT seems to possess anti-apoptotic properties in some tumor types (12, 38), we did not find any difference in cell growth or viability in breast cancer cells following QPRT depletion or ectopic QPRT expression. At the time of this manuscript preparation, Yue et al. reported that knocking down QPRT in MCF-7 and T47D cells increased the apoptosis rate, and QPRT overexpression marginally decreased apoptosis (39). The basis for such a difference is unclear, but our group and Yue et al. both showed that QPRT positively participates in regulating the migratory and invasive capacity of breast cancer cells.

We further examined whether the invasion-promoting effect of QPRT was mediated by NAD^+-consuming enzymes. Sirtuins are a family of histone deacetylases that require NAD^+ as a substrate for SIRT-mediated deacetylation reactions. Sirtuins can promote or suppress breast cancer metastasis, and several sirtuin modulators (including selisistat, a SIRT1 inhibitor) have been investigated in clinical trials (40). In breast cancer cells, SIRT1 depletion induced an epithelial shift and inhibited cell invasion (41). Nonetheless, we found that treatment with selisistat in QPRT-overexpressing cells resulted in an uprise of cell invasion. PARPs are also NAD^+-consuming enzymes, and poly(ADP)-ribosylation is a unique post-translational modification affecting various protein functions. The PARP inhibitor olaparib has been approved to treat patients whose cancer is positive for homologous recombination deficiency. MDA-MB-231 is a BRCA wild-type cell line with BRCA1 allelic loss and shows normal BRCA1 transcript levels (42). Although olaparib could partially reverse the QPRT-enhanced invasiveness, we were focusing on purinergic signaling as the potential link.

Nucleotides are prometastatic factors favoring tumor cell migration and tissue colonization, and purinergic receptors play an important role (43, 44). Given that NAD^+ is a $P2Y_{11}$ agonist (45), we evaluated the rescue effect of a $P2Y_{11}$ antagonist NF340 and found that NF340 effectively reversed the QPRT-enhanced invasiveness. The result was similar to that treatment with NF340 prevented ATP-induced stimulation of cell migration in hepatocellular carcinoma cells (46). Furthermore, we showed that both Rho GTPase and PLC pathways downstream to the $P2Y_{11}$ receptor were involved. Nonetheless, we could not exclude the possibility that additional NAD^+-independent mechanisms are operative in the QPRT-mediated increment in cell migration and invasion.

Currently, phthalic acid, a quinolinic acid analog, is the only competitive inhibitor of QPRT (11). Treatment with phthalic acid reduced intracellular NAD^+ levels, SIRT1 activity, and cell viability in a dose-dependent manner in human astrocytes and neurons (47). Although phthalates are widely used as plasticizing agents, phthalic acid is a germ cell mutagen (48). While newer selective QPRT inhibitors are under investigation, it would be interesting to determine the synergic or additive effects of combining QPRT and NAMPT inhibitors. Additionally, QPRT blockade might undoubtfully increase the upstream quinolinic acid, and quinolinic acid will lead to neurotoxicity. A combination with inhibitors against 3-hydroxyanthranilic acid oxygenase or other enzymes along the kynurenine pathway should be taken into consideration.

In summary, the present study demonstrated a significant role of QPRT in breast cancer. QPRT promotes cell migration and invasion of breast cancer cells through, at least in part, the phosphorylation of myosin light chain *via* Rho GTPase and PLC pathways downstream of purinergic receptors (**Figure 7**). QPRT might be a potential prognostic indicator and therapeutic target in breast cancer.

DATA AVAILABILITY STATEMENT

The raw data supporting the conclusions of this article will be made available by the authors, without undue reservation.

ETHICS STATEMENT

The animal study was reviewed and approved by Institutional Animal Care and Use Committee.

AUTHOR CONTRIBUTIONS

C-LL, S-NC, Y-HK, and C-HL carried out the experiment. C-LL and Y-CC wrote the manuscript with support from S-PC. M-JC helped supervised the project. Y-CC and S-PC conceived the original idea. Y-CC supervised the project. All authors contributed to the article and approved the submitted version.

FUNDING

This work was supported by MacKay Memorial Hospital (grants MMH-E-107-10, MMH-E-108-10, and MMH-E-109-10).

ACKNOWLEDGMENTS

We thank Dr. Ming-Shen Dai (Tri-Service General Hospital, Taipei, Taiwan) for providing MMTV-PyVT mice.

SUPPLEMENTARY MATERIAL

The Supplementary Material for this article can be found online at: https://www.frontiersin.org/articles/10.3389/fendo.2020.621944/full#supplementary-material

Supplementary Figure 1 | Effects of quinolinate phosphoribosyltransferase (QPRT) depletion on breast cancer cell growth. In MDA-MB-468 and BT-20 cells stably transfected with a control shRNA or QPRT-targeting shRNA, cell viability was determined by the CellTiter Aqueous One Solution Cell Proliferation (MTS) Assay at 24 to 96 h. Significance was calculated using an unpaired t-test (n = 3). Data represent means ± standard deviations.

Supplementary Figure 2 | Effects of ectopic quinolinate phosphoribosyltransferase (QPRT) expression on cell viability and chemotherapy sensitivity. MDA-MB-231 cells transfected with pCMV6-empty vector or pCMV6-QPRT were treated with cisplatin in serial dilutions. Cell viability was determined by the CellTiter Aqueous One Solution Cell Proliferation (MTS) Assay at 24 and 48 h. Significance was calculated using an unpaired t-test (n = 3). Data represent means ± standard deviations.

REFERENCES

1. Heer E, Harper A, Escandor N, Sung H, McCormack V, Fidler-Benaoudia MM. Global burden and trends in premenopausal and postmenopausal breast cancer: a population-based study. *Lancet Glob Health* (2020) 8(8):e1027–37. doi: 10.1016/S2214-109X(20)30215-1
2. Chen Z, Xu L, Shi W, Zeng F, Zhuo R, Hao X, et al. Trends of female and male breast cancer incidence at the global, regional, and national levels, 1990-2017. *Breast Cancer Res Treat* (2020) 180(2):481–90. doi: 10.1007/s10549-020-05561-1
3. Chiang CJ, Lo WC, Yang YW, You SL, Chen CJ, Lai MS. Incidence and survival of adult cancer patients in Taiwan, 2002-2012. *J Formos Med Assoc* (2016) 115(12):1076–88. doi: 10.1016/j.jfma.2015.10.011
4. Ho YR, Ma SP, Chang KY. Trends in regional cancer mortality in Taiwan 1992-2014. *Cancer Epidemiol* (2019) 59:185–92. doi: 10.1016/j.canep.2019.02.005
5. Katsyuba E, Romani M, Hofer D, Auwerx J. NAD(+) homeostasis in health and disease. *Nat Metab* (2020) 2(1):9–31. doi: 10.1038/s42255-019-0161-5
6. Verdin E. NAD(+) in aging, metabolism, and neurodegeneration. *Science* (2015) 350(6265):1208–13. doi: 10.1126/science.aac4854
7. Pramono AA, Rather GM, Herman H, Lestari K, Bertino JR. NAD- and NADPH-Contributing Enzymes as Therapeutic Targets in Cancer: An Overview. *Biomolecules* (2020) 10(3):358. doi: 10.3390/biom10030358
8. Lee YC, Yang YH, Su JH, Chang HL, Hou MF, Yuan SS. High visfatin expression in breast cancer tissue is associated with poor survival. *Cancer Epidemiol Biomarkers Prev* (2011) 20(9):1892–901. doi: 10.1158/1055-9965.EPI-11-0399
9. Ji C, Cong R, Wang Y, Wang Y, Zhang Q, Zhou X, et al. Relationship between NAMPT/PBEF/visfatin and prognosis of patients with malignant tumors: a systematic review and meta-analysis. *Ann Transl Med* (2019) 7(23):785. doi: 10.21037/atm.2019.11.32
10. Canto C, Menzies KJ, Auwerx J. NAD(+) Metabolism and the Control of Energy Homeostasis: A Balancing Act between Mitochondria and the Nucleus. *Cell Metab* (2015) 22(1):31–53. doi: 10.1016/j.cmet.2015.05.023
11. Jacobs KR, Castellano-Gonzalez G, Guillemin GJ, Lovejoy DB. Major Developments in the Design of Inhibitors along the Kynurenine Pathway. *Curr Med Chem* (2017) 24(23):2471–95. doi: 10.2174/0929867324666170502123114
12. Sahm F, Oezen I, Opitz CA, Radlwimmer B, von Deimling A, Ahrendt T, et al. The endogenous tryptophan metabolite and NAD+ precursor quinolinic acid confers resistance of gliomas to oxidative stress. *Cancer Res* (2013) 73(11):3225–34. doi: 10.1158/0008-5472.CAN-12-3831
13. Xu YH, Deng JL, Wang LP, Zhang HB, Tang L, Huang Y, et al. Identification of Candidate Genes Associated with Breast Cancer Prognosis. *DNA Cell Biol* (2020) 39(7):1205–27. doi: 10.1089/dna.2020.5482
14. Chen IC, Hsiao LP, Huang IW, Yu HC, Yeh LC, Lin CH, et al. Phosphatidylinositol-3 Kinase Inhibitors, Buparlisib and Alpelisib, Sensitize Estrogen Receptor-positive Breast Cancer Cells to Tamoxifen. *Sci Rep* (2017) 7(1):9842. doi: 10.1038/s41598-017-10555-z
15. N. Cancer Genome Atlas. Comprehensive molecular portraits of human breast tumours. *Nature* (2012) 490(7418):61–70. doi: 10.1038/nature11412
16. Subramanian A, Tamayo P, Mootha VK, Mukherjee S, Ebert BL, Gillette MA, et al. Gene set enrichment analysis: a knowledge-based approach for interpreting genome-wide expression profiles. *Proc Natl Acad Sci U.S.A.* (2005) 102(43):15545–50. doi: 10.1073/pnas.0506580102
17. Gyorffy B, Lanczky A, Eklund AC, Denkert C, Budczies J, Li Q, et al. An online survival analysis tool to rapidly assess the effect of 22,277 genes on breast cancer prognosis using microarray data of 1,809 patients. *Breast Cancer Res Treat* (2010) 123(3):725–31. doi: 10.1007/s10549-009-0674-9
18. Chen IC, Chang YC, Lu YS, Chung KP, Huang CS, Lu TP, et al. Clinical Relevance of Liver Kinase B1(LKB1) Protein and Gene Expression in Breast Cancer. *Sci Rep* (2016) 6:21374. doi: 10.1038/srep21374
19. Chang YC, Lin CH, Lin JC, Cheng SP, Chen SN, Liu CL. Inhibition of 3beta-Hydroxysteroid Dehydrogenase Type 1 Suppresses Interleukin-6 in Breast Cancer. *J Surg Res* (2019) 241:8–14. doi: 10.1016/j.jss.2019.03.024
20. Liu CL, Chen MJ, Lin JC, Lin CH, Huang WC, Cheng SP, et al. Doxorubicin Promotes Migration and Invasion of Breast Cancer Cells through the Upregulation of the RhoA/MLC Pathway. *J Breast Cancer* (2019) 22(2):185–95. doi: 10.4048/jbc.2019.22.e22
21. Chang YC, Chen CK, Chen MJ, Lin JC, Lin CH, Huang WC, et al. Expression of 3beta-Hydroxysteroid Dehydrogenase Type 1 in Breast Cancer is Associated with Poor Prognosis Independent of Estrogen Receptor Status. *Ann Surg Oncol* (2017) 24(13):4033–41. doi: 10.1245/s10434-017-6000-6
22. Cheng SP, Chen MJ, Chien MN, Lin CH, Lee JJ, Liu CL. Overexpression of teneurin transmembrane protein 1 is a potential marker of disease progression in papillary thyroid carcinoma. *Clin Exp Med* (2017) 17(4):555–64. doi: 10.1007/s10238-016-0445-y
23. Lin EY, Jones JG, Li P, Zhu L, Whitney KD, Muller WJ, et al. Progression to malignancy in the polyoma middle T oncoprotein mouse breast cancer model provides a reliable model for human diseases. *Am J Pathol* (2003) 163(5):2113–26. doi: 10.1016/S0002-9440(10)63568-7
24. Chang YC, Liu CL, Chen MJ, Hsu YW, Chen SN, Lin CH, et al. Local anesthetics induce apoptosis in human breast tumor cells. *Anesth Analg* (2014) 118(1):116–24. doi: 10.1213/ANE.0b013e3182a94479
25. Katoh K, Kano Y, Noda Y. Rho-associated kinase-dependent contraction of stress fibres and the organization of focal adhesions. *J R Soc Interface* (2011) 8(56):305–11. doi: 10.1098/rsif.2010.0419
26. Moreschi I, Bruzzone S, Nicholas RA, Fruscione F, Sturla L, Benvenuto F, et al. Extracellular NAD+ is an agonist of the human P2Y11 purinergic receptor in human granulocytes. *J Biol Chem* (2006) 281(42):31419–29. doi: 10.1074/jbc.M606625200
27. Communi D, Govaerts C, Parmentier M, Boeynaems JM. Cloning of a human purinergic P2Y receptor coupled to phospholipase C and adenylyl cyclase. *J Biol Chem* (1997) 272(51):31969–73. doi: 10.1074/jbc.272.51.31969
28. Lutz S, Freichel-Blomquist A, Yang Y, Rumenapp U, Jakobs KH, Schmidt M, et al. The guanine nucleotide exchange factor p63RhoGEF, a specific link between Gq/11-coupled receptor signaling and RhoA. *J Biol Chem* (2005) 280(12):11134–9. doi: 10.1074/jbc.M411322200
29. Amin E, Dubey BN, Zhang SC, Gremer L, Dvorsky R, Moll JM, et al. Rho-kinase: regulation, (dys)function, and inhibition. *Biol Chem* (2013) 394(11):1399–410. doi: 10.1515/hsz-2013-0181
30. Chowdhry S, Zanca C, Rajkumar U, Koga T, Diao Y, Raviram R, et al. NAD metabolic dependency in cancer is shaped by gene amplification and enhancer remodelling. *Nature* (2019) 569(7757):570–5. doi: 10.1038/s41586-019-1150-2
31. Guo J, Lam LT, Longenecker KL, Bui MH, Idler KB, Glaser KB, et al. Identification of novel resistance mechanisms to NAMPT inhibition via the de novo NAD(+) biosynthesis pathway and NAMPT mutation. *Biochem Biophys Res Commun* (2017) 491(3):681–6. doi: 10.1016/j.bbrc.2017.07.143
32. Thongon N, Zucal C, D'Agostino VG, Tebaldi T, Ravera S, Zamporlini F, et al. Cancer cell metabolic plasticity allows resistance to NAMPT inhibition but invariably induces dependence on LDHA. *Cancer Metab* (2018) 6:1. doi: 10.1186/s40170-018-0174-7
33. Hinsch N, Frank M, Doring C, Vorlander C, Hansmann ML. QPRT: a potential marker for follicular thyroid carcinoma including minimal invasive variant; a gene expression, RNA and immunohistochemical study. *BMC Cancer* (2009) 9:93. doi: 10.1186/1471-2407-9-93
34. Hornigold N, Dunn KR, Craven RA, Zougman A, Trainor S, Shreeve R, et al. Dysregulation at multiple points of the kynurenine pathway is a ubiquitous feature of renal cancer: implications for tumour immune evasion. *Br J Cancer* (2020) 123(1):13s7–147. doi: 10.1038/s41416-020-0874-y
35. Audrito V, Manago A, La Vecchia S, Zamporlini F, Vitale N, Baroni G, et al. Nicotinamide Phosphoribosyltransferase (NAMPT) as a Therapeutic Target in BRAF-Mutated Metastatic Melanoma. *J Natl Cancer Inst* (2018) 110(3):290–303. doi: 10.1093/jnci/djx198
36. Bolandghamat Pour Z, Nourbakhsh M, Mousavizadeh K, Madjd Z, Ghorbanhosseini SS, Abdolvahabi Z, et al. Up-regulation of miR-381 inhibits NAD+ salvage pathway and promotes apoptosis in breast cancer cells. *EXCLI J* (2019) 18:683–96. doi: 10.17179/excli2019-1431
37. Santidrian AF, Matsuno-Yagi A, Ritland M, Seo BB, LeBoeuf SE, Gay LJ, et al. Mitochondrial complex I activity and NAD+/NADH balance regulate breast cancer progression. *J Clin Invest* (2013) 123(3):1068–81. doi: 10.1172/JCI64264
38. Ullmark T, Montano G, Jarvstrat L, Jernmark Nilsson H, Hakansson E, Drott K, et al. Anti-apoptotic quinolinate phosphoribosyltransferase (QPRT) is a

target gene of Wilms' tumor gene 1 (WT1) protein in leukemic cells. *Biochem Biophys Res Commun* (2017) 482(4):802–7. doi: 10.1016/j.bbrc.2016.11.114
39. Yue Z, Shusheng J, Hongtao S, Shu Z, Lan H, Qingyuan Z, et al. Silencing DSCAM-AS1 suppresses the growth and invasion of ER-positive breast cancer cells by downregulating both DCTPP1 and QPRT. *Aging (Albany NY)* (2020) 12(14):14754–74. doi: 10.18632/aging.103538
40. Sinha S, Sharma S, Vora J, Shrivastava N. Emerging role of sirtuins in breast cancer metastasis and multidrug resistance: Implication for novel therapeutic strategies targeting sirtuins. *Pharmacol Res* (2020) 158:104880. doi: 10.1016/j.phrs.2020.104880
41. Shi L, Tang X, Qian M, Liu Z, Meng F, Fu L, et al. A SIRT1-centered circuitry regulates breast cancer stemness and metastasis. *Oncogene* (2018) 37 (49):6299–315. doi: 10.1038/s41388-018-0370-5
42. Elstrodt F, Hollestelle A, Nagel JH, Gorin M, Wasielewski M, van den Ouweland A, et al. BRCA1 mutation analysis of 41 human breast cancer cell lines reveals three new deleterious mutants. *Cancer Res* (2006) 66(1):41–5. doi: 10.1158/0008-5472.CAN-05-2853
43. Ferrari D, Malavasi F, Antonioli L. A Purinergic Trail for Metastases. *Trends Pharmacol Sci* (2017) 38(3):277–90. doi: 10.1016/j.tips.2016.11.010
44. Bellefeuille SD, Molle CM, Gendron FP. Reviewing the role of P2Y receptors in specific gastrointestinal cancers. *Purinergic Signal* (2019) 15(4):451–63. doi: 10.1007/s11302-019-09678-x
45. Kennedy C. P2Y11 Receptors: Properties, Distribution and Functions. *Adv Exp Med Biol* (2017) 1051:107–22. doi: 10.1007/5584_2017_89
46. Khalid M, Brisson L, Tariq M, Hao Y, Guibon R, Fromont G, et al. Carcinoma-specific expression of P2Y11 receptor and its contribution in ATP-induced purinergic signalling and cell migration in human hepatocellular carcinoma cells. *Oncotarget* (2017) 8(23):37278–90. doi: 10.18632/oncotarget.16191
47. Braidy N, Guillemin GJ, Grant R. Effects of Kynurenine Pathway Inhibition on NAD Metabolism and Cell Viability in Human Primary Astrocytes and Neurons. *Int J Tryptophan Res* (2011) 4:29–37. doi: 10.4137/IJTR.S7052
48. Jha AM, Singh AC, Bharti M. Germ cell mutagenicity of phthalic acid in mice. *Mutat Res* (1998) 422(2):207–12. doi: 10.1016/s0027-5107(98) 00151-1

Conflict of Interest: The authors declare that the research was conducted in the absence of any commercial or financial relationships that could be construed as a potential conflict of interest.

frontiers in Endocrinology

ORIGINAL RESEARCH
published: 30 April 2021
doi: 10.3389/fendo.2021.642928

Complications of Pregnancy and the Risk of Developing Endometrial or Ovarian Cancer: A Case-Control Study

Yang Liu[1], *Xingyu Chen*[1], *Jiayi Sheng*[1], *Xinyi Sun*[2], *George Qiaoqi Chen*[3], *Min Zhao*[4]* *and Qi Chen*[2]

[1] School of Medicine, Nanjing Medical University, Nanjing, China, [2] Department of Obstetrics & Gynaecology, The University of Auckland, Auckland, New Zealand, [3] School of Medicine, The University of Manchester, North Manchester, United Kingdom, [4] Department of Gynaecology, The Affiliated Wuxi Maternity and Child Health Care Hospital of Nanjing Medical University, Wuxi, China

OPEN ACCESS

Edited by:
Ralf Jockers,
Université de Paris, France

Reviewed by:
Giovanni Luca,
University of Perugia, Italy
Bei Xu,
Heart Research Institute, Australia

***Correspondence:**
Min Zhao
q.chen@auckland.ac.nz;
zmdoc2002@163.com

Specialty section:
This article was submitted to Cancer Endocrinology, a section of the journal Frontiers in Endocrinology

Received: 17 December 2020
Accepted: 25 March 2021
Published: 30 April 2021

Citation:
Liu Y, Chen X, Sheng J, Sun X, Chen GQ, Zhao M and Chen Q (2021) Complications of Pregnancy and the Risk of Developing Endometrial or Ovarian Cancer: A Case-Control Study. Front. Endocrinol. 12:642928. doi: 10.3389/fendo.2021.642928

Background: The association of complications of pregnancy and the risk of developing gynecological cancer is controversial with the limited study. In this study, we investigated the association of preeclampsia, or gestational diabetes mellitus (GDM), or large for gestational age (LGA), or intrauterine growth restriction (IUGR) and the risk of endometrial or ovarian cancer.

Methods: In this case-control study, 189 women with endometrial cancer and 119 women with ovarian cancer were included. 342 women without gynecological cancers were randomly selected as a control group. Data on the history of pregnancy and age at diagnosis of gynecological cancer as well as the use of intrauterine devices (IUDs) were collected.

Results: Women with a history of preeclampsia or IUGR did not have an increased risk of developing endometrial or ovarian cancer. While women with a history of GDM or with the delivery of LGA infant increased the risk of developing endometrial cancer but not ovarian cancer. The odds of women with a history of GDM or with the delivery of LGA infant developing endometrial cancer was 2.691 (95% CI: 1.548, 4.3635, p=0.0003), or 6.383 (95% CI: 2.812, 13.68, p<0.0001) respectively, compared to the controls. The odds ratio of women who did not use IUDs developing ovarian cancer was 1.606 (95% CI: 1.057, 2.434), compared to the controls. There was no association of age at first birth and developing endometrial or ovarian cancer.

Conclusion: Our observational data suggested that GDM and delivery of an LGA infant are associated with an increased risk of endometrial cancer.

Keywords: preeclampsia, GDM, IUGR, endometrial cancer, ovarian cancer

INTRODUCTION

Endometrial and ovarian cancers are most common gynecological cancer worldwide (1). Despite the risk of cancer being greatly dependent on lifestyle factors, which may in many ways be different between multiparous and nulliparous women, strong evidence has previously suggested that women with multiparous have significantly decreased the incidence of endometrial and ovarian cancer (2–6). A recent study further reported that women with multiparous delay the time of developing endometrial cancer (7). Interestingly a recent study reported that women with multiparous have a similar overall risk of developing non-gynecological cancers compared to women with a lower parity (8). This study further confirmed a negative association of pregnancy with developing gynecological cancer.

The underlying mechanism of this long-term protective effect by multiparous has been suggested by the shift in hormonal balance (reduced levels of estrogen and elevated levels of progesterone) and lack of ovulation during pregnancy (5, 9, 10), although a recent study indicated that the shift in hormonal balance (increased levels of progesterone in third trimester) is not the sole explanation for the protective effect of pregnancy (11). Hormonal changes may affect malignant transformation such as causing DNA damage (12) and new evidence further shows that in general estrogen has an impact on carcinogenesis (13). Elevated progesterone levels during pregnancy could inhibit estrogen-driven endometrial cell proliferation and promote differentiation and apoptosis of endometrial cells (14, 15). It is also well-known that breasting feeding significantly reduces gynecological cancer development (16), which could be due to the reduced ovulation.

During pregnancy, in addition to other organs (such as ovary and uterine) the placenta also produces large amounts of estrogen and progesterone (17). Recent evidences have showed aberrant maternal serum concentration of estrogen and progesterone in complications of pregnancy, such as preeclampsia, intra-uterine growth restriction (IUGR) and preterm birth (18–22). Imbalance between estrogen and progesterone could also impair fetal maturation and growth in IUGR infants (22). It is well believed that placental dysfunction is associated with most of obstetrical complications and contributes to the aberrant production of estrogen and progesterone.

The association of complications of pregnancy and developing gynecological cancer has been recently investigated with limited data. Preeclampsia was reported to increase the risk of developing endometrial cancer (23) or ovarian cancer (24, 25), however other studies did not find the increased risk for developing endometrial cancer in women with a history of preeclampsia (24–27). Gestational diabetes mellitus (GDM) was reported to increase the risk for developing endometrial cancer (28) or ovarian cancer (29). While recent studies reported there is no association of GDM and the development of endometrial or ovarian cancer later in women's life (30–32). These studies suggest that the association of complications of pregnancy with gynecological cancer is controversial. Therefore, in this observational case-control study, we investigated whether there is an association between complications of pregnancy and the incidence of endometrial and ovarian cancer.

METHODS

This study received approval by the Ethics Committee of The affiliated Wuxi Maternity and Child Health Care Hospital of Nanjing Medical University, China. Ethic Committees granted permission for data collection from hospital medical database.

Study Cohort

A total of 189 women who were diagnosed with endometrial cancers and 119 women who were diagnosed with ovarian cancer from January 2013 to December 2016 from Wuxi Maternity and Child Health Hospital, Nanjing Medical University, China were included. In addition, during the study period, 343 women without gynecological cancer were randomly selected as a control group. All these selected women had more than one live birth. Age at diagnosis of endometrial or ovarian cancers, age at first birth, status of menopause, history of complications of pregnancy including preeclampsia, GDM and IUGR, Large for gestational age (LGA) were collected. In addition, parity, gravida, the length of breastfeeding and use of intra uterine devices (IUDs) were collected from the hospital's electronic database.

Preeclampsia was defined as a maternal systolic blood pressure ≥140mmHg and/or diastolic blood pressure ≥ 90mmHg measured on two occasions separated by at least 6 hours, with or without proteinuria (>300 mg in a 24 hours period), and/or impaired liver function and/or lower platelet count, after 20 weeks of gestation in accordance with the guidelines of the International Society for the Study of Hypertension in Pregnancy (ISSHP) (33). GDM was defined as having any degree of glucose intolerance with onset or first recognition during pregnancy according to the World Health Organization (WHO) guidelines (http://www.who.int/iris/handle/10665/85975). LGA were defined as being of a birth weight at 90th percentile of greater for gestational age (34). IUGR was defined by an estimated fetal weight below the 10th percentile for its gestational age (35–37).

Statistical Analysis

Age at diagnosis or age at first delivery was expressed as median and range. ANOVA or Chi-square test was performed to analyze the difference in clinical characteristics of study cohort and the association of complications of pregnancy and endometrial or ovarian cancer. The odds ratio (OR) 95% confidence intervals (CI) for the association of GDM or LGA and the risk of developing endometrial or ovarian cancer was performed using GraphPad Prism version 8.4, GraphPad Software, La Jolla, CA. $p<0.05$ was considered as the threshold for statistical significance.

RESULTS

Clinical Characteristics of the Study Population

The general characteristics of study participants are summarized in **Table 1**. The median age was 53 (range 29-65) years in women with endometrial cancer, 50 (range 24-68) years in women with ovarian cancer and 43 (range 20-65) years in women in the control group. The age at first time of delivery was 25 (range 19-33) years in women with endometrial cancer, 24 (range 20-32) years in women with ovarian cancer, and 25 (range 18-36) years in controls. There was no difference in the age of first birth (p=0.248).

GDM Was Associated With Developing Endometrial Cancer

Of 189 women diagnosed with endometrial cancer, there were 33 (17.5%) patients with a history of GDM, which was significantly higher than that in controls (7.3%) (**Table 2**). The odds ratio of women with a history of GDM developing endometrial cancer was 2.691 (95% CI: 1.548, 4.3635, p=0.0003), compared to the controls. In addition, there were 25 (13%) patients who delivered an LGA infant in their previous pregnancies, which was significantly higher than that in controls (2.3%) (**Table 2**). The odds ratio of women who delivered an LGA infant developing endometrial cancer was 6.383 (95% CI: 2.812, 13.68, p<0.0001), compared to the controls.

In contrast, the portion of patients with a history of preeclampsia (1.6%) or with a history of IUGR (1.5%) was similar with controls (1.7% or 1.5%, respectively, **Table 2**). Due to the small sample size, we were not able to perform a statistical analysis. The portion of women diagnosed with endometrial cancer who used intrauterine devices (IUDs) (53%) was not statistically different to the controls (49%) (p=0.621). The portion of women diagnosed with endometrial cancer who had breastfeeding was also no difference to the controls (91% vs 93%, p=0.447).

Complications of Pregnancy Was Not Associated With Developing Ovarian Cancer

Of 119 women diagnosed with ovarian cancer, there were 5 (4.2%) patients with a history of GDM, which was no different to the controls (2.3%) (**Table 3**, p=0.239). There were 5 (4.2%) patients who delivered an LGA infant in their previous pregnancies, which was also not statistically different to the controls (7.3%) (**Table 3**, p=0.288). In addition, the proportion of women with a history of preeclampsia (1.7%) or with a history of IUGR (0.8%) in women diagnosed with ovarian cancer was also no different to the controls (1.7% or 1.5%). Due to the small sample size, we were not able to perform a statistical analysis. The portion of women with ovarian cancer who had breastfeeding (90%) was also no difference to the controls (93%, p=0.315). However, the portion of women diagnosed with ovarian cancer who used intrauterine devices (IUDs) (39%) was significantly lower than the controls (49%) (**Table 3**, p=0.029). The odds ratio of women without using IUDs developing ovarian cancer was 1.606 (95% CI: 1.057, 2.435, p=0.029), compared to the controls.

TABLE 2 | The association of complications of pregnancy and endometrial cancer.

	Women with endometrial cancer (n=189)	Women without endometrial cancer (n=343)	P value (Chi-square test)
GDM (n, %)	33 (17.5%)	25 (7.3%)	0.0003
LGA (n, %)	25 (13%)	8 (2.3%)	<0.0001
Breastfeeding (n, %) *	93 (90%)	311 (93%)	0.447
Preeclampsia (n, %)	3 (1.6%)	6 (1.7%)	0.889
IUGR (n, %)	1 (0.5%)	5 (1.5%)	N/A
Using IUD (n, %)	100 (53%)	167 (49%)	0.621

**, data on 36 cases with endometrial cancer and 8 controls missed; N/A, not applicable.*

TABLE 3 | The association of complications of pregnancy and ovarian cancer.

	Women with ovarian cancer (n=119)	Women without ovarian cancer (n=343)	P value (Chi-square test)
GDM (n, %)	5 (4.2%)	25 (7.3%)	0.239
LGA (n, %)	5 (4.2%)	8 (2.3%)	0.288
Breastfeeding (n, %) *	93 (90%)	311 (93%) n=335	0.315
Preeclampsia (n, %)	2 (1.7%)	6 (1.7%)	N/A
IUGR (n, %)	1 (0.8%)	5 (1.5%)	N/A
Using IUD (n, %)	46 (39%)	167 (49%)#	0.029

**, data on 16 cases with ovarian cancer and 8 controls missed; #, data on 11 controls missed; N/A, not applicable due to small same size.*

TABLE 1 | Clinical characteristics of study population.

	Endometrial cancer (n=189)	Ovarian cancer (n=119)	Controls (n=343)	P value
Age at diagnosis (years, median/range)	53 (29-65)	50 (24-68)	43 (20-64)	<0.00001 (ANOVA)
Age at first birth (years, median/range)	25 (19-33)	24 (20-32)	25 (18-36)	0.248 (ANOVA)
Parity (number, %)				Chi square
P=1	128 (68%)	94 (79%)	280 (82%)	0.001
P≥2	61 (32%)	25 (21%)	63 (18%)	
Abortion (number, %)	N=136	N=79	N=260	Chi square
Once	76 (56%)	39 (49%)	134 (51%)	0.691
Twice	39 (29%)	22 (28%)	80 (31%)	
≥ Thrice	21 (15%)	18 (23%)	46 (18%)	

DISCUSSION

In this case-control study in Chinese population, we found that women with a history of GDM or with delivery of LGA infants, but not preeclampsia increased the risk of developing endometrial cancer. In contrast, women with a history of preeclampsia or GDM or with delivery of LGA infants or IUGR did not increase the risk of developing ovarian cancer. Use of IUDs only reduced the risk for developing ovarian cancer.

The pathophysiology of cancer associated to pregnancy is not fully understood. However, the negative association of parity and the incidence of endometrial and ovarian cancer can be explained by hormonal changes, immunological suppression and increased permeability and vascularization during pregnancy. Increased level of estrogen is one of the risk factors for developing endometrial or ovarian cancer through stimulating the growth of estrogen-dependent tissue (14, 15). During pregnancy, placenta also produces large amounts of hormones and placental dysfunction is now recognized as one of the pathogenesis of complications of pregnancy. The aberrant maternal serum concentration of estrogen and progesterone are reported in complications of pregnancy (18–22). Recent study also reported that the expression of estrogen receptor α (ERα) was increased in extravillous trophoblasts in GDM (38). This consequently suggest that complications of pregnancy may increase the risk of developing gynecological cancer. However, the findings recently reported in the literature are not consistent, due to the limited studies.

To date two recent studies investigated the association of GDM and the risk of developing endometrial cancer. Study led by Wartko reported that GDM increased the risk for developing endometrial cancer later in women's life (28), while another study did not find this association (30). In our current study, we found that a history of GDM increased the risk of developing endometrial cancer with an odd ratio of 2.69, which is consistent with the Wartko's study (28). It is well-known that GDM is associated with delivery of LGA infants (39, 40) and the association of delivery of LGA infants and the risk of developing endometrial cancer has not been well investigated. In our current study, we also found that delivery of LGA infants in previous pregnancy significantly increased the risk of developing endometrial cancer. The odd ratio in women with a delivery of LGA infant developing ovarian cancer was 6.4 (95% CI: 2.812, 13.68), compared to the controls.

To date, only four studies investigated the association of GDM and the risk of developing ovarian cancer. Study led by Fuchs (29) reported a significant positive association of GDM and endometrial cancer, and other two studies reported a positive association of GDM and endometrial cancer, but the association did not reach statistical difference (30, 32). While, a recent study did not find this association (31). In our current study, we also did not find a significant association between GDM and the risk of developing ovarian cancer.

Prior studies investigating the association of preeclampsia and risk of developing endometrial cancer or ovarian cancer are limited in the literature due to the relatively low prevalence of preeclampsia. Although a recent study reported an increased risk of developing endometrial cancer in women with a history of preeclampsia (23), four previous studies reported that women with a history of preeclampsia did not have an increased risk of developing endometrial cancer (24–27). In our current case-control study, we also did not find an association of preeclampsia and endometrial cancer. Due to the small sample size of preeclampsia, previous studies including our current study were not able to analyze whether the time of onset of preeclampsia is associated with the risk of developing endometrial cancer. It is now believed that placental dysfunction is more related to the pathogenesis of early onset preeclampsia while maternal response is likely involved in the pathogenesis of late onset preeclampsia (41). One study reported that early onset preeclampsia increased the risk of developing endometrial cancer (26). In addition, in our current study, we found that preeclampsia did not increase the risk of developing ovarian cancer, although previous two studies reported an association of preeclampsia and risk of developing ovarian cancer. This difference could be due the small sample size seen in our study. Preeclampsia and IUGR share very similar uteroplacental pathology and the association of women with IUGR and risk of developing gynecological cancer has not been well investigated yet. In our current study we found that IUGR did not increase the risk of developing either endometrial or ovarian cancer.

Across the board, the IUD is known to lower risk for many gynecological cancers, including endometrial (42) and ovarian cancer (43). In our current study, we found that the number of women with ovarian cancer who used IUDs was significantly lower than the controls, suggesting use of IUDs has a protective effect on developing ovarian cancer. This finding was consistent with previous study. However, we did not find the lower number of women diagnosed with endometrial cancer who used IUDs, compared to the controls. We do not know the exact reason causing this difference between previous study and our study. This could be due to the types of IUD and the duration of use between two studies.

Age at first birth has been suggested to be associated with the risk of developing endometrial cancer, but this finding is not consistent. A recent study with two population-based prospective cohort studies reported that age at first birth is unlikely to increase the risk of developing endometrial cancer (44). In our current study, we also found that there was no difference in age at first birth between women diagnosed with endometrial or ovarian cancer and the controls. However, due to the previous One-Child Policy in China, the majority of cases included in this study were uniparous (one birth). This may result in that the age at first birth was relatively younger.

We acknowledge that the sample size in our current study is relatively small and all the data were collected from a single tertiary hospital. In addition, the association of subtypes of endometrial or ovarian cancer and complications of pregnancy were not able to be further analyzed. Future study with a large sample size and multicenter care is required.

In this study, we found that GDM and delivery of LGA increased the risk of developing endometrial but not ovarian

cancer. Although these two types of cancer are hormonal dependents, we do not know the exact reasons for our finding. Studies have reported that women with a history of GDM have a 7-fold higher risk of developing diabetes mellitus in women's later life (45). Previous studies also found an association of endometrial cancer, but not ovarian cancer and diabetes mellitus (46–48), suggesting diabetes mellitus is a risk factor for developing endometrial cancer.

In this study, we reported the difference in the association of endometrial cancer with complicated pregnancy between GDM and preeclampsia. We do not know the exact reason for this finding, but this could be due to the difference in the pathogenesis of these two complications. A study reported an increased placental leptin expression in GDM, and leptin is one of the most probable candidates involved in the pathophysiology of GDM (49). While, levels of human chorionic gonadotrophin (hCG) and corticotrophin-releasing hormone (CRH) which are produced by the placenta are significantly increased in women with preeclampsia.

In conclusion, our current study reported that women with a history of GDM or with a delivery of LGA infant increased the risk of developing endometrial cancer but not ovarian cancer. In contrast, women with a history of preeclampsia or IUGR did not increase the risk of developing either endometrial or ovarian cancer. Age at first birth is unlikely to be associated with the risk of developing endometrial or ovarian cancer.

During pregnancy, your placenta makes hormones that cause glucose to build up in your blood. Usually, your pancreas can send out enough insulin to handle it. But if your body can't make enough insulin or stops using insulin as it should, your blood sugar levels rise, and you get gestational diabetes.

DATA AVAILABILITY STATEMENT

The original contributions presented in the study are included in the article/supplementary material. Further inquiries can be directed to the corresponding author.

ETHICS STATEMENT

The studies involving human participants were reviewed and approved by the Ethics Committee of The affiliated Wuxi Maternity and Child Health Care Hospital of Nanjing Medical University, China. Written informed consent for participation was not required for this study in accordance with the national legislation and the institutional requirements.

AUTHOR CONTRIBUTIONS

All authors contributed to the article and approved the submitted version. In addition to this, each author contributed to the following work: YL, XC, JS: collected the data reported in this work. XS: literature data collection. GC, MZ, QC: designed study and wrote the manuscript draft.

FUNDING

This study received the support from Outstanding Talent Project of Wuxi Health and Family Planning Commission of China (ZDRC023).

REFERENCES

1. Bray F, Ferlay J, Soerjomataram I, Siegel RL, Torre LA, Jemal A. Global cancer statistics 2018: GLOBOCAN estimates of incidence and mortality worldwide for 36 cancers in 185 countries. *CA Cancer J Clin* (2018) 68(6):394–424. doi: 10.3322/caac.21492
2. Daly M, Obrams GI. Epidemiology and risk assessment for ovarian cancer. *Semin Oncol* (1998) 25(3):255–64.
3. Risch HA. Hormonal etiology of epithelial ovarian cancer, with a hypothesis concerning the role of androgens and progesterone. *J Natl Cancer Inst* (1998) 90(23):1774–86. doi: 10.1093/jnci/90.23.1774
4. Pike MC, Pearce CL, Wu AH. Prevention of cancers of the breast, endometrium and ovary. *Oncogene* (2004) 23(38):6379–91. doi: 10.1038/sj.onc.1207899
5. Karageorgi S, Hankinson SE, Kraft P, De Vivo I. Reproductive factors and postmenopausal hormone use in relation to endometrial cancer risk in the Nurses' Health Study cohort 1976-2004. *Int J Cancer* (2010) 126(1):208–16. doi: 10.1002/ijc.24672
6. Helmrich SP, Shapiro S, Rosenberg L, Kaufman DW, Slone D, Bain C, et al. Risk factors for breast cancer. *Am J Epidemiol* (1983) 117(1):35–45. doi: 10.1093/oxfordjournals.aje.a113513
7. Chen Q TM, Guo F, Lau S, Zhao M. Parity Correlates with the Timing of Developing Endometrial Cancer, But Not Subtype of Endometrial Cancer. *J Cancer* (2015) 6(11):1087. doi: 10.7150/jca.12736
8. Högnäs E, Kauppila A, Hinkula M, Tapanainen JS, Pukkala E. Incidence of cancer among grand multiparous women in Finland with special focus on non-gynecological cancers: A population-based cohort study. *Acta Oncol* (2016) 55(3):370–6. doi: 10.3109/0284186X.2015.1063775
9. Dossus L, Allen N, Kaaks R, Bakken K, Lund E, Tjonneland A, et al. Reproductive risk factors and endometrial cancer: the European Prospective Investigation into Cancer and Nutrition. *Int J Cancer* (2010) 127(2):442–51. doi: 10.1002/ijc.25050
10. Jordan SJ, Green AC, Nagle CM, Olsen CM, Whiteman DC, Webb PM, et al. Beyond parity: association of ovarian cancer with length of gestation and offspring characteristics. *Am J Epidemiol* (2009) 170(5):607–14. doi: 10.1093/aje/kwp185
11. Chen Q, Guo F, Jin HY, Lau S, Stone P, Chamley L. Phagocytosis of apoptotic trophoblastic debris protects endothelial cells against activation. *Placenta* (2012) 33(7):548–53. doi: 10.1016/j.placenta.2012.03.007
12. Roy D, Liehr JG. Estrogen, DNA damage and mutations. *Mutat Res* (1999) 424(1-2):107–15. doi: 10.1016/S0027-5107(99)00012-3
13. Chen GG, Zeng Q, Tse GM. Estrogen and its receptors in cancer. *Med Res Rev* (2008) 28(6):954–74. doi: 10.1002/med.20131
14. Kim JJ, Chapman-Davis E. Role of progesterone in endometrial cancer. *Semin Reprod Med* (2010) 28(1):81–90. doi: 10.1055/s-0029-1242998
15. Henderson BE, Feigelson HS. Hormonal carcinogenesis. *Carcinogenesis* (2000) 21(3):427–33. doi: 10.1093/carcin/21.3.427
16. Jordan SJ, Na R, Johnatty SE, Wise LA, Adami HO, Brinton LA, et al. Breastfeeding and Endometrial Cancer Risk: An Analysis From the Epidemiology of Endometrial Cancer Consortium. *Obstet Gynecol* (2017) 129(6):1059–67. doi: 10.1097/AOG.0000000000002057
17. Abbassi-Ghanavati M, Greer LG, Cunningham FG. Pregnancy and laboratory studies: a reference table for clinicians. *Obstet Gynecol* (2009) 114(6):1326–31. doi: 10.1097/AOG.0b013e3181c2bde8
18. Mazor M, Hershkovitz R, Chaim W, Levy J, Sharony Y, Leiberman JR, et al. Human preterm birth is associated with systemic and local changes in

progesterone/17 beta-estradiol ratios. *Am J Obstet Gynecol* (1994) 171(1):231–6. doi: 10.1016/0002-9378(94)90474-X
19. Berkane N, Liere P, Lefevre G, Alfaidy N, Nahed RA, Vincent J, et al. Abnormal steroidogenesis and aromatase activity in preeclampsia. *Placenta* (2018) 69:40–9. doi: 10.1016/j.placenta.2018.07.004
20. Hertig A, Liere P, Chabbert-Buffet N, Fort J, Pianos A, Eychenne B, et al. Steroid profiling in preeclamptic women: evidence for aromatase deficiency. *Am J Obstet Gynecol* (2010) 203(5):477 e1–9. doi: 10.1016/j.ajog.2010.06.011
21. Jobe SO, Tyler CT, Magness RR. Aberrant synthesis, metabolism, and plasma accumulation of circulating estrogens and estrogen metabolites in preeclampsia implications for vascular dysfunction. *Hypertension (Dallas Tex 1979)* (2013) 61 (2):480–7. doi: 10.1161/HYPERTENSIONAHA.111.201624
22. Baud O, Berkane N. Hormonal Changes Associated With Intra-Uterine Growth Restriction: Impact on the Developing Brain and Future Neurodevelopment. *Front Endocrinol* (2019) 10:179–9. doi: 10.3389/fendo.2019.00179
23. Trabert B, Troisi R, Grotmol T, Ekbom A, Engeland A, Gissler M, et al. Associations of pregnancy-related factors and birth characteristics with risk of endometrial cancer: A Nordic population-based case–control study. *Int J Cancer* (2020) 146(6):1523–31. doi: 10.1002/ijc.32494
24. Paltiel O, Friedlander Y, Tiram E, Barchana M, Xue X, Harlap S. Cancer after pre-eclampsia: follow up of the Jerusalem perinatal study cohort. *BMJ* (2004) 328(7445):919. doi: 10.1136/bmj.38032.820451.7C
25. Calderon-Margalit R, Friedlander Y, Yanetz R, Deutsch L, Perrin MC, Kleinhaus K, et al. Preeclampsia and subsequent risk of cancer: update from the Jerusalem Perinatal Study. *Am J Obstet Gynecol* (2009) 200(1):63.e1–63.e635. doi: 10.1016/j.ajog.2008.06.057
26. Hallum S, Pinborg A, Kamper-Jørgensen M. Long-term impact of preeclampsia on maternal endometrial cancer risk. *Br J Cancer* (2016) 114 (7):809–12. doi: 10.1038/bjc.2016.55
27. Mogren I, Stenlund H, Högberg U. Long-term impact of reproductive factors on the risk of cervical, endometrial, ovarian and breast cancer. *Acta Oncol* (2001) 40(7):849–54. doi: 10.1080/02841860152703481
28. Wartko PD, Beck TL, Reed SD, Mueller BA, Hawes SE. Association of endometrial hyperplasia and cancer with a history of gestational diabetes. *Cancer Causes Control* (2017) 28(8):819–28. doi: 10.1007/s10552-017-0908-9
29. Fuchs O, Sheiner E, Meirovitz M, Davidson E, Sergienko R, Kessous R. The association between a history of gestational diabetes mellitus and future risk for female malignancies. *Arch Gynecol Obstet* (2017) 295(3):731–6. doi: 10.1007/s00404-016-4275-7
30. Pace R, Rahme E, Dasgupta K. Gestational diabetes mellitus and risk of incident primary cancer: A population-based retrospective cohort study. *J Diabetes* (2020) 12(1):87–90. doi: 10.1111/1753-0407.12988
31. Peng Y-S, Lin J-R, Cheng B-H, Ho C, Lin Y-H, Shen C-H, et al. Incidence and relative risk for developing cancers in women with gestational diabetes mellitus: a nationwide cohort study in Taiwan. *BMJ Open* (2019) 9(2): e024583. doi: 10.1136/bmjopen-2018-024583
32. Han K-T, Cho GJ, Kim EH. Evaluation of the Association between Gestational Diabetes Mellitus at First Pregnancy and Cancer within 10 Years Postpartum Using National Health Insurance Data in South Korea. *Int J Environ Res Public Health* (2018) 15(12):2646. doi: 10.3390/ijerph15122646
33. Brown MA, Magee LA, Kenny LC, Karumanchi SA, McCarthy FP, Saito S, et al. The hypertensive disorders of pregnancy: ISSHP classification, diagnosis & management recommendations for international practice. *Pregnancy Hypertens* (2018) 13:291–310. doi: 10.1016/j.preghy.2018.05.004
34. Alexander GR, Himes JH, Kaufman RB, Mor J, Kogan M. A United States national reference for fetal growth. *Obstet Gynecol* (1996) 87(2):163–8. doi: 10.1016/0029-7844(95)00386-X
35. ACOG Practice bulletin no. 134: fetal growth restriction. *Obstet Gynecol* (2013) 121(5):1122–33. doi: 10.1097/01.AOG.0000429658.85846.f9
36. Lausman A, McCarthy FP, Walker M, Kingdom J. Screening, diagnosis, and management of intrauterine growth restriction. *J Obstet Gynaecol Can* (2012) 34(1):17–28. doi: 10.1016/S1701-2163(16)35129-5
37. Vayssiere C, Sentilhes L, Ego A, Bernard C, Cambourieu D, Flamant C, et al. Fetal growth restriction and intra-uterine growth restriction: guidelines for clinical practice from the French College of Gynaecologists and Obstetricians. *Eur J Obstet Gynecol Reprod Biol* (2015) 193:10–8. doi: 10.1016/j.ejogrb.2015.06.021
38. Knabl J, Hiden U, Hüttenbrenner R, Riedel C, Hutter S, Kirn V, et al. GDM Alters Expression of Placental Estrogen Receptor α in a Cell Type and Gender-Specific Manner. *Reprod Sci* (2015) 22(12):1488–95. doi: 10.1177/1933719115585147
39. Casey BM, Lucas MJ, McIntire DD, Leveno KJ. Pregnancy outcomes in women with gestational diabetes compared with the general obstetric population. *Obstet Gynecol* (1997) 90(6):869–73. doi: 10.1016/S0029-7844(97)00542-5
40. Yang J, Cummings EA, O'Connell C, Jangaard K. Fetal and neonatal outcomes of diabetic pregnancies. *Obstet Gynecol* (2006) 108(3 Pt 1):644–50. doi: 10.1097/01.AOG.0000231688.08263.47
41. Redman CW. Early and late onset preeclampsia: Two sides of the same coin. *Pregnancy Hypertens* (2017) 7:58. doi: 10.1016/j.preghy.2016.10.011
42. Felix AS, Gaudet MM, La Vecchia C, Nagle CM, Shu XO, Weiderpass E, et al. Intrauterine devices and endometrial cancer risk: a pooled analysis of the Epidemiology of Endometrial Cancer Consortium. *Int J Cancer* (2015) 136(5): E410–22. doi: 10.1002/ijc.29229
43. Wheeler LJ, Desanto K, Teal SB, Sheeder J, Guntupalli SR. Intrauterine Device Use and Ovarian Cancer Risk: A Systematic Review and Meta-analysis. *Obstet Gynecol* (2019) 134(4):791–800. doi: 10.1097/AOG.0000000000003463
44. Sugawara Y, Sugiyama K, Tomata Y, Kanemura S, Fukao A, Tsuji I. Age at First Birth and the Risk of Endometrial Cancer Incidence: A Pooled Analysis of Two Prospective Cohort Studies among Japanese Women. *J Cancer* (2018) 9(23):4422–9. doi: 10.7150/jca.26242
45. Bellamy L, Casas JP, Hingorani AD, Williams D. Type 2 diabetes mellitus after gestational diabetes: a systematic review and meta-analysis. *Lancet (London England)* (2009) 373(9677):1773–9. doi: 10.1016/S0140-6736(09)60731-5
46. La Vecchia C, Negri E, Franceschi S, D'Avanzo B, Boyle P. A case-control study of diabetes mellitus and cancer risk. *Br J Cancer* (1994) 70(5):950–3. doi: 10.1038/bjc.1994.427
47. Muti P, Quattrin T, Grant BJ, Krogh V, Micheli A, Schünemann HJ, et al. Fasting glucose is a risk factor for breast cancer: a prospective study. *Cancer Epidemiol Biomarkers Prev* (2002) 11(11):1361–8.
48. Adler AI, Weiss NS, Kamb ML, Lyon JL. Is diabetes mellitus a risk factor for ovarian cancer? A case-control study in Utah and Washington (United States). *Cancer Causes Control* (1996) 7(4):475–8. doi: 10.1007/BF00052674
49. Kampmann FB, Thuesen ACB, Hjort L, Bjerregaard AA, Chavarro JE, Frystyk J, et al. Increased leptin, decreased adiponectin and FGF21 concentrations in adolescent offspring of women with gestational diabetes. *Eur J Endocrinol* (2019) 181(6):691–700. doi: 10.1530/EJE-19-0658

Conflict of Interest: The authors declare that the research was conducted in the absence of any commercial or financial relationships that could be construed as a potential conflict of interest.

frontiers in Endocrinology

ORIGINAL RESEARCH
published: 07 June 2021
doi: 10.3389/fendo.2021.654975

The Impact of ^{68}Gallium DOTA PET/CT in Managing Patients With Sporadic and Familial Pancreatic Neuroendocrine Tumours

Daniel J. Cuthbertson[1,2†], Jorge Barriuso[3,4†], Angela Lamarca[3,4], Prakash Manoharan[5], Thomas Westwood[5], Matthew Jaffa[1], Stephen W. Fenwick[1], Christina Nuttall[4], Fiona Lalloo[6], Andreas Prachalias[7], Michail Pizanias[7], Hulya Wieshmann[1], Mairead G. McNamara[3,4], Richard Hubner[3,4], Raj Srirajaskanthan[8], Gillian Vivian[8], John Ramage[8], Martin O. Weickert[9], D Mark Pritchard[1,2], Sobhan Vinjamuri[1], Juan Valle[3,4] and Vincent S. Yip[10,11]*

[1] Liverpool University Hospitals NHS Foundation Trust, ENETS Centre of Excellence, Liverpool, United Kingdom, [2] Faculty of Health and Life Sciences, University of Liverpool, Liverpool, United Kingdom, [3] Division of Cancer Sciences, University of Manchester, Manchester, United Kingdom, [4] Department of Medical Oncology, The Christie NHS Foundation Trust, ENETS Centre of Excellence, Manchester, United Kingdom, [5] Department of Radiology and Nuclear Medicine, The Christie NHS Foundation Trust ENETS Centre of Excellence, Manchester, United Kingdom, [6] Department of Clinical Genetics, Manchester Centre for Genomic Medicine, Central Manchester University Hospitals NHS Foundation Trust, Saint Mary's Hospital, Manchester, United Kingdom, [7] Institute of Liver Studies, Kings College Hospital, London, United Kingdom, [8] Neuroendocrine Tumour Unit, KHP ENETS Centre of Excellence, Institute of Liver Studies, Kings College Hospital, London, United Kingdom, [9] The Arden Neuroendocrine Centre, ENETS Centre of Excellence, University Hospitals Coventry and Warwickshire, Coventry, United Kingdom, [10] Barts and the London HPB Centre, Royal London Hospital, London, United Kingdom, [11] Department of Pancreatobiliary Surgery, Royal Liverpool University Hospital, Liverpool, United Kingdom

OPEN ACCESS

Edited by:
Jianfeng Liu,
Huazhong University of Science and Technology, China

Reviewed by:
Dario Giuffrida,
Mediterranean Institute of Oncology (IOM), Italy
Simona Glasberg,
Hadassah Medical Center, Israel

***Correspondence:**
Daniel J. Cuthbertson
dan.cuthbertson@liv.ac.uk

[†]These authors have contributed equally to this work

Specialty section:
This article was submitted to Cancer Endocrinology, a section of the journal Frontiers in Endocrinology

Received: 18 January 2021
Accepted: 11 May 2021
Published: 07 June 2021

Citation:
Cuthbertson DJ, Barriuso J, Lamarca A, Manoharan P, Westwood T, Jaffa M, Fenwick SW, Nuttall C, Lalloo F, Prachalias A, Pizanias M, Wieshmann H, McNamara MG, Hubner R, Srirajaskanthan R, Vivian G, Ramage J, Weickert MO, Pritchard DM, Vinjamuri S, Valle J and Yip VS (2021) The Impact of ^{68}Gallium DOTA PET/CT in Managing Patients With Sporadic and Familial Pancreatic Neuroendocrine Tumours. Front. Endocrinol. 12:654975. doi: 10.3389/fendo.2021.654975

Objective: Pancreatic neuroendocrine tumours (panNETs) arise sporadically or as part of a genetic predisposition syndrome. CT/MRI, endoscopic ultrasonography and functional imaging using Octreoscan localise and stage disease. This study aimed to evaluate the complementary role of ^{68}Gallium (^{68}Ga)-DOTA PET/CT in managing patients with panNETs.

Design: A retrospective study conducted across three tertiary UK NET referral centres.

Methods: Demographic, clinical, biochemical, cross-sectional and functional imaging data were collected from patients who had undergone a ^{68}Ga-DOTA PET/CT scan for a suspected panNET.

Results: We collected data for 183 patients (97 male): median (SD) age 63 (14.9) years, 89.1 *vs.* 9.3% (n=163 vs. 17) alive *vs.* dead (3 data missing), 141 sporadic *vs.* 42 familial (MEN1, n=36; 85.7%) panNETs. Non-functional *vs.* functional tumours comprised 73.2 *vs.* 21.3% (n=134 *vs.* 39) (10 missing). Histological confirmation was available in 89% of individuals (n=163) but tumour grading (Ki67 classiifcation) was technically possible only in a smaller cohort (n=143): grade 1, 50.3% (n=72); grade 2, 46.2% (n=66) and grade 3, 3.5% (n=5) (40 histopathological classification either not technically feasible or biopsy not perfomed). 60.1% (n=110) were localised, 14.2% (n=26) locally advanced and 23.5% (n=43) metastatic (4 missing). 224 ^{68}Ga-DOTA PET/CT scans were performed in total for: diagnosis/staging 40% (n=88), post-operative assessment/clinical surveillance 53%

(n=117) and consideration of peptide receptor radionuclide therapy (PRRT) 8% (n=17) (2 missing). PET/CT results confirmed other imaging findings (53%), identified new disease sites (28.5%) and excluded suspected disease (5%). Overall, ^{68}Ga-DOTA PET/CT imaging findings provided additional information in 119 (54%) patients and influenced management in 85 (39%) cases.

Conclusion: ^{68}Ga-DOTA PET/CT imaging more accurately stages and guides treatment in patients with sporadic/familial panNETs with newly diagnosed/recurrent disease.

Keywords: pancreatic neuroendocrine tumours, ^{68}Gallium DOTA PET/CT, functional imaging, multiple endocrine neoplasia type 1, sporadic and familial

INTRODUCTION

Pancreatic neuroendocrine tumours (panNETs) are rare tumours accounting for ~2% of all pancreatic malignancies (1). However, national registry data suggest there is an increasing incidence of NETs (up to 2.5-fold higher) across all sites, stages and grade of disease (overall annual age-adjusted incidence rate of NETs ~7/100,000 US population; and panNETs specifically 0.48/100,000) (2). NET prevalence is considerably higher, with more patients presenting with earlier stage disease (3), better overall survival (4) and a variety of systemic treatments for grade (G), G1/G2 tumours that prolong progression-free or overall survival, including somatostatin analogues, ^{177}Lu-DOTATATE, systemic chemotherapy, everolimus and sunitinib (5–10).

An updated World Health Organisation (WHO) grading classification in 2017 suggested that pancreatic neuroendocrine neoplasms (p-NENs) be categorised according to the grade and degree of differentiation into *well-differentiated* pancreatic neuroendocrine tumours (panNETs) and *poorly differentiated* neuroendocrine carcinomas (NEC) (small cell and large cell subtypes) (11–13). Pancreatic NETs may be classified according to stage/disease extent (localised, regional or metastatic) and according to the histological grade using the Ki67 proliferation index from slower growing G1 and G2 tumours (G1/G2; Ki67 index <3% and 3-20% respectively) through to faster growing (well differentiated) G3 tumours (Ki67 index >20%) (14). Pancreatic NECs are characterised by a higher proliferative index (Ki67>20%) with usually a much more aggressive course (as for other poorly differentiated tumours). Histopathological data has validated prognostic value, independently predicting overall survival (15).

PanNETs may also be classified according to functionality, depending on secretion of hormones/peptides that cause specific symptoms/clinical syndromes. Patients with non-functional tumours, constituting the majority, tend to present late in the disease, often with distant metastases, and may have shorter life expectancy than those with functional panNETs (16). Finally, panNETs may arise sporadically or as part of a cancer-predisposing syndrome, such as in multiple endocrine neoplasia Type 1 (MEN1), von Hippel Lindau syndrome (VHL), tuberous sclerosis or neurofibromatosis (17). Functional panNETs occur more commonly in familial *vs.* sporadic panNETs (~40 *vs.* 10%); most commonly, insulinomas or gastrinomas (4). Indeed, panNETs occur in approximately two thirds of MEN1 patients and account for ~10% of all patients with panNETs (18).

Treatment of panNETs is dependent on multiple factors including tumour size, functionality, histological grade and stage. Imaging techniques used to stage NETs involve a combination of cross-sectional imaging (computer tomography [CT]/magnetic resonance imaging [MRI]) and endoscopic ultrasound (EUS). NETs generally over-express cell-surface somatostatin receptors (SSTRs), particularly subtypes 2a and 5, forming the basis for their detection and treatment using peptide receptor radionuclide therapy (PRRT) (19). In most NET specialist centres, functional imaging for staging of G1/G2 NETs involves somatostatin receptor scintigraphy (SRS), historically commonly using ^{111}In-labeled-DTPA-octreotide (Octreoscan) (20). However, its diagnostic utility is limited by poor image quality, less spatial resolution and a prolonged imaging protocol. More recently somatostatin receptor-based ^{68}Gallium positron emission tomography (^{68}Ga)-PET/CT imaging has been used due to the higher spatial resolution of PET *vs.* SPECT (3-6 mm *vs.* 10-15mm), allowing greater visualisation of small tumours, coupled with a 10-fold greater affinity of ^{68}Ga-DOTA peptides *vs.* ^{111}In-Octreotide for SSTRs (21). The higher sensitivity and specificity of ^{68}Ga DOTA PET/CT over conventional SRS has been shown previously (21). In a series of 51 patients with a histologically confirmed NET, who had evidence of disease biochemically or on cross-sectional imaging, but with a negative or equivocal ^{111}In-DTPA-octreotide scan, ^{68}Ga-DOTATATE PET was able to identify disease in 87% of cases, and in many revealed additional lesions, leading to a change in management in 71% of cases (22). This ability to provide information on primary tumour site, to facilitate accurate staging and influence management has meant it is considered the gold-standard functional imaging technique by many.

Several previous studies have determined the impact of ^{68}Gallium-DOTA based PET/CT imaging on patient management in individuals with lung carcinoids (23) or gastroenteropancreatic (GEP) NETS, but much less is known about its impact on patient management in patients specifically with panNETs (21, 24). The primary objective of this study was to determine to what extent ^{68}Ga-DOTA PET/CT imaging results provide complementary clinical information to cross-

sectional imaging (e.g., confirming suspected metastatic disease suspected on CT/MRI or identifying additional sites of local disease or regional/distant metastasis not seen on CT/MRI) and how this information may have led to an intra-or inter-modality change in management in a clinical population with both sporadic and hereditary panNETs.

METHODS

Inclusion Criteria

Patients referred to the NET multi-disciplinary team (NET MDT) meeting at 3 ENETS (European Neuroendocrine Tumour Society) Centres of Excellence (Liverpool, Manchester and London; representing four large hospitals: Aintree University Hospital, Liverpool; Royal Liverpool University Hospital, Liverpool; The Christie NHS Foundation Trust, Manchester; and King's College Hospital, London) were identified retrospectively from local electronic case-note records. All consecutive patients who underwent a ^{68}Ga-DOTA PET/CT scan between July 2015-July 2018 for a clinically suspected or histologically confirmed panNET were identified and included in the analysis (**Figure 1** shows a typical example of imaging findings using complementary cross-sectional and functional imaging). Where multiple/serial ^{68}Ga-DOTA PET/CT scans were performed in an individual, each episode was considered and analysed separately as the patient age, disease characteristics, previous treatments and scan findings may/will have been different. ^{68}Ga-DOTA PET/CT was used as part of the staging process for all patients with potentially-resectable disease, to detect recurrence in patients who had previous resections and to determine eligibility for PRRT. All patients had undergone comprehensive biochemical testing and cross-sectional imaging with CT/MRI and EUS where appropriate. A data collection template was created based on our related study in lung carcinoids (23).

Clinical Data

Clinical data were collected retrospectively. Demographic details (age and gender), current status (alive/deceased) and date of death or last follow up were recorded. We included patients with a sporadic panNET or with a familial predisposition to a panNET (multiple endocrine neoplasia type 1 (MEN type 1), von Hippel Lindau (VHL) syndrome, tuberous sclerosis (TSC), neurofibromatosis type 1 (NF1) or miscellaneous others including MUTYH-associated polyposis (MAP) or MAX mutation (familial paraganglioma syndrome)).

Biochemical Data

All patients underwent biochemical testing for chromogranin A/B and a full fasting gut hormone profile (glucagon, gastrin, somatostatin, pancreatic polypeptide (PP) and vasoactive

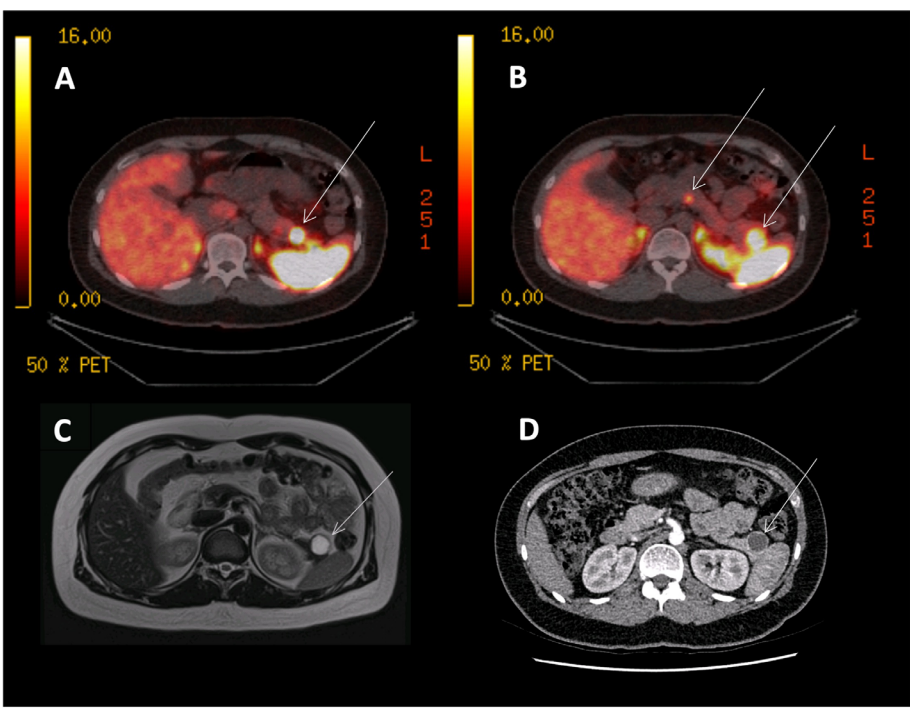

FIGURE 1 | ^{68}Ga-DOTANOC PET, CT and MRI images of an MEN1 patient with three panNETs (T3N0M0). **(A)** ^{68}Ga-DOTANOC PET/CT image showing a single panNET uptaking tracer in the pancreatic tail. **(B)** ^{68}Ga-DOTANOC PET/CT image showing two additional PanNETs in the tail and neck of the pancreas. **(C)** MRI scan showing a single lesion in the tail of the pancreas, commented as being 'cystic' and needing further imaging and discussion at MDT. **(D)** A CT scan showing a single cystic lesion in the tail of the pancreas, commented on as likely being a cyst.

intestinal polypeptide). The results recorded were those closest to the date of ^{68}Ga-DOTA PET/CT scanning, and pre-operatively if the scan was performed pre-operatively. Tumour functionality (functional *vs.* non-functional) was described according to either clinical symptoms (based on a hormonal hypersecretion syndrome) or biochemically (not based on immunohistochemistry analysis).

Treatment History

Details about treatments previously received were recorded (including disease surveillance). Surgical information included date of surgery, type (Whipple, distal pancreatectomy or enucleation), number of lymph nodes removed, and how many of them were involved with metastatic spread, resection margins (**R0**, cure or complete remission; **R1**, microscopic residual tumour; **R2**, macroscopic residual tumour) and whether there was tumour recurrence following surgery. Systemic therapy was also identified, including use of somatostatin analogues (SSAs), PRRT, molecular targeted therapies and chemotherapy.

Histopathological Data

Histopathological data was retrieved where tissue samples had been taken (using endoscopic ultrasound-guided fine-needle aspiration (EUS-FNA), fine needle biopsies (FNB) or surgical resection specimens) and undergone histopathological analysis; all histology was reviewed by dedicated experienced NET histopathologists at each centre. Data collected (where available) included the location of the primary pancreatic lesion (unclear, tail, body, head/neck or multifocal) and the number of panNETs.

Pathological data reported included the Ki67 index (%) and mitotic count (counts per High Power Field (HPF)) and the WHO staging (G1, 2 or 3). In some instances, particularly where EUS-FNA is employed, only tumour cytology is possible (to confirm a panNET), and grading (G1, 2 or 3 based on Ki67) is not always possible. This higher diagnostic sensitivity of FNB compared with EUS-FNA has been previously reported (25). Stage at first diagnosis was also recorded incorporating the TNM data measuring the tumour size (T1-T2 *vs.* T3) and determining the presence of lymph node/liver/lung/bone/other metastases.

Cross-Sectional Imaging Data

All patients underwent cross-sectional imaging with CT scanning of chest, abdomen and pelvis or MRI scanning of the abdomen. Dedicated CT/MRI pancreas specific protocols and endoscopic ultrasound examinations were performed where suggested by the NET MDT.

^{68}Ga-DOTA PET/CT Imaging Data

All patients underwent functional imaging with a ^{68}Ga-DOTA PET/CT scan in line with the local centre-specific imaging protocols acknowledging inherent differences in radiopharmaceutical preparation, scanning equipment and protocols. ^{68}Ga-DOTA PET/CT data included the scan date, the specific DOTA-peptide and stage of disease at time of ^{68}Ga-DOTA scan (categorised as not present, localised, locally advanced or metastatic). Representative PET/CT images are shown in **Figure 1**.

Indications for Performing the ^{68}Ga-DOTA PET/CT Scan

^{68}Ga-DOTA PET/CT scans (in preference to Octreoscan) were performed in all centres on the recommendation of the local MDT according to initial cross-sectional imaging (+/-histological) findings and according to a proposed management strategy decided by MDT consensus. The rationale for performing ^{68}Ga-DOTA PET/CT scanning was recorded as one of the following: i) diagnosis and staging for the initial presentation of a panNET ii) post-operative assessment/surveillance/monitoring for relapse; or iii) consideration of PRRT.

Findings From the ^{68}Ga-DOTA PET/CT Scan

Images from all ^{68}Ga-DOTA PET/CT images were independently reviewed by the dedicated NET MDT specialist radiologist/nuclear medicine physician (HW, SV, PM) with knowledge of relevant medical information and cross-sectional imaging or EUS findings. Information was collected regarding ^{68}Ga-DOTA PET/CT scan findings, including primary tumour (site and size), metastatic spread to the liver, regional lymph nodes, lung, bone and 'other' sites and whether the area of uptake was visible on CT, MRI or EUS. In addition, all PET scans were assessed according to whether uptake was equivalent to the background uptake by the liver. Many UK ENETS centres do not routinely report SUV_{max} measurements on ^{68}Ga-DOTA PET/CT scans in line with ENETS guidlelines/recommendations.

Findings were categorised as one of the following options: i) provided confirmatory information, concordant with other imaging techniques ii) identified sites of tumour not previously seen with other imaging (i.e., identification of occult metastases), iii) changed options of treatment (surgery/PRRT), iv) ruled out presence of metastases/disease suspected on previous imaging, v) confirmed resection/PRRT response after surgery or PRRT.

Impact on the Patient's Clinical Management

Treatment decisions endorsed by the local multi-disciplinary NET team and recorded formally as an MDT outcome were analysed. This was examined by looking at two components. First, we examined the number of episodes where ^{68}Ga-DOTA PET/CT provided either confirmatory information in suspected disease or additional information (either by identifying occult sites of disease or excluding suspected sites of disease). Secondly, we assessed the number of episodes where this information assisted or changed management (i.e. by confirmation of eligibility for PRRT or surgery or leading to an inter-modality change in treatment).

Statistical Analysis

Patient data were anonymised once data collection had been completed, and statistical analysis was carried out using IBM SPSS Statistics for Windows, Version 19.0. Armonk, NY: IBM Corp. (California, USA). Continuous variables were described with median, standard deviation (SD) and range. Categorical variables are presented as frequencies and percentages. Continuous variables were tested for normal distribution by

Shapiro-Wilk and Kolmogorov–Smirnov tests. Univariate analysis of categorical variables was performed with chi-square and Fisher's exact test when appropriate; continuous variables were analysed by Mann-Whitney test as the majority of the continuous variables were not normally distributed. Multivariable analysis consisted of logistic regression for the dichotomous variables and multivariable Mann-Whitney test.

Ethics

This work was registered as an audit at the lead site of analysis and did not require independent ethical committee approval. Furthermore, all data was completely anonymised and coded as it did not contain any patient-identifiable information it was not necessary to obtain individual patient consent.

RESULTS

A total of 183 patients with panNETs (97 males and 86 females) were included, for which 224 scans were identified (114 male, 110 female) and analysed. Forty one individuals underwent repeat ^{68}Ga-DOTA PET/CT scans (Liverpool Centre) at different points within their treatment pathway (data handling as outlined in Methods).

Baseline Characteristics

Baseline characteristics of the participants are shown in **Table 1**.

Genetic Data

Data for the whole cohort are shown, but additionally we compare data between sporadic panNETs and familial panNETs. Sporadic panNETs arose in 141 patients with panNET-associated familial syndromes in 42 individuals: 36 with MEN1, 2 with VHL, 1 each with TSC, NF1, paraganglioma, MAX mutation and MUTYH-associated polyposis.

Age

The median age of individuals with familial panNETs was younger than that for those with sporadic panNETs (51 *vs.* 66 years respectively).

Histopathological Classification

Where available, diagnosis was based on biopsy (either from EUS-FNA, tissue biopsy or from histopathological examination of a resected specimen) for the majority of cases (n=163; 89%); this proportion was similar for sporadic and panNETs (n=127; 90.1% *vs.* n=36, 85.7% respectively). In cases where a tissue biopsy was not performed, diagnosis was based on imaging characteristics. Frequency of tumour grades were G1, 2 and 3: 50.3%, 46.2% and 3.5% respectively for the whole cohort, and the proportions were similar between sporadic and familial panNETs. The reason for the overwhelming predominance of G1 and G2 tumours is likely because our retrospective analysis was based on identifying those patients who had undergone galluim PET/CT scanning. This investigation would usually be reserved for lower grade NETs.

Extent of Metastatic Spread

Similarly, most tumours were localised (60.1%) or only locally advanced (14.2%) at diagnosis with 23.5% metastatic; familial tumours tended to be more localised than sporadic tumours. The sites of metastatic spread were as expected: liver (60, 32.8% of the entire series), lung (18, 9.8% of the entire series), bone (26, 14.2% of the entire series) and peritoneum (1, 0.5%).

Functionality of the Tumour

Overall, the majority of tumours were non-functional (73.2%) (**Table 2**). As would be expected, functionality was more common in those with familial panNETs (40.5%) versus those with sporadic panNETs (21.3%).

TABLE 1 | Summary of patients' characteristics.

		Whole cohort (n=183)		Sporadic (n=141)		Familial (n=42)	
		n	%	n	%	n	%
Gender	Male	97	53	75	53.2	22	52.4
	Female	86	47	66	46.8	20	47.6
Median age (SD) years		63 (14.9)	N/A	66 (12.5)	N/A	51 (16.5)	N/A
Range (upper, lower)		13,89		13,89		17,79	
Diagnosis based on	Imaging	20	11	14	9.9	6	14.3
	Biopsy	163	89	127	90.1	36	85.7
Ki 67 index (Grade (G))	G1 (<3%)	72	50.3	58	41.1	14	33.3
	G2 (3-20%)	66		55	39	11	26.2
	G3 (>20%)	5	46.2	4	2.8%	1	2.4
	(range 22-42)	(missing n=40)	3.5	(missing n=24)		(missing n=16)	
Stage at diagnosis	Localised	110	60.1	83	58.9	27	64.3
	Locally advanced	26		19	13.5	7	16.7
		43	14.2	37	26.2	6	14.3
	Metastatic	(missing n=4)	23.5	(missing n=2)		(missing n=2)	
Status	Alive	163	89.1	124	87.9	39	92.9
	Deceased	17		15	10.6	2	4.8
		(missing n=3)	9.3	(missing n=2)		(missing n=1)	

TABLE 2 | Functional hormone secretory patterns.

	Whole cohort (n=183)		Sporadic (n=141)		Familial (n=42)	
	Number, n	%	Number, n	%	Number, n	%
Functionality						
Functional	39	21.3	22	15.6	17	40.5
Non-functional	134	73.2	110	78	24	57.1
Specific functional excess						
Insulinoma	13	7.1	9	6.4	4	9.5
Gastrinoma/Zollinger-Ellison syndrome	12	6.5	5	3.	4	9.5
Glucagonoma	7	3.8	3	2.1	4	9.5
PTHrP secreting	1	1	2	1.4	–	–
Ectopic ACTH secretion	1	0.5	1	0.7	–	–
Pancreatic polypeptide	1	0.5	–	–	1	2.4
Proinsulin	1	0.5	1	0.7	–	–
VIP and glucagon co-secretion	1	0.5	1	0.7	–	–

Specific functional excess does not include carcinoid syndrome. Missing data not displayed. Percentages are based on the whole sample including missing data in this table. PTHrP, parathyroid hormone-related peptide; ACTH, adrenocorticotrophic hormone; VIP, vasoactive intestinal polypeptide.

Treatment Characteristics

The majority of patients were treated with curative resection (68%) (**Table 3**). Only a small number received somatostatin analogues, chemotherapy or PRRT.

Indications for Performing ^{68}Ga DOTA PET/CT Scans

There were a variety of indications for performing the ^{68}Ga-DOTA PET/CT, including diagnosis in cases of suspected panNETs; completing staging in patients with suspected localised panNETs who were being considered for surgical resection (40%), in patients being considered for PRRT (8%), or in post-surgical patients assumed to be disease-free as part of surveillance or monitoring for relapse (53%) (**Table 4**).

The Impact of ^{68}Ga DOTA PET/CT Imaging on Patient Management

Findings from the scan were categorised as follows (**Table 5**): in 53.5% of episodes (n=107) the scan findings provided confirmatory evidence available from cross-sectional imaging. In 28.5% of episodes (n=57) the scan identified sites of disease not previously seen with other imaging. There was no evidence that functional imaging provided any advantages over cross-sectional imaging for any specific sites of disease.

In 12% of cases (n=24) this led to an inter-modality change in treatment and in 5% (n=10), the scan ruled out the presence of metastases/disease suspected on previous imaging. In 1% (n=2), the scan confirmed adequacy of resection/PRRT response. In 24 episodes these data were missing. In total, new information from the scan was provided in 53.8% of cases (n=119) and influenced management in 39.4% of episodes (n=85).

TABLE 4 | Rationale for performing Ga^{68} DOTA PET/CT scans.

	Whole cohort (n=224)		Sporadic (n=172)		Familial (n=52)	
	Number, n	%	Number, n	%	Number, n	%
Diagnosis and staging	88	40	62	36	26	50
Consideration for PRRT	17	8	15	9	2	4
Post-operative assessment/ surveillance/monitoring for relapse	117	53	93	55	24	46
Missing	2		2		0	

TABLE 3 | Characteristics of tumour staging and treatments. Percentages are calculated on the valid data excluding the missing data.

		Whole cohort (n=183)		Sporadic (n=141)		Familial (n=42)	
		n	%	n	%	n	%
Curative resection	Yes	124	67.8	98	69.5	26	61.9
	No	59	32.2	43	30.5	16	38.1
T pathological stage	**T1**	55	36.9	41	35.0	14	43.8
(based on resection specimen) (Tumour size)	**T2**	37	24.8	26	22.2	11	34.4
	T3	42	28.1	36	30.8	6	18.8
	T4	15	10.1	14	12.0	1	3.1
N pathological stage	**N0**	96	61.1	76	62.3	20	57.1
(based on resection specimen) (Lymph node)	**N1**	60	38.2	45	36.9	15	42.9
	N2	1	0.6	1	0.8	0	
Metastasis M at diagnosis	**M0**	130	74.7	98	72.6	32	82.1
	M1	44	25.3	37	27.4	7	17.9
Resection margins	**R0**	76	72.4	64	74.4	12	63.2
	R1	25	23.9	20	23.3	5	26.3
	R2	4	3.8	2	2.3	2	10.5
Type of treatment	**SSA** (Y/N)	39/97	40.2	32	82.1	7	17.9
	Chemotherapy	25/116	21.6	23	92.0	2	8.0
	PRRT (Y/N)	18/118	15.3	15	83.3	3	16.7

TABLE 5 | Findings from Ga^{68}-DOTA PET/CT imaging and the impact on patient management.

	Whole cohort (n=224)		Sporadic (n=172)		Familial (n=52)	
Findings form the Ga68 DOTA PET/CT imaging	**Number, n**	**Valid %**	**Number, n**	**Valid %**	**Number, n**	**Valid %**
Confirmed information derived from other imaging modalities	107	53.5	81	54.7	26	50.0
Identified sites of cancer not previously seen with other imaging	57	28.5	40	27.0	17	32.7
Inter-modality change of treatment	24	12	17	11.5	7	13.5
Ruled out presence of metastases/disease suspected on previous imaging	10	5	8	5.4	2	3.8
Confirmed resection/PRRT response	2	1	2	1.4	N/A	N/A
Missing	24	N/A	24	N/A		
Impact on patient management						
Additional information provided						
Yes	119	53.8	88	52.1	31	59.6
No	102	46.2	81	47.9	21	40.4
Missing	3	–	3	–	–	–
Influenced management						
Yes	85	39.4	64	39	21	40.4
No	131	60.6	100	61	31	59.6
Missing	8	–	8	–	–	

Death

Eighty nine percent of patients were still alive with only 9% deceased

Univariate analysis, comparing familial syndrome to sporadic, revealed that there were statistical differences in hormone related syndromes, favouring familial cases ($p<0.001$). The location of the primary was multifocal more frequently in familial cases ($p<0.001$) and in sporadic cases, the stage was more commonly metastatic ($p=0.009$). There was somatostatin analogue use more often in the sporadic cases ($p=0.03$). Also, there were significant differences in the outcome of the resection in the 2 groups ($p=0.025$); R0 was more often observed in the sporadic cases. However, no statistical difference was found regarding WHO grade, being predominantly G2 in both groups.

The multivariable analysis (logistic regression) did not show any significant independent variable associated with the change or impact on management.

DISCUSSION

The findings of this study, conducted in a large cohort of patients with sporadic and familial (predominantly MEN1-related) panNETs highlight the role of ^{68}Ga-DOTA PET/CT imaging in the diagnosis, staging and determination of treatment options in patients with panNETs. The scan identified sites of disease that had not been identified with other imaging in 28.5% of patients, excluded suspected disease sites in 5% and confirmed resection/PRRT response in 1% of cases. Overall ^{68}Ga-DOTA PET/CT imaging impacted on patient management by providing additional information over cross-sectional imaging in 53.8% of cases and influenced management in 39.4% of cases. Ga^{68}-DOTA PET/CT imaging may aid or change management by identification of additional sites of pancreatic or metastatic disease not observed using CT/MRI, or by modifying the intended surgical approach or leading to substitution of surgery for systemic therapy where unresectable disease is demonstrated. Similarly, ^{68}Ga-DOTA PET/CT was necessary prior to PRRT treatment to demonstrate eligibility by confirming avidity of the tumour to SSTR-based tracers (26).

Our findings are consistent with those of other studies that have examined the role of functional imaging in patients with panNETs. The choice of functional imaging modality depends on the biological characteristics of the NETs, where histological grade is available: ^{18}F-FDG PET/CT is preferred for more aggressive, higher grade and less well differentiated neuroendocrine neoplasms while ^{68}Ga-DOTA PET/CT was found to be superior to ^{18}F-FDG PET/CT in patients with low-grade tumours. In general, in patients with a NET with a lower Ki67 index, the use of ^{18}F-FDG PET/CT should be limited, while for higher G2 and G3 NETs, combined ^{68}Ga-DOTATATE and ^{18}F-FDG PET/CT can be considered (27). In the current study, we do not report findings of the ^{18}F-FDG PET/CT scans (if/where they were undertaken) in those patients with higher G2 and G3 NETs as this was not the focus of the research.

The role of ^{68}Ga-DOTA PET/CT imaging in patients with NETs has generally been well established (28, 29) and it is now acknowledged as the functional imaging modality of choice in the current standards of care, where available (26, 30). Although the potential utility of SRS is acknowledged in the diagnosis of panNETs, ^{68}Ga DOTA PET/CT is generally considered superior to conventional SRS. As no SRS was undertaken in this cohort, no comparative data between SRS and PET/CT is available. However, much of the previous analysis relating to ^{68}Ga-DOTA PET/CT imaging in patients with NETs has related to heterogeneous populations of gastroenteropancreatic (GEP) NETs, with far fewer studies evaluating the utility in panNETs exclusively (31–33). Reassuringly, a recent systematic review and meta-analysis of 14 studies including a total of 1,561 patients demonstrated that somatostatin receptor directed PET-CT effected a change in management in 44% (range 16-81%) consistent with our findings (34).

Furthermore, in the studies examining panNETs exclusively, most reflect analysis in sporadic panNETS, and few have included

MEN1-related panNETs specifically (**Supplementary Table 1**). The strength of this study is that it includes a large cohort of patients with MEN1-associated panNETs. Current clinical practice guidelines for the diagnosis and surveillance of non-functional panNETs suggest the use of biomarkers (such as chromogranin A), but the results of recent biomarker studies highlight a low diagnostic accuracy for MEN1-associated panNETs (35, 36). The MEN guidelines also recommend anatomical imaging modalities such as CT/MRI and EUS without mentioning these newer functional imaging modalities (17). The inclusion of the genetic cohort (who are under regular active clinical, biochemical and radiological surveillance) may explain the proportion of patients with localised disease permitting complete resection. There have been only a small number of both retrospective and prospective analyses of the role of ^{68}Ga DOTA PET/CT specifically considering MEN1-associated panNETs (21, 24, 37, 38). Applied to MEN1 specifically, ^{68}Ga DOTA PET/CT was more sensitive than Octreoscan or CT scan in a study of 26 cases comparing multiple imaging modalities (including ^{111}I-pentetreotide SPECT-CT and triple phase CT); in 38.5% of patients ^{68}Ga DOTA PET/CT detected additional metastases (24). In 31%, the addition of ^{68}Ga DOTA PET/CT scan findings caused a change in management recommendations (related to detection of metastases). The group recommended that this imaging modality should be integrated into screening and surveillance of panNETs in MEN1. In a larger cohort of 131 patients with GEP-NETS studied prospectively (of which a proportion were panNETs), ^{68}Ga DOTATE PET/CT was demonstrated to be significantly superior to CT and ^{111}In-pentetreotide (demonstrating 95.1, 45.3 and 30.9% of lesions respectively) (21). However, we would argue that functional imaging is only advocated in cases where surgical resection or PRRT is being considered or in general where the results may influence management.

A recent analysis of 5287 cases of panNET in the Surveillance, Epidemiology and End Results Program (SEER) US national database, demonstrated that the median survival from diagnosis was 4.1 years (95% CI 3.9-4.4), but this varied dramatically according to patient characteristics. Functioning (*vs.* non-functioning) panNETs, younger age at diagnosis, localised disease, lower tumour grade and surgical treatment were all associated with lower mortality. However, even the most favourable combination of risk factors were still associated with some reduction in normal life expectancy (16) and so there is a significant need for early detection and selection of the most appropriate treatment to improve patient outcomes. The optimal management of patients with panNETs depends on their size, functionality, tumour grade and stage. The decision as to whether management should consist of ongoing surveillance, surgical resection, medical or systemic therapy requires a multidisciplinary approach. The positive impact of surgical resection on survival in patients with nonfunctioning panNETs has been repeatedly demonstrated (39, 40). Current recommendations for surgical intervention suggest that resection should be considered for any functional panNET or for non-functional panNETs >2cm (41). Small nonfunctioning panNETs are often indolent neoplasms without lymph node metastasis. However, within the context of MEN1, analysis of the literature for MEN1-related panNETs highlighted a very low growth rate of small non-functioning (NF) panNETs suggesting a need for a re-evaluation of the timing and frequency of surveillance and optimal treatment approach (42).

Our results showed a lower percentage of R0 resection in familial cases. This could be related to a more conservative surgical approach. However, in our series, it could be partially explained by a higher number of missing data within this smaller group (the familial cases).

Limitations of this study are acknowledged. First, we acknowledge that this was a retrospective data collection with the inherent limitations (e.g., less comprehensive and a lack of standardisation of data collection) and secondly that we were also unable to record detailed justification of the management decisions other than *via* the written NET MDT outcomes. Histopathological data was available for the vast majority (89%) of patients but not for the entire cohort. This reflects real-world management where tissue sampling may not be feasible or clinically appropriate. Furthermore, we accept PET/CT scanning equipment and scanning protocols (including use of slightly different radiolabelled somatostatin analogues (DOTA-NOC *vs.* TOC *vs.* TATE) are not perfectly aligned between centres. We do not routinely quantify tracer uptake on the PET/CT scans e.g., using SUV_{max} or Krenning score however this may be a more relevant consideration to assess treatment response rather than initial treatment choice. Finally, we do not have simultaneous Octreoscans to highlight the superior sensitivity of somatostatin receptor-directed PET-CT over octreoscans. However, the significant strengths of the current study include the large size of the series including both sporadic and familial, inclusion of three ENETS centre of excellence and extensive multi-disciplinary involvement including 4 experienced nuclear medicine PET/CT physicians.

Thus, although we cannot comment on the role of functional imaging (*versus* cross-sectional or biochemical surveillance) as part of a surveillance protocol in patients who have received treatment for their NET, we have shown that ^{68}Ga-DOTA PET/CT has a significant complementary role in staging and guiding treatment in patients with sporadic and familial panNETs with newly diagnosed or recurrent disease, particularly where surgical resection or treatment with PRRT is considered.

DATA AVAILABILITY STATEMENT

The raw data supporting the conclusions of this article will be made available by the authors, without undue reservation.

ETHICS STATEMENT

Ethical review and approval was not required for the study on human participants in accordance with the local legislation and institutional requirements. Written informed consent for participation was not required for this study in accordance with the national legislation and the institutional requirements.

AUTHOR CONTRIBUTIONS

All authors contributed to data collection, drafting and editing the manuscript. Statistical analysis was undertaken by JB. All authors contributed to the article and approved the submitted version.

SUPPLEMENTARY MATERIAL

The Supplementary Material for this article can be found online at: https://www.frontiersin.org/articles/10.3389/fendo.2021.654975/full#supplementary-material

REFERENCES

1. Lawrence B, Gustafsson BI, Chan A, Svejda B, Kidd M, Modlin IM. The Epidemiology of Gastroenteropancreatic Neuroendocrine Tumors. *Endocrinol Metab Clin North Am* (2011) 40(1):1–18. vii. doi: 10.1016/j.ecl.2010.12.005
2. Dasari A, Shen C, Halperin D, Zhao B, Zhou S, Xu Y, et al. Trends in the Incidence, Prevalence, and Survival Outcomes in Patients With Neuroendocrine Tumors in the United States. *JAMA Oncol* (2017) 3 (10):1335–42. doi: 10.1001/jamaoncol.2017.0589
3. Hallet J, Law CHL, Cukier M, Saskin R, Liu N, Singh S. Exploring the Rising Incidence of Neuroendocrine Tumors: A Population-Based Analysis of Epidemiology, Metastatic Presentation, and Outcomes. *Cancer* (2015) 121 (4):589–97. doi: 10.1002/cncr.29099
4. Halfdanarson TR, Rabe KG, Rubin J, Petersen GM. Pancreatic Neuroendocrine Tumors (Pnets): Incidence, Prognosis and Recent Trend Toward Improved Survival. *Ann Oncol* (2008) 19(10):1727–33. doi: 10.1093/annonc/mdn351
5. Strosberg J, El-Haddad G, Wolin E, Hendifar A, Yao J, Chasen B, et al. Phase 3 Trial of 177Lu-Dotatate for Midgut Neuroendocrine Tumors. *N Engl J Med* (2017) 376(2):125–35. doi: 10.1056/NEJMoa1607427
6. Yao JC, Shah MH, Ito T, Bohas CL, Wolin EM, Van Cutsem E, et al. Everolimus for Advanced Pancreatic Neuroendocrine Tumors. *N Engl J Med* (2011) 364(6):514–23. doi: 10.1056/NEJMoa1009290
7. Raymond E, Dahan L, Raoul JL, Bang YJ, Borbath I, Lombard-Bohas C, et al. Sunitinib Malate for the Treatment of Pancreatic Neuroendocrine Tumors. *N Engl J Med* (2011) 364(6):501–13. doi: 10.1056/NEJMoa1003825
8. Rinke A, Muller HH, Schade-Brittinger C, Klose KJ, Barth P, Wied M, et al. Placebo-Controlled, Double-Blind, Prospective, Randomized Study on the Effect of Octreotide LAR in the Control of Tumor Growth in Patients With Metastatic Neuroendocrine Midgut Tumors: A Report From the PROMID Study Group. *J Clin Oncol* (2009) 27(28):4656–63. doi: 10.1200/JCO.2009.22.8510
9. Caplin ME, Pavel M, Ćwikła JB, Phan AT, Raderer M, Sedláčková E, et al. Lanreotide in Metastatic Enteropancreatic Neuroendocrine Tumors. *New Engl J Med* (2014) 371(3):224–33. doi: 10.1056/NEJMoa1316158
10. Strosberg JR, Fine RL, Choi J, Nasir A, Coppola D, Chen DT, et al. First-Line Chemotherapy With Capecitabine and Temozolomide in Patients With Metastatic Pancreatic Endocrine Carcinomas. *Cancer* (2011) 117(2):268–75. doi: 10.1002/cncr.25425
11. Chun YS, Pawlik TM, Vauthey JN. 8th Edition of the AJCC Cancer Staging Manual: Pancreas and Hepatobiliary Cancers. *Ann Surg Oncol* (2018) 25 (4):845–7. doi: 10.1245/s10434-017-6025-x
12. Perren A, Couvelard A, Scoazec JY, Costa F, Borbath I, Delle Fave G, et al. Enets Consensus Guidelines for the Standards of Care in Neuroendocrine Tumors: Pathology: Diagnosis and Prognostic Stratification. *Neuroendocrinology* (2017) 105(3):196–200. doi: 10.1159/000457956
13. Lloyd RV OR, Klöppel G, Rosai J. *Who Classification of Tumours of Endocrine Organs. 4th*. Lyon: International Agency for Research on Cancer (2017).
14. Auernhammer CJ, Spitzweg C, Angele MK, Boeck S, Grossman A, Nolting S, et al. Advanced Neuroendocrine Tumours of the Small Intestine and Pancreas: Clinical Developments, Controversies, and Future Strategies. *Lancet Diabetes Endocrinol* (2018) 6(5):404–15. doi: 10.1016/S2213-8587(17)30401-1
15. Yang M, Ke NW, Zeng L, Zhang Y, Tan CL, Zhang H, et al. Survival Analyses for Patients With Surgically Resected Pancreatic Neuroendocrine Tumors by World Health Organization 2010 Grading Classifications and American Joint Committee on Cancer 2010 Staging Systems. *Medicine* (2015) 94(48):e2156. doi: 10.1097/MD.0000000000002156
16. Brooks JC, Shavelle RM, Vavra-Musser KN. Life Expectancy in Pancreatic Neuroendocrine Cancer. *Clin Res Hepatol Gastroenterol* (2019) 43(1):88–97. doi: 10.1016/j.clinre.2018.08.005
17. Thakker RV, Newey PJ, Walls GV, Bilezikian J, Dralle H, Ebeling PR, et al. Clinical Practice Guidelines for Multiple Endocrine Neoplasia Type 1 (MEN1). *J Clin Endocrinol Metab* (2012) 97(9):2990–3011. doi: 10.1210/jc.2012-1230
18. McKenna LR, Edil BH. Update on Pancreatic Neuroendocrine Tumors. *Gland Surg* (2014) 3(4):258–75. doi: 10.3978/j.issn.2227-684X.2014.06.03
19. Vinjamuri S, Gilbert TM, Banks M, McKane G, Maltby P, Poston G, et al. Peptide Receptor Radionuclide Therapy With (90)Y-DOTATATE/(90)Y-DOTATOC in Patients With Progressive Metastatic Neuroendocrine Tumours: Assessment of Response, Survival and Toxicity. *Br J Cancer* (2013) 108(7):1440–8. doi: 10.1038/bjc.2013.103
20. Krenning EP, Kwekkeboom DJ, Bakker WH, Breeman WA, Kooij PP, Oei HY, et al. Somatostatin Receptor Scintigraphy With [111In-DTPA-D-Phe1]- and [123I-Tyr3]-octreotide: The Rotterdam Experience With More Than 1000 Patients. *Eur J Nucl Med* (1993) 20(8):716–31. doi: 10.1007/BF00181765
21. Sadowski SM, Neychev V, Millo C, Shih J, Nilubol N, Herscovitch P, et al. Prospective Study of 68Ga-DOTATATE Positron Emission Tomography/Computed Tomography for Detecting Gastro-Entero-Pancreatic Neuroendocrine Tumors and Unknown Primary Sites. *J Clin Oncol* (2016) 34(6):588–96. doi: 10.1200/JCO.2015.64.0987
22. Srirajaskanthan R, Kayani I, Quigley AM, Soh J, Caplin ME, Bomanji J. The Role of 68Ga-DOTATATE PET in Patients With Neuroendocrine Tumors and Negative or Equivocal Findings on 111In-DTPA-octreotide Scintigraphy. *J Nucl Med* (2010) 51(6):875–82. doi: 10.2967/jnumed.109.066134
23. Lamarca A, Pritchard DM, Westwood T, Papaxoinis G, Nonaka D, Vinjamuri S, et al. 68Gallium DOTANOC-PET Imaging in Lung Carcinoids: Impact on Patients' Management. *Neuroendocrinology* (2018) 106(2):128–38. doi: 10.1159/000472717
24. Sadowski S, Millo C, Cottle-Delisle C, Merkel R, Yang L, Herscovitch P, et al. Results of (68)Gallium-DOTATATE PET/CT scanning in patients with multiple endocrine neoplasia type 12015.
25. Eusebi LH, Thorburn D, Toumpanakis C, Frazzoni L, Johnson G, Vessal S, et al. Endoscopic Ultrasound-Guided Fine-Needle Aspiration vs Fine-Needle Biopsy for the Diagnosis of Pancreatic Neuroendocrine Tumors. *Endoscopy Int Open* (2019) 07(11):E1393–E9. doi: 10.1055/a-0967-4684
26. Sundin A, Arnold R, Baudin E, Cwikla JB, Eriksson B, Fanti S, et al. Enets Consensus Guidelines for the Standards of Care in Neuroendocrine Tumors: Radiological, Nuclear Medicine & Hybrid Imaging. *Neuroendocrinology* (2017) 105(3):212–44. doi: 10.1159/000471879
27. Panagiotidis E, Alshammari A, Michopoulou S, Skoura E, Naik K, Maragkoudakis E, et al. Comparison of the Impact of 68Ga-DOTATATE and 18F-FDG PET/CT on Clinical Management in Patients With Neuroendocrine Tumors. *J Nucl Med* (2017) 58(1):91–6. doi: 10.2967/jnumed.116.178095
28. Geijer H, Breimer LH. Somatostatin Receptor PET/CT in Neuroendocrine Tumours: Update on Systematic Review and Meta-Analysis. *Eur J Nucl Med Mol Imaging* (2013) 40(11):1770–80. doi: 10.1007/s00259-013-2482-z
29. Skoura E, Michopoulou S, Mohmaduvesh M, Panagiotidis E, Al Harbi M, Toumpanakis C, et al. The Impact of 68Ga-DOTATATE PET/CT Imaging on Management of Patients With Neuroendocrine Tumors: Experience From a National Referral Center in the United Kingdom. *J Nucl Med* (2016) 57(1):34–40. doi: 10.2967/jnumed.115.166017
30. Zandee WT, de Herder WW. The Evolution of Neuroendocrine Tumor Treatment Reflected by ENETS Guidelines. *Neuroendocrinology* (2018) 106 (4):357–65. doi: 10.1159/000486096
31. Sharma P, Arora S, Dhull VS, Naswa N, Kumar R, Ammini AC, et al. Evaluation of (68)Ga-DOTANOC PET/CT Imaging in a Large Exclusive Population of Pancreatic Neuroendocrine Tumors. *Abdom Imaging* (2015) 40 (2):299–309. doi: 10.1007/s00261-014-0219-5
32. Schmid-Tannwald C, Schmid-Tannwald CM, Morelli JN, Neumann R, Haug AR, Jansen N, et al. Comparison of Abdominal MRI With Diffusion-Weighted

Imaging to 68Ga-DOTATATE PET/CT in Detection of Neuroendocrine Tumors of the Pancreas. *Eur J Nucl Med Mol Imaging* (2013) 40(6):897–907. doi: 10.1007/s00259-013-2371-5
33. Naswa N, Sharma P, Kumar A, Nazar AH, Kumar R, Chumber S, et al. Gallium-68-DOTA-NOC PET/CT of Patients With Gastroenteropancreatic Neuroendocrine Tumors: A Prospective Single-Center Study. *AJR Am J Roentgenol* (2011) 197(5):1221–8. doi: 10.2214/AJR.11.7298
34. Barrio M, Czernin J, Fanti S, Ambrosini V, Binse I, Du L, et al. The Impact of Somatostatin Receptor-Directed PET/CT on the Management of Patients With Neuroendocrine Tumor: A Systematic Review and Meta-Analysis. *J Nucl Med* (2017) 58(5):756–61. doi: 10.2967/jnumed.116.185587
35. Qiu W, Christakis I, Silva A, Bassett RLJr., Cao L, Meng QH, et al. Utility of Chromogranin A, Pancreatic Polypeptide, Glucagon and Gastrin in the Diagnosis and Follow-Up of Pancreatic Neuroendocrine Tumours in Multiple Endocrine Neoplasia Type 1 Patients. *Clin Endocrinol* (2016) 85 (3):400–7. doi: 10.1111/cen.13119
36. de Laat JM, Pieterman CR, Weijmans M, Hermus AR, Dekkers OM, de Herder WW, et al. Low Accuracy of Tumor Markers for Diagnosing Pancreatic Neuroendocrine Tumors in Multiple Endocrine Neoplasia Type 1 Patients. *J Clin Endocrinol Metab* (2013) 98(10):4143–51. doi: 10.1210/jc.2013-1800
37. Albers MB, Librizzi D, Lopez CL, Manoharan J, Apitzsch JC, Slater EP, et al. Limited Value of Ga-68-DOTATOC-PET-CT in Routine Screening of Patients With Multiple Endocrine Neoplasia Type 1. *World J Surg* (2017) 41(6):1521–7. doi: 10.1007/s00268-017-3907-9
38. Froeling V, Elgeti F, Maurer MH, Scheurig-Muenkler C, Beck A, Kroencke TJ, et al. Impact of Ga-68 Dotatoc PET/CT on the Diagnosis and Treatment of Patients With Multiple Endocrine Neoplasia. *Ann Nucl Med* (2012) 26 (9):738–43. doi: 10.1007/s12149-012-0634-z
39. Hill JS, McPhee JT, McDade TP, Zhou Z, Sullivan ME, Whalen GF, et al. Pancreatic Neuroendocrine Tumors: The Impact of Surgical Resection on Survival. *Cancer* (2009) 115(4):741–51. doi: 10.1002/cncr.24065
40. Gomez-Rivera F, Stewart AE, Arnoletti JP, Vickers S, Bland KI, Heslin MJ. Surgical Treatment of Pancreatic Endocrine Neoplasms. *Am J Surg* (2007) 193 (4):460–5. doi: 10.1016/j.amjsurg.2006.10.016
41. Falconi M, Eriksson B, Kaltsas G, Bartsch DK, Capdevila J, Caplin M, et al. Enets Consensus Guidelines Update for the Management of Patients With Functional Pancreatic Neuroendocrine Tumors and Non-Functional Pancreatic Neuroendocrine Tumors. *Neuroendocrinology* (2016) 103 (2):153–71. doi: 10.1159/000443171
42. van Treijen MJC, van Beek DJ, van Leeuwaarde RS, Vriens MR, Valk GD. Diagnosing Nonfunctional Pancreatic NETs in MEN1: The Evidence Base. *J Endocr Soc* (2018) 2(9):1067–88. doi: 10.1210/js.2018-00087

Conflict of Interest: The authors declare that the research was conducted in the absence of any commercial or financial relationships that could be construed as a potential conflict of interest.

Advantages of publishing in Frontiers

OPEN ACCESS
Articles are free to read for greatest visibility and readership

FAST PUBLICATION
Around 90 days from submission to decision

HIGH QUALITY PEER-REVIEW
Rigorous, collaborative, and constructive peer-review

TRANSPARENT PEER-REVIEW
Editors and reviewers acknowledged by name on published articles

Frontiers
Avenue du Tribunal-Fédéral 34
1005 Lausanne | Switzerland

Visit us: www.frontiersin.org
Contact us: frontiersin.org/about/contact

REPRODUCIBILITY OF RESEARCH
Support open data and methods to enhance research reproducibility

DIGITAL PUBLISHING
Articles designed for optimal readership across devices

FOLLOW US
@frontiersin

IMPACT METRICS
Advanced article metrics track visibility across digital media

EXTENSIVE PROMOTION
Marketing and promotion of impactful research

LOOP RESEARCH NETWORK
Our network increases your article's readership